



**PROCEEDINGS OF THE 24<sup>TH</sup>  
INTERNATIONAL APPLIED GEOCHEMISTRY SYMPOSIUM  
FREDERICTON, NEW BRUNSWICK, CANADA**



**JUNE 1<sup>ST</sup>-4<sup>TH</sup>, 2009**

**EDITED BY**

**DAVID R. LENTZ, KATHLEEN G. THORNE, & KRISTY-LEE BEAL**



**VOLUME II**



All rights reserved.

This publication may not be reproduced in whole or in part, stored in a retrieval system or transmitted in any form or by any means without permission from the publisher.

ISBN 978-1-55131-137-1 (Volume 2)

©2009 AAG

**PROCEEDINGS OF THE 24<sup>TH</sup>  
INTERNATIONAL APPLIED GEOCHEMISTRY SYMPOSIUM  
FREDERICTON, NEW BRUNSWICK  
CANADA  
JUNE 1<sup>ST</sup>-4<sup>TH</sup>, 2009**

**EDITED BY**

**DAVID R. LENTZ  
KATHLEEN G. THORNE  
KRISTY-LEE BEAL**

**VOLUME II**



## TABLE OF CONTENTS (VOLUME II)

TECHNICAL EDITORS .....	IX
<b>NEW FRONTIERS FOR EXPLORATION IN GLACIATED TERRAIN .....</b>	<b>563</b>
Glacial dispersal from the Mount Fronsac North massive sulfide deposit, Bathurst Mining Camp, New Brunswick, Canada .....	565
<i>Heather Campbell<sup>1</sup>, Bruce E. Broster<sup>1</sup>, Michael Parkhill<sup>2</sup>, Nicholas Susak<sup>1</sup>, &amp; Paul Arp<sup>3</sup></i> .....	565
Geochemical and mineral dispersal patterns related to drift-covered copper-gold mineralization in central British Columbia, Canada .....	569
<i>Ray Lett</i> .....	569
Heavy mineral and till geochemical signatures of the NICO Co-Au-Bi deposit, Great Bear magmatic zone, Northwest Territories, Canada .....	573
<i>Isabelle McMartin<sup>1</sup>, Louise Corriveau<sup>2</sup> &amp; Georges Beaudoin<sup>3</sup></i> .....	573
Base metal exploration using indicator minerals in glacial sediments, northwestern Alberta, Canada .....	577
<i>Roger C. Paulen<sup>1</sup>, Suzanne Paradis<sup>2</sup>, Alain Plouffe<sup>1</sup> &amp; I. Rod Smith<sup>3</sup></i> .....	577
Imaging a buried diamondiferous kimberlite using conventional geochemistry and Amplified Geochemical Imaging <sup>SM</sup> Technology .....	581
<i>Jamil. A. Sader<sup>1</sup>, Harry. S. Anderson II<sup>2</sup>, Ray. F. Fenstermacher<sup>2</sup> &amp; Keiko Hattori<sup>1</sup></i> .....	581
New advances in geochemical exploration in glaciated terrain – examples from northern Finland .....	585
<i>Pertti Sarala</i> .....	585
Regional geochemical soil data as aid to the reconstruction of Mid-Pleistocene ice flows across central and eastern England .....	589
<i>Andreas J. Scheib, Jonathan Lee, Neil Breward &amp; Lister Bob</i> .....	589
Till geochemical and indicator mineral methods in mineral exploration: history and status .....	593
<i>L. Harvey Thorleifson</i> .....	593
Numerical Evaluation of Partial Digestions for Soil Analysis, Talbot VMS Cu-Zn Prospect, Manitoba, Canada .....	597
<i>Pim W.G. Van Geffen<sup>1</sup>, T. Kurt Kyser<sup>1</sup>, Christopher J. Oates<sup>2</sup>, &amp; Christian Ihlenfeld<sup>2</sup></i> .....	597
Multi-element soil geochemistry above the Talbot Lake VMS Cu-Zn Deposit, Manitoba, Canada .....	601
<i>Pim W.G. Van Geffen<sup>1</sup>, T. Kurt Kyser<sup>1</sup>, Christopher J. Oates<sup>2</sup>, &amp; Christian Ihlenfeld<sup>2</sup></i> .....	601
<b>APPLIED AQUEOUS GEOCHEMISTRY .....</b>	<b>605</b>
Application of calcite precipitation rate in predicting the utilization period of calcite scale affected wells, Philippines .....	607
<i>Gabriel M. Aragon<sup>1</sup>, Benson G. Sambrano<sup>1</sup>, &amp; James B. Nogara<sup>1</sup></i> .....	607
Sources of arsenic contamination and remediation of mine water at the historical Glen Wills mining area in Northeast Victoria, Australia .....	611
<i>Dennis Arne<sup>1</sup>, Andrew Nelson<sup>2</sup>, &amp; John Webb<sup>2</sup></i> .....	611
Geochemical and hydrogeological controls on naturally occurring arsenic in groundwater at a field site in West Bengal, India .....	615
<i>Roger D. Beckie<sup>1</sup>, Alexandre J. Desbarats<sup>2</sup>, Tarak Pal<sup>3</sup>, Cassandra E. M. Koenig<sup>1</sup>, Pradip K. Mukherjee<sup>3</sup>, Andrew Rencz<sup>2</sup>, &amp; Gwendy Half<sup>2</sup></i> .....	615

Flux of river active material flowing into the sea from Chinese continent: preliminary results .....	619
<i>Sun Binbin<sup>1,2,3</sup>, Zhou Guohua<sup>1,2</sup>, Wei Hualing<sup>1,2</sup>, Liu Zhanyuan<sup>1,2</sup>, &amp; Zeng Daoming<sup>1,2</sup></i> .....	619
Methods for obtaining a national-scale overview of groundwater quality in New Zealand	623
<i>Christopher J. Daughney, Uwe Morgenstern, Rob van der Raaij, Robert Reeves, Matthias Raiber, &amp; Mark Randall</i> .....	623
Genesis of smectite scales in Mindanao geothermal production field, Philippines .....	627
<i>Rosella G. Dulce<sup>1</sup>, Gabriel M. Aragon<sup>2</sup>, Benson G. Sambrano<sup>3</sup>, &amp; Lauro F. Bayrante<sup>4</sup></i> .....	627
Adding Value to Kinetic Testing Data I – Interpretation of Tailings Humidity Cell Data from the Perspectives of Aqueous Geochemistry and Mineralogy at the Crowflight Minerals, Bucko Lake Nickel Project .....	631
<i>David R. Gladwell<sup>1</sup> &amp; Catherine T. Ziten<sup>1</sup></i> .....	631
Large-scale hydrogeochemical mapping - insight into alteration processes and prospectivity mapping .....	635
<i>David J Gray, Ryan R.P. Noble, &amp; Nathan Reid</i> .....	635
Ontario's ambient groundwater geochemistry project .....	639
<i>Stewart M. Hamilton<sup>1</sup></i> .....	639
Distribution of cadmium forms and their correlation with organic matters in acid soils ....	643
<i>Wei Hualing<sup>1,2</sup> &amp; Zhou Guohua<sup>1,2</sup></i> .....	643
Adaptation of the OECD T/DP for metals and metal compounds to marine systems .....	647
<i>Philippa Huntsman-Mapila<sup>1</sup>, Jim Skeaff<sup>1</sup>, Marcin Pawlak<sup>1</sup>, Hayley Roach<sup>1</sup>, &amp; Dave Hardy<sup>1</sup></i> .....	647
Ferromanganese nodules in Lake George, New Brunswick .....	649
<i>Camilla Melrose<sup>1</sup> &amp; Tom Al<sup>1</sup></i> .....	649
Application of stable hydrogen isotope models to the evaluation of groundwater and geothermal water resources: case of the Padurea Craiului limestone aquifers system...	653
<i>Delia Cristina Papp<sup>1</sup> &amp; Ioan Cociuba<sup>1</sup></i> .....	653
The influence of soil and bedrock on trace metal concentrations and groundwater quality in northern Finland.....	657
<i>Raija Pietilä<sup>1</sup></i> .....	657
Geochemistry of arsenic in the sediment-water interface of an alluvial aquifer, Bangladesh .....	661
<i>Md. T. Rahman<sup>1</sup>, Akira Mano<sup>1</sup>, Keiko Udo<sup>1</sup>, &amp; Yoshinobu Ishibashi<sup>2</sup></i> .....	661
Groundwater as a medium for geochemical exploration in peatlands.....	665
<i>Jamil A. Sader<sup>1</sup>, Keiko Hattori<sup>1</sup>, &amp; Stewart M. Hamilton<sup>2</sup></i> .....	665
Quantification of injection fluids effects to Mindanao Geothermal Production Field productivity through a series of tracer tests, Philippines .....	669
<i>Benson G. Sambrano<sup>1</sup>, Gabriel M. Aragon<sup>2</sup>, &amp; James B. Nogara<sup>2</sup></i> .....	669
Organic and inorganic surface expressions of the Lisbon and Lightning Draw Southeast oil and gas fields, Paradox Basin, Utah, USA .....	673
<i>David M. Seneshen<sup>1</sup>, Thomas C. Chidsey, Jr<sup>2</sup>, Craig D. Morgan<sup>2</sup>, &amp; Michael D. Vanden Berg<sup>2</sup></i> 673	
Aqueous geochemistry of Pit Lake at EL mine site, Manitoba, Canada: Implications for site remediation. ....	677
<i>Nikolay V. Sidenko<sup>1</sup>, Donald Harron<sup>1</sup>, Karen H. Mathers<sup>1</sup>, &amp; J. Michael McKernan<sup>1</sup></i> .....	677
The case for logratio based grain-size normalization of sediment .....	681
<i>Robert C. Szava-Kovats<sup>1</sup></i> .....	681

<b>APPLIED GEOCHEMISTRY OF GEOLOGICAL STORAGE OF CO<sub>2</sub></b> .....	<b>685</b>
Composition and levels of groundwater in the CO <sub>2</sub> CRC Otway Project area, Victoria, Australia: establishing a pre-injection baseline.....	687
<i>Patrice de Caritat<sup>1</sup>, Dirk Kirste<sup>2</sup>, &amp; Allison, Hortle<sup>3</sup></i> .....	687
Carbon mineralization in mine tailings and implications for carbon storage in ultramafic-hosted aquifers .....	691
<i>Gregory M. Dipple<sup>1</sup>, James M. Thom<sup>1</sup>, &amp; Siobhan A. Wilson<sup>1</sup></i> .....	691
Comparison of CO <sub>2</sub> -N <sub>2</sub> -enhanced coalbed methane recovery and CO <sub>2</sub> storage for low- & high-rank coals, Alberta, Canada and Shanxi, China.....	695
<i>William D. Gunter<sup>1</sup>, Xiaohui Deng<sup>1</sup>, &amp; Sam Wong<sup>1</sup></i> .....	695
Geochemical modelling and formation water monitoring at the CO <sub>2</sub> CRC Otway Project, Victoria, Australia.....	699
<i>Dirk Kirste<sup>1</sup>, Ernie Perkins<sup>2</sup>, Chris Boreham<sup>3</sup>, Barry Freifeld<sup>4</sup>, Linda Stalker<sup>5</sup>, Ulrike Schacht<sup>6</sup>, &amp; James Underschultz<sup>5</sup></i> .....	699
Pembina Cardium CO <sub>2</sub> Monitoring Project, Alberta Canada – geochemical evaluation and modelling of the geochemical monitoring data .....	703
<i>Ernie Perkins<sup>1</sup>, Stephen Talman<sup>1</sup>, &amp; Maurice Shevalier<sup>2</sup></i> .....	703
Numerical assessment of CO <sub>2</sub> enhanced CH <sub>4</sub> recovery from the Mallik gas hydrate field, Beaufort-Mackenzie Basin, Canada .....	707
<i>Mafiz Uddin<sup>1</sup>, J.F. Wright<sup>2</sup>, William D. Gunter<sup>3</sup>, &amp; D. Coombe<sup>4</sup></i> .....	707
Geochemical monitoring of chemical and isotopic compositions of CO <sub>2</sub> fluids and calcite precipitation during injection tests at Ogachi Hot-Dry Rock site, Japan.....	711
<i>Akira Ueda<sup>1</sup>, Yoshihiro Kuroda<sup>1</sup>, Kazunori Sugiyama<sup>2</sup>, Akiko Ozawa<sup>2</sup>, Hiroshi Wakahama<sup>3</sup>, Saeko Mito<sup>3</sup>, Yoshikazu Kaj<sup>4</sup>, &amp; Hideshi Kaieda<sup>5</sup></i> .....	711
<b>NORTH AMERICAN SOIL GEOCHEMICAL LANDSCAPES PROJECT</b> .....	<b>715</b>
The landscape geochemistry of the Sacramento Valley, California .....	717
<i>Martin B. Goldhaber<sup>1</sup>, Jean M. Morrison<sup>1</sup>, Richard B. Wanty<sup>1</sup>, Christopher T. Mills<sup>1</sup>, &amp; JoAnn M. Holloway<sup>1</sup></i> .....	717
The North American Soil Geochemical Landscapes Project: preliminary results from Nova Scotia .....	721
<i>Terry A. Goodwin<sup>1</sup>, Peter W. B. Friske<sup>2</sup>, Ken L. Ford<sup>2</sup>, &amp; Eric C. Grunsky<sup>2</sup></i> .....	721
Testing the variants of aqua regia digestion using certified reference materials.....	725
<i>E. C. Grunsky, R.G. Garrett, P.W. Friske, &amp; M. McCurdy<sup>1</sup></i> .....	725
Preliminary results of the North American Soil Geochemical Landscapes Project, northeast United States and Maritime Provinces of Canada.....	729
<i>Eric C. Grunsky<sup>1</sup>, David B. Smith<sup>2</sup>, Peter W.B. Friske<sup>1</sup>, &amp; Laurel G. Woodruff<sup>3</sup></i> .....	729
The North American Soil Geochemical Landscapes Project in New Brunswick .....	733
<i>Toon Pronk<sup>1</sup>, Michael A. Parkhill<sup>2</sup>, Rex Boldon<sup>1</sup>, Marc Desrosiers<sup>2</sup>, Peter Friske<sup>3</sup>, &amp; Andy Rencz<sup>3</sup></i> .....	733
The North American Soil Geochemical Landscapes Project: overview, goals, progress.....	737
<i>David B. Smith<sup>1</sup>, Laurel G. Woodruff<sup>2</sup>, Andy Rencz<sup>3</sup>, &amp; Alfredo de la Calleja<sup>4</sup></i> .....	737
Continental-scale patterns in soil geochemistry and mineralogy: results from two transects of the United States and Canada.....	741
<i>Laurel G. Woodruff<sup>1</sup>, David B. Smith<sup>2</sup>, D.D. Eber<sup>3</sup>, &amp; William F. Cannon<sup>4</sup></i> .....	741
<b>SOURCES, TRANSPORT, AND FATE OF TRACE AND TOXIC ELEMENTS IN THE ENVIRONMENT</b> .....	<b>745</b>

Sources of lead in soils and uptake by plants: Lower Guadiana River basin, south Portugal and Spain .....	747
<i>Maria J. Batista<sup>1</sup>, Maria M. Abreu<sup>2</sup>, J. Locutura<sup>3</sup>, T. Shepherd<sup>4</sup>, D. Oliveira<sup>1</sup>, J. Matos<sup>1</sup>, A. Bel-Lan<sup>3</sup>, &amp; L. Martins<sup>1</sup></i> .....	747
Risk assessment of arsenic mobility in groundwaters in Langley, British Columbia using geochemical indicators .....	751
<i>Rafael Cavalcanti de Albuquerque<sup>1</sup>, Dirk Kirste<sup>1</sup>, &amp; Diana Allen<sup>1</sup></i> .....	751
Spatial assessment of trace elements in Taylor Valley Antarctic Glaciers: Dominance of eolian deposition .....	755
<i>Sarah K. Fortner<sup>1,2*</sup>, Kathleen A. Welch<sup>1</sup>, W. Berry Lyons<sup>1,2</sup>, John Olesik<sup>2</sup> &amp; Rebecca A. Witherow<sup>1,2</sup></i> .....	755
Heavy metal loads in sediments influenced by Mežica Pb-Zn abandoned mine, Slovenia .....	759
<i>Mateja Gosar<sup>1</sup> &amp; Miloš Miler<sup>1</sup></i> .....	759
Relationship of heavy metals between rice and soils in Zhejiang, China .....	763
<i>Zhou Guohua, Wei Hualing, Sun Binbin &amp; Liu Zhanyuan</i> .....	763
Anthropogenic Gadolinium as a Micropollutant in Drinking Water .....	767
<i>Serkan Kulaksiz<sup>1</sup> &amp; Michael Bau<sup>1</sup></i> .....	767
Correlation of Atmospheric Soil and Atmospheric Lead in Three North American Cities: Can Re-suspension of Urban Lead Contaminated Soil be a Major Source of Urban Atmospheric Lead and Cause Seasonal Variations in Children's Blood Lead Levels? ...	771
<i>Mark Laidlaw<sup>1</sup></i> .....	771
Impact of Evolving Hypoxia on the Remobilization of As and Se in the Lower St. Lawrence Estuary (Québec).....	775
<i>Stelly Lefort<sup>1</sup>, Gwenaëlle Chaillou<sup>2</sup>, Nathalie Molnar<sup>1,3</sup>, Alfonso Mucci<sup>1</sup>, &amp; Bjorn Sundby<sup>1,2</sup></i> ..	775
Geochemistry of catchment outlet sediments: evaluation of Mobile Metal Ion <sup>TM</sup> analyses from the Thomson region, New South Wales, Australia .....	779
<i>Alan Mann<sup>1</sup>, Patrice de Carita<sup>2</sup>, and John Greenfield<sup>3</sup></i> .....	779
Five-Year History of a Biologically Based Treatment System that Treats High Concentrations of Effluent from an Industrial (Smelter Operation) Landfill .....	783
<i>Al Mattes<sup>1</sup>, Bill Duncan<sup>2</sup>, D.Gould<sup>3</sup>, Les Evans<sup>1</sup>, Susan Glasuaer<sup>1</sup></i> .....	783
Urban geochemistry and health in New Orleans: .....	789
Soil Pb, blood Pb and student achievement by 4 <sup>th</sup> graders .....	789
<i>Howard W. Mielke<sup>1,2</sup>, Christopher R. Gonzales<sup>3</sup>, &amp; Eric Powell<sup>4</sup></i> .....	789
Mercury concentrations in fungal tissues, as influenced by forest soil substrates and moss carpets .....	793
<i>Mina Nasr &amp; Paul A. Arp</i> .....	793
Hydrogeochemical processes governing the origin, transport, and fate of major and trace elements from mine wastes and mineralized rock.....	797
<i>D. Kirk Nordstrom<sup>1</sup></i> .....	797
Geological controls concerning mercury accumulations in stream sediments across Canada.....	803
<i>Jae Ogilvie<sup>1</sup>, Mina Nasr<sup>1</sup>, Andy Rencz<sup>2</sup>, Paul A. Arp<sup>1</sup></i> .....	803
Quantifying hydrothermal, groundwater, and crater lake contributions to the hyperacid Banyu Pahit stream, East-Java, Indonesia.....	809
<i>Stephanie Palmer<sup>1</sup>, Jeffrey M. McKenzie<sup>1</sup>, Vincent van Hinsberg<sup>1</sup>, &amp; A.E. Williams-Jones<sup>1</sup></i> .....	809

Land use/land cover influences on the estimated time to recovery of inland lakes from mercury enrichment .....	815
<i>Matthew J. Parsons<sup>1</sup> &amp; David T. Long<sup>1</sup></i> .....	815
Potential for contamination of deep aquifers in Bangladesh by pumping-induced migration of higher arsenic waters .....	819
<i>Kenneth G. Stollenwerk</i> .....	819
<b>CURRENT CAPABILITIES AND FUTURE PROSPECTS OF REAL-TIME, IN-FIELD GEOCHEMICAL ANALYSIS .....</b>	<b>823</b>
LIBS-based geochemical fingerprinting for the rapid analysis and discrimination of minerals – the example of garnet .....	825
<i>Daniel C. Alvey<sup>1</sup>, Jeremiah J. Remus<sup>2</sup>, Russell S. Harmon<sup>3</sup>, Jennifer L. Gottfried<sup>4</sup>, &amp; Kenneth Morton<sup>2</sup></i> .....	825
The U-tube sampling methodology and real-time analysis of geofluids .....	829
<i>Bary Freifeld<sup>1</sup>, Ernie Perkins<sup>2</sup>, James Underschultz<sup>3</sup>, &amp; Chris Boreham<sup>4</sup></i> .....	829
LIBS as an archaeological tool – example from Coso Volcanic Field, CA .....	833
<i>Jennifer L. Gottfried<sup>1</sup>, Russell S. Harmon<sup>2</sup>, Anne Draucker<sup>3</sup>, Dirk Baron<sup>3</sup>, &amp; Robert M. Yohe<sup>3</sup></i> ..	833
The application of visible/infrared spectrometry (VIRS) in economic geology research: Potential, pitfalls and practical procedures .....	837
<i>Andrew Kerr, Heather Rafuse, Greg Sparkes, John Hinchey, &amp; Hamish Sandeman</i> .....	837
Analysis of gem treatments: comparison of nano-second and pico-second laser-induced breakdown spectroscopy .....	841
<i>Nancy J. McMillan<sup>1</sup>, Patrick Montoya, Carlos Montoya, &amp; Lawrence Bothern</i> .....	841
Laser ablation chemical analysis LIBS and LA-ICP-MS for geochemical and mining applications .....	843
<i>R.E. Russo<sup>1,2,3</sup>, J. Yoo<sup>2</sup>, J. Plumer<sup>1</sup>, J. Gonzalez<sup>2</sup>, &amp; X. Mao<sup>3</sup></i> .....	843
In-situ Mössbauer spectroscopy on Earth, Mars, and beyond .....	847
<i>Christian Schröder<sup>1</sup>, Göstar Klingelhöfer<sup>1</sup>, Richard V. Morris<sup>2</sup>, Bodo Bernhardt<sup>3</sup>, Mathias Blumers<sup>1</sup>, Iris Fleischer<sup>1</sup>, Daniel S. Rodionov<sup>1,4</sup>, &amp; Jordi Gironés López<sup>1</sup></i> .....	847
Archaeometry in the House of the Vestals: analyzing construction mortar with portable infrared spectroscopy .....	851
<i>Jennifer Wehby<sup>1</sup> &amp; Samuel E. Swanson<sup>1</sup></i> .....	851
Fluorescence analysis of dissolved organic matter (DOM) in landfill leachates .....	853
<i>Caixiang Zhang<sup>1</sup>, Yanxin Wang<sup>1</sup>, &amp; Zhaonian Zhang<sup>2</sup></i> .....	853
Innovation for the CHIM method .....	857
<i>Liu Zhanyuan, Sun Binbin, Wei Hualing, Zeng Daoming, &amp; Zhou Guohua</i> .....	857
<b>GEOCHEMICAL ASPECTS OF MINE WASTES .....</b>	<b>861</b>
Geochemistry of the Lake George Antimony mine tailings, Lake George, New Brunswick, Canada: Understanding antimony mobility in a tailings environment .....	863
<i>Pride T. Abongwa<sup>1</sup> &amp; Tom A. Al<sup>1</sup></i> .....	863
Contribution of <i>Cistus ladanifer</i> L. to natural attenuation of Cu and Zn in some mine areas of the Iberian Pyrite Belt .....	867
<i>Maria J. Batista<sup>1</sup> &amp; Maria M. Abreu<sup>2</sup></i> .....	867
The Diavik Waste Rock Project: Design, construction and preliminary results .....	871
<i>D. W. Blowes<sup>1</sup>, L. Smith<sup>2</sup>, D. Segó<sup>3</sup>, L.D. Smith<sup>1,4</sup>, M. Neuner<sup>2</sup>, M. Gup-ton<sup>2</sup>, B.L. Bailey<sup>1</sup>, N. Pham<sup>3</sup>, R.T. Amos<sup>1</sup>, &amp; W.D. Gould<sup>1</sup></i> .....	871

Prediction of acid mine generating potential: Validation using mineralogy .....	875
<i>Hassan Bouzazah<sup>1,2</sup>, Mostafa Benzaazoua<sup>1</sup>, Benoît Plante<sup>1</sup>, Bruno Bussière<sup>1</sup>, &amp; Eric Pirard<sup>2</sup></i>	
Preliminary investigation into tailings-ground water interactions at the former Steep Rock iron mines, Ontario, Canada .....	879
<i>Andrew G. Conly<sup>1</sup>, Peter F. Lee<sup>2</sup>, &amp; Chris Perusse<sup>1</sup></i> .....	
Long-term fate of ferrihydrite in uranium mine tailings .....	883
<i>Soumya Das<sup>1</sup> &amp; M. Jim Hendry<sup>1</sup></i> .....	
Methods for obtaining a national-scale overview of groundwater quality in New Zealand .....	887
<i>Christopher J. Daughney, Uwe Morgenstern, Rob van der Raaij, Robert Reeves, Matthias Raiber, &amp; Mark Randall</i> .....	
Mineralogical characterization of arsenic, selenium, and molybdenum in uranium mine tailings .....	891
<i>Joseph Essilfie – Dughan<sup>1</sup>, M. Jim Hendry<sup>1</sup>, Ingrid Pickering<sup>1</sup>, Graham George<sup>1</sup>, Jeff Warner<sup>2</sup>, &amp; Tom Kotzer<sup>3</sup></i> .....	
Spatial and temporal evolution of Cu-Zn mine tailings while dewatering .....	895
<i>D. Jared Etcheverry<sup>1</sup>, Barbara L. Sherriff<sup>1</sup>, Nikolay Sidenko<sup>1,2</sup>, &amp; Jamie VanGulck<sup>3</sup></i> .....	
Adding value to Kinetic Testing Data II – Interpretation of waste rock humidity cell data from an exploration perspective at the Adanac Molybdenum Corporation, Ruby Creek Molybdenum Project, BC, Canada .....	899
<i>David R. Gladwell<sup>1</sup> &amp; Catherine T. Ziten<sup>1</sup></i> .....	
Alteration of sulfides within an open air waste-rock dump: Application of synchrotron $\mu$ -XRD, $\mu$ -XRF, and $\mu$ -XANES analyses .....	903
<i>Pietro Marescotti<sup>1</sup>, Cristina Carbone<sup>1</sup>, Gabriella Lucchetti<sup>1</sup>, &amp; Emilie Chalmin<sup>2</sup></i> .....	
Arsenic speciation in wastes resulting from pressure oxidation, roasting and smelting .....	907
<i>Dogan Paktunc</i> .....	
Importance of sorption in the geochemistry of nickel in waste rock .....	911
<i>Benoît Plante<sup>1</sup>, Mostafa Benzaazoua<sup>1</sup>, Bruno Bussière<sup>1</sup>, &amp; Donald Laflamme<sup>2</sup></i> .....	
Distribution of elements of concern in uranium mine tailings, Key Lake, Saskatchewan, Canada .....	915
<i>Sean A. Shaw<sup>1</sup>, M. Jim Hendry<sup>1</sup>, Joseph Esselie-Dughan<sup>1</sup>, Tom Kotzer<sup>2</sup>, &amp; Harm Maathuis<sup>2</sup></i> ..	
Source, attenuation and potential mobility of arsenic at New Britannia Mine, Snow Lake, Manitoba .....	919
<i>Stephanie Simpson<sup>1</sup>, Barbara L. Sherriff<sup>1</sup>, Nikolay Sidenko<sup>1,2</sup>, &amp; Jamie Van Gulck<sup>3</sup></i> .....	
Geochemistry and mineralogy of ochre precipitates formed as waste products of passive mine water treatment .....	923
<i>Teresa M. Valente<sup>1</sup>, Marcel D. Antunes, Maria Amália S. Braga, &amp; Jorge M. Pamplona</i> .....	
Instability of AMD samples and evolution of ochre-precipitates in laboratory conditions .....	927
<i>Teresa M. Valente<sup>1</sup> Lúcia M. Guise, &amp; Carlos A. Leal Gomes</i> .....	
Arsenic mineralogy and potential for bioaccessibility in weathered gold mine tailings from Nova Scotia .....	931
<i>Stephen R. Walker<sup>1</sup>, Michael B. Parsons<sup>2</sup>, &amp; Heather E. Jamieson<sup>1</sup></i> .....	
<b>GEOCHEMICAL SURVEYS IN GOVERNMENT - NEW DEVELOPMENTS AND USES .....</b>	<b>935</b>
Presentation of regional geochemical data via Internet Earth browsers .....	937
<i>Stephen W. Adcock<sup>1</sup>, Wendy A. Spirito<sup>1</sup>, &amp; Eric C. Grunsky<sup>1</sup></i> .....	
The National Geochemical Survey of Australia: 2009 update on progress .....	941

<i>Patrice de Caritat<sup>1</sup>, Michelle Cooper<sup>1</sup> &amp; Paul Morris<sup>2</sup></i> .....	941
Multi-element geochemical mapping in Southwest China .....	945
<i>Zhizhong Cheng<sup>1</sup> &amp; Xuejing Xie<sup>1</sup></i> .....	945
Exploration geochemical surveys of the Taupo Volcanic Region, New Zealand .....	949
<i>Anthony B. Christie<sup>1</sup> &amp; Richard Carver<sup>2</sup></i> .....	949
The effect of geology on lake geochemical trends in Sudbury, Ontario, viewed through Google Earth.....	953
<i>Richard Dyer<sup>1</sup></i> .....	953
Developing an exploration/environmental geochemical database on a shoestring budget .....	957
<i>Ronald R. McDowell<sup>1</sup>, Katharine L. Avary<sup>1</sup>, David L. Matcher<sup>2</sup>, James Q. Britton<sup>1</sup>, J. Eric Lewis<sup>1</sup>, &amp; Paula J. Hunt<sup>1</sup></i> .....	957
The value of government-generated geochemical data, and an example of its delivery .....	961
<i>Paul Morris<sup>1</sup></i> .....	961
Using stream sediments for environmental geochemistry in Austria.....	965
<i>Sebastian Pfeleiderer<sup>1</sup>, Albert Schedl<sup>1</sup>, &amp; Herbert Pirk<sup>2</sup></i> .....	965
Surficial geochemical studies in support of non-renewable mineral resource assessments, Northwest Territories, Canada.....	969
<i>Toon Pronk<sup>1</sup>, Roger C. Paulen<sup>2</sup>, Andrea Mills<sup>3</sup>, &amp; Adrian Hickin<sup>4</sup></i> .....	969
Abundances of chemical elements in rocks, sediments, and the continental crust of China .....	973
<i>Chi Qinghua<sup>1</sup> &amp; Yan Mingcai<sup>2</sup></i> .....	973
CSIRO Exploration and Mining: the challenge of being pure, applied and relevant.....	979
<i>John L. Walshe<sup>1</sup></i> .....	979
Determination of platinum and palladium for geochemical mapping.....	983
<i>Yao Wensheng<sup>1,2</sup>, Yan Hongling<sup>3</sup>, Sun Aiqin<sup>3</sup>, &amp; Wang Xueqiu<sup>1,2</sup></i> .....	983
76 elements geochemical mapping in Southwest China .....	987
<i>Zhizhong Cheng<sup>1</sup> &amp; Xuejing Xie<sup>1</sup></i> .....	987
A Methodology of source tracking of cadmium anomalies and their quantitative estimation along the Yangtze River Basin, China .....	991
<i>Chuangdong Zhao<sup>1</sup> &amp; Hangxin Cheng<sup>1</sup></i> .....	991
<b>GENERAL SESSION.....</b>	<b>995</b>
Investigation of physical, chemical and microbiological processes in the development of forest rings in Ontario.....	997
<i>Kerstin Brauneder<sup>1</sup>, Stewart M. Hamilton<sup>2</sup>, Keiko H. Hattori<sup>1</sup>, &amp; Gordon Southam<sup>3</sup></i> .....	997
Geology and Geochemistry of the Lac Cinquante Uranium Deposit, Nunavut .....	1001
<i>Nathan J. Bridge<sup>1</sup>, Neil R. Banerjee<sup>1</sup>, Craig S. Finnigan<sup>1,2</sup>, Rob Carpenter<sup>2,3</sup>, &amp; Jeff Ward<sup>3</sup></i> .....	1001
The New Brunswick Groundwater Chemistry Atlas: a geographical representation of groundwater quality in New Brunswick.....	1005
<i>Annie E. Daigle<sup>1</sup>, Mallory Gilliss<sup>1</sup>, &amp; Darryl A. Pupek<sup>1</sup></i> .....	1005
Spatial geochemical trends of beach and dune sands from the Northeastern coast of Mexico: implications for provenance.....	1009
<i>Juan Jose Kasper-Zubillaga<sup>1</sup>, John S. Armstrong-Altrin<sup>1</sup>, &amp; Arturo Carranza Edwards<sup>1</sup></i> .....	1009
Biogeochemistry of Iron .....	1014
<i>A.L. Kovalevskii<sup>1</sup> &amp; O.M. Kovalevskaya<sup>1</sup></i> .....	1014

Correlation of atmospheric soil and atmospheric lead in three North American cities: can re-suspension of urban lead contaminated soil be a major source of urban atmospheric lead and cause seasonal variations in children's blood lead levels? .....	1018
<i>Mark Laidlaw</i> <sup>1</sup> .....	1018
Using Ground Penetrating Radar to delineate sub-surface calcrete in the Great Victoria Desert, South Australia: implications for gold exploration .....	1022
<i>Melvyn J. Lintern</i> <sup>1</sup> , <i>Anton W. Kepic</i> <sup>2</sup> & <i>Matthew Josh</i> <sup>3</sup> .....	1022
A new direction in searching for the atmospheric CO <sub>2</sub> sink: considering the joint action of carbonate dissolution, global water cycle and the photosynthetic uptake of dic by aquatic organisms .....	1025
<i>Zaihua Liu</i> <sup>1,2,*</sup> , <i>Wolfgang Dreybrodt</i> <sup>3</sup> , & <i>Haijing Wang</i> <sup>4</sup> .....	1025
Groundwater CO <sub>2</sub> : is it responding to atmospheric CO <sub>2</sub> ? .....	1029
<i>G. L. Macpherson</i> .....	1029
Lithological Identification of Rocks in Cape Smith Fold Belt Region; New Quebec Using Remote Sensing Applications .....	1033
<i>Yask N. Shelat</i> <sup>1</sup> & <i>James E. Mungall</i> <sup>1</sup> .....	1033
Selective geochemical extraction patterns in Cyprus soils: responses to geology and land use variations .....	1037
<i>Nyree Webster</i> <sup>1</sup> , <i>David Cohen</i> <sup>*1</sup> , <i>Neil Rutherford</i> <sup>12</sup> , <i>Andreas Zissimos</i> <sup>3</sup> , & <i>Eleni Morisseau</i> <sup>3</sup> ..	1037
The petrogenesis of the Ulsan carbonate rocks from the southeastern Kyongsang Basin, South Korea .....	1041
<i>Kyounghee Yang</i> .....	1041
Alteration-Mineralization Pattern and Geochemical Characteristics of Samli (Balikesir) Fe-Oxide-Cu-(Au) Deposit, Turkey .....	1045
<i>Erkan Yilmazer</i> <sup>1*</sup> , <i>Nilgün Gulec</i> <sup>1</sup> , & <i>İlkay Kuscu</i> <sup>2</sup> .....	1045
Total and soil organic carbon, and total sulfur determinations of soils from Cyprus .....	1051
<i>Andreas Zissimos</i> <sup>*1</sup> , <i>Eleni Morisseau</i> <sup>1</sup> , <i>Eleni Stavrou</i> <sup>1</sup> , & <i>David Cohen</i> <sup>2</sup> .....	1051

TECHNICAL EDITORS  
*(Listed in alphabetical order)*

Mark Arundell  
U. Aswathanarayana  
Roger Beckie  
Chris Benn  
Robert Howell  
Charles Butt  
Bill Coker  
Hugh deSouza  
Sara Fortner  
David Gladwell  
Wayne Goodfellow  
Eric Grunsky  
William Gunter  
Gwendy Hall  
Jacob Hanley  
Russell Harmon  
David Heberlein  
Brian Hitchon  
Andrew Kerr  
Dan Kontak  
Kurt Kyser

David Lentz  
Ray Lett  
Matthew Leybourne  
Steven McCutcheon  
Beth McClenaghan  
Nancy McMillan  
Paul Morris  
Lee Ann Munk  
Dogan Paktunc  
Roger Paulen  
Ernie Perkins  
David Quirt  
Andy Rencz  
David Smith  
Cliff Stanley  
Gerry Stanley  
Nick Susak  
Bruce Taylor  
Ed Van Hees  
James Walker  
Lawrence Winter



## **NEW FRONTIERS FOR EXPLORATION IN GLACIATED TERRAIN**

EDITED BY:

**BETH MCCLENAGHAN  
ROGER PAULEN  
BILL COKER  
CHRIS BENN**



## Glacial dispersal from the Mount Fronsac North massive sulfide deposit, Bathurst Mining Camp, New Brunswick, Canada

Heather Campbell<sup>1</sup>, Bruce E. Broster<sup>1</sup>, Michael Parkhill<sup>2</sup>,  
Nicholas Susak<sup>1</sup>, & Paul Arp<sup>3</sup>

<sup>1</sup> University of New Brunswick, Department of Geology, P.O. Box 4400, Fredericton,  
NB E3B 5L2 Canada (E-MAIL: [X5E5G@UNB.CA](mailto:X5E5G@UNB.CA))

<sup>2</sup> NEW BRUNSWICK DEPARTMENT OF NATURAL RESOURCES, GEOLOGICAL SURVEYS BRANCH, P.O.  
BOX 50, BATHURST,  
NB E2A 3Z1 Canada

<sup>3</sup> UNIVERSITY OF NEW BRUNSWICK, DEPARTMENT OF FORESTRY AND ENVIRONMENTAL MANAGEMENT,  
P.O. BOX 44555, FREDERICTON, NB E3B 6C2 Canada

**ABSTRACT:** Concentrations for 53 elements in till (C-horizon sediment) sampled over the Mount Fronsac North volcanogenic massive sulfide deposit were analyzed to determine whether geochemical concentrations were coincident with known glacial flow directions, and whether Hg could be used as a pathfinder element for massive sulfides. Based on data from these analysis, three patterns were observed in glacial till: palimpsest (Pb, Ag and Cu), related to local ice flow dispersal of mineralized gossan; ribbon (Ni, Co and Cr), related to flow of the Laurentide Ice Sheet over gabbroic intrusions and an arcuate pattern (Hg and Cd) related to post-glacial ionic mobility. Concentration gains of Mo, As, Sb and Hg in supergene gossan and gains of Zn, Au, Cd, Hg and Co in till were calculated using Sn as a conservative element. These results indicate that processes responsible for element signatures in till over the Mount Fronsac North deposit are: 1) pre-glacial weathering of primary sulfides resulting in gossan formation, 2) pre-glacial colluvial and hydromorphic redistribution of gossanous material, 3) west to east and southwest to northeast mechanical transport of mineralized bedrock by glaciers and 4) ionic migration of cations and anions due to electrochemical reactions between wall rock and sulfides.

**KEYWORDS:** *glacial, gossan, mobility, dispersal, till, geochemistry*

### INTRODUCTION

Two hundred and fifty three till (C-horizon) samples were collected and analyzed to determine suitable analytical methods to delineate till geochemical signatures that reflect Zn-Pb-Ag mineralization and to determine possible pathways of element migration from the bedrock to till. Results of a study conducted at the Mount Fronsac North deposit are discussed here.

### GEOLOGICAL SETTING

#### Location and Geology

The Mount Fronsac North (MFN) Zn-Pb-Ag deposit is located approximately 40 km southwest of Bathurst, in the Bathurst Mining Camp (BMC), New Brunswick. The MFN deposit lies stratigraphically in the Brunswick horizon between the Nepisiguit Falls Formation and the Flat Landing Brook Formation of the Ordovician Tetagouche Group (Figs. 1-3). Footwall

rocks consist of crystal tuffs, tuff lavas (ONFp), chloritic sedimentary and volcanic and volcanoclastic rocks (ONFs) of the Nepisiguit Falls Formation. The massive sulfides are enveloped by sericite-pyrite-chlorite schist alteration. Hanging wall units consist of ash and crystal tuff and interlayered sedimentary rocks (OFLBts), fine-grained crystal tuffs (OFLBft), rhyolites (OFLBr), mafic tuffs and flows (OFLbt) of the Flat Landing Brook formation. Late gabbroic intrusions intrude the hanging wall units (Gower & McCutcheon 1995; Walker & Graves 2006). Sulfide mineralization occurs in 2-20 m thick beds that dip to the east and plunge to the north with a high grade zone that grades 7.65% Zn, 2.18% Pb, 0.14% Cu, 40.3 g/t Ag and 0.40g/t Au (Walker & Graves 2006).

#### Host Rock & Sulfide Geochemistry

Massive sulphide chemistry used in this study were from diamond drill hole (DDH) MF-00-31 (Walker & Graves 2006) with concentrations (geometric mean) of 3650.41 ppm Zn, 1091.32 ppm Pb, 1038.01 ppm As, 8.55 ppm Ag, 124.67 ppb Au, 159.51 ppm Cu, and 68.22 ppm Sb. Rhyolite (OFLBr) contains up to 8 ppb Au. The gabbro contains the highest values of Ni (77 ppm), Cr (293 ppm) and Co (47 ppm) and moderately high values of Cu (41 ppm).

### PRE-GLACIAL ELEMENT CONCENTRATION IN GOSSANS

Pre-glacial weathering of BMC massive sulfide deposits during the Pliocene-Pleistocene (Boyle 2003; Symons *et al.* 1996) resulted in the formation of oxidized caps (gossans) that overlie many of the massive sulfide occurrences/deposits. Gossan occurs at MFN and outcrops on the northwest extent of the mineralized zone. Detailed studies on BMC gossans by Boyle (2003) showed that Sn volumetrically remained the same in the weathering process and thus could be used in mass balance calculations (1) to determine element mobility from the sulfide to the gossan.

% element gain / loss =

$$\frac{C_{\text{element in gossan}} \times \left( \frac{C_{\text{Sn Sulfides}}}{C_{\text{Sn Gossan}}} \right) - C_{\text{element in Sulfides}}}{C_{\text{element in Sulfides}}} \times 100$$

Calculations of gains and losses from the MFN deposit and gossan boulders on surface nearby show gains in Cu, As, Mo, V, Hg, Bi and Sb; which are consistent with other gossans in the BMC (Boyle 2003), with the exception of Cu.

### GLACIAL DISPERSAL

Two main glacial events are responsible for glacial dispersal from the MFN deposit; a west to east Laurentide Ice Sheet flow (090°) and later local southwest to northeast (070°) ice flow. Both these glacial events were primarily erosive (Pronk *et al.* 1989; Parkhill & Doiron 2003)

leaving a thin layer (<1 m) of sandy lodgement till overlying deformation till.

### METHODS

Bedrock samples were analyzed by aqua regia digestion/inductively coupled plasma mass spectrometry/emission spectrometry (ICP-MS/ES), 4-acid digestion/ICP-MS/ES (total digestion), INAA and XRF. The 253 till samples were collected at 25 m intervals along a grid extending 200 m outward from the mineralized zone. Gridlines with 50 m sample spacing were added to complete the survey and to cover approximately the 1 km x 1 km area over the deposit. Till samples were split, and the <0.063 mm fraction analyzed by aqua regia digestion - ICP-MS/ES. Splits (not sieved) were analyzed at the University of New Brunswick Forestry & Environmental Laboratories for cold vapor atomic fluorescence spectrometry (CVAFS).

### TILL GEOCHEMISTRY AND DISTRIBUTION

Results for Hg from ICP-MS/ES and CVAFS showed excellent correlation ( $r_s=0.87$ ) despite different sample preparation (sieving and pre-digestion for ICP-MS/ES; no sieving or digestion for CVAFS). Thresholds between anomalous and background populations were determined using methods of Sinclair (1974). Bubble plots of element distribution (Figs. 1-3) show four main geochemical patterns; 1) a slight arcuate pattern in the moderately anomalous (66-275 ppb) population for Hg and Cd contents, 2) a west to east ribbon-shaped train for Ni, Cr and Co concentrations, 3) a diffuse pattern for Zn content and 4) a southwest to northeast zone of elevated concentrations of Ag, As, Sb, Pb, Cu, Au, Hg and Mo.

Mass balance calculations were performed on till samples using Sn concentrations. Tin concentrations in till are sensitive to grain size partitioning and differing analytical methods, thus results from these calculations are qualitative. In the till, concentration gains relative to Sn in Zn, Au, Cd, Hg and Co were obvious after performing the calculations; all of

these elements show concentrations losses from the gossan.

**DISCUSSION**

Mechanical and chemical weathering is responsible for element transport in MFN till. The later northeastward – southwestward ice flow and resultant glacial dispersal (070°) is interpreted as palimpsest and defined by elements concentrated in the gossan along with Ag, Au and Pb. The ribbon-shaped train (090°) is defined by elements concentrated in the gabbroic intrusions. An arcuate concentration pattern is apparent for Hg and Cd in till surrounding the bedrock sulfide zone, thus it is thought that electrochemical mechanisms may be a factor in mobilizing these elements to the surface. The pattern for Zn (not shown) is diffuse and appears to be the result of down slope (hydromorphic) post-glacial transport.

**CONCLUSIONS**

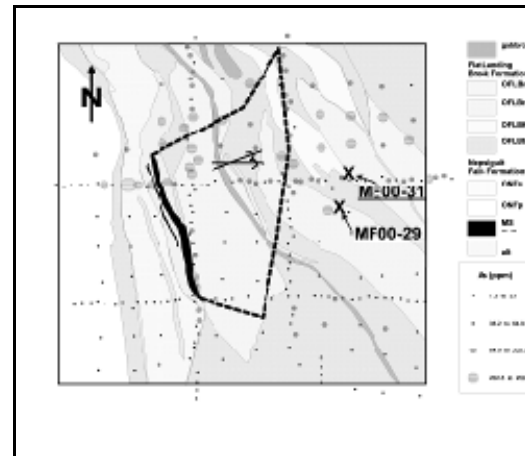
Excellent correlation between ICP-MS/ES and CVAFS analysis of Hg ( $r_s=0.87$ ) show that sieving does not affect anomalous concentrations of this element in till.

Element distribution patterns in till around the MFN deposit are most likely the result of concentration of anionic species in the gossan, glacial dispersal of metal-rich bedrock, and mobilization of

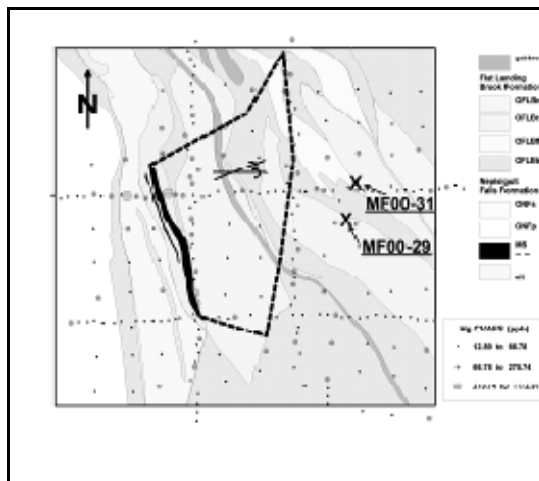
**Fig. 1.** Distribution of Hg (and Cd) in till at the MFN deposit. DDH MF00-31 and DDH MF00-29 are marked with an “X”; subcropping mineralization is marked by a dashed line. Arrows indicate ice flow directions, the youngest flow was northeastward.

elements by electrochemical mechanisms and hydromorphic dispersal. These conclusions are supported by qualitative mass balance calculations and variable geochemical distribution patterns in till, in the context of local and regional ice flow.

Till geochemical distribution patterns are coincident with known glacial dispersal directions; however post-glacial processes overprint the primary glacial dispersal



**Fig. 2.** Distribution of As (Ag, Sb, Pb, Cu, Au, Hg and Mo) in till at the MFN deposit. DDH MF00-31 and DDH MF00-29 are marked with an “X”; subcropping mineralization is marked by a dashed line. Arrows indicate ice flow directions, the youngest flow was northeastward.



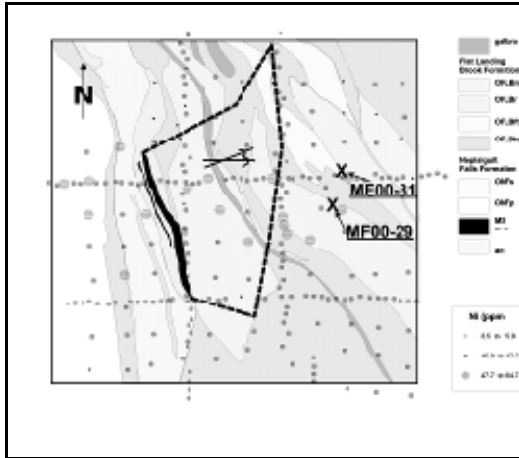


**Fig. 3.** Distribution of Ni (Cr, Co) in till at the MFN deposit. DDH MF00-31 and DDH MF00-29 are marked with an "X"; subcropping mineralization is marked by a dashed line. Arrows indicate ice flow directions, the youngest flow was northeastward. signature of the deposit. Thus both processes should be considered when using till geochemical methods in areas of thin till cover in the BMC.

#### ACKNOWLEDGEMENTS

This abstract benefited greatly from discussions with J. Walker, D. Lentz, S. Vetter, and B. McClenaghan. C. Stanley is thanked for observations on statistical processing and data presentation. We are grateful to DNR-NB for their financial and field support. This project was funded as part of the Geological Survey of Canada's Targeted Geoscience Initiative-3 Program, aimed at finding methods for delineating buried sulfide mineralization.

#### REFERENCES

BOYLE, D. 2003. Preglacial weathering of massive sulfide deposits in the Bathurst Mining Camp; economic geology, geochemistry, and exploration applications. In: GOODFELLOW, W., MCCUTCHEON, S. & PETER, J. *Massive sulfide deposits of the Bathurst Mining Camp, New Brunswick, and northern Maine*. Economic Geology Monographs, **11**, 689-721.

GOWER S. & MCCUTCHEON S. 1995. Geology of the Portage Brook area (NTS 21 O/7h and part of 21 O/10a), northwestern Bathurst Mining Camp, New Brunswick, EXTECH-II. MRR-20, 3-14.

PARKHILL, M. & DOIRON, A. 2003. Quaternary geology of the Bathurst Mining Camp and implications for base metal exploration using drift prospecting. In: GOODFELLOW, W., MCCUTCHEON, S. & PETER, J. *Massive sulfide deposits of the Bathurst Mining Camp, New Brunswick, and northern Maine*. Economic Geology Monographs, **11**, 631-660.

PRONK, A., BOBROWSKY, P., & PARKHILL, M. 1989. An interpretation of late Quaternary glacial flow indicators in the Baie des Chaleurs region, northern New Brunswick. *Geographie Physique et Quaternaire*, **43**, 179-90.

SINCLAIR, A. 1974. Selection of threshold values in geochemical data using probability graphs. *Journal of Geochemical Exploration*, **3**, 129-149.

SYMONS D., LEWCHUCK, M., & BOYLE, D. 1996. Pliocene-Pleistocene genesis for the Murray Brook and Heath Steele Au-Ag gossan ore deposits, New Brunswick, from paleomagnetism. *Canadian Journal of Earth Sciences*, **33**, 1-11.

WALKER, J. & GRAVES, G. 2006. The Mount Fronsac North volcanogenic massive sulfide deposit; a recent discovery in the Bathurst mining camp, New Brunswick. *Exploration and Mining Geology*, **15**, 221-240.

## Geochemical and mineral dispersal patterns related to drift-covered copper-gold mineralization in central British Columbia, Canada

Ray Lett

Geological Survey Branch, British Columbia Ministry of Energy, Mines and Petroleum Resources, PO Box 9333, STN PROV GOV'T, Victoria, BC CANADA (e-mail: [Ray.Lett@gov.bc.ca](mailto:Ray.Lett@gov.bc.ca))

**ABSTRACT:** Commercial selective extraction methods, such as Enzyme Leach<sup>SM</sup>, MMI<sup>SM</sup>, and Bio Leach<sup>SM</sup> have become increasingly popular for geochemical soil surveys in areas where the mineralization is buried beneath unconsolidated sediments. A soil (B horizon soil) and till (C horizon soil) orientation survey on the Shiko Lake copper-gold porphyry mineral occurrence in central British Columbia reveals asymmetric soil geochemical profiles typical of mineralised bedrock entrained in till. Abundant, fresh gold grains in till samples close to a copper anomaly peak suggest a local source for the anomalous soil. A close association of MMI<sup>SM</sup> and Bio Leach<sup>SM</sup> B horizon soil anomalies with metal extracted by aqua regia from C horizon soil samples suggests that the selective extractions reflect till rather than bedrock composition.

**KEYWORDS:** *till, copper, gold, MMI, Bio Leach, aqua regia.*

### INTRODUCTION

Mesozoic volcanic rocks and coeval intrusive complexes within the Quesnel geotectonic terrain of central British Columbia host several major porphyry copper-gold mines. Exploration for new deposits in this region has been met with limited success, because prospective bedrock is mantled by Late Pleistocene glacial sediment (e.g., till) and Late Oligocene to Pleistocene plateau basalt. However, subcropping mineral deposits can be found by detecting the geochemical signature of mineralized bedrock in till. These down-ice dispersal trains are typically ribbon-shaped and are areally more extensive than their bedrock target. For example, Levson (2001) reports anomalous Cu values in the <0.063 mm till fraction up to 4 km down-ice from the Bell Cu-Au mine. In these trains, metal values typically decreased exponentially in the down-ice direction (Klassen 2001).

This paper documents a soil and till survey of the Shiko Lake porphyry copper-gold mineral occurrence near Quesnel Lake, British Columbia, and the comparison of Cu, Au, and other elements by partial extraction geochemical analysis with the distribution of gold and other heavy mineral grains (Lett & Doyle 2009).

### BEDROCK AND SURFICIAL GEOLOGY

At Shiko Lake (Fig. 1) a Jurassic complex composed of diorite, monzonite, and syenite intrudes basalt and volcanoclastic rocks. Chalcopyrite, bornite, and gold occur disseminated and in veins mainly within the syenite (Fig. 2).



**Fig. 1.** Location of the Shiko Lake mineral property in western Canada.

Much of the bedrock is covered with up to 3 m of a sandy till deposited during a southeast to northwest ice-flow event. Soil formed on the glacial sediment is typically a well-drained brunisol.

**Sampling and analysis**

Samples from the B and C soil horizons, collected from profiles exposed in pits dug along traverses crossing the mineralized zone (Fig. 2) were prepared and analysed for 63 elements by a combination of aqua regia digest-inductively coupled plasma-mass spectrometry (ICPMS) and neutron activation (INAA). Analyses were carried out on the <0.063 mm fraction of the C horizon and the <0.177 mm fraction of the B soil horizon. The B horizon samples were also analysed for by SGS's propriety Mobile Metal Ion<sup>SM</sup> (MMI) and Activation Lab's propriety Bio Leach<sup>SM</sup> and Enzyme Leach<sup>SM</sup> techniques and for hydrocarbons by the soil gas hydrocarbon<sup>SM</sup> (SGH) method. Gold and other heavy mineral grains were identified and counted in a heavy mineral concentrate of the C soil horizon (till) sample.

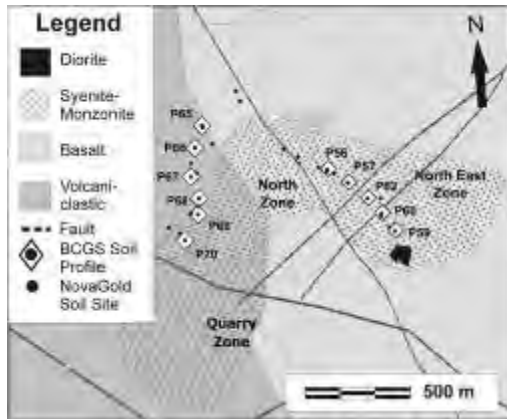


**Fig. 2.** Shiko Lake bedrock geology and soil sample locations. Geochemical data described here were compiled from BC Geological Survey studies by Lett & Doyle (2009) and a Novagold Resources till survey (Petsel 2006).

**Results**

A strong positive correlation exists between Cu, Ag, Co, Au, W, and Se in the B and C horizon soil and suggests that these elements are geochemical pathfinders for sulfide mineralization at the Shiko Lake mineral occurrence. Glacial dispersal of Cu and Co in C horizon soil samples is characterized by the shape of geochemical profiles. These typically

show a sharp up-ice peak and exponential down-ice decay curve of metal values.

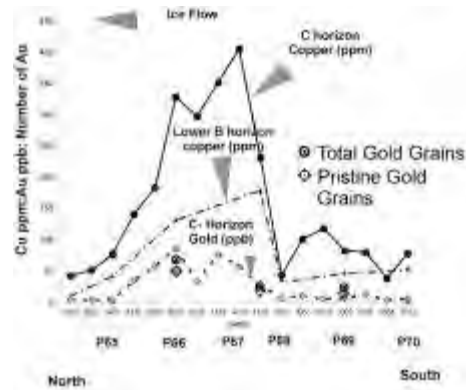


**Fig. 3.** Distribution of Cu and Au in B and C horizon soil west of the north zone, Shiko Lake. C horizon geochemical data are from BCGS studies by Lett & Doyle (2009) and a Novagold Resources till survey by Petsel (2006). Gold abundance in the C horizon samples was determined by an aqua regia digestion and instrumental analysis.

Figure 3 shows an example of this dispersal curve for Cu concentration along one traverse west of the North East zone. In addition to Cu, there are also abundant Au grains in the same C horizon sample suggesting a local bedrock source for both Cu and Au-rich debris in the till. The greater anomaly contrast for Cu, Au, and Co in the C horizon sample, compared to the lower B, may be explained by the fact that in this case analyses were conducted on the -0.063 mm fraction of the C horizon sample compared to the -0.180 mm fraction of the B horizon soil.

Two commercial partial extraction techniques improve anomaly contrast in B horizon soil samples compared to aqua regia-ICPMS for Cu and Au. However, whereas the MMI<sup>SM</sup> and Bio Leach<sup>SM</sup> Cu profiles are similar, the MMI<sup>SM</sup> Au signal is much larger than that for Bio Leach<sup>SM</sup>. Analysis of samples at different depths down the B soil horizon profile indicates that the geochemical response from these methods is depth dependant.

An exact source for the anomalous metal content and the gold grains in the samples presented here cannot be

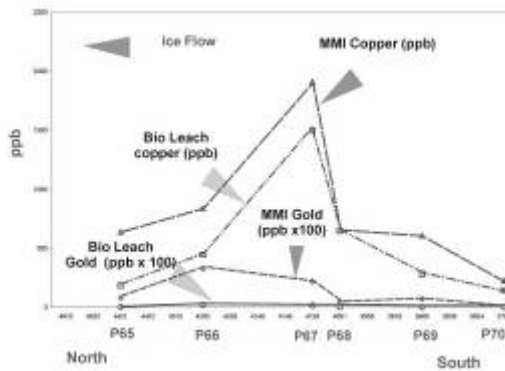


**Fig. 4.** Distribution of Cu and Au in B horizon soil west of the north zone, Shiko Lake, by MMI<sup>SM</sup> and Bio Leach<sup>SM</sup>.

confirmed, but a most likely source is mineralized bedrock close to the syenite – volcaniclastic contact, near Profile Site 68. A close relationship between the aqua regia-ICPMS, MMI<sup>SM</sup> and Bio Leach<sup>SM</sup> determined element patterns suggests that the partial extraction methods reflect metal-rich debris in till mechanically dispersed x m from a mineralized source rather than metal dispersion to surface directly from underlying mineralized bedrock.

#### CONCLUSIONS

A study of soil geochemistry and gold grain mineralogy over the Shiko Lake porphyry copper-gold mineral occurrence in central British Columbia has revealed:

- (1) That an asymmetric soil Cu profile and abundant fresh gold grains in C horizon soil samples most likely reflects mineralised bedrock entrained in till from a local source.
- (2) MMI<sup>SM</sup> and Bio Leach<sup>SM</sup> selective extract anomalies most likely reflect till geochemistry.

#### ACKNOWLEDGEMENTS

S. Petsel, Consultant, Vancouver, BC, and R. Durfeld, Durfeld Geological Management Ltd. Williams Lake, BC are thanked for providing information about the Shiko Lake property. The Geological Survey of Canada generously funded much of the sample preparation and analysis. SGS Laboratories, Toronto carried out the mobile metal ion<sup>SM</sup> (MMI) analysis, Activation Laboratories, Ancaster, performed the Enzyme Leach<sup>SM</sup>, Bio Leach<sup>SM</sup> and SGH<sup>SM</sup> analysis and Acme Analytical, Vancouver and analysed the samples by aqua regia-ICPMS. Overburden Drilling Management, Nepean prepared the heavy mineral concentrates from till samples and identified and counted the mineral grains in the concentrates.

#### REFERENCES

- KLASSEN, R.A. 2001. A Quaternary geological perspective on geochemical exploration in glaciated terrains. In: McCLENAGHAN, M.B., BOBROWSKY, P.T., HALL, G.E.M. & COOK, S.J. (eds). *Drift Exploration in Glaciated Terrain*, Geological Society, Special Publication, **185**, 1–17.
- LETT, R.E. & DOYLE, J. 2009. Geochemistry projects by the British Columbia Geological Survey. *British Columbia Ministry of Energy, Mines & Petroleum Resources*, Paper **2008-1**, 219–229.
- LEVSON, V.M. 2001. Regional till geochemical surveys in the Canadian Cordillera: sample media, methods, and anomaly evaluation. In: McCLENAGHAN, M.B., BOBROWSKY, P.T., HALL, G.E.M. & COOK, S.J. (eds). *Drift Exploration in Glaciated Terrain*, Geological Society, Special Publication, **185**, 45–68.
- PETSEL, S.A. 2006. Rock and soil sampling survey assessment report on the Shiko Lake property; *British Columbia Ministry of Energy, Mines and Petroleum Resources Assessment Report 2866*, 182 p.



## Heavy mineral and till geochemical signatures of the NICO Co-Au-Bi deposit, Great Bear magmatic zone, Northwest Territories, Canada

Isabelle McMartin<sup>1</sup>, Louise Corriveau<sup>2</sup> & Georges Beaudoin<sup>3</sup>

<sup>1</sup> Geological Survey of Canada, 601 Booth Street, Ottawa, ON, K1A 0E8, Canada (e-mail: [imcmarti@nrcan.gc.ca](mailto:imcmarti@nrcan.gc.ca))

<sup>2</sup> Geological Survey of Canada, 490 rue de la Couronne, Québec, QC, G1K 9A9, Canada

<sup>3</sup> Laval University, 1065 avenue de la Médecine, Québec, QC, G1V 0A6, Canada

**ABSTRACT:** To establish a practical guide to geochemical and mineralogical exploration for iron oxide copper-gold deposits in glaciated terrain, an orientation study around the NICO Co-Au-Bi deposit in the Great Bear magmatic zone of Northwest Territories was initiated in 2007. Bedrock and till samples, collected up-ice (background), proximal and down-ice from mineralization and host rocks, were analyzed to characterize their heavy mineral and geochemical signatures. Heavy mineral analysis demonstrates that, apart from gold and magnetite, few mineral species present at NICO have some clear potential as indicator minerals in surficial sediments. The non-ferromagnetic heavy minerals are either not chemically stable in surface glacial sediments (arsenopyrite, chalcopyrite, pyrite), not sufficiently coarse-grained (bismuthinite, tourmaline), not abundant enough in the mineralized bedrock (scheelite, molybdenite, cobaltite), or not sufficiently heavy (ferroactinolite). Although the Co-rich composition of arsenopyrite is possibly the strongest vector to Au-rich polymetallic mineralization in the study area, arsenopyrite is completely oxidized in surface tills. Iron oxide composition using preliminary discriminant diagrams shows some potential, namely with the Ni/(Cr+Mn) versus Ti+V plot. Till geochemistry reflects major differences in composition between the country/barren host rocks versus the mineralized rocks, and several elements (As-Bi-Co-Au-Cu-Sb-W-Cd) are identified as pathfinders for IOCG mineralization.

**KEYWORDS:** *indicator minerals, till geochemistry, IOCG, NICO, arsenopyrite*

### INTRODUCTION

The Great Bear magmatic zone (GBMZ) in the Northwest Territories (NWT) is now considered the most prospective setting for iron oxide copper-gold (IOCG) deposits in Canada (Corriveau 2007) and hosts two economic IOCG deposits: the magnetite-group IOCG NICO Co-Au-Bi deposit and the nearby hematite-group IOCG Sue-Dianne Cu-Ag-Au deposit (Fig. 1). Moreover, many past-producing vein-type uranium, silver and copper mines and Kiruna-type showings are now recognized to be parts of large polymetallic IOCG systems (Mumin *et al.* 2009). As part of a joint government-industry-academia research project taking place under the government Targeted Geoscience Initiative 3, Geo-mapping for Energy and Minerals, and Strategic Investments in Northern Economic Development programs, the Co-Au-Bi NICO deposit was selected as a first test site to characterize the heavy mineral and geochemical

signature of IOCG±U deposits and derived glacial sediments and assess if some heavy minerals have a potential as indicator minerals for IOCG deposits. The mineralogy and chemistry of heavy minerals from bedrock and C-horizon till samples collected in 2007, as well as till geochemistry, are summarized below.

### REGIONAL SETTING

The NICO deposit is located at the south end of the GBMZ in the Proterozoic Bear Structural Province of the Canadian Shield, about 160 km northwest of Yellowknife, Northwest Territories (Fig. 1). It represents an economically significant source of Co-Au-Bi-Cu-Fe with calculated reserves of 21.8 Mt with 1.08g/t Au, 0.13%Co and 0.16% Bi (Fortune Minerals 2008). Mineralization at NICO consists of a number of mineral showings predominantly hosted in brecciated and altered siltstone and wacke of the 1.88 Ga



**Fig. 1.** The Great Bear magmatic zone in the Wopmay orogen and known mineralization. The NICO deposit is located in the southern part of the GBMZ.

Treasure Lake Group, overlain by felsic ignimbrite sheets of the Faber Group (Goad *et al.* 2000). Ore minerals mainly consists of Fe-, As-, Co- and Cu-sulphides, native Au and Bi. Intense, pervasive, polyphase iron-oxide (magnetite-dominant)-hornblende-biotite-tourmaline-K-feldspar-carbonate replacive alteration occurs in the upper metasedimentary sequence below the volcanic-sedimentary unconformity (Corriveau *et al.* 2009; Mumin *et al.* 2009).

Ice-flow indicators indicate the area was influenced primarily by the Laurentide Ice Sheet flowing to the WSW during the last Wisconsinan glaciation. Pebble lithology data show that surface till composition reflects local provenance of the underlying

bedrock. The area is underlain by extensive discontinuous permafrost with mixed deciduous and conifer open forest vegetation.

## METHODS

Thirteen till samples were collected over or immediately down-ice (<100 m) from known mineralized zones, offset from mineralization (barren), and up-ice (NE) from the NICO deposit area (background). The samples were collected from hand dug pits in the upper C horizon, at an average depth of 50 cm. Twenty-seven representative bedrock samples were collected from both mineralized and unmineralized host rocks and from regional rocks. Till and bedrock samples were processed to separate a heavy mineral fraction (specific gravity > 3.2 g/cm<sup>3</sup>), indicator mineral picking (0.25-2 mm) and gold grain counts. Selected mineral grains considered to have possible IOCG affinities were hand picked, mounted and microprobed. Till samples (<2 and <63 µm fractions) were analysed geochemically for trace and major elements using ICP-ES+MS (aqua regia) and INAA. Analysis of duplicate and analytical standards were used to monitor analytical precision and accuracy of geochemical results.

## RESULTS AND DISCUSSION

### Heavy mineral signature

Six sulphide species were observed in the non-ferromagnetic heavy mineral concentrates (NFM-HMCs) of bedrock samples: arsenopyrite >> pyrite > chalcopyrite > bismuthinite = molybdenite = cobaltite. Chalcopyrite, pyrite and bismuthinite do survive in near-surface till but only in minor amounts (<8 grains/sample). Although the Co-rich composition of arsenopyrite is possibly the strongest vector to Au-rich polymetallic mineralization in the study area, sand-sized arsenopyrite is absent in C-horizon tills, suggesting that arsenopyrite more readily oxidizes than chalcopyrite and pyrite in till, and therefore is an impractical indicator mineral to detect mineralization using surficial sediments at NICO.

Tourmaline occurs in three bedrock samples in considerable amounts (up to 650 grains/sample) but in two of these samples, both from barren brecciated porphyry, tourmaline occurs as very small grains (<0.05 mm) intercalated with quartz so that few grains are heavier than 3.2 g/cm<sup>3</sup> in the 0.25-0.5 mm fraction. The fragmental nature of the tourmaline grains in crackle breccias hampers the use of tourmaline as an indicator mineral for the NICO deposit.

Ferroactinolite, although forming a pervasive alteration mineral in mineralized bedrock at NICO, is present only in minor amounts in several bedrock concentrates. The grains are not sufficiently heavy to be concentrated in the NFM-HMCs, except where they contain inclusions of magnetite (Fig. 2). Ferroactinolite also typically occurs as loose, silt-size aggregates of prismatic crystals in mineral grains of several bedrock samples (Fig. 3). These mineral inclusions are likely destroyed during glacial transport and comminution.

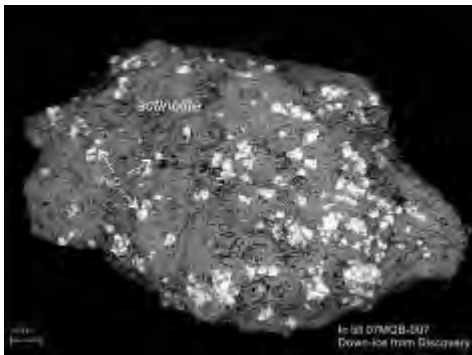


**Fig. 2.** Fe-oxide grains occurring as small inclusions in an actinolite grain from a till sample collected near the Discovery outcrop. Scale bar is 100 µm in length.

Relatively high concentrations of gold grains are found in surface tills collected over and near mineral showings of the NICO deposit area (up to 39 grains/10 kg sample) in comparison with those collected over barren host rocks (up to 10) and background terrain (up to 4). Pristine gold grains indicating a local source and a short distance of glacial transport are mostly abundant close to mineralized

zones indicating that documenting gold grain abundance, size, shape and fineness remains a valuable surface exploration method for gold-bearing IOCG deposits in the GBMZ.

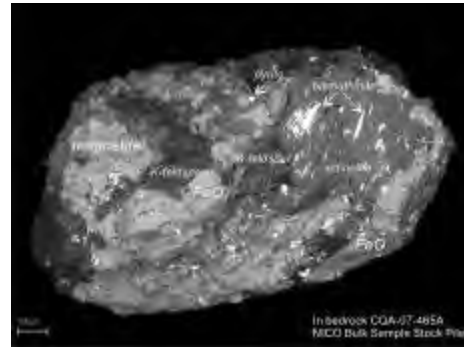


**Fig. 3.** Magnetite grain from a sub-surface bedrock sample occurring in association with a mixture of other minerals common to the mineralization zones. Scale bar is 100 µm in length.

Magnetite occurs in all bedrock and till samples in varied concentrations, as individual grains but also disseminated in bedrock fragments (Fig. 3) or as inclusions in mineral grains (Fig. 2). Variations in Fe-oxide composition are such that they fall within distinct fields in discriminant diagrams and can fingerprint a range of mineral deposit types (Beaudoin & Dupuis 2009). In the Ni/(Mn+Cr) vs. Ti+V diagram (Fig. 4), most grains from background till have higher Ti+V compositions compared to grains from till collected over NICO and a similar composition to grains collected in nearby metasediments at the Tan Fe-U showing. There is a good correspondence between the composition of grains from NICO metasediments and that of grains from till collected over NICO, and a reasonable differentiation between NICO metasediments and background metasediments. These preliminary results indicate the potential use of discriminant diagrams for iron oxides to fingerprint IOCG deposits.

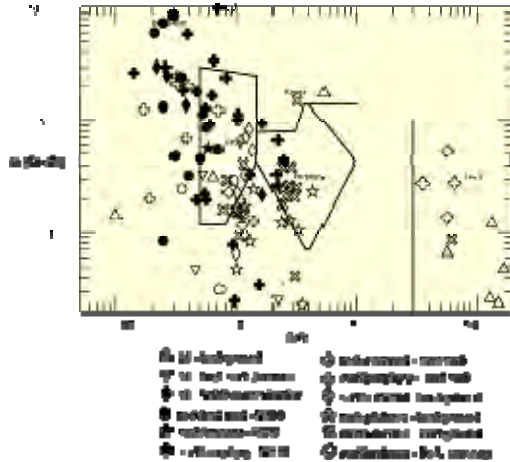


**Fig. 4.** Ni/(Cr+Mn) vs. Ti+V for magnetite grains from all till and bedrock samples.

### Till geochemistry

Several trace elements show anomalous concentrations in the fine fractions of till. Increasing metal concentrations from background to mineralization for As-Cu-Bi-Co-Au-Sb-W-Cd are observed, by over three orders of magnitude for As (up to 1512 ppm in <63 µm). This geochemical signature reflects major differences in composition between the country/barren host rocks versus the mineralized rocks.

### CONCLUSIONS

Study of the heavy mineral signature of the NICO deposit area and overlying glacial sediments demonstrates that gold grain abundance, size and shape, as well as magnetite composition, have the best potential to fingerprint the IOCG mineralization. Till geochemistry re-mains a useful and effective exploration tool for IOCG deposits in the GBMZ with As-Cu-Bi-Co-Au-Sb-W-Cd as the most effective pathfinder elements. The de-velopment of indicator mineral methods, together with till geochemistry, will be further tested with detailed bedrock and drift sampling around the Sue-Dianne deposit in 2009.

### ACKNOWLEDGEMENTS

We are grateful to Fortune Minerals for logistical support at NICO, K. Venance (GSC) for microprobe analysis, the DIVEX research network for supporting the iron

oxide mineral chemistry studies, and Overburden Drilling Management for heavy mineral processing. R. Paulen is thanked for providing a careful review.

### REFERENCES

- BEAUDOIN, G. & DUPUIS, C. 2009. Iron-oxide trace element fingerprinting of mineral deposit types. In: CORRIVEAU, L. & MUMIN, H. (eds) *Exploring for Iron Oxide Copper-Gold Deposits: Canada and Global Analogues*. Geological Association of Canada, Short Course Volume, **19**, 107-121.
- CORRIVEAU, L. 2007. Iron oxide copper-gold deposits: a Canadian perspective. In: GOODFELLOW, W.D. (ed) *Mineral deposits of Canada: a synthesis of major deposit-types, district metallogeny, evolution of geological provinces, and exploration methods*. Geological Association of Canada, Mineral Deposits Division, Special Publication, **5**, 307-328.
- CORRIVEAU, L., WILLIAMS, P.J. & MUMIN, H. 2009. Alteration vectors to IOCG mineralization: from uncharted terranes to deposits. In: CORRIVEAU, L. & MUMIN, H. (eds) *Exploring for Iron Oxide Copper-Gold Deposits: Canada and Global Analogues*. Geological Association of Canada, Short Course Volume, **19**, 87-106.
- FORTUNE MINERALS LTD. 2008. Annual Report.
- GOAD, R.E., MUMIN, A.H., DUKE, N.A., NEALE, K.L., MULLIGAN, D.L. & CAMIER, W.J. 2000. The NICO and Sue-Dianne Proterozoic, Iron Oxide-hosted, Polymetallic Deposits, Northwest Territories: Application of the Olympic Dam Model in Exploration. *Exploration and Mining Geology*, **9** (2), 123-140.
- MUMIN, H., SOMARIN, A.K., JONES, B., CORRIVEAU, L., OOTES, L. & CAMIER, J. 2009. The IOCG-Porphyry-Epithermal Continuum of Deposits types in the Great Bear Magmatic Zone, Northwest Territories, Canada. In: CORRIVEAU, L. & MUMIN, H. (eds) *Exploring for Iron Oxide Copper-Gold Deposits: Canada and Global Analogues*. Geological Association of Canada, Short Course Volume, **19**, 57-75.

## Base metal exploration using indicator minerals in glacial sediments, northwestern Alberta, Canada

Roger C. Paulen<sup>1</sup>, Suzanne Paradis<sup>2</sup>, Alain Plouffe<sup>1</sup> & I. Rod Smith<sup>3</sup>

<sup>1</sup> Geological Survey of Canada, 601 Booth Street, Ottawa, ON, K1A 0E8 CANADA (e-mail: [ropaulen@nrcan.gc.ca](mailto:ropaulen@nrcan.gc.ca))

<sup>2</sup> Geological Survey of Canada, 9860 West Saanich Road, Sidney, BC, V8L 4B2 CANADA

<sup>3</sup> Geological Survey of Canada, 3303 – 33rd Street NW, Calgary, AB, T2L 2A7 CANADA

**ABSTRACT:** An indicator mineral survey in northwest Alberta has discovered a glacial dispersal train containing highly elevated concentrations of sphalerite grains and minor galena within the sand-sized fraction of glacial sediments. High concentrations of dark grey to black, angular, brittle grains of sphalerite were found (100 to >1000 grains) in nine bulk till samples (~30 kg). The presence of high sphalerite grain counts in nine samples situated within a geographically restricted area argues against long-distance glacial transport, comminution, and deposition of erratic material from the carbonate-hosted Pine Point Zn-Pb deposits, located 330 km to the northeast. The Pb isotopic composition of the galena grains recovered from till is similar to values obtained from other Mississippi Valley-type deposits in the Cordillera and Pine Point suggesting the galena is derived from sulphide occurrences situated along the Great Slave Lake Shear Zone. However, sphalerite grains from the till have a sulphur isotopic composition much different from values recorded from Mississippi Valley-type deposits in the northern and southern Cordillera;  $\delta^{34}\text{S}$  values are interpreted to indicate bacterial reduction of coeval seawater sulphate. These results highlight the prospect of base metal deposits hosted within the Cretaceous shale bedrock of northern Alberta.

**KEYWORDS:** *indicator minerals, sphalerite, galena, Great Slave Lake Shear Zone*

### INTRODUCTION

The Cretaceous sedimentary rocks of the Western Canada Sedimentary Basin (WCSB), renowned for their hydrocarbon resources, are seldom considered to have potential to host base metal sulphide mineralization. These sedimentary rocks have also discouraged those who presumed that the Precambrian rocks of the Canadian Shield to the east and north are more favourable hosts of base metal mineralization (*cf.*, Macqueen 1997).

In northwestern Alberta, Canada, the Alberta Geological Survey (AGS) and the Geological Survey of Canada (GSC) conducted reconnaissance-scale sampling of glacial sediments to assess the potential occurrence of economic minerals (Fig. 1). This sampling program represents the first systematic regional geochemical and mineralogical survey of northwestern Alberta (Plouffe *et al.* 2006; 2008).

### REGIONAL SETTING

The uppermost bedrock in northwest Alberta consists of a Cretaceous succession of nearly horizontal and poorly-indurated marine shales of the Fort St. John Group (Loon River and Shaftesbury formations) and Smoky Group, separated by deltaic to marine sandstones of the Dunvegan Formation (Okulitch 2006). A large structural feature, the Great Slave Lake Shear Zone (GSLSZ) cuts across the study area (Eaton & Hope 2003).

Northwest Alberta is mantled by an extensive cover of unconsolidated glacial and nonglacial sediments of varying thicknesses. During the Late Wisconsin, the Keewatin-sourced Laurentide Ice Sheet flowed west and southwest across northern Alberta towards the Rocky Mountains (Paulen *et al.* 2007).

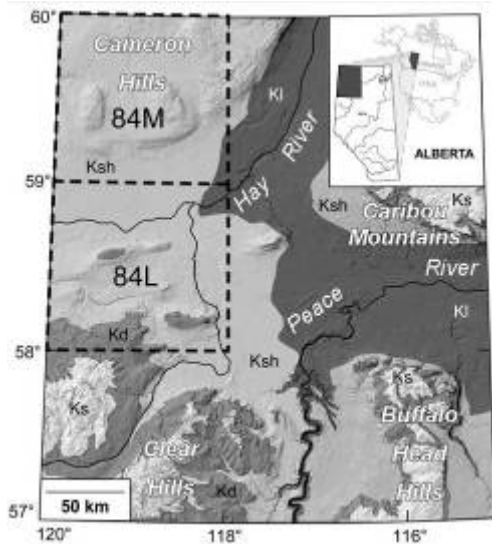


**Fig. 1.** Physiography and bedrock geology of northwest Alberta in which the sampling survey (National Topographic System sheets 84M and 84L) was undertaken. Cretaceous bedrock units listed from oldest to youngest (after Hamilton *et al.* 1998): Loon River Formation (Kl), Shaftesbury Formation (Ksh), Dunvegan Formation (Kd) and Smoky Group (Ks).

## METHODS

Bulk sediment samples (~30 kg) of till (n=63) and glaciofluvial sediments (n=7) were collected in C soil-horizon (>1 m depth) from hand-dug pits, natural bluffs, and man-made exposures. Samples underwent heavy mineral separation ( $SG \geq 3.2 \text{ g/cm}^3$ ) using a shaking table and heavy liquid separation. Heavy indicator minerals were visually identified and picked from the sand-sized fraction (0.25 – 2.00 mm).

Selected sphalerite grains (n=15) were mounted and analyzed by electron microprobe. Isotopic analyses of Pb were conducted on galena and sphalerite grains at Carleton University. Sulphur isotope analyses were performed on sphalerite powders at the University of Ottawa.

## RESULTS AND DISCUSSION

### Heavy Mineral Signature

A sphalerite dispersal train occurs in the centre of the study area (Fig. 2). Dark grey to black, brittle grains of sphalerite were found in high concentrations (>100 grains)

in nine till samples including one sample with 1047 sphalerite grains (normalized to 30 kg sample weight; (Plouffe *et al.* 2006). Background concentration in local till is zero grains. Grains exhibit pristine morphology with angular to sub-angular edges. The mineralogical anomaly extends over an area of approximately 4000 km<sup>2</sup>. One to four angular to sub-angular galena grains were recovered in eight of the till samples from the anomalous region.

### Sphalerite Chemistry

The average composition of the 15 sphalerite grains analyzed is 33.4 wt.% S, 65.4 wt.% Zn, 0.7 wt.% Fe and 0.43 wt.% Cd with trace amounts (0.3 to 0.1 wt.%) of Cu, Ag, Se, and In (Plouffe *et al.* 2007). Compared to the composition of sphalerite from the world class Pine Point Mississippi Valley-type Zn-Pb deposit, 330 km to the northeast (Kyle 1981), sphalerite from this study contains lower levels of Pb and Fe and higher Cd concentrations.

### Isotopic Fingerprinting

Of the ten galena grains recovered from the till, nine cluster into one population which exhibit very small variations in  $^{206}\text{Pb}/^{204}\text{Pb}$ ,  $^{207}\text{Pb}/^{204}\text{Pb}$ , and  $^{208}\text{Pb}/^{206}\text{Pb}$ . These nine galena grains lie within the “Pine Point lead” cluster that includes data from the Pine Point orebodies (Cumming *et al.* 1990), other Zn-Pb occurrences in the Pine Point district (Paradis *et al.* 2006), and subsurface sulphide occurrences in drill cores from carbonate sequences of the WCSB located along the GSSLZ. One galena grain is more enriched in  $^{206}\text{Pb}/^{204}\text{Pb}$  and plots below the “shale curve.” The only two sphalerite grains analyzed for Pb isotopes plot below the “shale curve” away from the “crustal evolution curve” (Fig. 3).

The “Pine Point lead” isotopic signature is quite distinctive (Fig. 3). It shows remarkable homogeneity, with  $^{206}\text{Pb}/^{204}\text{Pb}$  values in a narrow range of 18.167 - 18.189, indicating either a homogeneous source or a thorough mixing of Pb during extraction, transport, and precipitation (Cumming *et al.* 1990; Paradis *et al.*

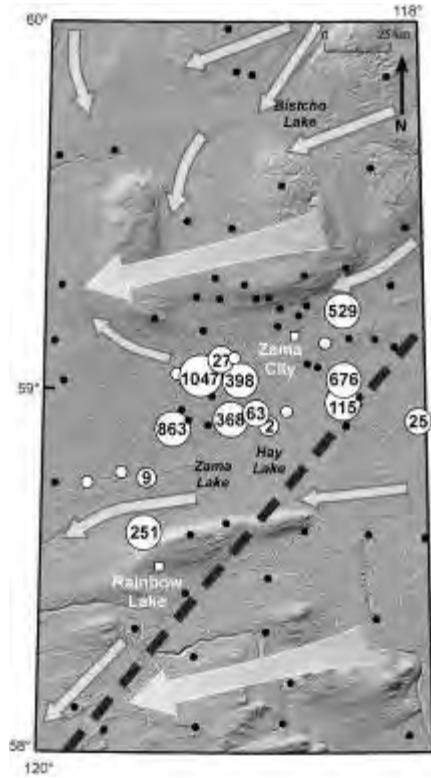


**Fig. 2.** Spherulite grains recovered from glacial sediments, normalized to 30 kg sample weights, plotted on a Shuttle Radar Topography Mission (SRTM) generated digital elevation model. Small white circles represent a single grain count; small solid black circles indicate samples with no recovered spherulite. The GSLSZ, projected to surface (Eaton & Hope 2003), is shown as the thick dashed line. Large arrows depict ice flow during glacial maximum and smaller arrows indicate local lobes of flow during deglaciation.

2006). Modelling of U and Pb concentrations and ratios suggest a depleted lower crustal source consistent with Pb derivation from basement rocks (Nelson *et al.* 2002; Paradis *et al.* 2006).

Spherulite from the till displays a range of  $\delta^{34}\text{S}$  values from -14.1 to -6.0 per mil with a mean value of -9.0 per mil. These low values are interpreted to be the result of bacterial reduction of coeval seawater sulphate. These values are different than those reported for Mississippi Valley-type deposits in the northern and southern Cordillera, which are dominantly much heavier (Fig. 4). Sulphur isotope values

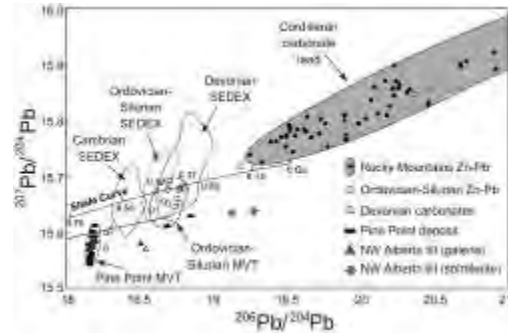


**Fig. 3.** Lead isotopic data ( $^{207}\text{Pb}/^{204}\text{Pb}$  versus  $^{206}\text{Pb}/^{204}\text{Pb}$ ) from till of northwest Alberta compared with data from the Pine Point district, Cordilleran Zn-Pb deposits, and known WCSB occurrences (Paradis *et al.* 2006).

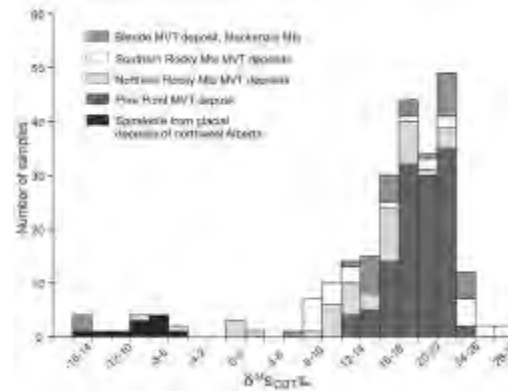


**Fig. 4.** Histogram of  $\delta^{34}\text{S}$  values for spherulite grains from NW Alberta till samples, the Pine Point Pb-Zn deposit and other Pb-Zn deposits in the Rocky and Mackenzie mountains (Paradis *et al.* 2006).

from the Pine Point deposits range from 12.2 to 27.0 per mil (Evans *et al.* 1968).

**CONCLUSION**

The bedrock source(s) of the spherulite and galena grains recovered from till in northwest Alberta remains unknown. Data presented here indicate that this mineralogical anomaly in till is not derived from the nearest known Zn-Pb deposit, Pine Point. The anomaly occurs in close proximity to the GSLSZ (Eaton & Hope 2003). The Pb isotopic values of the galena samples from the till samples in northwest Alberta are identical to those of the Pine Point district and other occurrences along the GSLSZ. Therefore,

we suggest that the bedrock source(s) for the sphalerite and galena grains in the till is probably local sulphide occurrence(s) situated along the GSSLZ, hosted in Cretaceous sediments of the WCSB.

#### ACKNOWLEDGEMENTS

The authors would like to acknowledge geologists at the AGS for insight into the regional Quaternary and bedrock geology of northern Alberta. Isabelle McMartin and Beth McClenaghan (GSC) critically reviewed the manuscript. This research was conducted as part of the GSC-AGS NRD Project 4450, GSC contribution number 20080715.

#### REFERENCES

- CUMMING, G.L., KYLE, J.R., & SANGSTER, D.F. 1990. Pine Point: A case history of lead isotopic homogeneity in a Mississippi Valley-type district. *Economic Geology*, **85**, 133-144.
- EATON, D.W. & HOPE, J. 2003. Structure of the crust and upper mantle of the Great Slave Lake shear zone, northwestern Canada, from teleseismic analysis and gravity modelling. *Canadian Journal of Earth Sciences*, **40**, 1203-1218.
- EVANS, T. L., CAMPBELL, F. A., & KROUSE, H. R. 1968. A reconnaissance study of some western Canadian lead-zinc deposits. *Economic Geology*, **63**, 349-359.
- HAMILTON, W.N., PRICE, M.C. & LANGENBERG, C.W. 1998. Geological map of Alberta. Alberta Geological Survey, Map 236, map scale 1:1,000,000.
- KYLE, J. R. 1981. Geology of the Pine Point lead-zinc district. In: WOLF, K. H. (ed) *Handbook of Strata-bound and Stratiform Ore Deposits*. Elsevier, Volume 9, part III, Chapter 11, Amsterdam, 643-741.
- MACQUEEN, R.W. 1997. Introduction. In: MACQUEEN, R.W. (ed) *Exploring for Minerals in Alberta*. Geological Survey of Canada Geoscience Contributions, Canada-Alberta Agreement on Mineral Development (1992-1995). Geological Survey of Canada, Bulletin 500, 1-12.
- NELSON, J., PARADIS, S., CHRISTENSEN, J. & GABITES, J. 2002. Canadian Cordilleran Mississippi Valley-type deposits: A case for Devonian-Mississippian back-arc hydrothermal origin. *Economic Geology*, **97**, 1013-1036.
- OKULITCH, A. 2006. Bedrock geology, Peace River, Alberta. Geological Survey of Canada, Open File 5282, map scale 1:1 000 000.
- PARADIS, S., TURNER, W.A., CONIGLIO, M., WILSON, N. & NELSON, J.L. 2006. Stable and radiogenic isotopic signatures of mineralized Devonian carbonates of the Northern Rocky Mountains and the Western Canada Sedimentary Basin. In: HANNIGAN, P.K. (ed) *Potential for carbonate-hosted lead-zinc Mississippi Valley-type mineralization in northern Alberta and southern Northwest Territories: Geoscience Contributions, Targeted Geoscience Initiative*, Geological Survey of Canada, Bulletin 591, 75-104.
- PAULEN, R.C., PRIOR, G.J., PLOUFFE, A., SMITH, I.R., MCCURDY, M.W. & FRISKE, P.W.B. 2007. Cretaceous shale of northern Alberta: A new frontier for base metal exploration. In: MILKEREIT, B. (ed.) *Exploration in the New Millennium, Proceedings of the Fifth Decennial International Conference on Mineral Exploration*, 1207-1213.
- PLOUFFE, A., PAULEN, R.C. & SMITH, I.R. 2006. Indicator mineral content and geochemistry of glacial sediments from northwest Alberta (NTS 84L, M): new opportunities for mineral exploration. *Geological Survey of Canada*, Open File 5121 and Alberta Geological Survey, Special Report **77**.
- PLOUFFE, A., PAULEN, R.C., SMITH, I.R. & KJARSGAARD, I.M. 2007. Chemistry of kimberlite indicator minerals and sphalerite derived from glacial sediments of northwest Alberta. *Geological Survey of Canada*, Open File 5545 and Alberta Geological Survey, Special Report **87**.
- PLOUFFE, A., PAULEN, R.C., SMITH, I.R. & KJARSGAARD, I.M. 2008. Sphalerite and indicator minerals in till from the Zama Lake region, northwest Alberta (NTS 84L and 84M). *Geological Survey of Canada*, Open File 5692 and Alberta Geological Survey, Special Report **96**.

## Imaging a buried diamondiferous kimberlite using conventional geochemistry and Amplified Geochemical Imaging<sup>SM</sup> Technology

Jamil. A. Sader<sup>1</sup>, Harry. S. Anderson II<sup>2</sup>,  
Ray. F. Fenstermacher<sup>2</sup> & Keiko Hattori<sup>1</sup>

<sup>1</sup>University of Ottawa, Earth Sciences Department, Ottawa, Ontario K1N 6N5 CANADA  
(e-mail: [jamilsader@yahoo.com](mailto:jamilsader@yahoo.com))

<sup>2</sup>W. L. Gore & Associates, Inc. 100 Chesapeake Blvd, Elkton, MD, UNITED STATES OF AMERICA

**ABSTRACT:** Accurate mapping of mineral deposits buried by tens to hundreds of meters of overburden will focus an exploration program, minimizing costs and time expended. Traditional surface geochemical techniques often focus on measuring and mapping metal ions in the soil or vegetation, water/soil chemical properties, and by-product gases such as oxygen and carbon dioxide. A new technique, Amplified Geochemical Imaging<sup>SM</sup> Technology, focuses on high sensitivity measurements of volatile compounds emanating from the mineral deposit itself, its contact zone, or associated redox systems. Compounds ranging from light sulphur species to organics with 18 carbon atoms, which are found at the surface, are collected and analyzed using a sensitive and sophisticated analytical technique. Differentiation of compounds associated with the mineralization and a robust image of the buried deposit are then obtained by processing the data using advanced modelling systems and multivariate statistical methods. This new technique works well with high content sulphur minerals such as those deposits hosted in Volcanogenic Massive Sulphide, porphyry Cu, Mississippi Valley-type, and some gold systems. In this paper, Amplified Geochemical Imaging<sup>SM</sup> Technology, along with conventional surface geochemical analysis, was used to image a kimberlite.

**KEYWORDS:** *diamond, kimberlite, soil geochemistry, imaging, volatile*

### INTRODUCTION

In regions where bedrock is covered by thick sediments, application of surficial geochemical exploration methods has led to a great deal of success. This paper identifies responses of Gore Amplified Geochemical Imaging<sup>SM</sup> (GAGI) compounds ranging from light sulphur species to organics with 18 carbon atoms (Anderson 2006) over kimberlites, which correlate well with geochemical responses in soil.

### GEOLOGICAL SETTING

The Honerat kimberlite is approximately 45 km east of the town of Ville-Marie, western Quebec, Canada (Fig. 1). Gravity surveys and drilling have indicated that the kimberlite was emplaced along a normal fault structure trending NW-SE. Kimberlites in this region are of Jurassic age. The Honerat kimberlite is approximately 85 m in diameter, based on company drill logs. The subcropping

surface of the kimberlite consists of hypabyssal facies kimberlite. Country rocks are dominantly Archean felsic to intermediate metavolcanics and the surficial sediments sampled at Honerat consisted of clay with minor silt to silt with minor clay. Continental-scale glaciation has affected the region several times during the Quaternary. The most recent glaciation retreated from the study area approximately 8000 years BP (Veillette 1994), during which time thick deposits (45 to 90 m) of unconsolidated glacial, glaciofluvial and glaciolacustrine sediments were deposited over the Honerat kimberlite.

A second location approximately 5 km south of the Honerat kimberlite was also studied (named Unknown) (Fig. 1).

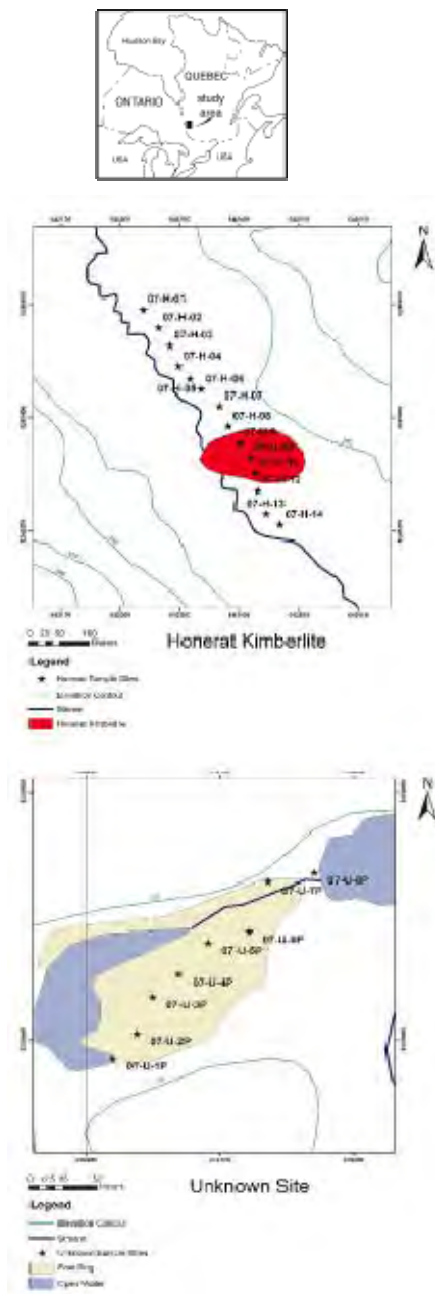


**Fig. 1.** The Honerat kimberlite and the Unknown Site are located in western Quebec, Canada. The labeled points represent sample collection sites along transects at Honerat and Unknown.

Although no kimberlite is known of in this second area, kimberlite boulders and elevated kimberlite indicator mineral counts in glacial sediments have been

found within 300 m of the Unknown site. This location was also interpreted to be a possible site for a kimberlite pipe because it is along a NE-SW trending graben structure. The terrain at Unknown is saturated peat, between 1 and 4 m deep, which overlies fine gravel. Depth to bedrock at this test site is not known.

## METHODS

Soil samples were collected along a traverse over the Honerat kimberlite and extended off the kimberlite approximately 75 m SE and 225 m NW from the pipe's centre (Fig. 1). Although it is common practice to collect samples from upper B-horizon soil (Levinson 1980; Bajc 1998; Mann *et al.* 2005) our samples were collected from C-horizon soil because GAGI samplers were placed at a depth of 60 cm (well below the B horizon). Within 8 hours of sampling, a portion of each soil sample was mixed with Milli-Q water (1:1) to create a slurry. The values of pH and oxidation-reduction potential (ORP) were determined in each slurry. Ammonia acetate leach of the soil samples were performed at Acme Analytical Laboratories, Vancouver, where 20 ml of ammonium acetate was mixed with 1 g soil sample and elements were determined by inductively coupled plasma-mass spectrometry. The GAGI samplers installed at Unknown were placed in piezometers and submerged in water at a depth of approximately 1 m below ground surface.

The GAGI samplers, installed along traverses at both Honerat and Unknown, were left in place for 5 months before being retrieved. Retrieved samplers from both locations were sent to Gore Laboratories where they were heated, and compounds were thermally desorbed and analyzed with a gas chromatograph/mass spectrometer (GC/MS).

## RESULTS AND DISCUSSION

Soil slurry ORP values are lower over the Honerat kimberlite (near 0 mV) compared to other locations along the sampling traverse (up to 100 mV). Over this kimberlite there is also a marked depletion

in concentrations of a variety of elements such as Ni, Mg, Co, K, and total REEs in soil directly over the kimberlite (Fig. 2). Conversely, enrichments of these elements at the margin(s) of the kimberlite are evident. The elemental results are similar to the soil geochemical signature over the 95-2 kimberlite, approximately 60 km to the west (McClenaghan *et al.* 2006).

Reduced ions from the Honerat kimberlite are accumulating in the surface soil producing low ORP values. Low ORP values over the kimberlite with high values near the margins suggest the presence of a “reduced chimney” (Hamilton *et al.* 2004a, 2004b), where reduced species (such as Fe<sup>2+</sup>) are migrating from the underlying kimberlite through glacial sediments to surface.

The partial leach results from soil samples identify the location of the buried Honerat kimberlite. The depletion of Ni, Mg, Co, K, and total REEs in C-horizon soils over the Honerat kimberlite suggests that numerous kimberlite pathfinder elements are not adsorbed on to soil particles. Instead, they are remaining in the dissolved phase in solution due to the more reducing environment inside compared with outside the kimberlite. However, as elements migrate out of the kimberlite “reduced chimney” environment into a more oxidizing environment, they may adsorb to soil particles, possibly oxyhydroxide complexes and produce elevated element responses at the margins of the kimberlite.

The data obtained by GAGI correlate well with soil geochemical data for the Honerat kimberlite. Individual components of the Gore analysis such as elevated dimethyl sulfide, and lower concentrations of methyl butane (Fig. 3a & b) are found at the same locations as low relative element concentrations and more reducing conditions. The spatial correlation between changes in the redox conditions, the depletion of metals, and some GAGI compounds suggests either the upward migration of GAGI compounds from the kimberlite or their formation/depletion in soil due to changing redox conditions. We suggest the latter interpretation based on

the variation of  $\delta^{13}\text{C}$  for dissolved inorganic carbon (DIC) in peat groundwaters from Unknown. The values of  $\delta^{13}\text{C}$  compared with concentrations of sulfide and hydrocarbons suggest biogenic reactions with inorganic carbon.

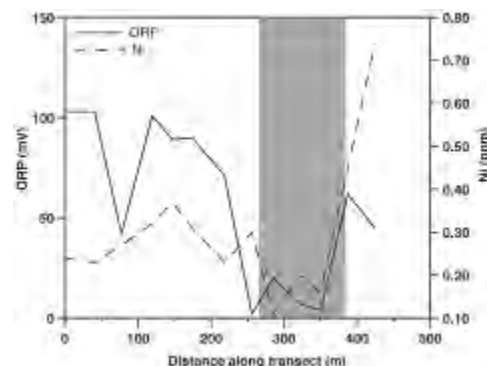


**Fig. 2.** Low relative ORP values correlate with low Ni values in soils over the Honerat kimberlite (depicted as the grey zone).

## CONCLUSIONS

This paper demonstrates that, in addition to soil geochemical exploration techniques, Gore Amplified Geochemical Imaging<sup>SM</sup> is another tool for the exploration geochemist.

- 1) Kimberlite bodies can be identified at ground surface using soil geochemistry where 90 m of glacial sediment overlies a kimberlite. This is based on variations in element concentrations of pathfinder elements such as Ni, Mg, Co, K, and total REEs over versus off a kimberlite.
- 2) The Gore Amplified Geochemical Imaging<sup>SM</sup> technique, like soil geochemistry, shows anomalous concentrations of sulfides and hydrocarbons in soils over the kimberlite.
- 3) Values of  $\delta^{13}\text{C}$ -DIC correlate with some hydrocarbons at the Unknown Site and suggest that Amplified Geochemical Imaging<sup>SM</sup> responses could be the result of surficial bacterial communities that thrive over kimberlites.

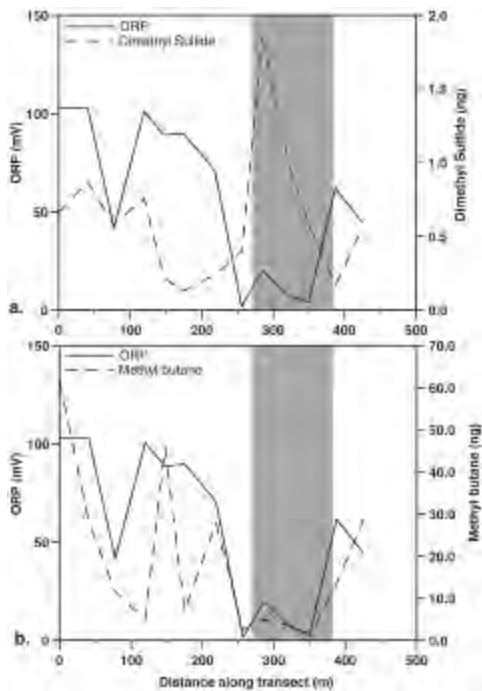


**Fig. 3.** High concentrations of dimethyl sulfide (a) and depleted concentrations of methyl butane (b) correlate with reducing soils over the kimberlite (depicted as the grey zone).

#### ACKNOWLEDGEMENTS

We thank Dr. Thomas Morris, President and CEO, and Mr. Matthew Sooley of Northern Superior Resources for providing information on, and access to the site. Field expenses and analytical costs were supported by an NSERC Discovery Grant. Funding for this project was also provided in part by an Ontario Graduate Scholarship (support for Jamil Sader's Ph.D.) and a student research grant from the Society of Economic Geologists.

#### REFERENCES

- ANDERSON, H.S. II. 2006. Amplified Geochemical Imaging: An Enhanced View to Optimize Outcomes. *EAGE First Break*, 24, August 2006, 77–80.
- BAJC, A.F. 1998. A comparative analysis of enzyme leach and mobile metal ion selective extractions; case studies from glaciated terrain, northern Ontario. *Journal of Geochemical Exploration*, **61**, 113-148.
- HAMILTON, S.M., CAMERON, E.M., McCLENAGHAN, M.B., & HALL, G.E.M. 2004a. Redox, pH and SP variation over mineralization in thick glacial overburden. Part I: methodologies and field investigation at the Marsh Zone gold property. *Geochemistry: Exploration, Environment, Analysis*, **4**, 33-44.
- HAMILTON, S.M., CAMERON, E.M., McCLENAGHAN, M.B., & HALL, G.E.M. 2004b. Redox, pH and SP variation over mineralization in thick glacial overburden; Part II, Field investigation at Cross Lake VMS property. *Geochemistry - Exploration, Environment, Analysis*, **4**, 45-58.
- LEVINSON, A.A. 1980. *Introduction to Exploration Geochemistry*. Applied Publishing, Wilmette, Illinois.
- MANN, A.W., BIRRELL, R.D., FEDIKOW, M.A.F., & DE SOUZA, H.A.F. 2005. Vertical ionic migration; mechanisms, soil anomalies, and sampling depth for mineral exploration. *Geochemistry - Exploration, Environment, Analysis*, **5**, 201-210.
- McCLENAGHAN, M.B., HAMILTON, S.M., HALL, G.E.M., BURT, A.K., & KJARSGAARD, B.A. 2006. Selective Leach Geochemistry of Soils Overlying the 95-2, B30, and A4 Kimberlites, Northeastern Ontario. *Geological Survey of Canada*, Open File 5069.
- VEILLETTE, J.J. 1994. Evolution and paleo-hydrology of glacial lakes Barlow and Ojibway. *Quaternary Science Reviews*, **13**, 945-971.

## **New advances in geochemical exploration in glaciated terrain – examples from northern Finland**

**Pertti Sarala**

*Geological Survey of Finland, P.O. Box 77, FI-96101 Rovaniemi, Finland (e-mail: [pertti.sarala@gtk.fi](mailto:pertti.sarala@gtk.fi))*

**ABSTRACT:** New geochemical sampling and analysis methods were tested in northern Finland. The purpose was to test new applications for regional and/or target-scale exploration by using surficial till as a sample material. The tests were carried out as part of a gold, nickel and PGE exploration project. One of the tested methods was mobile metal ion method of which results were compared with the results of enzyme leaching, soil gas and partial leaching methods. Sampling was carried out using small, hand-dug test pits. Another method tested was using an on-line XRF method, using continuous, 5 to 20 m long till and weathered bedrock samples from test excavations, and at the second stage from 0.5 km to 3 km long sampling lines (50 m interval) with percussion drilling. Based on these results, all methods have potential for exploration purposes in glaciated terrain, although the detection limits can cause some limitations. For example, using on-line XRF methods it is possible to find out elevated contents of trace elements in till as a mark of mineralization or mineralized alteration zones in the bedrock, and to direct target-scale sampling and research.

**KEYWORDS:** *geochemical methods, weak leach, XRF, till, exploration*

### **INTRODUCTION**

Till geochemistry is a widely used method in regional- and target-scale exploration and mineral potential mapping in Finland. Sampling is usually carried out by using percussion drilling and/or test pit surveys with following partial leaching and analyses of inductively coupled plasma atomic emission spectrometry (ICP-AES) and/or graphite furnace atomic absorption spectrometry (GAAS). However, this sampling procedure is often expensive and time-consuming.

Based on this background new sampling and analytical methods have been tested in northern Finland to seek new applications for exploration by using surficial till as a sample material with emphasis on decreasing analytical costs and increasing sample efficiency. This study was carried out as a part of on-going Au, Ni and PGE exploration project of the Geological Survey of Finland.

### **METHODS**

In the first test phase, several weak leach methods were tested. Samples were collected from the small hand-dug test pits

(Fig. 1) for mobile metal ion (MMI), enzyme leaching and soil gas analyses. The results were compared against known results of analyses based on partial leaching. MMI sampling procedure as outlined by SGS Group Laboratories ([http://www.geochem.sgs.com/sampling\\_f\\_or\\_mmi\\_geochem](http://www.geochem.sgs.com/sampling_f_or_mmi_geochem)). Trace element analyses were completed in the ALS Chemex laboratory.

In the second test phase, the application of a new on-line XRF-scanner was tested for 1) continuous till and weathered bedrock samples and 2) till profiles with sampling interval of about 100 m. Continuous samples were taken from the tractor excavated test trenches both from the surface of the pre-Quaternary weathered bedrock and from the till about 0.5 m above the weathered bedrock surface.

For the profile (length from 0.5 to 3 km, point interval of 50 m) sampling, both small hand-dug test pits (depth about 50 cm) and percussion drilling (sampling depth 1 to 1.5 m) have been used. Measurements were made using the ScanMobile system which is a moving



**Fig. 1.** Sampling point for the weak leach analytical samples, northern Finland.

scanning unit produced by the Mine On-line Services Limited. New sample handling methods were developed for the XRF scanning process. After removing pebbles >1 cm, till samples with natural moisture were put into the wooden boxes: continuous samples, 6 m per box (Fig. 2), and profile samples, 48 pieces per box (Fig. 3).

## RESULTS

The test of weak leach methods shows that glacial till and stratified sediments are usable material for mobile metal ion tracing. The thickness of overburden is not an essential factor for affecting the mobile ion concentrations in the upper soil horizon. However, the influence of complex till stratigraphy is not clear for ion mobilization from the bedrock source of surface.

The large number of trace elements available in weak leach analytical packages is effective for many types of ore exploration. In surveys for Au, Ni and PGE deposits, many anomalies in surficial sediments have been found, and detailed studies have shown that these anomalies reflect bedrock (source) mineralization. As an example, Figure 4 shows a Ni anomaly

in surface sediment with a mineralized zone sourced in the bedrock at the contact



**Fig. 2.** Continuous pre-Quaternary weathered bedrock sampling, placed into core boxes that allow for 6 m of continuous length.

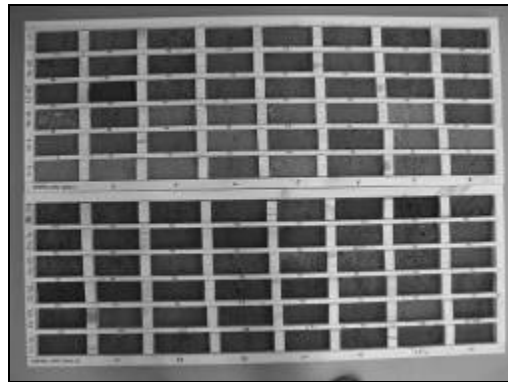


**Fig. 3.** Profile till samples placed into the wooden boxes ready for XRF-scanning.

of metakomatiitic volcanic rocks and quartzite (Fig. 4).

Mobile, on-line XRF methods have been tested in the Au exploration targets. Analysis of continuous till and weathered bedrock samples shows clear variation of the contents of pathfinder elements of hydrothermal alteration. Particularly, in the weathered bedrock, the presence of narrow mineralized veins is seen (Fig. 5). One interesting feature is that the indication of the weathered bedrock sources can be traced 2 to 5 m down-ice in the till. These results suggest very short glacial transport of mineralized debris from the bedrock sources. Information on

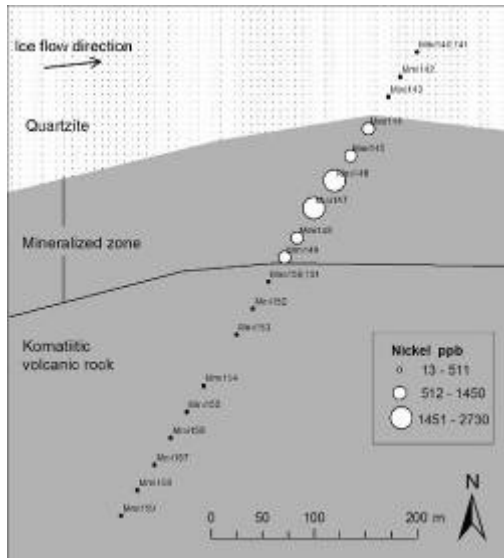


**Fig. 4.** An example of Ni (MMI) anomaly in till indicating mineralization in the bedrock.

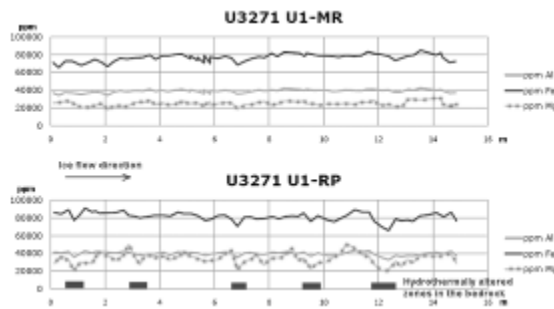


**Fig. 5.** An example of Al, Fe and Mg contents in continuous weathered bedrock and till samples analyzed with on-line XRF method. MR = till, RP = weathered bedrock.

transport distance and is very important for planning other till geochemistry sampling within the region.

XRF analyses of the profile till sampling reflects lower variation of trace element content. However, it is possible to see indications of mineralized bedrock as relatively higher element concentrations particularly, if overburden is thin.

**CONCLUSIONS**

Use of weak leach methods shows that mobile ion concentrations in the upper soil horizons can be used for tracing mineralization or mineralized structures in

the bedrock. Au, Ni and PGE type deposits have been found based on the studies carried out in northern Finland. This method is also usable for bedrock mapping in the areas of thick glacial overburden.

Mobile, on-line XRF-scanning is a new tool for exploration when using till and weathered bedrock samples. Detailed geochemical mapping is possible if continuous samples are taken. The most prospective regional- or target-scale zones in the bedrock can be traced with long till sampling profiles using light-weight sampling methods (e.g., shallow hand-dug test pits or percussion drilling). The benefit of this method is low analytical costs and faster turn around time for results.

**ACKNOWLEDGEMENTS**

I want to thank a large group of geologists in the Geological Survey of Finland (Esko Korhikoski, Olli Sarapää, Markku Iljina, Eelis Pulkkinen, Veikko Keinänen, Helena Hulkki, Tuomo Törmänen, Pertti Heikura, Anne Peltoniemi-Taivalkoski) and Juhani Ojala from the Store Norske Gull As who have participated this project during 2007-2008. Also, Paula Haavikko, Martti Melamies, Ilkka Keskitalo, Pertti Telkkälä, Reijo Puljujärvi, Jorma Valkama, Jaakko Hietava, Irmeli Huovinen, Janne Hokka, Mikko Numminen, Matti Mäkikyrö and Mikko Savolainen are thanked for the assistance in the field. The abstract has been reviewed by Roger Paulen and Beth McClenaghan (Geological Survey of Canada).



## Regional geochemical soil data as aid to the reconstruction of Mid-Pleistocene ice flows across central and eastern England

Andreas J. Scheib, Jonathan Lee, Neil Breward & Lister Bob

British Geological Survey, Kingsley Dunham Centre, Keyworth, Nottingham, NG12 5GG UNITED KINGDOM  
(e-mail: [ascheib@bgs.ac.uk](mailto:ascheib@bgs.ac.uk))

**ABSTRACT:** Principal component analysis of high-density, regional soil geochemical data was used to reveal element associations within Mid-Pleistocene glacial till deposits across Central and Eastern England. Results have helped to characterise tills by their geochemical composition at a regional scale, leading to a better understanding of, (i) which parent materials tills have been derived from, (ii) sediment transportation paths and flow trajectories of the British Ice Sheet, and (iii) the evolution of the British Ice Sheet during the Mid-Pleistocene.

**KEYWORDS:** *Soil geochemistry, glacial till deposits, PCA, ice flow reconstruction*

### INTRODUCTION

Tills are the most difficult superficial deposits to interpret and classify, but are crucial to the reconstruction of former glaciations and understanding the coupling between ice sheet behaviour and climate change (Evans 2007). Geochemical surveys of tills in Finland and Canada have successfully demonstrated that geochemical data contain vital information for refining glacial stratigraphy, determining till sediment provenance, and reconstructing ice flow trajectories (McClenaghan *et al.* 1992; Klassen 2001; Sarala 2005). Anglian-age (c. 450 ka) glacial deposits of Central and Eastern England are complex and have been studied in various detail, but studies have not yet utilised the vast resource of high-density soil geochemical data held by the British Geological Survey (BGS). The aim of this study was to investigate the potential of this regional soil geochemical data help to characterise and classify glacial till deposits as well as to reconstruct glacial flow trajectories and its sediment sources. This was tested by using multivariate principal component analysis (PCA), which is a helpful means to manipulate and interpret multi-element geochemical data as shown by Grunsky and Smee (1999) and Ali *et al.* (2006).

### MATERIALS AND METHODS

#### Study area and data

The study benefits from access to a geochemical database containing analytical data from ~ 27,500 soil samples collected since 1986 by the Geochemical Baseline Survey of the Environment (G-BASE) (Johnson *et al.* 2005). The area presented in this study covers more than 40,000 km<sup>2</sup> of Central and Eastern England (Fig.1). Soils were collected at a density of one sample every two km<sup>2</sup> of the British National Grid (BNG). At each site, samples were collected, from (5-20 cm) and (35-50 cm), of which latter were used in this study. Each sample comprising a composite of material of five sub-samples collected at the corners and centre of a 20 m square. A more detailed account on the sampling procedures used and sample preparation can be found in Johnson *et al.* (2005). Major and trace element determinations were carried out by X-ray fluorescence spectrometry (XRFS) giving a range of up to 53 elements. However, this study used only 25 elements (Ba, Ca, Co, Cr, Cu, Fe, Ga, K, La, Mg, Mn, Mo, Nb, Ni, P, Pb, Rb, Sn, Sr, Ti, U, V, Y, Zn and Zr) as some elements were excluded on quality issues. Prior to PCA, analytical data were log-transformed, as investigated by Reimann *et al.* (2002).

A spatial join of the analytical data with BGS DiGMapGB-50 Superficial Geology returned data for ~ 4,700 soil samples, which had been collected over glacial till deposits (Fig.1) of Mid-Pleistocene, Anglian age.

**Geological setting**

Central and Eastern England is almost entirely underlain by sedimentary rocks that young from west to east. Four major geological sub-divisions are presented in Figure 1. Permian and Triassic mudstone and sandstone dominate the East Midlands and parts of Yorkshire; Jurassic clays crop out within the centre of the study area and Cretaceous chalk underlies most of Central East Anglia.

Figure 1 shows the distribution of sample sites located directly over Anglian till deposits, covering approximately a quarter of the study area. North of the Devensian limit (also known as Dimlington re-advance) occur younger till deposits of the Devensian glaciation. More than half of the sample sites were located over diamictons of the Lowestoft Formation (LOFT) of East Anglia. The remaining tills are classified as Mid-Pleistocene diamictons (TILMP), and the Oadby Till (ODT) and Thrussington Till (THT) members of the Wolston Formation in the Midlands. Several possible ice flow scenarios could account for the spatial and lithological distribution of these tills (Perrin *et al.* 1979).

Ice trajectory scenarios are A) ice flowing southwards from the North Sea Basin and into northern East Anglia, B) ice flowing into East Anglia and East Midlands through The Wash Basin radiating to the east and C) west. The fourth scenario (D) describes ice moving down from northern Central England into the Midlands in southerly direction and then radiating into East Anglia.

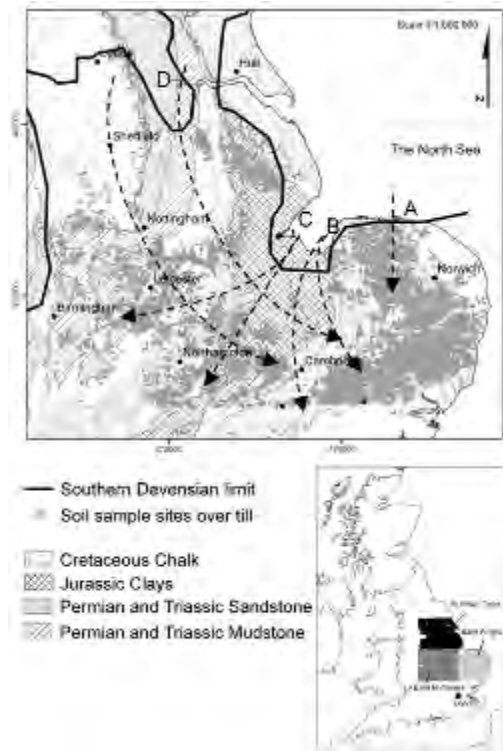


**Figure 1.** Distribution of soil sample sites collected over glacial till deposits, ice flow scenarios (A to D) and main bedrock strata of the study area.

**RESULTS**

PCA is a popular approach for analysing large multi-element datasets for two reasons. Firstly, the reduction of the number of variables to form a small number of independent principal components and secondly, the creation of more interpretable combined variables (Ali *et al.* 2006). The analysis was carried out using a correlation matrix in order to reduce the effects of magnitude that are attributed to elements such as Ca, Fe, K and Mg (Grunsky & Smee 1999). A total of 15 principal components were calculated until 95 % of the variance was explained. Eigenvalues returned from PCA were plotted in a scree plot (Fig. 2), which gives an indication as to the significance of the derived PCs (Grunsky & Smee 1999).

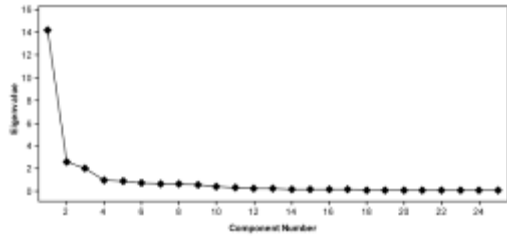


**Fig. 2.** Scree plot of eigenvalues

PCs with high eigenvalues are assumed to best represent the geochemical variability and characteristics of the data. Components 4 and higher returned Eigenvalues below 1.0 and were excluded from further interpretation, as discussed by Mandal *et al.* (2008).

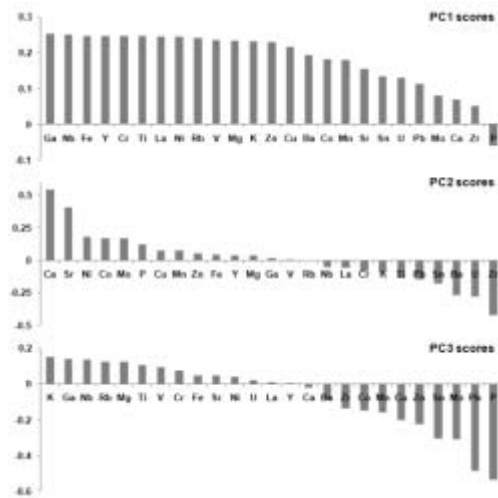


**Fig. 3.** Score loadings for PC1 to 3

PC1 represents 57% of the total variance of the data with an eigenvalue of 14.2. PC2 accounts for a further 10 % and PC3 for 8.0% of the total variance with eigenvalues of 2.6 and 2.0 respectively.

Element loadings of the first three PCs are displayed in Figure 3. PC1 includes all selected elements with only P being inversely related. Loadings of PC2 present a much clearer variation in the data and correspond to Ca-Sr association, thought to be related to limestone and chalk bedrock.

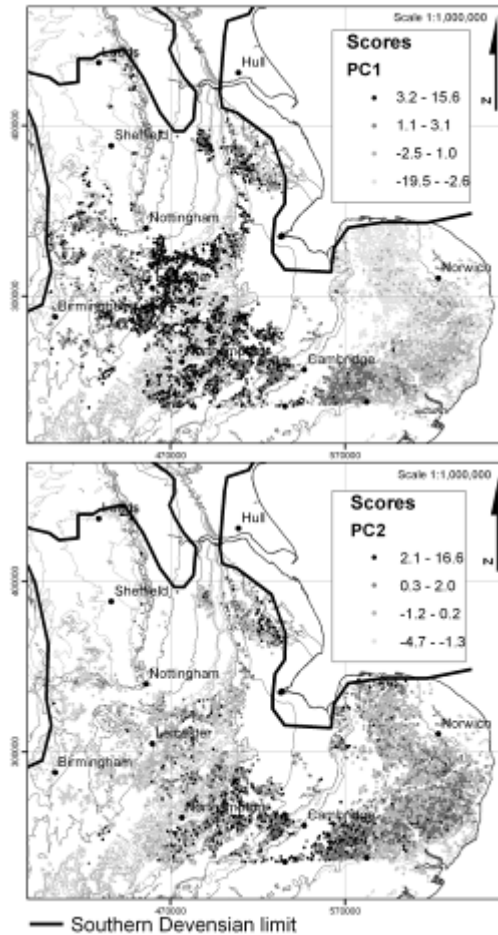


**Fig. 4.** Spatial distribution of PC1 and PC2 loading scores across Central and Eastern England.

Positive loadings of K, Ga and Nb in PC3 are indicators for clay rich soils. Negative loadings correspond to heavy metals and may indicate an anthropogenic component. Figure 4 displays spatial distribution of scores of PC1 and PC2. High scores of PC1 are mainly located over the East Midlands area, whilst the northern half of East Anglia, with low or negative scores, appears relatively deficient in these elements. High scores of PC2 are located between Northampton and the east of Cambridge, south of the Humber estuary at Hull and along the northern coastline of East Anglia. Tills in these areas were derived from calcareous and Sr-bearing strata, most likely Cretaceous Chalk (Fig. 1).

## CONCLUSIONS

This study is in progress and gives only preliminary results. However, the application of multivariate analysis has already highlighted various geochemical characteristics and associations within soils collected over Mid-Pleistocene tills. Findings can be summarised as follows:

(1) Regional geochemical soil data can provide vital information on the composition and provenance of glacial till deposits in Central and Eastern England.

(2) PCA has highlighted some clear regional divisions within the tills, especially between the East Midlands and East Anglia

(3) Ice flow scenario A is unlikely. Scenarios B and C have occurred mainly in a southerly direction, carrying chalky material and possibly overriding earlier ice flow D.

(4) To classify tills, most significant indicator elements are Ga, Mg, K, Rb, Ca, Sr and P.

(5) Further investigation should involve the integration of lithological and grain-size data as well as other methods of data analysis.

## ACKNOWLEDGEMENTS

This abstract is published with the permission of the Director of the British Geological Survey (NERC).

## REFERENCES

ALI, K., CHENG, Q., LI, W. & CHEN, Y. 2006. Multi-element association analysis of stream sediment geochemistry data for predicting gold deposits in south-central Yunnan Province, China. *Geochemistry: Exploration, Environment, Analysis*, **6**, 341-348.

EVANS, D.J.A. 2007. Glacial Landforms – Tills. In: *Encyclopedia of Quaternary Science*. Elsevier, 808-818.

GRUNSKY, E.C. & SMEE, B.W. 1999. The differentiation of soil types and mineralization from multi-element geochemistry using multivariate methods and digital topography. *Journal of Geochemical Exploration*, **67**, 287-299.

JOHNSON, C.C., BREWARD, N., ANDER, E.L. & AULT, L. 2005. G-BASE: Baseline geochemical mapping of Great Britain and Northern Ireland. *Geochemistry: Exploration, Environment, Analysis*, **5(4)**, 347-357.

KLASSEN, R.A. 2001. The interpretation of background variation in regional geochemical surveys – an example from Nunavut, Canada. *Geochemistry: Exploration, Environment, Analysis*, **1**, 163-173.

MANDAL, U.K., WARRINGTON, D.N., BHARDWAJ, A.K., BAR-TAL, A., KAUTSKY, L. MINZ, D., & LEVY, G.J. 2008. Evaluating impact of irrigation water quality on a calcareous clay soil using principal component analysis. *Geoderma*, **144**, 189-197.

MCCLENAGHAN, M.B., LAVIN, O.P., NICHOL, I. & SHAW J. 1992. Geochemistry and clast lithology as an aid to till classification, Matheson, Ontario, Canada. *Journal of Geochemical Exploration*, **42**, 237-260.

PERRIN, R.M.S., ROSE, J. & DAVIES, H. 1979. The distribution, variation and origins of pre-Devensian tills in eastern England. *Philosophical Transactions of the Royal Society of London*, **B287**, 535-570.

REIMANN, C., FILZMOSE, P. & GARRETT, G. 2002. Factor analysis applied to regional geochemical data: problems and possibilities. *Applied Geochemistry*, **17**, 185-206.

SARALA, P. 2005. Till geochemistry in the ribbed moraine area of Peräpohjola, Finland. *Applied Geochemistry*, **20**, 1714-1736.

## Till geochemical and indicator mineral methods in mineral exploration: history and status

L. Harvey Thorleifson

Minnesota Geological Survey, 2642 University Ave W, St Paul, MN 55114, USA (e-mail: [thorleif@umn.edu](mailto:thorleif@umn.edu))

**ABSTRACT:** Detection of clastic debris transported from mineralized sources is the basis of mineral exploration methods ranging from boulder tracing to elemental and indicator mineral methods. Essential to successful application of these methods to tracing of mineralized debris to bedrock sources in recently glaciated environments are an understanding of glacial process and history, combined with sound survey design and interpretation. In North America and Fennoscandia, advances in mineral exploration and glacial geology were mutually supportive in the latter 20th century, concurrent with a shift in exploration to overburden-covered regions. Developments during this time began with recognition of the relevance of glacial process and history to prospecting, and progressed with increased comprehension of the textural and mineralogical tendencies of glacial sediments. Development of logistics suited to glaciated environments such as reverse circulation drilling followed, and in the 1990s, the discovery of diamonds in Canada resulted in much progress in application and awareness of drift prospecting methods. As a result, the discipline now centres on intricate indicator mineral and elemental methods that bring together the most current insights into glacial geology, mineral deposit geology, and mineral chemistry, in the search for a full range of commodities.

**KEYWORDS:** *till, geochemistry, indicator mineral, mineral exploration, glacial sediment*

### INTRODUCTION

In glaciated terrain, mineral exploration may take advantage of clastic dispersal of mineralized boulders, indicator minerals, and fine detrital debris or their weathering products that may be detected by elemental analysis. Whereas what might be regarded as purely geochemical methods rely on elements that have been dispersed from primary or secondary sources by aqueous or gaseous chemical processes, indicator mineral and till geochemical methods utilized in glaciated terrain are based on mineral grains transported by mechanical processes.

Elemental analyses of, for example, soils, may be used to detect a combination of chemical and clastic signals, although an exploration strategy usually is directed at either one or the other. For example, the B horizon might be sampled and appropriate analytical procedures applied to seek a dominantly chemical signal, while the C horizon might be sampled and analyzed to seek primarily a clastic signal residing in mineral grains or their weathering

products. In the case of indicator mineral grains, however, the signal is attributable to mechanical dispersal processes alone.

In glaciated environments, labile minerals may be detected 100s of km from source (Fig. 1). Tracing of glacial indicators therefore requires assessment of indicator character and mapping of concentration gradients, supported by knowledge of ice flow history, processes of sediment transport, and factors such as glacial sediment thickness, bedrock topography, and bedrock erodibility.

The principle that underpins these methods holds that sediments bearing traceable clastic debris carried down the transport trend by glacial processes will be detected during exploration, mapping, or research, if sample spacing and signal to noise ratio are adequate. Exploration surveys carried out by industry test for the presence of mineralization, to aid decisions regarding property acquisition and follow-up. Mapping surveys typically conducted by government agencies serve as a reference for exploration by defining trends in background, identifying

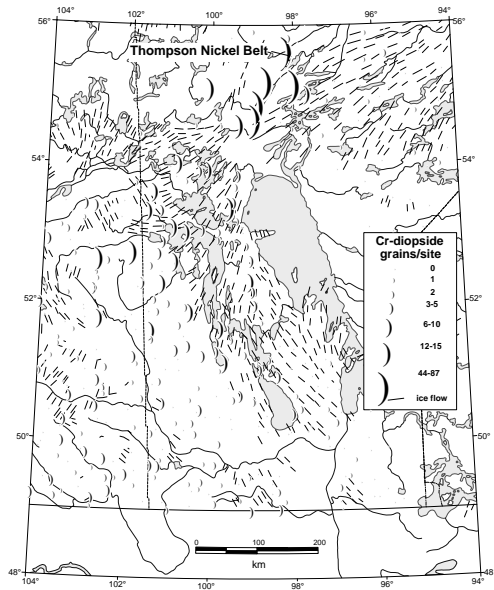


**Fig. 1.** An indicator mineral plume consisting of Cr-diopsides glacially dispersed from the Thompson Nickel Belt in Manitoba, Canada, detected in ~20 litre till samples at a 30-km spacing (Thorleifson *et al.* 1994; Thorleifson & Matile 1997).

problematic areas, and by providing examples of anomalies (Fig. 2). Research surveys are carried out to enhance methods, understand processes, and improve the effectiveness of both exploration and mapping, commonly as case studies around known mineral deposits.

The dispersed signal characteristically has a much larger aerial footprint than the source. Dispersal train size and contrast with background are governed by size of the source, concentration at source, dilution, background level, visual distinctiveness of the debris, and the nature of the processes of sediment transport (Averill 2001). Detection method also affects signal to noise ratio in relation to sample size, the degree to which the textural, density, and/or magnetic fraction in which the target preferentially resides is concentrated, and analytical methods.

Indicator minerals recovered for morphological and mineralogical analyses include those from kimberlite and

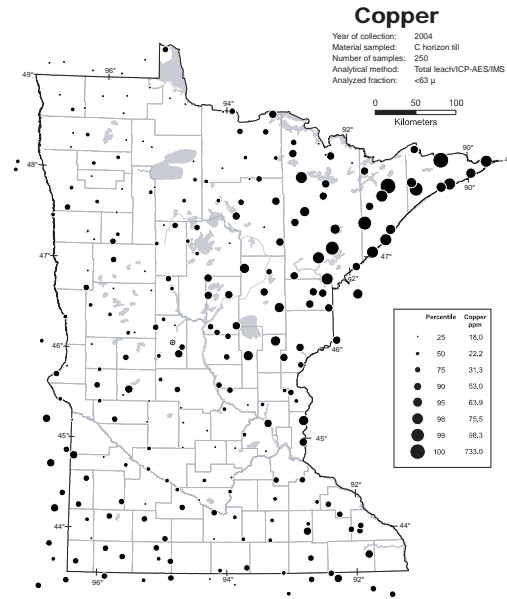


**Fig. 2.** Mapping of sediment composition by government agencies provides a reference for exploration by mapping background, identifying problematic areas, and by providing examples of anomalies (Thorleifson *et al.* 2007).

lamproite, gold grains, sulphides, and other minerals indicative of mineral deposits and associated alteration. In addition to visual and mineralogical analysis of mineral grains, and to reduce cost or seek a signal not recoverable as mineral grains, elemental methods may be used to detect elements diagnostic of specific mineral grains or their weathering products, typically in a fraction defined by texture, density, and/or magnetic susceptibility. To avoid mixing clastic and chemical signals, C-horizon or deeper sediments in soil profiles are sampled. The gravel, sand, and finer size fractions may also be analyzed to trace provenance, in order to assist interpretation.

Several syntheses have reviewed the application of till geochemical and indicator mineral methods to mineral exploration in glaciated terrain (Coker & DiLabio 1989; DiLabio & Coker 1989; Kujansuu & Saarnisto 1990; Kauranne *et al.* 1992; Bobrowsky *et al.* 1995; Shilts 1996; McClenaghan *et al.* 1997, 2001; Thorleifson & McClenaghan 2003, 2007;

McClenaghan 2005; Paulen & McMartin 2009).

## HISTORY

Pre-20th century literature includes reference to glacially transported boulders and mineral grains being recognized as indicators of mineral potential (e.g., Tilas 1740), and early 20th century literature confirms that glacial transport of mineral deposit indicators was understood (e.g., Prest 1911). In the latter 20th century, there was rapid progress in glacial geology, and concurrent progress in its application of its principles to mineral exploration (e.g., Dreimanis *et al.* 1957). Progress was stimulated by publication of case studies that recognized glacially transported kimberlite indicator minerals (Lee 1968), and development of logistics, such as reverse circulation drilling, that are well suited to glaciated terrain (Skinner 1972).

Much further effort was required, however, to establish the textural and mineralogical tendencies of glacial sediments, and to clarify how survey design and interpretation requires a comprehension of these tendencies. Dreimanis & Vagners (1971), for example, demonstrated how varying rocks tend toward differing size fractions during glacial comminution, such as carbonate preferentially producing silt, and granite preferentially producing sand. Shilts (1971) demonstrated the striking compositional differences between the clay, silt, and sand fractions of till, thus indicating the great significance of textural partitioning with respect to till geochemistry. Similarly, a comprehension of the controls on sulphide preservation in glacial sediments, with sulphides virtually absent above the water table due to aeration while being well preserved in deeper sediments, was fundamental to facilitation of progress in the discipline (Shilts 1975). With these principles in place, and with improved insights into glacial processes, the boom in gold exploration in the 1980s resulted in broader application and awareness of drift prospecting, and the ensuing explosion of

diamond exploration in the 1990s brought advanced methods in mineral chemistry to the discipline.

## STATUS

Current developments in till geochemical and indicator mineral methods in mineral exploration largely relate to more intricate and confident survey design and interpretation that take into account an enhanced comprehension of glacial process and history. Concurrently, developments in field and laboratory, elemental and isotopic analytical technology are progressing, as is the integration of knowledge from the fields of glacial geology, mineral deposit geology, and mineral chemistry. As a result, the range of targets being sought has broadened to encompass all commodities, for example with the development of indicator mineral methods suitable for the search for base metals (Averill 2001).

## REFERENCES

- AVERILL, S.A. 2001. The application of heavy indicator mineralogy in mineral exploration with emphasis on base metal indicators in glaciated metamorphic and plutonic terrains. In: MCCLENAGHAN, M.B., BOBROWSKY, P.T., HALL, G.E.M. & COOK, S.J. (eds) *Drift Exploration in Glaciated Terrain*, Geological Society of London, Special Publication No. **185**, 69-81.
- BOBROWSKY, P.T., SIBBICK, S.J., NEWELL, J.H. & MATESEK, P.F. (eds) 1995. *Drift Exploration in the Canadian Cordillera*. British Columbia Ministry of Energy, Mines and Petroleum Resources, Paper 1995-2.
- COKER, W.B. & DiLABIO, R.N.W. 1989. Geochemical exploration in glaciated terrain: geochemical responses. In: GARLAND, G.D. (ed.) *Proceedings of Exploration '87*, Ontario Geological Survey, Special Volume **3**, 336-383.
- DiLABIO, R.N.W. & COKER, W.B. (eds) 1989. *Drift Prospecting*. Geological Survey of Canada, Paper **89-20**.
- DREIMANIS, A., KNOX, K.S., MORETTI, F.J., & REAVELY, G.H. 1957. Heavy mineral studies in tills of Ontario and adjacent areas. *Journal of Sedimentary Petrology*, **27**, 148-161.
- DREIMANIS, A. & VAGNERS, U.J. 1971. Bimodal distribution of rock and mineral fragments in basal tills. In: GOLDTHWAIT, R.P. (ed) *Till, A*

- Symposium*, Ohio State University Press, 237-250.
- KAURANNE, K., SALMINEN, R., & ERIKSSON, K., (eds) 1992. Regolith exploration geochemistry in arctic and temperate terrains. *Handbook of Exploration Geochemistry*, **5**, Elsevier.
- KUJANSUU, R. & SAARNISTO, M. (eds) 1990. *Glacial Indicator Tracing*. A.A. Balkema, Rotterdam, Netherlands.
- LEE, H.A. 1968. An Ontario kimberlite occurrence discovered by application of the glaciofocus method to a study of the Munro Esker. *Geological Survey of Canada*, Paper 68-7.
- McCLENAGHAN, M.B. 2005. Indicator mineral methods in mineral exploration. *Geochemistry: Exploration, Environment, Analysis*, **5**, 233-245.
- McCLENAGHAN, M.B., THORLEIFSON, L.H. & DiLABIO, R.N.W. 1997. Till Geochemical and Indicator Mineral Methods in Mineral Exploration. In: GUBINS, A.G. (ed) *Proceedings of Exploration 97*, 233-248.
- McCLENAGHAN, M.B., BOBROWSKY, P.T., HALL, G.E.M. & COOK, S.J. (eds) 2001. *Drift Exploration in Glaciated Terrain*. Geological Society, London, Special Pub. No. 185.
- PAULEN, R.C. & McMARTIN, I. (eds) 2009. *Application of till and stream sediment heavy mineral and geochemical methods to mineral exploration in western and northern Canada*; Geological Association of Canada Short Course Notes 18.
- PREST, W.H. 1911. Prospecting in Nova Scotia. *Nova Scotia Mining Society Journal*, **16**, 73-91.
- SHILTS, W.W. 1971. Till studies and their application to regional drift prospecting. *Canadian Mining Journal*, **92**, 45-50.
- SHILTS, W.W. 1975. Principles of geochemical exploration for sulphide deposits using shallow samples of glacial drift. *Canadian Institute of Mining and Metallurgy Bulletin*, **68**, 73-80.
- SHILTS, W.W. 1996. Glacial drift exploration. In: MENZIES, J. (ed) *Past Glacial Environments: Sediment Forms and Techniques*. Butterworth-Heinemann, 411-438.
- SKINNER, R.G. 1972. Drift prospecting in the Abitibi Clay Belt; overburden drilling program methods and costs. *Geological Survey of Canada*, Open File 116.
- THORLEIFSON, L.H. & MATILE, G.L.D. 1997. Till geochemical and indicator mineral reconnaissance of northeastern Manitoba. *Geological Survey of Canada*, Open File D3449.
- THORLEIFSON, L.H., GARRETT, R.G. & MATILE, G.L.D. 1994. Prairie kimberlite study – indicator mineral geochemistry. *Geological Survey of Canada*, Open File 2875.
- THORLEIFSON, L. H., HARRIS, K.L., HOBBS, H.C., JENNINGS, C.E., KNAEBLE, A.R., LIVELY, R.S., LUSARDI, B.A., & MEYER, G.N. 2007. Till geochemical and indicator mineral reconnaissance of Minnesota. *Minnesota Geological Survey*, Open File Report OFR-07-01.
- THORLEIFSON, L.H. & McCLENAGHAN, M.B. 2003. *Indicator mineral methods in mineral exploration*. Prospectors and Developers Association of Canada, Short Course Notes, Toronto, March 8, 2003.
- THORLEIFSON, L.H. & McCLENAGHAN, M.B. 2007. *Indicator Mineral Methods in Mineral Exploration*. Exploration 07, Short Course Notes, Toronto, Canada, September 9, 2007.
- TILAS, D. 1740. Tanckar om Malmletande, i anledning af löse gråstenar. *Kongl. Svenska Vetenskaps. Academiens Handlingar* 1739-1740, I, 190-193.

## Numerical Evaluation of Partial Digestions for Soil Analysis, Talbot VMS Cu-Zn Prospect, Manitoba, Canada

Pim W.G. Van Geffen<sup>1</sup>, T. Kurt Kyser<sup>1</sup>,  
Christopher J. Oates<sup>2</sup>, & Christian Ihlenfeld<sup>2</sup>

<sup>1</sup>Dept. Geological Sciences & Geological Engineering, Queen's University, Miller Hall, Kingston, Ontario, K7L 3N6  
Canada (e-mail: [pvgeffen@geoladm.geol.queensu.ca](mailto:pvgeffen@geoladm.geol.queensu.ca))

<sup>2</sup>Anglo American plc, 20 Carlton House Terrace, London SW1Y 5AN UK

**ABSTRACT:** To enhance the subtle geochemical expression of ore deposits in surface soils developed on exotic sediment cover, various partial digestions and selective extraction methods have been developed, targeting specific phases in the soil or cation sorption sites. Eleven extraction methods were assessed for their exploration performance on soil samples from a 1000 m transect across the Paleoproterozoic Talbot VMS deposit, hosted by metavolcanic and metasedimentary sequences of the Flin Flon – Snow Lake terranes that are overlain by 100 m of Paleozoic dolomite and 0 to 2 m of Holocene glacial and glaciolacustrine sediments. As a numerical screening tool for exploration performance, Student's *t* test and *t* probability ( $P_t$ ) statistics were applied to evaluate the magnitude and spatial accuracy of anomalies in each data set. In the surface soils that were analyzed, Zn anomalies have the highest contrast for most methods, followed by P and Cd. Extraction methods by which Zn anomalies were identified within the >95% confidence interval (i.e.  $P_t < 5\%$ ) were ranked numerically, in decreasing order of exploration performance (increasing  $P_t$ ): Enzyme Leach (0.3%), deionized water (0.8%), sodium pyrophosphate (0.9%), MMI (1.6%), clay fraction aqua regia (2.2%), and ammonium acetate at pH 7 (2.3%).

**KEYWORDS:** soil geochemistry, partial digestion, Student's *t* distribution, VMS Cu-Zn

### INTRODUCTION

Soil geochemistry is widely applied in mineral exploration, and with advancing knowledge of speciation and residence phases of trace elements in soils, a variety of partial and selective extractions for chemical analysis have been developed over the past decades. Each of these methods has been designed to target and dissolve only those elements that are adsorbed onto labile phases in soil, from carrier fluids and gases that transported them from a deposit to the surface (e.g. Hall *et al.* 1996).

In this case study, 11 different extraction methods (Table 1) were applied to a 1000 m line of 15 B/C-horizon soil samples (<0.25 mm) across the Talbot VMS Cu-Zn deposit in northern Manitoba, Canada (Fig. 1), followed by ICP-MS analysis. Student's *t* test and minimum *t* probability statistics provide a tool to rank the 'exploration performance' of each method (Stanley 2003; Stanley & Noble 2008). By

comparing the means and standard deviations of the anomalous and background sub-populations of the soil data set, the probability that they are derived from the same parent population can be calculated as a percentage ( $P_t$ ). The greater the contrast between the anomalous and background sub-populations, the smaller  $P_t$ , and the better the element indicates the anomaly.  $T$  probability was calculated for all elements in each extraction method, with Zn showing the strongest anomalies for most extraction methods.

### GEOLOGICAL SETTING

The Talbot VMS Cu-Zn prospect is situated in the eastern extension of the Paleoproterozoic Flin Flon Belt (1.92 – 1.88 Ga), north-western Manitoba (Stern *et al.* 1999). The prospect is located just northeast of Lake Talbot, about 160 km SE of Flin Flon (Fig. 1). Mineralization is hosted by medium to high-grade

**Table 1.** Partial digestions and selective extractions applied to Talbot soil samples (<250 µm fraction)

Method (ICP-MS)	Target Phases	Laboratory
Deionised water	Soluble components <sup>1</sup>	GSC
Ammonium acetate at pH 7	Exchangeable cations, soluble <sup>1</sup>	GSC
Ammonium acetate at pH 5	Fine carbonates, exchangeable cations <sup>1</sup>	GSC
Sodium pyrophosphate	Organic complexes <sup>1</sup>	GSC
Hydroxylamine hydrochloride	Amorphous Fe-Mn oxides <sup>1</sup>	GSC
1% Nitric acid	Carbonates, adsorbed components <sup>1</sup>	GSC
Aqua regia	All but silicates and stable oxides <sup>2</sup>	ACME Labs
Aqua regia clay fraction (<2 µm) <sup>†</sup>	All but silicates and stable oxides <sup>2</sup>	ACME Labs
Enzyme Leach <sup>SM</sup> (proprietary)	Enzymatic, bio-available <sup>3</sup>	Actlabs
Bioleach (proprietary)	Bio-available <sup>3</sup>	Actlabs
MMI <sup>TM</sup> (proprietary)	"Mobile metal ion" <sup>4</sup>	SGS

<sup>1</sup>Hall 1996a & b, Geological Survey of Canada (GSC); <sup>2</sup>ACME Labs 2009; <sup>3</sup>Actlabs 2009; <sup>4</sup>SGS 2009

<sup>†</sup>Physical extraction by suspension and centrifugation in deionized water



**Fig. 1.** Location of the Talbot prospect (inside black circle), Manitoba, Canada .

metamorphic arc assemblages (Syme & Bailes 1993) and occurs as coarse grained, massive to semi-massive and disseminated sulphides: chalcopyrite + sphalerite + pyrite ± pyrrhotite (Bailes & Galley 1999). The Proterozoic rocks are overlain by 100 m of Palaeozoic carbonate sequences of the Western Interior Basin and 0 to 2 m of Quaternary glacial and glaciolacustrine sediments.

Minor intra-plate tectonics and isostatic rebound after glaciation have fractured the

carbonate cover (Elliott 1996). Normal faulting of the carbonate cover with vertical offsets over 5 m has been observed in the Talbot area. These fractures, as well as many smaller cracks and joint sets, may allow fluids and gases to migrate upward and transport elements from the basement to the surface.

The soil in the study area is developed in clays and fine grained till (clay to sand - rich matrix), and soil horizons are poorly developed in the boreal climate. Vertical relief around the prospect is minimal, less than 10 m in general, and standing water occupies low-lying areas most of the year. The area was glaciated between 13 ka and 10 ka, after which it was covered by the large water body of Lake Agassiz, until ~8 ka (Teller & Leverington 2004) in which glaciolacustrine sediments were deposited. The local vegetation consists mostly of sphagnum moss and coniferous trees.

## RESULTS

Student's *t* test statistics and *t* probability were calculated to quantify the contrast between 'anomalous' and 'background' populations in each extraction method data set (Student 1908; Stanley & Noble 2008). Sample sites were designated 'anomalous' based on the projection of mineralization and a fault zone in the cover rocks. For most methods, Zn

**Table 2.** Numerical ranking of extractions, based on *t* probability distribution of Zn

Method, Zn <i>t</i> probability	%
Enzyme Leach	0.3
Deionized water	0.8
Sodium pyrophosphate	0.9
MMI	1.8
Aqua regia clay fraction (<2 μm)	2.2
AA7	2.3
AA5	6.5
Aqua regia	11.7
Hydroxylamine hydrochloride	17.6
1% Nitric acid	46.8
Bioleach (negative <i>t</i> , as $\mu_a < \mu_b$ )	(-)80.0

anomalies have the greatest contrast between anomaly and background, followed by P (if detected) and Cd (Fig. 2). Enzyme Leach produces the greatest contrast for Zn (Table 2), Bioleach the weakest.

**CONCLUSIONS**

Although the number of samples in this case study is small, *t* probability analysis provides a robust screen for comparing and ranking different geochemical methods applied to the same soil samples. High contrast anomalies of Zn, Cd, and P in most methods, including sodium pyrophosphate and Enzyme Leach, may indicate an affinity with organic phases in the <250μm soil fraction. The proprietary nature of the Enzyme Leach, Bioleach, and MMI restricts the geochemical interpretation of the results. From an exploration point of view, clay separation with aqua regia digestion gives the most reproducible and interpretable results for the Talbot soils (*in progress*).

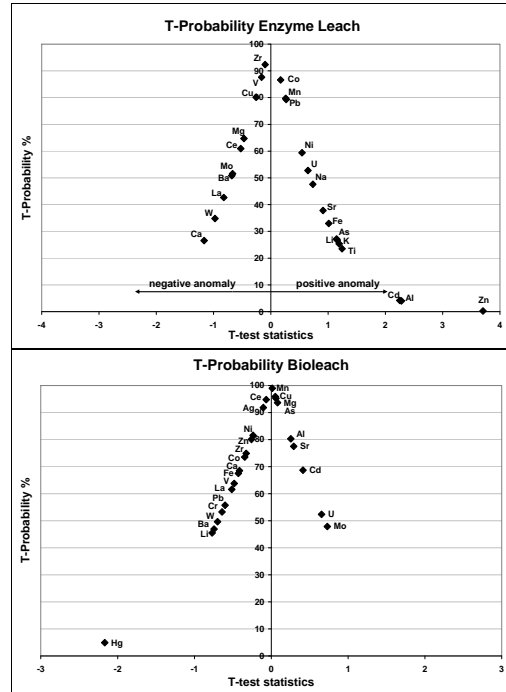


**Fig. 2.** *t* probability as a function of Student's *t* statistics for Enzyme Leach (a; "best case") and Bioleach (b; "worst case")

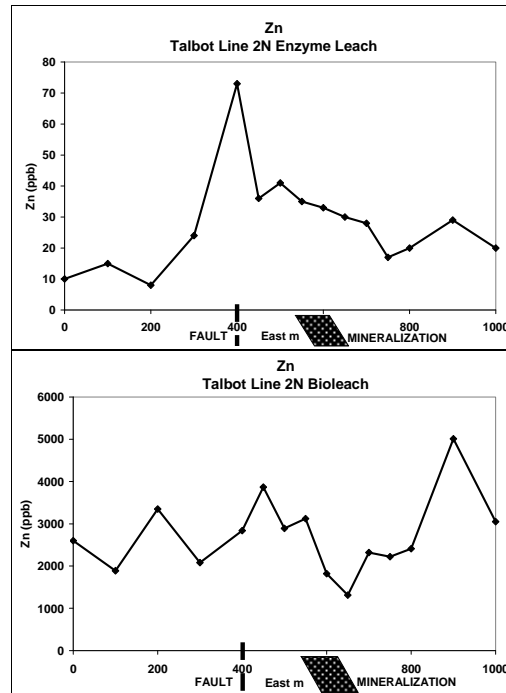


**Fig. 3.** Line plots of Zn concentration (ppb) in soils determined by Enzyme Leach (a) and Bioleach (b), with respective *t* probabilities of 0.3% and (-)80% ( $\mu_a < \mu_b$ ).

## ACKNOWLEDGEMENTS

We would like to thank Gwendy Hall for contributing a major part of the partial digestions and analyses at the Geological Survey of Canada, and Kelly Gilmore, chief geologist at HBED, for accommodating us and allowing access to the Talbot property.

## REFERENCES

- ACME Labs service guide 2009: [http://www.acmelab.com/downloads/Acme\\_2009.pdf](http://www.acmelab.com/downloads/Acme_2009.pdf)
- ACTLABS Service Guide 2009: [http://www.actlabs.com/pricelist/serviceguide09\\_canada.pdf](http://www.actlabs.com/pricelist/serviceguide09_canada.pdf)
- AULER, A.S. & SMART, P.L. 2003. The influence of bed-rock derived acidity in the development of surface and underground karst: evidence from the Precambrian carbonates of semi-arid northeastern Brazil", *Earth Surface Processes and Landforms*, **28**, 157–168
- BAILES, A.H. & Galley, A.G., 1999. Evolution of the Paleoproterozoic Snow Lake arc assemblage and geodynamic setting for associated volcanic-hosted massive sulphide deposits, Flin Flon Belt, Manitoba, Canada. *Canadian Journal of Earth Sciences*, **36**, 1789–1805.
- ELLIOTT, C.G. 1996. Phanerozoic deformation in the "stable" craton, Manitoba, Canada. *Geology*, **24**, 909–912.
- GOVETT, G.J.S. 1976. Detection of deeply buried and blind sulphide deposits by measurement of H<sup>+</sup> and conductivity of closely spaced surface soil samples. *Journal of Geochemical Exploration*, **6**, 359–382.
- HALL, G.E.M., HAMILTON, S.M., MCCLENAGHAN, M.B., & CAMERON, E.M. 2004. Secondary geochemical signatures in glaciated terrain. *Extended Abstracts*, SEG 2004 – Predictive Mineral Discovery Under Cover Symposium, no. 33, University of Western Australia, Perth.
- HALL, G.E.M., VAIVE, J.E., BEER, R., & HOASHI, M. 1996. Phase selective leaches for use in exploration geochemistry. In: EXTECH I; a multidisciplinary approach to massive sulphide research in the Rusty Lake-Snow Lake greenstone belts, Manitoba. *Geological Survey of Canada Bulletin*, 169-200.
- HALL, G.E.M., VAIVE, J.E., & MACLAURIN, A. 1996. Selective leaching of the labile organic component of humus and soils with sodium pyrophosphate solution. In: EXTECH I; a multidisciplinary approach to massive sulphide research in the Rusty Lake-Snow Lake greenstone belts, Manitoba). *Geological Survey of Canada Bulletin*, 201-213.
- SGS MMI™ 2009: [http://www.sgs.com/mmi\\_process\\_geochem](http://www.sgs.com/mmi_process_geochem)
- STANLEY, C.R. 2003. Statistical evaluation of anomaly recognition performance. *Geochemistry: Exploration, Environment, Analysis*, **3**, 3–12.
- STANLEY, C.R. & NOBLE, R.R.P. 2008. Quantitative assessment of the success of geochemical exploration techniques using minimum probability methods. *Geochemistry: Exploration, Environment, Analysis*, **8**, 1-13.
- STERN, R.A., MACHADO, N., SYME, E.C., LUCAS, S.B., & DAVID, J. 1999. Chronology of crustal growth and recycling in the Paleoproterozoic Amisk collage (Flin Flon Belt), Trans-Hudson Orogen, Canada. *Canadian Journal of Earth Sciences*, **36**, 1807-1827.
- STUDENT (W.S. GOSSET), 1908. The probable error of a mean. *Biometrika*, **6**, 1–25.
- SYME, E.C. & BAILES, A.H. 1993. Stratigraphic and tectonic setting of early Proterozoic volcanogenic massive sulfide deposits, Flin Flon, Manitoba. *Economic Geology*, **88**, 566-589.
- TELLER, J.T. & LEVERINGTON, D.W. 2004. Glacial Lake Agassiz: A 5000 yr history of change and its relationship to the δ<sup>18</sup>O record of Greenland. *GSA Bulletin*, **116**, 729-742.

## Multi-element soil geochemistry above the Talbot Lake VMS Cu-Zn Deposit, Manitoba, Canada

Pim W.G. Van Geffen<sup>1</sup>, T. Kurt Kyser<sup>1</sup>,  
Christopher J. Oates<sup>2</sup>, & Christian Ihlenfeld<sup>2</sup>

<sup>1</sup>Dept. Geological Sciences & Geological Engineering, Queen's University, Miller Hall, Kingston, ON K7L 3N6  
CANADA (email: [pvgeffen@geoladm.geol.queensu.ca](mailto:pvgeffen@geoladm.geol.queensu.ca))

<sup>2</sup>Anglo American plc, 20 Carlton House Terrace, London SW1Y 5AN UNITED KINGDOM

**ABSTRACT:** Future discoveries of economic mineral deposits increasingly rely on the identification of secondary expressions of deeply buried, metal bearing systems. The Talbot VMS prospect, located in the Paleoproterozoic Flin Flon belt in northern central Manitoba, hosts Cu-Zn mineralization in meta-volcanic sequences that are overlain by 100 m of Paleozoic sandstone and dolomite formations of the Western Interior Platform, that are covered by a thin (0 to 2 m) blanket of Quaternary glacial and glaciolacustrine sediments. Soil profiles up to 50 cm depth were sampled at 50-100 m intervals over a 1000 m transect across the deposit. Trace element chemistry of the clay fraction (<2 µm) of soils displays a strong geochemical signature of the underlying deposit. Anomalous concentrations of Ag, Cu, Au, Cd, Co, Bi, Se, and Mn in clay separates are related to the presence of the underlying Talbot ore body, showing that deposits at considerable depths of allochthonous cover can be detected using a multi-element approach, at low cost and small environmental impact.

**KEYWORDS:** soil geochemistry, deep cover exploration, VMS Cu-Zn, Manitoba, Canada

### INTRODUCTION

Most major ore deposits that intersect the earth's surface have probably been identified. To satisfy the increasing demand for metals, buried deposits lacking primary surface expressions have become targets for exploration. Future discoveries of economic mineral deposits increasingly rely on the identification of subtle, secondary expressions of deeply buried metal bearing systems (Govett 1976; Kelly *et al.* 2006).

Novel geochemical methods that can indicate the presence and composition of deep seated mineralization are therefore essential. In this study, the multi-element geochemistry of soils and their clay-sized fractions are compared for the deeply buried Talbot VMS Cu-Zn prospect, northern Manitoba, Canada.

### GEOLOGICAL SETTING

The Talbot VMS Cu-Zn prospect is situated in the eastern extension of the Paleoproterozoic Flin Flon Belt (1.92-1.88 Ga), northwestern Manitoba (Stern *et al.* 1999). The prospect is located just

northeast of Lake Talbot, about 160 km SE of Flin Flon and 200 km SW of Thompson (Fig. 1). Mineralization is hosted by medium to high-grade metamorphic arc assemblages (Syme & Bailes 1993; Lucas *et al.* 1996) and occurs as coarse grained, massive to semi-massive and disseminated sulfides: chalcopyrite + sphalerite + pyrite ± pyrrhotite (Bailes & Galley 1999). The Proterozoic rocks are overlain by 100 m of Palaeozoic carbonate sequences of the Western Interior Platform (Stern *et al.* 1995). The deposit was first discovered through diamond drilling in 2003, and is currently in an advanced stage of exploration by Hudson Bay Exploration and Development. Diamond drilling has indicated significant mineralization, including a major intersection of massive sulphide, containing 11.2 ppm Au, 184 ppm Ag, 12.4% Cu and 3.50% Zn, over 9.65 m (HudBay Minerals Inc. 2006).

The crystalline host rocks are covered by Palaeozoic sediments of the Western Interior Basin. These consist of Ordovician



**Fig. 1.** Location of the Talbot prospect (inside black circle), Manitoba, Canada.

sandstones (Winnipeg Fm) and sequences of dolomite and limestone (Red River, Stonewall, and East Arm Fms) that contain chert and small pyrite-marcassite accretions (Bezys 2000). Minor intra-plate tectonics and isostatic rebound after glaciation have fractured the carbonate cover rocks (Elliott 1996). Acids produced by sulfide oxidation in the basement are interpreted to have caused partial dissolution of the basal limestone, in a manner similar to that described for rocks in eastern Brazil (Auler & Smart 2003). Increased void space and glacial loading may have caused the carbonate cover to collapse locally, and normal faulting of the carbonate cover with vertical offsets over 5 m has been observed in the Talbot area. These fractures, as well as many smaller cracks and joint sets, may allow fluids and gases to migrate upward and transport elements from the basement to the surface.

The area was glaciated between 13 ka and 10 ka, after which it was covered by the large water body of Lake Agassiz, until ~8 ka (Teller & Leverington, 2004), in which up to 2 m of fine grained glacial and glaciolacustrine sediments were deposited. The Talbot soil is developed on inhomogeneous glacial sand and clay,

and soil horizons are poorly developed. Vertical relief around the prospect is minimal, less than 10 m in general, and standing water occupies low-lying areas most of the year, forming swamps. The local vegetation consists mostly of sphagnum moss and coniferous trees.

## METHODS AND RESULTS

At 15 sites along a 1000 m transect across the Talbot deposit, soil profiles were sampled in 10 cm depth intervals, up to 50 cm. The <250  $\mu\text{m}$  (silt + clay) and <2 $\mu\text{m}$  (clay) fractions of the soil samples were analysed using an aqua regia digestion and ICP-MS measurement of 53 elements.

Most elements of interest in the Talbot 250  $\mu\text{m}$  and <2 $\mu\text{m}$  separates are well above analytical detection limits, except PGEs. Clay separates have, on average, 50% higher concentrations of most elements than silt + clay fraction of the soils.

The clay content (wt. %) (Fig. 2) shows a strong positive correlation with most element concentrations in the <250 $\mu\text{m}$  soil analyses, e.g. Cu (Fig. 3), with distinctly low values at 400 m east. In contrast, the clays show a well defined anomaly at the bottom of the profile at 400 m east (Fig. 4), with high concentrations of Ag, Cu, Au, Cd, Co, Bi, Se, and Mn.

## CONCLUSIONS

The results of this research have implications for the application of exploration geochemistry in boreal forest terrains, especially when soils developed on glaciolacustrine sediments are used as the main sample medium. The choice of sampling depth, or soil horizon, can greatly impact the geochemical results, and the optimum should therefore be established in orientation surveys, by describing and sampling depth profiles. Separation of the clay fraction from the soil reduces the variability in the mineralogy of the sample medium, and subtle geochemical anomalies are not obscured by variations in the silt content of the bulk soil. Although the locations of anomalies are partly controlled by

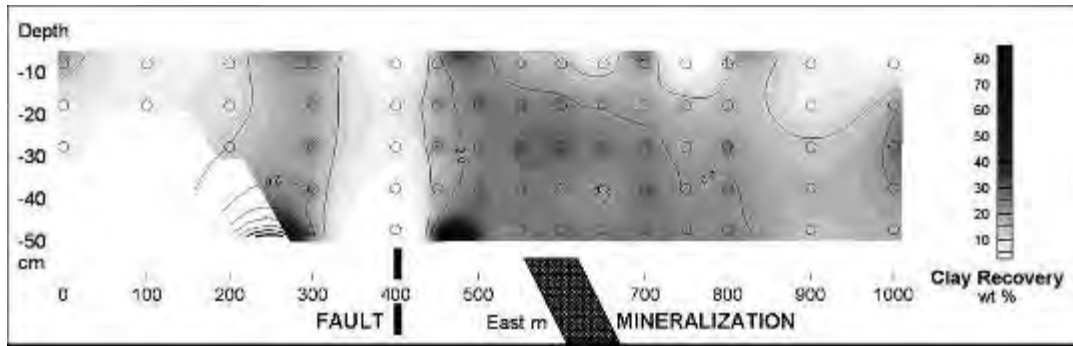


Fig. 2. Clay recovery (wt %) from soils, depth profile (vertical scale 500 x exaggerated).

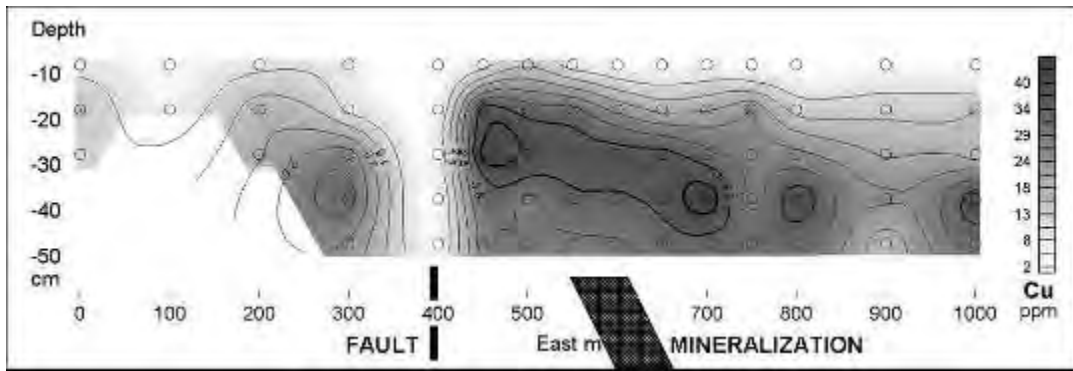


Fig. 3. Cu concentrations (ppm) in bulk soil, depth profile.

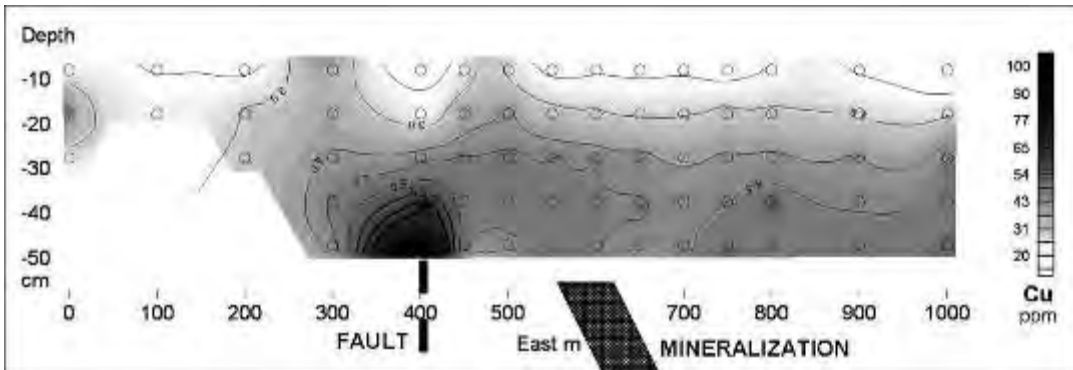


Fig. 4. Cu concentrations (ppm) in clay fraction, depth profile.

structures in cover rocks, the presence of the Talbot ore body is evident in the geochemistry of the clay sized fraction of soils through more than 100 m of cover rocks and glacial sediments.

#### ACKNOWLEDGEMENTS

We would like to thank Kelly Gilmore, chief geologist, and other staff at HBED, for accommodating us and allowing access to the property.

#### REFERENCES

- AULER, A.S. & SMART, P.L. 2003. The influence of bed-rock derived acidity in the development of surface and underground karst: evidence from the Precambrian carbonates of semi-arid northeastern Brazil. *Earth Surface Processes and Landforms*, **28**, 157–168.
- BAILES, A.H. & GALLEY, A.G. 1999. Evolution of the Paleoproterozoic Snow Lake arc assemblage and geodynamic setting for associated volcanic-hosted massive sulphide deposits, Flin Flon Belt, Manitoba, Canada. *Canadian Journal of Earth Sciences*, **36**, 1789–1805.
- BEZYS, R.K. 2000. Stratigraphic investigations and corehole drilling program, 2000. In: *Report of Activities 2000*, Manitoba Industry, Trade and Mines, Manitoba Geological Survey, 196-201.
- ELLIOTT, C.G. 1996. Phanerozoic deformation in the “stable” craton, Manitoba, Canada. *Geology*, **24**, 909–912.
- GOVETT, G.J.S. 1976. Detection of deeply buried and blind sulphide deposits by measurement of H<sup>+</sup> and conductivity of closely spaced surface soil samples. *Journal of Geochemical Exploration*, **6**, 359–382.
- HUDBAY MINERALS Inc. 2006. Second Half 2006 Exploration Update Data. <http://www.hudbayminerals.com/ourBusiness/exploration.php>
- KELLEY, D.L., KELLEY, K.D., COKER, W.B., CAUGHLIN B., & DOHERTY M.E. 2006. Beyond the Obvious Limits of Ore Deposits: The Use of Mineralogical, Geochemical, and Biological Features for the Remote Detection of Mineralisation” 100<sup>th</sup> Anniversary Special Paper: Remote Detection of Mineralisation, *Economic Geology*, **101**, 729–752.
- LUCAS, S.B., STERN, R.A., SYME, E.C., REILLY B.A., & THOMAS, D.J. 1996. Intraoceanic tectonics and the development of continental crust: 1.92–1.84 Ga evolution of the Flin Flon Belt, Canada. *GSA Bulletin*, **108**, 602–629.
- STERN, R.A., SYME, E.C., BAILES, A.H., & LUCAS S.B. 1995. Paleoproterozoic (1.90-1.86 Ga) arc volcanism in the Flin Flon Belt, Trans-Hudson Orogen, Canada. *Contributions to Mineralogy and Petrology*, **119**, 117–141.
- STERN, R.A., MACHADO, N., SYME, E.C., LUCAS, S.B., & DAVID, J. 1999. Chronology of crustal growth and recycling in the Paleoproterozoic Amisk collage (Flin Flon Belt), Trans-Hudson Orogen, Canada. *Canadian Journal of Earth Sciences*, **36**, 1807–1827.
- SYME, E.C. & BAILES, A.H. 1993. Stratigraphic and tectonic setting of early Proterozoic volcanogenic massive sulfide deposits, Flin Flon, Manitoba. *Economic Geology and the Bulletin of the Society of Economic Geologists*, **88**, 566 – 589.
- TELLER, J.T. & LEVERINGTON, D.W. 2004. Glacial Lake Agassiz: A 5000 yr history of change and its relationship to the δ<sup>18</sup>O record of Greenland. *GSA Bulletin*, **116**, 729–742

# **APPLIED AQUEOUS GEOCHEMISTRY**

EDITED BY:

**DAVE GLADWELL  
RAY LETT  
ROGER BECKIE**



## Application of calcite precipitation rate in predicting the utilization period of calcite scale affected wells, Philippines

Gabriel M. Aragon<sup>1</sup>, Benson G. Sambrano<sup>1</sup>, & James B. Nogara<sup>1</sup>

<sup>1</sup>Energy Development Corporation, Merritt Road, Fort Bonifacio, Makati City, Taguig PHILIPPINES  
(e-mail: aragon.gm@energy.com.ph)

**ABSTRACT:** The empirically determined precipitation rate law was applied to calculate the utilization period of calcite scale affected wells where pipe geometry and varying boiling temperatures were considered. The results using the empirical precipitation rate law method showed extended utilization periods for saturation ratio (Q/K) less than or equal to 1.72, and shorter utilization periods for saturation ratios above 1.72 compared to the direct deposition of excess calcite method. The applicability of the calcite precipitation rate law method in predicting the utilization period of the calciting wells depends on the determination of the actual flash point temperature and calibration of the empirical equation to the field observations. The empirical equation was derived under laboratory conditions using stirred reactor tanks at 100°C and extrapolated to higher temperatures. The laboratory test set-up is perceived to be an approximation and does not mimic the complexity of the flow regime observed in geothermal wells. Information on the utilization period of calciting wells derived from the modified rate law method will assist in a refined evaluation of steam availability from geothermal fields as well as providing a well maintenance schedule.

**KEYWORDS:** precipitation rate, calciting, saturation ratio, boiling temperatures, Mindanao Geothermal Production field

### INTRODUCTION

The majority of available speciation software only reveals the characteristics of the geothermal fluids in terms of degree of saturation with respect to calcite. This does not directly translate into the duration during which the well will sustain the discharge. The utilization period of calciting wells can be derived from the discharge history, assuming that the well has had stable chemistry. Variations of the utilization period through time is expected because of geothermal reservoirs are very dynamic due to the effects of mass extraction and injection, which particularly affects the fluid chemistry.

The initial methodology used assumed that all excess calcite from the solution would be deposited in a predetermined volume of the geothermal pipe. This approach is conservative considering that calcite deposition is an instantaneous process. However, the literature frequently states that calcite deposition is kinetically-controlled where the process of deposition could either be slower or faster (Sjöberg &

Rickard 1984; Compton & Unwin 1990; Lebron 1996; Shiraki & Brantley 1995) developed a precipitation rate equation for high salinity fluid in laboratory conditions at a temperature of 100°C using a reactor tank. This was modified through extrapolation to extend the application up to 300°C and currently used in the program code of *FRACHEM* (Andre *et al.* 2006).

This paper evaluates the applicability of the modified precipitation rate equation in predicting the discharge duration of a calciting well compared to the observed utilization history and the results of the conservative method from direct deposition of excess calcite. Three wells in Mindanao Geothermal Production Field (MGPF) with documented output decline due to calcite deposition were studied, namely APO1D, SP4D, and MD1D.

### THE GEOTHERMAL FIELD

The Mindanao Geothermal Production Field (MGPF), with an area of ~30 sq km, is situated on the northwest flanks of Mt.

Apo volcano located in the southwestern part of Mindanao Island (Fig. 1). Commercial exploitation of the field started in March 1997 with commissioning of the 52-MWe Mindanao-1 geothermal power plant (M1). An additional 52-MWe power plant (M2) commissioned in June 1999 increased the total capacity to 104 MWe. Each power plant requires a minimum energy off-take at the end of the year. This necessitates an updated total steam availability of the field and realistic forecast to ensure realization of steam production. The unexpected drop in output in the calcite-affected wells upset the steam availability of the field and required immediate well intervention utilizing a drilling rig to regain the initial capacity.

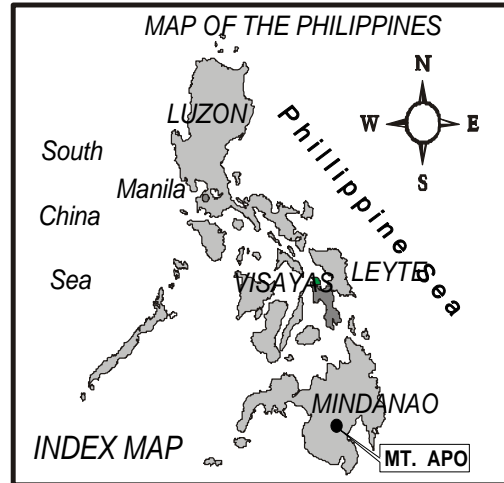


Fig. 1. Philippine map showing the location of the project sites

**PRECIPITATION RATE**

The general rate law equation is given by:

$$Rate = Kp(\Omega - 1)^n A_{kgw} \quad (1)$$

where:

- Rate – precipitation rate, mole/kgw-s
- Kp – rate constant, mole/m<sup>2</sup>-s
- Ω - saturation ratio (Q/K)
- A<sub>kgw</sub> – surface area for deposition per kilogram water
- n – empirically determined

The following equations are derived from Eq. 1 depending on the saturation levels (Q/K) which is modified to include higher temperature range:

For Q/K < 1.72:

$$R_p = 1.927 \times 10^{-2} T \exp\left(\frac{-41840}{RT}\right) A_{kgw} \left(\frac{Q}{K} - 1\right)^{1.93} \quad (2)$$

For Q/K > 1.72:

$$R_p = 1.011 T \exp\left(\frac{-41840}{RT}\right) A_{kgw} \exp\left(\frac{-2.36}{\ln\left(\frac{Q}{K}\right)}\right) \quad (3)$$

where:

- R – 8.315 J/mol-K
- T – Temperature in Kelvin
- Q/K – Saturation ratio taken from WATCHWORKS
- A<sub>kgw</sub> – Surface area for deposition per kilogram water in m<sup>2</sup>
- R<sub>p</sub> – Precipitation rate, mole/Kgw-s

The following are the assumptions made in applying the precipitation rate equation:

- Deposition occurred at boiling point
- The fluid is supersaturated with calcite mineral
- Complete adhesion of the calcite mineral on the inner wall of the pipe
- Moderate flow in the pipe to mimic the stirring experiment

The last two assumptions may not be true under actual well conditions, where instantaneous boiling and turbulent flow in the pipe occur. However, these conditions do not allow certain calcite crystals to deposit immediately and fractions may be removed by the fluid.

**RESULTS AND DISCUSSION**

**Fluid Chemistry**

The Ca<sup>2+</sup> concentration of the wells range between 87 to 211 mg/L at different boiling temperatures and near neutral to slightly alkaline pH is comparable to the quartz reservoir temperature. For instance, APO1D had the lowest reservoir temperature at 228°C had the highest calcium value of 211 mg/L among the three. This is followed by SP4D with a temperature of 236°C and Ca<sup>2+</sup> value of 139 mg/L while the hottest well MD1D with reservoir temperature of 270°C has the lowest Ca<sup>2+</sup> value of 87 mg/L. Except for MD1D, the wells at reservoir condition are almost saturated with respect to calcite, while the residual liquid becomes oversaturated following boiling as the

liquid flows to the well bore due to the pressure difference. This boiling process as a triggering mechanism for calcite formation is proven in the depths of the calcite minerals. The majority of the calcite blockages were found at flash point depths of the production wells.

**Utilization Rate**

**Well APO1D**

The utilization periods for APO1D given by the direct deposition of the excess calcite method has a minimum of 1 month and maximum of 6 months as shown in Fig. 2. It should be noted that the calcite precipitation rate equation at a saturation ratio above 1.72 provided shorter utilization time than the direct deposition method, indicating that the rate law overestimated the amount of calcite deposited. At a saturation ratio below 1.72, however, the rate law indicated a longer utilization period, which was expected since the calcite deposition is kinetically controlled rather than instantaneous deposition of the excess calcite.

**Well SP4D**

The actual utilization period of the well prior to maintenance ranged from 10 to 15 months. Using the calcite precipitation rate equation, the utilization period indicated 235°C as the first boiling temperature coinciding to a period of 11 months (Fig. 3). Again the 205°C was not considered here since it occurred at the surface pipeline and the calcite blockages were found in the production liner. The equivalent utilization period for the direct deposition of excess calcite at this condition is only 5 months. The simulated flash temperature of SP4D is 234°C which is comparable to actual and calculated utilization periods. Similar to APO1D, the calculated utilization periods for saturation ratio above 1.72 indicated shorter duration than the direct deposition of excess calcite.

**Well MD1D**

This well has no saturation values obtained below 1.72. Thus the utilization

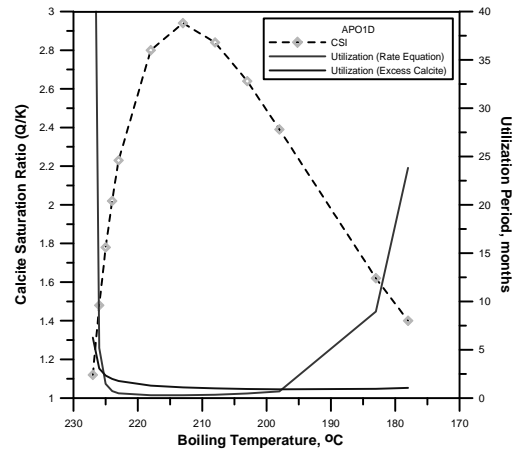


**Fig. 2.** APO1D saturation ratio and utilization periods at different boiling temperatures.

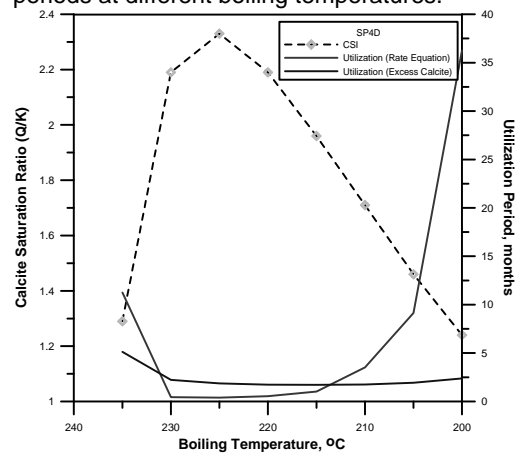


**Fig. 3.** SP4D saturation ratio and utilization periods at different boiling temperatures.

period based on precipitation rate (Eq. 1) consistently resulted in a short utilization (maximum of 15 days) compared to the utilization from direct deposition of excess calcite (maximum 6 months). Based on the last maintenance, the actual utilization period of the well is almost 6 months. This actual utilization period corresponded to the value from the direct deposition of excess calcite at the boiling temperature of 270°C.

Notably, well MD1D has high calcite saturation values and yet produces for longer than the calculated utilization periods than APO1D and SP4D using the direct deposition method (Fig. 4). This can be attributed to the lower equilibrium constant of calcite at higher temperatures. Thus, despite the inherently lower calcium

concentration of MD1D, the well has a high degree of saturation.

## CONCLUSIONS

(1) The precipitation rate (Eq. 1) indicates comparable values for utilization period at calcite saturation ratio below 1.72 since the results are closer to the observed

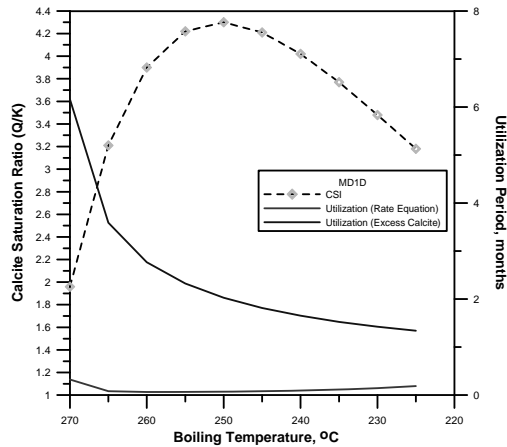


**Fig. 4.** MD1D saturation ratio and utilization periods at different boiling temperatures.

utilization period.

(2) The calcite precipitation rate (Eq. 1) should be further refined by calibrating the equation to the field condition particularly for saturation ratio above 1.72.

(3) The calcite saturation ratio is more responsive with regards to detecting the onset of calcite deposition through the sudden shift of the saturation ratio from consistently  $> 1$  to  $< 1$ .

(4) The direct deposition of excess calcite method should be used in predicting the utilization period in cases where the flash point temperature of the well is known and the saturation ratio at this condition is above 1.72.

## ACKNOWLEDGMENTS

The authors wish to thank EDC for allowing the presentation and publication of this paper.

## REFERENCES

ANDRE, L., SPYCHER, N., XU T., VUATAZ, F.D., &

PRUESS, K. 2006. Modelling brine-rock interactions in an enhanced geothermal system deep fractured reservoir at Soultz-Sous-Forêts (France): a joint approach using two geochemical codes: frachem and toughreact. *Lawrence Berkley National Laboratory, University of California*.

BERNER, R.A. & MORSE, J.M. 1974. Dissolution kinetics of calcium carbonate in seawater. IV. Theory of calcite dissolution. *American Journal of Science*, **274**, 108-134.

BUSENBERG, E. & PLUMMER, L.N. 1986. A comparative study of the dissolution and crystal growth kinetics of calcite and aragonite. *U.S. Geological Survey Bulletin*, **1578**, 139-168.

COMPTON R. G. & UNWIN P. R. 1990. The dissolution of calcite in aqueous solution at pH  $< 4$ : Kinetics and mechanism. *Philosophical Transactions of the Royal Society, London Series A*, **330**, 1-46.

DULCE, R.G., NOGARA, J.B., & SAMBRANO, B.G. 2000. Calcite scale deposition in production wells in Mindanao Geothermal Production Field, Philippines. *PNOC-EDC Internal Report*. **2000**.

KLEIN, C. & CHAPPELL, N. 1998. WATCHWORKS V 1.0. GeothermEx, Inc., 5221 Central Ave., Suite 201, Richmond, CA 94804, USA.

LEBRON, I. & SUAREZ, D.L. 1996. Calcite nucleation and precipitation kinetics as affected by dissolved organic matter at 25°C and pH  $> 7.5$ . *Geochimica et Cosmochimica Acta*, **60**(15), 2765-2776.

MORSE, J.W. 1978. Dissolution kinetics of calcium carbonate in sea water; VI, The near-equilibrium dissolution kinetics of calcium carbonate-rich deep sea sediments. *American Journal of Science*, **278**, 344-353.

PLUMMER L.N., WIGLEY T.M.L., & PARKHURST, D.L. 1978. The kinetics of calcite dissolution in CO<sub>2</sub>-water systems at 5° to 60°C and 0.0 to 1.0 atm CO<sub>2</sub>. *American Journal of Science*, **278**, 179-216.

SHIRAKI, R. & BRANTLEY, S.L. 1995. Kinetics of near-equilibrium calcite precipitation at 100°C: An evaluation of elementary reaction-based and affinity-based rate laws. *Geochemica et Cosmochimica Acta*, **59**, 1457-1471.

SJÖBERG, E.L. & RICKARD, D.T. 1984. Calcite dissolution kinetics: surface speciation and the origin of the variable pH dependence, *Chemical Geology*, **42**, 119-136.

## Sources of arsenic contamination and remediation of mine water at the historical Glen Wills mining area in Northeast Victoria, Australia

Dennis Arne<sup>1</sup>, Andrew Nelson<sup>2</sup>, & John Webb<sup>2</sup>

<sup>1</sup>*ioGlobal, 469 Glen Huntley Road, Elsternwick, Victoria, 3185 AUSTRALIA  
(email: dennis.arne@ioGlobal.net)*

<sup>2</sup>*Department of Environmental Geoscience, La Trobe University, Bundoora, 3086, Victoria AUSTRALIA*

**ABSTRACT:** Arsenic in Glen Wills Creek is seasonally elevated to levels exceeding Australian drinking water guidelines and environmental trigger values of 7 µg/L and 13 µg/L, respectively. Arsenic enters the creek from both surface and groundwater drainage from sulfidic mine tailings in and adjacent to Glen Wills Creek. Arsenic was also previously contributed to the creek by natural outflow from the Maude Mine No. 5 adit, but this water is now retained in a storage dam on site. Mine waters are reduced, contain between 2.8 and 3.5 mg/L Fe and an average of 1.87 mg/L As, mainly as As<sup>3+</sup>. This water becomes progressively oxidised as it flows from a sump at the adit mouth down to the storage dam. Up to 98% of the As is removed through passive oxidation and the precipitation of ferrihydrite. The remaining As can be removed through the use of coagulating agents, such as poly-aluminium chloride and ferric chloride.

**KEYWORDS:** arsenic, mine water, tailings, Glen Wills, Australia

### INTRODUCTION

Glen Wills is a historical gold mining area located in the headwaters of the Mitta Mitta River in the highlands region of eastern Victoria (Fig. 1). Mining involved the processing of arsenical gold ore and the production of ~200,000 t of waste rock and tailings, mainly prior to 1970. Most of the tailings were deposited either directly in or adjacent to Glen Wills Creek. A long-term water quality monitoring program for Glen Wills Creek was initiated by Australian Gold Mines in late 2003 to establish baseline data for future development of the mine. Analysis of the data collected between 2003 and 2005 has revealed arsenic levels downstream of historical mine workings and tailings deposits generally exceed the maximum allowable guideline value for Australian drinking water of 7 µg/L and are often in excess of the Australian and New Zealand Environment and Conservation Council trigger value for the protection of 95% of species in freshwater aquatic ecosystems of 13 µg/L. Possible arsenic sources include natural discharge water from the No. 5 adit of the Maude Mine, both ground and surface water discharging from the

Yellow Girl tailings (~20,000 t), and groundwater discharging from the combined Maude/Yellow Girl tailings (~85,000 t).

### GEOLOGICAL SETTING

The Glen Wills area occurs within Ordovician sedimentary rocks the Omeo Zone (Pinnak Sandstone), which underwent medium grade metamorphism during the Silurian Benambran Orogeny (Morand *et al.* 2005). The rocks in the immediate vicinity of Glen Wills consist largely of corderite- and andalusite- or sillimanite-bearing schists intruded by the



**Fig.1.** Location of Glen Wills in eastern Victoria, Australia.

Silurian Mt. Wills Granite. Gold mineralisation is structurally-hosted and accompanied by the presence of pyrite, arsenopyrite, sphalerite, aurostibite, and a variety of sulfosalts (Crohn 1958). Gangue phases include quartz and ferroan dolomite.

**METHODOLOGY**

Water from Glen Wills Creek was sampled monthly over a two-year period from eight monitoring sites. These samples were not filtered or acid-stabilised in the field. However, the samples were chilled and shipped overnight to the laboratory for analysis. Surface waters emanating from the No. 5 adit of the Maude Mine and the Yellow Girl tailings, as well as discharge waters from the No. 5 adit that are stored in a sump and dam near the adit entrance were sampled less frequently. Groundwater within the Yellow Girl tailings was sampled from a diamond drill exploration hole, and mine water from the internal shaft in the Maude Mine was sampled using a 1L stainless steel sampling bomb. Both filtered (<0.45 µm) and unfiltered samples were collected from contaminated sources, and samples for heavy metal analysis were acidified with HNO<sub>3</sub> in the field. No special preservation for Hg was undertaken. Samples for arsenic speciation were stabilised with HCl. Heavy metals (As, Se, Zn, Pb, Ni, Cu, Cr, Cd, Mn, Fe, Hg) were determined using ICP-MS. Arsenic speciation was determined using High Performance Liquid Chromatography-Inductively Coupled Plasma-Mass Spectrometry (HPLC-ICP-MS).

Net acidity of tailings was determined using a modification of the procedure described by Ahern *et al.* (2000). Potential sulfidic acidity was determined from XRF S determinations. Net acidity was taken as the sum of the potential sulfidic acidity and titratable actual acidity, less the acid neutralisation capacity.

**GLEN WILLS CREEK**

Average As levels measured in Glen Wills Creek between 2003 and 2005 increase downstream, beginning from where mine

waters from the No. 5 adit discharge into the creek (Fig. 2). A clear positive correlation also exists between As and total Fe in solution (Fig. 3) because As is present in the form of arsenopyrite in the deposit.

Arsenic levels in the creek show a seasonal variation with the highest levels occurring during the summer and autumn months when water flow levels in the creek are at their lowest. Major cations and anions for the water samples are illustrated in Figure 4. Group 1 samples are relatively fresh surface water samples, whereas Group 4 samples are highly contaminated waters. Groups 2 and 3 represent varying degrees of mixing between these two end members.

**MINE WATER**

Mine water from a depth of up to 80 m from the internal shaft has a total Fe content of between 2.8 to 3.5 mg/L, an average As content of 1.87 mg/L, an average pH of 6.63 and a negative Eh.

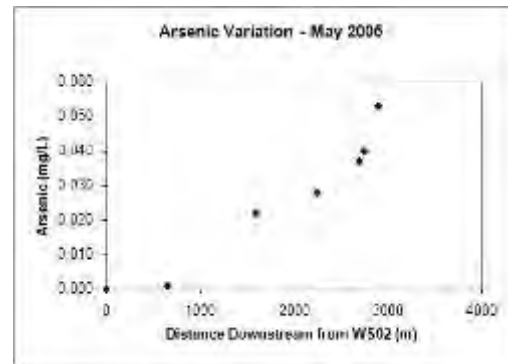


Fig. 2. Average As levels in Glen Wills Creek during May, 2005.

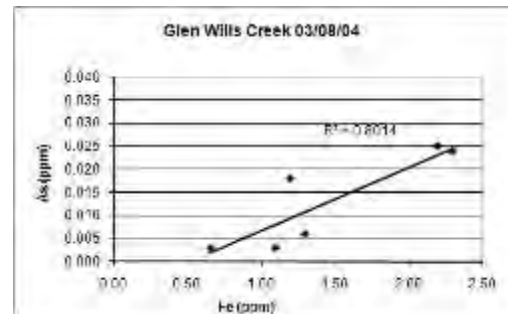
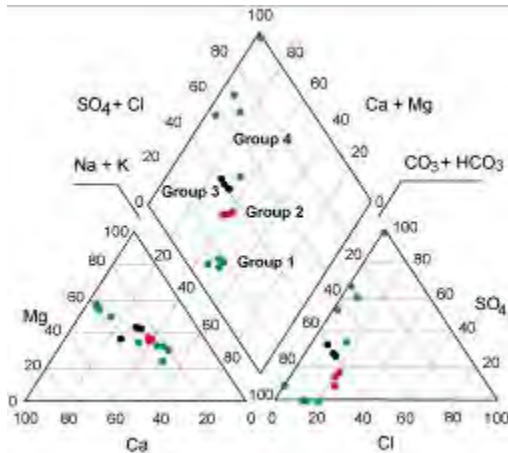


Fig.3. Relationship between As and Fe in Glen Wills Creek.



**Fig. 4.** Piper diagram comparing water monitoring data (Groups 1-3) and contaminated samples (Group 4). From Arne (2005).

The majority of the As in mine water from the internal shaft occurs as  $As^{3+}$ , with only a minor component of  $As^{5+}$  (Fig. 5). Iron and As are predominantly in solution in these waters. Water from the internal shaft oxidises as it flows from the sump to the storage dam, and the amount of Fe and As in solution drops sharply as As is absorbed onto precipitating ferrihydrite (Fig. 6). The dominant As species in the sump and dam is  $As^{5+}$ . Natural attenuation through passive oxidation removes ~98% of the As in solution from the mine waters.

**WATER TREATMENT**

To determine the most practical and cost effective method of treatment to remove the remaining As in the dam water, a number of bench-scale trials have been performed, testing commercial products which utilise the enhanced coagulation, fixed-bed adsorption, and ion exchange methods of arsenic removal. Fixed-bed adsorbents (activated alumina and granular ferric oxyhydroxide) and ion exchange resin displayed a relatively poor efficiency for arsenic removal. However, the coagulating agents poly-aluminium chloride and ferric chloride reduced arsenic concentrations to  $\leq 13$  ppb; achieving near 100 percent arsenic removal efficiencies at minimum dose rates of 7.1 mg/L and 16.3 mg/L,

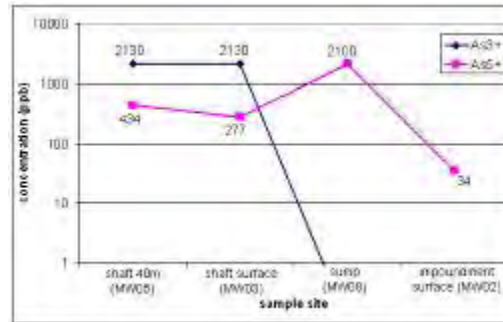


**Fig. 5.** Variation in As species during oxidation of mine waters from the internal shaft, Maude Mine. Measured values are indicated. From Nelson (2008).

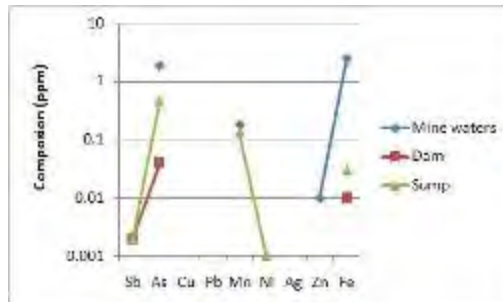


**Fig. 6.** Scholler plot showing variation in dissolved metals during oxidation of Maude Mine water.

respectively.

**TAILINGS**

Analyses of six sulfidic tailings samples indicate a range of net acidities ranging between 294 mole  $H^+$ /tonne in un-oxidized tailings and -115 mole  $H^+$ /tonne in oxidised tailings. The wide range of net acidities reflects both the effects of historic sulfide oxidation and the presence of carbonate gangue phases. Groundwater from the Yellow Girl tailings is sulfate-rich, with a lower pH (5.9) than mine water and contains elevated Ca, Mg and Fe, as well as dissolved As, Mn, Hg, Ni and Zn.

**CONCLUSIONS**

Arsenic and Fe are being released from mine water emanating from the No. 5 adit of the Maude Mine, and from surface and ground water draining from variably oxidized sulfidic tailings. From both a drinking water and ecosystem perspective this As contaminates Glen Wills Creek.

Passive oxidation of mine water from the Maude Mine removes up to 98% of the contained As through precipitation of ferrihydrite and scavenging of As from solution. The remaining arsenic in the water can be removed by the use of the coagulating agents poly-aluminium chloride or ferric chloride.

#### **ACKNOWLEDGEMENTS**

This project would not have been possible without the support of Australian Gold Mines and, more recently, Synergy Metals Ltd.

#### **REFERENCES**

- ARNE, D.C. 2005. *Groundwater Management at the Glen Wills Historic Mining Area, Victoria*. Unpublished Graduate Diploma Thesis, University of Technology, Sydney.
- AHERN, C.R., MCELNEA, A.E., LATHAM, N.P., & DENNY, S.L. 2000. A modified acid sulfate soil method for comparing net acid generation and potential sulfide oxidation - POCASm. In: AHERN, C. R., HEY, K. M., WATLING, K. M., & ELDERSHAW, V. J. (eds.), *Acid sulfate soils: Environmental issues, assessment and management*. Department of Natural Resources, Brisbane, 21/21 - 22/12.
- CROHN, P.W. 1958. Geology of the Glen Wills and Sunnyside Goldfields, northeastern Victoria. *Bulletin of the Geological Survey of Victoria*, **56**.
- MORAND, V.J., SIMONS, B.A., TAYLOR, D.H., CAYLEY, R.A., MAHER, S., WOHI, K.E., & RADOJKOVIC, A.M. 2005. Bogong 1:100,000 map area geological report, *Geological Survey of Victoria Report 125*.
- NELSON, A. 2008. *Geochemical Characterization and Arsenic Remediation of Mine Discharge Water at the Glen Wills Historic Mining Area, Victoria*. Unpublished Honours Thesis, La Trobe University, Bundoora.

## Geochemical and hydrogeological controls on naturally occurring arsenic in groundwater at a field site in West Bengal, India

Roger D. Beckie<sup>1</sup>, Alexandre J. Desbarats<sup>2</sup>, Tarak Pal<sup>3</sup>,  
Cassandra E. M. Koenig<sup>1</sup>, Pradip K. Mukherjee<sup>3</sup>,  
Andrew Rencz<sup>2</sup>, & Gwendy Hall<sup>2</sup>

<sup>1</sup>Department of Earth and Ocean Sciences, University of British Columbia, Vancouver, BC, V6T 1Z4 CANADA  
(e-mail: rbeckie@eos.ubc.ca)

<sup>2</sup>Geological Survey of Canada, Ottawa, ON, K1A 0E8 CANADA

<sup>3</sup>Central Petrological Laboratories, Geological Survey of India, Kolkata-700016 INDIA

**ABSTRACT:** Since 2004, the Geological Surveys of India and Canada in collaboration with the University of British Columbia have been investigating naturally occurring arsenic in groundwater at a field site near the village of Gotra, West Bengal, India. At the field site, high (> 50 ppb) and low arsenic groundwater zones are separated by a transition zone less than 30 m wide. There is no clear distinction in major-element chemistry between high-dissolved-arsenic and low-dissolved-arsenic zones. Sediment cores show arsenic values between 1 ppm As in sandy zones up to 20 ppm As in finer-grained material. The distinguishing feature of the site is that groundwater with high concentrations of arsenic (> 50 ppb) is found in the aquifer below and proximal to an in-filled channel. Shallow wells completed in the low-permeability soft, gray clayey-silt channel fill within 5 m from the edge of a pond provide strong evidence for near surface arsenic release. Water proximal to another pond away from the channel is not associated with high arsenic. All geochemical indicators point to organic-matter driven reductive release processes. Indeed, groundwater with high arsenic is associated with high phosphate, low sulfate, high ammonia, high alkalinity, abundant methane, high dissolved organic carbon and  $\text{PCO}_2$  between  $10^{-1.2}$  and  $10^{-0.7}$  bars. The degree of super-saturation with respect to vivianite and siderite increases with arsenic concentration. Sediments contained solid-phase arsenic concentrations of 1 to several ppm As in sandy zones up to 20 ppm As in finer-grained channel material.

**KEYWORDS:** *arsenic, groundwater, Bengal Basin*

### INTRODUCTION

Since its initial discovery in 1978 in West Bengal, India, arsenic has been found in groundwater at concentrations above World Health Organization (WHO) recommended threshold for human consumption in a large area of the Bengal Basin. It is now well-accepted that the groundwater arsenic is naturally occurring, derived from the Himalayan sediments in the basin, and that arsenic release into the groundwater is related to reduction processes driven by organic matter (Acharyya *et al.* 1999; Nickson *et al.* 2000; Harvey *et al.* 2002). However, the location and detailed mechanism of arsenic release into groundwater has yet to be clearly defined by any of the numerous groups working in the Bengal Basin. While arsenic is found in groundwater in many

regions of the Bengal Basin, locally the arsenic distribution is very patchy. Wells separated by 10's of meters can produce groundwater with arsenic concentrations that differ by 100's of parts per billion. In addition, the source of the organic matter driving reduction is unclear, with both subsurface peat and pond-derived organic matter proposed. In this paper we present results from detail characterization of the site established by the Geological Surveys of India and Canada (GSI/GSC) where low and high arsenic concentrations are found in close proximity.

### SITE

The study site is located approximately 56 km northeast of Kolkata India in the village of Gotra in Nadia District, West Bengal, (2546396N 662938E UTM, 88.59 N,

23.018 E). The village is approximately 1 km long and 500 m wide, oriented on a south-east to north-west trend. The village is bounded to the south west by a line of south-east to north-west trending ponds that mark the trace of an abandoned channel. The north-east limit of the village is defined by four ponds that trend on a similar orientation, but it is less clear if these ponds were dug or are abandoned channels.

**SAMPLING**

Groundwater samples were collected from approximately 50 domestic wells in and surrounding the village of Gotra and from approximately 15 monitoring piezometers and multilevel wells installed by the GSI/GSC. Sediments were collected in 2004 from two continuous 40 – m and from finer grained units during drilling of monitoring piezometers by the indigenous hand-flapper method.

**RESULTS**

The water chemistry results from the shallow aquifer at the site reveal a zone of low arsenic concentrations (<50 ppb) adjacent to high arsenic concentrations. These zones are separated by a 10 – 30 m transition.

Arsenic concentrations vary from below detection to above 500 parts per billion (ppb) (Fig. 1). The highest dissolved arsenic concentrations in the aquifer occur below the in-filled abandoned channel. Groundwater flow data provides strong evidence for near surface arsenic release.

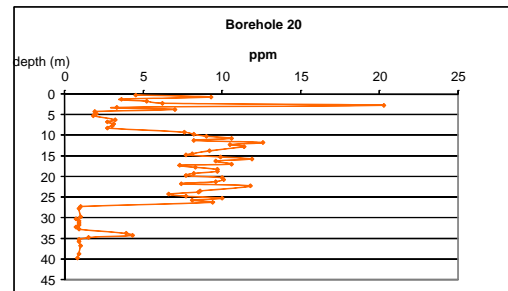
Sequential extractions carried out by the Geological Survey of Canada show that arsenic is distributed among a number of

**Fig. 1.** Arsenic concentration in ppb versus depth in m for all wells in Gotra area, 2004 sampling event.

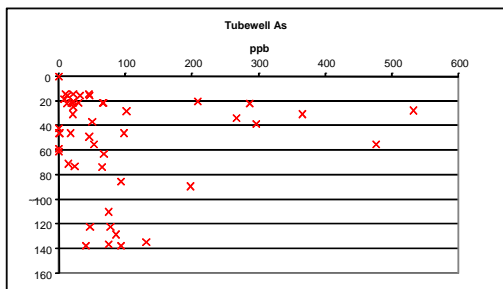
pools: weakly absorbed, amorphous and crystalline iron oxides and in sulfides and silicates. The dominant solid phase arsenic pools are iron oxides and sulfides and silicates. From 30 % - 50 % of the arsenic is in a form that can be considered easily releasable. The release of 1 ppm solid-phase arsenic can result in approximately 5 ppm aqueous - phase arsenic.

Solid – phase arsenic concentrations are low in aquifer sands in both high and low arsenic zones – generally 2 parts per million (ppm) or less. In fine grain sediments, arsenic levels are typically 5 – 10 ppm in both the low and high arsenic zones, peaking at 20 ppm near the surface in the channel-fill silts (borehole 20, Fig. 2).

The groundwater is dominantly calcium-



**Fig. 2.** Solid-phase arsenic in ppm versus depth in m from a continuous core. The core consists of clayey silt to depth of 28 m, and fine sand thereafter with a silt horizon at 34 m depth. As was measured by digestion with an HCl-HNO<sub>3</sub>-H<sub>2</sub>O aqua regia solution followed by inductively coupled plasma mass spectrometry and inductively coupled plasma atomic emission spectroscopy analysis.



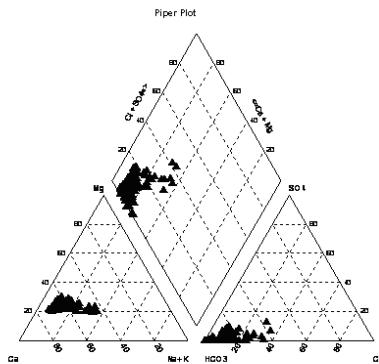


**Fig. 3.** Piper plot of Gotra – area groundwater.

bicarbonate type, with remarkably little variation in proportions of major elements between low and high arsenic zones (Fig. 3). Specific conductance ranges from a low of ~300  $\mu\text{S}/\text{cm}$  in locations with sand to the surface to ~1800  $\mu\text{S}/\text{cm}$  in fine-grained sediments. The groundwaters are almost all anoxic, with iron concentrations up to 21 mg/L. Sulfate concentrations are generally less than a few mg/L, and are typically below detection in high arsenic zones and the highest in low arsenic zones.

Dissolved arsenic is correlated with ammonia (Fig. 4), consistent with a release mechanism associated with the oxidation of organic carbon. Other chemical data not shown here provide clear evidence of iron, manganese and sulfate reduction and abundant methane in some samples indicates that methanogenesis is also occurring. It is not clear however if arsenic is released primarily by a desorption process associated with reduction of sorbed arsenic or by release after the reductive dissolution of the iron oxide sorbent. Phreeqc analysis shows  $\text{PCO}_2$  between  $10^{-1.2}$  and  $10^{-0.7}$  bars and that high arsenic waters are supersaturated with both siderite and vivianite.

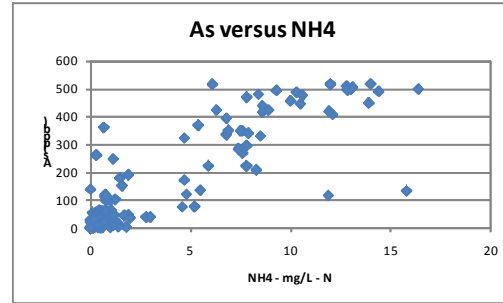


**Fig. 4.** Solid phase arsenic in ppm versus depth in m. The core consists of silty clay to depth of 28 m, and fine sand thereafter.

### REFERENCES

- ACHARYYA, S.K., CHAKRABORTY, P., LAHIRI, S., RAYMAHASHAY, B.C., GUHA, S., & BHOWMIK, A. 1999. Arsenic poisoning in the Ganges delta. *Nature*, **401**, 545-545.
- HARVEY, C.F., SWARTZ, C.H., BADRUZZAMAN, A. *et al.* 2002. Arsenic mobility and groundwater extraction in Bangladesh. *Science*, **298**, 1602-1606.
- NICKSON, R.T., MCARTHUR, J.M., RAVENSCROFT, P., BURGESS, W.G., & AHMED, K.M. 2000. Mechanism of arsenic release to groundwater, Bangladesh and West Bengal. *Applied Geochemistry*, **15**, 403-413.



## Flux of river active material flowing into the sea from Chinese continent: preliminary results

Sun Binbin<sup>1,2,3</sup>, Zhou Guohua<sup>1,2</sup>, Wei Hualing<sup>1,2</sup>,  
Liu Zhanyuan<sup>1,2</sup>, & Zeng Daoming<sup>1,2</sup>

<sup>1</sup> Institute of Geophysical and Geochemical Exploration, CAGS, Langfang 065000, Hebei CHINA  
(e-mail: sunbinbin@igge.cn)

<sup>2</sup> Laboratory for Applied Geochemistry, CAGS, Langfang, 065000, Hebei CHINA

<sup>3</sup> School of Earth Sciences and Resources, China University of Geosciences, Beijing 100083 CHINA

**ABSTRACT:** It's one of the key tasks for current regional eco-geochemical assessments proceeding in China to find out the flux flowing into the sea through rivers, especially for dissolved and suspended particulate matter (SPM) forms, which are active parts in water body and of high eco-environmental significance. This paper presents the method of the survey and gives the approximately primary heavy metal and nutritious elements' flux and proportion of water-soluble and SPM forms when the elements migrate to the sea for the whole Chinese continent, which bases on the actual SPM, filtering water and bed mud sampling, analysis and rivers' runoff data of main 35 rivers eastern coastline of China.

**KEYWORDS:** *element flux, filtering water, suspended particulate matter (SPM), active mass, transport way.*

### INTRODUCTION

River is the most consanguineous natural water body to human being and is the channel between terrene and ocean. The length of Chinese coastline is over 18000km. There are over 1500 and 80 rivers flowing into the sea that watershed area respectively exceed 1000km<sup>2</sup> and 10000km<sup>2</sup>. Furthermore, the rivers included like Yangtze River, Yellow River and Pearl River are all world-class. These rivers span wide latitude, various climate-landscape and different geological setting, and many of them have been polluted seriously. Research of inorganic and organic chemical components, flux flowing into the sea and transport form for great rivers like Yangtze, Yellow and Pearl River has been doing systemically since 1990s, and plenty of fruits in theory, mechanism and methodology have been showed (Zhang *et al.* 1995; Ye 2001; Pan *et al.* 2005; Ying *et al.* 2005; Wu *et al.* 2006; Zhou *et al.* 2008). Few rivers, limited index (most studies give just the content of total heavy metal) and hydrologic data in different terms are the same points of these studies. This survey designed to trace the source and transport form of

heavy metals in shallow sea environment, and then to make forecast and precaution through evaluating its potential ecological effect. This work includes systemic survey of 35 main rivers flowing into the sea in China.

### METHOD

In this survey, we collected SPM and filtering water samples respectively in wet and dry seasons and bottom mud in dry. Water was collected by plastic bucket below 30cm of the river surface at the place where the river is wide and lowly velocity relatively. In addition, we did this in the middle of the river. Conductivity, water temperature, pH and salinity were determined in field. Water samples were pumped through 0.45µm nylon membranes at stationed place. Then both membranes and filtering water samples were preserved. Membranes were folded, then put into sealing plastic envelop. Two bottles of filtering water were collected to 250ml plastic bottle. One was infused 2.5ml HNO<sub>3</sub>(1:1) for common elements analysis. Another was infused 2.5ml HNO<sub>3</sub>(1:1) and 12.5ml K<sub>2</sub>Cr<sub>2</sub>O<sub>7</sub>(5%) for mercury. Nylon membranes' drying and

weighting were proceeded before field work and after both for calculating the quality of SPM.

**ANALYSIS**

The membrane is put into 30ml quartz crucible after drying and weighting. Add 15ml aqua regia and 10ml distilled water into crucible. Then put it to platen heater for 1 hour, use 5ml distilled water to rinse the crucible and heat up for another hour. Displace the liquid to 25ml polythene pipe by water and add water to the calibration. Finally, determine the contents by ICP-MS, ICP-OES and AFS after shaking up and clarify. Insert 2 pieces of nothingness membranes to SPM samples for background value evaluation. All membrane samples are analyzed in duplicate for no reference material monitoring.

**RESULTS**

We calculate the flux by the formula blow:

$$T_i = C_{SPM-F} \times C_{SPM-Fi} \times Q_F + C_{SPM-K} \times C_{SPM-Ki} \times Q_K + C_{W-Fi} \times Q_F + C_{W-Ki} \times Q_K$$

where  $T_i$  is the flux of one or other element(i) flowing into the sea,  $C_{SPM-F}$  and  $C_{SPM-K}$  are concentrations of SPM in wet and dry season respectively,  $C_{SPM-Fi}$  and  $C_{SPM-Ki}$  are contents of element “i” in SPM respectively,  $C_{W-Fi}$  and  $C_{W-Ki}$  are contents of element “i” in filtering water respectively,  $Q_F$  and  $Q_K$  are runoffs respectively. Base on the publications, ratios of  $Q_F$  and  $Q_K$  in whole runoff are approximately determined to 8:2 and 6:4 for north and south (Yellow river is concluded) of Yellow river respectively. Sum of 32 (we get only 32 rivers runoff data as yet) main rivers’ runoff is 1526.97 billion  $m^3$ , while the runoff of Chinese continent is 1592.3 billion  $m^3$ . Ratio between former and later is 95.90%. Flux of Chinese continent flowing into the sea is calculated blow:

$$T_t = \frac{\sum T_i}{95.90\%}$$

where  $T_t$  is the flux of the whole Chinese

continent flowing into the sea,  $\sum T_i$  is the flux of 32 rivers flowing into the sea.

Table 4 shows the flux of main heavy metals and nutritious elements for 32 rivers (R-Flux) and Chinese continent (T-Flux) flowing into the sea. Furthermore, it shows the average ratio of SPM and dissolved forms (SPM-rate and Water-rate) when rivers reach to shallow sea. From it, variation of flux is very large among different elements, flux of major elements like as Ca, Fe, K, Mg, Na can get to a few or decades million tons, while trace elements including Cd and Hg have only decades to one hundred tons. In the same boat, transport forms of different elements vary largely too. Ratio of dissolved form for Ca, K, Mg and Na when river water migrates to sea takes up over 90%, while for Fe and Pb SPM form takes up domination.

**PROBLEMS AND DISCUSSION**

Flux showed in this paper exist some problems that:

Runoff, which changes greatly in different seasons and years, is one of the key factors influencing flux’s calculation. So, exact calculation needs long-term, dynamic and synchronic hydrologic data.

Hydrological characters are very complex in estuary. Flocculation, agglomeration, deposition and resuspension occur together. Element in river water is in condition of dynamic changes. Therefore, sample site plays a key role in flux survey. Near to downriver more, it should be affected by ocean

**Table 4.** Total flux of elements flowing into the sea and main transport forms for Chinese continental rivers(flux units: ton)

Element	R-Flux	T-flux	SPM-rate	Water-rate
As	4301	4494	27.5	72.5
Ca	69089129	72181089	3.3	96.7
Cd	110.9	115.8	64.5	35.5
Cu	10221	10678	62.9	37.1
Fe	4029673	4210014	97.5	2.5
Hg	24.7	25.8	42.9	57.1
K	5476964	5722075	7.8	92.2
Mg	17145829	17913160	6.2	93.8
Na	35814027	37416819	0.2	99.8
P	246259	257279	42.3	57.7
Pb	7309	7636	89.1	10.9
Zn	66834	69825	24.7	75.3

more, whereas influence aroused by violent industrial activities couldn't be displayed at estuary area. Furthermore, it's in estuary where many branches' afflux into the main river. To consider these branches we should add sample sites, in other words, we have to increase survey cost.

Besides, publications of rivers' runoff and ratio in wet and dry season are usually out of data or average values, which have been changed greatly by human in past decades. To this day, we can't get exact runoff data for different departments' data share difficulty.

On the other hand, this survey is mainly about active material flux, which is less affected by hydrological conditions than coarse particles. Accordingly, flux of this can provide reference data in some respects.

#### REFERENCES

PAN, Y.J. GUO, Z.G., YANG, Z.S., FAN, D.J., & SUN, X.G. 2005. Comparative Study on the

Composition of Grain Size of Suspended Sediments from the Yangtze and Yellow Rivers. *Journal of Ocean University of Qingdao*, **35(3)**, 417-422 (in Chinese).

WU, H.L., SHEN, H.T., YAN, Y.X., & WANG, Y.H. 2006. Preliminary study on sediment flux into the sea from Yangtze Estuary. *Journal of Sediment Research*, **6**, 75-81(in Chinese).

YE, L.Q. 2001. Discussion on the Flux of Heavy Metals into the sea from the Pearl River. *Environment and Exploitation*, **16(2)**, 52-54(in Chinese).

YING, M., LI, J.F., WAN, X.N., & SHEN, H.T. 2005. Study on Time Series of Sediment Discharge at Datong Station in the Yangtze River. *Resources and Environment in the Yangtze Basin*, **14(1)**, 83-87(in Chinese).

ZHANG, C.S., WANG, L.J., & ZHANG, S. 1995. Metal speciation in sediments and suspended matter in the middle-lower reaches of the Changjiang River. *China Environmental Science*, **15(5)**, 342-347 (in Chinese).

ZHOU, G.H., SUN, B.B., LIU, Z.Y., WEI, H.L., & ZENG, D.M. 2008. Flux of River Active Material Flowing into the Sea: Concept and Methodology. *Geological Bulletin of China*, **27(2)**, 182-187 (in Chinese).



## Methods for obtaining a national-scale overview of groundwater quality in New Zealand

Christopher J. Daughney, Uwe Morgenstern, Rob van der Raaij,  
Robert Reeves, Matthias Raiber, & Mark Randall

GNS Science, 1 Fairway Drive, Avalon NEW ZEALAND (e-mail: c.daughney@gns.cri.nz)

**ABSTRACT:** This study presents methods developed to summarise groundwater quality in New Zealand, based on data collected since 1990 from over 100 monitoring sites comprising the National Groundwater Monitoring Programme (NGMP). Site-specific groundwater age determinations based on measured concentrations of tritium, CFCs and SF<sub>6</sub> range from less than one year to more than 100 years, with the 25<sup>th</sup>, 50<sup>th</sup> and 75<sup>th</sup> percentiles (across the entire NGMP) being approximately 10, 40 and 100 years, respectively. Hierarchical cluster analysis based on median concentrations of 15 major and minor constituents reveals three dominant water types across the NGMP. At 42% of the monitoring sites, groundwater quality shows some level of human influence, with nitrate, chloride and/or sulphate concentrations in excess of natural background levels. At 32% of the monitoring sites, groundwater quality shows little or no evidence of human influence, but due to high levels of oxygen in the aquifer, any introduced nitrate or sulphate will persist and accumulate. At the remaining 26% of the monitoring sites, the groundwater is oxygen-poor and is not likely to accumulate significant nitrate, but due to natural processes, it commonly accumulates concentrations of iron, manganese, arsenic and/or ammonia.

**KEYWORDS:** *hydrochemistry, groundwater age, multivariate statistics, New Zealand*

### INTRODUCTION

The objective of this study is to provide an overview of groundwater quality across all of New Zealand (NZ). This is achieved by analysis of data collected through the NZ National Groundwater Monitoring Programme (NGMP). The NGMP, established in 1990, is a long-term research programme that aims to identify spatial and temporal trends in NZ groundwater quality and relate them to specific causes. The data analysis methods of interest in this study include hierarchical classification of monitoring sites from hydrochemistry (Daughney & Reeves 2005, 2006), and groundwater age determination based on measured concentrations of tritium, CFCs (*chlorofluorocarbons*) and SF<sub>6</sub> (Daughney *et al.* 2009).

Hierarchical Cluster Analysis (HCA) is a multivariate statistical method that can be used to assign groundwater samples or monitoring sites to distinct categories (hydrochemical facies). HCA offers several advantages over other methods of

grouping or categorising groundwaters. HCA does not require *a priori* assumptions about the number of groups or the criteria that control the groupings, such as aquifer lithology or confinement. HCA can be based on any number of variables, and these variables can be of any type (chemical, physical, biological; distributed or non-distributed). HCA can thus provide a more holistic approach to sample comparison than most other methods, which are limited in terms of the number of variables that can be simultaneously presented clearly. HCA produces a set of average parameter values (a centroid) for each cluster in the original units of the input variables, and hence the results of HCA can be more readily interpreted in the geological or hydrochemical context than multivariate methods based on transformation, e.g. Principal Components Analysis. The output of HCA can be displayed as a membership table, where each site or sample is unambiguously assigned to a single group. By contrast, for most graphical methods (e.g. Piper

diagrams), it is difficult to determine exactly where the boundaries of each group should be placed, how many groups there should be, or which samples should be assigned to each group.

Determination of groundwater age is valuable for a variety of reasons covering the spectrum from applied resource management to fundamental scientific research. Groundwater dating relies on measurement of one or more tracer substances, followed by fitting of the tracer concentration data with a lumped-parameter model (Zuber *et al.* 2005). Tritium, CFCs and SF<sub>6</sub> are the tracers most commonly used for dating young groundwater (less than about 100 years old).

It is often useful to estimate groundwater age independently of the tracer method in order to overcome ambiguities that can arise in age determinations based on limited tracer data at some sites and in some hydrogeological conditions. Ambiguity in groundwater age can be overcome by fitting the convolution integral to time series tracer data, but it may not be practical to make several measurements over perhaps several years, as might be necessary to permit detection of significant change in the tracer concentrations relative to analytical uncertainty. Major ion hydrochemistry and well depth can be used to estimate groundwater age independently from the direct method of measuring tracer concentrations.

Discriminant Analysis (DA) is a multivariate statistical method that generates a set of classification functions that can be used to predict into which of two or more categories an observation is most likely to fall, based on a certain combination of input variables. DA may be more effective than regression for relating groundwater age to major ion hydrochemistry and well construction because it can account for complex, non-continuous relationships between age and each individual variable used in the algorithm while inherently coping with uncertainty in the age values used for

calibration, and there is no need to assume that the sites involved are within the same aquifer or even within the same catchment.

## METHODS

The NGMP includes 112 long-term monitoring sites across New Zealand; four sites that are no longer included in the NGMP were also considered as part of this study. NGMP sites are situated in discrete aquifers (or on discrete flow lines in large aquifer systems) and are selected to encompass a range of aquifer lithology, confinement and surrounding land use that is representative of New Zealand aquifers in general. Median well depth is 26 m below ground surface (b.g.s.), and the minimum, lower quartile, upper quartile and maximum well depths across all NGMP sites are 3, 10, 55 and 337 m b.g.s., respectively.

Samples are collected quarterly on an on-going basis from each NGMP site according to a standardized protocol. Electrical conductivity, pH and temperature are measured in the field using portable meters, and three different types of samples are collected for laboratory analysis of various parameters. An unfiltered, unpreserved sample is analysed in the laboratory for alkalinity, conductivity and pH using an autotitrator. A filtered (0.45 µm) unpreserved sample is analyzed for Cl, Br, F, SO<sub>4</sub>, NO<sub>3</sub>-N and PO<sub>4</sub>-P by ion chromatography, and for NH<sub>4</sub>-N by automated phenohypochlorite method. A filtered, acid-preserved (HNO<sub>3</sub>) sample is analyzed for Na, K, Ca, Mg, Fe, Mn and SiO<sub>2</sub> by inductively coupled plasma optical emission spectrometry. The length of the historical record differs for each NGMP site but on average covers a period of seven years.

Groundwater age at each NGMP site has been assessed using multiple tracers. Tritium was analyzed in a 1 L unfiltered unpreserved sample using 70-fold electrolytic enrichment prior to ultra-low level liquid scintillation spectrometry (Morgenstern & Taylor 2005). Samples for analysis of CFCs and SF<sub>6</sub> (125 ml and 1 L, respectively) were collected in strict

isolation from the atmosphere and analysed by gas chromatography using an electron capture detector (Busenberg & Plummer 1992; van der Raaij 2003). Dissolved Ar and N<sub>2</sub> concentrations were used to estimate the temperature at the time of recharge and the excess air concentration, which allowed calculation of the atmospheric partial pressure of CFCs and SF<sub>6</sub> at the time of recharge.

The convolution integral and the Exponential Piston Flow Model (EPM) were used to relate measured tracer concentrations to historical tracer input. The tritium input function is based on tritium concentrations measured monthly since the 1960s near Wellington, New Zealand. CFC and SF<sub>6</sub> input functions are based on measured and reconstructed data from southern hemisphere sites. The EPM was applied consistently in this study because statistical justification for selection of some other response function requires a substantial record of time-series tracer data which is not yet available for the majority of NGMP sites, and for those NGMP sites with the required time-series data, the EPM and other response functions yield similar results for groundwater age.

HCA and DA were conducted using log-transformed site-specific median concentrations of various parameters as described by Daughney & Reeves (2005) and Daughney *et al.* (2009). HCA was conducted with median concentrations of Br, Ca, Cl, F, Fe, HCO<sub>3</sub>, K, Mg, Mn, Na, NH<sub>4</sub>-N, NO<sub>3</sub>-N, PO<sub>4</sub>-P, SiO<sub>2</sub> and SO<sub>4</sub> using the Nearest-Neighbour and Wards linkage rules. DA was conducted using electrical conductivity, well depth, and the median concentrations of Ca, Mg, Na, K, HCO<sub>3</sub>, Cl and SO<sub>4</sub>.

### SUMMARY OF RESULTS

The range of hydrochemistry encountered across the NGMP can be summarized by assigning each site to one of three categories (hydrochemical facies) defined via HCA. 32% of the NGMP monitoring sites are assigned to the *natural-fresh* category and are typified by oxic groundwater showing little or no evidence

of human or agricultural impact. 42% of the NGMP sites are assigned to the *impacted* category, and are also typified by oxic groundwater, but with evidence of some degree of human or agricultural impact in the form of above-background concentrations of NO<sub>3</sub>-N, often co-occurring with elevated concentrations of Cl and/or SO<sub>4</sub>. The level of impact observed at these sites is variable, with 15% of sites having median NO<sub>3</sub>-N concentration above the guideline for safe human consumption (11.3 mg/L). The remaining 26% of the NGMP sites are assigned to the *natural-evolved* category and are typified by reduced (anoxic) groundwater, often with measurable concentrations of NH<sub>4</sub>-N, dissolved Fe and/or dissolved Mn, and relatively high total dissolved solids concentrations.

Site-specific groundwater age values ranged from less than one year to more than 100 years, with the 25<sup>th</sup>, 50<sup>th</sup> and 75<sup>th</sup> percentiles being approximately 10, 40 and 100 years, respectively, across the entire NGMP. Classification functions derived from DA allowed assignment of 71% of the sites to the correct of four age categories (mean residence time ten years or less, 11 to 40 years, 41 to 100 years, or more than 100 years).

Groundwater age displays a generally expected relationship to well depth, but the age category cannot be predicted from well depth alone. In line with expectation, over all NGMP sites, well depth has a weak positive correlation to groundwater age, with the youngest and oldest age categories generally being associated with shallow and deep bores, respectively. However, shallow wells do not always tap young groundwater: there were a small number of NGMP sites at which groundwater from the oldest age category was found in a well less than 10 m deep. This situation occurred in both confined and unconfined aquifers, corresponding to upward-moving groundwater at the discharge end of a flow system.

Likewise, despite certain expected relationships between groundwater age and hydrochemistry, a particular site's groundwater age category cannot be

predicted from its hydrochemistry alone. For example, the older the groundwater is, the more likely it is to be assigned to the natural-evolved hydrochemical category. This is expected because the longer the groundwater is in the aquifer and isolated from the atmosphere, the more likely it is to become anoxic and to accumulate dissolved substances through water-rock interaction. However, only 85% of the NGMP sites assigned to the oldest age category display the natural-evolved hydrochemical signature, indicating that groundwater can remain oxic in some New Zealand aquifers for more than 100 years. Conversely, the natural-evolved hydrochemical signature is found at a small proportion (5%) of NGMP sites in the youngest age category, indicating that in some situations groundwater can become anoxic in less than a decade. Not surprisingly, this confirms that the rates of hydrochemical reactions are variable, as would be expected for aquifers with varied or mixed lithologies.

There is no significant partitioning of the different age categories between the natural-fresh and impacted hydrochemical categories. In other words, the number of sites having oxic impacted groundwater is always roughly equal to the number of sites with oxic unimpacted groundwater, regardless of groundwater age category. This implies that the impact of human and agricultural activity on New Zealand's groundwater quality is of similar extent over the last ten years as over the previous century.

#### ACKNOWLEDGEMENTS

The authors thank personnel from New

Zealand regional councils for assistance with sample collection. This research was funded by the New Zealand Foundation for Research, Science and Technology (Contract C05X0706).

#### REFERENCES

- BUSENBERG, E. & PLUMMER, L.N. 1992. Use of chlorofluorocarbons (CCl<sub>3</sub>F and CCl<sub>2</sub>F<sub>2</sub>) as hydrologic tracers and age dating tools: the alluvium and terrace system of Central Oklahoma. *Water Resources Research*, **28**, 2257-2283
- DAUGHNEY, C.J., MORGENSTERN, U., VAN DER RAAIJ, R., & REEVES, R.R. 2009. Groundwater age in New Zealand aquifers: Tracer measurements and age estimation from hydrochemistry. *Hydrogeology Journal*, in press.
- DAUGHNEY, C.J. & REEVES, R.R. 2005. Definition of hydrochemical facies in the New Zealand National Groundwater Monitoring Programme. *Journal of Hydrogeology New Zealand*, **44**, 105-130.
- MORGENSTERN, U. & TAYLOR, C.B. 2005. Low-level tritium measurement using electrolytic enrichment and LSC. *Proc. Int. Symp. Quality Assurance for Analytical Methods in Isotope Hydrology*. International Atomic Energy Agency.
- VAN DER RAAIJ, R.W. 2003. *Age dating of New Zealand groundwaters using sulphur hexafluoride*. M.Sc. thesis, School of Earth Sciences, Victoria University of Wellington, New Zealand.
- ZUBER, A., WITCZAK, S., RÓZAŃSKI, K. *et al.* 2005. Groundwater dating with <sup>3</sup>H and SF<sub>6</sub> in relation to mixing patterns, transport modelling and hydrochemistry. *Hydrological Processes*, **19**, 2247-2275.

## Genesis of smectite scales in Mindanao geothermal production field, Philippines

Rosella G. Dulce<sup>1</sup>, Gabriel M. Aragon<sup>2</sup>,  
Benson G. Sambrano<sup>3</sup>, & Lauro F. Bayrante<sup>4</sup>

<sup>1</sup>Energy Development Corporation, Merritt Road, Fort Bonifacio, Taguig City 1634 PHILIPPINES  
(e-mail: dulce.rg@energy.com.ph)

**ABSTRACT:** Smectite [Al<sub>4</sub>Si<sub>8</sub>O<sub>20</sub>(OH)<sub>4</sub>n•H<sub>2</sub>O], a hydrated expanding clay mineral is present in significant amounts in the surface facilities of the Mindanao Geothermal Production Field. It is the dominant constituent of total deposits in the low-pressure flash vessel station, and Separator Vessels (SV) 100 and 101. It is found in minor quantities of total deposits downstream of these vessels. The fragmental clay deposits cause recurrent operational problems, such as flooding of brine surge tank and flash vessel, clogging of pump at the LP station, and subsequent power plant trip. Petrologic and scanning electron microscopy analyses of clay samples reveal micro-textural features and mineral association suggesting that they deposited directly from the brine in the surface facilities, and are not hydrothermal alteration minerals transported from production wells. Moreover, simulation using SV-100 brine chemistry gives a high saturation index of smectite (log Q/K of 10-24) indicating high potential for depositing smectite. Very high saturation index is due to the brine's elevated aluminum content of 640 ppb. Since aluminum is the major parameter that controls smectite saturation index, clay scaling may be controlled by brine treatment with Al-sequestering or complexing agent (Gallup, 1997).

**KEYWORDS:** *smectite, scale, saturation index, deposits, brine*

### INTRODUCTION

Smectite refers to a hydrated expanding clay mineral with a general chemical formula of Al<sub>4</sub>Si<sub>8</sub>O<sub>20</sub>(OH)<sub>4</sub>n•H<sub>2</sub>O (Read 1970). Aside from being commonly observed as a hydrothermal alteration of rock cuttings from geothermal wells, this clay mineral is noticeably present in the surface facilities of the Mindanao Geothermal Production Field (MGPF). It is abundant in the Low-Pressure (LP) Flash Vessel Station, particularly in the brine surge tank, flash vessel, bypass line and valve, and pump. It occurs in lesser amounts upstream of this station: in the solid trap, main brine line 1 (MBL-1), brine line sampling points after SV-100/101 and SV-602, and at the bases of SV-100 and SV-101. The huge amounts of fragmental clay deposits cause recurrent operational problems such as flooding of brine surge tank and flash vessel, clogging of pump at the LP station, and subsequent power plant trip.

This study attempts to determine the probable origin of abundant smectite in

the LP station of MGPF. Samples were collected and analyzed using polarizing microscope and scanning electron microscope (SEM), and energy dispersive x-ray (EDX). Brine chemistry at selected sampling locations was also studied, and simulation using WATCH speciation software was done to determine the potential of the brine to directly deposit smectite. The conduct of this study will focus on the root cause of the problem, *i.e.*, the formation of huge amounts of smectite scales.

### SMECTITE CHARACTERIZATION

#### Petrologic Analysis

Abundant fragmental sand- to pebble-sized deposits at several Fluid Collection and Recycling System (FCRS) locations in MGPF (Fig. 1 and Table 1) were collected and analyzed using a polarizing microscope.

The abundant dark brown to black soft minerals in the collected samples are identified as smectite, based on optical properties under a polarizing microscope.

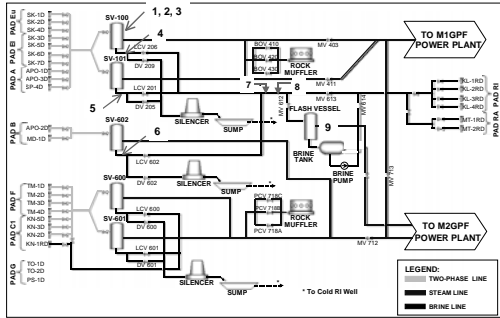


Fig. 1. Process flow diagram of MGPF.

Sampling Location	Smectite	Amorphous Silica	Corrosion Products	Rock Cuttings	Calcite
1. SV100 sidewall	5	80	15	-	-
2. SV100 stand pipe	10	70	20	-	-
3. SV100 base	5	85	10	-	-
4. SV100 brine line	80	6	7	5	2
5. SV101 brine line	55	15	10	15	5
6. SV602 brine line	3	70	15	5	7
7. MBL-1 (main brine line)	83	2	7	5	3
8. Solid trap	20	40	35	5	-
9. Low Pressure Flash Vessel station					
Brine surge tank	85	5	2	7	1
Flash vessel wall	-	97	1	1	-
Flash vessel base	3	85	5	7	-
Bypass valve	80	8	2	10	-
Bypass line	80	15	-	3	2
Brine line pump	4	90	6	-	-

Table 1. Sampling locations in MGPF.

Under the microscope, smectite is light to dark brown, or greenish to yellowish brown mineral. It has a grain size range of 0.07-7.00 μm. Smectite is present together with other fine-sized fragmental amorphous silica, corrosion products and rocks. Smectite comprises from 5% to 85% of the total deposits in MGPF FCRS.

Smectite occurs commonly as rounded

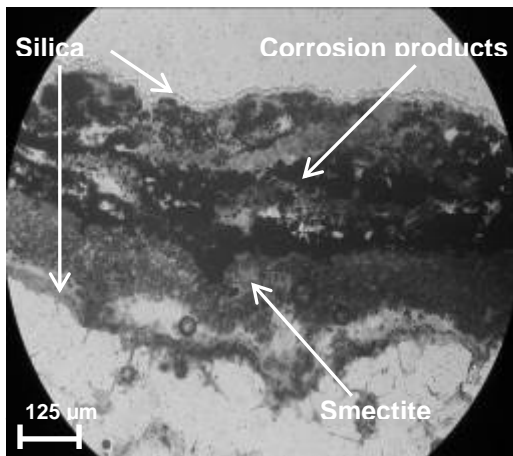


Fig. 2. Smectite scales interlayered with amorphous silica and corrosion products.

birefringent crystalline masses. Occasionally, it exists as amorphous to microcrystalline materials. Smectite exhibits fibrous, radiated, or daisy-like textures, very typical of smectite scales, but not observed in smectite as hydrothermal alteration mineral. It also shows very fine ripple marks which are displayed by amorphous silica scales in geothermal brine lines. In addition, smectite also has wavy extinction like amorphous silica. Smectite is occasionally thinly (1-2 mm) interlayered with amorphous silica and corrosion products (Fig. 2). It is embedded with abundant minute dendritic opaque minerals.

### Determination of the Chemical Formulae of Clay Samples using EDX Analysis

The elemental compositions in weight percent of the four samples coded Brine Surge 1, Brine Surge 2, MBL-1A and MBL-1B collected from brine surge tank and MBL-1 sampling points were determined by EDX analysis. The clays are composed dominantly of O<sub>2</sub> (~70-80 wt. %) and Si (~10-15 wt. %), and minor amounts of Na, Mg, and Al (below 5 wt.%). Trace to nil K, Ca, Fe, Mn, Zn, and Cl are also present. In MBL-1B, however, significant amounts of Fe (~6.5 wt. %) is present in the sample. These elemental compositions are consistent with the general formula of smectite as will be discussed later.

All four clay samples have been identified as smectite on a polarizing microscope. Deciphering their chemical formulae can be done using the atomic percentages (Aragon 2006). Smectite has a general chemical formula of  $Al_4Si_8O_{20}(OH)_4.nH_2O$  (Read 1970), with substitution of Mg for part of the Al. As a result of this substitution, positive ions such as Na<sup>+</sup> or Ca<sup>2+</sup> are attached to the surfaces or edges of the minute crystals, thus balancing the negative charges, which result when Mg<sup>2+</sup> takes the place of Al<sup>3+</sup>. In this way, variants known as sodium-smectite and calcium-smectite are formed. The positive ions (Na<sup>+</sup>, Ca<sup>2+</sup>) are

exchangeable bases, and their presence accounts for the high base-exchange capacity of the mineral.

Table 2 gives the compositions of the same four clay samples in atomic percent. The atomic percent is defined as the number of atoms of an element per unit volume divided by the number of atoms per unit volume of the substance containing the element. This is similar to mole fraction when the atomic percent is converted to fractional value.

Thus, the chemical formula of smectite (Table 3) is slightly complex since deficiency in Al<sup>3+</sup> will be directly sufficed by Mg<sup>2+</sup> and indirectly by Na<sup>+</sup> and Ca<sup>2+</sup>.

The chemical formula may be in the form of Al<sub>w</sub>Mg<sub>x</sub>Na<sub>y</sub>Ca<sub>z</sub>Si<sub>8</sub>O<sub>20</sub>(OH)<sub>4</sub>.nH<sub>2</sub>O where w, x, y, and z are the subscripts for each cation. The subscript is variable and highly dependent on the availability of the cations when the clay mineral was formed.

**CLAY FORMATION SIMULATION USING SV-100 BRINE CHEMISTRY**

Simulation of clay formation using SV-100 fluid was done using WATCH speciation program. Table 4 shows the data (Urbino & Lam, 2005) used for the clay simulation study. The speciation program calculates the saturation index in terms of log Q/K of the four clay minerals: Ca-smectite, Mg-smectite, K-smectite, and Na-smectite. Based on simulation, the log Q/K values at separator temperature of 170°C are **23.8, 22.6, 9.6,** and **10.8** for Ca-smectite, Mg-smectite, K-smectite, and Na-smectite, respectively. Thus, the brine fluid from the separator vessel is super saturated with respect to all clay minerals due to its very high aluminum content of 640 ppb. The inherently high potential for smectite deposition of the SV-100 separated brine fluid explains the presence of abundant clay minerals in the FCRS, most particularly in the second flash separator (LP station) where the separated brine from SV-100, SV-101, and SV-602 is further flashed at low pressure (120°C) to produce steam for the power plant.

**CONCLUSIONS**

(1) Abundant fragmental smectite deposits

Element	Brine Surge 1	Brine Surge 2	MBL-1A	MBL-1B
O	79.39	85.07	83.49	82.69
Na	2.08	2.08	0.83	2.37
Mg	1.79	2.30	5.34	3.31
Al	2.16	1.33	0.41	0.94
Si	13.86	8.78	8.47	7.71
K	0.26	0.07	0.09	0.15
Ca	0.28	0.15	0.15	0.23
Fe	0.19	0.16	0.75	2.15
Mn	---	0.05	0.30	0.27
Zn	---	---	0.17	0.03
Cl	---	---	---	0.14
Total	100.00	100.00	100.00	100.00

**Table 2.** Compositions in atomic % based on EDX analysis.

Sample Code	Chemical Formulae for Smectite
Brine Surge 1	Al <sub>2.0</sub> Mg <sub>1.7</sub> Na <sub>2.0</sub> Ca <sub>0.3</sub> Si <sub>8</sub> O <sub>20</sub> (OH) <sub>4</sub> .51H <sub>2</sub> O
Brine Surge 2	Al <sub>1.5</sub> Mg <sub>2.5</sub> Na <sub>2.3</sub> Ca <sub>0.2</sub> Si <sub>8</sub> O <sub>20</sub> (OH) <sub>4</sub> .69H <sub>2</sub> O
MBL-1A	Al <sub>0.4</sub> Mg <sub>4.9</sub> Na <sub>0.8</sub> Ca <sub>0.1</sub> Si <sub>8</sub> O <sub>20</sub> (OH) <sub>4</sub> .53H <sub>2</sub> O
MBL-1B	Al <sub>0.9</sub> Mg <sub>2.9</sub> Na <sub>2.3</sub> Ca <sub>0.2</sub> Si <sub>8</sub> O <sub>20</sub> (OH) <sub>4</sub> .57H <sub>2</sub> O

**Table 3.** Chemical formulae of clay samples.

	SV-100	SV-602	MBL-1	LPBL*
Date	4/21/2005	4/18/2005	4/18/2005	4/7/2005
Sampling Pressure (MPaa)	0.79	0.83	0.74	0.89
Temp. (°C)	172	172	167	175
pH (@20°C)	6.92	7.02	6.92	6.95
Na	3462	3378	3821	3549
Mg	0.20	0.07	0.28	0.12
Al	0.64	0.58	---	0.64
K	549	674	546	531
Ca	165	137	93.5	182
Fe	1.53	0.72	---	0.06
Zn	0.0246	0.0212	---	0.0188
Cl	6063	6095	6220	6167
SO <sub>4</sub>	47.9	88.2	33.5	37.6
B	117	61.9	61.1	120
SiO <sub>2</sub>	541	688	566	574
H <sub>2</sub> S	---	3.7	---	4.11
SSI		0.91	0.78	0.742

**Table 4.** Brine chemistry at SV-100, SV-602, MBL-1 & LPBL (\*low pressure brine line).

in the low-pressure flash vessel station and other surface facilities in the Mindanao geothermal production field cause recurrent operational problems.

(2) Petrologic and SEM analyses of these clay samples reveal micro-textural and structural features and mineral association suggesting that they deposited directly from the brine in the surface facilities, and are not hydrothermal alteration minerals transported from production wells.

(3) The chemical formulae of the clays based on atomic % are: Al<sub>1.5</sub>Mg<sub>2.5</sub>Na<sub>2.3</sub>Ca<sub>0.2</sub>Si<sub>8</sub>O<sub>20</sub>(OH)<sub>4</sub> •69H<sub>2</sub>O in brine surge tank, and

$\text{Al}_{0.9}\text{Mg}_{2.9}\text{Na}_{2.3}\text{Ca}_{0.2}\text{Si}_8\text{O}_{20}(\text{OH})_4 \cdot 57\text{H}_2\text{O}$  in MBL-1.

(4) Simulation using SV-100 brine chemistry gives a tremendously high saturation index of smectite (log Q/K of 10-24) indicating high potential for depositing smectite. Very high saturation index is due to the brine's elevated aluminum content of 640 ppb. Thus, abundant smectite scales likely form in LP station where separated brine from SV-100/101/602 is further flashed at 120°C. These soft clay deposits are easily removed from the vessels and transported as fragmental materials downstream of these facilities.

#### REFERENCES

- ARAGON, G.M. 2006. Determining the chemical formulae of clay samples from the Mindanao geothermal production field, Philippines. *PNOC-EDC internal report*.
- GALLUP, D.L. 1997. Aluminum silicate scale formation and inhibition: scale characterization and laboratory experiments. *Geothermics*, **26**, 483-499.
- READ, H.H. 1970. Rutley's elements of mineralogy. c. George Allen & Unwin (Publishers) Ltd.
- URBINO, G.A. & LAM, J.C. 2005. Mindanao geothermal production field water test report. *PNOC-EDC internal report*.

## Adding Value to Kinetic Testing Data I – Interpretation of Tailings Humidity Cell Data from the Perspectives of Aqueous Geochemistry and Mineralogy at the Crowflight Minerals, Bucko Lake Nickel Project

David R. Gladwell<sup>1</sup> & Catherine T. Ziten<sup>1</sup>

<sup>1</sup>Wardrop Engineering Inc., 900 – 330 Bay Street, Toronto, ON, M5H 2S8 (e-mail david.gladwell@wardrop.com)

**ABSTRACT:** Kinetic testing of tailings is often focused on issues of acid mine drainage or metal leaching from an environmental perspective. Data is presented from 76 weeks of kinetic testing of bench test rougher tailings from the Crowflight Minerals, Bucko Lake Nickel Project. Statistical examination of the kinetic test data indicates that the data set is highly auto-correlated, a common feature of kinetic test data. Auto-correlated data is difficult to interpret without a prior knowledge of the dataset, therefore mineralogy determined during metallurgical testing was used to define the sample mineralogy and PHREEQC software was used to compute the equilibrium concentrations of ionic species according to ion pair theory. The sulfide mineral assemblage includes pyrrhotite, pentlandite, pyrite and chalcopyrite. Periods of oxidation of specific sulfide minerals and carbonate phases were identified from leachate chemistry using both ion pair molalities and sliding correlation coefficients. Pentlandite was observed to begin oxidizing first, followed by iron sulfides (pyrite and pyrrhotite) and chalcopyrite. The ability to define reaction products associated with oxidation of specific minerals in kinetic test data facilitates operational tailings management.

**KEYWORDS:** *Kinetic Testing, AMD, Tailings, Aqueous Speciation, PHREEQC, Nickel Mining.*

### INTRODUCTION

Estimation and prediction as to whether waste rock and tailings will produce acid mine drainage (AMD) are precursory to environmental certification, and therefore are a critical step in mine development. Kinetic tests are carried out using a cell or column that are operated over a period of typically 1 year, whereas static tests are a onetime measurement to determine the acid producing potential (AP) and neutralization potential (NP) when exposed to oxidation, but cannot provide information on reaction rates (Morin & Hutt 1997; Jambor *et al.* 2002; Blowes *et al.* 2003). Humidity cell testing is a standard protocol (ASTM, 2001) involving periodic rinsing of tailings samples over time to remove all reaction products that accumulated following the previous rinsing (Morin & Hutt 1997; Price *et al.* 1997) and subsequently analyzing the leachate for relevant parameters (Lapakko & White 2000; Sapsford *et al.* 2009). The results elucidate how tailings/waste rock will behave over time with the onset of

oxidation, assist in calculating oxidation rates, mineral reaction rates, and with respect to prediction of acid generation facilitate estimation of the rate of NP depletion and the period when AMD commences (Day *et al.* 1997; Morin & Hutt 1997; Price *et al.* 1997; Frostan *et al.* 2002; Howell & Parshley 2005; Ardaub *et al.* 2008).

This paper outlines a novel approach to maximising the value of kinetic data by combining mineralogy (from petrological studies) and aqueous geochemistry to reveal oxidation of relevant mineral assemblages based on changes in unique element suites. PHREEQC<sub>i</sub> was used to calculate equilibrium ion pair concentrations. PHREEQC<sub>i</sub> and its precursors have been used extensively for sensitive acid precipitation studies (Meranger *et al.* 1986) and for AMD projects (Morin 1985).

### GEOLOGICAL SETTING

The Bucko Lake Nickel Project is located in north-central Manitoba and owned by

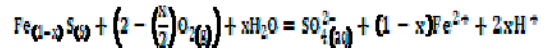
Crowflight Minerals Inc. The ore deposit consists of Apehbian ultramafic sills intruded into Archean gneisses (Wardrop 2008). Rougher tails were produced from lock cycle testing of bulked drill core samples.

**KINETIC TEST DATA**

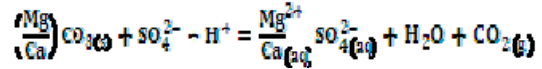
Kinetic testing of the rougher tails sample was carried out in accordance with standard ASTM, 2001. Leachate samples were collected each week for 76 weeks and analyzed for a range of parameters including: conductivity, pH, acidity, total alkalinity, sulfate and a suite of dissolved metals. Dissolved metals and metalloids were determined by ICP-MS, other parameters by titration or selective ion electrode methods.

Data such as that generated by the Bucko kinetic testing (and most other kinetic testing) is difficult to interpret due to its highly auto-correlated content (Cerioli & Riani 2005). The high degree of auto-correlation frustrates the extraction of meaningful information from the data and may be part of the reason why most interpretations of kinetic data are restricted to prediction of potential AMD or metal leaching. Prior knowledge of sample mineralogy is necessary to untangle the complex web of inter-correlated data. Based on metallurgical studies the Bucko rougher tails samples are known to contain several sulfide phases including Pentlandite (Fe,Ni)<sub>9</sub>S<sub>8</sub>, Pyrrhotite (Fe<sub>7</sub>S<sub>8</sub> to FeS), Chalcopyrite (CuFeS<sub>2</sub>), and Pyrite (FeS<sub>2</sub>). Calcite (CaCO<sub>3</sub>) and Magnesite (MgCO<sub>3</sub>) are also present and the balance of the sample is composed of varieties of talc (Mg<sub>6</sub>[Si<sub>8</sub>O<sub>20</sub>](OH)<sub>4</sub>).

The most likely mineral phases to oxidize under the kinetic testing conditions are the sulfides. Acidity generated from their oxidation is likely to react with calcite and to a lesser extent magnesite. Talc minerals are unlikely to react with leachate. Expected reactions are therefore of the forms:



(1)



(2)

**CALCULATION OF ION PAIR CONCENTRATION**

PHREEQC version 2.15 was used to calculate equilibrium concentrations of ion pairs from the leachate chemistry. PHREEQC was initially developed by the United States Geological Survey and a substantial library of thermodynamic constants has built up over the ongoing development period (Appelo & Postma 2005).

Considering the other sulfides present as well, likely ion pairs present in the leachate include FeSO<sub>4</sub>, CaSO<sub>4</sub>, NiSO<sub>4</sub>, CuSO<sub>4</sub> and MgSO<sub>4</sub>.

The distributions of CuSO<sub>4</sub> and NiSO<sub>4</sub> molality (m), determined using PHREEQC, are presented as Figure 1. NiSO<sub>4</sub> m is maximum at week 15 and decreases thereafter with peaks at week 34 and around week 60.

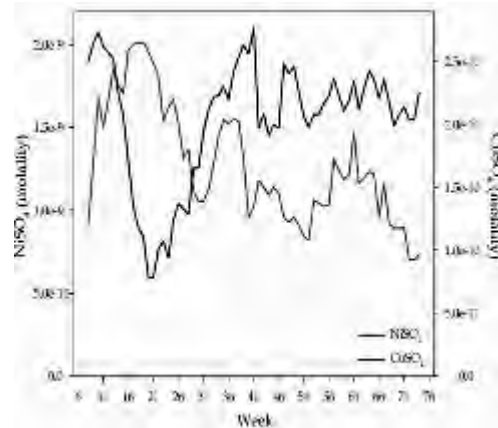


**Fig. 1.** Distribution of Ni and Cu Sulfate Ion Pair Molality (5 point boxcar filtered).

**Table 1.** Mean dissolved concentrations for chalcopyrite and pentlandite periods of kinetic tests

	Acidity	Alkalinity	Ca <sup>2+</sup>	B	Mg	Ni	K	Si	Na	Sr	NiCO <sub>3</sub> *	NiHCO <sub>3</sub> *
Pentlandite (weeks 10-29)	0.96	28	37	0.086	4.5	0.0027	16	0.95	0.87	0.059	1.80E-09	1.70E-09
Chalcopyrite (weeks 31-47)	0.89	20	40	0.025	3.9	0.0012	14	0.8	0.68	0.044	7.50E-10	6.40E-10

All concentrations in mg/L except \* denotes molality

CuSO<sub>4</sub> shows minimum concentrations around weeks 10 through 29 after which it increases and appears to approach a steady state concentration. The distribution of FeSO<sub>4</sub> molality (not shown) is less variable, which is expected since Fe is present in all sulfide phases. The distributions of NiSO<sub>4</sub> and CuSO<sub>4</sub> suggest that Pentlandite oxidizes before Chalcopyrite since the molality of the sulfates are the products of these reactions. The products of each oxidation reaction are linked by the oxidation reaction of type (Eq.1). Correlation in the analytical data for these parameters should be higher when these reactions are occurring. Correlation coefficients for the Ni/SO<sub>4</sub> and Cu/SO<sub>4</sub> ion pairs are presented in Figure 2. The coefficients are calculated using an un-weighted seven point sliding window and the results are smoothed using an un-weighted three point window.

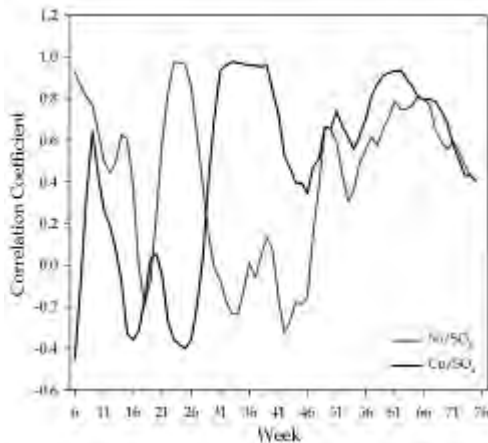


**Fig. 2.** Smoothed 7-point Sliding Correlation Coefficients for Ni/SO<sub>4</sub> and Cu/SO<sub>4</sub>.

High values of NiSO<sub>4</sub> and CuSO<sub>4</sub> correspond to high values of the appropriate correlation coefficients, confirming the interpretation that

pentlandite oxidizes first, around weeks 10 through 29, but also from weeks 50 through 70. Chalcopyrite appears to be actively oxidizing from approximately week 31 through the end of the kinetic test. The ability to identify periods of the tailings kinetic testing when individual sulfide minerals are oxidizing makes the testing data much more useful for design of the tailings management strategy, especially regarding potential changes in ore composition or metallurgical processing. For example, for the Bucko test, during weeks 10 through 29 there is minimal chalcopyrite oxidation and during weeks 31 through 47 there is minimal pentlandite oxidation. Table 1 compares leachate chemistry for the periods of pentlandite and chalcopyrite oxidation. Periods of pyrrhotite and pyrite oxidation cannot be discriminated using the above methodology since iron is present in all sulfides, therefore pyrrhotite and pyrite may also be oxidizing during the two periods compared.

The most significant differences are for B and Ni, which are both over twice the concentrations when pentlandite is oxidizing compared to the period of chalcopyrite oxidation. Ni carbonate and bicarbonate species show the greatest increases in concentration. Leachate generated during periods of increased chalcopyrite oxidation does not show increases in any parameters. Clearly, changes in pentlandite content of the tailings, either from changes in ore, metallurgical processes or sulfide segregation at deposition potentially present a higher environmental concern than changes in chalcopyrite content. The ability to characterize differences of this nature is of significant benefit in management of tailings facility and deposition design and also provides

valuable input into metallurgical process design criteria.

## CONCLUSIONS

Periods of kinetic testing of tailings where individual sulfide phases are oxidizing were identified in highly auto-correlated data from the Crowflight Minerals Bucko Lake Nickel Project using PHREEQC modelling and sliding correlation coefficients in tandem with mineralogical data. This capability provides significant added value to kinetic testing data through the increased ability to utilize the data in tailings management.

## ACKNOWLEDGEMENTS

The authors acknowledge and thank Crowflight Mineral Inc for permission to use the case study and Wardrop Engineering Inc. for support and reviews.

## REFERENCES

- APELLO, C.A.J. & POSTMA, D. 2005. *Geochemistry, Groundwater and Pollution, 2<sup>nd</sup> Edition*. CRC Press; Boca Raton.
- ARDAU, C., BLOWES, D.W. & PTACEK, C.J. 2009. Comparison of laboratory testing protocols to field observations of the weathering of sulfide-bearing mine tailings. *Journal of Geochemical Exploration*, **100**, 182-191.
- ASTM. 2001. Standard test method for accelerated weathering of solid materials using a modified humidity cell. **Method D5744-96**.
- BLOWES, D.W., PTACEK, C.J., JAMBOR, J.L., & WEISNER, C.G. 2003. The geochemistry of acid mine drainage. In: LOLLAR, B.S. (ed.) *Environmental Geochemistry, Treatise on Geochemistry* (eds. HOLLAND, H.D.; TUREKIAN, K.K.) Elsevier-Pergamon, Oxford. **9**, 149-204.
- BOWELL, R.J. & PARSHLEY, J.V. 2005. Mineralogical controls on Pit Lake geochemistry, summer Camp Pit, Nevada. *Chemical Geology*, **215**, 373-385.
- CERIOLI, A. & RIANI, M. 2005. Studies in Classification, Data Analysis, and Knowledge Organization. *Data and Information Analysis to Knowledge Engineering. The 29th Annual Conference of the German Classification Society*. University of Magdeburg.
- DAY, S.J., HOPE, G., & KUIT, W. 1997. Waste rock management planning for the Kudz Ze Kayah project, Yukon Territory: 1. Predictive Static and Kinetic Test Work. *Proceedings of the 4<sup>th</sup> International Conference on Acid Rock Drainage*. Vancouver, **I**, 81-98.
- FROSTAD, S., KLEIN, B., & LAWRENCE, R.W. 2002. Evaluation of laboratory kinetic test methods for measuring rates of weathering. *Mine Water and the Environment*, **21**, 183-192.
- JAMBOR, J.L., DUTRIZAC, J.E., GROAT, L.A., & RAUDSEPP, M. 2002. Static tests of neutralization potentials of silicate and aluminosilicate minerals. *Environmental Geology*, **43**, 1-17.
- LAPAKKO, K.A. & WHITE, W.W.III. 2000. Modification of the ASTM 5744-96 kinetic test. *Proceedings from the 5<sup>th</sup> International Conference on Acid Rock Drainage*. Littleton, 631-639.
- MERANGER, J.C., GLADWELL, D.R., & LETT, R.E. 1986. Application of a conceptual model to assessing the impact of acid rain on drinking water quality. *WHO Water Quality Bulletin*, **11**, 179-186.
- MORIN, K. 1985. Simplified explanations and examples of computerized methods for calculating chemical equilibria in water. *Computers and Geoscience*, **11**, 409-416.
- MORIN, K.A. & HUTT, N.M. 1997. *Environmental Geochemistry of Minesite Drainage: Practical Theory and Case Studies*. MDAG Publishing, Vancouver.
- PRICE, W.A., MORIN, K.A., & HUTT, N.M. 1997. Guidelines for the prediction of acid rock drainage and metal leaching for mines in British Columbia: Part II. Recommended procedures for static and kinetic testing. In: *Proceedings of the 4<sup>th</sup> International Conference on Acid Rock Drainage*. Vancouver, **I**, 15-30.
- SAPSFORD, D.J., BOWELL, R.J., DEY, M., & WILLIAMS, K.P. 2009. Humidity cell tests for the prediction of acid rock drainage. *Minerals Engineering*, **22**, 25-36.

## Large-scale hydrogeochemical mapping - insight into alteration processes and prospectivity mapping

David J Gray, Ryan R.P. Noble, & Nathan Reid

CSIRO Exploration and Mining, 26 Dick Perry Ave, Kensington, WA, 6117 AUSTRALIA  
(e-mail: david.gray@csiro.au)

**ABSTRACT:** The hydrogeochemistry of the northern Yilgarn Craton of Western Australia has been examined to assess the utility of groundwater for regional exploration for Ni, Au, Zn and U mineralization. The objective was to develop reliable regional hydrogeochemical vectors to mineralization in the study area, as well as establish size of geochemical haloes from various systems, and determine regional background concentrations for environmental and exploration purposes. Approximately 1400 samples were collected across an area of 500 x 300 km with additional samples from selected sites near differing mineralisation styles. Results corroborate established geochemical weathering models around sulfide mineralisation, clearly depict major U systems, and have been valuable for understanding background concentrations of elements, particularly those of environmental importance such as Cr, As and NO<sub>3</sub>. Regional groundwater chemistry shows potential for discovering large mineralised systems in deeply covered terrains that are often uneconomical to explore with more traditional methods.

**KEYWORDS:** groundwater, Yilgarn, Western Australia, sulfide weathering, exploration

### INTRODUCTION

Following on from a successful groundwater sampling study along the Leonora-Wiluna Belt (Gray & Noble 2007), a hydrogeochemical mapping project for the northern Yilgarn was established as a proof of concept for broad scale hydrogeochemistry, with potential for mapping, environmental background establishment and mineral exploration across many other areas of Western Australia, especially outside recognized mineralisation belts.

### GEOLOGICAL SETTING

The Archaean Yilgarn Craton is composed mainly of granite, with mafic, volcanic and sedimentary "greenstone" rocks. It is one of the world's principal mineral provinces, with considerable resources of primary and supergene Au, sulfide-hosted and lateritic nickel, bauxite, as well as a wide range of other commodities.

Much of the Yilgarn (~70%) is under transported cover and exploration has relied heavily on geochemical sampling either at surface or from depth (drilling). Two broad regions (north and south) are

identified based on their regolith history, vegetation, rainfall pattern and groundwater characteristics. The boundary between these regions is quite sharp, approximately coincident with latitude 30°S – commonly called the *Menzies Line*. In the north, groundwaters are fresh and neutral, trending more saline in the valley axes, whereas in the south, groundwaters are commonly neutral to acid, saline to hyper-saline and reducing. These regional variations have major effects on the dispersion of many elements and their distribution in the regolith.

### METHODS AND MATERIALS

Approximately 1400 samples were collected from predominantly farm wells and bores, although dewatering bores and groundwater monitoring bores were also sampled. Water was collected from the outflow pipe when the bore or well was operational, or bailed using a flow-through system with one-way valves. Additional samples were added to the assessment from previous work to enhance the study around key mineralised sites such as

those shown in Figures 1 and 2.

Field measurements included pH, Eh, EC, temperature, depth of water table and depth of sample collection. Separate, field preserved sub-samples were collected for cation (ICP-MS/OES), anion (IC), alkalinity (titration), DOC, PO<sub>4</sub> and Au and PGE analysis (using carbon sorption).

One litre of unfiltered water was rolled with a carbon sachet and 10g NaCl for 7 days. The carbon was then dried, ashed, digested in aqua regia and analysed by ICP-MS, for Ag, Au, Pd, and Pt. Field and analytical blanks, as well as duplicates were used in all analyses to ensure accuracy (Gray *et al.* 2001).

**GROUNDWATER CHARACTERISTICS OF DIFFERING DEPOSIT TYPES**  
**Orogenic Gold**

South of the Menzies Line, gold dissolves as Au halide (Gray *et al.* 2001). Dissolved Au concentrations reach µg/L levels, with groundwater anomalies greater than 200 m spatial extent. To the north, anomalous Au

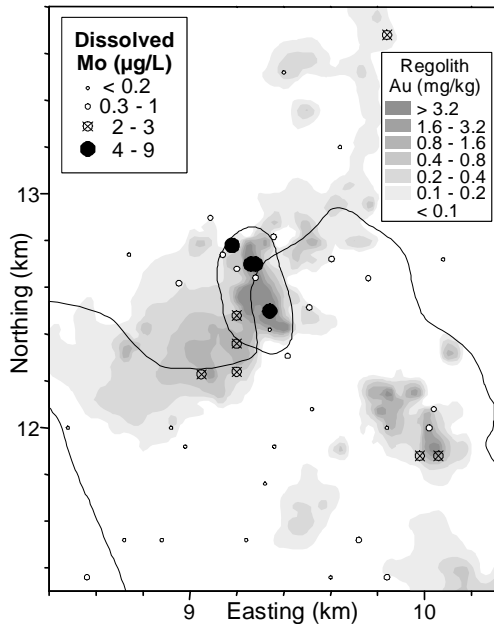


**Fig. 1.** Dissolved Mo distribution at the Baxter deposit in Western Australia has a much greater and consistent anomaly compared to dissolved Au (not shown). The results are superimposed on maximum Au contents in the regolith to show the extent of mineralisation.

concentrations are much lower (> 5 ng/L is anomalous), though the spatial extent is similar.

In the northern Yilgarn and surrounding areas, such as the Baxter deposit) chalcophile elements are enriched in groundwaters contacting with weathering sulfides (e.g., As, Mo, Ag, Sb, W, Tl, and Bi) and these may be more useful regional exploration tools than dissolved Au itself (Fig. 1).

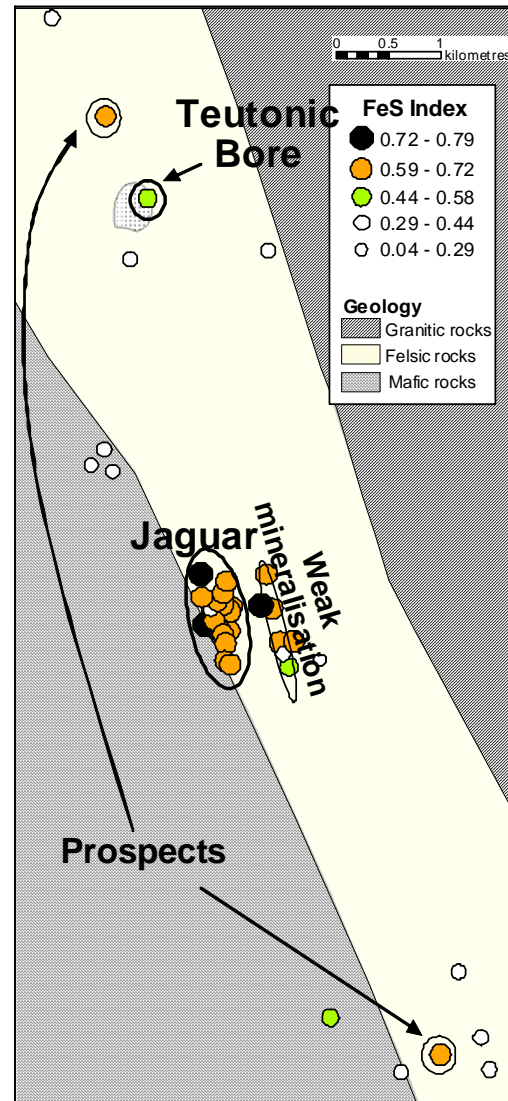


**Fig. 2.** The distribution of the calculated FeS index from groundwater results at the Teutonic Bore / Jaguar VMS camp. Results correlate closely with known ore bodies and prospects.

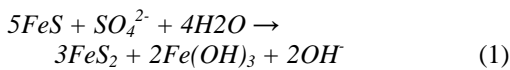
### Nickel Sulfides

The development of reliable regional and smaller-scale hydrogeochemical vectors to Ni sulfide mineralisation in weathered terrains requires understanding of controls on Ni-S weathering.

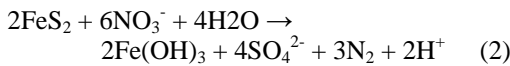
The first alteration phase is the partial sulfide oxidation: pyrrhotite → pyrite and pentlandite → violarite, which can utilise either sulfate or bicarbonate as oxidants:

This causes sulfate and bicarbonate depletion in deep groundwaters around mineralisation.

In shallow groundwaters, dissolved nitrate is a strong oxidant in high concentrations (> 100 mg/L) across much of central Australia, and is possibly derived from “leakage” from nitrogen



fixing nodules in *Acacia* sp. roots. The reduction of nitrate and the oxidation of pyrite and violarite results in nitrate depletion and sulfate enrichment in groundwater:



Thus use of sulfate and nitrate is effective at detecting the presence of sulfides. Other indices, consistent with the model for groundwater evolution around weathering sulfides, delineate the sulfide signature independent of the type of water i.e. varied Eh and pH. The better performing indices for mineralization targeting are:

- Mineralised* (Ni+Co+W+Pt)
- Acid Sulfides* (Mo+Ba+Li+Al) and FeS (pH-Eh+Fe+Mn)

*Combined indices* use the *mineralised* signature and take away the *acid sulfides* or the *FeS index*. Massive NiS gave stronger groundwater signatures than disseminated mineralisation, which commonly were only clearly delineated using these combined indices.

### Volcanic Massive Sulfides

VMS exploration using groundwaters uses similar principles to NiS exploration using a combination of parameters for finding sulfides (Fig. 2), then distinguishing VMS using other parameters including Ag, Pt, W. Metals such as Cu or Zn can give very high (>> mg/L) anomalism, although the spatial distribution is highly variable.

### Palaeochannel Uranium

Secondary uranium (carnotite;  $K_2(UO_2)_2(VO_4)_2 \cdot 3H_2O$ ) commonly shows a strong groundwater signature (Fig. 3), and hydrogeochemical exploration is likely to be successful, particularly in the northern parts of the Yilgarn Craton (Gray & Noble 2007; Fig. 3) and elsewhere in central Australia. Uranium mineral saturation indices are also valuable for exploration targeting.

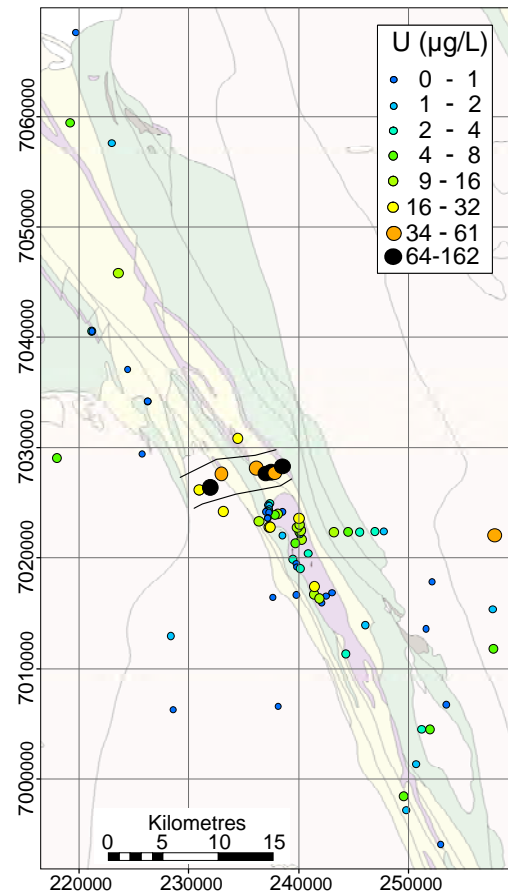


**Fig. 3.** Dissolved uranium at Honeymoon Well. The Centripede Palaeochannel uranium deposit is clearly delineated.

Another area for research is how groundwater fluxes of vanadium (critical for carnotite precipitation) and phosphate (enhances uranium mobility) are controlled by geology and geomorphology. This may assist in targeting economic from sub-economic targets.

#### **HYDROGEOCHEMICAL MAPPING**

Large-scale groundwater results from the regional mapping show patterns stretching 10s of kms. Mineralisation signatures are also evident, particularly for U systems. Nitrate, Cr and As are also found in large concentrations and are valuable for assessing water resources for human and agricultural purposes. Other lithological changes between granites and greenstones, and different types of granites are also evident on the regional scale. Numerous underexplored regions have also been highlighted that, based on their groundwater signature, may warrant further exploration.

#### **CONCLUSIONS**

Results which corroborate established geochemical weathering models around sulfide mineralisation, clearly depict major U systems, and have been valuable for

understanding background concentrations of elements, particularly those of environmental importance such Cr, As and NO<sub>3</sub>. The use of NO<sub>3</sub> and SO<sub>4</sub> for exploration is an important new development for exploration targeting of sulfide systems. Regional groundwater chemistry shows good potential for discovering large mineralised systems in deeply covered terrains that are often uneconomical to explore with more traditional methods.

#### **ACKNOWLEDGEMENTS**

We thank CSIRO and the Minerals Down Under Flagship, as well as a number of companies for the support for this research. The most recent regional study was supported by the exploration industry, GSWA, MERIWA, WA DoW, and GA.

#### **REFERENCES**

- GRAY, D.J. 2001. Hydrogeochemistry in the Yilgarn Craton. *Geochemistry: Exploration, Environment, Analysis*, 1, 253–264.
- GRAY D.J. & NOBLE R.R.P. 2007. Nickel hydrogeochemistry of the NE Yilgarn Craton, Western Australia. CSIRO Division of Exploration and Mining Restricted Report P2006/524. CRC LEME *Open File Report* **243R**, 133 p.

## Ontario's ambient groundwater geochemistry project

Stewart M. Hamilton<sup>1</sup>

<sup>1</sup>Ontario Geological Survey, 933 Ramsey Lake Road, Sudbury, ON CANADA  
(e-mail: [stew.hamilton@ontario.ca](mailto:stew.hamilton@ontario.ca))

**ABSTRACT:** The Ontario Geological Survey has recently completed the second year of a multi-year groundwater sampling project that is intended to cover all the accessible areas of the one million square kilometre province of Ontario. The project will provide baseline groundwater quality for policy makers and other stakeholders. Areas of natural groundwater quality hazards are being outlined and the chemistry of groundwater will be established with a specific focus on the effect of geology on water quality. Samples are being collected from domestic wells on a regular 10x10 km grid with one sample being collected from an overburden well and another from bedrock in each node. The study is helping to establish 'normal' levels of over 80 parameters in groundwater, many of which have poorly understood range and distribution in natural groundwaters. Preliminary results demonstrate that geology indeed plays an important role in the distribution of dissolved constituents. Concentrations of natural hazards such as fluoride are controlled by the nature and distribution of the host rock.

**KEYWORDS:** *groundwater geochemistry, background concentrations, well sampling*

### INTRODUCTION

Ontario encompasses approximately one million km<sup>2</sup> and is Canada's 2<sup>nd</sup> largest province. Across Ontario, natural water quality variations exist in groundwater-sourced water supplies that have the potential to impact human health and limit the usability of the resource. Most of these variations, including well-known regional water quality problems, can be attributed to easily definable geological conditions. Until recently no detailed province-wide groundwater geochemical study had ever been carried out that delineates areas of poor water quality and attempts to relate them to variations in rock and soil type despite very large amounts of geochemical data that exist in the public domain. Part of the reason for this is that the available data were collected in myriad studies by different groups and, as such, sampling was carried out over limited areas at various scales, with analysis being done to various standards of precision and accuracy. In addition, many analyses did not determine a wide enough range of parameters to allow comparison of any one parameter across the province as a whole or even within particular geological units. This project was initiated

by the OGS initiated in part to address these knowledge gaps.

### THE RELATIONSHIP BETWEEN GEOLOGY AND WATER GEOCHEMISTRY

The OGS regularly receives requests from the public, other government agencies and private sector companies for data that show 'normal' levels of dissolved constituents in waters. Since the geochemistry of groundwater is strongly influenced by the nature of aquifer materials, a 'normal' level for parameters in groundwater such as mercury, arsenic or nitrate is meaningless outside its geological context.

Rainwater is the ultimate source of recharge and resupply of all terrestrial waters. The total dissolved solids (TDS) content of rainwater rarely exceeds 10 parts per million (ppm) but is much higher for groundwater, river water and lake water (Fig. 1).

The increased solute-loading in terrestrial waters is due to dissolution of minerals in rock, soil and overburden materials as rainwater infiltrates them. Groundwater experiences the largest degree of water-rock interaction and consequently has the highest average

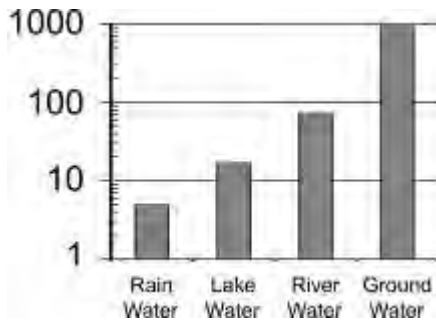


**Fig. 1.** Typical total dissolved solid (TDS) concentrations (mg/L) in terrestrial waters (from various sources listed in Hamilton *et al.* 2007).

TDS loading; lake-water experiences the least and has correspondingly lower loading. River water is a mixture of rainwater runoff and groundwater base flow and has intermediate amounts of TDS. This project seeks to collect representative numbers of groundwater samples in the major rock and overburden units in the province. This will help to establish background levels in an appropriate geological context and to understand the sources of minerals, nutrients and potential hazards in groundwater.

### SAMPLING APPROACH

Groundwater samples are collected from domestic wells on a regular 10x10 km grid. One sample within each grid node is collected from a well finished in bedrock and another from overburden.

Only untreated water is collected and samples are taken from the point in the domestic plumbing that is closest to the well. Information on the pump, plumbing and well are also collected from the homeowner or from Ontario Ministry of Environment water well records database.

Wells are purged until stable readings are obtained for field chemical parameters including pH, temperature, dissolved oxygen, redox and electrical conductivity. Samples are then collected for a wide variety of chemical parameters. Time sensitive parameters are analyzed within specific holding times. For example, alkalinity and hydrogen sulphide are measured at the time of sampling, iodide

within 24 hours and nitrogen parameters and bacteria within 48 hours.

Good quality control procedures are crucial to allowing the results of this project to integrated year upon year. More than 10% of all samples analyzed are for quality control. About half of these are duplicates; the others are blanks, certified or internal reference standards and spiked samples.

### RESULTS TO DATE

The 2007 and 2008 study areas covered 9,700 and 12,000 km<sup>2</sup> respectively and collected close to 500 groundwater samples (Fig. 2). The results of analyses for the second year are complete and are currently being processed. Results for the first year and preliminary results for 2008 demonstrate the remarkable effect that geology has on groundwater geochemistry. Most of the more than 80 geochemical parameters show correlation with at least one of the 10 major rock units in the study areas. For example F, a health related parameter, and H<sub>2</sub>S are elevated in the Hamilton Group shales. Light rare earth elements also show enrichment in this unit but the heavy rare earth elements are more enriched in the stratigraphically higher Kettle Point shales.

### CONCLUSIONS

The results from the first 2 years of the Ambient Groundwater Geochemistry project demonstrate very clearly that:

- (1) anthropogenic contaminants only occur locally in isolated areas and very rarely in bedrock wells;
- (2) geology is the ultimate source of most chemical constituents in groundwater; and
- (3) the geological context must be considered when determining the 'normal' level of any parameter.

This project will be an ongoing part of the OGS program for the foreseeable future. In addition to maintaining high sampling and analytical standards, a key challenge will be the seamless integration of the data year upon year as analytical methods improve. This and related problems are the subject of ongoing research at the OGS.

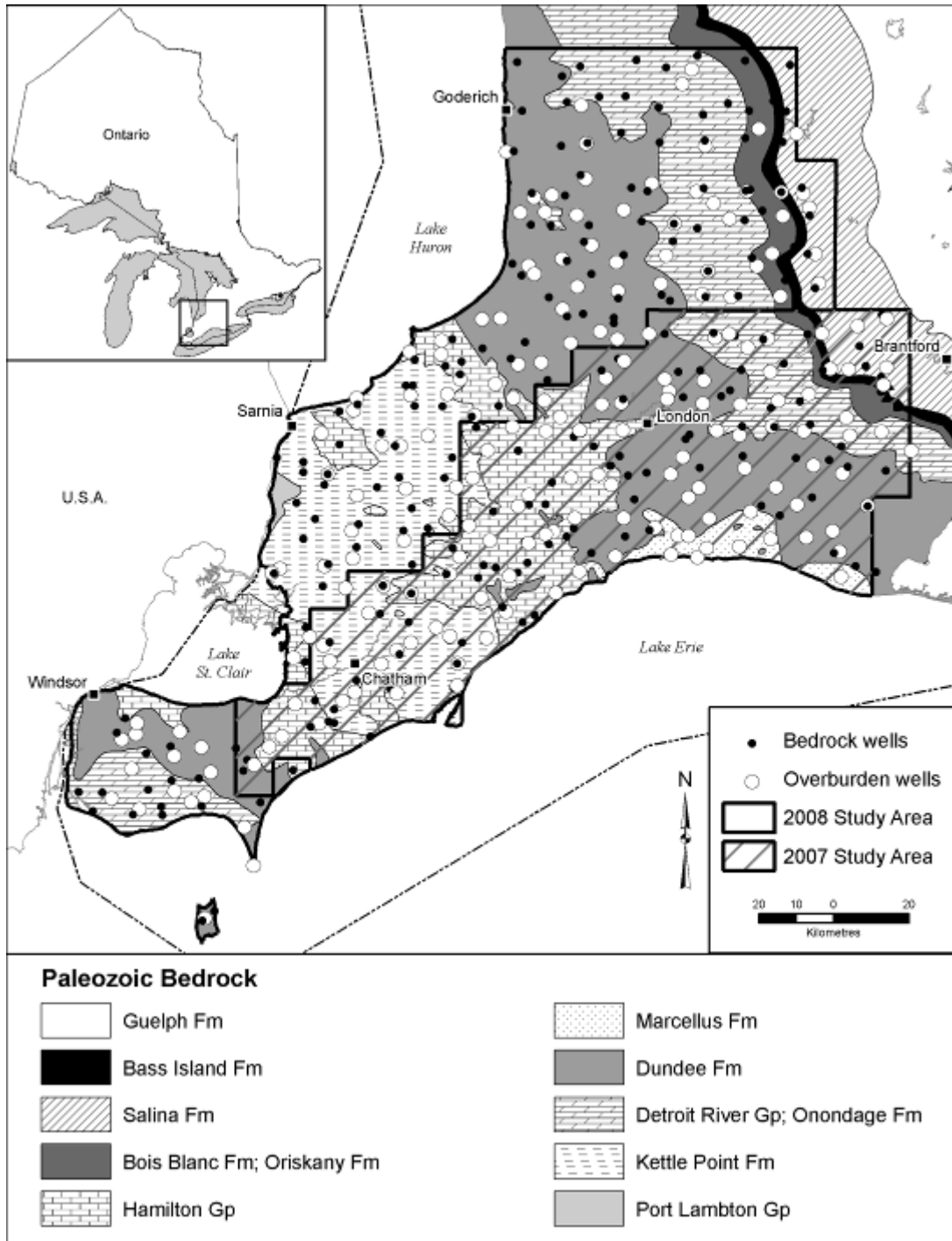


**Fig. 2.** Ambient Groundwater Geochemistry study areas and sample distribution for the 2007 and 2008 seasons (from Hamilton & Braunerder 2008).

**REFERENCES**

HAMILTON, S.M. & BRAUNEDER, K. 2008. The Ambient Groundwater Geochemistry Project: Year 2; in *Summary of Fieldwork and Other Activities*, Ontario Geological Survey Open File Report **6226**, 34-1 to 34-7.

HAMILTON, S.M., BRAUNEDER, K., & MELLOR, K.J. 2007. The Ambient Groundwater Geochemistry Project – Southwestern Ontario; in *Summary of Fieldwork and Other Activities*, Ontario Geological Survey Open File Report **6213**, 23-1 to 23-5.



## Distribution of cadmium forms and their correlation with organic matters in acid soils

Wei Hualing<sup>1,2</sup> & Zhou Guohua<sup>1,2</sup>

<sup>1</sup> Institute of Geophysical and Geochemical Exploration, Langfang, CO, 065000, Hebei China  
(e-mail: weihualing@igge.cn)

<sup>2</sup> Key Laboratory of Applied Geochemistry, CAGS, Langfang, CO, 065000, Hebei China

**ABSTRACT:** The activation, migration, transformation of heavy metals in soils can have environmental impact on human being and animals. Cadmium forms in soil can be classified into water-extractable, adsorbed and exchangeable, carbonate bounded, humic acid bounded, occluded metals onto Fe-Mn oxides, organically bounded and residual metals. This study focused on the distribution of Cd forms and their correlation with organic matters in the acid soils of Zhejiang, eastern China. The results show that Cadmium in soils mainly occurs as adsorbed and exchangeable forms and carbonate bounded forms in the acid soils, and its contents are relatively low as other forms. Organic matter is one of major factors controlling Cd forms.

**KEYWORDS:** Cadmium forms, organic matter, acid soils

### INTRODUCTION

Heavy metals in the environment, especially their accumulation in soils, is a serious environmental problem which the whole world faces (Du *et al.* 2005). The farmland soils are an important media of the ecological cycle of Cadmium, and its harm to human health can't be neglected (Wu *et al.* 2004). Heavy metal migration, transformation and toxicity to plants in soil are directly influenced by the quantity proportions of various forms (Zhu *et al.* 2002). The toxicity of water-extractable and adsorbed and exchangeable metals are the greatest, and residual metals is the lowest (Liu *et al.* 2002). Different forms have different bioavailability thus their influences on the environment and human health are different. It is critical to have a good understanding of Cadmium forms in soil. This paper describes the Cadmium forms in the acid soils of eastern China.

### SAMPLING AND ANALYSIS

In this study, 30 soil samples from rice farmland in Zhejiang province, in eastern China. We sampled the cultivation layer soils during rice harvest season. The soils are acidified and the average value of pH is 5.82. A sequential extraction procedure

with seven steps was used to extract the cadmium forms which was determined by ICP-MS (technical requirements of sample analysis in ecological geochemical assessment (trial Implementation), 2005). Water-extractable forms was extracted by distilled water, adsorbed and exchangeable forms by MgCl<sub>2</sub>, carbonate bounded metals by NaAc, acid glacial acetic acid, Humic acid bounded forms by sodium pyrophosphate, occluded forms onto Fe-Mn oxides by hydroxylamine Hydrochloride, organically bounded forms by H<sub>2</sub>O<sub>2</sub> and residual forms by hydrofluoric acid acids.

### RESULTS AND DISCUSSION

#### Cd Forms in the Soils

The proportion of various Cd forms in soils are shown in Figure 1. water-extractable forms make up 2.0%, adsorbed and exchangeable forms, 57%, carbonate bounded forms, 10.9%, humic bounded forms, 4.8%, occluded forms onto Fe-Mn oxides, 8.1%, organically bounded forms, 8.1%, and residual forms, 9.0%. Proportions of adsorbed and exchangeable forms >carbonate bounded forms>residual forms> occluded forms onto Fe-Mn oxides =organically bounded forms> Humic acid bounded forms

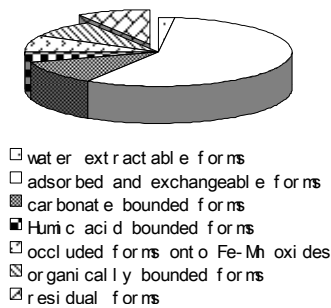


**Fig. 1.** Pie showing the proportion of Cd forms.

>water-extractable forms. The results show that Cd mainly occurs as non-residual forms in soils, and its proportion accounts for 90% of the total Cd. And among non-residual forms, adsorbed and exchangeable forms are dominated, which is bioavailable forms (Tu 1997; Wang 1997).

**Correlation Between Cd Forms and Organic Matter**

The amount of organic matters not only determines the nutrition of the soils, but also form complex compound with heavy metals to influence metal migration and bioavailability (Liu *et al.* 2002). From table 1, we can found that extractable Cd contents, especially occluded Cd onto Fe-Mn oxides and organically bounded Cd has a prominent positive correlation with organic matters ( $\alpha = 0.05, n = 30, F = 0.361$ ), (Fig. 2). Organic matters are one of the major factors which influence Cd occurrence forms. Bioavailable Cd increases with the content increase of soil organic matter.

**CONCLUSIONS**

- (1) Cadmium in acid soils mainly occurs as adsorbed and exchangeable forms.
- (2) There is a good correlation between organic matters and contents of various Cd forms. Organic matters can make Cadmium activate in the soils and lead to, biological toxicity.

**ACKNOWLEDGEMENTS**

We thank all the members of Key Laboratory of Applied Geochemistry, who

**Table 1.** Correlation coefficient of Cd forms and organic matters.

Cd forms	organic matters
Water-extractable Cd	0.399
adsorbed and exchangeable Cd	0.478
carbonate bounded Cd	0.480
Humic Cd	0.480
occluded Cd onto Fe-Mn oxides	0.559
organically bounded Cd	0.559
residual forms	0.248

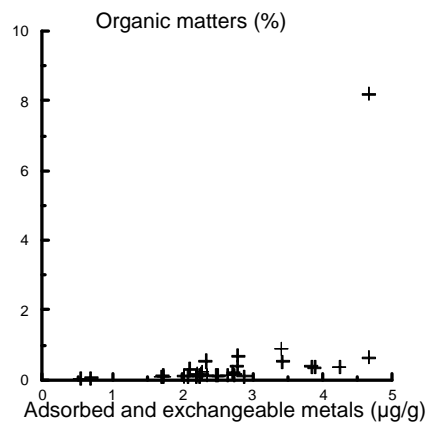


**Fig. 2.** Plot showing correlation between contents of adsorbed and exchangeable Cd and organic matters.

have helped with collecting sampling, analysis and data processing.

**REFERENCES**

CHINA GEOLOGICAL SURVEY. 2005 Technical Requirements of Sample Analysis in Ecological Geochemical Assessment (trial Implementation). DD2005-03 (in Chinese).  
 DU CAIYAN, ZU YANQUN, & LI YUAN. 2005. Effect of pH and Organic Matter on the Bioavailability Cd and Zn in Soil. *Journal of Yunnan Agricultural University*, **20**(4), 539-543 (in Chinese with English abstract).  
 LIU XIA, LIU SHUQING, & TANG ZHAOHONG. 2002. The Relationship Between Cd and Pb Forms and Their Availability to Rape in Major Soils of Hebei Province. *Acta ecologica Sinica*, **22**(10), 1688-1694 (in Chinese with English abstract).  
 TU CONG. 1997. Bioavailability of Ni fractions in

- soils. *Acta Scientiae Circumstantiae*, **17**(2), 179-185.
- WANG, P.X., QU, E.F., LI, Z.B., & SHUMAN, L. M. 1997. Fractions and availability of nickel in Loessial soil amended with sewage sludge or sewage. *Environ Qual.*, **26**, 795-800. (in Chinese with English abstract).
- WU TAO, ZENG YING, & NI SHIJUN. 2004. A Study on Cadmium Forms in Farmland Soil in the Suburb of Chengdu. *Shanghai Environment Sciences*, **23**(6), 236-23.
- ZHU BO, QING CHANGLE, & MU SHUSEN. 2002. Bioavailability of exotic zinc and cadmium in purple soil. *Chinese Journal of Applied Ecology*, **13**(5), 555-558 (in Chinese with English abstract).



## Adaptation of the OECD T/DP for metals and metal compounds to marine systems

Philippa Huntsman-Mapila<sup>1</sup>, Jim Skeaff<sup>1</sup>, Marcin Pawlak<sup>1</sup>,  
Hayley Roach<sup>1</sup>, & Dave Hardy<sup>1</sup>

<sup>1</sup>CANMET-MMSL, 555 Booth St., Ottawa, Ontario, K1A 0G1 CANADA  
(e-mail: phuntsma@nrcan.gc.ca)

**ABSTRACT:** The transformation/dissolution (T/D) characteristics of metals and alloys in a marine medium in seven- and twenty eight- day tests are being evaluated in this project. The two metals tested to date were selected based on data availability from freshwater T/D testing: cuprous oxide powder (Cu<sub>2</sub>O) and nickel metal powder (Ni). Prior to T/D testing, trace metals are initially removed from the marine medium with a Chelex-100 resin, while following T/D testing they are separated from the saltwater matrix by a metal chelation step with flow injection and analysed by ICP-AES. The marine media T/D data yields useful comparisons with data reported earlier for the freshwater OECD 203-based media at pH 6 and 8 and provides insight into the behaviour of metal-bearing substances in commerce under marine transformation/dissolution protocol (T/DP) conditions. Furthermore, the collected data supports an approach directed to the extension of the application of the T/DP to derive hazard classification proposals with respect to the marine environment.

**KEYWORDS:** *metals, marine systems, transformation/dissolution protocol*

### INTRODUCTION

The United Nations Globally Harmonized System of Classification and Labelling of Chemicals (GHS) includes an internationally standardized guidance procedure on Transformation/Dissolution Protocol (T/DP) for metals and sparingly soluble metal compounds (United Nations, 2007), recently validated by the OECD (Organization for Economic Cooperation and Development). To establish the acute aquatic hazard classification level of a metal-bearing substance under the GHS, data from the T/DP are compared with an acute ecotoxicity reference value (ERV) derived under conditions similar to those of the T/DP.

Industry is obligated to submit mandatory dossiers to the REACH (Registration, Evaluation and Authorisation of Chemicals) registry, an environmental protection regulation within the framework of the European Union (EU), and are to include a GHS aquatic hazard classification proposal. Both REACH and the GHS have significant implications for environmental protection

and market access for chemicals in commerce.

Freshwater media based on the OECD 203 ecotoxicity testing medium for fish and daphnia have been used in all T/DP testing of metals, metal compounds and alloys in the pH range 6-8.5 to date. However, the composition of a marine medium is also given in the T/DP section of the GHS, and by implication, a method for marine T/D testing is open for development and validation. While not currently required for REACH dossiers, T/D data in marine media and attendant classification proposals may be required in the future for marine shipping.

### ANALYTICAL PROCEDURE

We followed the OECD guidance document [United Nations 2007, p. 548] for the preparation of a standardized marine test medium. The document states that trace metals should be removed from the test medium before T/D tests are performed. For this step we used a Chelex-100 resin in a column set-up with a flow rate of 5 ml/min.

Prior to analysis, solutions from seven-day T/D tests on cuprous oxide (Cu<sub>2</sub>O) and nickel metal powder (Ni) were passed through a column with iminodiacetate functional groups using an ammonium acetate buffer. The alkali and alkali earth metals are not bound to the column thereby separating the cations associated with the saltwater matrix from the transition metals of interest which are subsequently eluted with nitric acid and analysed by ICP-AES (inductively-coupled plasma-atomic emission spectrometry).

## RESULTS

The reactivity and transformation to yield soluble bioavailable species of metal-bearing substances are expected to be significantly affected by the high chloride content and other unique chemical characteristics of marine waters.

Results of the T/DP testing of copper and nickel on freshwater medium can be found in the CANMET-MMSL report (Skeaff & Hardy 2005). At pH 6 and 100 mg/L loadings, the concentrations of copper and nickel dissolved from cuprous oxide and nickel metal powder attained average seven-day concentrations of about 3,250 and 540 µg/L, respectively. The average seven-day concentrations at pH 8 and 100 mg/L loadings of copper and nickel dissolved from cuprous oxide and nickel metal powder were significantly lower than those at pH 6: about 105 and 315 µg/L, respectively. Preliminary results from the pH 8 marine testing suggest that cuprous oxide powder has a greater reactivity in marine water to the pH 8

freshwater, while nickel metal powder is significantly less reactive in the marine media than in the pH 8 freshwater.

## CONCLUSIONS

This is an on-going project aimed at examining the T/D characteristics of metals and alloys in a marine medium in seven- and twenty eight-day tests. The data obtained to date on seven-day tests of cuprous oxide (Cu<sub>2</sub>O) and nickel metal powder (Ni) provides useful comparisons with those reported earlier for the freshwater OECD 203-based media at pH 6 and 8 (Skeaff & Hardy 2005) and insight into the behaviour of metal-bearing substances used in commerce under marine conditions of the T/DP. The data supports an approach directed to the eventual adaptation, validation and application of the OECD T/DP to marine systems for the purposes of marine hazard classification of metals, metal compounds and alloys.

## REFERENCES

- UNITED NATIONS. 2007. *Globally Harmonized System of Classification and Labelling of Chemicals*, ST/SG/AC.10/30/Rev.2. [http://www.unece.org/trans/danger/publi/ghs/ghs\\_rev02/02files\\_e.html](http://www.unece.org/trans/danger/publi/ghs/ghs_rev02/02files_e.html)
- SKEAFF, J.M. & HARDY, D.J. 2005. Validation Study of the Draft OECD Transformation/Dissolution Protocol for Metals and Sparingly Soluble Metal Compounds, Mining and Mineral Sciences Report-MMSL 04-45(CR)/-Contract No. 6028210, Natural Resources Canada, Ottawa K1A 0G1

## Ferromanganese nodules in Lake George, New Brunswick

Camilla Melrose<sup>1</sup> & Tom Al<sup>1</sup>

<sup>1</sup>Department of Geology, University of New Brunswick, 2 Bailey Drive, Fredericton NB E3B 5A3 CANADA  
(e-mail: camilla.melrose@unb.ca)

**ABSTRACT:** Ferromanganese nodules have been found in temperate freshwater lakes around the world. They form around a central nucleus of detrital rock in concentric iron- and manganese-rich bands. These nodules form when anoxic groundwater carrying dissolved metals seeps into oxygenated lake water, resulting in the formation of oxide minerals. Radiometric dating has shown that the nodules can be as old as the age of the lakes, after the retreat of the last glaciers approximately 10,000 years ago. Transects across nodules from two locations in Lake George, New Brunswick, were analyzed using LA-ICP-MS to determine compositional variations as the nodules grew. The nodules show enrichment in trace metals near the centre that decreases outwards, reflecting changes in groundwater composition over time.

**KEYWORDS:** ferromanganese, nodules, lakes, trace metals, LA-ICP-MS

### INTRODUCTION

Ferromanganese nodules have been identified and described in temperate lakes around the world. These nodules were first described by Honeyman (1881) who thought they were fragments of prehistoric pottery. Further investigation showed that the nodules were composed of iron and manganese oxides (Honeyman 1881).

Ferromanganese nodules found in freshwater lakes show concentric, alternating, iron- and manganese-rich bands radiating out from a central nucleus of detrital rock (e.g. Harriss & Troup 1970). The nodules are found primarily in shallow (1-5 meters depth) regions of lakes, in regions with little to no fine-grained sediment accumulation (e.g. Kindle 1935).

### GEOGRAPHIC SETTING

Ferromanganese nodules found in Lake George, New Brunswick are the focus of this project. Lake George is situated approximately 35 km southwest of Fredericton (Fig. 1).

Lake George is approximately 2.5 km wide and 3.5 km long, with a maximum depth of approximately 4 meters. Nodules were sampled from two locations on either side of the lake for this study (Fig. 2).

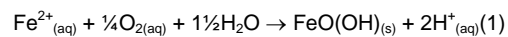


**Fig. 1.** Map of the Maritime Provinces showing the location of Lake George, to the southwest of Fredericton.

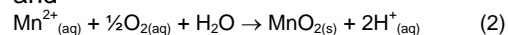
### FORMATION OF NODULES

The nodules form when anoxic groundwater carrying dissolved metals seeps up through the ground-water interface (Fig.3). The dissolved oxygen present in the lake water oxidizes the metals, resulting in the precipitation of iron- and manganese-oxides that form coatings on rock fragments.

Iron and manganese oxidize to form insoluble precipitates by the following reactions:



and



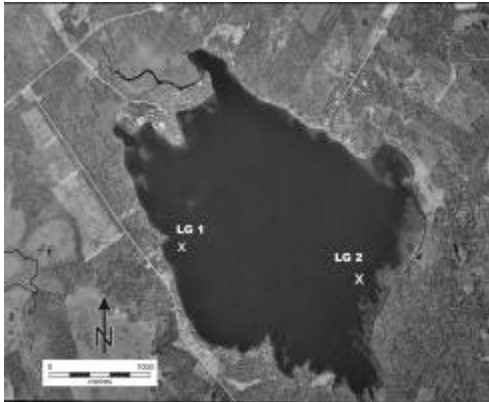


**Fig. 2.** Aerial photograph of Lake George showing the two sampling locations LG1 and LG2.

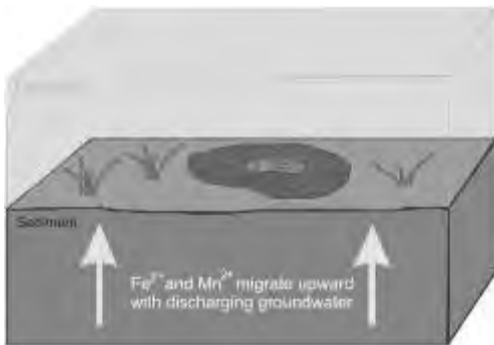


**Fig. 3.** Diagram illustrating the formation of ferromanganese nodules.

$\text{Fe}^{2+}$  will spontaneously oxidize to  $\text{Fe}^{3+}$  by the process shown in reaction 1 under neutral pH conditions in the presence of oxygen (Apello & Postma 1995). Under the same conditions, however,  $\text{Mn}^{2+}$  will remain as a dissolved ion (Apello & Postma 1995). Manganese oxidizing bacteria are common in freshwater lakes (Gregory & Staley 1982), and have been shown to control manganese cycling in the environment (Chapnick *et al.* 1982). As a result, Fe-oxidation is thought to continue year-round, while Mn-oxidation can only occur during the warmer months, when bacteria populations can flourish (Chapnick *et al.* 1982). This episodic pattern of Mn precipitation may explain the concentric banding observed in the

nodules (Fig. 4). Mn-rich bands form during the spring and summer, when the oxidation of manganese is bacterially mediated, and Fe-rich bands would form during the winter, when iron continues to oxidize and precipitate, but Mn-oxidation is arrested (Harriss & Troup 1970).

### AGE OF NODULES

Initial estimates of the growth rates of the nodules, and thus the age of the nodules, were based on the idea that one pair of Fe-rich and Mn-rich bands represent one year's growth. Growth rates of 0.1 to 1.5 mm/yr were calculated based on the thicknesses of the concentric bands (Harriss & Troup 1969). Based on this estimation the largest nodules would be approximately 1600 years old (Harriss & Troup 1969).

Radiometric isotope dating provides a more reliable way to estimate the growth rates and ages of the nodules. Moore and Dean (1979) studied nodules from Oneida Lake, USA, and found that, in cross-section, the nodules were characterized by regions showing little change in the amount of  $^{226}\text{Ra}$  present, followed by sharp decreases in  $^{226}\text{Ra}$  at specific ring boundaries. Such profiles can be explained by a pattern of short periods of concretion growth followed by periods with either no growth or with dissolution of the nodules (Moore & Dean 1979). These measurements give growth rates of 0.009 to 0.016 mm/yr with periods of no growth or dissolution of 500 to 1000 years. At these growth rates the largest nodules would be 10 000 years old (Moore & Dean 1979).

### COMPOSITION OF NODULES

Since the nodules form by precipitation of Fe and Mn in groundwater, and other dissolved constituents originating either from the groundwater or the lake water, the composition of the nodules varies according to their location on the lake bed. A comparison of the groundwater and lake

water at Lake George shows that the groundwater contains relatively high concentrations of dissolved ions compared to the lake water. Table 1 compares the elemental composition of representative groundwater and lake water samples collected at LG2 on Sept 11 2008.

The bulk Fe and Mn composition of the nodules is variable and, they contain a variety of trace elements, including significant amounts of P, Ba and As (Table 2).

LA-ICP-MS was used to determine the compositional variation in the nodules along transects from the central rock nucleus toward the outside edge. Analytical transects were conducted across nodules from LG1 and LG2 (Fig. 4). On each sample, one transect followed the shortest axis (from the nucleus to the top of the nodule) and a second followed the longest axis (from the nucleus to the

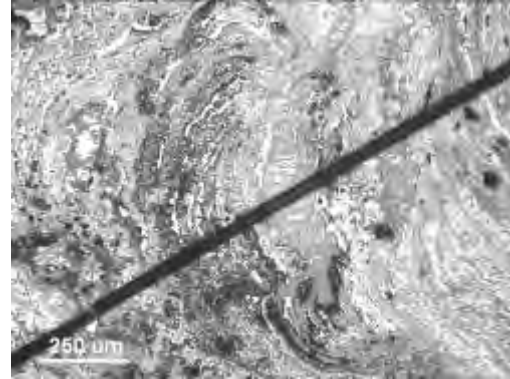


**Fig. 4.** Photograph from a portion of a thin section of a nodule from LG2. The dark line crossing the section shows the path of the laser used during LA-ICP-MS.

**Table 1.** Comparison of the groundwater and lake water composition (μg/L) at LG2 on September 11, 2008.

	Height above lake bed (cm)		
	55	5	-100
<b>Fe</b>	<2	<2	64
<b>Mn</b>	0.6	0.8	616
<b>As</b>	0.14	0.1	89
<b>P</b>	<5	1.5	411
<b>Ca</b>	803	1048	25553
<b>Na</b>	1450	1420	34600
<b>Mg</b>	211	249	3417
<b>B</b>	2.9	3.2	26
<b>Pb</b>	0.19	0.04	0.06

**Table 2.** Bulk composition of four nodules, two from location LG1 and two from location LG2, determined by XRF analysis.

Wt %	LG1		LG2	
	A	B	A	B
<b>Fe<sub>2</sub>O<sub>3</sub></b>	70.24	53.49	35.63	47.47
<b>MnO</b>	16.56	29.75	36.47	35.96
<b>P<sub>2</sub>O<sub>5</sub></b>	0.49	0.33	0.37	0.32
<b>Ba (ppm)</b>	5680	5138	11412	11437
<b>As (ppm)</b>	664.7	287.7	645.5	645.5

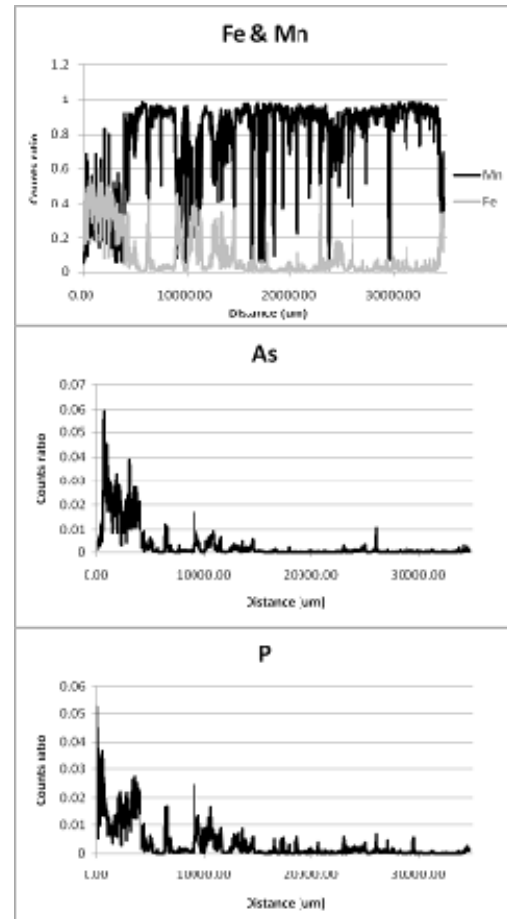


**Fig. 5.** Compositional variation along a transect across a nodule from LG1 analysed by LA-ICP-MS.

MS. The data are presented as count ratios where the counts for each element are normalized to the total counts.

outer rim).

Figure 5 shows the analytical results for Fe, Mn, As and P along a transect across a nodule from LG1. This nodule is enriched in Fe, As and P at the centre. The As and P enrichment are spatially correlated with the Fe-rich areas of the nodule, indicating co-precipitation of these trace elements with the Fe oxyhydroxide minerals. This compositional variation is assumed to reflect changes in the groundwater chemistry over time, potentially since the lake formed.

### CONCLUSIONS

Ferromanganese nodules have formed in temperate lakes around the world. The nodules form by the oxidation of dissolved Fe and Mn in regions of groundwater discharge. Radiometric dating has shown that the nodules grow slowly (Moore & Dean 1979), and can be as old as the lakes in which they are found. LA-ICP-MS transects across the nodules show variable enrichment in trace metals that reflect changes in the groundwater chemistry over time. This characteristic presents significant opportunities for

investigations of paleoclimate and hydrology.

### REFERENCES

- APPELO, C.A.J. & POSTMA, D. 1995. *Geochemistry, groundwater and pollution*. A.A. Balkema Publishers, United States of America.
- CHAPNICK, S.D., MOORE, W.S., & NEALSON, K.H. 1982. Microbially Mediated Manganese Oxidation in a Freshwater Lake. *Limnology and Oceanography*, **27**, 1004-1014.
- GREGORY, E. & STALEY, J.T. 1982. Widespread Distribution of Ability to Oxidize Manganese Among Freshwater Bacteria. *Applied and Environmental Microbiology*, **44**, 509-511.
- HARRISS, R.C. & TROUP, A.G. 1969. Freshwater Ferromanganese Concretions: Chemistry and Internal Structure. *Science*, **166**, 604-606.
- HARRISS, R.C. & TROUP, A.G. 1970. Chemistry and Origin of Freshwater Ferromanganese Concretions. *Limnology and Oceanography*, **15**, 702-712.
- HONEYMAN, D. 1881. Nova Scotia Geology (Superficial). *Proceedings and Transactions of the Nova Scotian Institute of Natural Science*, **5**, 319-331.
- KINDLE, E.M. 1935. Manganese Concretions in Nova Scotia Lakes. *Transactions of the Royal Society of Canada*, **29**, 163-180.
- MOORE, W.S. & DEAN, W.E. 1979. Growth Rates of Manganese Nodules in Oneida Lake, New York. *Earth and Planetary Science Letters*, **46**, 191-200.

## Application of stable hydrogen isotope models to the evaluation of groundwater and geothermal water resources: case of the Padurea Craiului limestone aquifers system

Delia Cristina Papp<sup>1</sup> & Ioan Cociuba<sup>1</sup>

<sup>1</sup> Geological Institute of Romania, Cluj-Napoca Branch, P.O. Box 181, 400750, Cluj-Napoca ROMANIA  
(email: deliapapp@yahoo.com)

**ABSTRACT:** The case of the present free waters system from the Padurea Craiului Mountains and the north-eastern extremity of the Pannonian Basin (Oradea – Felix) is investigated based on the correlation between deuterium, global salt content, and major solutes. All types of groundwaters (springs, drillings, wells) display  $\delta D$  values (-76.1 to -62.3‰) similar to the surface running waters (-76.5‰ to -50.7‰), suggesting that they are meteoric in origin. The global salt content ranges from 48.9mg/l to 1299.9mg/l for the groundwaters and from 47.5mg/l to 665.0mg/l for the surface waters. From the co-variation between the  $\delta D$  values, the global salt content, and the major solutes, as well as from the seasonal variation of these parameters, genetic links could be established. The mineralization of the groundwaters took place by means of an intense underground circulation, markedly on the karst system developed within the Mesozoic deposits of the Padurea Craiului Mountains.

**KEYWORDS:** *deuterium, global salt content, groundwater, Padurea Craiului, Oradea*

### INTRODUCTION

Application of integrated stable hydrogen isotope and hydrogeochemical models to the present free waters systems provides important information on their sources, mixing phenomena and underground dynamics that can be profitably used in problems of groundwater resources management, as well as in environmental protection.

Our work represents an extension of previous studies made by a research team from the Institute of Isotopic and Molecular Technology, Cluj-Napoca (Blaga *et al.* 1981) on the present free waters system from Padurea Craiului - Oradea area (Romania), that includes different sources of groundwaters, surface waters, as well as geothermal waters.

### GEOLOGICAL SETTING

The area under study comprises the western part of the Padurea Craiului Mountains in conjunction with the north eastern extremity of the Pannonian Basin (Oradea – Felix zone). The Padurea Craiului Massif had a long-lasting evolution with a pre-Hercynian start, being

mainly shaped during alpine orogenesis. Most of its formations belong to the Bihor tectonic unit (Ivanovici *et al.* 1976).

The basement is made up of crystalline schists of the meso-metamorphic Somes Series. Sedimentation started during Permian with detritic deposits interbedded with rhyolites. The overlying Triassic deposits are unconformable and include detritic formations (Lower Triassic) and massive layers of carbonate rocks (Middle Triassic). The absence of the Upper Triassic is due to the uplift of the region during the Kimmeric tectonic phase.

The Lower Jurassic deposits include the detritic formation (Hettangian – Lower Sinemurian), the limestone formation (Upper Sinemurian – Pliensbachian) and the marl formation with ammonites and belemnites (Toarcian).

The Middle Jurassic consists mainly of marls. The Upper Jurassic formations are massive (over 100 m thick) and are made up exclusively of limestones. During Upper Jurassic and Lower Cretaceous the limestone deposits have been uplifted and resulted in a paleo-karst surface that hosts discontinuous bauxite deposits. Lower

Cretaceous sedimentation started with the deposition of fresh-water limestones (Hauterivian) followed by successive layers of marine limestones (Barremian), marls (Aptian), marine limestones (Aptian), glauconitic sandstone (Aptian-Albian) and ended with a package of red detritic deposits.

Subsequent positive epirogenetic movements and two main phases of magmatic activity (Upper Cretaceous – Paleocene and Badenian – Pliocene) completed the morphogenesis of the Piatra Craiului Mountains and the formation of the Pannonian basin at the east. The post tectonic cover of the Pannonian basin starts with the Senonian through the Paleogene, Neogene (Miocene and Pliocene) to the Quaternary. The Pliocene deposits of the Pannonian Basin develop on the north-western part of the area under study. They are predominantly pelitic (Bessarabian – Meotian) and psammitic (Pontian – Upper Pliocene).

The most important aquifer systems existing in the region are connected to the Pliocene deposits, and to the Lower Cretaceous – Upper Jurassic and Triassic limestone deposits respectively, all containing cold and thermal waters with varying hydrochemical properties (Tenu 1981). From a hydrogeological point of view, the area (maximum elevation range of 900 – 1020 m) is a heavy-rain area (~1000 - 13000 mm/year), with a snow cap that lasts for 2 - 3 months in the winter (Pascu 1983). The density of the hydrographical network is about 0.5 km/km<sup>2</sup>. Due to the economic and balneological interest of geothermal springs (40 – 50 °C) two well known spas have been founded – Baile Felix and Baile 1 Mai (Oradea).

**SAMPLING AND ANALYTICAL METHODS**

Ninety water sources have been sampled. Deuterium content and global salt content were measured both in the underground sources (springs, drillings, wells) and in the surface sources (running water, precipitation), in order to include all the water types that might interact.

The Institute of Isotopic and Molecular Technology, Cluj-Napoca, performed all the analyses. The routine isotopic analyses were run on a Thomson THN 202D mass spectrometer, with a working precision of ±0.3‰. The uranium method was used to release hydrogen from water. All isotopic data are expressed in conventional δ notation as the permil deviation of D/H ratios with respect to the V-SMOW standard.

The global salt content was measured using a digital densimeter, and is expressed as the density difference of sample water relative to standard distilled water, at 25°C. It is noted as Δd and expressed in units of mg/l. Major solutes within the groundwater samples (Li, Na, K, Mg, Ca, and Sr) were analysed using absorption spectroscopy.

**RESULTS AND DISCUSSION**

Figure 1 summarises the experimental data. All displayed values represent the mean values for one year of observation.

All types of groundwaters display δD values (-76.1‰ to -62.3‰) similar to the surface waters from the studied area (-76.5‰ to -50.7‰) (Table 1), suggesting that they are meteoric in origin. The δD values of the local precipitations vary between -104.7‰ and -45.9‰ during one year of observation. The Δd values range from 48.9mg/l to 1299.9mg/l for the groundwaters and from 47.5mg/l to 665.0mg/l for the surface waters. The

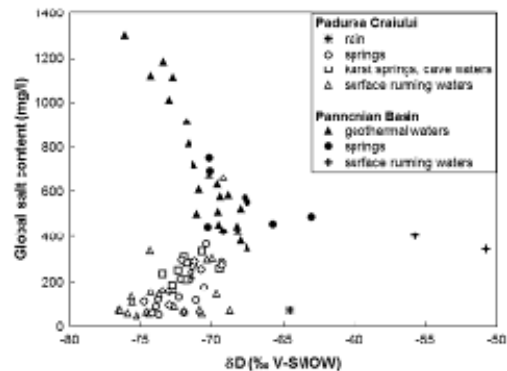


**Fig. 1.** Scatter plot of the δD values and the global salt content of the present free waters from the Padurea Craiului Mountains and the Pannonian Basin (Oradea - Felix).

**Table 1.** Summary of the distribution of the  $\delta D$  values, global salt content and major solutes of waters from the Padurea Craiului Mountains and Oradea - Felix.

	Mean value	Min. value	Max. value	Standard deviation
<b>Padurea Craiului</b>				
<i>Springs (no. of obs. 22)</i>				
$\delta D$ (‰)	-72.0	-74.7	-69.3	1.5
$\delta d$ (mg/l)	180.7	48.9	366.2	92.9
<i>Karst waters (no. of obs. 8)</i>				
$\delta D$ (‰)	-71.8	-73.4	-69.4	1.3
$\delta d$ (mg/l)	257.3	182.1	333.6	49.9
<i>Surface waters (no. of obs. 25)</i>				
$\delta D$ (‰)	-72.9	-76.5	-68.7	2.4
$\delta d$ (mg/l)	154.7	47.6	665.0	138.5
<i>Precipitations (no. of obs. 14)</i>				
$\delta D$ (‰)	-66.8	-104.7	-45.9	20.0
$\delta d$ (mg/l)	74.1	29.0	164.0	34.8
<b>Oradea - Felix</b>				
<i>Geothermal waters (no. of obs. 21)</i>				
$\delta D$ (‰)	-70.6	-76.1	-67.5	2.3
$\delta d$ (mg/l)	706.7	348.0	1299.5	288.8
Li (mg/l)	30.3	0.1	423.3	113.1
Na (mg/l)	28.5	9.5	76.4	19.8
K (mg/l)	9.6	2.6	17.2	5.4
Mg (mg/l)	27.1	1.1	59.6	13.9
Ca (mg/l)	153.13	70.45	245.75	53.1
Sr (mg/l)	2.7	0.3	5.9	1.8
<i>Fossil waters (no. of obs. 2)</i>				
$\delta D$ (‰)	-35.4	-37.3	-33.5	2.7
$\delta d$ (mg/l)	7204.8	5161.7	9248.0	2889.4
Li (mg/l)	3.1	1.2	5.0	2.7
Na (mg/l)	2532.9	2470.9	2595.0	87.7
K (mg/l)	70.2	46.4	94.0	33.7
Mg (mg/l)	14.0	5.1	22.9	12.6
Ca (mg/l)	62.2	13.4	111.0	69.0
Sr (mg/l)	1.4	1.1	1.7	0.4
<i>Springs (no. of obs. 9)</i>				
$\delta D$ (‰)	-67.3	-70.2	-62.3	3.1
$\delta d$ (mg/l)	579.1	423.3	822.0	145.1
<i>Running waters (no. of obs. 2)</i>				
$\delta D$ (‰)	-53.2	-55.7	-50.7	3.5
$\delta d$ (mg/l)	372.9	343.8	401.9	41.1

geothermal waters are characterized by much higher global salt content as compare to other groundwater sources from the study area, suggesting long-way underground circulation.

The higher deuterium content (-35.4‰) and higher global salt content (7204.8mg/l) correspond to two drillings from Oradea (Table 1). The chemical composition, characterized by high Na and K content, distinguish these waters from other groundwaters in the area. In addition, the correlation coefficients between  $\delta D$  and  $\Delta d$  are not significant. These findings are explained by a mixing phenomenon between a major component

of fossil water and a minor component of fresh waters of meteoric origin.

Evidence of the meteoric origin is also based on a series of specific isotopic effects. For waters belonging to the meteoric cycle, temperature variations are the essential factor, which controls their isotopic composition. Both running waters and groundwaters show seasonal variation of the  $\delta D$  values, as well as of the global salt content. Due to the evaporation produced during warm seasons, which determines the enrichment both in deuterium and salts, a positive correlation between the  $\delta D$  values and the global salt content was expected for the running waters. As an example, for the Lesului Valley the correlation coefficient,  $r$ , is 0.72 ( $n=14$ ). However, in many cases a low correlation coefficient or even a negative correlation was obtained, indicating relationships with phreatic waters.

The geothermal waters are less affected by the seasonal variation of temperature, and this suggests deep circulation. However, we could emphasize analogous seasonal variations of the  $\delta D$  values and the global salt content between the geothermal waters and water sources from Padurea Craiului, implying genetic relationships (Fig. 2). In many cases, a shift of 30 – 45 days could be observed in the variation sequences, pleading for a relatively rapid underground circulation.

Significant negative correlations between the  $\delta D$  values and Ca, Sr, and K contents of the geothermal waters have been found, suggesting similar leaching and transportation patterns for these elements. Mg also show negative correlations with the  $\delta D$  values, but less significant, while Li and Na display a slightly positive correlation. Significantly positive correlation coefficient between Ca, Sr, Mg, were obtained for most of the geothermal springs (0.77 to 0.86 ( $n=14$ )). This finding clearly indicates that the mineralization arises from the leaching of salts mainly from carbonate rocks.

## CONCLUSIONS

The results of this study show that:

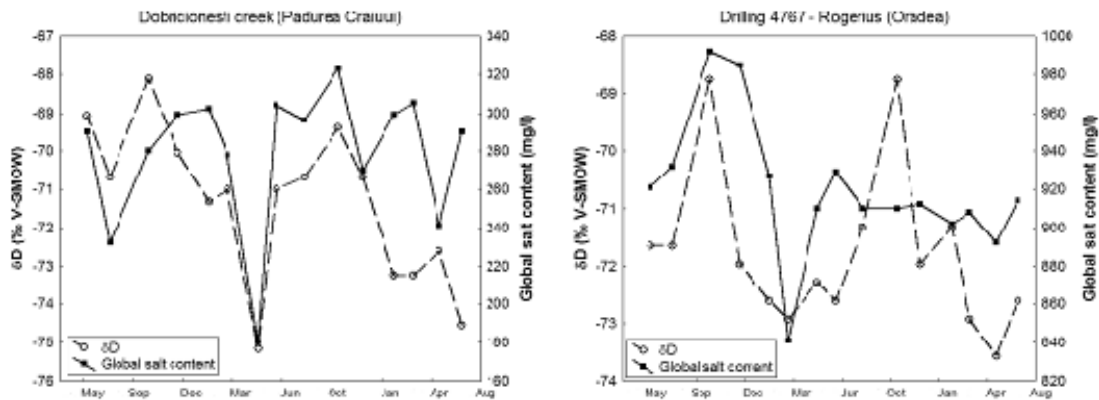


**Fig. 2.** Analogous seasonal variation of the  $\delta D$  values and the global salt content between surface water (Padurea Craiului Mountains) and geothermal water (Oradea).

- (1) the majority of the groundwaters, belong to the meteoric cycle and therefore can be influenced by climatic changes and pollution factors;
- (2) the mineralization of the groundwaters took place by means of an intense underground circulation, markedly on the fracture system developed within the carbonate deposits of the Padurea Craiului Mountains;
- (3) the infiltration of local precipitation is considered the main source of recharge to the groundwater system;
- (4) the high deuterium concentration and global salt content of the water from two drillings from Oradea can be explained by a mixing phenomenon between fossil water and fresh waters of meteoric origin;
- (5) even though the water sources are spread over a relatively extensive area, the similarities in the evolution of their  $\delta D$  values and global salt content emphasise common genetic links. As underground circulation is relatively fast it follows that

pollution of one source has a significant and rapid impact on the whole system.

#### ACKNOWLEDGEMENTS

Liviu Blaga is thanked for the access to his analytical data. The field work was partially funded by the Romanian National University Research Council (PN II, Programme: IDEAS).

#### REFERENCES

- BLAGA, L., BLAGA, L. M., FEURDEAN, V., & BINDEA, C. 1981. Cercetari privind originea si dinamica apelor geotermale din zona Oradea – Felix - 1 Mai, Institute of Isotopic and Molecular Technology, Cluj-Napoca, Romania, *Technical report*.
- INOVICI, V. BOROS, M., BLEAHU, M., PATRULIUS, D., LUPU, M., DIMITRESCU, R., & SAVU, H. 1976. Geologia Muntilor Apuseni. Ed. Academiei RSR, Bucuresti.
- PASCU, M. 1981. *Apele subterane din Romania*. TEHNICA, B. (ed).
- TENU, A. 1981. *Zacamintele de ape hipertermale din NV Romaniei*. Ed. Academiei RSR, Bucuresti.

## The influence of soil and bedrock on trace metal concentrations and groundwater quality in northern Finland

Raija Pietilä<sup>1</sup>

<sup>1</sup>Geological Survey of Finland, Northern Finland Office, P.O. Box 77, 96101, Rovaniemi FINLAND  
(e-mail: raija.pietila@gtk.fi)

**ABSTRACT:** Trace metal concentrations in groundwater in relation to local soil and bedrock were studied at twenty-six sites in the province of Oulu, Finland. The soil at the sites varies from coarse-grained sand to silty till. Soil samples were taken from all the genetic horizons of the podzol profile (A<sub>0</sub>, A, B, C) to a depth of 1 to 2 meters. The trace metal concentrations of the samples were analyzed using three different digestion methods; total digestion (HF-HClO<sub>4</sub>), partial digestion with Aqua Regia and digestion with NH<sub>4</sub>Ac. Synthetic rainwater dissolution was also used for some of the samples. Groundwater samples were collected from springs and observation wells three times a year during 1995-1998 and 2006-2007. The effect of atmospheric wet fallout on pH, anions and the concentration of trace metals in the groundwater was estimated by analyzing rainwater and snowpack samples from the same sampling sites.

**KEYWORDS:** groundwater, soil geochemistry, Oulu, Finland

### INTRODUCTION

Trace metal concentrations in groundwater and their relation to local soil and bedrock as well as seasonal changes in water quality in the province of Oulu, northern Finland (Fig. 1) were studied. Rural study sites were mainly chosen in order to rule out human or industrial impact on samples. Groundwater samples were collected three times a year during two separate time periods (1995-1998 and 2006-2007). The shallow springs (natural or captured) and wells represented mainly short groundwater residence time and samples from plastic pipes in the esker formations represents groundwater with long residence time.

### STUDY AREA

#### Regional Geology

In a broad outline the bedrock of the study area is mainly composed of Archean granitoids and gneisses in the eastern part of the province. The western parts are characterized by Svecokarelian schists and gneisses, and granites and granodiorites in Oulu, Muhos and Vihanti areas. In the southern part there are granitoids, in Puolanka, quartzite and in

the Kajaani and Vuolijoki areas the main bedrock is granite (Fig. 2). However, the composition of bedrock varies considerably within the areas. In the schist areas the presence of calcium- and magnesium-rich interlayers is reflected by elevated concentrations of these elements in the local soil. The major minerals in the granite gneiss areas where bedrock is highly resistant to weathering, especially in Pudasjärvi, are quartz, potassium feldspar, micas and sodium-rich plagioclases (Simonen 1980).

The topography rises towards the east from the coastal area in the west. Half of the study sites are situated in the esker formations and the other half in the basal till areas. The fine-rich tills are mainly composed of quartz, feldspars, amphiboles, chlorites and micas. The sand components are composed of mainly quartz and feldspars and poorly reflect the underlying bedrock (Räisänen *et al.* 1992).

### ANALYTICAL METHODS

The water samples were analysed for pH, redox potential, dissolved oxygen, electrical conductivity, nitrate, nitrite, sulphate, chloride, fluoride, phosphate and

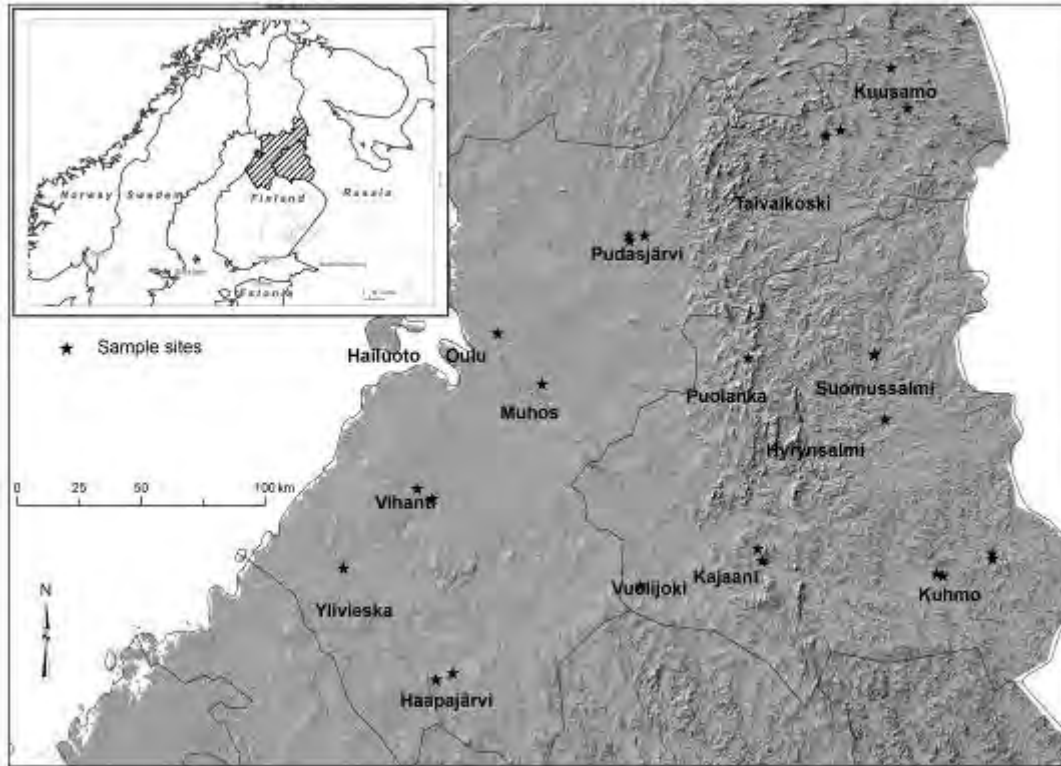


Fig. 1. Shaded relief map of the study area.

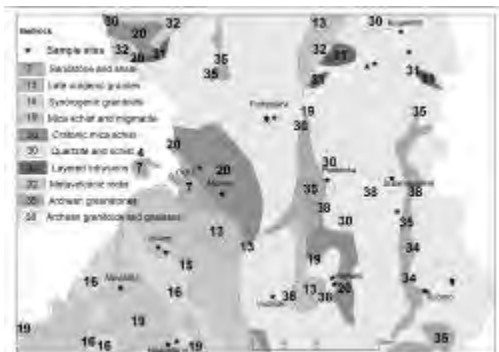


Fig. 2. Bedrock of the study area.

21 elements in the first sampling period. In the later sampling period there were more than 40 analyzed elements.

The podzol profile samples were taken from the groundwater catchment areas from humus ( $A_0$ ) eluvial (A) and illuvial (B) horizons and the parent material (C). In coarse-grained sand areas the profile was poorly developed and mainly 20 cm thick. the thickness in till areas ranged from 40 to 80 cm.

The soil samples were determined for pH, redox potential, electrical conductivity and 15 elements, using total digestion (HF-HClO<sub>4</sub>), partial digestion (Aqua Regia) and with NH<sub>4</sub>Ac.

## CONCLUSIONS

Preliminary results indicate that the character of bedrock significantly affects groundwater quality, especially in Haapajärvi, the south-western parts of the study area (Fig. 3). The arsenopyrite-bearing quartz dikes in mica schists are reflected by higher concentration of As both in local soil and groundwater samples. Arsenic in soil samples was found to be soluble in both weak acid and synthetic rainwater digestions. Mean As concentration of groundwater in the Haapajärvi (HaT in Fig. 4) site is 42 µg/l while the mean for the remainder of the province is less than 1 µg/l. In the eastern part of the province, the soils in the gneiss areas are depleted in most alkali metals

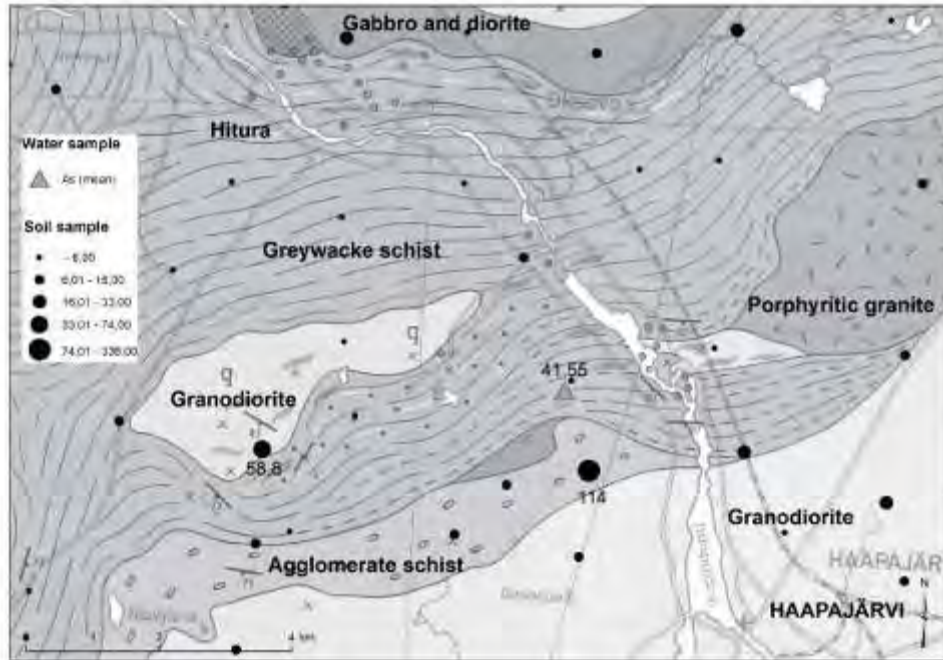


Fig. 3. Arsenic in soil and groundwater in Haapajärvi area

and elements including As, Cr, Fe, Mg, Ni, Pb, and V. The underlying geology is apparent in the groundwater chemistry of the area, which is slightly more diluted than the groundwaters near the coast, where mean concentrations of Ni, Pb, Cr, and Al are higher.

#### REFERENCES

- RÄISÄNEN, M.L., TENHOLA, J., & MÄKINEN, J. 1992. Relationship between mineralogy and physico-chemical properties of till in central Finland. *Bulletin of the Geological Society of Finland*, **64**, 25-58.
- SIMONEN, A. 1980. The Precambrian in Finland. *Geological Survey of Finland, Bulletin*, **304**, 58.



Fig. 4. Arsenic in groundwater.



## Geochemistry of arsenic in the sediment-water interface of an alluvial aquifer, Bangladesh

Md. T. Rahman<sup>1</sup>, Akira Mano<sup>1</sup>, Keiko Udo<sup>1</sup>, & Yoshinobu Ishibashi<sup>2</sup>

<sup>1</sup>Disaster Control Research Center, School of Civil and Environmental Engineering, Tohoku University, Sendai-980-8579 JAPAN (e-mail: litor2005@gmail.com)

<sup>2</sup>Dept. of Civil and Environmental Engineering, Tohoku Gakuin University, 1-13-1 Chuo, Tagajo, Miyagi, 985-8537 JAPAN

**ABSTRACT:** This paper is aiming to unearth the geochemical partitioning of Arsenic in the sediment-water interface with a view to explaining the mechanisms of the occurrence of high Arsenic (As) in the Holocene alluvial aquifer of the South-western Bangladesh. Observed relatively strong correlations of As with Fe, Al, HCO<sub>3</sub> and DOC in groundwater and also with Fe, Al, in sediment reflect the significant role of these elements in leaching As from the brown clay and the grey sand in the sediment-water interface. Sequential extractions followed by mineralogical investigation of the subsurface sediment revealed that Fe and Al minerals may not only be the principal source minerals in releasing As in the upper aquifers but may also be the adsorbent surfaces for As in the deeper aquifer. Potential As source mineral iron-pyrite was detected with XRD and TEM image successfully captured the Fe<sub>2</sub>O<sub>3</sub> contents in the clay sediments. Vivianite and siderite are the two Fe minerals as suggested by the geochemical code PHREEQC that may control the GW Fe and As concentrations. Partition coefficient  $K_d$  was found to vary between 10 to 190 L/Kg. Low  $K_d$  computed for the upper aquifer suggests that leaching that has still been occurring may explain the As mobilization.

**KEYWORDS:** arsenic, contaminated aquifer, leaching, adsorbent surface, mineralogy

### INTRODUCTION

High Arsenic (As) contamination detected in shallow sandy Holocene aquifers in different parts of Bangladesh has been recognized as a severe environmental catastrophe, since the early 1990s. About 45 million people who are heavily dependent on in collecting drinking water from these groundwater sources, are increasingly exposed to this elevated As pollution (Nickson *et al.* 2000; BGS & DPHE 2001; Anawar *et al.* 2002; Smedley 2003; Rahman *et al.* 2009).

Leaching and desorption of As from its associated mineral surfaces such as iron, aluminum and manganese oxides under the influence of the aquifer complex geochemistry, largely take part in its transport from sediment to aquifer pore-water. Adsorption has widely been considered as the retardation of As transport (Smedley 2003).

The objective of this paper is to evaluate the dominant geochemical mechanisms of the Holocene sandy aquifers so as to

focus particularly the partitioning of As in the sediment-water interface.

### STUDY SITE

Samples of groundwater and subsurface sediments were collected from one of the Arsenic hot spots located at a village named as Koyla (22° 51' 03.1" N, 89° 03' 50.9" E, around 300 km from capital city Dhaka) under Kalaroa upazilla of Satkhira district of South-Western part of Bangladesh (Fig. 1). This site is situated on the river Betna and also not so far from a tributary, Kabodak of the Ganges River. The topographic surface of that area is very flat and the land elevation with



Fig.1. Location map of Study area, Kalaroa

respect to the mean sea level does not exceed even 5 m.

**METHODOLOGY**

Groundwater chemical analysis was done with ICP-MS to identify the major anions and cations. Sequential leaching (Koen 2001) coupled with mineralogical investigation was performed to get an account of the mineral compositions of the affected sediments. XRD (X-ray diffraction), SEM (Scanning Electron Microscope), TEM (Transmission Electron Microscope) were utilized for mineralogical study. Speciation analysis was performed and mineral saturation indices were calculated by using the geochemical code PHREEQC (USGS 1998). Sediment-water equilibrium distribution coefficient,  $K_d$  was computed from the ratio of adsorbed As that was found in sediment extraction with the As that was determined to be remaining as dissolved in the groundwater.

**RESULTS AND DISCUSSIONS**

The sequential extractions of As presented in Fig. 2 shows that significant amount of As can be liberated at oxalic extraction phase. This phase is relating with the Fe-mineral adsorption. Strong relationship of the oxalic extracted As and Fe shown in Fig.3 suggests that As should possibly have experienced with desorption together with co-dissolution during the Fe-mineral have undergone partial dissolution process. Fe mineral might be the most dominant one in controlling the As mobilization (Rahman *et al.* 2009a).

Considerable correlation of As with Fe ( $R^2= 53\%$ ), Al ( $R^2= 49\%$ ),  $HCO_3$  ( $R^2= 45\%$ ) and DOC ( $R^2= 42\%$ ) in groundwater (Fig. 4 and 5) suggests that reductive dissolution of Fe and Al hydroxides triggered by microbial activities might have been taken place in releasing As from sediment (Nickson *et al.* 2000; Rahman *et al.* 2009). Solid phase such as bulk mineralogical analysis by XRD, elemental analysis by XRF, elemental mapping by SEM and TEM could further reflect the wide-spread presence of the adsorbent

minerals like iron oxy-hydroxide minerals (Rahman *et al.* 2009).

Roughly, 0.18% of the total mineral composition containing  $Fe_2O_3$  in the brown clay was detected by XRD. Other minerals like quartz, K-feldspar, muscovite, microcline, mica, and pyrite were also identified by XRD data.

The very irregular mineral surfaces of the sediment grains that may suitably offer other anions or cations to be adsorbed

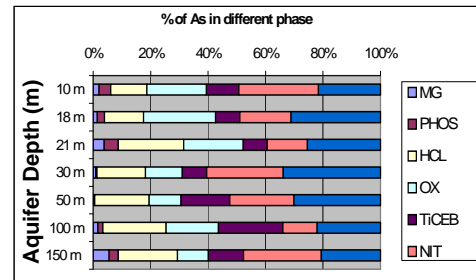


**Fig. 2.** Sequential extraction of Arsenic (MG-magnesium chloride, PHOS-sodium hypo phosphate, HCL-hydrochloric acid, OX-oxalic acid, ToCEB- titanium chloride with EDTA, NIT- nitric acid).

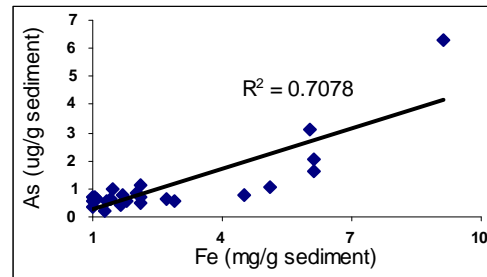


**Fig. 3.** Relationship between oxalic extracted As and Fe.

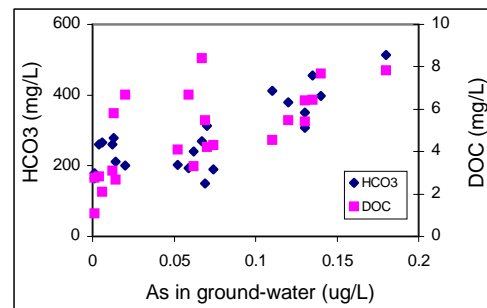


**Fig. 4.** Correlation of As with DOC and  $HCO_3$  in groundwater.

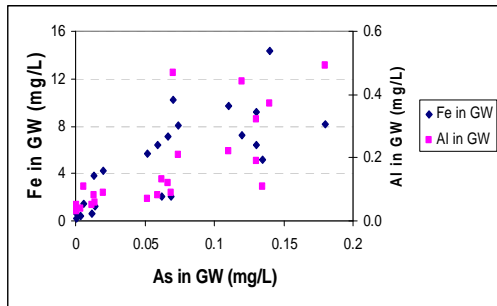


**Fig. 5.** Correlation of As with Fe and Al in groundwater.

can clearly be recognized with this SEM image (Fig. 6).

Observations of the same clay sample in a very finer scale (500 nm) by TEM, may help to identify the potential Fe-oxhydroxide surfaces attached on a sediment grain (Fig.6). Moreover, abundances of wide spread oxides that may have formed oxide minerals after binding with other elements such as Si, Fe and Al can easily be recognized from the right part of the TEM image (Fig. 7).

The variation of As in groundwater ranges between 1 to 180 µg/L and most of elevated concentrations were recorded for the upper shallow aquifers where mostly fine sandy sediments have frequently been noticed (Fig. 8). Oxalic extractable As in sediment has also been observed high in the fine sandy grains (8 µg/g) (Fig. 9). In contrast, the deeper aquifer was found to have contained low As in groundwater as well in sediment.

The partitioning of As in the aquifer solid-water interface can best be explained with the distribution coefficient,  $K_d$  (a ratio of solute adsorbed in sediment to that of dissolved in groundwater). Due to being simplistic in nature,  $K_d$  has long been well appreciated as well as applied by geochemical modelers.

In principle, smaller  $K_d$  values reflects the higher leaching potentiality of adsorbed As from the mineral surfaces in the sediment, whereas larger

$K_d$  values suggest the possible sorption of As onto the Fe as well as other minerals.

The  $K_d$  was found to vary between 10 to 190 L/kg (Fig. 10). A high  $K_d$  was found

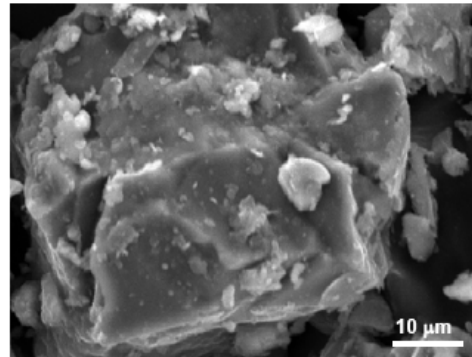


**Fig. 6.** Fe and Al minerals on sediment grain detected by SEM image.

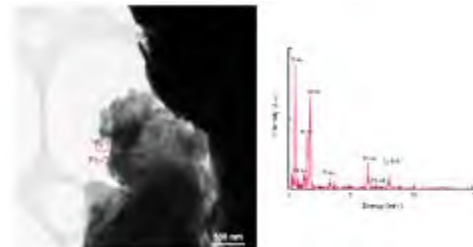


**Fig. 7.** Fe-oxhydroxide minerals on sediment grain detected by TEM.

for the deeper aquifer whereas a low  $K_d$  was computed for upper shallow aquifer. Also, the  $K_d$  was found to vary strongly with the variation of the aquifer parameters including pore water pH, Fe and Al contents of the sediments (Rahman *et al.* 2009). Having a larger amount of Fe, Al minerals, the deeper aquifer sediment may usually contain significant amount of adsorptive sites as compared to the upper aquifer and so the  $K_d$  of the deeper part was also high. Moreover, the mineral dissolution process in the shallower aquifer may have been occurring at a relatively higher rate compared to dissolution at depth. Due to this high dissolution, the potential sorption sites may have been diminishing significantly in number with time. Further more, As absorptive sites in the shallow aquifer may have already been occupied with other competing ions such as  $PO_4$ ,  $HCO_3$  (Rahman *et al.* 2009), These are the probable causes of the differences in As partitioning in the shallow as well as in the deeper aquifer. Thus, the As in the

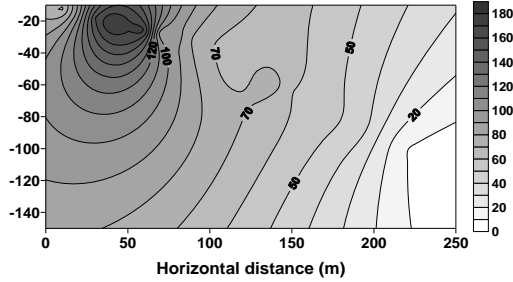


Fig. 8. Variation of Arsenic in groundwater.

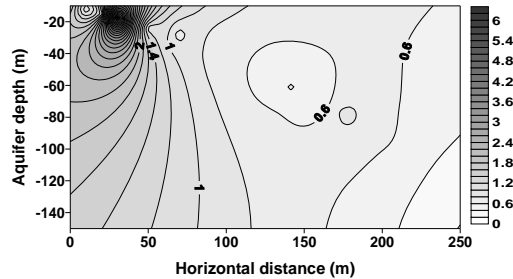


Fig. 9. Variation of Arsenic in aquifer Sediment.

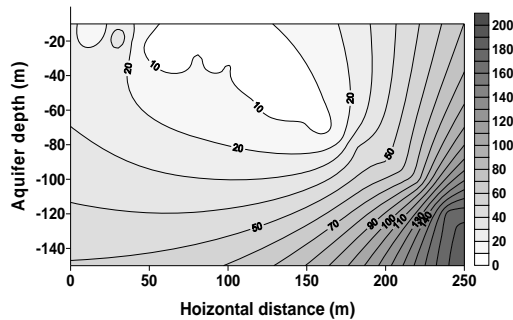


Fig. 10.  $K_d$  variation in the aquifer.

upper shallow aquifer can certainly be reductive dissolution of Fe and Al oxihydroxide mineral under the direct influence of the microbial degradation. Low  $K_d$  values computed in this study strongly support this view. Moreover, the strong correlation of As with Fe, Al, DOC, and  $\text{HCO}_3^-$  also reflect the likely occurrence of reductive dissolution type geochemical phenomena in the studied aquifer. Mineralogical study, further, show the evidences of the presences of the Fe, Al oxide minerals.

### CONCLUSIONS

Results of this present study can be summarized as:

- (1) Arsenic in upper finer sediment has been releasing due to the microbial degradation driven by the dissolution of the Fe-Al minerals;
- (2) computed low  $K_d$  values reflect the likely occurrence of As leaching reactions;
- (3) the deeper aquifer may act as a sink for the leached arsenic, and
- (4) due to the ion competition in groundwater parameters, leached As cannot be re-adsorbed and so high As predominates in the upper shallow aquifer

### ACKNOWLEDGEMENTS

The financial support by the Grant in Aid for Scientific Research from the Japan Society for the Promotion of Science (B-18404009) is sincerely acknowledged.

### REFERENCES

- ANAWAR, H.M., AKAI, J., MOSTAFA, K.M.G., SAFIULLAH, S., & TAREQ, S.M. 2002. Arsenic poisoning in groundwater: Health Risk and geochemical sources in Bangladesh. *Environ. Int.* **27**: 597-604
- BGS & DPHE. 2001. Arsenic Contamination of Groundwater of Bangladesh, Kinniburgh. In: D.G. & SMEDLEY, P.L. (ed.), Vol. 2: Final Report; *British Geological Survey Report WC/00/19*.
- KEON, N.E., SWARTZ, C.H., BRABANDER, D.J., HARVEY, C., & HEMOND, H.F. 2001. Validation of an arsenic sequential extraction method for evaluating mobility in sediments. *Environmental Science and Technology*, **35**, 2778-2784.
- NICKSON, R.T., MCARTHUR, J.M., RAVENSCROFT, P., BURGESS, W.B. & AHMED, K.Z. 2000. Mechanism of Arsenic Poisoning of Groundwater in Bangladesh and West Bengal. *Applied Geochemistry*, **15**, 403-413
- RAHMAN, M.T., MANO, A., UDO, K., & ISHIBASHI, Y. 2009. Geochemistry of Arsenic in the Holocene Aquifer, South-Western Bangladesh. In: PARK, N.S. (ed.), *Advances in Geosciences, Hydrological-Vol*, World Scientific Publication, Singapore (Accepted)
- PHREEQC USGS. 1998. [http://www.brr.cr.usgs.gov/projects/GWC\\_coupled/phreeqc/index.html](http://www.brr.cr.usgs.gov/projects/GWC_coupled/phreeqc/index.html)
- SMEDLEY, P.L. 2003. Arsenic in groundwater South and East Asia. Welch. In: A.H. & STOLLENWERK, K.G. (ed.), *Arsenic in Groundwater Geochemistry and Occurrence*, Springer Science, New York, USA.

## Groundwater as a medium for geochemical exploration in peatlands

Jamil A. Sader<sup>1</sup>, Keiko Hattori<sup>1</sup>, & Stewart M. Hamilton<sup>2</sup>

<sup>1</sup>University of Ottawa, Earth Sciences Department, Ottawa, ON, K1N 6N5 CANADA  
(e-mail: jamilsader@yahoo.com)

<sup>2</sup>Ontario Geological Survey, Sudbury, ON, P3E 6B5 CANADA

**ABSTRACT:** Shallow groundwater in peat displays chemical responses indicating the presence of underlying kimberlites in the Attawapiskat region in the James Bay Lowlands, Canada. The responses include high concentrations of Ni, Cr, Fe, Mg and REEs and elevated values of electrical conductivity, saturation index of CaCO<sub>3</sub>, and alkalinity. These chemical responses are produced by deep groundwaters reacting with kimberlites and upwelling into shallow groundwater. Several elements are conservative and are observed in peat groundwater down the horizontal hydraulic gradient. This study suggests that it is preferable to collect peat groundwater samples deeper into the saturated zone where waters are more reducing and are likely to have higher concentrations of metals. Oxidized groundwaters near the surface tend to produce oxyhydroxides that can adsorb to peat and lower metal concentrations in peat groundwater.

**KEYWORDS:** kimberlite, exploration, geochemistry, groundwater, peat

### INTRODUCTION

In regions where bedrock is hidden by thick sediments, surficial geochemical exploration has been used with a great deal of success. A variety of models and methods have been proposed to explain the migration of elements through the overburden to the surface from hidden kimberlites and other ore deposits (i.e., Hamilton *et al.* 2004a,b; Hattori & Hamilton 2008; Mann *et al.* 2005; McClenaghan *et al.* 2006). These models have focused on geochemical responses in mineral soil.

In many northern regions, peat bogs are widespread. Our study shows that peat groundwater can have geochemical responses consistent with its interaction with kimberlite rocks (Sader *et al.* 2007). The geochemical responses can be different from those in mineral soil. Therefore, exploration in peat bog terrains requires specific sampling methods.

### GEOLOGICAL SETTING

The kimberlites in this study are located in the James Bay Lowlands and are in close proximity to the DeBeers Victor Mine. The kimberlites are mid Jurassic (~170 Ma) in age and have been emplaced into

Paleozoic limestone (Webb *et al.* 2004). These kimberlites all have similar groundmass mineralogies consisting mainly of carbonate, spinel, and serpentine with lesser monticellite, mica, apatite, and perovskite (Kong *et al.* 1999) and they are all of volcanoclastic facies near ground surface. Varying thicknesses of clay and fine marine sediments of the Tyrell Sea (~ 4000 – 12000 years BP) and 1 to 4 m of peat overlie kimberlites (Fraser *et al.* 2005). Bioherms composed of coral and skeletal remains of other marine organisms sometimes outcrop.

### METHODOLOGY

Fieldwork was conducted at Attawapiskat kimberlites (Yankee, Zulu, Alpha-1, Bravo-1, and X-ray), and at the Control location August 14-23, 2007 and October 14-18, 2007. Shallow piezometers were used to collect peat groundwater. At the Yankee and Zulu kimberlites piezometers were installed along transects between 25 to 50 m apart. Between 3 and 5 piezometers were installed at Alpha-1, Bravo-1, and X-ray. Piezometers were typically pushed into the peat 1.1 m with a loosely fitting plastic champagne cork at the end to prevent peat entering the pipe while it was

being pushed down. The pH, oxidation-reduction potential (ORP), electrical conductivity (EC), dissolved oxygen content (DO), temperature, and CaCO<sub>3</sub> alkalinity were measured on-site at the time of sampling for all piezometer, monitoring well, and borehole water samples.

Waters collected from piezometers and monitoring wells were analyzed for metals using an ICP-AES and ICP-MS at the Ontario Geological Survey. Anion contents were also determined at the Ontario Geological Survey using an ion chromatograph.

### RESULTS AND DISCUSSION

Our results indicate that peat groundwater can be an effective medium for surficial geochemical exploration. The dilute, acidic peat groundwaters contrast well with groundwaters that have interacted with kimberlite.

Elevated Ca, CaCO<sub>3</sub>-SI, alkalinity, and EC in peat groundwaters are good indicators of the upwelling of deep groundwater. The data are supported by measured groundwater levels that indicate upwelling (elevated water levels in piezometers and monitoring wells). These parameters are especially good indicators in peatlands because of high contrast between groundwaters that have interacted with rocks and dilute peat groundwaters.

We could identify groundwaters that have interacted with kimberlite rather than host limestone by identifying elevated concentrations of a suite of elements that are related to kimberlites. These elements include Mg, Ni, Cr, and REEs. For example, elevated Mg is found only where waters are discharging over the Yankee kimberlite even though Ca is elevated over the kimberlite plus where groundwater is discharging from the bioherm (Fig. 1). Select elements appear to be more chemically conservative in acidic peat groundwater and can sometimes be found down gradient of the kimberlite margin.

A “reduced chimney” is visible in the peat groundwater over both the Yankee and Zulu kimberlites, where elevated ORP responses correspond with low to non-detectable DO (Fig. 2). The “reduced chimney” model was first described by (Hamilton *et al.* 2004a, b). Elevated ORP and depletion of DO are due to the consumption of oxygen by ascending reduced ions from the kimberlite.

The depth of sampling is important. Deeper samples yield increased elemental concentrations. Our results also indicate

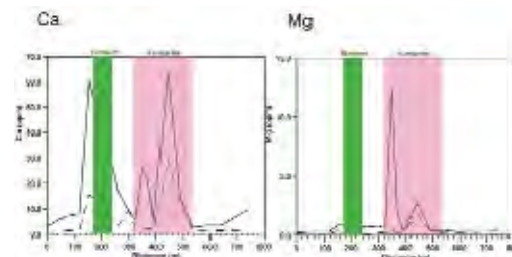


**Fig. 1.** Calcium exhibits a strong response over the kimberlite, but it shows elevated concentration near the bioherm. Magnesium, generally high in kimberlite rock, only shows responses over the kimberlite.

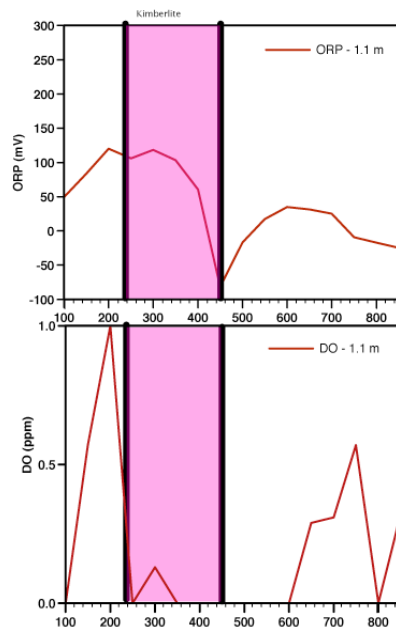


**Fig. 2.** The high ORP values and the corresponding low DO concentration in peat groundwaters along a transect at Zulu is an indication of reduced ions moving to the surface and oxidizing.

that absolute depth below surface is not the only important aspect to consider during sample collection. Samples that are collected deeper below the vadose/saturated boundary tend to be more reducing and have the potential to contain higher elemental concentrations (Fig. 3). Although piezometers were installed at a uniform depth into peat from the surface in this study, the water sampled from the piezometer was not necessarily from the same depth into the saturated zone. These variations can lead to imprecise results and misleading interpretations. A sample that is collected deep into the saturated zone will likely contain higher element concentrations relative to other samples along a transect where groundwaters are not collected as deep. This can erroneously indicate the presence of a buried kimberlite when none really exist.

### CONCLUSIONS

This contribution can be summarized in the following points:

- (1) Kimberlites can be detected in shallow peat groundwater, organic-rich environments using surficial geochemistry.
- (2) Elements that are common to kimberlite rock are elevated in peat groundwater over buried kimberlite.
- (3) The elevated concentrations of reduced ions that are migrating from a kimberlite produce a “reduced chimney” over the kimberlite.
- (4) Unlike the protocol associated with the sampling of the upper B horizon, where reddish-brownish oxidized soil, sitting just below the more leached grayish soil, there are few visual signs in peat to indicate that sample collection is at the appropriate depth. Therefore we are reliant on geochemical and hydrogeological parameters in the field to guide us where best to collect a peat groundwater sample.

### ACKNOWLEDGEMENTS

We thank NSERC Collaborative Research Development Program and DeBeers Canada for financial and in-kind support of this project. We also like to express our gratitude to the Ontario Geological Survey

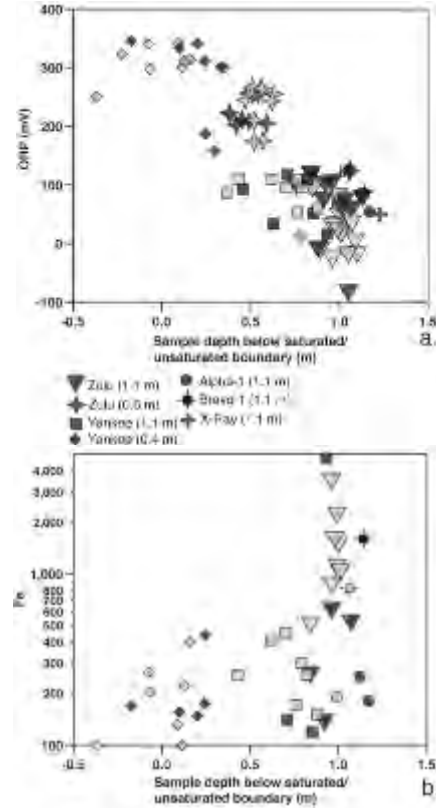


**Fig. 3.** Sample collection deeper into the saturated zone results in more reducing conditions (a) and increase in redox sensitive elements such as Fe (b).

for providing us with invaluable field equipment.

Funding for this project was provided in part by an Ontario Graduate Scholarship (support for Jamil Sader's Ph.D.) and a student research grant from the Society of Economic Geologists.

### REFERENCES

FRASER, C., HILL, P.R., & ALLARD, M. 2005. Morphology and facies architecture of a falling sea level strandplain, Umiujaq, Hudson Bay, Canada. *Sedimentology*, **52**, 141-160.

HAMILTON, S.M., CAMERON, E.M., McCLENNAGHAN, M.B., & HALL, G.E.M.. 2004a. Redox, pH and SP variation over mineralization in thick glacial overburden. Part I: methodologies and field investigation at the Marsh Zone gold property. *Geochemistry: Exploration, Environment, Analysis*, **4**, 33-44.

- HAMILTON, S.M., CAMERON, E.M., McCLENAGHAN, M.B., & HALL, G.E.M. 2004b. Redox, pH and SP variation over mineralization in thick glacial overburden; Part II, Field investigation at Cross Lake VMS property. *Geochemistry - Exploration, Environment, Analysis*, **4**, 45-58.
- HATTORI, K.H. & HAMILTON, S. 2008. Geochemistry of peat over kimberlites in the Attawapiskat area, James Bay Lowlands, northern Canada. *Applied Geochemistry*, **23**, 3767-3782.
- KONG, J., BOUCHER, D.R., & SCOTT SMITH, B.H. 1999. Exploration and geology of the Attawapiskat kimberlites, James Bay lowlands, northern Ontario, Canada. In: GURNEY, J.J., GURNEY, M.D., PASCOE, M.D., & RICHARDSON, S.H.J.D. (eds.), *Proc. 7th Int. Kimb. Conf. Red Roof Design*.
- MANN, A.W., BIRRELL, R.D., FEDIKOW, M.A.F., & DE SOUZA, H.A.F. 2005. Vertical ionic migration; mechanisms, soil anomalies, and sampling depth for mineral exploration. *Geochemistry - Exploration, Environment, Analysis*, **5**, 201-210.
- McCLENAGHAN, M.B., HAMILTON, S.M., HALL, G.E.M., BURT, A.K., & KJARSGAARD, B.A. 2006. Selective Leach Geochemistry of Soils Overlying the 95-2, B30, and A4 Kimberlites, Northeastern Ontario. *Open-File Report - Geological Survey of Canada No 5069*.
- SADER, J.A., LEYBOURNE, M.I., McCLENAGHAN, M.B., & HAMILTON, S.M. 2007. Low-temperature serpentinization processes and kimberlite ground water signatures in the Kirkland Lake and Lake Timiskiming kimberlite fields, Ontario, Canada; implications for diamond exploration. *Geochemistry - Exploration, Environment, Analysis*, **7**, 3-21.
- WEBB, K.J., SCOTT SMITH, B.H., PAUL, J.L., & HETMAN, C.M. 2004. Geology of the Victor Kimberlite, Attawapiskat, northern Ontario, Canada: cross-cutting and nested craters. *Lithos*, **76**, 29-50.

## Quantification of injection fluids effects to Mindanao Geothermal Production Field productivity through a series of tracer tests, Philippines

Benson G. Sambrano<sup>1</sup>, Gabriel M. Aragon<sup>2</sup>, & James B. Nogara<sup>2</sup>

<sup>1</sup>Energy Development Corporation, Merritt Road, Fort Bonifacio, Makati City, Taguig PHILIPPINES  
(e-mail: sambrano.bg@energy.com.ph)

**ABSTRACT:** Tracer tests using naphthalene disulfonates were conducted in Mindanao Geothermal Production Field, Philippines in 2003 and 2006 to describe the extent of the re-injection fluids encroachment to the production sector and quantify its effects to wells performance and over-all field productivity. Modelling was done to predict the effects of RI fluids in terms of output and temperature declines in each production wells using the Icebox<sup>®</sup> software package. Majority of the production wells drilled in this sector indicated positive tracer response with % tracer recovery ranging from 2% to as high as 40%. These substantial amounts of injected fluid could lead to significant decrease in production temperature ranging from 13 to as high as 39°C. The timing of the temperature decline (thermal breakthrough) is highly dependent in the matrix porosity it could be as early as 2 years (porosity = 60 %) or as long as 15 years (porosity = 5 %) in the case of SK2D. The steam availability of the field has an average decline rate of 0.8 kg/month which is solely attributed to reservoir cooling. Changes in the reservoir management were implemented resulting to thermal recovery of the Marbel production sector and sustained overall Mindanao field productivity.

**KEYWORDS:** Mindanao Geothermal Production Field, naphthalene disulfonates, Icebox<sup>®</sup> TRMASS, TRINV, TRCOOL, Marbel, Sandawa

### INTRODUCTION

Mindanao Geothermal Production (MGP) field is geographically divided into three sectors from the northwest to southeast, namely: Kullay-Matingao, Marbel and Sandawa. Steam is produced from Marbel and the Sandawa sectors. There are three injection sinks in the field, namely: Kullay Matingao and Kanlas (Fig.1).

Commercial production began in two-fold with Mindanao-1 (M1) in 1997 and followed by Mindanao-2 (M2) in 1999. M1 draws steam from the Marbel sector and M2 from the Sandawa sector. Geochemical monitoring of the well discharges after nearly a year of production in M1 indicated that injection returns were affecting Marbel sector. Two tracer tests were conducted to establish injection breakthrough from well MT2RD.

The first and second tracer tests used ~20 kgs of sodium fluorescein dye in March 1998 and 1 curie of I<sup>131</sup> in December 1998. The results of these tests

are discussed in the reports of Malate *et al.* (1999) and Delfin *et al.* (1999).

The 2003 tracer tests were conducted in two wells by injecting 400 kg of 1,6 NDS into MT2RD on March 28, 2003 and

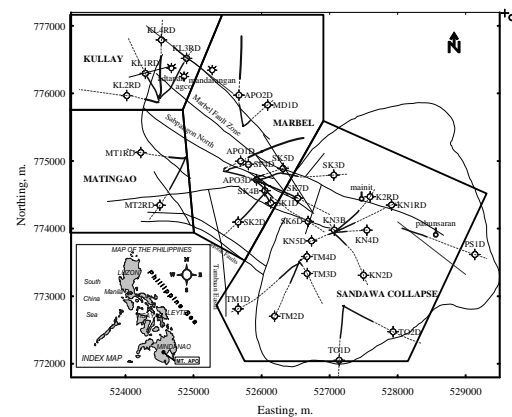


**Fig. 1.** Map of Mindanao geothermal production field (MGPF) showing the geographical boundaries. Philippine map (insert) shows the regional location of the geothermal project (Mt. Apo).

another 400 kg of 2,6 NDS into KL1RD on April 8, 2003. Subsequently in October 2006, 400 kg of 1,5 NDS and 1,3,6 NTS into MT1RD and KL4RD, respectively, and ~350 kg of 2,7 NDS into KN2RD, an injection well within Sandawa production sector. The tracer tests essentially evaluate the injected fluids coming from Matingao and Kullay due to high brine load injection into these sectors. This report presents an update of the tracer tests conducted in the Mindanao Geothermal Production Field.

**STRUCTURAL CORRELATION**

Detailed structural assessment by Pioquinto (1997) established that there are several structural routes connecting Matingao and Kullay injection sinks to the Marbel production sector. The preferential flow of the injection fluids from Matingao and Kullay was further enhanced due to high extraction rate concentrated at the Marbel production sector since majority of the production wells (mostly with high total mass flow, e.g. APO3D at 70 kg/s, SK2D at 72 kg/s and SP4D at 55 kg/s) were drilled and produced from this region.

The probable route and structures included are identified using the following hierarchical criteria: 1) direct and shortest structural connection, 2) interconnection of faults, 3) average breakthrough time of tracer which is directly correlated to tracer concentration and 5) the location of major and minor feed zones within the respective wells.

**NAPHTHALENE DI-SULFONATES**

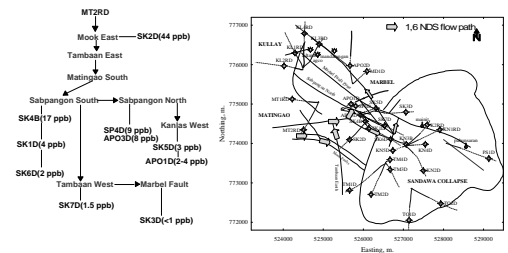
Two injection wells are located inside the Matingao injection sink namely: MT1RD and MT2RD. The combined load of these injection wells averages 220 kg/s with > 120 kg/s being injected at MT2RD. The Matingao sector accepts almost 70% of the total brine effluent obtained from the Marbel production sector. Positive tracer responses were detected in the following production wells in order of decreasing tracer concentrations: SK2D, SK4B, SP4D, APO3D, APO1D, SK1D, SK5D, SK6D, SK7D, SK3D and APO2D after injecting 400 kg each of 1,5 and 1,6

naphthalene di-sulfonate (NDS) in MT1RD and MT2RD, respectively. The most probable passageways of injected fluid from MT2RD as it moves to production sector are shown in Figure 2.

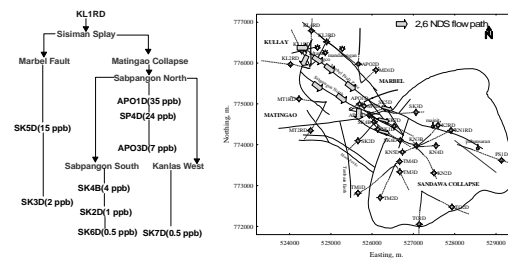
In over a year of monitoring since March 2003, the wells that showed positive tracer responses for 2,6 NDS enumerated in order of decreasing tracer concentrations are APO1D, SP4D, SK5D, APO3D, SK4B, SK3D, SK2D, SK1D, SK7D, SK6D and APO2D. While the same wells in the Marbel production sector indicated 1,3,6 NTS tracer response except for SK2D, SK6D and SK7D. The tracer remains undetected in Sandawa production wells as of this writing.

Figure 3 summarizes the flow paths of the reinjected fluid coming from well KL1RD elucidated through the injection of 2,6-naphthalene disulfonate.

Tracer injected (2,7 NDS) in well KN2RD from within the Sandawa sector were observed in nearly all Marbel production wells except for SK3D at less than 1 per cent overall injected fluid returns. Well APO1D indicated the highest percentage returns at 0.7 % with respect to the 2,7 NDS tracer suggesting a structural flow path through Kinuhaan fault



**Fig. 2.** Most probable flow paths of injected brine in MT2RD to the production sectors.



**Fig. 3.** Most probable flow paths of injected brine in KL1RD to the production sectors.

to Marbel Fault Zone reaching as far as well APO1D. Well SK2D indicated the least transit time of 3.5 months through Tabaco East Splay and Sabpangon South fault. Notably the tracer is undetected as of this writing in nearby Sandawa wells, namely KN3B, KN2D, TM1D and TM2D.

## RESULTS AND DISCUSSION

### Transit Time, Tracer Recovery and injection Fraction

The injection fractions were calculated using the following equation.

$$RI_{\text{Frac}} = (q \times M_r) / (100 \times Q) \quad (6)$$

Where:  $q$  = stable injection rate of injection well,  $M_r$  = % tracer recovered, and  $Q$  = stable production rate.

The profile of the tracer recovery curves (breakthrough curves) is best approximated and simplified using a single channel communication between the injection and production wells both for 1,6 and 2,6 NDS tracers.

The tracer breakthrough for 1,6 NDS injected in MT2RD (Matingao) is relatively faster and more pronounced compared to 2,6 NDS injected in KL1RD (Kullay). The earliest average breakthrough time is 4.7 months with a distance of 1100 meters and maximum tracer concentration of 44 ppb as given by well SK2D. While in 2,6 NDS, the earliest average breakthrough time is 11 months having a distance of 2400 m and maximum tracer concentration of 35 ppb as observed in well APO1D. The data seem logical because of the proportionate spatial differences of the two well pairs.

The total mass of tracer recovered for 1,6 NDS is about 48% or 192 kg out of 400 kg injected (combined mass tracer recovery on all wells affected by 1,6). The residual 52% of the tracer injected possibly dispersed to the reservoir. The bulk of the tracer recovered was obtained in well SK2D amounting to 31% of the tracer mass injected (124 kg) or 65% of the total tracer recovered. Presence of direct structural connection between MT2RD and SK2D through Mook East and proximity of the two wells to each

other explain this observation. Wells located at the margin of the Marbel production sector opposite to Matingao injection sink such as SK5D and SK6D gave minimal tracer recovery of < 2.0%. This implies that the tracer has vastly dispersed upon reaching the northeastern region of the reservoir.

Insufficient data sets were obtained for most of the wells monitored for 2,6 NDS. Data insufficiency is due to the generally longer transit time for 2,6 NDS requiring extended periods of monitoring. Wells APO1D and SP4D indicated a combined tracer mass recovery of about 30% or 120 kg 2,6 NDS out of 400 kg injected following the extended monitoring. Figure 4 shows the combined iso-contours of 1,6 NDS, 2,6 NDS maximum concentrations of both tracers in Mindanao geothermal field reflecting the spatial encroachment of both tracers to the production sectors which mimic the injected fluid coming from the two injection wells (MT2RD and KL1RD).

### Cooling Prediction

Wells with direct communication and closer to the injection sinks have the highest predicted decline in temperatures like SK2D (32°C), APO1D (13°C) and SP4D (13°C). The measured decline in temperatures for these wells based on silica geothermometer in 8 years of utilization is generally lower amounting to 3°C. As mentioned earlier, the timing of decline is uncertain due to unknown porosity value and the 3°C decline observed in these wells could possibly be the signal of the actual onset of thermal decline. Thus, further declines in the production temperatures are expected in the near future if the current injection scheme will be maintained.

In contrast, wells with low predicted reservoir temperature declines like SK5D and SK6D yielded higher actual values in 8 years of utilization. The actual temperature decline observed for SK5D and SK6D are 12°C and 9°C, respectively, but the maximum predicted temperature decline is about 1°C in both wells. The faster decline rates observed for these two

wells cannot solely be attributed to injection returns but possibly to other reservoir and well-bore processes like interplay of feed-zones, formation of scales, e.g. calcite that blocks the contribution of the hotter feed, and movement of other neighbouring fluids that are relatively cooler but with comparable reservoir chloride to the wells involved.

## CONCLUSIONS

- Positive tracer responses were noted in nine (9) production wells located inside the Marbel and three (3) production wells inside the Sandawa.
- Well SK2D has the highest decline value of around 39°C followed by wells APO1D and SP4D with similar decline value of 13°C. The timing of decline is greatly dependent on the actual porosity of the flow-channel where lower porosity value will prolong induction time for thermal decline.
- Temperature declines are also attributed to other reservoir and well-bore processes, e.g. interplay of feed-zones, scaling and inflow of other neighbouring cooler fluids.
- The 1,3,6 NTS injected in KL4RD validated the cold injection in-flow in APO2D which resulted to the continuous decline in the salinity of the well.
- Wells MD1D and SK5D are significantly affected by injected fluids from well KL4RD.
- Brine load reduction in well MT1RD should precede MT2RD since MT1RD has significantly affected well APO3D which has marginal production temperature at ~220°C.
- Brine inflow towards the Marbel production sector from the in-field injection well, KN2RD resulted to abnormal temperature declines in SK3D, SK7D and SK6D which could not be attributed to Matingao and Kullay injection sectors.
- Tracer test in KN2RD suggests a permeability barrier rather than limited

sector capacity which is evident by the positive tracer response of the Marbel production wells.

- Permanent utilization of the in-field Injectors may be detrimental in the long term as it affects the sustainability of the Marbel sector since it blocks the hot recharge towards this sector by creating a fluid barrier.

## ACKNOWLEDGMENT

The authors wish to thank EDC for allowing the presentation and publication of this paper.

## REFERENCES

- ARASON, I. 1993. TRINV: Tracer Inversion Program. Orkustofnun
- ARASON, I. 1993. TRMASS: A program to integrate observed data and give total recovered mass of tracer. Orkustofnun.
- AXELSSON, G., BJORNSSON, G., & ARASON, I. 1993. TRCOOL: A program to calculate cooling of production water due to injection of cooler water to a nearby well. Orkustofnun.
- AXELSSON, G. *et al.* 1994. Injection experiments in low temperature geothermal areas in Iceland. *Proceedings, World Geothermal Congress, 1995, 1991-1996.*
- DELFIN, F.G. JR., MALATE, R.C.M., & ARAGON, G.M. 1999. Tracer tests and injection returns at MGPF. *PNOC-EDC Internal Report, 1999.*
- DELFIN, F.G. JR. & PIOQUINTO, W.P.C. 1999. Alternative analysis of reservoir permeability in the Mt. Apo geothermal project. *PNOC-EDC Internal Report, 1999.*
- GONZALEZ, R.C. *et al.* 1994. Mindanao 1 Geothermal Project: *Resource Assessment Update. PNOC-EDC Internal Report, 1994.*
- HERRAS, E.B. 2004. The Naphthalene Disulfonate Tracer Test in the Mahanagdong Field, Leyte. *Proceedings, 25th Annual PNOC-EDC Geothermal Conference. 2005.*
- NOGARA, J.B. 2004. Tracer Tests Using Naphthalene Disulfonates in Mindanao Geothermal Production Field, Philippines. *Proceedings, 25th Annual PNOC-EDC Geothermal Conference. 2004.*
- PIOQUINTO, W.P.C. 1997. Probable passageways of injection returns and proposed alternative pads of MGPF. *PNOC-EDC Internal Report. 1997.*

## Organic and inorganic surface expressions of the Lisbon and Lightning Draw Southeast oil and gas fields, Paradox Basin, Utah, USA

David M. Seneshen<sup>1</sup>, Thomas C. Chidsey, Jr.<sup>2</sup>,  
Craig D. Morgan<sup>2</sup>, & Michael D. Vanden Berg<sup>2</sup>

<sup>1</sup>Vista Geoscience, 130 Capital Drive, Suite C, Golden, CO, 80401 USA  
(e-mail: dseneshen@vistageoscience.com)

<sup>2</sup>Utah Geological Survey, 1594 West North Temple, Salt Lake City, UT, 84114 USA

**ABSTRACT:** Exploration for Mississippian Leadville Limestone-hosted oil and gas reservoirs in the Paradox Basin is high risk in terms of cost and low documented success rates (~10% based on drilling history). This study was therefore initiated to evaluate the effectiveness of low-cost, non-invasive, organic and inorganic surface geochemical methods for predicting the presence of underlying Leadville hydrocarbon reservoirs. Lisbon field was chosen for testing because it is the largest Leadville oil and gas producer in the Paradox Basin, and the recently discovered Lightning Draw Southeast field with nearly virgin reservoir pressure is also available for comparison. In comparison with Lisbon field, Lightning Draw Southeast field, San Juan County, Utah, is smaller, with more carbon dioxide, nitrogen and helium, and has productive intervals in the overlying Ismay zone of the Pennsylvanian Paradox Formation.

The main conclusion of this study is that hydrocarbon-based surface geochemical methods can discriminate between productive and non-productive oil and gas reservoir areas. Variables in surface soils that best distinguish productive and non-productive areas are ethane and *n*-butane and heavy (C<sub>24</sub>+) aromatic hydrocarbons. Heavy metals (U, Mo, Cd, Hg, Pb) are possibly indirect indicators of hydrocarbon microseepage, but they are more difficult to link with the reservoirs.

**KEYWORDS:** *Lisbon, hydrocarbons, microseeps, metals, exploration*

### INTRODUCTION

Previous work has shown the potential of remote-sensing techniques for identifying kaolinite-enriched, bleached redbed Triassic Wingate sandstones over productive parts of Lisbon field, San Juan County, Utah (Fig. 1) (Conel & Alley 1985; Segal *et al.* 1986). These studies used Landsat Thematic Mapper (TM) data to recognize the presence of kaolinite as well as reduced iron (i.e., bleached redbed sandstones). Other than this work, there are no published surface geochemical studies in the Lisbon field area. The Utah Geological Survey (UGS) therefore initiated this study to test the effectiveness of several conventional and unconventional surface geochemical methods in the Lisbon area. The main objective for testing these techniques is to find effective geochemical exploration

methods to pre-screen large areas of the Paradox Basin for subsequent geophysical surveys and lease acquisition specifically for Leadville Limestone oil and gas reservoirs.

The premise behind surface geochemical exploration for petroleum is that light volatile hydrocarbons (i.e., C<sub>1</sub>-C<sub>5</sub>) ascend rapidly to the surface from a pressured reservoir as buoyant colloidal-size "microbubbles" along water-filled fractures, joints, and bedding planes (Klusman 1993; Saunders *et al.* 1999). In some cases, liquid C<sub>5</sub>+ hydrocarbons also ascend to surface along faults to produce oil seeps at surface. Partial aerobic and anaerobic bacterial consumption of the ascending hydrocarbons produces carbon dioxide and hydrogen sulfide that can significantly alter the chemical and mineralogical composition of overlying

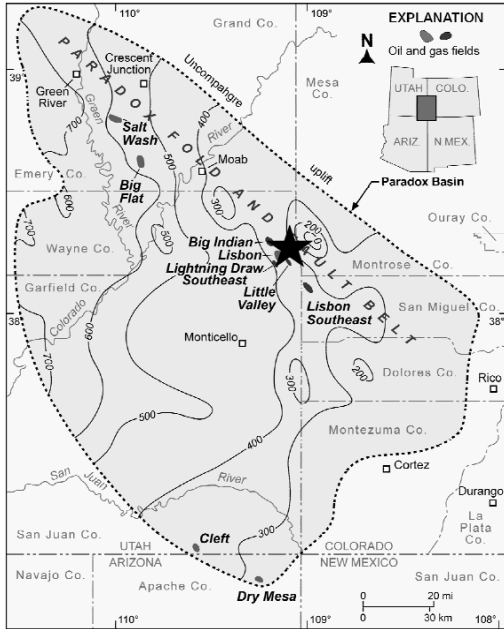


**Fig. 1.** Location of the Lisbon and Lightning Draw Southeast fields in the Paradox Basin of eastern Utah.

sediments and soils (Schumacher 1996). Changes include decreased iron and potassium concentration and increased silica, carbonate, magnetic minerals and uranium.

Both direct and indirect methods were tested in the Lisbon area. Direct methods include the assessment of hydrocarbon compositional signatures in surface soils, outcrop fracture-fill soils and mosses, and 6-ft (2 m) deep free-gas samples. Indirect methods pertain to the major and trace element chemistry of soils to look for alteration effects resulting from hydrocarbon microseepage.

**HYDROCARBON ANOMALIES IN SOILS**

Soil samples were collected at 200 to 500 meter intervals over the Lisbon and Lightning Draw fields and analyzed for thermally desorbed C<sub>1</sub> to C<sub>12</sub> alkanes by GC-FID and solvent-extractable C<sub>6</sub> to C<sub>36</sub> aromatics by fluorescence spectrophotometry.

Aromatic hydrocarbon anomalies are evident in soils over both fields (Fig. 2). The anomalous 4-, 5-, and 6-ring aromatic hydrocarbons, which correspond with

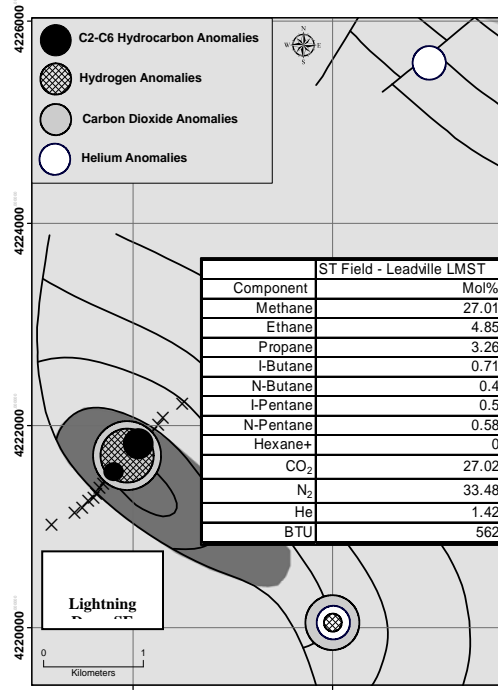


**Fig. 2.** Distribution of 395 to 470nm factor scores in soils over the Lisbon and Lightning Draw Southeast fields, which correspond to high correlation of 4- to 6-ring aromatic hydrocarbons.

395nm, 431nm and 470nm fluorescence peaks suggests the presence of heavy oil seeps at surface. Light alkanes (ethane and n-butane) are the most important variables for discriminating between the productive fields and down-dip water-legs.

**FREE GAS ANOMALIES**

Free gas samples were collected from 6-foot depth with a GeoProbe drill at 50-meter intervals over Lightning Draw Southeast. The samples were analyzed for C<sub>1</sub> to C<sub>6</sub> hydrocarbons by GC-FID and fixed gases (He, H<sub>2</sub>, CO<sub>2</sub>, CO, O<sub>2</sub>, N<sub>2</sub>, Ne, and Ar) by GC-TCD. The gas produced from the Leadville Formation is particularly rich in CO<sub>2</sub> and He, and thus these are key variables for identifying microseepage (Fig. 3). Light alkanes (C<sub>2</sub>-C<sub>6</sub>), H<sub>2</sub> and CO<sub>2</sub> are anomalous over the Lightning Draw field, but He is only anomalous off-structure to the southeast and over the water-leg of Lisbon (Fig. 3).

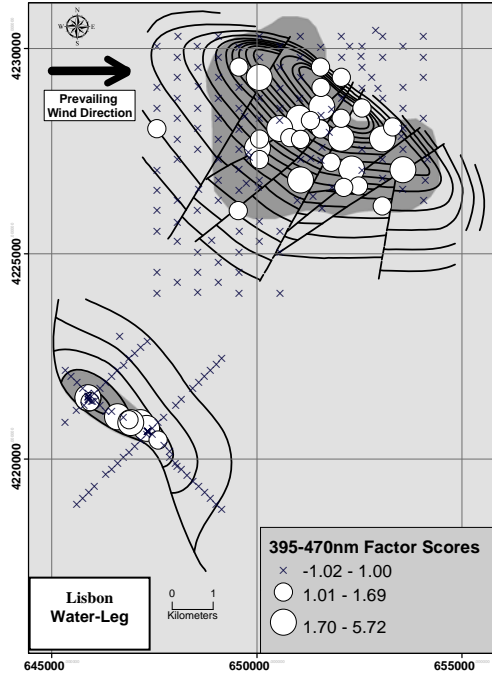


**Fig. 3.** Distribution of alkanes, H<sub>2</sub>, CO<sub>2</sub> and the anomalies in 6-foot deep free gas over the Lightning Draw Southeast field.

### HEAVY METAL ANOMALIES IN SOILS

Soil samples were analyzed for 53, aqua regia extractable elements by ICP-MS/ES. Cadmium, uranium and molybdenum are anomalous over part of the Lisbon field and most of the Lightning Draw Southeast field (Fig. 4). Mercury, lead and organic carbon are also anomalous over both fields.

### DISCUSSION

Light alkane and heavy aromatic anomalies over the Lisbon and Lightning Draw Southeast fields suggest that both volatile and liquid hydrocarbons are ascending to surface from the Leadville Limestone reservoir. The free gas C<sub>2</sub> to C<sub>6</sub>, CO<sub>2</sub> and H<sub>2</sub> anomalies over the crest of the Lightning Draw Southeast field also support the ascent of volatiles from the reservoir. In the case of Lightning Draw Southeast, however, there is also historic oil production from the stratigraphically higher Ismay Zone, and some of the hydrocarbon microseepage may therefore be partially or entirely sourced from this reservoir. The higher CO<sub>2</sub> in free gas over

the field suggests that there is leakage also from the lower CO<sub>2</sub>-rich Leadville Limestone reservoir. The lack of helium anomalies over the field is puzzling, but the anomalies on the margins of both fields may indicate leakage along faults related to salt collapse.

The heavy metal anomalies over both fields are interesting, but more difficult to explain in terms of leakage from the reservoir. The Cd-U-Mo anomalies over Lisbon can be explained by outcropping uranium mineralization in the Chinle Formation (Fig. 4), but there are no outcrops of Chinle exposed at Lightning Draw Southeast. An alternative explanation could be that uranium mineralization eroded from Morrison Formation deposits to the southeast (Fig. 4) is being “fixed” by the hydrocarbon microseepage at Lightning Draw Southeast. The anomalies would therefore be an indirect indication of hydrocarbon microseepage. The mercury and lead anomalies observed over both fields may be derived from the oil seeping to surface.

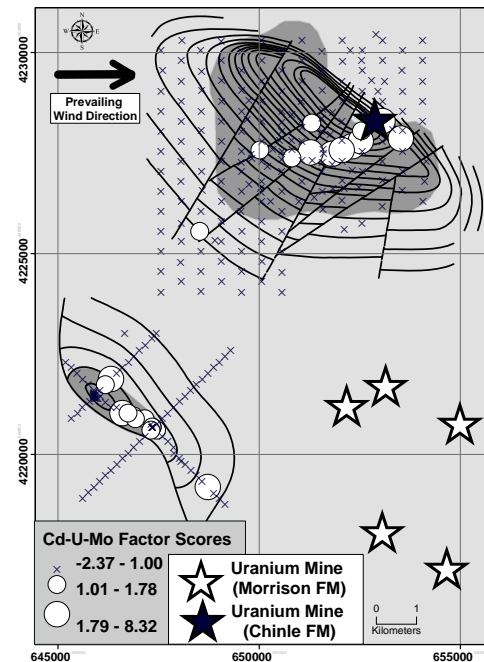


**Fig. 4.** Distribution of aqua regia extractable Cd-U-Mo factor scores in soils over the Lisbon and Lightning Draw Southeast fields

### CONCLUSIONS

The main conclusion drawn from this study is that hydrocarbon- and fixed gas-based geochemical exploration methods in the Paradox Basin are cost-effective tools for pre-screening large areas to focus subsequent lease acquisition and seismic surveys for oil and gas exploration. Heavy metal anomalies are more difficult to link with the reservoir.

### ACKNOWLEDGEMENTS

The Utah Geological Survey and the US Department of Energy are acknowledged for providing funding and logistical support for this study.

### REFERENCES

- CONEL, J.E. & ALLEY, R.E. 1985. Lisbon Valley, Utah uranium test site report. In: ABRAMS, M.J., CONEL, J.E., LANG, H.R., & PALEY H.N. (eds.), *The joint NASA Geosat test case project – final report: AAPG Special Publication, pt. 2, 1, 8-1 - 8-158.*
- KLUSMAN, R.W. 1993. *Soil gas and related methods for natural resource exploration.* Chichester, John Wiley & Sons, 483 p.
- SAUNDERS, D.F., BURSON, K.R., & THOMPSON, C.K., 1999. Model for hydrocarbon microseepage and related near-surface alterations: *AAPG Bulletin*, **83**, 170-185.
- SCHUMACHER, D. 1996. Hydrocarbon-induced alteration of soils and sediments. In: SCHUMACHER, D. & ABRAMS, M.A. (eds.), *Hydrocarbon migration and its near-surface expression: AAPG Memoir*, **66**, 71-89.
- SEGAL, D.B., RUTH, M.D., & MERIN, I.S. 1986. Remote detection of anomalous mineralogy associated with hydrocarbon production, Lisbon Valley, Utah. *The Mountain Geologist*, **23** (2), 51-62.
- CONEL, J.E. & ALLEY, R.E. 1985. Lisbon Valley, Utah uranium test site report. In: ABRAMS,

## **Aqueous geochemistry of Pit Lake at EL mine site, Manitoba, Canada: Implications for site remediation.**

**Nikolay V. Sidenko<sup>1</sup>, Donald Harron<sup>1</sup>,  
Karen H. Mathers<sup>1</sup>, & J. Michael McKernan<sup>1</sup>**

<sup>1</sup>*TetrES Consultants Inc., 603-386 Broadway, Winnipeg, MB, R3C 3R6 CANADA  
(e-mail: nsidenko@tetres.ca)*

**ABSTRACT:** Geochemistry of the Pit Lake was studied to understand processes controlling migration of metals in order to make recommendations for rehabilitations of EL – mine site, Lynn Lake Manitoba. After the closure of Cu-Ni EL Mine in 1963, the former open pit and the shaft were apparently connected (by blasting the crown pillar). Subsequent flooding of the former shaft caused the formation of Pit Lake. Pit Lake was found to be meromictic with a thermocline and a chemocline coinciding at depth of ~20 m, where former open pit was connected to the shaft. The mixolimnion (0-20m) has lower pH (~5) and higher concentrations of Al, Cu and Zn, but lower concentrations of Ni, Fe and major ions in comparison with the monimolimnion (20-130 m). The chemistry of mixolimnion appears to be controlled by acidic runoff and seepage from the overburden. Within the monimolimnion, slow processes of neutralization and metal attenuation dominate over acid generation and release of metals. The monimolimnion of Pit Lake can therefore be considered as having potential for serving as a long-term repository for different sulfide wastes occurring around Lynn Lake.

**KEYWORDS:** *open pit lakes, metal leaching, mine waste, rehabilitation*

### **INTRODUCTION**

Environmental assessments of open-pit mines include an understanding of geochemical processes, which control production of acidity and migration of metals (Davis & Ashenberg 1998, MEND 1991).

The EL Mine site was located 3.5 km south of the Town of Lynn Lake, Manitoba (Fig. 1). The mine was operated between 1954 and 1963 using open pit and underground mining techniques. Copper-nickel ore was associated with gabbro, pyroxenites and peridotites. At mine closure, a crown pillar was apparently blasted, connecting the underground workings to the open pit. The workings and the pit started to flood in 1976 forming Pit Lake. Pit Lake was surrounded by piles of overburden in order to divert water from the open pit during the mining (Fig. 1). The overburden contains fragments of sulfides and has negative net neutralization potential, which causes acid generation and metal leaching (TetrES 2009).

The objective of this study was to understand the geochemistry of the Pit Lake in order to recommend effective options for site remediation.

### **METHODS**

Bathymetry of Pit lake was studied using sonar. Sampling of the water column was performed with a Kemmerer sampler on August 18 and September 20, 2008. Temperature, pH, redox potential and conductivity were measured immediately after sampling using meters calibrated against standard solutions. Samples were field filtered through 0.45 mm filter and divided into two aliquots, for analyses of metals and major ions. The aliquot for metals was preserved with nitric acid to pH<2. All samples were kept at temperature near 4°C until delivered and analyzed by ALS laboratory, Winnipeg. Saturation indexes were calculated using the WATEQ4f computer program (Ball & Nordstrom 1999). The activities of the Fe redox couple were calculated from measured Eh.

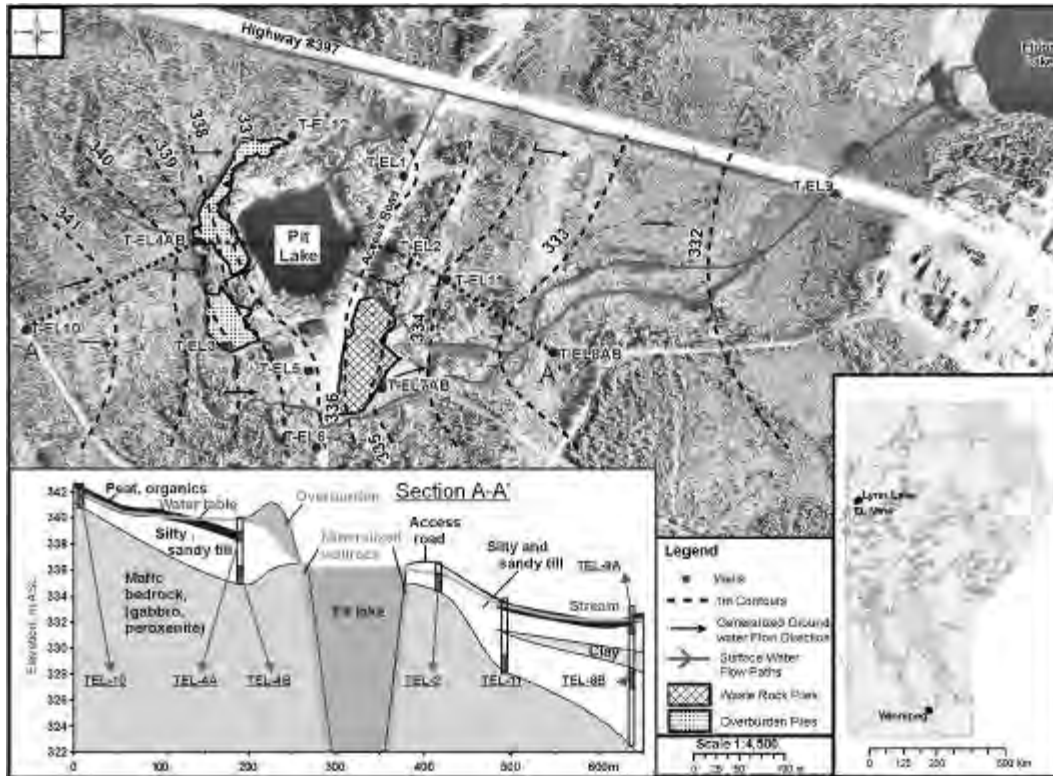


Fig. 1. Surface- and groundwater flows at former EL mine, Lynn Lake, Manitoba.

## RESULTS AND DISCUSSION

Bathymetry shows that the shape of Pit Lake resembles of a funnel with the an upper surface diameter of ~110 m and the diameter of the “neck” of ~50 m. The depth from the surface of the lake to the “funnel neck” is approximately ~20 m (the approximate position of the former crown pillar) and the total depth of the lake is ~130 m. Lake outflow is controlled by a culvert at elevation 236.4 m above sea level. Field investigation indicates that the lake is fed by surface runoff and seepage of groundwater through the overburden and fractured walls of the pit (Fig. 1).

Depth profiles of physical and chemical properties of Pit Lake indicate that the lake is divided into two zones with a boundary at the depth at ~20 m. The upper zone (mixolimnion) is characterized by variable temperature, redox and pH compared to lower zone (Figure 2). Lower zone (monimolimnion) is anoxic, and has relatively stable temperature, redox

conditions and pH. Concentrations of total dissolved solids (TDS) increase with depth and have an inflection point near the boundary between the zones (~20 m). Calculations of water density from different temperature and TDS across water column indicate that the lake does not have a complete turnover. Therefore, the lake can be classified as meromictic with a thermocline and a chemocline coinciding at the depth ~20 m, which are controlled by the morphology of the lake. Concentrations of major ions (Ca, Mg, K, Na sulfate and bicarbonate) are similar to profile of TDS and increase with depth (Fig. 2). Iron concentrations sharply increase near the thermocline and remain constant below, indicating anoxic conditions at the monimolimnion, deeper than 20 m (Fig. 2). Thermodynamic calculation shows that the water column is close to ferrihydrite saturation indicating that redox conditions in Pit Lake are likely controlled by  $Fe^{2+}/Fe(OH)_3$  couple (Fig. 3).

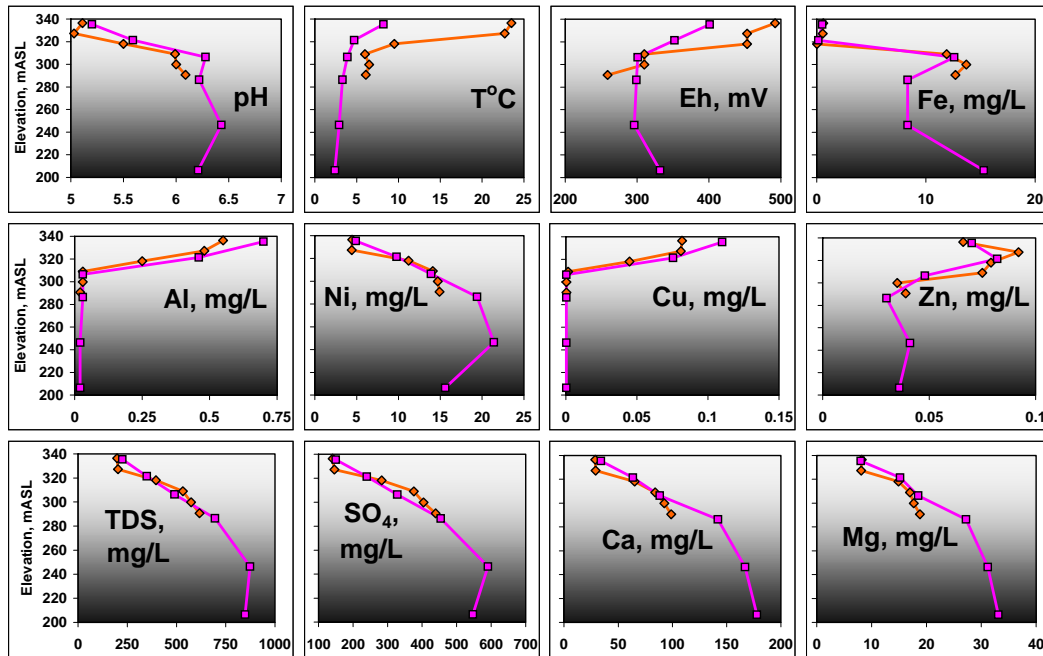


**Fig. 2.** Depth profiles of physical and chemical parameters in Pit Lake, August (diamonds) and September (boxes).

Aluminum concentrations are greater in the mixolimnion and negatively correlate with pH. Pit Lake is slightly supersaturated with respect to amorphous Al-hydroxide (Fig. 3). This fact indicates that concentrations of aluminum appears to be controlled by the solubility of  $Al(OH)_3$ , which is pH-sensitive. Concentrations of Ni are four times lower in the upper zone of the lake than in the lower zone. By contrast, significantly more Cu and Zn are found in the mixolimnion compared with the monimolimnion. Such distinction in the behaviour of elements that originated from the oxidizing sulfides can be explained by different rates of metal release or attenuation in two zones of the lake. The lower zone (monimolimnion) likely represents the chemistry of Pit Lake after the flooding of EL mine, with some later changes associated with adsorption of metals onto the Fe-hydroxides and neutralization resulting from dissolution of Ca and Mg pyroxenes, amphiboles and basic pascioclase (Jambor 2003). Metal affinity for Fe-hydroxides decreases in the order  $Cu > Zn > Ni$  (Walton-Day 2003). Therefore, Cu and Zn were likely more

easily scavenged from solution than Ni in the monimolimnion. The upper zone (mixolimnion) receives acidic runoff and seepage from the overburden, which lower pH and causes Cu, Zn and Al to be more mobile than in the lower zone. The mixolimnion was diluted with respect to Ni since Pit Lake was formed.

### CONCLUSIONS

- (1) Pit lake at the former El Mine is a meromictic lake with a thermocline and a chemocline coinciding at the depth ~20 m, where former open pit was connected to the shaft.
- (2) The chemistry of mixolimnion (0-20m) appears to be controlled by acidic runoff and seepage from the overburden, which contains fragments of sulfide minerals.
- (3) Below the chemocline, slow processes of neutralization and metal attenuation dominate over generation of acid and release of metals. Pit Lake, can therefore be considered as a potential long-term repository for different sulfide wastes occurring around the site and the town of Lynn Lake.

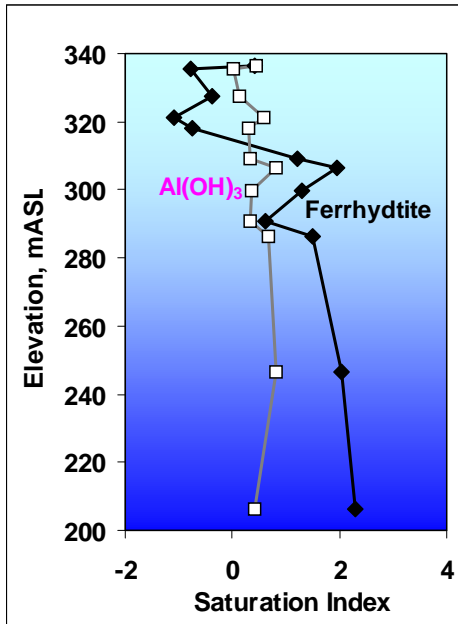


Fig. 3. Saturation indices of Fe (diamonds) and Al (boxes) and hydroxides in Pit Lake.

#### ACKNOWLEDGEMENTS

This study was funded by Division of Science, Technology Energy and Mines of Manitoba Province.

#### REFERENCES

- BALL, J.W. & NORDSTROM, D.K. 1991. User's manual for WATEQ4f, with revised thermodynamic data base and test cases for calculating speciation of major, trace, and redox elements in natural waters. *US. Geological Survey Open-File Report 91-183*.
- DAVID, A. & ASHENBERG, D. 1988. The aqueous geochemistry of Berkly Pit, Butte, Montana, USA. *Applied Geochemistry*, **4**, 23-36.
- JAMBOR, J.L. 2003. Mine waste mineralogy and mineralogical perspectives of acid-base accounting. In JAMBOR, J.L., BLOWES, D.W., & RITCHIE, A.M.I. (eds.), *Environmental aspects of mine waste, Mineralogical Association of Canada Short Course*, **31**, 117-147.
- MEND 1995. Review of in-pit disposal practices for the prevention of acid drainage – case studies. *MEND Report 2.36.1*.
- TETRES CONSULTANTS INC. 2009. *Environmental Site Assessment for EL-Mine Site, Lynn Lake, Manitoba*. Report to Manitoba Mines Branch, Winnipeg.
- WALTON-DAY, K. 2003. Passive and active treatment of mine drainage. In: JAMBOR, J.L., BLOWES, D.W., RITCHIE, & A.M.I. (eds.), *Environmental aspects of mine waste, Mineralogical Association of Canada Short Course*, **31**, 117-147.

## The case for logratio based grain-size normalization of sediment

Robert C. Szava-Kovats<sup>1</sup>

<sup>1</sup>*Inst. Of Ecology and Earth Sciences, University of Tartu, Lai 40, Tartu, 51005 ESTONIA  
(e-mail: robszav@ut.ee)*

**ABSTRACT:** Normalization of sediment is performed to mitigate the confounding effects of grain-size and mineralogical differences on the distribution of contaminants, such as heavy metals. Normalization has typically entailed linear regression analysis of a contaminant by a normalizing agent, either an element or compound. This method fails to recognize the inherent risk of statistical analysis of “raw” compositional data. Reanalysis of published data with a multivariate log-ratio approach reveals that the assumption that the normalizing agent maintains a linear relationship with clay content is nebulous. Furthermore, relationships between contaminants and normalizing agents are likely confounded by spurious correlation with other components. Therefore, the traditional approach to normalization is suspect and may lead to erroneous interpretations. Log-ratio methods are recommended.

**KEYWORDS:** *grain-size, normalization, compositional data, trends, principal component analysis*

### INTRODUCTION

The ability of sediments to adsorb contaminants makes sediment analysis an effective tool with which to assess and monitor contamination in marine environments. This ability is largely a joint function of grain-size distribution and mineralogy. Normalization is a common approach to compensate for grain-size and mineralogical differences in sediment (Horowitz 1991). Normalization often entails regression analysis of a contaminant against a ‘conservative’ element, (e.g. Al, Li, Fe) – one thought to represent the clay-sized fraction and/or presumed to have no anthropogenic input – or some other compound, such as organic carbon. The normalizing agent is usually selected based on the strength of the correlation with the contaminant (e.g. Aloupi & Angelidis 2001).

This approach, however, fails to consider the inherent nature of ‘compositional data’, i.e. all components are restricted to positive values with the sum of all components totalling 100%. These restrictions make suspect statistical analysis based on “raw”, untransformed data. Log-ratio transformations, developed by Aitchison (1982), rid compositional data

of these constraints and allow statistical analysis within Euclidean space.

We examine grain-size normalization by means of multivariate log-ratio techniques. Specifically, published data are reanalyzed to explore the relationship between normalizing agents and grain-size composition, and to compare the log-ratio method with the traditional approach of heavy metal normalization.

### DATA SOURCES

The data for this reanalysis comes directly or has been derived from two published studies of marine sediments: the Gulf of Trieste (Covelli & Fontolan 1997) and the Aegean Sea (Aloupi & Angelidis 2001). The former study provides grain-size data and measurements of Al<sub>2</sub>O<sub>3</sub>, Fe<sub>2</sub>O<sub>3</sub>, CaO, MgO, as well as total and organic carbon, from which non-organic carbon – expressed as CO<sub>2</sub> – was calculated. The latter study provides potential normalizing agents: CaCO<sub>3</sub>, organic C, Al<sub>2</sub>O<sub>3</sub>, Fe<sub>2</sub>O<sub>3</sub>, Mn, and Li, and heavy metal concentrations, of which we examine Zn. Both datasets also contain a component, “other”, the remainder of the composition. Instrumental analysis for major elements in both studies was preceded by a so-

called “total” (hydrofluoric-nitric-perchloric-hydrochloric) digestion.

### MATHEMATICAL METHODS

The constraints on compositional data create induced correlations on the components in a composition: a change in the value of any component must be compensated by corresponding changes in other components. However, log-ratio transformation rids compositional data of these constraints, thus enabling components to vary independently. For a detailed description, readers are referred to Aitchison (1982) or Buccianti *et al.* (2006).

Grain-size and geochemical trends in this reanalysis were calculated from the first component derived from a Principal Component Analysis (PCA) of covariance matrices resulting from *centered log-ratio* transformation (van Eynatten 2004; Szava-Kovats 2008). Given a  $d$ -part composition,  $\mathbf{x}=[x_1, \dots, x_d]$ , the log-ratio transformation to composition  $\mathbf{y}$  is

$$y_n = \ln (x_n/x_G) \quad n = 1, \dots, d \quad (1)$$

where  $x_G$  is the geometric mean of the  $d$  components of  $\mathbf{x}$ . The retransformation from  $\mathbf{y}$  to  $\mathbf{x}$  is

$$x_n = \exp(y_n)/\sum[\exp(y_1), \dots, \exp(y_n)] \quad (2)$$

The first PC provides a set of  $d$ -dimensional loadings, which can be transformed by (2) into a compositional data array,  $\mathbf{L}$ , and a PC score,  $S$ , for each  $\mathbf{y}$ . The first PC expressed as compositional data is calculated by the perturbation operation

$$\mathbf{x} = C[g_1L_1^S, \dots, g_dL_d^S] \quad (3)$$

where  $g$  is the geometric mean for a given component and  $C$  is the closure operation to sum to 100%. The compositional trends of each component of the first PC is calculated from (3) as a continuous function of  $S$ . The percentage of the total variance expressed by the first PC is a measure of goodness-of-fit.

### GRAIN-SIZE TRENDS (GULF OF TRIESTE)

The first PC accounts for 83.6% of the total variability. Linear log-ratio analysis often features markedly non-linear trends when transformed into compositional data (Fig. 1). As the clay content increases from 0, the trend reveals a rapid decline in sand, compensated largely by an increase in the silt fraction. Once the clay content approaches 40%, the sand content becomes exhausted and the silt fraction then begins to decrease with increasing clay. The log-ratio approach realistically models a theoretical transition from a high to low-energy environment (Szava-Kovats 2008). The chemical composition trend sees  $\text{Al}_2\text{O}_3$  and  $\text{Fe}_2\text{O}_3$  increasing concurrently with increasing clay content, whereas  $\text{CaO}$ ,  $\text{MgO}$  and  $\text{CO}_2$  exhibit a similar decrease. Organic C displays a slight increase and “other” – dominated by  $\text{SiO}_2$  and alkali metals – shows an initial rise followed by a decline.

This set of chemical trends suggests carbonates dominate the coarser fractions and Al-silicates dominate the finer grained fractions. However, the Al-Fe trend is non-linear, which, combined with the decline in “other”, suggests replacement of coarser-grained Al-silicates by clay minerals with increasing clay. Because clay minerals have surface areas orders of magnitude greater than silt or sand, the absorption potential of sediment is governed largely by clay content. Thus, a normalizing agent, such as Al, may not necessarily reflect the true absorption capacity. In this example, not only is the trend non-linear, but sediment with very little clay contains considerable amounts of Al.

### Zn NORMALIZATION (AEGEAN SEA)

The authors of this study divided their dataset into harbour and offshore sediments, assuming that the latter are contaminant-free, and used Li as the normalizing agent. All samples were compared to the regression equation based on the offshore sediments, which indicated considerable Zn contamination – with some samples >3 times background

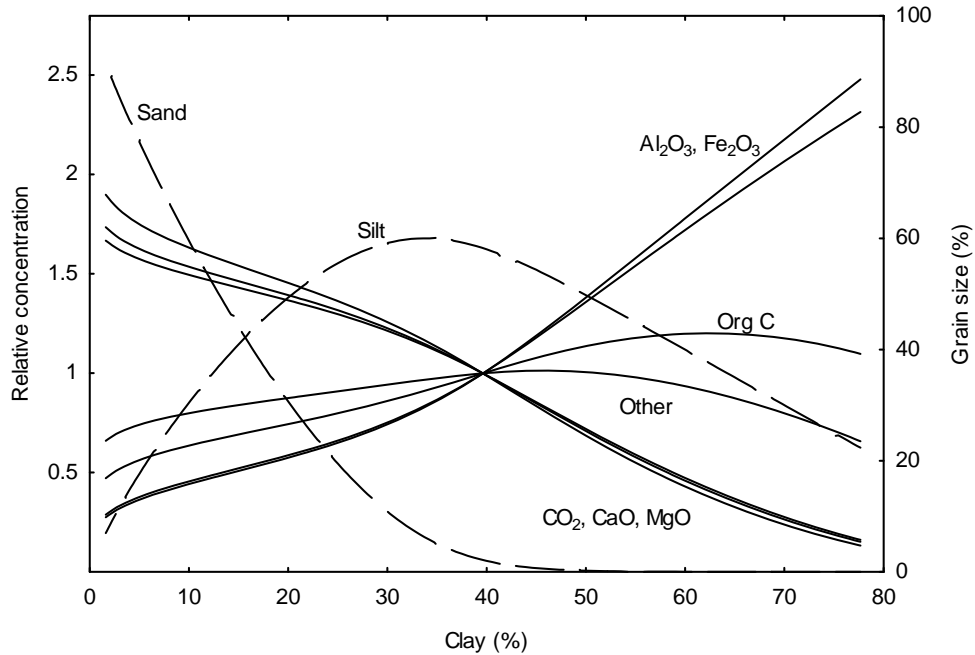


**Fig. 1.** Log-ratio-based normalization trends for Gulf of Trieste sediments. Grain-size fractions measured in %, chemical components scaled to relative abundance.

concentration – in most of the harbour samples (Fig. 2). Analysis of the complete dataset results in a significantly different regression fit and subsequently a vastly different interpretation.

Normalization was performed with the log-ratio method on both the entire dataset and the offshore subset. Biplots of the factor loadings show little difference between the two analyses (Fig. 3). The first PC accounts for no less than 75% of the variance and the loadings of the individual components are similar. Although the original study was based on Li normalization, the log-ratio PCA suggests greater affinity of Zn with organic C. More importantly, the similarity of the two sets of factor loadings indicates that the relationship among Zn and the other components changes little by limiting the analysis to offshore samples. In other words, the only genuine difference among the two datasets is the location of central tendency, and that the visual distinction between harbour and offshore samples in the Zn-Li scatterplot is largely an artefact of the effects of other components.

Log-ratio analysis reveals that, although the harbour samples display elevated Zn content, the degree of enrichment is considerably lower than suggested by the

traditional regression method. The log-ratio analysis calculates the enrichment

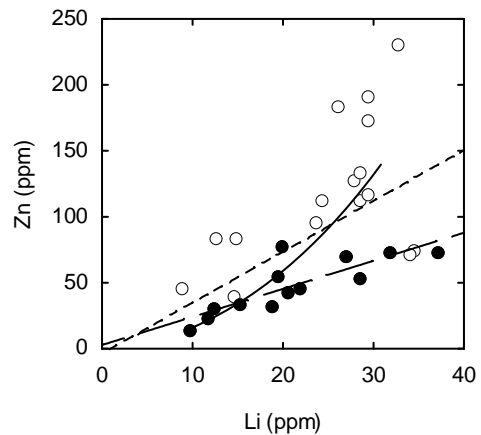


**Fig. 2.** Scatterplot of Zn and Li for Aegean Sea sediments. Open circles, harbour samples; full circles, offshore samples. Short dashed trend, regression for complete dataset; long dashed trend, regression for offshore samples; solid trend, log-ratio trend for all samples.

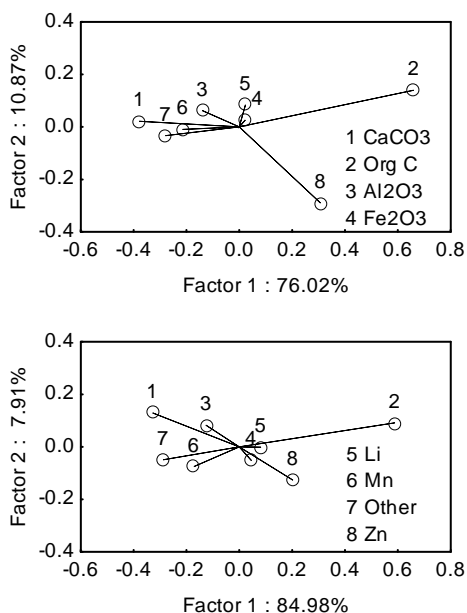


**Fig. 3.** Biplots of log-ratio factor loading for Aegean Sea sediments. Upper plot, complete dataset; lower plot, offshore samples. Percentages indicate variance accounted for by factor.

in the harbour samples as averaging about 40% greater than the offshore samples, whereas the traditional approach suggest the harbour samples average twice the background.

### CONCLUSIONS

The traditional approach to grain-size normalization – simple linear regression of “raw” data – is likely to result in dubious interpretation:

(1) the normalizing agent and the clay

content in sediment is unlikely to have a linear relationship,

(2) the relationship between potential contaminants and normalizing agents can be confounded by other, unaccounted for components,

(3) a log-ratio approach is recommended for grain-size normalization.

### ACKNOWLEDGEMENTS

This research was funded by Estonian Science Foundation Grant no. 7016.

### REFERENCES

- AITCHISON, J. 1982. The statistical analysis of compositional data. *Journal of the Royal Statistical Society*, **44**, 139-177.
- ALOUPI, M. & ANGELIDIS, M.O. 2001. Geochemistry of natural and anthropogenic metals in the coastal sediments of the island of Lesbos, Aegean Sea. *Environmental Pollution*, **113**, 211-219.
- BUCCIANTI, A., MATEU-FIGUERAS, G., & PAWLOWSKY-GLAHN, V. (eds.). 2006. *Compositional data analysis in the geosciences: from theory to practice*. Geological Society, London.
- COVELLI, S. & FONTOLAN, G. 1997. Application of a normalization procedure in determining regional geochemical baselines. *Environmental Geology*, **30**, 34-45.
- HOROWITZ, A.J. 1991. *A primer on Sediment – trace element chemistry*. Lewis Publishers Ltd., Chelsea, MI.
- SZAVA-KOVATS, R.C. 2008. Grain-size normalization as a tool to assess contamination in marine sediments: Is the <63 µm fraction fine enough? *Marine Pollution Bulletin*, **56**, 629-632.
- VAN EYNATTEN, H. 2004. Statistical modelling of compositional trends in sediments. *Sedimentary Geology*, **171**, 79-89.

**APPLIED GEOCHEMISTRY OF GEOLOGICAL STORAGE OF CO<sub>2</sub>**

EDITED BY:

**WILLIAM D. GUNTER  
ERNIE H. PERKINS  
BRIAN HITCHON**



## Composition and levels of groundwater in the CO2CRC Otway Project area, Victoria, Australia: establishing a pre-injection baseline

Patrice de Caritat<sup>1</sup>, Dirk Kirste<sup>2</sup>, & Allison, Hortle<sup>3</sup>

Cooperative Research Centre for Greenhouse Gas Technologies, CO2 CRC

<sup>1</sup>Geoscience Australia, GPO Box 378, Canberra, ACT 2601 AUSTRALIA

(email: Patrice.deCaritat@ga.gov.au)

<sup>2</sup>Department of Earth Sciences, Simon Fraser University, Burnaby, BC, V5A 1S6 CANADA

<sup>3</sup>Division of Petroleum Resources, CSIRO, Kensington, WA, 6151 AUSTRALIA

**ABSTRACT:** Groundwater monitoring around the CO2CRC Otway Project CO<sub>2</sub> injection site aims to (1) establish baseline aquifer conditions prior to CO<sub>2</sub> injection, and (2) enable detection monitoring for CO<sub>2</sub> leakage, in the unlikely event any should occur in the future. The groundwater composition was monitored at 24 bores around the site for nearly 2 years before injection started. The water samples were analysed for standard bulk properties, and inorganic chemical and isotopic compositions. In addition to sampling, standing water levels were monitored continuously in 6 of the bores using barometric loggers.

The shallow groundwaters have compositions typical of carbonate aquifer-hosted waters, being fresh (EC 800-4000 µS/cm), dominated by Ca<sup>2+</sup>, Na<sup>+</sup>, HCO<sub>3</sub><sup>-</sup> and Cl<sup>-</sup>, cool (T 12-23°C), and near-neutral (pH 6.6-7.5). Most of the deep groundwater samples are fresher (EC 400-1600 µS/cm), also dominated by Ca<sup>2+</sup>, Na<sup>+</sup>, HCO<sub>3</sub><sup>-</sup> and Cl<sup>-</sup>, cool (T 15-21°C), but are more alkaline (pH 7.5-9.5). Time-series reveal that most parameters measured have been relatively stable over the sampling period, although some bores display changes that appear to be non-seasonal. Groundwater levels in some of the shallow bores show a seasonal variation with longer term trends evident in both aquifers.

**KEYWORDS:** groundwater, carbon dioxide, geosequestration, carbon capture and storage

### INTRODUCTION

The CO2CRC Otway Project aims to demonstrate the feasibility of large-scale carbon capture and storage (CCS) in Australia. Up to 100,000 tonnes of supercritical CO<sub>2</sub>-rich gas (~80% CO<sub>2</sub>, ~20% CH<sub>4</sub>) are being injected into a depleted gas reservoir ~2100 m below ground (Fig. 1) in south-western Victoria. This naturally occurring gas is produced from the nearby Buttress-1 well, piped to the injection site, and injected into the Naylor field (Waarre C Formation) at the CRC-1 well. Early on during the injection history, the gas was tagged with a flush of tracers (CD<sub>4</sub>, SF<sub>6</sub> and Kr) (Underschultz *et al.* 2008).

An extensive world-class monitoring and verification (M&V) program (Hennig *et al.* 2008), of which the present work is but a component, was initiated before injection started to **(1)** document the natural state of the formation water, groundwater, soils and atmosphere, **(2)** monitor migration of

the CO<sub>2</sub> plume, and **(3)** detect leakage, should any occur. The groundwater monitoring project allows the natural groundwater composition and levels to be determined before any injection started [point **(1)** above]. In the unlikely event of CO<sub>2</sub> leakage into the aquifers overlying the Waarre C Formation, this work may also allow the chemical and/or isotopic detection of changes in water-mineral interactions in the aquifer systems [point **(3)** above].

### GROUNDWATER MONITORING

As part of the M&V effort, groundwater was sampled biannually from 21 bores in the shallow, unconfined Port Campbell Limestone aquifer and from 3 bores in the deeper, confined Dilwyn Formation aquifer (Fig. 1). All these bores are within a radius of ~10 km from CRC-1 (Fig. 2). The pre-injection monitoring, which took place between June 2006 and March 2008, was limited to pre-existing water bores. These

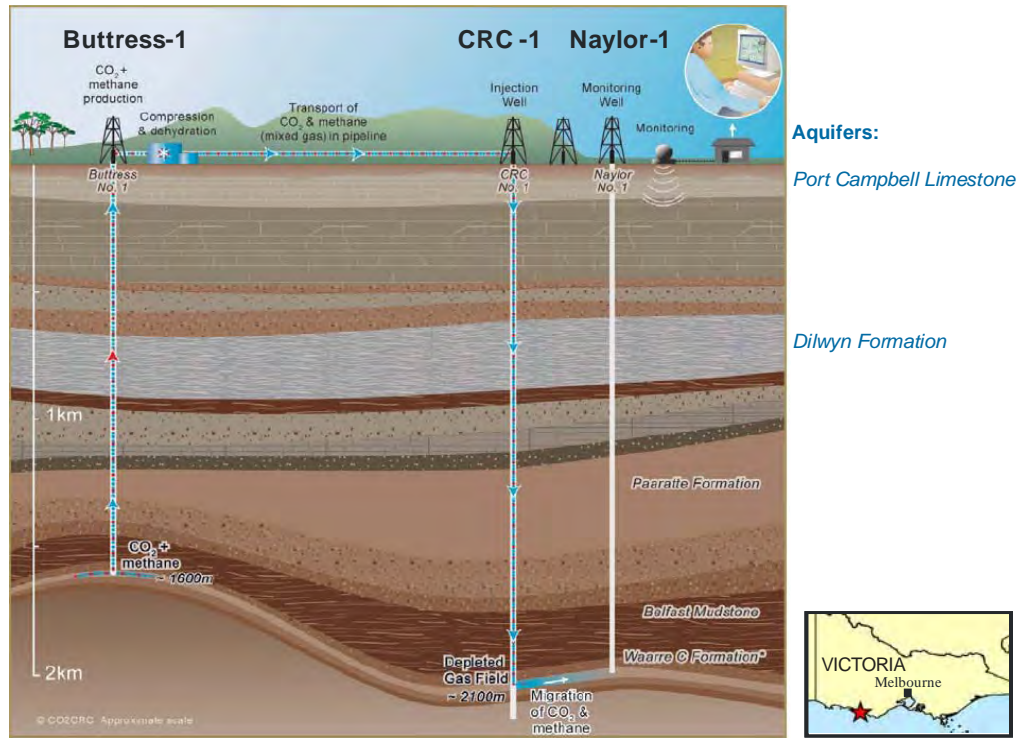


Fig. 1. CCS concept in the Otway Project ([www.co2crc.com.au](http://www.co2crc.com.au)).

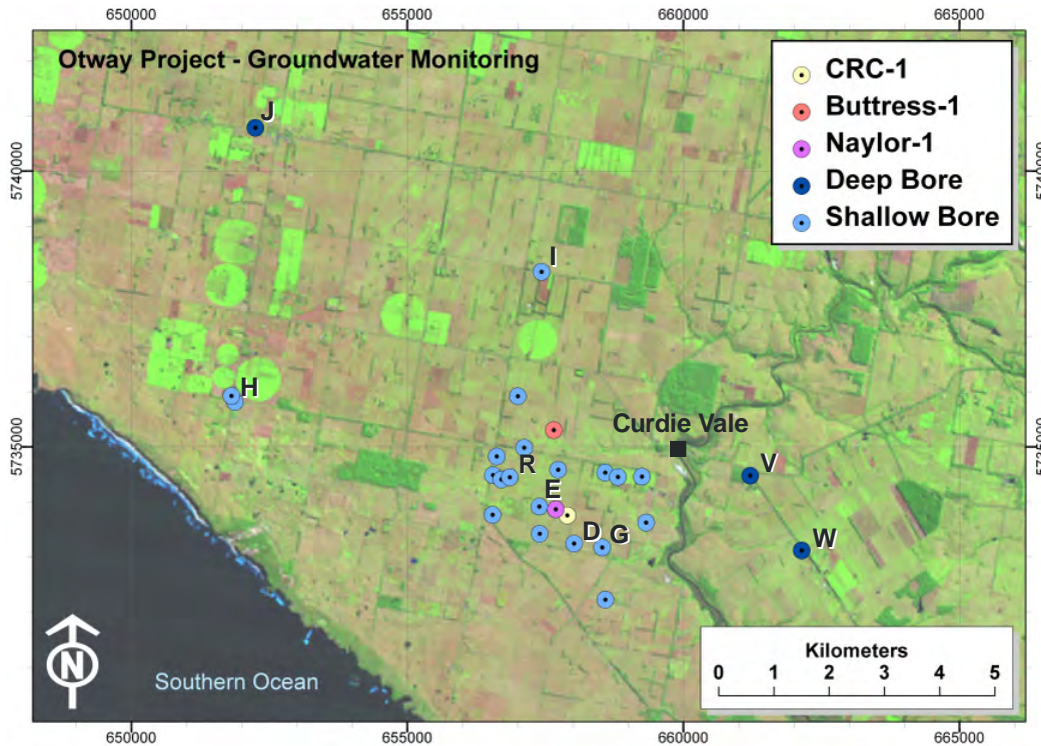


Fig. 2. Location of deep and shallow groundwater monitoring bores and CCS wells CRC-1, Buttriss-1 and Naylor-1 (see Fig. 1). Bores mentioned elsewhere in this paper are labelled.

are used locally for domestic, small-scale industry (dairy farming) and environmental monitoring purposes. In addition to groundwater sampling, standing water levels (SWL) have been monitored continuously in 6 of the bores using pressure and temperature data loggers.

**METHODS**

The water samples were analysed for pH, electrical conductivity (EC), temperature (T), dissolved oxygen (DO), redox potential (Eh), reduced iron (Fe<sup>2+</sup>) and alkalinity (dissolved inorganic carbon, DIC, as HCO<sub>3</sub><sup>-</sup>) in the field. A few special water samples were collected to determine background levels of CD<sub>4</sub>, SF<sub>6</sub> and Kr in the headspace gas. SWL and T were recorded hourly in 3 shallow (Sites H, I, R) and 3 deep (Sites J, V, W) open bores using automatic data loggers, which were downloaded biannually.

A suite of major, minor and trace inorganic species were analysed in the laboratory. Stable isotopes of O and H in water, of S in sulfate and of C and O in DIC were also determined.

**COMPOSITIONAL TRENDS**

The shallow groundwaters have compositions typical of carbonate aquifer-hosted waters, being fresh (EC 800-4000 µS/cm), dominated by Ca<sup>2+</sup>, Na<sup>+</sup>, HCO<sub>3</sub><sup>-</sup> and Cl<sup>-</sup> (Fig. 3a), cool (T 12-23°C), and near-neutral (pH 6.6-7.5). Most deep groundwater samples (Sites J, V, W) are fresher (EC 400-1600 µS/cm), also dominated by Ca<sup>2+</sup>, Na<sup>+</sup>, HCO<sub>3</sub><sup>-</sup> and Cl<sup>-</sup> (Fig. 3a), and cool (T 15-21°C), but are more alkaline (pH 7.5-9.5).

Time-series reveal that measured parameters have generally been stable over the sampling period. Some shallow bores, however, display increasing EC and T trends, and others, located mostly around the injection site, show decreasing then increasing alkalinity (Fig. 3b). Some bores located mostly further away from CRC-1 show steadily increasing alkalinity (with or without increasing Cl<sup>-</sup> and Na<sup>+</sup>, and decreasing Ca<sup>2+</sup>) (Fig. 3c). Alkalinity of the deep groundwater decreased slightly over the period. Most isotope

trends are stable over the period, except perhaps for an increase in δ<sup>2</sup>H<sub>water</sub> for instance at Sites D (from -34 to -25‰ VSMOW) and G (-35 to -26‰) and a decrease at Site I (-26 to -32‰).

**WATER LEVELS**

Data collected between January 2007 and March 2008 shows a seasonal climatic response in the shallow aquifer (Fig. 4a), which correlates well with the historic record. SWL in the Dilwyn aquifer varies little and T is essentially constant over the period (Fig. 4b); agreement with historic records, where they exist, is also good. Neither aquifer shows a response to significant perturbation such as the drilling of CRC-1 during February-March 2007.

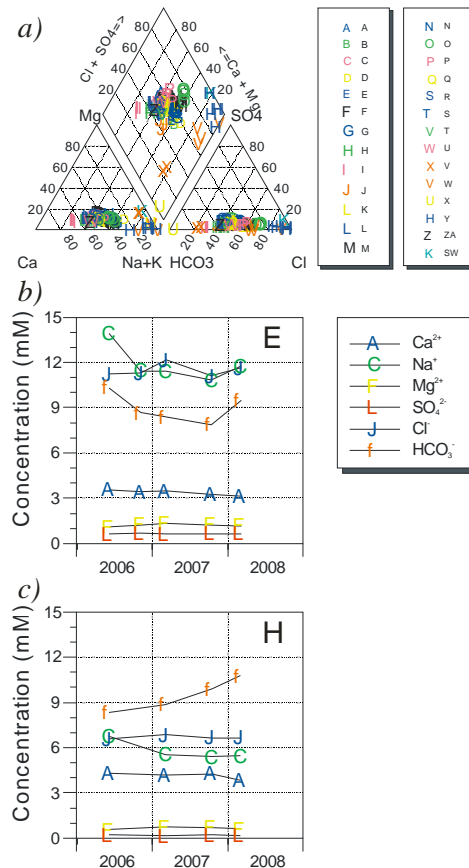


**Fig. 3.** Piper diagram of all water samples (symbols represent Sites; SW = seawater) (a), time-series of major elements at Site E (b), and at Site H (c).

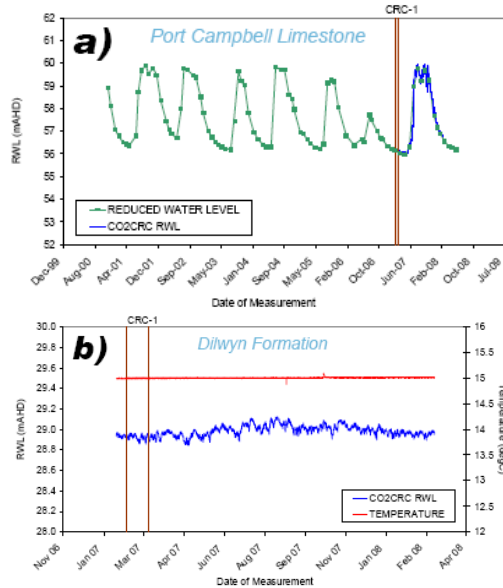


**Fig. 4.** Reduced water levels (RWL, in m relative to Australian Height Datum) in shallow aquifer at Site I compared to historical data (a), and in deep aquifer at Site J shown with temperature (b).

**CONCLUSIONS**

Monitoring of the composition and levels of the shallow and deep groundwaters in the Otway Project area has provided a pre-injection baseline revealing both seasonal and non-seasonal changes. Continued monitoring is recommended at the same frequency for at least 2 years

after the completion of CO<sub>2</sub> injection in order to detect any changes that it may cause. Headspace gas sampling for analysis of the chemical tracers added to the injected gas is in progress for selected bores.

**ACKNOWLEDGEMENTS**

Funding from the Australian Government's Cooperative Research Centres Program and CO2CRC sponsors made this work possible. We thank our colleagues within the CO2CRC for discussions and support. Chris Boreham, Rick Causebrook and Rob Langford provided internal reviews. Published with permission from the CEO of Geoscience Australia.

**REFERENCES**

HENNIG, A., ETHERIDGE, D., CARITAT, P *et al.* 2008. Assurance monitoring in the CO2CRC Otway Project to demonstrate geological storage of CO2: review of the environmental monitoring systems and results prior to the Injection of CO2. *Australian Petroleum Production & Exploration Association Journal*, **48**, Conference Proceedings (DVD).  
 UNDERSCHULTZ, J., FREIFELD, B., BOREHAM, C. *et al.* 2008. Geochemistry monitoring of CO2 storage at the CO2CRC Otway Project, Victoria. *Australian Petroleum Production & Exploration Association Journal*, **48**, Conference Proceedings (DVD).

## Carbon mineralization in mine tailings and implications for carbon storage in ultramafic-hosted aquifers

Gregory M. Dipple<sup>1</sup>, James M. Thom<sup>1</sup>, & Siobhan A. Wilson<sup>1</sup>

<sup>1</sup>Mineral Deposit Research Unit, University of British Columbia, Vancouver, B.C., V6T 1Z4 CANADA  
(e-mail: gdipple@eos.ubc.ca)

**ABSTRACT:** Atmospheric carbon dioxide is trapped within magnesium carbonate minerals during mining and processing of ultramafic-hosted ore. The extent of mineral-fluid reaction is consistent with laboratory experiments on the rates of mineral dissolution. Incorporation of new serpentine dissolution kinetic rate laws into geochemical models for carbon storage in ultramafic-hosted aquifers may therefore improve predictions of the rates of carbon mineralization in the subsurface.

**KEYWORDS:** carbon sequestration, tailings, serpentinite, mineral dissolution, weathering

### INTRODUCTION

Recent documentation of the formation of magnesium carbonate minerals via reaction of CO<sub>2</sub> with ultramafic rocks and mine wastes suggests that these reactions may be very rapid under near-surface conditions. For example, Wilson *et al.* (2006, 2009) have documented the rapid uptake of atmospheric CO<sub>2</sub> during weathering of chrysotile mine tailings, and Keleman & Matter (2008) have documented similar rates of CO<sub>2</sub> uptake during weathering of the Samail ophiolite. The rates of carbon uptake in these studies are broadly consistent with experimental kinetic data for mineral dissolution and carbonation. The implications of these new rate law data for mineralization of CO<sub>2</sub> in serpentinite-hosted aquifers used for carbon storage is explored here.

### CARBON MINERALIZATION IN MINE TAILINGS

Sulfate, halide, and carbonate minerals form in mine waste as a result of chemical weathering reactions and as a by-product of mineral processing. The formation of carbonate minerals is of particular interest for its potential in offsetting greenhouse gas emissions associated with mining. We have documented secondary carbonate mineral precipitation at the Mount Keith Nickel Mine (Western Australia) and the

Diavik Diamond Mine (Northwest Territories, Canada). Data from these active mines are compared to similar data from two closed chrysotile mines at Clinton Creek (Yukon, Canada) and Cassiar (British Columbia, Canada) as reported by Wilson *et al.* (2006, 2009).

Exposed surfaces contain secondary halide, sulfate, and carbonate mineralization. Halide and sulfate minerals are not generally present at depth, suggesting that they are dissolved upon burial. However, secondary carbonate minerals persist at depth within the tailings, but show signs of having been reworked upon burial. Differences in climate and tailings management practices have resulted in widespread mineralization and preservation of secondary carbonate minerals at Mount Keith, and limited carbonate mineralization in the tailings at Diavik, where underwater storage of tailings may have restricted mineralization.

Secondary mineralization at Mount Keith produces hydromagnesite, while mineralization at Diavik includes carbonates of Mg, Ca and Na: nesquehonite, calcite, vaterite, natrite, thermonatrite, natron, trona, gaylussite and northupite. The rate of carbon mineralization at the two mine sites was assessed using quantitative powder X-ray diffraction analysis and the Rietveld

method, as described by Wilson *et al.* (2006). Carbon uptake at Mount Keith occurs at a rate of about 50,000 tonnes CO<sub>2</sub> per year. The rate at Diavik is not significant. Carbon and oxygen isotope analysis of the precipitated carbonate minerals indicates that most of the bound carbonate is derived from the atmosphere. Serpentine, which is the most abundant mineral in mine tailings at Mount Keith, is implicated as the source of Mg for hydromagnesite.

### SERPENTINE DISSOLUTION KINETICS FROM EXPERIMENTAL DATA AND IMPLICATIONS FOR CARBON STORAGE

The steady-state dissolution rate of chrysotile in 0.1m NaCl solutions was measured at 22°C and pH ranging from 2 to 8. Dissolution experiments were performed in a continuously stirred flow-through reactor with the input solutions pre-equilibrated with atmospheric concentrations of CO<sub>2</sub>. Both magnesium and silicon steady-state fluxes from the chrysotile surface were regressed and the following empirical relationships were obtained:

$$F_{Mg} = -0.22 \text{ pH} - 10.02$$

$$F_{Si} = -0.19 \text{ pH} - 10.37$$

where  $F_{Mg}$  and  $F_{Si}$  are the log<sub>10</sub> Mg and Si flux in mol/m<sup>2</sup>/s from the chrysotile mineral surface, respectively (Fig. 1). Dissolution was typically non-stoichiometric. These element fluxes were used in reaction-path calculations to constrain the rate of CO<sub>2</sub> sequestration in two geological environments that have been proposed to mitigate anthropogenic increases of atmospheric CO<sub>2</sub>. Results indicate that CO<sub>2</sub> injection into serpentinite tailings at 10°C is approximately an order of magnitude faster than CO<sub>2</sub> injection into a serpentinite reservoir at 60°C on a per kilogram of water basis. Aquifer injection, while slower, provides a larger sequestration capacity.

### ACKNOWLEDGEMENTS

This study was supported by research

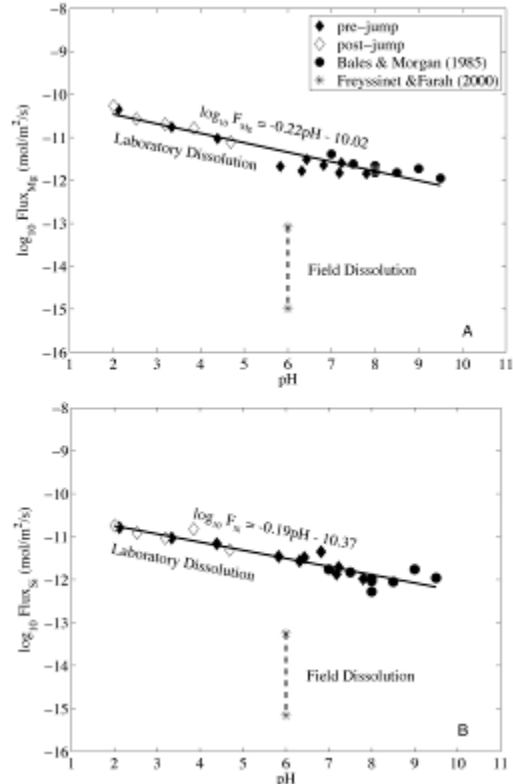


**Fig. 1.** Summary of chrysotile-steady state element fluxes: (A) Mg and (B) Si as a function of pH. Filled and open diamonds are steady-state fluxes determined after the onset of an experiment and after a pH-jump, respectively. Circles are Bales & Morgan (1985) element fluxes; their rates were determined in CO<sub>2</sub>-free solutions. The solid line is the linear least square fit to all the data. The stars are the range in fluxes determined from field serpentinite weathering (Freyssinet & Farah 2000).

grants from the Natural Sciences and Engineering Research Council of Canada, BHP Billiton Limited, and Diavik Diamond Mine Incorporated.

### REFERENCES

- BALES, R.C. & MORGAN, J.J. 1985. Dissolution kinetics of chrysotile at pH 7 to 10. *Geochimica et Cosmochimica Acta*, **49**, 2281-2288.
- FREYSSINET, P. & FARAH, A.S. 2000. Geochemical mass balance and weathering rates of ultramafic schists in Amazonia. *Chemical Geology*, **170**, 133-151.
- KELEMAN, P.B. & MATTER, J. 2008. In situ carbonation of peridotite for CO<sub>2</sub> storage.

- Proceedings of the National Academy of Sciences*, **105**, 17295-17300.
- WILSON, S.A., DIPPLE, G.M., POWER, I.M. *et al.* 2009. Carbon dioxide fixation within mine wastes of ultramafic-hosted ore deposits: Examples from the Clinton Creek and Cassiar chrysotile deposits, Canada. *Economic Geology*, **104**, in press.
- WILSON, S.A., RAUDSEPP, M., & DIPPLE G.M. 2006. Verifying and quantifying carbon fixation in minerals from serpentine-rich mine tailings using the Rietveld method with X-ray powder diffraction data. *American Mineralogist*, **91**, 1331-1341.



## Comparison of CO<sub>2</sub>-N<sub>2</sub>-enhanced coalbed methane recovery and CO<sub>2</sub> storage for low- & high-rank coals, Alberta, Canada and Shanxi, China

William D. Gunter<sup>1</sup>, Xiaohui Deng<sup>1</sup>, & Sam Wong<sup>1</sup>

<sup>1</sup>Alberta Research Council, 250 Karl Clark Road, Edmonton, AB, T6N 1E4 CANADA  
(e-mail: gunter@arc.ab.ca)

**ABSTRACT:** CO<sub>2</sub>-ECBM Micro-Pilots have been carried out in Canada and China to assess the response of low- and high-rank coal reservoirs to CO<sub>2</sub> injection. The selectivity of coals for CO<sub>2</sub>, compared to methane, can vary from 10 to 1 depending on coal rank. Although the CO<sub>2</sub> is more efficiently stripped by coals of low rank, permeability impairment is greater and the amount of methane recovered is less than for high-rank coals, providing other reservoir properties are similar. If a pure CO<sub>2</sub> source is not available, N<sub>2</sub>-CO<sub>2</sub> mixtures may produce more favourable economics.

**KEYWORDS:** CO<sub>2</sub> storage, coals, sorption, swelling, methane production

### INTRODUCTION

Coal gas reservoirs are dual storage reservoirs consisting of primary and secondary storage systems. The primary storage system makes up 98% or greater of the reservoir volume and contains organic matter, inorganic material, inherent water, and gas stored within very small pore spaces. Primary system gas storage is dominated by sorption phenomena because of the small size of the pores. During sorption, the molecules are within very close proximity to solid surfaces, are attracted to the solid, and are packed closer together than expected from the pressure conditions. The primary porosity system is relatively impermeable and mass transfer is dominated by diffusion (driven by gas concentration gradients). Commercially productive coal gas reservoirs contain a well-developed secondary storage system dominated by natural fractures. Without these natural fractures, commercial production would not be possible. Flow through the secondary storage system is due to pressure gradients between the fracture system and production wells. The majority of gas in a coal gas reservoir diffuses through the primary storage system, desorbs at the interface between the primary and secondary systems, and then

flows through the secondary system to wells.

### ENHANCED COALBED METHANE PRODUCTION

The CO<sub>2</sub> storage/enhanced coalbed methane (ECBM) process works by replacing sorbed methane (CH<sub>4</sub>) molecules in the primary storage system with sorbed CO<sub>2</sub> molecules (Mavor *et al.* 2002, 2004). The CH<sub>4</sub> molecules are displaced into the coal natural fracture system and to producing wells. The CO<sub>2</sub> is trapped in the primary storage system and there is little breakthrough to production wells until the majority of the well pattern is swept. A storage project terminates at breakthrough.

An alternative gas for ECBM is N<sub>2</sub>, which has a different enhanced recovery mechanism from CO<sub>2</sub>. N<sub>2</sub> is less sorptive than methane, with a sorptive capacity roughly 40% that of methane for high volatile bituminous B coal (Fig. 1). The N<sub>2</sub> process works by reducing the partial pressure of methane in the secondary system, increasing the rate of desorption from the primary system, and the rate of methane diffusion through the primary system. Some N<sub>2</sub> sorbs into the primary system but the majority remains in the secondary system. N<sub>2</sub> also increases the

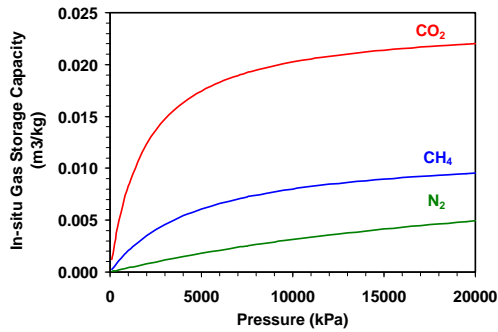


**Fig. 1.** CO<sub>2</sub> and methane sorption isotherms for the Lower Cretaceous Mannville Group high volatile bituminous B coal, Alberta.

total pressure in the natural fracture system, thereby, increasing the driving force to push gas through the fracture system to producing wells. One significant difference between N<sub>2</sub> and CO<sub>2</sub> injection is that the N<sub>2</sub> breaks through to the production wells and dilutes the well stream. When N<sub>2</sub> production becomes excessive, the production stream must be processed to reject N<sub>2</sub>.

Figure 2 shows examples of simulation computations of ECBM recovery, which schematically illustrate the methane recovery rate for two enhanced recovery scenarios, the first due to injection of pure N<sub>2</sub> and the second due to injection of pure CO<sub>2</sub>. Also illustrated is the expected recovery without injection (primary production).

N<sub>2</sub> injection rapidly increases the methane production rate. The timing and magnitude depends on the distance between injection and production wells, on the natural fracture porosity and permeability, and on the sorption properties. N<sub>2</sub> breakthrough at the production well occurs at about half the time required to reach the maximum methane production rate in this ideal case. The N<sub>2</sub> content of the produced gas continues to increase until it becomes excessive, i.e., 50% or greater.

The production increase due to CO<sub>2</sub> injection takes longer to develop. This is due to sorption of CO<sub>2</sub> relatively near the well with the sorbed CO<sub>2</sub>-methane front growing elliptically out from the injection wells. After a sufficient volume of methane

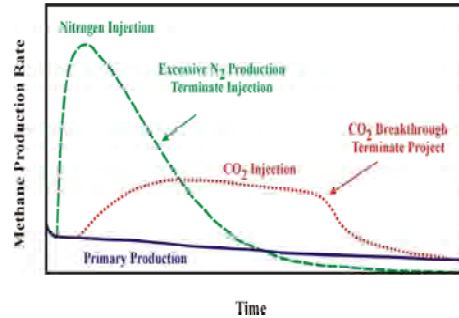


**Fig. 2.** Relative rates of methane production for the Mannville high volatile bituminous B coal.

has been displaced (roughly 20% of the reservoir volume), the methane productivity increases by a factor of 2 compared to primary production (Fig. 2). Eventually, CO<sub>2</sub> will breakthrough to the production well when sufficient CO<sub>2</sub> has been injected. At breakthrough, in the ideal case, 70% of the reservoir has been swept and the project is terminated.

In the absence of government incentives, the storage/ECBM process must be commercially attractive to interest investors for the large funding required for well facilities and flue gas collection systems. The source of the injected gases may be flue gas emissions from power plants (~13% CO<sub>2</sub>, ~80% N<sub>2</sub>, ~7% others), fertilizer plants, hydrogen plants, or the byproducts of gas treatment plants (CO<sub>2</sub> and mixtures of CO<sub>2</sub> and H<sub>2</sub>S). Flue gas injection may enhance the process economics to the point that large-scale commercial application is possible. Compared to pure CO<sub>2</sub>, flue gas injection requires a higher amount of compression for injecting the same amount of CO<sub>2</sub> downhole. One important component of the process design will be efficient compressors that minimize the volume of CO<sub>2</sub> created relative to the CO<sub>2</sub> injected. This design must also incorporate the economics of pre-treating the flue gas to increase CO<sub>2</sub> concentration and to reject the nitrogen from produced methane.

The optimum mix of N<sub>2</sub> and CO<sub>2</sub> in the injection gas depends on the technical and commercial requirements of the process. If CO<sub>2</sub> storage volume is the only consideration, the injected gas should be

100% CO<sub>2</sub>. If rapid maximization of hydrocarbon gas recovery is the only consideration, the injected gas should be 100% N<sub>2</sub>. The commercial and storage compromise will be between these two cases. We expect that the optimum commercial application will involve injecting variable gas composition to control storage volumes and the amount of N<sub>2</sub> in the produced gas stream. The range of the N<sub>2</sub> content in the injected gas is likely to be between 25% and 75%.

### THE EFFECT OF COAL RANK

Lower rank coals, often found at shallow depths, such as the subbituminous C coal of the Fort Union Formation of the Powder River Basin, Wyoming, have a great affinity for CO<sub>2</sub>, ten times (Mavor *et al.* 1999) that of methane. While this low-rank coal may be excellent for storage in the right reservoir setting (i.e., depth and pressure), the ECBM process will not be effective. Injection of ten volumes of CO<sub>2</sub> will displace only one volume of methane. As a result, the cost of injecting CO<sub>2</sub> cannot be significantly reduced by the sale of methane. However, in high volatile bituminous B coals, (such as those found in the Mannville Group, in Alberta, Canada, injection of two to three volumes of CO<sub>2</sub> will displace roughly one volume of methane (Fig. 1). The increase in the ratio of methane to CO<sub>2</sub> raises the chance for significant reduction in the cost of CO<sub>2</sub> storage. At the highest coal ranks, such as those found in the anthracitic coals of Shanxi Formation in Shanxi, China (Wong *et al.* 2007) injection of 1.2 volumes of methane will displace roughly one volume of methane (Fig. 3) resulting in production enhancements of more than five times.

### CONCLUSIONS

Other reservoir properties being similar, high-rank coals are more favorable for CO<sub>2</sub> storage because of their methane displacement efficiency (related to lower sorption selectivity for CO<sub>2</sub> compared to methane and higher absolute sorption of methane with increasing rank; see Figs 1 and 3). Higher ranks of coal are also more

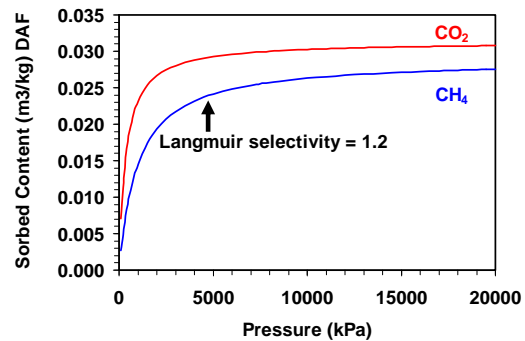


Fig. 3. CO<sub>2</sub> and methane sorption isotherms for the Shanxi anthracite.

favourable because the permeability is less affected by the swelling of the coal when it sorbs the CO<sub>2</sub> (Mavor & Gunter, 2006). Economics may demand that impure gas mixtures containing both nitrogen and CO<sub>2</sub> are used for enhanced recovery. However, for projects where the primary objective is storage of CO<sub>2</sub> in coal, pure CO<sub>2</sub> streams should be used.

### REFERENCES

- MAVOR, M.J. & GUNTER, W.D. 2006. Secondary porosity and permeability of coal vs gas composition and pressure. *SPE Reservoir Evaluation and Engineering Journal*, April, 114-125.
- MAVOR, M.J., GUNTER, W.D., & ROBINSON, J.R. 2004. Alberta multi-well micro-pilot testing for CBM properties, enhanced coalbed methane recovery and CO<sub>2</sub> storage potential. *Paper SPE 90256, presented at SPE Annual Technical Conference and Exhibition*, Houston, Texas.
- MAVOR, M.J., GUNTER, W.D., ROBINSON, J.R., LAW, D.H-S, & GALE, J. 2002. Testing for CO<sub>2</sub> sequestration and enhanced methane production from coal. *Paper SPE 75683, presented at SPE Gas Technology Symposium*, Calgary, Alberta.
- MAVOR, M., PRATT, T., & DEBRUYN, R. 1999. Study Quantifies Powder River Coal Seam Properties. *Oil & Gas Journal*, **97**, No. 17, 35-40.
- WONG, S., LAW, D., DENG, X., ROBINSON, J. *et al.* 2007. Enhanced coalbed methane and CO<sub>2</sub> storage in anthracitic coals: Micro-pilot test at South Qinshui, Shanxi, China. *International Journal of Greenhouse Gas Control*, **1**, No. 2, 215-222.



## Geochemical modelling and formation water monitoring at the CO2CRC Otway Project, Victoria, Australia

Dirk Kirste<sup>1</sup>, Ernie Perkins<sup>2</sup>, Chris Boreham<sup>3</sup>, Barry Freifeld<sup>4</sup>, Linda Stalker<sup>5</sup>,  
Ulrike Schacht<sup>6</sup>, & James Underschultz<sup>5</sup>

Cooperative Research Centre for Greenhouse Gas Technologies (CO2CRC)

<sup>1</sup>Department of Earth Sciences, Simon Fraser University, Burnaby, BC, V5A 1S6 CANADA;  
(email: dkirste@sfu.ca)

<sup>2</sup>Alberta Research Council, Edmonton, AB, T6N 1E4 CANADA

<sup>3</sup>Geoscience Australia, GPO Box 378, Canberra, ACT, 2601 AUSTRALIA

<sup>4</sup>Lawrence Berkeley National Laboratory, Berkeley, CA, 94720 USA

<sup>5</sup>Division of Petroleum Resources, CSIRO, Kensington, WA, 6151 AUSTRALIA

<sup>6</sup>ASP, University of Adelaide, Adelaide, SA 505 AUSTRALIA

**ABSTRACT:** Formation water monitoring and geochemical modelling of the Otway Project CO<sub>2</sub> injection site has been carried out to determine the physical and chemical processes that take place during the injection and migration of CO<sub>2</sub> into a depleted gas reservoir. A U-tube downhole assembly enabled the collection of high quality samples of the gas and the aqueous phases. Integration of the fluid compositional data with numerical modelling of the system indicates the pH is buffered by CO<sub>2</sub>-water-rock interactions both prior to and after the arrival of the CO<sub>2</sub>. The target formation, the Waarre C sandstone, has low reactivity with respect to CO<sub>2</sub>-driven geochemical reactions but contains sufficient calcite to buffer the pH. However, compositional changes predicted in the formation water are not observed implying that the formation waters sampled have not experienced extensive interaction with the CO<sub>2</sub>. The interpreted compositional changes and controls appear to reflect the dynamics of a system displaying 3-phase behaviour with separate methane gas, supercritical CO<sub>2</sub>, and aqueous phases.

**KEYWORDS:** formation water chemistry, carbon dioxide, geosequestration, geochemical modelling

### INTRODUCTION

The Otway Project of The Cooperative Research Centre for Greenhouse Gas Technologies (CO2CRC) is a demonstration site for the storage of CO<sub>2</sub>. The site is the first extensively monitored carbon storage research study of a depleted gas reservoir. Approximately 100,000 tonnes of an 80:20 CO<sub>2</sub>:CH<sub>4</sub> mixture will be injected into the Waarre C sandstone over the lifetime of phase 1 of the project. Monitoring was undertaken (1) to help determine the physical and chemical processes taking place during and after the introduction of CO<sub>2</sub> and (2) to validate numerical models describing the migration of the CO<sub>2</sub> and any geochemical interactions occurring during migration. To facilitate the monitoring and verification process during the initial injection, tracers (CD<sub>4</sub>, SF<sub>6</sub>, Kr) were included in the gas

injection stream to help establish breakthrough and for leakage detection.

Physical and chemical monitoring is carried out through a U-tube downhole installation (Freifeld *et al.* 2005) that allows the collection of high quality liquid and gas samples from targeted depths. The multi-level U-tube assembly is completed in the Waarre C unit approximately 300 m distant and up dip from the injector well (CRC-1). The Naylor-1 monitoring well is perforated from 2028.3 – 2032.2 m RT and 2039 – 2055 m RT. The U-tube assembly is constructed to sample from U1 at 2027 m RT (gas cap), U2 2040 m RT and U3 2045 m RT both initially below the gas-water contact.

This study describes the results of the formation water monitoring and the interpretation of the physical and geochemical processes from that data,

together with numerical simulations of the CO<sub>2</sub>-water-rock interactions.

## METHODS

On-site monitoring during sample collection includes in-line probes measuring temperature, pH, and electrical conductivity (EC). Samples were collected in high pressure vessels to limit compositional changes resulting from the exsolution of gases during collection. The high pressure vessels were transported to University of Adelaide for bench top analyses and preparation for further analytical procedures. Bench top analyses included measuring pH, Eh, T, EC, and alkalinity, and determining Fe, NO<sub>3</sub>, PO<sub>4</sub> and SiO<sub>2</sub> using spectrophotometry. The remaining fluid was then filtered and aliquots were prepared for major, minor and trace species analyses using IC (ion chromatography), ICP-OES (optical emission spectrometry) and ICP-MS (mass spectrometry) as well as IRMS (isotope ratio mass spectrometry) for isotopes of O, H and C. Table 1 shows some of the major species chemistry for samples collected from U2.

Fluid and gas samples were also collected for hydrocarbon and non-hydrocarbon gas compositional analyses (GC), carbon isotopes of CO<sub>2</sub> (GCIRMS), and for tracer analyses (GC-MS).

Mineral content and composition of core plugs from the reservoir rock were determined using petrologic examination, XRF, XRD, and microprobe analyses. Geochemical modelling was carried out using SOLMINEQ.88, the Geochemist's Workbench and TOUGHREACT.

## RESULTS AND DISCUSSION

Prior to injection, aqueous samples were collected from U2 and U3 in order to establish the methodology and baseline conditions. The samples were contaminated with kill fluid and the succession from the first samples shows a decrease in K and increase in most other species. Subsequent samples continued to show some contamination but it was determined that essentially baseline conditions had been achieved except for

the K. Later minor fluctuations in the K content are interpreted to indicate changes in the degree of kill fluid contamination that relate to permeability variations in the preferred interval.

The first indication of breakthrough of the CO<sub>2</sub> occurred in samples from all 3 U-tube samplers on 17 July, 2008 with slightly elevated CO<sub>2</sub> content and the presence of tracers. In mid-August, U2 became gassy and the pH dropped significantly. There was no coincident change in either the alkalinity or cation concentrations. By early September, U2 had converted entirely to gas lift. Over the same time frame, as the pH decreases, the per cent of CO<sub>2</sub> in the U2 samples (for gas exsolved from the water sample through decrease from formation to atmospheric pressure) increased from ~4% to >40%.

U3 samples contained high gas content in late October and reached gas lift by early January 2009. The pH followed a trend similar to that in U2 with decreases occurring with increased gas content in the sample. Alkalinity showed some increase but did not fully match the pH changes. The major cations showed changes more consistent with increased contamination than significant CO<sub>2</sub>-water-rock interaction.

Where interactions between the (supercritical) gas and water are possible, there is rapid isotopic equilibration between the oxygen in CO<sub>2</sub> and H<sub>2</sub>O. The potential to use this isotopic exchange equilibria as a measure of the extent of CO<sub>2</sub>-water interaction, and thus as an indicator of CO<sub>2</sub> migration, is discussed in Kharaka *et al.* (2006). Unlike the results of Kharaka *et al.* (2006), there are no consistent changes in the oxygen isotopic composition of the fluid samples at the Otway site.

## GEOCHEMICAL MODELLING

Geochemical modelling of the system at reservoir T and P were carried out to determine the relations between the CO<sub>2</sub>, pH, and mineral phases present. SOLMINEQ.88 was used to recalculate the pH at reservoir P and T conditions.

**Table 1.** U2 selected data.

Date	pH	pH	Alk	K	Mg	Na	Ca	Cl
	field	lab	[mmol/l]	mg/L	mg/L	mg/L	mg/L	mg/L
11/10/2007	-	6.69	13.2	1213	92.1	5783	458	11993
31/01/2008	6.50	6.38	12.8	452	100	6331	513	12211
31/03/2008	-	6.41	10.9	295	97.6	7126	590	12525
25/05/2008	6.06	5.85	10.8	308	97.8	7207	602	12410
11/06/2008	6.23	5.91	11.0	317	97.8	7123	598	12319
26/06/2008	6.03	6.37	12.1	252	102	6809	627	12390
17/07/2008	5.85	6.17	11.5	245	98.9	6850	646	12459
31/07/2008	5.92	6.10	11.9	256	98.5	6718	642	12441
7/08/2008	6.23	6.11	11.8	261	99.1	6845	640	12350
21/08/2008	5.04	5.58	11.7	329	88.0	6734	596	12280
28/08/2008	5.14	5.34	11.3	312	90.6	6844	601	12309
4/09/2008	4.66	5.94	11.3	-	-	-	-	-

The simulated CO<sub>2</sub> fugacity matches the initial reservoir CO<sub>2</sub> content and indicates that the pH is buffered by CO<sub>2</sub>-calcite equilibrium. Further modelling was carried out using the Geochemists Workbench React and Tact modules with the thermodynamic database modified to reflect the elevated P conditions and kinetic rate parameters consistent with the Waarre C mineralogy. The Waarre C shows low reactivity and short-term predictive modelling of the system under elevated CO<sub>2</sub> content changes little with time (Fig. 1).

The only significant changes anticipated are in the pH, and in the HCO<sub>3</sub> and Ca content if the system has calcite present, as suggested by the petrology and the SOLMINEQ.88 modelling. The field data show the decrease in pH but not the predicted increases in HCO<sub>3</sub> and Ca. This suggests that either there is no calcite present in the region around the Naylor-1 monitoring well or that the formation water has not had sufficient contact time with elevated CO<sub>2</sub> in the formation. The numerical model with calcite present predicts a pH similar to the observed pH just before gas lift (Fig. 2). Without calcite buffering the pH remains low (pH = 4.1).

It would appear that the system shows pH change and buffering but the other predicted compositional changes of the fluid are not observed. The preliminary interpretation of this data is that injection

of the CO<sub>2</sub> mixture has resulted in a 3 phase system, represented by the methane gas cap, the injected CO<sub>2</sub> mixture, and the formation water. If the CO<sub>2</sub> had mixed significantly with the methane gas cap changes in the total gas composition in U1 should mimic those of U2 and U3. However, this was not observed, and the CO<sub>2</sub> content in U1 until early November 2008. If the CO<sub>2</sub> had migrated in the aqueous phase there should be some evidence of CO<sub>2</sub>-water-rock interaction and this is also not observed. As a separate phase, the supercritical CO<sub>2</sub>:CH<sub>4</sub> mixture would only partially mix with the methane gas cap as the density and viscosity contrast is less than the CO<sub>2</sub>-water difference (Oldenburg 2003). As the CO<sub>2</sub> migrates up dip to the Naylor-1 monitoring well the plume would increase in thickness forcing the (supercritical) gas-water contact down resulting in U2 then U3 reaching gas lift. There is little opportunity for the CO<sub>2</sub> to dissolve in the water except in the wellbore and at the CO<sub>2</sub>-water interface. Thus there is no compositional change observed in the sampled water.

## CONCLUSIONS

Compositional changes in the formation water sampled from the Waarre C sandstone at the Otway Project pilot site provide information on the physical and chemical processes taking place during the injection and migration of CO<sub>2</sub>. By

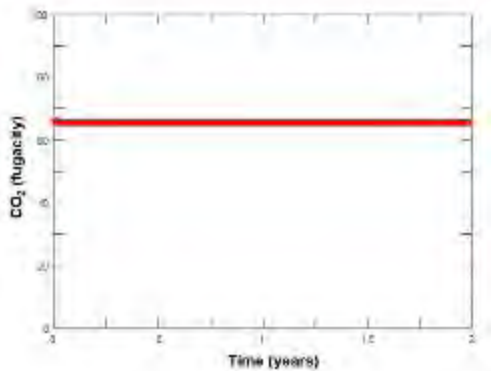


**Fig. 1.** Change of modelled CO<sub>2</sub> fugacity with time.

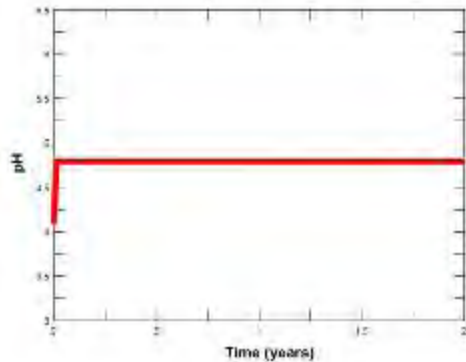


**Fig. 2.** Modelled pH with calcite buffering.

comparing the observed results with the chemistry predicted through numerical modelling, controls on the pH and composition are made evident. In the case of the Waarre C sandstone, the low content of mineral phases other than calcite that will react with CO<sub>2</sub>-rich water allows several observations and interpretation to be made.

(1) pH appears to be buffered by CO<sub>2</sub>-

calcite equilibrium both before and after the arrival of the CO<sub>2</sub>-rich plume.

(2) The evolution of the fluid composition reflects a lack of significant contact between the aqueous phase and the CO<sub>2</sub> while in the pore space of the reservoir.

(3) The CO<sub>2</sub> migrates as an immiscible phase with respect to both the methane gas cap and the formation water.

#### ACKNOWLEDGEMENTS

Funding from the Cooperative Research Centres Program of the Australian Government and CO2CRC sponsors made this work possible. We thank our colleagues within the CO2CRC for discussions and support. Sample collection and analysis were greatly assisted by staff of Deakin University, Australian National University, and Monash University.

#### REFERENCES

- FREIFELD, B.M., TRAUTZ, R.C., KHARAKA, Y.K., PHELPS, T.J., MYER, L.R., HOVORKA, S.D., & COLLINS, D. 2005. The U-tube: A novel system for acquiring borehole fluid samples from a deep geologic CO<sub>2</sub> sequestration experiment. *Journal of Geophysical Research*, **110**, B10203.
- KHARAKA, Y.K., COLE, D. R., HOVORKA, S.D., GUNTER, W.D., KNAUSS, K.G., & FREIFELD, B.M. 2006. Gas-water-rock interactions in Frio Formation following CO<sub>2</sub> injection; implications for the storage of greenhouse gases in sedimentary basins. *Geology*, **34**, 577-580.
- OLDENBURG, C.M. 2003. Carbon dioxide as a cushion gas for natural gas storage. *Energy and Fuels*, **17**, 240-246.

## Pembina Cardium CO<sub>2</sub> Monitoring Project, Alberta Canada – geochemical evaluation and modelling of the geochemical monitoring data

Ernie Perkins<sup>1</sup>, Stephen Talman<sup>1</sup>, & Maurice Shevalier<sup>2</sup>

<sup>1</sup>Alberta Research Council, Edmonton, AB, T6N 1E4 CANADA

<sup>2</sup>Applied Geochemistry Group, University of Calgary, Calgary, AB, T2N 1N4 CANADA

**ABSTRACT:** A CO<sub>2</sub> monitoring pilot was initiated at the Penn West Energy Trust CO<sub>2</sub>-EOR operations within the Cardium Formation of the Pembina Field. The Penn West Pembina Cardium CO<sub>2</sub>-EOR Monitoring Research Program focused on well integrity, local and regional geology and hydrology, extensive geochemical and geophysical monitoring, and short- and long-term predictive modelling.

Changes in the composition of the produced fluids were studied within the geochemical modelling program of the Penn West Monitoring Project. These changes clearly demonstrate directional heterogeneity within the reservoir, and give a clear indication of the short-term chemical reactions controlling the produced water chemistry. Equilibrium speciation calculations demonstrated that many of the produced waters are undersaturated with respect to calcite. This is most easily explained when mixtures of waters of quite different chemical compositions are produced from a single producing well. This observation has important implications for the interpretation of produced water compositions and demonstrates that flow within the reservoir must be understood to fully interpret the chemical signatures. Finally, chemical responses associated with oil field operational procedures such as well workovers could be seen for months after the events.

**KEYWORDS:** *formation water chemistry, carbon dioxide, geosequestration, geochemical modelling*

### INTRODUCTION

The Cardium Formation of the Pembina Field is located approximately 115 kilometres southwest of Edmonton, Alberta, Canada. The Pembina Field was discovered in 1953 and put on primary production in 1955. It was converted to a water flood starting in 1958. In March, 2005, a CO<sub>2</sub> monitoring pilot was initiated by Penn West Energy Trust at their CO<sub>2</sub>-EOR operations within the field. CO<sub>2</sub> was injected into two wells and water into several wells around the immediate pilot area. Early in 2007, the pilot was converted to a WAG (Water Alternating Gas) EOR scheme, where on an approximately monthly basis, the injection of water and CO<sub>2</sub> are switched to the other well.

The Penn West Pembina-Cardium CO<sub>2</sub>-EOR Monitoring Research program focused on establishing: (1) the state of the reservoir and wells, (2) the regional, local and site-specific geology and hydrology, (3) the movement of CO<sub>2</sub> in the

Cardium reservoir using seismic and monitoring of pressure, temperature, and composition of produced fluids, and (4) the short- and long-term fate of CO<sub>2</sub> through predictive modelling (Lakeman 2008).

The goals of the Penn West Monitoring Project were to deduce chemical processes within the reservoir, to track the path and fate of the injected CO<sub>2</sub> (flood performance), and to quantify the long-term CO<sub>2</sub> storage capacity of the reservoir. The necessary data to undertake this assessment were taken from other research in the Penn West Pembina Cardium Monitoring Research Program. This included detailed geological and reservoir studies, modelling based on history matches of the oil, gas, water production and detailed mineralogical investigations (Nightingale *et al.* 2008).

The injected and produced gases and fluids were sampled and analysed for a broad range of chemical and isotopic parameters (Shevalier *et al.* 2008). The

initial produced water chemistry was evaluated through three 'baseline' sampling trips carried out between February and April, 2005. CO<sub>2</sub> injection was initiated in March, 2005. From May 2005 to March 2008, monthly samples were taken, depending on operational conditions. Additionally, historical data on the Pembina Field waters were available (Melrose *et al.* 1976).

**RESULTS AND DISCUSSION**

The data set collected at the Penn West site is extensive, with 28 sampling trips undertaken to date. Selective data are shown in Figures 1 and 2 which show, respectively, the changes in the calculated partial pressure of carbon dioxide in equilibrium with the produced fluid, and the measured wellhead pH of the produced fluid as a function of the sampling date. These data show the response through the three baseline and the subsequent sampling trips. Some data are missing as not all the wells were operational, or producing enough water for a sample to be recovered on a given sampling trip.

The chemical effects of carbon dioxide breakthrough can be clearly seen on the right hand side of each of the figures. There is a strong directional trend reported in the reservoir, which is reflected in the geochemical signal. The producing wells which lie 'on trend' with the CO<sub>2</sub> injectors show a rapid chemical response in contrast to the 'off trend' wells for which the response is considerably delayed.

Figure 3 shows a schematic diagram of the CO<sub>2</sub>-EOR site, together with the calculated calcite saturation index for each produced water sample as a function of time and for each well. This figure also shows that there is a clear difference between those wells on the fracture trend and those off-trend. For most of the on-trend wells, the calcite saturation drops shortly after the onset of CO<sub>2</sub> injection, becoming negative. This is contrasted by the off-trend well behavior, for which the SI remains nearly constant, and positive through most of the period represented. The rapid decrease seen in a few wells

near the end of the monitoring period is associated with the arrival of a strong signal due to injected CO<sub>2</sub>. It is somewhat unexpected that some many of the samples were undersaturated with respect to calcite; we interpret this as indicating mixtures of waters with quite different chemical compositions are produced from these wells.

Melrose *et al.* (1976) noted that the waters produced from the Cardium reservoir under water flooding changed in composition from the initial formation water (a concentrated NaCl-dominated fluid) to a diluted Na (Cl,HCO<sub>3</sub>) water. This evolution in water composition is associated with ion exchange reactions coupled with calcite dissolution and CO<sub>2</sub> stripping from the oil phase. These ion exchange reactions can control the short-term response of the produced water chemistry to any changes in the injected fluid composition. Transient responses can occasionally be seen in the composition of the produced water recovered during this study. These

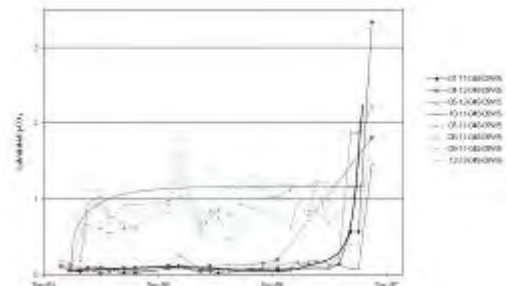


**Fig. 1.** Calculated partial pressure of CO<sub>2</sub> in equilibrium with the produced fluids.

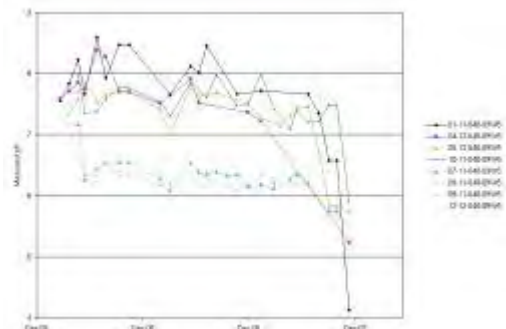


**Fig. 2.** Measured pH of the produced waters at the wellhead.

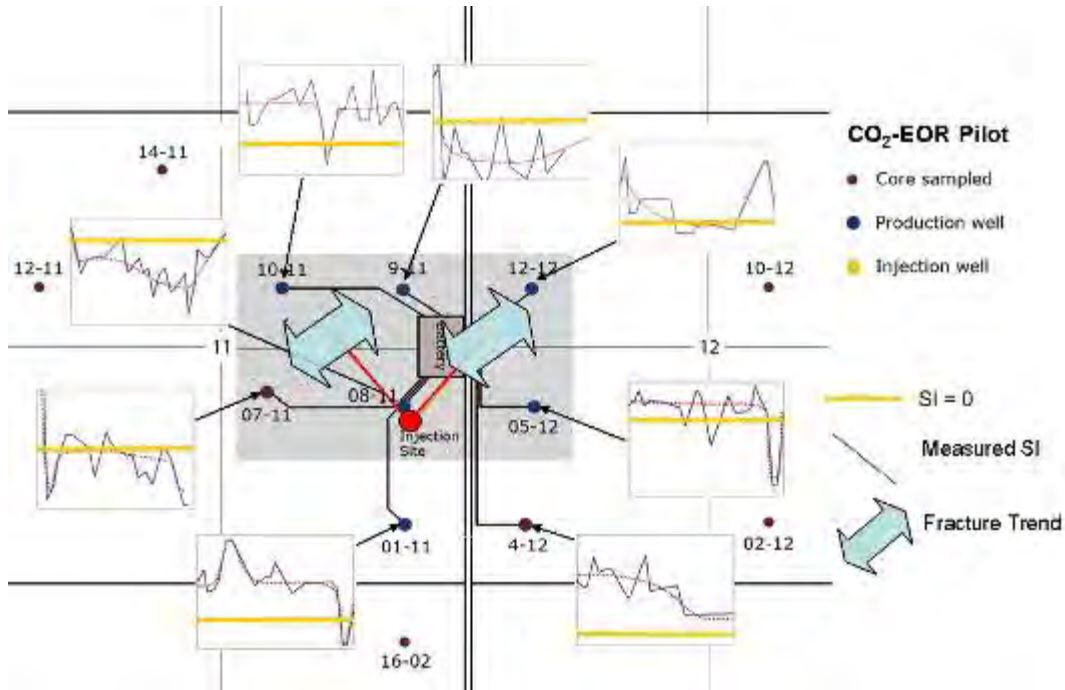


**Fig.3.** Schematic representation of the Penn West Cardium CO<sub>2</sub> EOR project together with the time evolution of the calcite saturation index. The horizontal line in each SI figure represents an SI of 0. The maximum SI on each figure is 0.8 and the minimum is -0.4, with the exception of well 08-11 with a maximum SI of 0.4 and a minimum of -1.6.

transient responses are often related to well workover events. Often, highly concentrated solutions are used as weighting fluids during well maintenance. These fluids can induce a shift in many of the equilibria which control the produced water chemistry under 'normal' operating conditions. These geochemical changes are transitory but have been observed to last for months after the operational procedures that initiated them was completed (Talman *et al.* 2009).

Filtering out the operationally induced changes from the produced fluid compositions clarified the changes induced through reactions with the injected carbon dioxide and helps establish the normal variations in fluid composition.

**CONCLUSIONS**

The results of this study demonstrate that geochemical analysis of CO<sub>2</sub>-EOR operations can yield important insights into the reactions which will ultimately

determine the fate of the injected CO<sub>2</sub>. Detailed geochemical sampling and analysis have provided the necessary data to interpret the processes occurring in the reservoir. The observed trends in the data are consistent with known geochemical process in the reservoir. The occasional large perturbations are the results of field operations, typically well workovers.

Observations of the arrival of the CO<sub>2</sub> acid front at different wells clearly demonstrates that there is a great deal of heterogeneity in the reservoir. Furthermore, the arrival of waters which are undersaturated with respect to calcite suggests that single producing wells are recovering waters with widely different CO<sub>2</sub> contents. These observations have important implications for the interpretation of produced water compositions; in complex reservoirs it must be done in conjunction with detailed reservoir flow models.

Geochemical examination of the

produced water composition has established that the primary controls on the produced water compositions are the injection fluid compositions, the formation fluid composition, and the formation mineralogy, and their interaction through mixing, dissolution, and ion exchange. Detailed historical data is critical to the interpretation of the current produced water compositions.

#### **ACKNOWLEDGEMENTS**

This work was carried out with the strategic guidance and financial support of Penn West Energy Trust, AERI (Alberta Energy Research Institute), Western Economic Diversification Canada, Natural Resources Canada, and the Alberta Government.

#### **REFERENCES**

LAKEMAN, B. 2008. Monitoring CO<sub>2</sub> at the Penn West Pembina Cardium Pilot. *3<sup>rd</sup> Annual Enhanced Oil Recovery Conference,*

*Calgary, Alberta. April 30, 2008.*

MELROSE, J.C., JOHNSON, W.F., & GEORGE, R.A. 1976. Water-rock interactions in the Pembina Field, Alberta. *Society of Petroleum Engineers, SPE Paper Number 6059.*

NIGHTINGALE, M., SHEVALIER, M., HUTCHEON, I., PERKINS, E., & MAYER, B. 2008. Impact of injected CO<sub>2</sub> on reservoir mineralogy during CO<sub>2</sub>-EOR. *9th International Conference on Greenhouse Gas Control Technologies, Washington DC, 16-20 November, 2008.*

SHEVALIER, M., NIGHTINGALE, M., JOHNSON, G., MAYER, B., HUTCHEON, I., & PERKINS, E. 2008. Geochemical monitoring of the Penn West CO<sub>2</sub>-EOR Pilot, Drayton Valley, Alberta. *7th Annual Conference on Carbon Capture and Sequestration, Pittsburgh, Pa.*

TALMAN, S., SHEVALIER, M., PERKINS, E., NIGHTINGALE, M., & MAYER, B. 2009. Impact on geochemical monitoring of CO<sub>2</sub>-EOR operations by well workovers and field operations at the Pembina Cardium CO<sub>2</sub> Monitoring Project. Presented at the *8th Annual Conference on Carbon Capture and Sequestration, Pittsburgh, Pa.*

## Numerical assessment of CO<sub>2</sub> enhanced CH<sub>4</sub> recovery from the Mallik gas hydrate field, Beaufort-Mackenzie Basin, Canada

Mafiz Uddin<sup>1</sup>, J.F. Wright<sup>2</sup>, William D. Gunter<sup>3</sup>, & D. Coombe<sup>4</sup>

<sup>1</sup> Alberta Research Council Inc., 250 Karl Clark Road, Edmonton, AB, T6N 1E4 CANADA

<sup>2</sup> Geological Survey of Canada, Terrain Sciences Division, Box 6000, 9860 West Saanich Road, Sidney, BC, V8L 4B2 CANADA

<sup>3</sup> Principal Consultant for the Alberta Research Council (CO<sub>2</sub> Geological Storage) & CEO of G BACH Enterprises Inc., 11239 63 Street, Edmonton, AB, T5W 4E5 CANADA

<sup>4</sup> Computer Modelling Group Ltd., 3512-33 Street NW, Calgary, AB, T2L 2A6 CANADA

**ABSTRACT:** The Mallik gas hydrate field represents an onshore permafrost-associated gas hydrate accumulation in the Mackenzie Delta on the coast of the Beaufort Sea, Northwest Territories, Canada. This deposit contains a high concentration of natural gas hydrate with an underlying aquifer or free-gas zone at the base of the hydrate stability field. The physical and chemical properties of CH<sub>4</sub> and CO<sub>2</sub> hydrates indicate the possibility of coincident CO<sub>2</sub> sequestration and CH<sub>4</sub> production from the Mallik gas hydrate bearing zones. This study presents a numerical assessment of CO<sub>2</sub> sequestration and the recovery of CH<sub>4</sub> from the gas hydrates at the Mallik site, Mackenzie Delta, Canada.

**KEYWORDS:** CH<sub>4</sub> hydrate; hydrate kinetics, hydrate stability, CO<sub>2</sub> sequestration; numerical simulation

### INTRODUCTION

Gas hydrates are crystalline compounds in which smaller gas molecules (<0.9 nm) are engaged inside the lattices of hydrogen-bonded ice crystals. The gas molecules in the crystalline solids are effectively compressed, volumetrically, by a factor of 164. A comprehensive review of the physical and chemical properties of gas hydrates can be found in Sloan (1998, 2003).

The Beaufort-Mackenzie Basin hosts immense unconventional natural gas hydrate reserves that are often co-located with conventional petroleum resources. Osadetz *et al.* (2005) reported that the conventional resources are co-located with an immense gas hydrate resource estimated between  $2.4 \times 10^{12}$  and  $87 \times 10^{12}$  m<sup>3</sup> of raw natural gas. Because the expected decline in conventional natural gas production from the Western Canada Sedimentary Basin cannot be replaced by conventional production from frontier regions alone, this immense hydrate resource offers a solution to replace the expected decline in conventional gas reserves.

Majorowicz & Osadetz (2001) reported that the Mallik gas hydrate-bearing deposit in permafrost regions tends to occur at depths of 700 m to 1400 m where the permafrost is 100 m to 900 m thick. The Mallik 2002 Gas Hydrate Production Research Well Program conducted scientifically constrained production tests of the natural gas from the Mallik gas hydrate deposit, which is situated in the Mackenzie Delta on the coast of the Beaufort Sea, Northwest Territories, Canada (Dallimore *et al.* 2005a; Satoh *et al.* 2005). Gas hydrate production tests demonstrated the potential for possible commercial production. Japan intends to establish commercial production from gas hydrates within the time frame of conventional natural gas production from the Mackenzie Delta (Yonezawa 2003).

Currently, there are three possible gas recovery processes for hydrates: (1) thermal stimulation, (2) depressurization and (3) inhibitor injection. Very limited thermal stimulation and depressurization tests were reported for the Mallik natural gas hydrate reservoirs, together with numerical simulations (Moridis *et al.* 2004,

and Kurihara *et al.* 2005). However, there is no sustainable and environmental friendly recovery technology for the Arctic gas hydrates.

The objective of this study is to evaluate the feasibility of CO<sub>2</sub>-enhanced CH<sub>4</sub> recovery technology for the Beaufort-Mackenzie Basin gas hydrates. The physical and chemical properties of CH<sub>4</sub> and CO<sub>2</sub> hydrates indicate the possibility of coincident CO<sub>2</sub> sequestration and CH<sub>4</sub> production from the Mallik gas hydrate-bearing deposits.

### MALLIK GAS HYDRATES

The production research well, JAPEX/JNOC/GSC Mallik 5L-38 showed three gas hydrate-bearing zones at depths from 892 to 930 m, 942 to 993 m, and 1060 to 1120 m with gas hydrate

saturations ranging from 50 to 85%, 40 to 80%, and 80 to 90%, respectively. Fig. 1 presents important geophysical log data, and estimated porosity, permeability, and hydrate saturation, and identifies three major hydrate-bearing zones. The hydrate-aquifer interface marks the bottom of the stability zone at a pressure of 12,962 kPa, temperature of 12.2°C, and pore water salinity of 45,000 ppm (45 ppt – parts per thousand) (Wright *et al.* 2005).

In the JAPEX/JNOC/GSC program, small-scale field production tests were conducted by using pressure-drawdown experiments. Data measured in response to depressurization are: pressure, temperature, gas flow, and water flow. During our study, these data were not available to us.

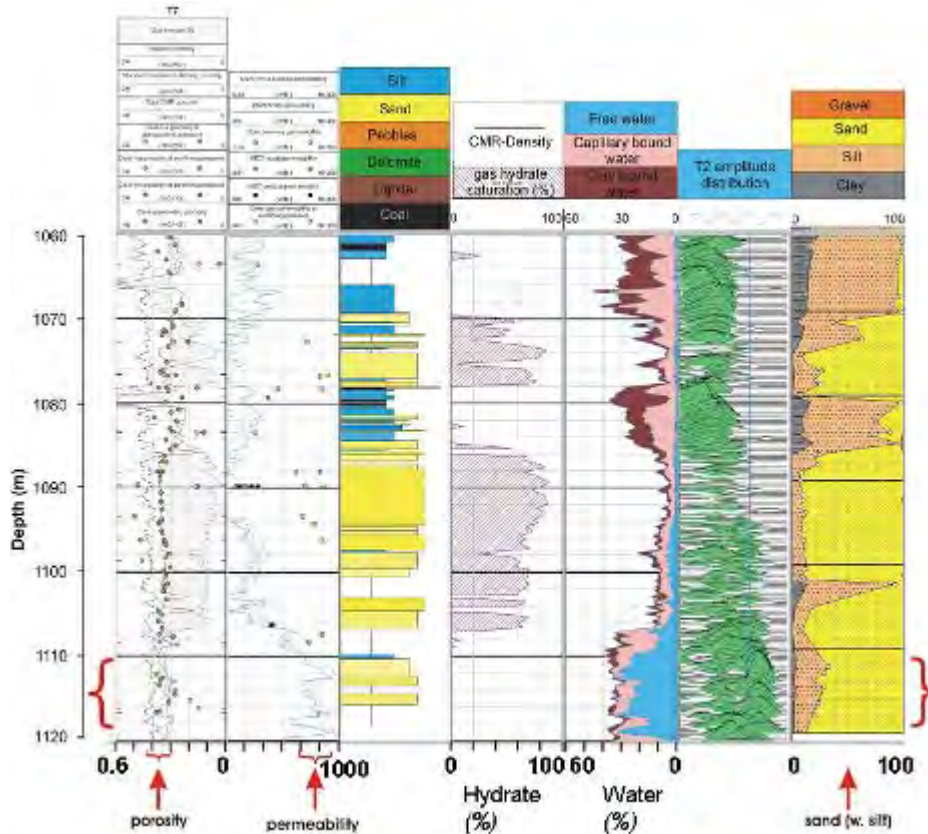


**Fig. 1.** Log data showing the variation of porosity, permeability, and gas hydrate saturation for the Mallik Gas Hydrate Research Program Well-5L-38 (Uddin *et al.* 2008b).

### CH<sub>4</sub> PRODUCTION FROM THE MALLIK GAS HYDRATES

A unified gas hydrate kinetic model (developed at ARC) coupled with a thermal reservoir simulator (CMG STARS) was applied to simulate the dynamics of CH<sub>4</sub> production and CO<sub>2</sub> sequestration processes in the Mallik geological zones. The kinetic model contains two mass transfer equations: one equation transfers gas and water into hydrate, and a decomposition equation transfers hydrate into gas and water (Uddin *et al.* 2008a).

Uddin *et al.* (2008b) conducted several depressurization simulations for the Mallik 5L-38 well. Their results showed that the Mallik gas hydrate layer with its underlying aquifer could yield significant amounts of gas originating entirely from gas hydrates, the volumes of which increased with the production rate. However, large amounts of water were also produced. Sensitivity studies indicated that the methane release from the hydrate accumulations increased with the decomposition surface area, the initial hydrate stability field (P-T conditions), and the thermal conductivity of the formation. Methane production appears to be less sensitive to the specific heat of the rock and of the gas hydrate.

Fig. 2 highlights a serious practical limitation in the depressurization technology due to the drop in temperature from the heat loss during the breakdown of the hydrate (Uddin *et al.* 2008b). This leads to a new stability field at lower salinities. The stability paths in such a progressive depressurization could lead into a complex ice formation domain.

### CO<sub>2</sub> SEQUESTRATION IN THE MALLIK GAS HYDRATES

Uddin *et al.* (2008b) presented CO<sub>2</sub> hydrate formation simulations for several generic reservoirs similar to Mallik 5L-38. The plots of P-T conditions (see Figs 5 to 10 in Uddin *et al.* 2008b) shows a significant increase in temperature with CO<sub>2</sub> hydrate formation. This leads to a new stability field at higher salinities and highlights a practical limitation in CO<sub>2</sub> hydrate formation (Fig. 3).

### CO<sub>2</sub> ENHANCED CH<sub>4</sub> PRODUCTION

The combination of CO<sub>2</sub> injection and methane production over specific PT regimes allows the heat effects of CO<sub>2</sub> hydrate formation and methane hydrate decomposition to nullify each other resulting in a sustainable delivery process which both reduces CO<sub>2</sub> emissions to combat global warming and recovers methane to supplement the declining reserves of conventional natural gas (Fig. 4). This gas hydrate phase-behaviour in response to the dissociation and formation processes clearly demonstrates the potential of CO<sub>2</sub> enhanced CH<sub>4</sub> recovery from the Mallik gas hydrate deposit.

### ACKNOWLEDGEMENTS

The authors gratefully acknowledge the

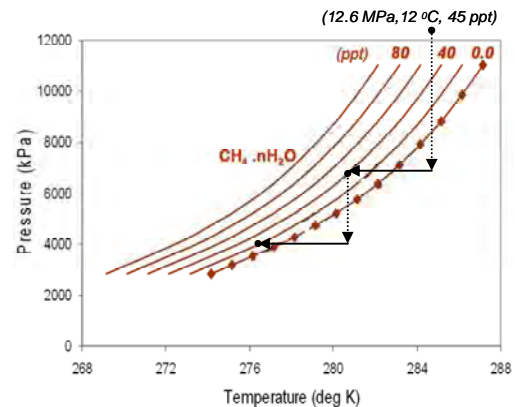


Fig. 2. CH<sub>4</sub> hydrate stability curves (laboratory data) showing CH<sub>4</sub> hydrate dissociation paths (schematic) in the depressurization method.

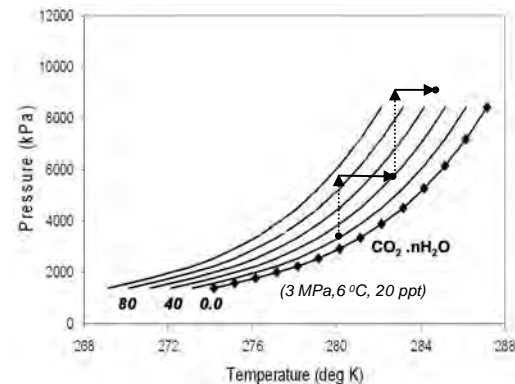
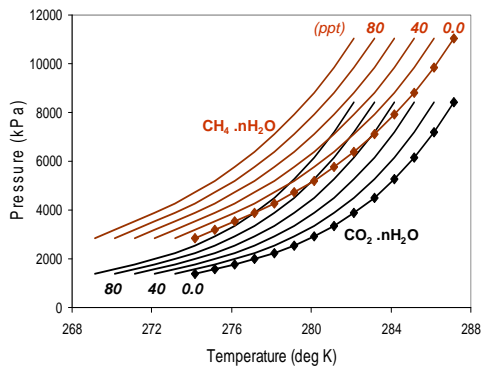


Fig. 3. CO<sub>2</sub> hydrates stability curves (lab data) showing CO<sub>2</sub> hydrate formation paths (schematic) by injection of CO<sub>2</sub> gas.



**Fig. 4.** CH<sub>4</sub> - and CO<sub>2</sub> hydrates stability curves showing CO<sub>2</sub> enhanced CH<sub>4</sub> hydrate dissociation zone.

support from the Alberta Research Council and the Geological Survey of Canada.

**REFERENCES**

DALLIMORE, S.R., COLLET, T.S., UCHIDA, T., & WEBER, M. 2005a. Overview of the science program for the Mallik 2002 Gas Hydrate Production Research Well Program., In: DALLIMORE, S.R. & T.S. COLLETT, T.S. (eds.), *Scientific Results from the Mallik 2002 Gas Hydrate Production Research Well Program, Mackenzie Delta, Northwest Territories, Canada*. Geological Survey of Canada, Bulletin 585.

KURIHARA, M., OUCHI, H., INOUE, T., YONEZAWA, T., MASUDA, Y., DALLIMORE, S.R., & COLLETT, T.S. 2005. Analysis of the JAPEX/JNOC/GSC et al. Mallik 5L-38 gas hydrate thermal-production test through numerical simulation. *Geological Survey of Canada, Bulletin 585*.

MAJOROWICZ, J.A. & OSADETZ, K.G. 2001. Basic geological and geophysical controls bearing on gas hydrate distribution and volume in Canada. *American Association of Petroleum Geologists Bulletin*, **85**, 1211-1230.

MORIDIS, G.J., COLLETT, T.S., DALLIMORE, S.R., SATOH, T., HANCOCK, S., & WEATHERILL, B. 2004. Numerical studies of gas production from several CH<sub>4</sub> hydrate zones at the Mallik site, Mackenzie Delta, Canada. *Journal of Petroleum Science and Engineering*, **43**, 219-238.

OSADETZ, K.G., MORRELL, G.R., DIXON, J., DIETRICH, J.R., SNOWDON, I.R., DALLIMORE, S.R., & MAJOROWICZ, J.A. 2005. Beaufort-Mackenzie Basin: A review of conventional and nonconventional (gas hydrate) petroleum reserves and undiscovered resources. *Geological Survey of Canada, Bulletin 585*.

SATOH, T., DALLIMORE, S.R., COLLETT, T.S., INOUE, T., HANCOCK, S.H., MORIDIS, G., & WEATHERILL, B. 2005. Sedimentology of the cored interval, JAPEX/JNOC/GSC et al. Mallik 5L-38 gas hydrate production well. *Geological Survey of Canada, Bulletin 585*.

SLOAN, E.D. 1998. *Clathrate Hydrates of Natural Gases*. 2nd edition, Marcel Dekker, 513-537.

SLOAN, E.D. 2003. Fundamental principles and applications of natural gas hydrates. *Nature*, **426**, 353-359.

UDDIN, M., COOMBE, D., LAW, D., & GUNTER W,D. 2008a. Numerical studies of gas hydrate formation and decomposition in a geological reservoir. *ASME, Journal of Energy Resources Technology*, **130**, paper 032501.

UDDIN, M., COOMBE, D., & WRIGHT, F. 2008b. Modelling of CO<sub>2</sub> hydrate formation in geological reservoirs by injection of CO<sub>2</sub> gas. *ASME, Journal of Energy Resources Technology*, **130**, paper 032502.

WRIGHT, J.F., DALLIMORE, S.R., NIXON, F.M., & DUCHESNE, C. 2005. In situ stability of gas hydrate in reservoir sediments of the JAPEX/JNOC/GSC et al. Mallik 5L-38 gas hydrate production research well. *Geological Survey of Canada, Bulletin 585*.

YONEZAWA, T. 2003. unpublished <http://www.netl.doe.gov/scngo/Natural%20Gas/hydrates/newsletter/HMNewspring03.pdf>, viewed 2005-03-22, spring 2003, 8.

## Geochemical monitoring of chemical and isotopic compositions of CO<sub>2</sub> fluids and calcite precipitation during injection tests at Ogachi Hot-Dry Rock site, Japan

Akira Ueda<sup>1</sup>, Yoshihiro Kuroda<sup>1</sup>, Kazunori Sugiyama<sup>2</sup>, Akiko Ozawa<sup>2</sup>, Hiroshi Wakahama<sup>3</sup>, Saeko Mito<sup>3</sup>, Yoshikazu Kaji<sup>4</sup>, & Hideshi Kaieda<sup>5</sup>

<sup>1</sup>Kyoto University, C1-2-155, Katsura, Nishikyo-ku, Kyoto, 616-8540 JAPAN  
(e-mail: a-ueda@earth.kumst.kyoto-u.ac.jp)

<sup>2</sup>Mitsubishi Materials Techno Corp., 1-14-16 Kudan-kita, Chiyoda-ku, Tokyo, 102-8205 JAPAN

<sup>3</sup>Research Institute of Innovative Technology for the Earth, 9-2 Kizugawadai, Kyoto, 619-0292 JAPAN

<sup>4</sup>Chuo Kaihatsu Corp., 3-4-2 Nishi-aoki, Kawaguchi, Saitama, 332-0035 JAPAN

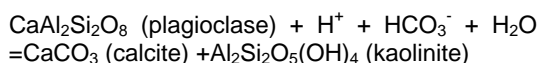
<sup>5</sup>Central Research Institute of the Electric Power Industry, 1646 Abiko, Chiba, 270-1194 JAPAN

**ABSTRACT:** Field experiments of CO<sub>2</sub> sequestration into the Ogachi hot dry rock (HDR; the temperature is 200°C) site are performed to investigate mineralization of a part of CO<sub>2</sub> as carbonates by interaction with rocks (Georeactor; Ca extraction from rocks and carbonate fixation). In 2007, CO<sub>2</sub> dissolved water (river water with dry ice) was directly injected into OGC-2 (from September 2nd to 9th) and Run #2 (from September 11th to 16th). Several tracers were also injected at the same time. Water samples are collected at the depth of ca. 800m by a sampler (500ml in volume) and monitored for their chemical and isotopic compositions. During the Run #2 experiment, river water was injected into OGC-1 at 2 days after injection of CO<sub>2</sub> water into OGC-2. During the field experiments, dissolution or precipitation rates of calcite were determined by using a technique of “in situ analyses”. Calcite crystals covered with Au film is hold in a crystal cell and set in a crystal sonde. The crystal sonde is then put into OGC-2 and water samples at the certain depth is introduced into the sonde. After 1 hour, the sonde is recovered and the calcite crystal is observed by a newly developed phase shift interferometer to analyze the dissolution or precipitation rates of calcite from the reservoir fluids. The “in situ analyses” show that calcite precipitation was observed within 2 day after the injection. This supports the view that most of CO<sub>2</sub> injected might be fixed as carbonate.

**KEYWORDS:** georeactor, CO<sub>2</sub>, mineralization, calcite, Ogachi

### INTRODUCTION

Several research programs have been proceeded on CO<sub>2</sub> sequestering, where the temperatures of CO<sub>2</sub> reservoirs are less than 100°C and pressures are a few tens to hundreds of bars (ex. Perkins & Gunter 1996; Holloway 1996; Gale 2004). In countries such as Japan, where have many active volcanic areas, one possibility is to sequester CO<sub>2</sub> into hydrothermal regions. The chemical reaction rates between CO<sub>2</sub>-saturated water and rocks are usually faster than those at room temperature. For example, the following reaction can proceed to the right side at high temperature (Gale & Shane 1905).



(1)

Carbonate-rich rock formations can be observed in most Japanese geothermal fields. In the Sumikawa field, Akita, Japan, for example, CO<sub>2</sub>-rich ground waters are thought to have reacted with reservoir rocks according to reaction (1), to form a carbonate and kaolinite alteration assemblage. An isotopic investigation of

calcites at Sumikawa indicated that the reaction occurred at 100 to 250 °C by interaction of reservoir rocks with meteoric waters (Ueda *et al.* 2001).

### THE CONCEPT OF “GEOREACTOR”

Reaction (1) moves towards the right side at higher temperature, reflecting the fact that calcite solubility decreases with increasing temperature. The calcite and kaolinite (clay)-rich rock is produced through the reaction and acts as a cap rock for the geothermal reservoir. These considerations, together with the increasing reaction rates as temperatures are elevated and the fact that precipitation of carbonate minerals fixes CO<sub>2</sub> suggest that CO<sub>2</sub> sequestration could be practicable by injection into geothermal fields (Georeactor; Fig.1).

In Japan, total rock volume in high (>150°C) and intermediate (90-150°C) temperature fields are estimated to be 2100 and 2800 km<sup>3</sup> respectively. CO<sub>2</sub> storage capacity is calculated to be about 20 billion tons CO<sub>2</sub> (ca. 17 times Japan's total annual CO<sub>2</sub> emissions). The CO<sub>2</sub>/(Ca+Mg) mole ratio of typical igneous rocks is 0.012-0.12. If

1-12% of Ca and Mg would be released, CO<sub>2</sub> may be fixed in carbonate minerals (Ohsumi *et al.* 2005).

In our laboratory experiments, a part of CO<sub>2</sub> can be precipitated as carbonate during interaction with rocks at 100 to 250°C (Ueda *et al.* 2005). To examine this phenomena in the field, CO<sub>2</sub> saturated water was injected into the Ogachi HDR site.

**FIELD EXPERIMENTS**

The Ogachi hot dry rock (HDR) field is situated at the northeast Japan and has been studied to produce geothermal electricity by Central Research Institute of the Electric Power Industry for 20 years. There are two injection/production wells (OGC-1 and -2) and an observation one (OGC-3). Two major feed zones were formed by hydro fracturing at depth of 700m and 1100m, where their temperatures are 170 and 210°C, respectively.

Field experiments of CO<sub>2</sub> sequestration into the Ogachi HDR have been examined for 4 years by our group (Metcalf *et al.*, 2006; Ueda *et al.* 2007). In 2007, CO<sub>2</sub> dissolved water (river water with dry ice) was directly injected into OGC-2 (Fig.3; Run #1 (from September 2nd to 9th) and Run #2(from September 11th to 16th)). Several tracers were also injected at the same time. Water samples are collected at the depth of ca. 800m by a sampler (500ml in volume) and monitored for their

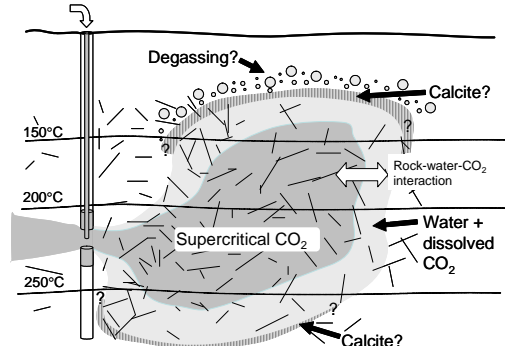


**Fig. 1.** Outline of CO<sub>2</sub> sequestration into geothermal fields.

chemical and isotopic compositions ( $\delta D$ ,  $\delta^{18}O$ ,  $\delta^{13}C_{CO_2}$ ). During the Run #2 experiment, river water was injected into OGC-1 at 2 days after injection of CO<sub>2</sub> water into OGC-2.

During the field experiments, dissolution or precipitation rates of calcite were determined by using a technique of “in site

analyses” (Sato *et al.* 2007a). Calcite crystals covered with Ti rod or Au film is hold in a crystal cell and set in a crystal sonde. The crystal sonde is then put into OGC-2 and water samples at the certain depth is introduced into the sonde. After 1 hour, the sonde is recovered and the calcite crystal is observed by a newly developed phase shift interferometer

**Injexction of CO2 and river water**

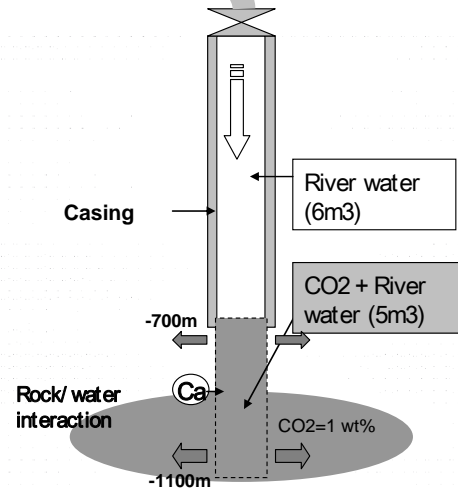


**Fig. 2.** . CO<sub>2</sub>-water injection test at OGC-2 in 2007.

(Ueda *et al.* 2005; Sato *et al.* 2007b) to analyze the dissolution or precipitation rates of calcite from the reservoir fluids.

**RESULTS AND DISCUSSION**

During the 2007 field experiments, CO<sub>2</sub> concentrations of the water samples under the reservoir pressure could not be correctly monitored due to the broken of the water sampler. This means that water samples were collected around 800m depth and a part of CO<sub>2</sub> must be degassed during ascending to the surface from the sampler. Therefore, CO<sub>2</sub> concentrations of the reservoir fluids are calculated on the basis of the observed pH and charge balance of each samples (Case 1) and the tracer concentration (Case 2). The Case 2 means that CO<sub>2</sub> in the injected water did not react with rocks. Fig.3 shows the calculated CO<sub>2</sub> concentration with iodine. Iodine concentration decreases from 1000 to 200µg/L with the elapsed time. From Fig.4, the fraction of the injected CO<sub>2</sub> water (1 wt.% CO<sub>2</sub>) is almost zero. This means that

the injected water was completely diluted with the reservoir fluid. The calculated CO<sub>2</sub> concentrations vary from 900 to 600 mg/L .

From the chemical compositions of water samples, the saturation index of calcite is calculated as follows;

$$S.I. \text{ (Saturation Index)} = \text{Log} (Q/K) \quad (2)$$

where Q and K are activity and solubility products of calcite, (Ca<sup>2+</sup>)(CO<sub>3</sub><sup>2-</sup>), respectively. If S.I.>0, the fluid is saturated with respect to calcite (calcite precipitation).

Fig. 4 shows the change of the S.I. during the experiments (Run2). In the case 1, the S.I. is above zero except for the sample collected just after CO<sub>2</sub> injection. In contrast, the S.I. is close to zero in the case 2 implying that the reservoir fluid mixed with the injected CO<sub>2</sub> water is almost in equilibrium with calcite. Fig. 6 also shows the observed dissolution or precipitation rates of calcites which are determined by in site analyses. From these results, the injected CO<sub>2</sub> water is

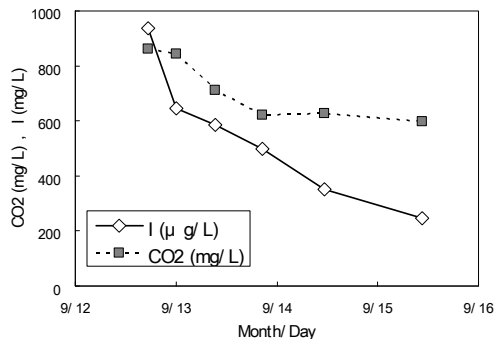


Fig. 3. Concentrations of iodine and CO<sub>2</sub>.

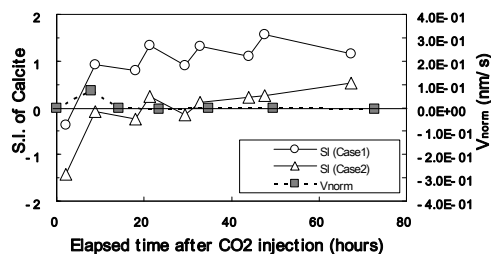


Fig. 4. Saturation index of calcite.

diluted with the reservoir fluid with 3 days and most CO<sub>2</sub> in them might be deposited by interaction with granitic rocks. According to the material balance, only 1μm thickness of the granitic rocks is enough to react with the CO<sub>2</sub> water to precipitate as carbonate

minerals. In the previous field experiments in 2002 and 2003, Ca concentration in the water samples increased from 10 to 80 mg/L with 1 day and quickly decreased to the background. These results also support

### CONCLUSIONS

The injected CO<sub>2</sub> water is diluted with the reservoir fluid within 3 days. Most CO<sub>2</sub> in them might be deposited as calcite by interaction with granitic rocks. Ca concentration in the water samples increased from 10 to 80 mg/L with 1 day and quickly decreased to the background. These results also support the view that CO<sub>2</sub> injected is precipitated as carbonates within few days.

### ACKNOWLEDGEMENTS

This research is partly supported by the grants of the Programmed Research "Development of evaluation technology for the CO<sub>2</sub> in the exhaust gas sequestration into geothermal fields" of RITE under the fund from METI (Ministry of Economy, Trade and Industry). We thank Odashima, Tokumaru and other members at Ogachi for their kind help during laboratory and field experiments.

### REFERENCES

GALE, J. 2004. Geological storage of CO<sub>2</sub>: What do we know, where are the gaps and what more needs to be done? *Energy*, **29**, 1329-1338.

GALES, C. & SHANE, H. 1905. About a case of kaolinitisation in granite by a cold CO<sub>2</sub> bearing water. *Zenit. Geol. Min. Palisant.*, 427-467.

HOLLOWAY, S. (ed.). 1996. *The underground disposal of carbon dioxide*, Final report, Contract No. JOU2 CT92-0031, 355 p.

METCALFE, R., UEDA, A., KATO, K. et al. 2006. The feasibility of sequestering CO<sub>2</sub> in geothermal systems: a theoretical evaluation, abstr. GHGT8.

OHSUMI, T., YAJIMA, T., KAIEDA, H., ITO, H., ITO, Y., KATO, K., & UEDA, A. 2005. CO<sub>2</sub> sequestration into geothermal fields: (1) The capacity and possibility, *Abst. Goldschmidt Conference*.

PERKINS, E.H. & GUNTER, W.D. 1996. Mineral traps for carbon dioxide. In: HITCHON, B. (ed.), *Aquifer disposal of carbon dioxide*, 93-113.

SATO, H., YAJIMA, T., UEDA, A., OZAWA, A., KATO, K., & KAJI, Y. 2007a. CO<sub>2</sub> injection experiment at Ogachi hot dry rock: In-situ test of calcite production using a crystal-growth sonde, *Abst. Meetings Geothermal Society of Japan*.

- SATOH, H., NISHIMURA, Y., TSUKAMOTO, K., UEDA, A., KATO, K., & UETA, S. 2007b. In-situ measurement of dissolution of anorthite in Na-Cl-OH solutions at 22° using phase-shift interferometry. *American Mineralogist*, **92**, 503-509.
- UEDA, A., AJIMA, S., & YAMAMOTO, M. 2001. Isotopic study of carbonate minerals from the Sumikawa geothermal area and its application to water movement. *Journal of the Geothermal Research Society of Japan*, **23**, 181-196.
- UEDA, A., KATO, K., OHSUMI, T. *et al.* 2005. Experimental studies of CO<sub>2</sub>-rock interaction at elevated temperatures under hydrothermal conditions. *Geochemical Journal*, **39**, 417-425.
- UEDA, A., UETA, S., KATO, K., TSUKAMOTO, K., SATOH, H., & NISHIMURA, Y. 2006. A preliminary report of development of high resolution phase shift interferometry for the assessment of nuclear waster disposal. *Journal Geochemical Exploration*, **88**, 355-357.
- UEDA, A., YAJIMA, T., SATOH, H. *et al.* 2007. Preliminary geochemical results on the CO<sub>2</sub> Georeactor sequestration test at the Ogachi HDR site, *Abst. Goldschmidt Conference*.

# **NORTH AMERICAN SOIL GEOCHEMICAL LANDSCAPES PROJECT**

EDITED BY:

**DAVID SMITH  
ANDY RENCZ**



## The landscape geochemistry of the Sacramento Valley, California

Martin B. Goldhaber<sup>1</sup>, Jean M. Morrison<sup>1</sup>, Richard B. Wanty<sup>1</sup>,  
Christopher T. Mills<sup>1</sup>, & JoAnn M. Holloway<sup>1</sup>

<sup>1</sup>US Geological Survey, Denver Federal Center, Lakewood, CO, 80225 USA (e-mail: mgold@usgs.gov)

**ABSTRACT:** We have conducted a holistic 'geochemical landscape' study of the Sacramento Valley (the northern portion of the Great Valley of California, U.S.A). Our data sets consist of regional soil and ground-water chemical analyses coupled with more focused geochemical studies comprising smaller portions of the area. Both the soil and ground-water data exhibit systematic distribution patterns reflecting geologic, geomorphic, hydrologic, and anthropogenic processes. Sacramento Valley soil samples are differentiated east to west due to the effect of a levee along the Sacramento River, which bisects the valley. Eastern valley soils reflect inputs of glacial debris from the Sierra Nevada as well as material washed down to the valley from extensive placer gold mining. Western valley soils contain a significant chemical signature derived from ultramafic rocks in the Coast Ranges to the west of the valley. Ground water is similarly differentiated east to west in part reflecting this geologic differentiation of valley fill materials. Chromium in the (VI) oxidation state (a potentially toxic constituent) is present in somewhat elevated concentrations, particularly in the western valley. This elevated ground-water Cr content also may reflect the relative abundance of Cr in western valley soil.

**KEYWORDS:** *Geochemical landscapes, chromium, California, soil geochemistry*

### INTRODUCTION

The field of Landscape Geochemistry (LG) deals with the study of the environment that occurs at or near the surface of the earth. As a discipline, LG integrates the interactions of the lithosphere with the hydrosphere, atmosphere and biosphere. As described in a series of papers and a book by Fortescue (1992), LG was conceptually developed largely in the former Soviet Union. The evolution of a geochemical landscape involves the interaction of processes occurring over a range of time and spatial scales. Humans are increasingly intervening and even dominating these processes, making LG studies especially relevant to understanding global environmental change. We have conducted an LG study of a large portion of the Sacramento Valley, in the state of California, U.S.A. This study originated as a pilot project for the soil geochemical survey of North America (North American Soil Geochemical Landscapes Project) and links regional soil and rock geochemistry, hydrochemistry, geophysics, and remote

sensing with existing geomorphic, geologic and land use studies. Our research encompasses regional-scale studies, supplemented by research on specific processes at the local and microscopic scales.

### Overview of study area

Most of the study area is located in the drainage basin of the Sacramento River, which flows near the center of the Sacramento Valley in the northern third of the Great Valley, or Central Valley, of California. This valley was extensively transformed during the past 150 years of human settlement through urbanization, agriculture, mining, and flood control activities (Kelley 1998). The Central Valley is one of the great agricultural regions of the world (Johnson *et al.* 1993) and has rapidly expanding urban and suburban population centers.

The Sacramento Valley is a tectonically controlled basin bounded on the east by the Sierra Nevada, on the west by the Coast Ranges, and on the north by the Klamath Mountains. The alluvium of the valley reflects inputs from these bounding

source areas. Useful geochemical tracers are derived from the chemically and mineralogically distinctive ultramafic rocks (e.g., serpentinite) that crop out extensively in both the Coast Range and Sierra Nevada. These rocks, and the soils derived from them, have particularly high concentrations of Cr and Ni.

#### **Methodology**

Our study uses archived samples supplemented by newly collected material. The archived sample set consists of more than 1300 soil samples collected on a 1-km grid spacing throughout the 1:250,000-scale Sacramento Quadrangle during the late 1970s and early 1980s by the U.S. Department of Energy's National Uranium Resource Evaluation Hydrogeochemical and Stream Sediment Reconnaissance (NURE HSSR) Program (Smith 1997). Each sample represents the upper 10-15 cm of soil. We reanalyzed these archived samples using ICP-MS and ICP-AES. Details on the methods and the analytical results are available in Morrison *et al.* (2008). We also collected soil and rock samples along the western and eastern drainages feeding the valley to characterize potential sources of alluvium.

In addition, chemical data for 661 ground-water and 627 surface-water samples were obtained from the USGS National Water Information System database. Only subsets of all available data that included analyses for major cations, anions, and pH, and had cation-anion charge balances within  $\pm 20\%$  were utilized.

## **RESULTS**

### **Soil Geochemistry**

The soil geochemical results segregate broadly into distinct element groups whose distribution reflects the interplay of geologic, hydrologic, geomorphic, and anthropogenic factors. One group includes the elements Cr, Ni, V, Co, Cu, and Mg associated with mafic and ultramafic rocks. Using Cr as an example, elevated concentrations occur in soils overlying ultramafic rocks in the foothills of the Sierra Nevada (median Cr = 3500 mg/kg) as well as in the northern Coast Ranges.

Low concentrations of these elements occur in soils located further upslope in the Sierra Nevada, where they overly Tertiary volcanic, metasedimentary and plutonic rocks (granodiorite and diorite). Eastern Sacramento Valley soil samples, defined as those collected east of the Sacramento River, are lower in Cr (median Cr = 150 mg/kg) and are systematically lower in the ultramafic suite of elements compared to soils from the west side of the Sacramento Valley (median Cr = 250 mg/kg). A second group of elements showing a coherent pattern, including Ca, K, Sr, and rare earth elements (REE), is derived from relatively silicic rock types. This group occurs at elevated concentrations in soils overlying volcanic and plutonic rocks at higher elevations in the Sierras (e.g., median La = 28 mg/kg). The same elements are elevated on the east side of the Sacramento Valley (median La = 20 mg/kg) compared to soils overlying ultramafic rocks in the Sierra Nevada foothills (median 15 mg/kg) and the western Sacramento Valley (median 14 mg/kg). The segregation of soil geochemistry into distinctive groupings separated by the Sacramento River arises from the former presence of a natural levee (now replaced by an artificial one) along the banks of the river. This levee has been a barrier to cross-valley sediment transport. Sediment transport to the valley by glacial outwash from higher elevations in the Sierra Nevada and, more recently, debris from placer gold mining in the Sierra foothills has dominated sediment sources in the eastern valley. High content of mafic elements (and low content of silicic elements) in surface soils of the west side of the valley is due to the transport of ultramafic rock material from the Coast Ranges and input of sediment from the late Mesozoic marine Great Valley Group. The Great Valley Group lies between the Coast Range ultramafic rocks and the Sacramento Valley and is itself enriched in mafic elements.

The distribution pattern of a third group of elements, including Zn, Cd, As, and Cu, reflects the impact of historical mining.

Soil with elevated content of these elements occurs along the Sacramento River in both levee and adjacent flood basin settings. We interpret that transport of sediment impacted by large metal sulfide mines located in the Klamath Mountains at the north end of the Valley has caused this pattern.

Lead and, to some extent, Zn distribution patterns are strongly affected by anthropogenic inputs. Elevated soil Pb content is localized around major cities and along major highways due to inputs from leaded gasoline. Zinc has a similar distribution pattern, but the likely source is tire wear.

#### **Ground-water Geochemistry**

Ground water on the west side of the Sacramento Valley contains greater concentrations of Na, Ca, Mg, B, Cl, and SO<sub>4</sub>, while the east-side ground water contains greater concentrations of Si and K. These differences in ground-water composition result, in part, from chemical reactions between water and aquifer materials. As such, they reflect the chemical differences of the sediments that fill the western Sacramento Valley, which are higher in Mg and lower in K than eastern valley sediments. The elevated Na, B, and Cl may, in part, reflect input from saline thermal springs that are common along the west side of the Sacramento Valley.

Ground water on the west side of the Sacramento Valley has particularly high concentrations of dissolved Cr ranging up to 50 µg/L and averaging 16.4 µg/L. We interpret that this pattern reflects the enrichment in soil/alluvium Cr content on the west side of the Valley.

#### **Mechanism of Cr(VI) Generation**

Chromium occurs in both the Cr(III) and Cr(VI) valence states. The rock and soil Cr reported in this study is dominantly insoluble and non-toxic Cr(III), whereas the aqueous Cr reported in ground water is soluble and potentially toxic Cr(VI). We have analyzed core material (up to ~30 m depth) from an area of the valley that exhibits elevated Cr(VI) concentrations in

ground water. This core material contains up to 2200 mg/kg total Cr of which only a minute fraction is Cr(VI) (up to 42 µg/kg). Our data suggests that the majority of the total Cr is contained in the refractory spinel mineral chromite, which is the dominant residence of Cr in ultramafic rocks. The core samples contain abundant Mn oxides, an oxidizing agent for Cr(III), and are able to oxidize up to 26 mg of added Cr(III) (as CrCl<sub>3</sub>) per kg of soil. The relative insolubility of chromite in the pH range of ~7 to 9 inhibits the dissolution of Cr(III) from this mineral and its resulting transport to Mn-oxide surfaces. We are currently performing laboratory investigations into possible roles of microbial activity and anthropogenic inputs in the mobilization of Cr(III) and its subsequent oxidation by native Mn oxides.

#### **CONCLUSIONS**

(1) We have studied the interaction of geologic, geochemical, geomorphic, hydrologic, and anthropogenic processes in the Sacramento Valley of north-central California, U.S.A.

(2) Our results demonstrate significant spatial differentiation in the geochemistry of Sacramento Valley soil between the eastern and western sides of the valley that is related to the geomorphic separation of the valley by a levee along the Sacramento River. The western valley contains an elevated component of material derived from ultramafic rocks compared to the eastern side.

(3) This east-west difference reflects dominance in sediment source in the eastern valley by material derived from glacial debris and placer mining, and the presence of ultramafic rocks in the headwaters of western streams and ultramafic constituents in sediments on the west side of the valley.

(4) Ground water in the Sacramento Valley likewise has an east-west differentiation that reflects the geologic differentiation in valley materials

(5) Chromium in ground water is elevated in parts of the Sacramento Valley, particularly the western side.

(6) The rate of Cr(VI) formation is limited by the insolubility of Cr(III) oxides.

#### ACKNOWLEDGEMENTS

We thank Dave Smith of the USGS, and Toby O'Geen, Mike Singer, and Randy Southard of the University of California at Davis for help with this study.

#### REFERENCES

- Fortescue, J.A.C. 1992. Landscape geochemistry; retrospect and prospect-1990. *Applied Geochemistry*, **7**, 1-53.
- JOHNSON, S., HALSAM, G., & DAWSON, R. 1993. *The Great Central Valley; California's Heartland*. University of California Press, Berkeley, California.
- KELLEY, R. 1998. *Battling the Inland Sea; Floods, Public Policy and the Sacramento Valley*. University of California Press, Berkeley, California.
- MORRISON, J.M., GOLDHABER, M.B., HOLLOWAY, J.M., & SMITH, D.B. 2008. Major- and trace-element concentrations in soils from northern

California: Results from the Geochemical Landscapes Project Pilot Study. *U.S. Geological Survey Open-File Report 2008-1306*. Available from: <<http://pubs.usgs.gov/of/2008/1306/>>.

SMITH, S. M. 1997. National Geochemical Database: Reformatted data from the National Uranium Resource Evaluation (NURE) Hydrochemical and Stream Sediment Reconnaissance (HSSR) Program. *U.S. Geological Survey Open-File Report 97-492*. Available from: <<http://pubs.usgs.gov/of/1997/ofr-97-0492/index.html>>..

## The North American Soil Geochemical Landscapes Project: preliminary results from Nova Scotia

Terry A. Goodwin<sup>1</sup>, Peter W. B. Friske<sup>2</sup>, Ken L. Ford<sup>2</sup>, & Eric C. Grunsky<sup>2</sup>

*1Nova Scotia Department of Natural Resources, Mineral Resources Branch, 1701 Hollis Street, Halifax, NS, B3J 2T9 CANADA (e-mail: goodwita@gov.ns.ca)*

*2Geological Survey of Canada, 601 Booth Street, Ottawa, ON, K1A 0E8 CANADA*

**ABSTRACT:** The North American Soil Geochemical Landscapes Project (NASGLP) is a tri-national initiative that involves the federal, provincial and state geological surveys of Canada, the United States and Mexico. Soil samples were collected, prepared and analyzed using a common set of field and analytical protocols. One outcome of this initiative will be the release of the first-ever continental-scale map of the soil geochemistry of North America. Preliminary results for Nova Scotia indicate maximum arsenic soil concentrations are associated with the Meguma Supergroup, host to the majority of the province's gold districts, while maximum uranium and radon concentrations are associated with highly evolved leucomonzogranite. This type of information is required for land-use planners and policy makers to ensure effective land-use planning minimizes human health risks by identifying areas where the natural background elemental concentrations are elevated.

**KEYWORDS:** *Nova Scotia, soil, geochemical surveys, arsenic, uranium, radon, human health*

### INTRODUCTION

Nova Scotia is a small province located on the east coast of Canada and is characterized by a relatively complex bedrock and surficial geologic history. As a result, large regions of the province are known to contain naturally elevated background concentrations of various elements. In addition to areas of naturally elevated background, significant sub-economic to economic mineralization also exists for a wide variety of elements. Anthropogenic inputs also contribute to the variation in the geochemical landscape at both local and regional scales.

### FIELD SAMPLING

In order to assess natural soil geochemical background concentrations, samples were collected from various soil horizons and discrete depth intervals from hand-dug pits. A total of 72 sites were sampled during the 2007 and 2008 field seasons yielding an average density of approximately 1 site per 800 km<sup>2</sup> that is double the nominal density of a site per 1600 km<sup>2</sup> for the NASGLP. Samples were collected from the surface layer (0 to 5

cm) as well as the A, B and C soil horizons. At each site, (1) soil gas radon (kBq/m<sup>3</sup>); (2) K (pct), eU (ppm) and eTh (ppm) concentrations by in situ gamma ray spectrometry; and (3) soil permeability values were also determined.

### SAMPLE PREPARATION AND ANALYSIS

Soil samples were sieved to two size fractions: <63 µm and <2 mm. Samples were analyzed for multi-element geochemistry by inductively coupled plasma/mass spectrometry (ICP/MS) following a "near total" 4-acid digestion.

Radon concentrations were determined using an RM-2 portable soil radon monitoring system while in situ soil permeability values were determined using Radon-JOK portable sampling equipment.

### RESULTS – ARSENIC

Preliminary results for As in the <63-µm fraction indicate C-horizon soil concentrations range from a low of 2.2 ppm to a high of 345 ppm with a mean of 22.3 ppm (Fig. 1). The highest As sample site is located within the Late Neoproterozoic/Cambrian Meguma



**Fig. 1.** Arsenic concentrations (ppm) in C-horizon soil samples, Nova Scotia.

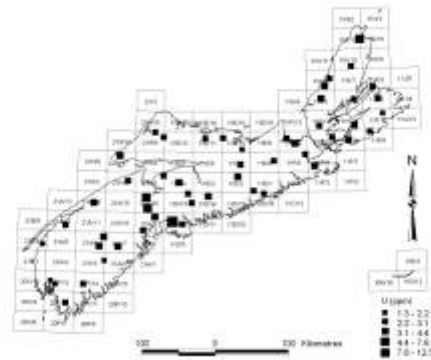


**Fig. 2.** Uranium concentrations (ppm) in C-horizon soil samples, Nova Scotia.

Supergroup, a deepwater succession of marine metasandstones fining upwards into slate. This site also reported the highest arsenic in the <2-mm fraction of the A-horizon (229 ppm), B-horizon (284 ppm) and the C-horizon (228 ppm). The Meguma Supergroup hosts the majority of the province's gold districts that are characterized by the regional presence of arsenopyrite and locally by gold-arsenopyrite mineralization.

### URANIUM

Uranium concentrations in the <63- $\mu\text{m}$  fraction of C-horizon soil range from a low of 1.3 ppm to a high of 12.5 ppm with a mean of 3.0 ppm (Fig. 2). The highest U concentration is associated with highly evolved Middle-to-Late Devonian leucomonzogranite of the South Mountain Batholith, one of the largest granitoid bodies in eastern North America and occupying an area of approximately 7300  $\text{km}^2$ . Several other highs are associated with Middle-to-Late Devonian leucomonzogranite or Carboniferous age Horton Group sedimentary rocks.

### RADON

Radon in soil gas is present everywhere throughout the province in all geologic terrains. Soil gas Rn concentrations range from a low of 0.1  $\text{kBq/m}^3$  to a high of 207.0  $\text{kBq/m}^3$  with a mean of 25.3  $\text{kBq/m}^3$  (Fig. 3). The highest Rn soil gas concentrations are also associated with Middle-to-Late Devonian leucomonzogranite of the South



**Fig. 3.** Mean soil gas radon concentrations ( $\text{kBq/m}^3$ ), Nova Scotia.

Mountain Batholith and, to a lesser degree, with sedimentary rocks of the Carboniferous age Horton and Pictou groups.

### DISCUSSION

All results represent regional, natural background soil concentrations unaffected by obvious anthropogenic influences such as garbage or proximity to industrial, residential or transportation sources.

Exposure to elements such as As, U and Rn may represent an increased human health risk, particularly in areas where the natural background concentrations are elevated.

In order to ensure effective land-use planning, geochemical sampling and mapping are required to identify areas where the natural background concentrations are elevated so that

human exposure to these elements can be minimized.

The identification of elevated U in the C-horizon soil and elevated Rn in the soil gas associated with the Middle-to-Late Devonian leucomonzogranite of the South Mountain Batholith are examples of the type of information generated by the

NASGLP for predicting areas of potential natural geologic hazards.

#### **ACKNOWLEDGEMENTS**

Funding for the project was provided by the Geological Survey of Canada and by the Radiation Protection Bureau of Health Canada.



## Testing the variants of aqua regia digestion using certified reference materials

E. C. Grunsky, R.G. Garrett, P.W. Friske, & M. McCurdy<sup>1</sup>

<sup>1</sup>Geological Survey of Canada, Natural Resources Canada, Ottawa, ON, K1A 0E8 CANADA  
(e-mail: egrunsky@nrcan.gc.ca)

**ABSTRACT:** The North American Soil Geochemical Landscapes Project requires an analytical protocol that will: 1) provide consistent data across North America; and 2) provide data that would be to the greatest extent possible compatible with current data holdings. The primary method involves a near-total digestion using hydrochloric, nitric, perchloric, and hydrofluoric acids followed by ICP-AES and ICP-MS. The project is also investigating the use of an aqua regia digestion because environmental regulatory agencies frequently use this “total recoverable” extraction to set soil action levels and remediation levels. To select the specific aqua regia protocol, eight Certified Reference Materials (CRMs) were analyzed, in triplicate random order, for 53 elements by four “aqua regia” digestion protocols and the EPA 3050B digestion method. From the results, we have concluded that there are few significant differences among the different aqua regia extractions for the elements of greatest environmental concern (e.g., As, Cd, Co, Cu, Hg, Ni, Pb, U, and Zn). Elements where agreement among the protocols is significantly lacking include Cr, Mn, Mo, Sb, and Zr. The final decision was to use the “aqua regia” variant of the US EPA 3050B protocol.

**KEYWORDS:** *aqua regia digestion, certified reference materials, analysis of variance, Tri-national soil survey*

### INTRODUCTION

A variety of strong acid dissolutions, e.g., 4-acid (near-total) extraction and aqua regia (total recoverable) extraction, are used by different agencies for the purpose of determining trace-element concentrations in environmental materials.

The North American Soil Geochemical Landscapes Project requires an analytical protocol that will: 1) provide consistent data across North America; and 2) provide data that would be to the greatest extent possible compatible with current data holdings. In a 2003 workshop decision, a near-total extraction using hydrochloric, nitric, perchloric, and hydrofluoric acids followed by ICP-AES and ICP-MS was chosen as the core analytical protocol for the continental-scale survey. However, it was also recognized that many environmental regulatory agencies use some variety of aqua regia extraction in setting soil action levels and remediation levels. For this reason, an experiment was devised to select an aqua regia extraction that would be optimum for the project.

Eight Certified Reference Materials (CRMs) (Table 1) were analyzed, in triplicate random order, for 53 elements by five digestion protocols (Table 2) as shown in the experimental design (Table 3). All final determinations were by ICP-AES and -MS in a single batch using a randomized ordering of the prepared digestions.

### RESULTS

Of the 53 elements determined, 48 had useful values above the method detection limits. The data for As and Cr are shown as dotplots (Figs. 1 and 2) as examples of metals and metalloids that occur in both soluble and acid-resistant mineral phases. Dotplots highlight the varying analytical precision for each material and each analytical protocol.

Chromium (Fig. 2) shows the greatest variability across the CRMs, which is consistent with the presence of Cr in both strong-acid soluble minerals and as acid-resistant chromite. On the other hand, As shows good repeatability for the range of

**Table 1.** Certified Reference Materials

Certified Reference Material	Description
LKSD-1	GSC-CCRMP lake sediment
LKSD-4	GSC-CCRMP lake sediment
STSD-1	GSC-CCRMP stream sediment
STSD-4	GSC-CCRMP stream sediment
TILL-1	GSC-CCRMP glacial till (diamicton)
TILL-4	GSC-CCRMP glacial till (diamicton)
SoNE-1	USGS Nebraska soil
2711	USGS Montana soil

**Table 2.** Variants of strong-acid digestion.

**M1 [AR-111]**

1 g sample in a test-tube digest with 3 ml of 1:1:1 HCl-HNO<sub>3</sub>-H<sub>2</sub>O in a heated shaker block at 95° C for an hour, then make up to 10 ml volume with 5% diluted HCl and homogenize the solution with a shaker.

**M2 [AR31] Classical AR digestion**

1 g sample in a test-tube, cold digest with 0.75 ml of HNO<sub>3</sub> for half an hour to oxidize any excess organic matters; follow by adding 2.25 ml of HCl. Place the samples in a heated shaker block at 95° C for an hour. Make up to 10 ml volume with 5% diluted HCl and homogenize the solution with a shaker.

**M3 [AR13] Reverse classical AR digestion (Lefort)**

1 g sample in a test-tube, cold digest with 2.25 ml of HNO<sub>3</sub> for half an hour to oxidize any excess organic matters, follow by adding 0.75 ml of HCl. Place the samples in a heated shaker block at 95° C for an hour. Make up to 10 ml volume with 5% diluted HCl and homogenize the solution in a shaker.

**M4 [AR11]**

1:1 HCl-HNO<sub>3</sub>. Cold digest 0.5 g sample in a test tube with 1.5 ml of conc. HNO<sub>3</sub> until reaction subsides. Further oxidize the sample in a hot water bath at 95° C until brown fumes almost disappear. Remove samples and cool, then add 1.5 ml of conc. HCl and mix. Place the samples in a heated shaker block at 95° C for an hour. Make up to 10 ml volume with 5% diluted HCl and homogenize the solution in a shaker.

**M5 [EPA3050] Modified US-EPA 3050B**

1 g sample in a test-tube, digest with 1 ml of 1:1 HNO<sub>3</sub>-H<sub>2</sub>O in a hot water bath until no brown fumes given off. Allow the samples to cool, add further 0.5 ml of conc. HNO<sub>3</sub> and place samples back to hot water bath and continue heating until no brown fumes are given off. Cool the samples and add 0.5 ml of 30% H<sub>2</sub>O<sub>2</sub>, reheat the samples in hot water bath until the reaction subsides, cool the samples and continue adding another 0.5 ml of 30% H<sub>2</sub>O<sub>2</sub> and repeat the heating until the reaction subsides. Cool the sample and make up to 10 ml volume with 5% diluted HCl and mix the solution well by shaking.

**CRMs and analytical protocols.**

Figures 3 and 4 display what are known as, “interaction plots”, where the mean of triplicate analyses is plotted with respect to CRM and analytical protocol. Where all methods extract a similar amount of the element, the lines representing CRMs will be parallel. In cases where the lines cross, there is an “interaction” between the mineralogy of the CRM and the analytical protocols. For Cr, this latter effect is clearly demonstrated, whereas for As, the methods consistently extract proportionally similar amounts.

ANOVA (ANalysis Of VAriance) provides a formal statistical procedure for analyzing the data arising from the experimental design used here (Table 3).

The details, beyond the model, are not presented, however, the key conclusions are for some of the elements there is no statistical difference between the standard Aqua Regia digestions analytical protocols and a significant difference for some elements with the EPA 3050B digestion. These differences are shown in the interaction plots of Figure 4.

**CONCLUSIONS**

From the experiment undertaken, it is concluded that there are few significant differences between the results yielded by the aqua regia-based extractions for the elements of greatest environmental concern (e.g., As, Cd, Co, Cu, Hg, Ni, Pb, U, and Zn). Elements where agreement between the protocols is significantly lacking include Cr, Mn, Mo, Sb and Zr. Clearly, US-EPA 3050B, an all-oxidizing reagent, HNO<sub>3</sub>-H<sub>2</sub>O<sub>2</sub>, protocol, ([www.epa.gov/epawaste/hazard/testmethods/sw846/pdfs/3050b.pdf](http://www.epa.gov/epawaste/hazard/testmethods/sw846/pdfs/3050b.pdf)) extracts, in almost all instances, less of the metals and metalloids than the various HCl-HNO<sub>3</sub> strong-acid mixtures, including “classic” aqua regia (M2 - AR31). Notable exceptions are Hf, Nb, Th, and Zr, where US-EPA3050B extracts more of these elements than the “aqua regias”.

Our objective was to select an analytical

**Table 3.** Experimental design and statistical model.

Table 3. Experimental Design and Statistical Model

CRM	Extraction Method				
	1	2	3	4	5
1	1, 2, 3	1, 2, 3	1, 2, 3	1, 2, 3	1, 2, 3
2	1, 2, 3	1, 2, 3	1, 2, 3	1, 2, 3	1, 2, 3
3	1, 2, 3	1, 2, 3	1, 2, 3	1, 2, 3	1, 2, 3
4	1, 2, 3	1, 2, 3	1, 2, 3	1, 2, 3	1, 2, 3
5	1, 2, 3	1, 2, 3	1, 2, 3	1, 2, 3	1, 2, 3
6	1, 2, 3	1, 2, 3	1, 2, 3	1, 2, 3	1, 2, 3
7	1, 2, 3	1, 2, 3	1, 2, 3	1, 2, 3	1, 2, 3
8	1, 2, 3	1, 2, 3	1, 2, 3	1, 2, 3	1, 2, 3

Analysis of Variance Model:

Two-Way with Interaction and Replication within CRMs

$$Y_{ijk} = \mu + \alpha_i + \beta_j + (\alpha\beta)_{ij} + \gamma_{jk} + \epsilon_{ijk}$$

Where:

Y<sub>ijk</sub> = the k-th replicate analysis by the i-th Method of the j-th CRM

μ = the grand mean

α<sub>i</sub> = the main effect due to the i-th Method

β<sub>j</sub> = the effect due to the j-th CRM (Sample)

(αβ)<sub>ij</sub> = the interaction effect between the i-th Method and j-th CRM

γ<sub>jk</sub> = the effect due to the k-th analysis of the j-th CRM

ε<sub>ijk</sub> = the pooled residual variability

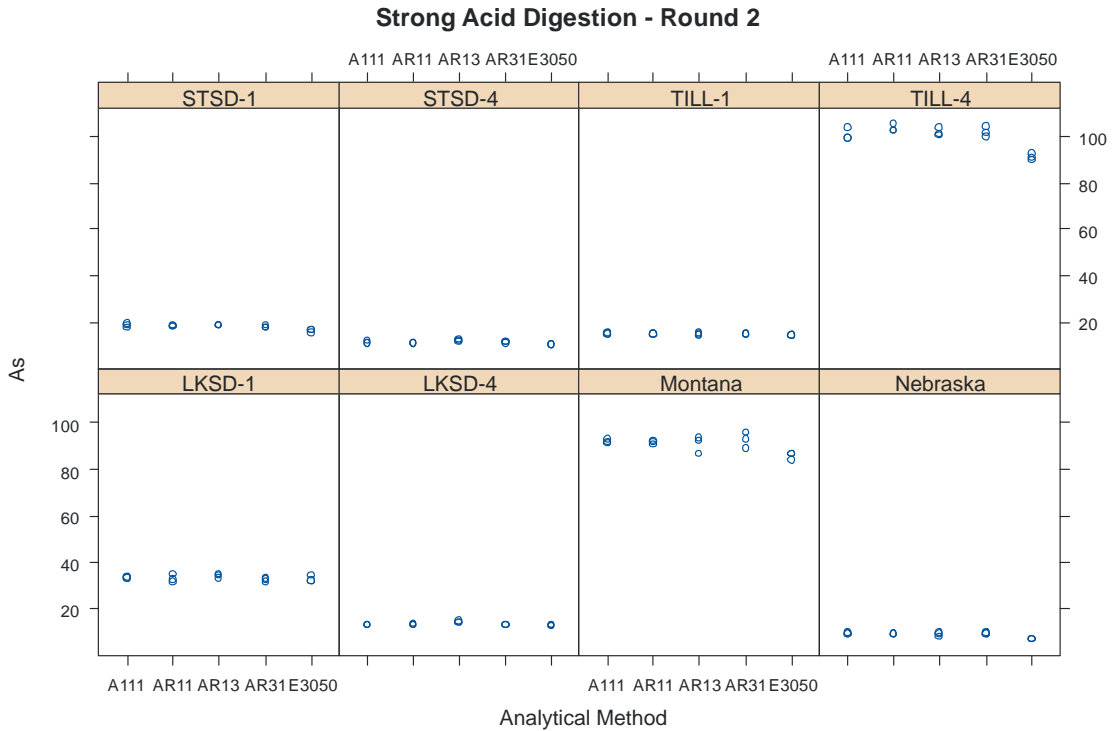


**Fig. 1.** Dotplot for arsenic factored by certified reference material. The x-axis represents the different digestions.

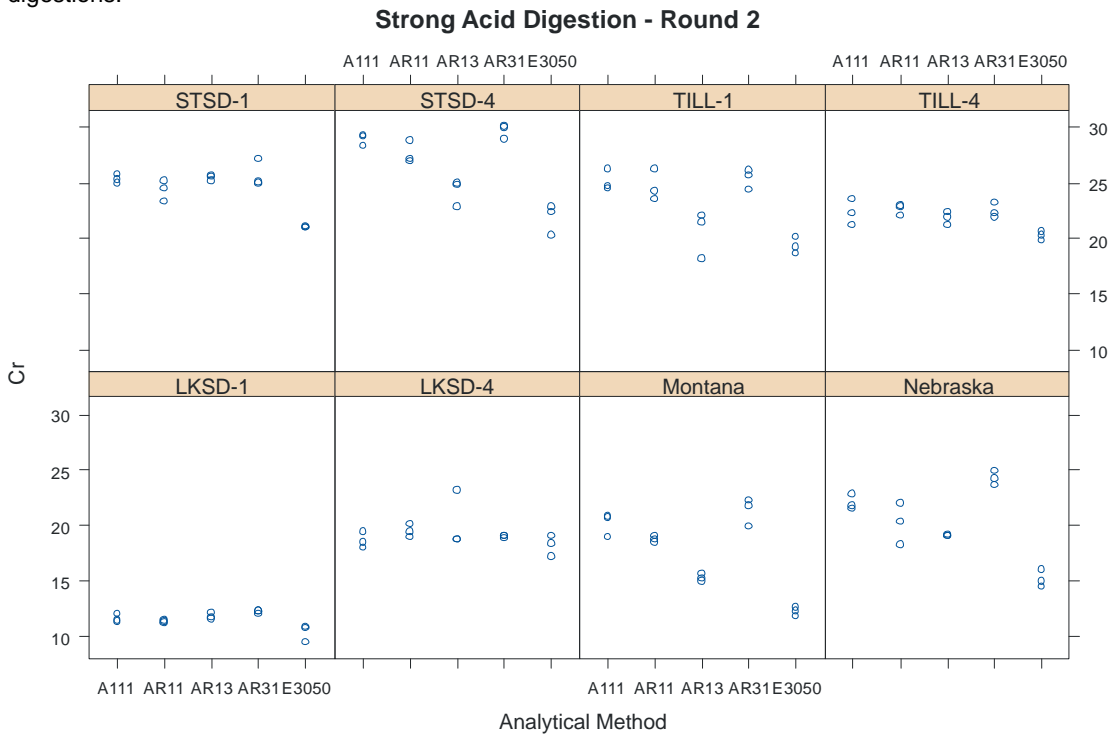


**Fig. 2.** Dotplot for chromium factored by certified reference material. The x-axis represents the different digestions.

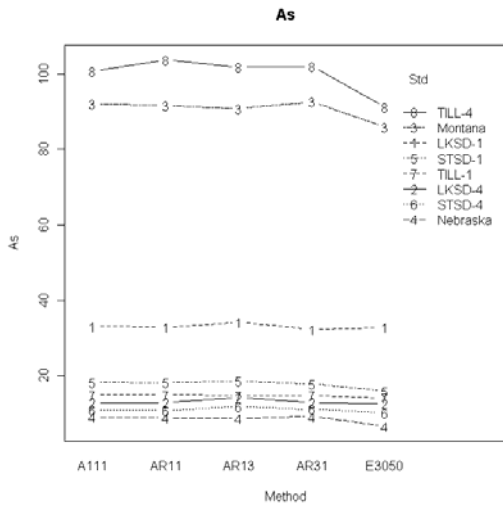


Fig. 3. Interaction plot for As.

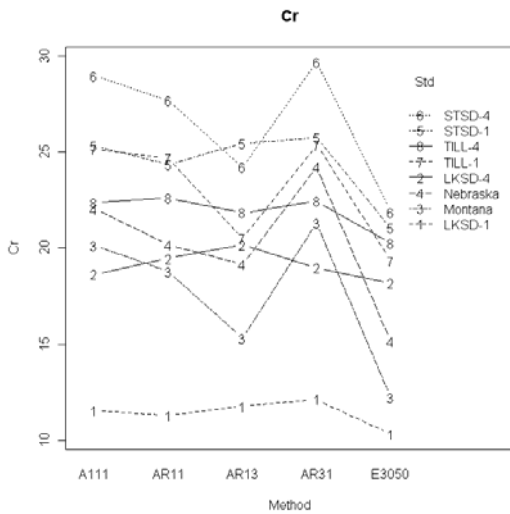


Fig. 4. Interaction plot for Cr.

protocol that will yield data that are consistent with both the majority of the regulatory regimes and the existing data holdings. The “classic” aqua regia (M2 – AR31) protocol meets this requirement. However, this may not be widely accepted in the environmental community. Therefore, we recommend that the aqua regia variant of US-EPA 3050B (i.e. without H<sub>2</sub>O<sub>2</sub>) be the basis of an analytical protocol for use in the North American Soil Geochemical Landscapes. This procedure uses a 4:1 HCl-HNO<sub>3</sub> mix rather than the 3:1 of “classical” aqua regia. However, on the basis of this study, we expect that this change in reagent ratio will not cause any geochemically significant variation.

## Preliminary results of the North American Soil Geochemical Landscapes Project, northeast United States and Maritime Provinces of Canada

Eric C. Grunsky<sup>1</sup>, David B. Smith<sup>2</sup>, Peter W.B. Friske<sup>1</sup>, & Laurel G. Woodruff<sup>3</sup>

<sup>1</sup>Geological Survey of Canada, 601 Booth St., Ottawa, ON, K1A 0E8 CANADA  
(e-mail: egrunsky@nrcan.gc.ca)

<sup>2</sup>U.S. Geological Survey, Denver Federal Center, MS 973, Denver, CO, 80225 USA

<sup>3</sup>U. S. Geological Survey, 2280 Woodale Dr., St. Paul, MN, 55104 USA

**ABSTRACT:** The results of a soil geochemical survey of the Canadian Maritime provinces and the northeast states of the United States are described. The data presented are for the <2-mm fraction of the surface layer (0-5 cm depth) and C horizons of the soil. Elemental determinations were made by ICP-MS following two digestions, aqua regia (partial dissolution) and a strong 4-acid mixture (near-total dissolution). The preliminary results show that Hg and Pb exhibit elevated abundances in the surface layer, while As and Ni exhibit abundances that can be attributed to the geological provenance of the soil parent materials.

**KEYWORDS:** *soil geochemistry, Northeast United States, Maritime Provinces of Canada, As, Hg, Ni, Pb, Zn*

### INTRODUCTION

Initial results of the North American Soil Geochemical Landscapes project (NASGLP) are presented from the Northeast United States (Maine, New Hampshire, Vermont, Massachusetts, Connecticut, Rhode Island and New York) and the Maritime provinces of Canada (Nova Scotia, New Brunswick and Prince Edward Island).

Soil sampling was conducted across the Canadian Maritime provinces and the US states during 2007 using an established field protocol by the United States Geological Survey (USGS), the Geological Survey of Canada (GSC) and the New Brunswick and Nova Scotia provincial surveys.

The surface layer (0-5 cm depth), A, B and C soil horizons were sampled where available. The B horizon was not sampled by the USGS. Due to the thin and relatively discontinuous nature of the A horizon at many of the Canadian sites and difficulty in distinguishing between H- and A-horizon material, some of the A-horizon samples have organic content greater than the >17% upper pedological limit. Reclassification based on the organic content and other factors will be done

before any detailed interpretation is undertaken on these "A-horizon" samples.

The Canadian maritime component of the NASGLP consists of 171 sites and the US component is comprised of 180 sites. Nominal sample densities were one site per 1600 km<sup>2</sup> in the United States and one site per 800 km<sup>2</sup> in Canada. Not all sites provided sufficient material to undertake chemical analyses for all horizons.

The results presented here are for As, Hg, Ni, and Pb, which are elements of interest for issues in human health.

Results are plotted on a base map of Ecoprovinces, which reflect geological, pedological, meteorological and topographic conditions (<http://sis.agr.gc.ca/cansis/nsdb/ecostrat/intro.html>).

### FOUR-ACID DIGESTION RESULTS FOR 0-5-CM AND C-HORIZON SOILS

Figure 1 presents As in 0-5-cm soils. Elevated levels occur along the eastern shore of Nova Scotia (Meguma terrane), in the Belledune area of northern New Brunswick, the northeast part of Maine, southwest New Hampshire, and south eastern New York State. The elevated values of As may also reflect



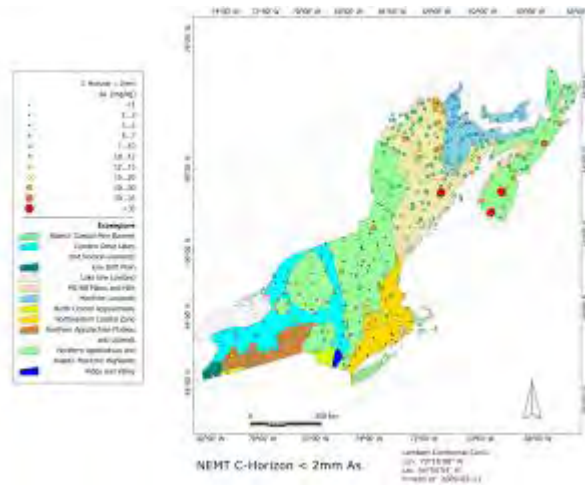


Fig. 2. As in C horizon; 4-acid digestion, < 2mm size fraction, ICP-MS.

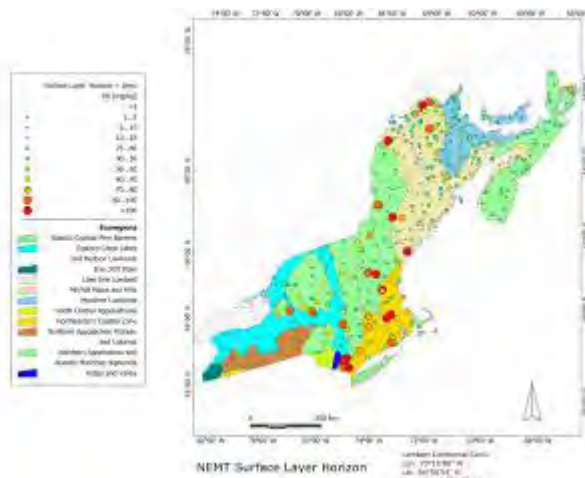


Fig. 3. Pb in 0-5-cm soils; 4-acid digestion, < 2mm size fraction, ICP-MS.

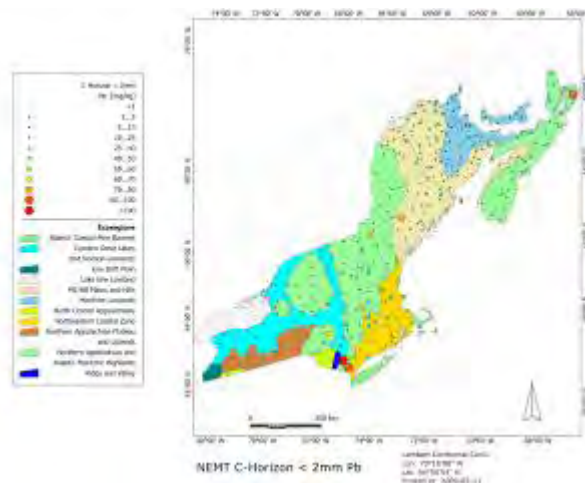


Fig. 4. Pb in C horizon; 4-acid digestion, < 2mm size fraction, ICP-MS.

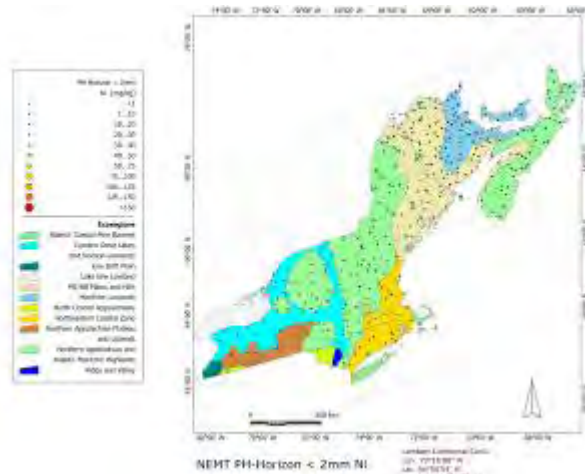


Fig. 5. Ni in 0-5-cm soils; 4-acid digestion, < 2mm size fraction, ICP-MS.

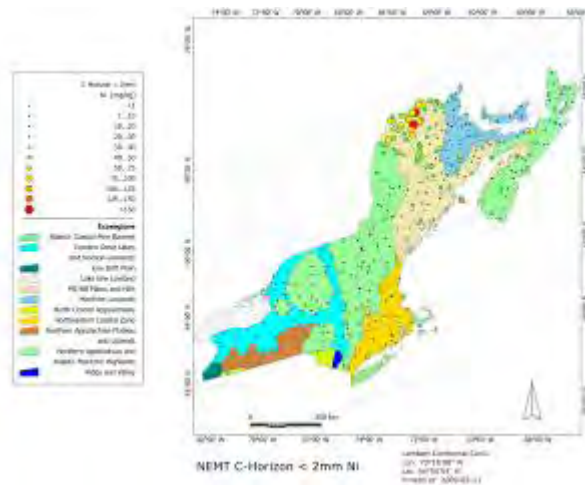


Fig. 6. Ni in C horizon; 4-acid digestion, < 2mm size fraction, ICP-MS.

## The North American Soil Geochemical Landscapes Project in New Brunswick

Toon Pronk<sup>1</sup>, Michael A. Parkhill<sup>2</sup>, Rex Boldon<sup>1</sup>, Marc Desrosiers<sup>2</sup>,  
Peter Friske<sup>3</sup>, & Andy Rencz<sup>3</sup>

<sup>1</sup>Geological Surveys Branch, New Brunswick Department of Natural Resources, P.O. Box 6000, Fredericton, NB, E3B 5H1 CANADA (e-mail: toon.pronk@gnb.ca)

<sup>2</sup>Geological Surveys Branch, New Brunswick Department of Natural Resources, P.O. Box 50, Bathurst, NB, E2A 3Z1 CANADA

<sup>3</sup>Geological Survey of Canada, 601 Booth Street, Ottawa, ON, K1A 0E8 CANADA

**ABSTRACT:** The New Brunswick field component of the North American Soil Geochemical Landscapes Project (NASGLP) was carried out in 2008. A total of 118 sites were sampled following the NASGLP sampling protocol for Canadian projects. A total of 19 different samples for 7 separate government agencies were collected at each site. Initial analytical results indicate consistent regional patterns that largely follow geological and ecosystem boundaries. The cross-disciplinary aspect of the project has attracted collaborators from environment, health and resource sectors. The existence of large till, stream, and water geochemical databases provides background information for ongoing research, data extrapolation, and possibly spin-off map products that can be used for health, environmental and land use planning studies.

**Keywords:** *New Brunswick, soil chemistry, environment, radon, health, background values*

### INTRODUCTION

New Brunswick's diverse geology, excellent accessibility, and extensive geochemical database, make it a logical place to start 'testing' the protocols and methodology of the North American Soil Geochemical Landscapes Project (NASGLP) within Canada. Cooperation and coordination between the federal and provincial geological surveys, as well as Health Canada (HC), Environment Canada - Atlantic (ECA), and Agriculture Canada (AAFC) assured methodological continuity across the country and involvement of the user groups from the project outset.

New Brunswick Quaternary geologists have dug more than 18,000 soil pits during the last 25 years in all parts of the province and have an intimate knowledge of the landscape and its soils. New Brunswick's diverse geology and relatively small areal extent led us to sample at double the national/continental density, i.e. two sample sites per 1600 km<sup>2</sup> (Fig. 1). The second site within each sample block was taken at a National Forest

Inventory (NFI) site and will thus help link the newly acquired data with that database. Partly because of the "pilot" aspect of the project and partly because of all the partners involved (7 different departments/ agencies), a large number (19) of samples from various soil horizons was collected at each site (Fig. 2). Such

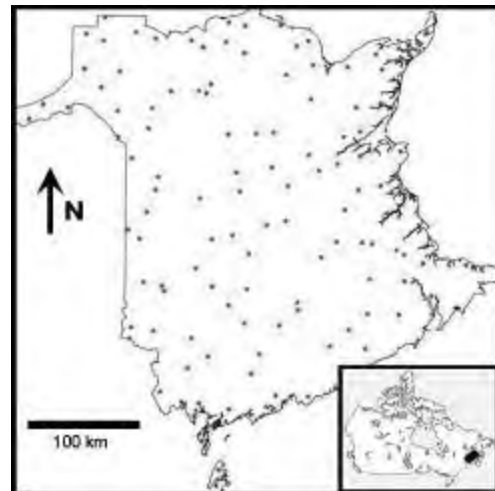


**Fig. 1.** Distribution of NASGLP sample sites in New Brunswick.



**Fig. 2.** Array of samples collected for 7 different agencies at each NASGLP site. Soil gas radon concentration and radiometric measurements were recorded at each site as well.

thorough sampling will make the resulting database a very robust one that will undoubtedly form the base of many future research projects and play an important role in decision making processes related to environment, health, and more general chemical background questions.

For agriculture and environment related projects, the <2-mm soil fraction is routinely analyzed and used as a standard, whereas for mineral exploration the <63- $\mu$ m fraction is used. The latter better reflects bio-accessibility and both fractions are analyzed using different chemical digestions.

### **GEOLOGICAL SETTING**

New Brunswick's bedrock geology is well mapped and largely well understood. Because of NB's mineral wealth, a great deal of mineral exploration work has been carried out since the 1950s. The bedrock in NB is also diverse in age. The oldest Precambrian rocks can be found in the Saint John area, whereas some of the younger ones, in the form of Triassic basalts, occupy more than half of the Island of Grand Manan. Most of NB's rocks are of Middle Paleozoic age. The triangle between Moncton, Fredericton, and Bathurst is occupied by a thick sequence of Carboniferous rocks that host

economic quantities of salt, potash, oil and gas, as well as numerous uranium occurrences. This diverse bedrock geology is covered by a generally thin layer of Quaternary glacial and glacio-fluvial and minor fluvial, aeolian, and marine deposits. Few areas of the province are dominated by bedrock outcrop and soil composition is thus often a mixture of several lithological components. The chemistry and texture of our soils is a reflection of New Brunswick's complex geological history.

The chemistry of the earth's surface, or active layer, influences our health and well being. Natural background variation of surface chemistry is rather high because of the variety in age and depositional environment of our bedrock. This variety is captured by the New Brunswick component of the NASGLP.

### **SAMPLING METHODOLOGY**

Sampling was carried out by two field parties, one in the north and one in the southern part of the province. Several times during the campaign, crews got together in the 'overlap' area and confirmed sampling was consistent between the two crews.

Sample locations (Fig. 1) were selected by using the methodology developed by the Geological Survey of Canada (Geological Survey of Canada Report, in prep.) during the start-up of the NASGLP. Canadian protocols differ somewhat from the American and Mexican protocols, partly because our sampling environments differ and partly because in the Canadian context several add-on projects were developed in cooperation with other interested agencies. Target sample sites were randomly generated by the GSC's generalized random tessellation stratified (GRTS) sampling design (Garrett 1983), but sampling crews had the option to reject a site if it was not representative of the area or if access was extremely difficult. The latter was a logistical issue as the sample gear and instrumentation were rather voluminous and heavy, and could only be carried from roads for a short distance. If the target site was rejected,

the next randomly generated site was evaluated in the same manner. It was only necessary once to go to a third option. In addition to the core Canadian sampling protocol, New Brunswick crews gathered soil radon data for Health Canada and composite surface and mineral soil samples for use by Environment Canada - Atlantic for toxicology studies.

### **SELECTED RESULTS**

One of the most revealing results is the chromium plot, which shows high values over part of the sedimentary cover rocks in the northwestern corner of the province. This regionally elevated area has been investigated in the past when stream sediment geochemical surveys revealed highly anomalous Cr-Ni-Co values. It was never satisfactorily explained and it was concluded that higher than normal background levels were responsible for the anomalies. The present survey seems to confirm that conclusion. The two sample sites on Grand Manan gave us some of the highest values (369 ppm in C-horizon parent material) which is not surprising in light of the bedrock geology represented by Triassic basalts. Several other elements (e.g., Se) are also highest at the Grand Manan sites.

There is also (as expected) a strong regional correlation between the uranium and radon soil gas concentrations in general, though not always site-to-site. Arsenic distribution is of special interest because of its toxicological effects and the fact that there are a couple of areas within New Brunswick that historically have high arsenic levels in drinking water and soils. These include areas underlain by Carboniferous volcanic rocks near Harvey, and the Bathurst/Belledune area in northern New Brunswick. The Harvey area seemingly defies detection at the scale NASGLP sampling because of the low sample density.

Comparisons of the chemistry of different soil horizons (Fig. 3) will reveal some of the natural variability and may highlight areas of potential health concern. If we compare the lead values for the <2-mm fraction for the surficial 0-5-cm, layer,

which is the horizon typically looked at for health studies, and the C horizon, we can detect some interesting differences. Lead in the C horizon has a generally 'flat' appearance with slightly elevated background over the northern part of the Miramichi Highlands, especially the Bathurst base-metal camp. The 0-5-cm material shows a more diverse distribution, which may be partly related to the higher organic content of that layer and/or to anthropogenic sources.

### **RADON FOLLOW-UP STUDY IN THE FREDERICTON – NEW MARYLAND AREA**

A follow-up study on soil radon gas and indoor radon gas was carried out in the Fredericton area. It was found that the individual correlation between soil gas radon and indoor radon on individual properties was not very high, but there was definitely a regional correlation. The reasons for the low individual correlation can be traced to other important variables such as age and type of construction of the homes.

### **TOXICOLOGY STUDY (ENVIRONMENT CANADA - ATLANTIC)**

Toxicology and environmental health studies often lack a firm foundation of baseline data, and the NASGLP is a perfect starting point for a baseline data survey. During the field component of the survey, the crews collected two composite samples. One represented the top 5 cm of the soil directly below the litter layer (which will include a lot of the airborne components if they are present), and a second came from the 0-30-cm interval, independent of which soil horizon this may represent. Within this interval (the active layer), most of the interactions between biota and the non-living soil components take place, and thus is the important interval for this type of study. Environment Canada's Biological Methods Division selected one of the northern New Brunswick sites to collect a bulk sample in an attempt to create reference sites across Canada for standardized toxicity test methods.



**Fig. 3.** Podzol profile at NASGLP sample site NB072009. Podzols were the soil type at approximately 100 of the 118 sites.

#### **ACKNOWLEDGEMENTS**

We would like to thank Ken Ford, Rick McNeil and other staff at the GSC for their

continued support; Rita Mroz at Environment Canada – Atlantic for data and thoughts on the toxicology data; our director Les Fyffe and managers Malcolm McLeod and Steve McCutcheon for their understanding and support in this project that extends well beyond provincial as well as disciplinary boundaries; Jing Chen at HC for supplying us with instrumentation and support for the radon survey; all our field support especially Heather Campbell, Parrish Arnott, and Louis-Philippe Cyr that not only brought physical ability, but also computer and instrument savvy as well as ideas to the project. Constructive criticism by Reg Wilson greatly improved the abstract.

#### **REFERENCES**

- GARRETT, R.G. 1983. Sampling Methodology. In: HOWARTH, R.J. (ed.), *Handbook of Exploration Geochemistry, Vol.2, Statistics and Data Analysis in Geochemical Prospecting*. Elsevier, **83-110**.
- GEOLOGICAL SURVEY OF CANADA REPORT, 2009 (in prep), *North American Soil Geochemical Landscapes Project, Field Protocol Manual – Canadian project*.

## The North American Soil Geochemical Landscapes Project: overview, goals, progress

David B. Smith<sup>1</sup>, Laurel G. Woodruff<sup>2</sup>, Andy Rencz<sup>3</sup>, & Alfredo de la Calleja<sup>4</sup>

<sup>1</sup>U.S. Geological Survey, Denver Federal Center, MS 973, Denver, CO, 80225 USA  
(e-mail: dsmith@usgs.gov)

<sup>2</sup>U.S. Geological Survey, 2208 Woodale Drive, St. Paul, MN, 55112 USA

<sup>3</sup>Geological Survey of Canada, 601 Booth Street, Ottawa, ON, K1A 0E8 CANADA

<sup>4</sup>Servicio Geológico Mexicano, Av. Mariano Jiménez No. 465, Col. Alamos, San Luis Potosí, S.L.P., C.P., 78280 MEXICO

**ABSTRACT:** In 2002, the U.S. Geological Survey (USGS), the Geological Survey of Canada (GSC), and the Mexican Geological Survey (Servicio Geológico Mexicano, or SGM) initiated a long-term effort called the North American Soil Geochemical Landscapes Project to map the geochemistry of North American soils using standardized sample collection and analytical protocols. The purpose of this geochemical survey is to improve our understanding of the baseline concentrations of chemicals and elements that are normally found in soil and the location and causes of elevated or depleted concentrations. Protocols were developed through recommendations of stakeholders at a series of workshops in 2002 – 2004 and tested and refined during a 3-year pilot phase from 2004 – 2006. Sampling for the continental-scale survey, initiated in 2007, will be done at a density of 1 site per 1,600 km<sup>2</sup> (13,500 sites).

**KEYWORDS:** *soil geochemistry, low-density geochemical mapping, geochemical background, continental-scale geochemical mapping, soil*

### INTRODUCTION

Soil is a critical natural resource that plays a key role in determining human health and ecosystem integrity, supporting food production, and the natural recycling of carbon and essential nutrients in the environment. On the other hand, many communities dispose of solid and liquid wastes from households and from agricultural and industrial processes by dumping them onto, or burying them in, the soil. Either through ingestion, inhalation, or dermal absorption, soil can be a pathway for potentially toxic chemicals of natural or anthropogenic origin to enter the human body (Oliver 1997; Abrahams 2002; Plumlee & Ziegler 2003). Although soil is so important in our everyday lives, our knowledge of the concentration and distribution of naturally occurring and man-made chemicals in the soils of North America is limited. At present, agencies involved with human health and environmental risk assessment and management have no common

understanding of soil geochemical background variation for the continent of North America and the processes that control this variation.

In 2002, the North American Soil Geochemical Landscapes Project, a tri-national initiative among the United States, Canada, and Mexico, was initiated with the goals to (1) develop a continental-scale framework for generating soil geochemical data and (2) provide soil geochemical data that are useful for a wide range of applications and disciplines.

### PROJECT DEVELOPMENT

A series of three workshops held in 2002 – 2004 included stakeholders representing about 50 North American governmental agencies, academia, environmental consultancies, and the medical community. The workshops resulted in a set of recommended sampling and analytical protocols for a soil geochemical survey that would meet the needs of this diverse set of customers. The Project is

based on low-density sample collection over a spatially balanced array of 13,500 sites for the North American continent (1 sample site per approximately 1,600 km<sup>2</sup>). There is a core set of samples to be taken at each site, and each country may add additional sample types to meet the needs of users.

The core sampling protocols represent both depth-based and horizon-based samples. One depth-based sample is taken from 0-to-5 cm, regardless of what soil horizon this represents. A composite of the A horizon (the uppermost mineral soil) and a composite of the C horizon (usually the weathered parent material of the overlying soil) are also collected at each site. The 0-5-cm and A-horizon samples are more likely to represent anthropogenic influence on soil composition, and the C-horizon sample is more representative of geologic influence. Each sample is sieved to <2 mm and then ground to <150 µm prior to chemical analysis for over 40 major and trace elements. The core analytical protocol, consistent among the three countries, involves a near-total 4-acid (hydrochloric, nitric, perchloric, and hydrofluoric) digestion followed by inductively coupled plasma-atomic emission spectrometry and inductively coupled plasma-mass spectrometry. Mercury is determined by cold-vapor atomic absorption spectrometry (AAS) and Se and As are determined by hydride generation AAS. Total carbon is determined by combustion at 1370°C and carbonate carbon is determined as CO<sub>2</sub> by coulometric titration. Organic carbon can then be determined by difference. Each country may include additional analytical methods as desired.

In addition to the standard geochemical protocols, the survey has a microbiological

component. A separate sample of 0-5-cm soil is collected at each site for the determination of *Bacillus anthracis* (anthrax).

### PILOT STUDIES

A three-year pilot phase was conducted from 2004 – 2006 to test and refine the sampling and analytical protocols and to optimize logistics for the survey. This pilot phase was conducted at both a continental- and a regional-scale. The continental-scale pilot study consisted of sampling at approximately 40-km intervals along two transects across the US, Canada, and Mexico. A north-south transect extended from northern Manitoba to the Pacific coast of Mexico west of Acapulco. An east-west transect followed the 38<sup>th</sup> parallel from just north of San Francisco, California to the Virginia shore (Smith *et al.* 2005). The regional-scale study, designed to represent a more detailed follow-up investigation of an area of interest identified from the larger scale study, was conducted in an area of northern California located just north of San Francisco and extending from the Pacific coast to the California-Nevada border (Morrison *et al.* 2008).

### INITIATION OF CONTINENTAL-SCALE SAMPLING

The full-scale sampling of North American soils was initiated in 2007 with completion of the Maritime Provinces of New Brunswick, Nova Scotia, and Prince Edward Island in Canada and the New England states and New York in the US. Sample coverage at the end of 2008 is shown in Fig. 1. It is anticipated that this project will take approximately ten years to complete.

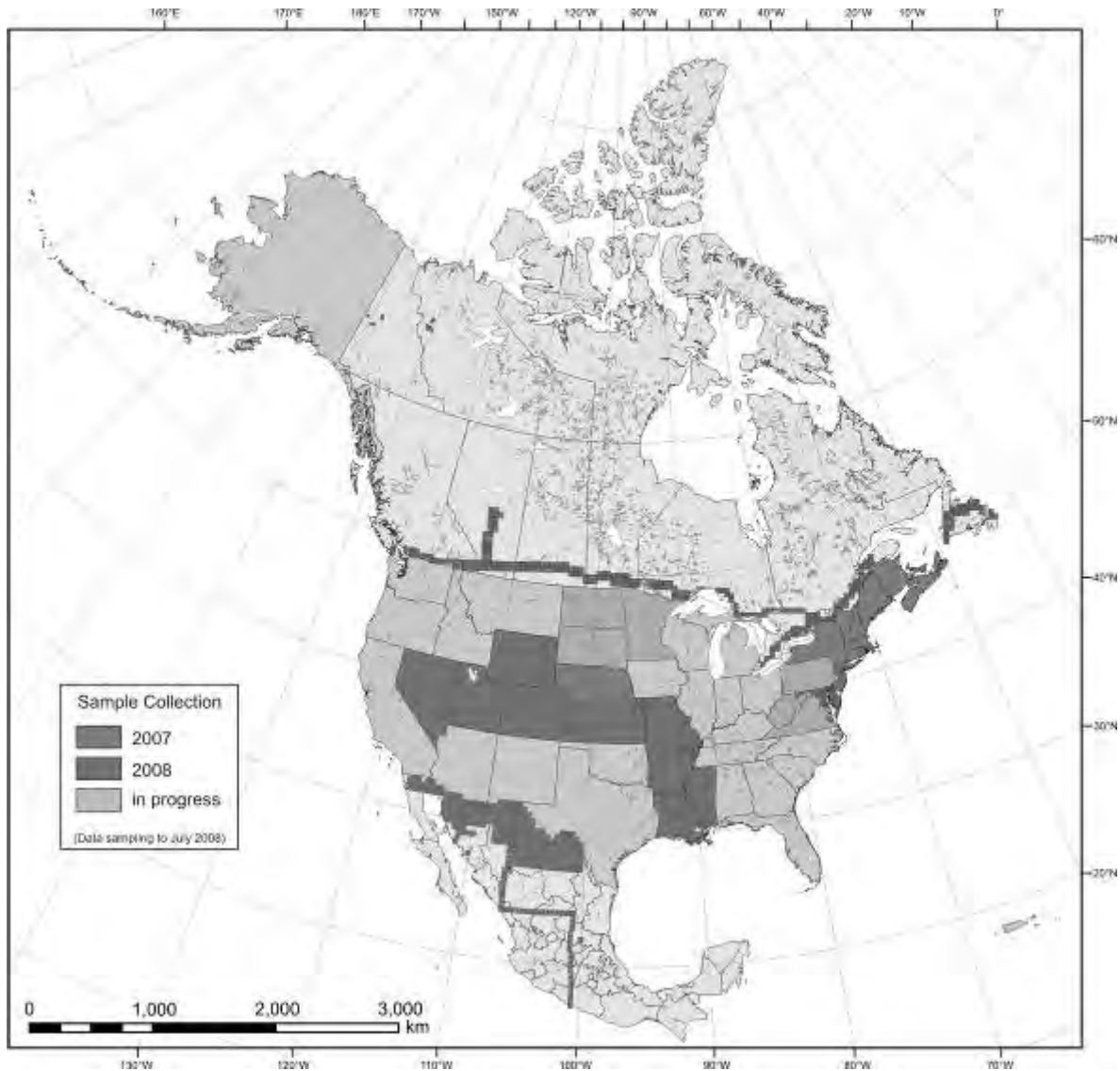


**Fig. 1.** Map showing status of sampling for the North American Soil Geochemical Landscapes Project as of December 31, 2008.

#### ACKNOWLEDGEMENTS

We thank the many stakeholders who participated in the various workshops and provided valuable guidance in the design of the continental-scale soil geochemical survey. We also thank all the people who have, to date, participated in sampling in all three countries.

#### REFERENCES

ABRAHAMS, P.W. 2002. Soils: their implications to human health. *Science of the Total Environment*, **291**, 1–32.

MORRISON, J.M., GOLDHABER, M.B., HOLLOWAY, J.M., & SMITH, D.B. 2008. Major- and trace-element concentrations in soils from northern California: Results from the Geochemical Landscapes Project Pilot Study. *US Geological Survey Open-File Report 2008-1306*.

OLIVER, M.A. 1997. Soil and human health: a review. *European Journal of Soil Science*, **48**, 573–592.

PLUMLEE, G.S. & ZIEGLER, T.L. 2003. The medical geochemistry of dusts, soils, and other Earth materials. In: HOLLAND, H.D. AND TUREKIAN, K.K. (executive eds.), LOLLAR, B.S.

(volume ed.), *Treatise on Geochemistry*, **9**,  
Pergamon Press, Oxford, 263–310.  
SMITH, D.B., CANNON, W.F., WOODRUFF, L.G. *et*  
*al.* 2005. Major- and trace-element

concentrations in soils from two continental-  
scale transects of the United States and  
Canada. *US Geological Survey Open-File*  
*Report* **2005-1253.**

## Continental-scale patterns in soil geochemistry and mineralogy: results from two transects of the United States and Canada

Laurel G. Woodruff<sup>1</sup>, David B. Smith<sup>2</sup>, D.D. Eberl<sup>3</sup>, & William F. Cannon<sup>4</sup>

<sup>1</sup>U.S. Geological Survey, 2208 Woodale Drive, St. Paul, MN, 55112 USA

<sup>2</sup>U.S. Geological Survey, Mail Stop 973, Denver, CO, 80225 USA

<sup>3</sup>U.S. Geological Survey, 3215 Maine Street, Boulder, CO, 80303 USA

<sup>4</sup>U.S. Geological Survey, Mail Stop 954, Reston, VA, 20192 USA

**ABSTRACT:** In 2004, the U.S. Geological Survey and the Geological Survey of Canada initiated a pilot study that collected more than 1,500 soil samples along two transects across Canada and the United States. The two transects crossed a wide array of soil types, surficial materials, soil ages, climatic conditions, landforms, land covers, and land uses. Geochemical and mineralogical data for the transect samples display coherent, robust regional and continental-scale patterns that are the result of broad-scale geochemical processes acting at the scale of mapping. The patterns can often be related to profound differences in soil parent material and to hemisphere-wide climate effects. The geochemical data also demonstrate that at the continental-scale changes can occur in the dominance of any of the major factors that control soil geochemistry, abruptly in some regions. The transect study served as a pilot project to develop and refine field and analytical protocols for a comprehensive North American soil geochemistry sampling project.

**KEYWORDS:** *continental-scale, soil geochemistry, soil mineralogy, transects*

### INTRODUCTION

In the United States, a large-scale soil geochemical survey was conducted from 1961 through 1974 (Shacklette & Boerngen 1984), but a continental-scale database of soil geochemistry for North America using consistent protocols and modern analytical methods is currently not available. To address this, the U.S. Geological Survey (USGS), the Geological Survey of Canada (GSC), and the Mexican Geological Survey (SGM) are collaborating on a soil geochemical survey of the entire North American continent (Smith *et al.* 2009). As a pilot study for this effort, the USGS and GSC sampled soils along two transects across the US and Canada in 2004.

The two transects crossed multiple, complex environments with widely diverse surficial materials, topography, climate, landforms, land covers, and land uses. A north-to-south (N-S) transect extended from northern Manitoba, Canada, to the US-Mexico border near El Paso, Texas. A west-to-east (W-E) transect followed the 38<sup>th</sup> parallel from just north of San

Francisco, California, to the Virginia shore (Fig. 1).

At each site, soils representing 0-to-5 cm depth, and the A, and C horizons, if present, were collected and analyzed for more than 40 major and trace elements. Soils from 0-to-5 cm depth also were analyzed of a suite of organic compounds.

The W-E transect crosses significant gradients in precipitation, with generally humid conditions along the west coast, arid to semiarid conditions in the interior



Fig. 1. Location of two transects.

western half of the US, and increasingly humid conditions in the eastern half of the country. The N-S transect has less dramatic precipitation changes, but does have significant differences in mean annual temperature from very cold in the north to very hot in the south.

Despite the highly variable settings of the sample sites, transect soil data show regional- to continental-scale patterns in mineralogy and geochemistry that can be related to soil-forming factors and processes acting at broad scales (Woodruff *et al.* 2009). To illustrate large-scale patterns revealed by transect soils, geochemical results have been grouped into ten coherent, sub-continental areas based on physiographic characteristics, including commonalities of surficial processes, climate, landform, soil parent materials, and soil age.

### CONTINENTAL-SCALE MINERALOGY AND GEOCHEMISTRY

At the continental- to subcontinental-scale the relative proportions of major minerals in soils are largely controlled by parent material and climate factors. In turn, the distributions of many major and trace elements are strongly influenced by soil mineralogy, especially the presence or absence of quartz (Eberl & Smith 2009; Bern 2009).

#### West to East Transect

Mineralogy and soil geochemistry along the W-E transect reflect both the influence of soil parent materials and effect of hemispheric climate gradients. The quartz dilution effect described by Bern (2009) dominates the distribution of a number of elements; Al is given as an example in Figure 2.

Higher quartz contents in soils occur in areas where the soil parent materials include quartz-rich materials, such as sandstone bedrock or eolian deposits (area 3; Fig. 2) and in regions where high precipitation accelerates soil weathering and leaching, resulting in high contents of residual, inert quartz (areas 9 and 10; Fig. 2). In Fig. 2 the distribution of Al is nearly

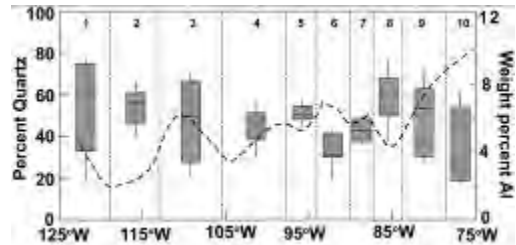


**Fig. 2.** Percent quartz in C horizon (dashed trend line) and weight percent Al (filled boxes) in C horizon soils along the W-E transect (truncated box plot; boxes include 50% of data, extent of lines include 80% of data; solid line is the median). Geochemical data shown by the box plots were grouped into 10 areas (vertical dashed lines, numbers at top of plot) defined by commonalities of physiographic features.

a mirror image of the distribution of quartz as the presence of quartz dilutes the presence of other minerals or elements other than Si.

The continental pattern for Na matches the pattern for total feldspar percentages, as Na values are primarily correlated with plagioclase (Eberl & Smith 2009). Feldspars are much more susceptible to chemical dissolution than quartz and, with sufficient time and precipitation, will weather mainly to clay minerals. As a result, total feldspar contents and Na contents decrease with increasing precipitation from west to east (Fig. 3).

Interpreting vertical chemical trends in soils along the transects is complicated by the diverse combination of parent materials, soil age, and climate, which all influence vertical element distributions. However, there is a common pattern for a number of elements in vertical soil profiles along the W-E transect that is apparently reflective of the strong west to east gradient in precipitation along the 38th parallel. The variability of mean annual precipitation minus mean annual potential evapotranspiration (PMPE) provides an index of relative moisture conditions at the ground surface (McCabe & Wolock 2002). Positive PMPE values indicate water in excess of climate demands, and negative values indicate a scarcity of water for climate demands (McCabe & Wolock 2002). Along the W-E transect, these hydrologic landscape-derived climate

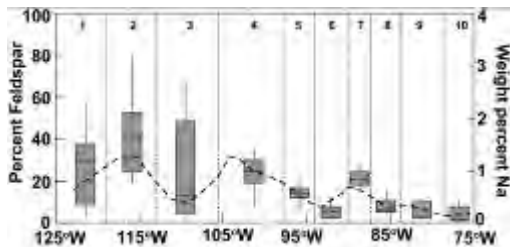


**Fig. 3.** Percent feldspar in C horizon (dashed trend line) and weight percent Na in C horizon soils along the W-E transect (filled boxes). Plot specifics as in Figure 2.

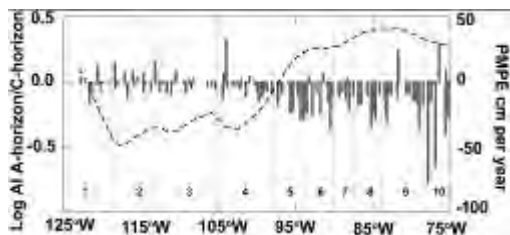


**Fig. 4.** Trend line for PMPE (dashed line) plotted with a bar anchor plot of the log A-horizon/C-horizon Al ratios (dark boxes) for the W-E transect.

conditions roughly correspond to the general west (arid) to east (humid) pattern of increasing precipitation. In Figure 4, the log A-horizon/C-horizon ratio for Al is plotted as individual values with a base of 0 (ratio of 1). Also shown is a trend line for PMPE values for each sample site.

The log Al A-horizon/C-horizon ratio is variable for sites in the western half of the transect, but east of ~ 103.5°W longitude, the ratio becomes consistently <0, indicating that Al is higher in the C horizon than the A horizon. The vertical distributions for a diverse group of elements, including Fe, Ce, Cr, Cs, Ga, In, La, Ni, Rb, Sc, Th, and V, match the pattern observed for Al with a transition to log ratios consistently <0 east of the break point near 103.5°W longitude. This agreement for multiple elements suggests that this pattern represents a profound characteristic of soil geochemistry along the transect that appears independent of the very diverse soil parent materials and soil ages. The west-to-east shift in the A-horizon/C-horizon ratios for these elements corresponds with the west-to-east climatic shift from drier, more arid

conditions to wetter, more humid conditions. Where PMPE values are positive, excess surface soil moisture and its consequences, such as enhanced plant activity, soil leaching, and formation of secondary minerals, apparently dominate over the influence of soil parent material and soil age, and strongly influence the vertical distributions of many elements.

### North to South Transect

Data from the N-S transect reveal complex patterns for soil mineralogy and geochemistry. Marked transitions in both mineralogy and chemistry are noted where the N-S transect crosses the southern glacial limit. North of the glacial limit, soils record mixed glacial provenances while south of the limit, soils from a number of sites developed on transported and sorted parent materials, including loess and alluvium. An increase in clay content in loess south of the glacial limit compared to tills and outwash north of the glacial limit results in markedly higher concentrations of a number of elements in loess, including Al, Sc, Ti, Ba, Be, Bi, Ce, Cs, Ga, La, Nb, Pb, Rb, Sb, Sn, Th, U, and W.

Seventy-three soil samples from 0-to-5 cm depth along the N-S transect collected by ultraclean methods were analyzed for selected organochlorine pesticides. Only three of the samples had pesticide concentrations greater than the detection limit of the analytical method.

### CONCLUSIONS

Lessons learned from the field sampling for the transects and recognized in the geochemical data lead to the following:

- (1) A 40-km x 40 km sample spacing for the North American project will provide soil geochemical and mineralogical data that will display coherent and robust regional to continental-scale patterns, as also demonstrated by Smith and Reimann (2008).
- (2) Collecting soils from the A and C horizons eliminates variability resulting from mixing of soil horizons in random

percentages when using only a depth-based sampling. This provides the greatest chance for success in relating soil geochemistry to pedogenic processes. A 0-to-5 cm depth sample represents soils with a high potential of human contact.

(3) The distribution of Al and a number of other elements in soil profiles across the W-E transect appears to be strongly dependant on climate gradients rather than significant changes in soil parent materials and soil age. This observation provides important information about the relative importance of a number of geochemical processes that are not revealed in studies at more detailed (local) scales.

#### ACKNOWLEDGEMENTS

We thank John Horton, Jim Kilburn, Robert Garrett, Rodney Klassen, Jean Morrison, and Harley King for field assistance during sampling along the transects. We thank the many people who participated in the USGS workshops where the sample design protocols and analytical framework for the transects were developed. We also thank the many landowners who provided access to sites.

#### REFERENCES

BERN, C. 2009. Soil chemistry in lithologically diverse datasets: The quartz dilution effect. *Applied Geochemistry*, in press.

EBERL, D.D. & SMITH, D.B. 2009. Mineralogy of soils from two-continental-scale transects across the United States and Canada and its relation to soil geochemistry and climate. *Applied Geochemistry*, in press.

MCCABE, G.J. & WOLOCK, D.D. 2002. Trends and temperature sensitivity of moisture conditions in the conterminous United States. *Climate Research*, **20**, 19-29.

SHACKLETTE, H.T. & BOERNGEN, J.G. 1984. Element concentrations in soils and other surficial materials of the conterminous United States. *U.S. Geological Survey Professional Paper* **1270**.

SMITH, D.B., CANNON, W.F., WOODRUFF, L.G., GARRETT, R.G., KLASSEN, R.D., KILBURN, J.E., HORTON, J.D., KING, H.D., GOLDHABER, M.B., & MORRISON, J.M. 2005. Major- and trace-element concentrations in soils from two continental-scale transects of the United States and Canada. *U.S. Geological Survey Open-File Report* **2005-1253**.

SMITH, D.B. & REIMANN, C. 2008. Low-density geochemical mapping and the robustness of geochemical patterns. *Geochemistry: Exploration, Environment, Analysis*, **8**, 219-227.

SMITH, D.B., WOODRUFF, L.G., O'LEARY, R.M., CANNON, W.F., GARRETT, R.G., KILBURN, J.E., & GOLDHABER, M. B. 2009. Pilot studies for the North American Soil Geochemical Landscapes Project – site selection, sampling protocols, analytical methods, and quality control. *Applied Geochemistry*, in press.

WOODRUFF, L.G., CANNON, W.F., EBERL, D.D., SMITH, D.B., KILBURN, J.E., HORTON, J., GARRETT, R.G., & KLASSEN, R.D. 2009. Continental-scale patterns in soil geochemistry and mineralogy: Results from two transects of the United States and Canada. *Applied Geochemistry*, in press.

**SOURCES, TRANSPORT, AND FATE OF TRACE AND TOXIC ELEMENTS IN  
THE ENVIRONMENT**

EDITED BY:

**LEE ANN MUNK  
SARAH FORTNER**



## Sources of lead in soils and uptake by plants: Lower Guadiana River basin, south Portugal and Spain

Maria J. Batista<sup>1</sup>, Maria M. Abreu<sup>2</sup>, J. Locutura<sup>3</sup>, T. Shepherd<sup>4</sup>, D. Oliveira<sup>1</sup>, J. Matos<sup>1</sup>, A. Bel-Lan<sup>3</sup>, & L. Martins<sup>1</sup>

<sup>1</sup>INETI- Dep. Prospeção Minérios Metálicos, Ap. 7586, 2721-866 Alfragide, Portugal (joao.batista@ineti.pt);

<sup>2</sup>ISA-Dep. Ciências do Ambiente, Univ. Técnica de Lisboa, Tapada da Ajuda, 1349-017 Lisboa, Portugal;

<sup>3</sup>Instituto Geológico e Minero de España, R. Rio Rosas, Madrid, España;

<sup>4</sup>GEOMEDIC, Nottingham, UK;

**ABSTRACT:** This study forms part of a larger multidisciplinary environmental study of the Lower Guadiana River basin carried out by a joint Portuguese-Spanish research team. It describes the mobility of lead in soil profiles taken over varied lithologies of the Iberian Pyrite Belt and the distribution of this metal with the root, stems and leaves of three plant species native to the area (*Cistus ladanifer* L., *Lavandula luisieri* and *Thymus vulgaris*). Results indicate that at all sample sites the mobility of lead is very low.

**KEYWORDS:** Lead, soils, plants; Guadiana River, Portugal, Spain

### INTRODUCTION AND SETTING

The purpose of this study was to identify and quantify the sources of heavy metals, especially lead, in soils and plants of the Lower Guadiana River basin and thereby model the potential mobility of lead. Other than direct pollution from mining, the main sources of heavy metal pollution in the environment are by diffuse pollution (Callender, 2004). In agricultural areas this can include lead from the use of pesticides, fertilizers and municipal sludge (Alloway, 1985). Metals can be attached or associated with different mineral phases in the soil, this along with environmental parameters determinesthe availability to plants.

The Guadiana Basin occupies a total area of 66,850 km<sup>2</sup> in Spain and Portugal, 8,350 km<sup>2</sup> of which comprises the Iberian Pyrite Belt (IPB); one of the world's largest concentrations of base metal sulphide deposits (Leistel et al., 1997; Ribeiro et al., 1990). Three plant species (*Cistus ladanifer*, *Lavandula luisieri* and *Thymus vulgaris*) were utilized in this study. The soils in which these plants were sampled are developed over varied geological formations. The oldest formation (PQ Group, Upper Devonian) consists of a thick sequence of arenites and shales

overlain by the Volcanic Sedimentary Complex (Upper Devonian). This unit hosts the IPB massive sulphide deposits and consists of volcanics and metal-rich shales. Both Devonian sequences are overlain by unmineralised, Carboniferous shales and sandstones of the Culm sequence that covers most of the southern part of the Lower Guadiana Basin.

### METHODOLOGY

Sampling of the superficial soils was carried out at 353 sites. At 66 of these sites, samples were collected at two depths: a near-surface sample at 0-20 cm and a sub-surface sample at 20-40 cm where the soil profile was deep enough to allow sampling. The plant species sampled were 136 *Cistus ladanifer* L., 9 *Lavandula luisieri* (Rozeira) Rivas-Martinez and 3 *Thymus vulgaris* L. To complete the understanding of bedrock control on soil lead concentrations, representative samples of the main IPB formations were sampled including sulphide ores from the main ore deposits (Sao Domingos in Portugal; Cabezas de Pasto, Romanera, Lagunazo, Isabel Mn, Cármen 1 and 2, Herrerias, Sierrencilla

Matutera and Vuelta Falsa-Trimpancho in Spain).

Chemical analysis of the soils and plants were made by INAA and ICP-OES following digestion by HCl+HNO<sub>3</sub>+HF+HClO<sub>4</sub>.

Soils were further characterized by the determination of pH in water and potassium chloride in the proportions 1:2.5, total organic carbon (TOC) and cation exchange capacity (CEC). Transfer coefficients between soil and plant and enrichment in soils were determined. The results for Pb were represented in the form of relative enrichments for soils (Kabata-Pendias, 1985) and transfer coefficients in plants (Kovalevskii, 1979).

A Principal Components Analysis (PCA) was performed on the data to determine the relationship of Pb to other chemical elements.

## RESULTS AND DISCUSSION

High concentrations of lead were detected in the wine-coloured and black shales of the Volcanic Sedimentary Complex with 96 mg kg<sup>-1</sup> and 52 mg kg<sup>-1</sup>, respectively. The highest concentrations were reported for the Cu-Pb-Zn massive sulphide ore samples from the abandoned mines of Cabezas del Pasto, Romanera and Serrencillas where concentrations of Pb exceeded 5000 mg kg<sup>-1</sup>.

The median value of Pb for the soils is 25 mg kg<sup>-1</sup> which is coincident with the world median concentration (Kabata-Pendias *et al.* 1985). However, the range of concentrations is between 5 and 25700 mg kg<sup>-1</sup>. In the sub-surface samples the mean value is 23 mg kg<sup>-1</sup> and a range of 9 to + 5000 mg kg<sup>-1</sup> (Table 1). In the Sao Domingos mine area, the enrichment in Pb is very significant probably due to wind dispersed mine wastes but the high concentrations are proportional as a function of depth in the surrounding soils. However, the sub-surface concentrations are significantly lower than the near - surface concentrations illustrating the

**Table 1-** Statistical parameters in soils

Parameters	N <sup>o</sup> samples	Average.
Pb Superficial	355	133,09
Pb_ sub-superficial	66	103,30
Ca	353	4,36
Mg	353	1,91
K	353	0,24
Na	353	0,14
CEC	353	9,81
V	353	66,78
pH (H2O)	353	5,55
pH (KCl)	353	4,36
Org. Carbon	353	13,37
Parameters	Minimum	Maximum
Pb Superficial	5,00	25700,00
Pb_ sub-superficial	9,00	5000,000*
Ca	0,21	17,97
Mg	0,16	13,59
K	0,00	1,54
Na	0,001	7,99
S	0,70	22,11
CEC	1,77	21,78
V	14,20	265,78
pH (H2O)	2,22	8,22
pH (KCl)	1,80	7,64
Org. Carbon	1,24	55,93

limited vertical mobility of Pb under the prevailing climatic conditions. From all the 66 soil profiles in the lower Guadiana basin, lead shows a low vertical mobility.

The factors that influence mobility and availability of lead are the mineralogy of clay fraction, pH, CEC and organic matter content. However, correlation coefficients indicate no clear relationship of lead to these parameters and are consistently low.

The PCA statistical treatment of both near-surface and sub-surface soil pairs shows that in general Pb is associated with the same group of elements irrespective of depth. This may be a

Parameters	Geom. Mean	Median
Pb Superficial	29,94	25,00
Pb_sub-superficial	24,78	23,00
Ca	3,58	3,60
Mg	1,57	1,52
K		0,19
Na	0,09	0,09
CEC	9,38	9,51
V	60,61	62,94
pH (H2O)	5,50	5,52
pH (KCl)	4,32	4,25
Org. Carbon	11,71	12,17
Parameters	Variance	St.Dev
Pb Superficial	189605	1376,97
Pb_sub-superficial	375046	612,41
Ca	8	2,91
Mg	2	1,46
K	0	0,18
Na	0	0,43
S	15	3,92
CEC	8	2,87
V	974	31,22
pH (H2O)	1	0,74
pH (KCl)	0	0,66
Org. Carbon	46	6,77

Org. carbon – Organic carbon; CEC cations exchange capacity

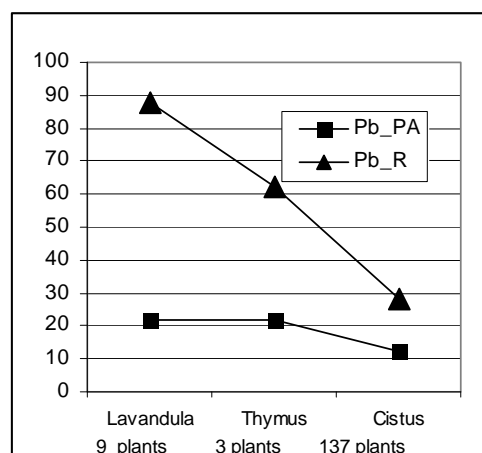
consequence of the shallow depth of these soils.

The concentrations of lead in plants are in general higher in the roots than in the aerial parts (stems and leaves), with 25 to + 5000 mg kg<sup>-1</sup> and 11 to 15 mg kg<sup>-1</sup>, respectively in *Lavandula luisieri* (Rozeira) Rivas-Martinez roots and aerial parts; 3 to 982 mg kg<sup>-1</sup> and 3 to 308 mg kg<sup>-1</sup>, respectively in *Cistus ladanifer* L. roots and aerial parts; and 35 to 70 mg kg<sup>-1</sup> and 8 to 29 mg kg<sup>-1</sup>, respectively in *Thymus vulgaris* L. roots and aerial parts.

Although the number of plant samples is not equally divided per species, due to availability it was nevertheless noted that

the highest concentrations of lead were determined in *Lavandula luisieri* (Rozeira) Rivas-Martinez (Figure 1).

Lead is known to have a very low transport within plants. It is absorbed by the roots but effectively immobilized there (Adriano, 1986). In fact, plants such as *Cistus ladanifer* L. present low transfer coefficients, consequently the animals that eat these plants have a very low risk of ingesting significant amounts of lead. The bi-plot diagram of soil lead/aerial part lead



PA –aerial part; R-roots  
**Fig. 1.** Median results of leaves and roots for thr three plant species

versus soil lead/roots lead in the case of *Cistus ladanifer* L. shows that most of the individuals plot within a claw near the origin. The points that plot outside the claw are samples that were collected near roads or old mines.

### CONCLUSIONS

The low mobility of lead is reflected in the vertical concentrations of lead in the soil and the distribution of lead within the plant system. Lead seems to preferentially concentrate in roots rather than aerial parts of the sampled species. This is agreement with the frequent behaviour of most species in relation to this heavy metal.

### ACKNOWLEDGEMENTS

This study was part of a larger multi-disciplinary environmental project carried out in the framework of an INTERREG IIA Programme of the European Community between Portugal and Spain.

### REFERENCES

- ADRIANO, D.C. 1986. Trace Elements in the Terrestrial Environment. *Springer-Verlag New York Inc.*, 533 p.
- ALLOWAY B.J. 1995. Heavy metals in soils. London: *Blackie Academic & Professional*.
- CALLENDER, E. 2004. Heavy metals in the environment- Historical trends. *Environmental Geochemistry, Elsevier*.
- KABATA-PENDIAS, A. & PENDIAS, H. 1985. Trace elements in soils and plants, 3rd edition, *CRC Press, Inc.*
- KOVALEVSKII, A.L. 1979. Biogeochemical Exploration for Mineral Deposits. *Oxonian Press PVT., Nova Deli*.
- LEISTEL, J.M., MARCOUX, E., THIEBLEMONT, D., QUESADA, C., SANCHEZ, A., ALMODOVAR, G.R., PASCUAL, E. & SAEZ, R. 1997. The volcanic-hosted massive sulphide deposits of the Iberian Pyrite Belt: Review and preface to special issue, **33**, 2-30.
- RIBEIRO, A., QUESADA, C., & DALLMEYER, R.D. 1990. Geodynamic evolution of the Iberian massif. In: Pre-Mesozoic Geology of Iberia. R. D. Dallmeyer & E. M. Garcia (Eds), Springer-Verlag, Berlin, 383-395.

## Risk assessment of arsenic mobility in groundwaters in Langley, British Columbia using geochemical indicators

Rafael Cavalcanti de Albuquerque<sup>1</sup>, Dirk Kirste<sup>1</sup>, & Diana Allen<sup>1</sup>

<sup>1</sup>Department of Earth Sciences, Simon Fraser University, Burnaby, British Columbia, Canada (e-mail: [rca41@sfu.ca](mailto:rca41@sfu.ca))

**ABSTRACT:** Arsenic is mobilized in groundwater under reducing and alkaline conditions as a result of its sorption properties. High arsenic concentrations have been associated with elevated concentrations of a number of specific anions and oxianions species, such as F, V, B, Mo, U, Be and Se, under alkaline conditions, and with redox sensitive species, as Fe, Mn and SO<sub>4</sub>, under reducing conditions. In this study, these species are used as indicators of arsenic mobility in a historical well water geochemistry dataset that contains sample entries with no arsenic data. The study area is the Township of Langley, British Columbia, where arsenic has been reported to be above the Canadian guideline (0.010 mg/l) in groundwater present in Quaternary sediments. A multi-proxy approach is used where a sample or well is only considered to potentially have high arsenic mobility if more than one indicator is observed. Sampling and laboratory analyses will take place during the summer of 2009 in order to test the results of the study.

**KEYWORDS:** *groundwater geochemistry, arsenic mobility, redox, sorption, Quaternary aquifers*

### INTRODUCTION

Arsenic is an element deleterious to human health. Although the World Health Organization guideline for drinking water is set at 0.010 mg/l, studies have shown that this guideline far exceeds tolerable cancer risks (Lindberg & Vahter 2006). Groundwater contamination by arsenic is commonly the result of factors influencing arsenic mobility rather than issues relating to arsenic sources (Smedley & Kinniburgh 2002). Due to sorption properties related to the charge of its dissolved species, arsenic is desorbed from solids and mobilized in water under specific groundwater conditions. The dissolved species formed by the oxidized form of arsenic, arsenate [As (V)], is negatively charged in the pH range typical of natural waters. This causes arsenate to be adsorbed to solids under acidic conditions, and to be released to solution at higher pH. Conversely, the dissolved species of the reduced form of arsenic, arsenite [As (III)], is uncharged. As a result, arsenite tends to be mobile in reducing environments regardless of water pH (Pierce & Moore 1982; Matsunaga *et al.* 1996; Howell 1994). Dissolution of arsenic

bearing minerals as a result of groundwater redox is also a recognized contributor to elevated arsenic levels in groundwater. Examples are the reduction of oxides and oxidation of sulphides containing arsenic (Smedley & Kinniburgh 2002).

In alkaline environments dissolved arsenic concentrations have been observed to correlate positively with other elements that occur in solution as anions and oxianions species, such as F, V, B, Mo, U, Be and Se (Smedley *et al.* 2002). In reducing environments, correlations have been observed between arsenic and redox sensitive species, such as dissolved organic carbon, Fe, Mn and SO<sub>4</sub> (Smedley *et al.* 2003).

The objective of the study is to carry out a risk assessment for arsenic mobility in groundwater on an aquifer system in a temperate climate region. The targeted region is the Township of Langley, British Columbia for which an extensive historical database of groundwater chemistry exists. However, as is typical for many groundwater systems, this database is variable in terms of the quality and extent of the hydrogeochemical and hydrogeological information. These

historical datasets will be evaluated to develop arsenic mobility risk maps for the different aquifer units and then tested by comparing the risk maps with arsenic data contained within more comprehensive datasets.

#### **HYDROGEOLOGICAL AND HYDROGEOCHEMICAL SETTING**

The Township of Langley is located in the Lower Fraser Valley of southern British Columbia, 40 kilometres to the southeast of downtown Vancouver. The groundwater system studied consists of aquifers in Quaternary surficial sediments that were deposited during and since the Fraser Glaciation. The Quaternary deposits are composed of a complex mixture of glacio-fluvial, glacial-marine and postglacial fluvial sediments (Armstrong 1976; Halstead 1986). The four major Quaternary units from oldest to youngest are: the deltaic, marine and glacial marine sediments of the Capilano Sediments; the stony clay and silty clay interbedded marine, glaciomarine and glacial sediments of the Fort Langley Formation; the Sumas Drift made up of till, glaciofluvial and glaciomarine sediments; and the postglacial fluvial, lacustrine and colluvial deposits of the Salish Sediments (Halstead 1986). The local bedrock geology is composed of sedimentary rocks deposited within the Tertiary Georgia Basin (Monger 1990).

Arsenic concentrations in drinking water from wells in Quaternary sediments in the Township of Langley have been reported to be above the Canadian guideline (0.010 mg/l) (Wilson *et al.* 2008a,b). In their studies of arsenic contamination of groundwater in the Langley/Surrey region, Wilson *et al.* (2008a,b) found that the highest arsenic concentrations in groundwater were in samples collected from waters in organic-rich silty loam and clay of the Salish Sediments and marine and glacial-marine deposits of the Capilano Sediments. They also found that in these two units the concentration of arsenic tended to increase at greater depths. The bedrock is not known to be rich in arsenic. This, coupled with the

correlations observed between arsenic concentrations and surficial geology, implies that local bedrock geology is not an important contributor to the observed arsenic concentrations in groundwater (Wilson *et al.* 2008a).

#### **DISCUSSION**

Historical well water geochemistry datasets, available through the British Columbia Ministry of the Environment and Environment Canada, are used to evaluate which samples, wells and geographical areas of Langley have groundwater conditions that suggest arsenic mobility. The datasets contain data collected throughout the study region over several years. Some of the sample entries in the datasets are extensive in geochemical information as they contain pH, and concentrations of major, minor and trace elements, including arsenic. Most of the data entries however are limited, lacking arsenic and other minor and trace species. Most samples were not analysed for redox potential or for the speciated concentrations of arsenite and arsenate. Sample collection methods varied making the quality of the analytical data suspect because important indicators of arsenic mobility, such as pH and the concentrations of redox sensitive elements, can be altered when samples are not properly collected or stored (Ficklin & Mosier 1999). Geochemistry data from an excess of 300 wells is available. Some of this data is however not used in the study due to unreliability and incompleteness of its geochemical entries.

For the first stage of the study, available geological and hydrogeological information is used to develop a conceptual model and the hydrogeological framework of the study area. By doing so, potential geochemical processes leading to arsenic mobility in groundwater can be inferred. The potential geochemical processes are evaluated using published studies on arsenic mobility in order to determine which of the processes are more likely to be exerting a greater control on arsenic mobility and which primary and

secondary hydrogeochemical criteria best serve as indicators of arsenic mobility in the region. These indicators are then queried within the local historical dataset to develop distribution maps. The results obtained are plotted on an arsenic mobility risk assessment map. The produced arsenic risk assessment map is tested against available arsenic data in the region as a means of evaluating the effectiveness of the indicators chosen. It should be noted that tagging samples and wells as having high risk of arsenic mobility does not necessarily imply that the water contains high arsenic concentrations. Other factors that often control arsenic concentrations that are not widely evaluated in the study include hydrogeological processes and local variations of sources of arsenic in bedrock geology and sediments.

This study will test the applicability of the discussed indicators to historical geochemical datasets with little or no arsenic data available. These indicators should help determine which areas are more likely to have higher arsenic concentrations in water and where more sampling is needed. Extensive well water sampling will ultimately be conducted in order to test the arsenic mobility risk assessment presented. Sample analyses will include field measured Eh, arsenite and arsenate concentrations and a number of redox sensitive and pH sensitive species so that appropriate suggestions on redox and pH controls to arsenic mobility can be made. The observations made with this study will help determine which other areas of British Columbia with similar groundwater environments may have arsenic mobility conditions that triggers the need for further water sampling.

### CONCLUSIONS

At the time of the submission of this extended abstract the background research on arsenic mobility is complete and the acquisition of the hydrogeological and geochemical datasets as well as the development of the preliminary conceptual model and hydrogeological framework is

underway, thus comprehensive results and conclusions will be presented at the conference. Preliminary data analyses show a positive correlation between arsenic and pH, with the highest arsenic concentrations occurring at a pH above 8. Weak correlations were found between arsenic and anionic species, such as  $\text{HCO}_3^-$ , Mo, B and F. Fe concentrations range from 0.001 mg/l to values as high as 100 mg/l, which, coupled with the correlation observed by Wilson *et al.* (2008a) of arsenic and water depth within the Salish and Capilano units, may be an indicator of reduction. Arsenic mobility may therefore be occurring as a result of both high pH and reduction. Due to the variability of data quality and completeness within the historical datasets, a variety of indicators are used in the production of the mobility risk map. These include pH, and the concentrations of  $\text{HCO}_3^-$ , Mo, B, F, Fe, Mn,  $\text{SO}_4$  and  $\text{NH}_4$ . Further study is needed in order to better evaluate processes leading to observed arsenic concentrations. This will be addressed with the historical data analysis presented at the conference, and appropriately tested with subsequent field work and laboratory analyses.

### ACKNOWLEDGEMENTS

We thank the British Columbia Ministry of Environment, Environment Canada, Hans Schreier and Martin Suchy for providing historical groundwater geochemistry datasets and Michael Simpson for logistical help.

### REFERENCES

- ARMSTRONG, J.E. 1976. Quaternary geology, stratigraphic studies and revaluation of terrain inventory maps, Fraser Lowland, British Columbia. *Geological Survey of Canada*, Paper 75-1, Part A, 377-380.
- BOWELL, R.J. 1994. Sorption of arsenic by iron oxides and oxyhydroxides in soils. *Applied Geochemistry*, 9, 279-286.
- FICKLIN, W.H. & MOSIER, E.L. 1999. Field methods for sampling and analysis of environmental samples for unstable and selected stable constituents. *Reviews in Economic Geology*, 6A, 249-260.

- HALSTEAD, E.C. 1986. Ground Water Supply - Fraser Lowland, British Columbia. National Hydrology Research Institute Paper No. 26, IWD Scientific Series No. 146, National Hydrology Research Centre, Saskatoon, 80 p.
- LINDBERG, A. & VAHTER, M. 2006. Health effects of inorganic arsenic. In: *NETHERLANDS NATIONAL COMMITTEE - INTERNATIONAL ASSOCIATION OF HYDROGEOLOGISTS. Arsenic in groundwater: A world problem.* Netherlands National Committee of the IAH, Utrecht, The Netherlands, 64-81.
- MATSUNAGA, H., YOKOYAMA, T., ELDRIDGE, R.J., & BOLTO, B.A. 1996. Adsorption characteristics of arsenic(III) and arsenic(V) on iron(III)-loaded chelating resin having lysine-Na,Nα-diacetic acid moiety. *Reactive and Functional Polymers*, 29, 167-174.
- MONGER, J.W.H. 1990. Georgia Basin: Regional setting and adjacent Coast Mountains geology, British Columbia. *Geological Survey of Canada*, Paper 90-1F, 95-107.
- PIERCE, M.L. & MOORE, C.B. 1982. Adsorption of arsenite and arsenate on amorphous iron hydroxide. *Water Research*, 16, 1247-1253.
- SMEDLEY, P.L. & KINNIBURGH, D.G. 2002. A review of the source, behaviour and distribution of arsenic in natural waters. *Applied Geochemistry*, 17, 517-568.
- SMEDLEY, P.L., NICOLLI, H.B., MACDONALD, D. M.J., BARROS, A.J., & TULLIO, J.O. 2002. Hydrogeochemistry of arsenic and other inorganic constituents in groundwaters from La Pampa, Argentina. *Applied Geochemistry*, 17, 259-284.
- SMEDLEY, P.L., ZHANG, M., ZHANG, G., & LUO, Z. 2003. Mobilisation of arsenic and other trace elements in fluviolacustrine aquifers of the Huhhot Basin, Inner Mongolia. *Applied Geochemistry*, 18, 1453-1477.
- WILSON, J. E., BROWN, S., SCHREIER, H., SCOCILL, D., & ZUBEL, M. 2008a. Arsenic in Groundwater Wells in Quaternary Deposits in the Lower Fraser Valley of British Columbia. *Canadian Water Resources Journal*, 33, 397-412.
- WILSON, J. E., SCHREIER, H., & BROWN, S. 2008b. Arsenic in Groundwater in the Surrey-Langley Area. *British Columbia Ministry of the Environment*.

## Spatial assessment of trace elements in Taylor Valley Antarctic Glaciers: Dominance of eolian deposition

Sarah K. Fortner<sup>1,2\*</sup>, Kathleen A. Welch<sup>1</sup>, W. Berry Lyons<sup>1,2</sup>, John Olesik<sup>2</sup> & Rebecca A. Witherow<sup>1,2</sup>

<sup>1</sup>Byrd Polar Research Center, 1090 Carmack Road, Columbus, Ohio, 43210, USA

<sup>2</sup>School of Earth Sciences, 125 S Oval Mall Road, Columbus, Ohio, 43210, USA (\*e-mail: fortner.27@osu.edu)

**ABSTRACT:** We have examined the major ion and trace element chemistry in four 60 to 110 cm deep snowpits from three Taylor Valley (TV) glaciers (Commonwealth, Canada, and Howard) all located within 20 kilometers of the Ross Sea. Taylor Valley (77° 30' S, 163° 15' E) in South Victoria Land and is part of the McMurdo Dry Valleys (MCM), the largest ice-free area in Antarctica. On the north side of TV, Commonwealth and Canada glaciers originate in the Asgard Range, whereas Howard Glacier flows from the Kukri Hills in the south side of the valley. Snow chemistry of these glaciers is strongly influenced by cross-valley winds that deposit eolian materials, including mineral dust and soluble salts. Trace elements (As, Cd, Cu, Eu, Mo, Nd, Pr, Rb, Sm, Sn, Sr, and U) in recent TV glacier snow are almost exclusively derived from eolian dust. Variability in spatial trace element concentrations and concentrations at depth reflect the episodic nature of TV wind events.

**KEYWORDS:** eolian deposition, Antarctica, snow, trace elements

### INTRODUCTION

Lithogenic eolian deposition is a primary chemical contributor to TV snow (Lyons *et al.*, 2003; Williamson *et al.*, 2007; Witherow *et al.*, 2006). Eolian transport of local soils and lake sediments is a documented dispersal mechanism for valley floor life as well as life immured in glacier ice and cryoconite holes (Christener *et al.*, 2003; Nkem *et al.*, 2006). The solubilization of eolian soil on MCM glacier surfaces may be an important, but previously undocumented, source of trace elements to the streams and lakes (Green *et al.*, 1986; Green *et al.*, 2005). Understanding chemical variation associated eolian deposition is especially important as the availability of trace elements may be essential to the ecosystems reliant on glaciers and glacier melt waters (Bargagli, 2000).

### SITE DESCRIPTION

#### Taylor Valley, Antarctica

TV spans 34 km northeast to southwest from the Ross Sea to the Taylor Glacier and has an area of 400 km<sup>2</sup>. To the north, TV is bounded by the Asgard Range and

to the south, the Kukri Hills (Figure 1). Taylor Valley contains numerous valley glaciers (35% of the total area) whose melt produces perennial streams and three closed-basin lakes (Fountain *et al.*, 1999). The valley floor is covered with lacustrine sediment and poorly developed soil of various ages (Marchant *et al.*, 1996). These soils and sediments are readily mobilized and transported through-

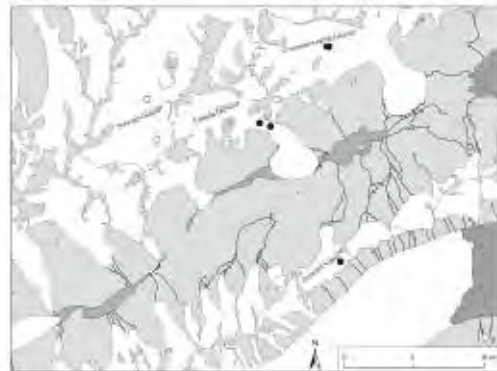


**Fig. 1.** Taylor Valley, Antarctica: glaciers in white, soil in light grey, streams and lakes in dark grey. Snow pit sampling locations are identified with black circles.

out the valley (Lancaster, 2002) with the primary pathway being along the valley floor corridor from the SE to NW or from the NW to SE (Nylen *et al.*, 2004).

### Canada, Commonwealth and Howard Glacier

The Commonwealth Glacier, originating in the Asgard Range, is the second easternmost glacier in the Taylor Valley. Canada Glacier is further inland. Directly across the valley from Canada Glacier is Howard Glacier, which flows from the Kukri Hills. The south-facing glaciers in the Asgard Range cover a greater area than those in the Kukri Hills. Eight years of stake measurements suggest that Commonwealth Glacier may be gaining mass, whereas Howard Glacier is in equilibrium (Fountain *et al.*, 2006). Overall mass balance is not known for Canada Glacier. However, the Canada Glacier ablation zone generally loses mass (up to 12 cm weq/yr) year-round (Fountain *et al.*, 2006). Although mass balance varies between glaciers, all TV glaciers are at their maximum extent since the Last Glacial Maximum (Denton *et al.*, 1989; Fountain *et al.*, 2006).

### METHODS

Four snowpits ranging from 0.6 to 1.1 m were excavated from the upper accumulation zones of Commonwealth, Canada and Howard glaciers were sampled for trace elements and major ions. Canada Glacier was sampled in both January and December 2006 less than 0.5 km apart. Commonwealth (60 cm) and Howard glaciers (110 cm) were sampled only during December 2006. Using the methods of Witherow *et al.*, 2006 snowpits are estimated to represent between 5 and 15 years of accumulation, with some sites potentially wind-redistributed.

LDPE bottles for trace element analyses were soaked in a 10% (v/v) Fisher<sup>TM</sup> trace metal grade HCl/DI. Bottles were then triple rinsed with DI and filled with 10% (v/v) Fisher<sup>TM</sup> trace metal grade HNO<sub>3</sub>/DI. After rinsing with DI, bottles were filled with 1% ultraclean Optima<sup>TM</sup> grade HNO<sub>3</sub>/DI and stored in plastic bags in a

class 100 clean hood. To minimize contamination, samples were collected using “clean hands, dirty hands” techniques (Fitzgerald, 1999).

Trace element samples were acidified to 2% (v/v) using Optima<sup>TM</sup> HNO<sub>3</sub> prior to melting for analyses. Snow samples were not filtered, so the results represent dissolved and colloidal species as well as acid soluble concentrations dissolved from particulates. Trace elements added through acidification were negligible.

A Thermo Finnigan Element 2 Inductively Coupled Plasma Sector-Field Mass Spectrometer (ICP-SF-MS) with guard electrode was employed for trace element analyses. RSD values derived from internal check standard never exceeded 10%. Accuracy was better than 15% for all elements as determined by analyzing the certified reference standard NWRI TM-RAIN 95 trace metal fortified rainwater, every 5 to 8 samples.

### RESULTS/DISCUSSION

#### Sources of trace elements to Taylor Valley Glaciers

To determine the non-seasalt (nSS) contributions of trace elements we have normalized mean concentrations of ions to Cl<sup>-</sup> and subtracted the contributions from seasalt (Nozaki, 1997). We assume that all of the Cl<sup>-</sup> in the sample was from marine aerosol or marine-derived salt and nSS major ions and trace elements can be calculated. For example the percentage of nSS-SO<sub>4</sub><sup>2-</sup> is calculated as:

$$\%nSS-SO_4^{2-} = \left[ \frac{[X]_{snow} - [X]_{ocean}}{[Cl^-]_{snow} - [Cl^-]_{ocean}} \right] \times 100$$

Trace element concentrations in Canada, Commonwealth, and Howard glaciers were 100% nSS. In fact, all trace elements measured had median element:Cl<sup>-</sup> ratios 3 or more orders of magnitude greater than seawater averages (Nozaki, 1997).

We compared snowpit element:S ratios to average annual emission rates measured in December 1986, December 1988, December 1989, and January 1991

from Mount Erebus, the closest active volcano (<80 km) (Zreda-Gostynska and Kyle, 1997). By normalizing trace element concentrations to sulfate we found that the volcanic contributions of As, Cd, Cu, Mo, Pb, Rb, Sn, and V snowpit concentrations were less than 1%.

Our results suggest that crustally derived-material represents the major source of trace element contributions to TV snow. Crustal contributions to the TV glaciers are particularly high due to their proximity to local soil sources and their low annual snow accumulation rates (Welch *et al.*, 1993; Witherow *et al.*, 2006). Furthermore, exposure to strong winds appears to influence the amount of eolian material received. Only the Howard Glacier snowpit lacked shielding from surrounding peaks. Therefore, Howard Glacier snow had significantly greater maximum concentrations of all trace elements with the exception of Rb and Sr than the other three snowpits (Fig. 2).

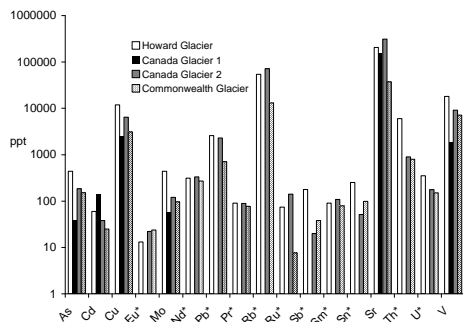


**Fig. 2.** Maximum concentrations observed in Taylor Valley glacier snowpits in parts-per-trillion (\* not measured in Canada Glacier 1).

Furthermore, elemental concentrations at depth, and hence through time, ranged several orders of magnitude in all snowpits because wind events are episodic and variable in speed and duration (Nylen *et al.*, 2004). Howard Glacier is plotted for example (Fig. 3).

**CONCLUSIONS**

TV glaciers are the primary source of water to life-supporting streams and lakes. Understanding the spatial and temporal variation in glacier snow geochemistry

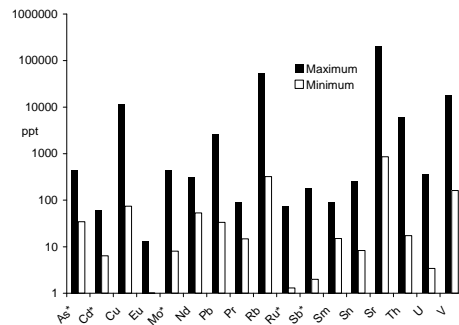


**Fig. 3.** Maximum and minimum concentrations observed in Howard Glacier snow in parts-per-trillion (\* minimum value is below the detection limit).

may begin to elucidate the chemical and hence, ecological, variation observed in streams and lakes. This study suggests that:

- (1) Eolian deposition dominates the deposition of trace elements on TV snow.
- (2) Wind exposure is, therefore, important controls of eolian deposition. Howard Glacier snow was the most wind exposed and had the greatest trace element concentrations
- (3) Episodic wind events explain the wide range in trace element and Ca concentrations observed TV snow.

**ACKNOWLEDGEMENTS**

We thank Anthony Lutton for his assistance with the ICP-MS and Joel Barker and Cecelia Mortenson for their help in the field. Thank you also to Dave Lape for constructing a snow sampler.

**REFERENCES**

CHRISTNER, B.C., KVITKO, B.H., II & REEVE, J.N. 2003. Molecular identification of bacteria and eukarya inhabiting an Antarctic cryoconite hole. *Extremophiles*, **7**, 177-183.

FITZGERALD, W.F. 1999. Clean Hands: Clair Patterson's Crusade Against Environmental Lead Contamination. *Nova Science*, 119-137.

FOUNTAIN, A.G., LYONS W.B., BURKINS, M.B., DANA, G.L., DORAN, P.T., LEWIS, K.J., MCKNIGHT, D.M., MOOREHEAD D.L., PARSON, A.N., PRISCU, J.C., WALL D.H., WHARTON, JR. R.A. & VIRGINIA, R.A. 1999. Wind dispersal of

- soil invertebrates in the McMurdo Dry Valleys, Antarctica. *Bioscience*, **49**, 961-971.
- FOUNTAIN, A.G., NYLEN, T., MACCLUNE, K.L., DANA, G.L. 2006. Glacier mass balances (1993-2001), Taylor Valley, McMurdo Dry Valleys, Antarctica. *Journal of Glaciology*, **52**, 451-462.
- GREEN, W.J., CANFIELD, D.E., LEE, G.F. & JONES, R., A. 1986. Mn, Fe, Cu, and Cd distributions and residence times in closed basin Lake Vanda (Wright Valley, Antarctica). *Hydrobiologia*, **134**, 237-248.
- GREEN, W.J., STAGE, B.R., PRESTON, A., WAGERS, S., SHACAT, J. & NEWELL, S. 2005. Geochemical processes in the Onyx River, Wright Valley, Antarctica: major ions, nutrients, trace metals. *Geochemica et Cosmochimica Acta*, **69**, 839-850.
- HINKLEY, T.K., LAMOUTHE, P.J., WILSON, S.A., FINNEGAN, D.L. & GERLACH, T.M. 1999. *Earth and Planetary Science Letters*, **170**, 315-325.
- LANCASTER, N. 2002. Flux of aeolian sediment in the McMurdo Dry Valleys, Antarctica: a preliminary assessment. *Arctic, Antarctic, and Alpine Research*, **34**, 318-323.
- LYONS, W.B., WELCH, K.A., FOUNTAIN, A.G., DANA, G.L., VAUGHN, B.H. & MCKNIGHT, D.M. 2003. Surface glaciochemistry of Taylor Valley, southern Victoria Land, Antarctica and its relationship to stream chemistry. *Hydrological Processes*, **17**, 115-130.
- MARCHANT D.R., DENTON G.H., SWISHER C.C. & POTTER N. 1996. Late Cenozoic Antarctic paleoclimate reconstructed from volcanic ashes in the dry valleys region of southern Victoria Land *Geological Society of America Bulletin*, **108**, 181-194.
- NKEM, J.N., WALL, D.H., VIRGINIA, R.A., BARRETT, J.E., BROOS, E.J., PORAZINSKA, D. & ADAMS, B.J., 2006. Wind dispersal of soil invertebrates in the McMurdo Dry Valleys, Antarctica. *Polar Biology*, **29**, 346-352.
- NOZAKI, Y. 1997. A fresh look at element distribution in the North Pacific Ocean. *Eos, Transactions American Geophysical Union*, **78**, 221-221.
- NYLEN, T.H., FOUNTAIN, A.G., & DORAN, P.T. 2004. Climatology of katabatic winds in the McMurdo dry valleys, southern Victoria Land, Antarctica, *Journal of Geophysical Research*, **109**, 9.
- WELCH K. A. 1993. Glaciochemical investigations of the Newall Glacier, Southern Victoria Land, Antarctica In *Earth Sciences*. University of New Hampshire; 92.
- WELCH, K.A., MAYEWSKI, P.A. & WHITLOW, S.I. 1993. Methanesulfonic acid in coastal Antarctic snow related to sea-ice extent. *Geophysical Research Letters*, **20**, 443-446.
- WITHEROW R.A., LYONS W.B., BERTLER N.A.N., WELCH K.A., MAYEWSKI P.A., SNEED S.B., NYLEN T., HANDLEY M.J., & FOUNTAIN A.G. 2006. The aeolian flux of calcium, chloride, and nitrate to the McMurdo Dry Valleys landscape: evidence from snow pit analysis. *Antarctic Science*, **18**, 497-505.

## Heavy metal loads in sediments influenced by Mežica Pb-Zn abandoned mine, Slovenia

Mateja Gosar<sup>1</sup> & Miloš Miler<sup>1</sup>

<sup>1</sup>Geological Survey of Slovenia, Dimičeva 14, 1000 Ljubljana, Slovenia  
(e-mail: [mateja.gosar@geo-zs.si](mailto:mateja.gosar@geo-zs.si), [milos.miler@geo-zs.si](mailto:milos.miler@geo-zs.si))

**ABSTRACT:** The main objective of this study was to identify heavy-metal concentrations and associated mineral phases using an ICP and SEM-EDS in the heavily metal polluted sediments of the Meža River Valley, characterize them according to their source and genesis, and assess the degree of negative impact arising from Pb-Zn mining and smelting activities in the Mežica mining district and the ironworks in the Ravne area (Meža River Valley, NNE part of Slovenia). The highest Pb and Zn concentrations were measured in stream sediments of the Meža River and its tributaries in the areas of former mining and smelting activities in Mežica and Žerjav and the highest contents of Co, Cr, Cu and Ni were identified in the area of the Ravne ironworks.

**KEYWORDS:** heavy-metal bearing phases, mining, ironworks, SEM-EDS

### INTRODUCTION

In the Meža Valley around 19 million tons of lead-zinc ore were produced and processed for more than 300 years. Previous investigations of Meža River sediments have shown elevated concentrations of lead and some other metals (Fux & Gosar 2007). At the end of the 20<sup>th</sup> century, the Meža River had the highest concentrations of heavy metals in any Slovenian stream (Lapajne *et al.* 1999). After the mine and processing plants ceased operation, the direct transfer of heavy metals into the environment decreased sharply. However, deposits of poor ore and ore processing wastes have persisted as a source of heavy metal pollution. From those places heavy metals have washed out into the nearby streams, including the Meža River and more downstream locations such as the Drava River.

Previous investigations of soil and river sediments, carried out by Vreča *et al.* (2001), Šajn & Gosar (2004), and Šajn (2006) have shown that the upper Meža Valley is still highly polluted from past mining activities that ceased more than 10 years ago.

### SAMPLING AND ANALYTICAL METHODS

In the upper stream of the Meža River, including significant tributaries (e.g. Topla, Helenski potok, Mušenik, Jazbinski potok, Junčarjev potok), the stream sediment samples were collected approximately 1 km apart. From Mežica to the Drava River the sampling distance was increased to 10 km. Additionally, two samples of the Drava River sediments were taken before and after its confluence with the Meža River (Fig. 1).

Two fractions (< 0.125 mm and < 0.063 mm) of air-dried and sieved sediments

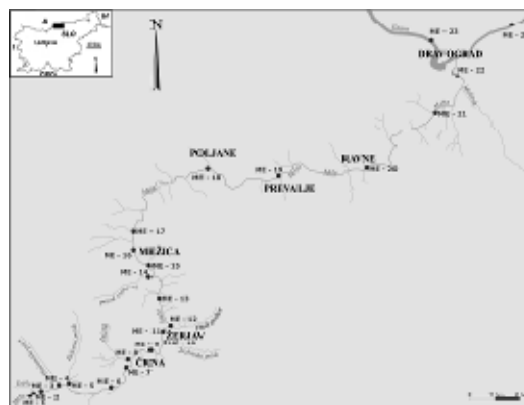


**Fig. 1.** Location of study area with sampling locations.

were analyzed at the ACME Analytical Laboratories Ltd. (Vancouver, Canada).

The content of heavy metals in sediments was determined by sample digestion with 10 ml of the mixture of HClO<sub>4</sub>, HCl, HNO<sub>3</sub> and HF at 200°C, followed by Inductively Coupled Plasma Emission Spectrometry (ICP) (ACME, 2003).

Identification of heavy metal-bearing particles in seven stream sediment samples (grain size fraction < 0.063 mm), coated with gold, was performed in the BSE mode on a JEOL JSM 6490LV SEM coupled with an Oxford INCA Energy EDS. Semi-quantitative chemical analysis was performed on polished, carbon-coated samples of river sediment embedded in araldite resin, using EDS point analysis and X-ray mapping. Heavy metal mineral phases were assessed from the atomic proportions of the constituent elements, obtained by semi-quantitative analysis. EDS data correction was performed using the standard ZAF-correction procedure included in the INCA Energy software© (Oxford Instruments, 2006).

## **HEAVY METALS IN STREAM SEDIMENTS**

### **Lead (Pb) and Zinc (Zn)**

Lead content varies between 80 mg/kg and 14,200 mg/kg in the < 0.063 mm fraction and between 76 mg/kg and 19,300 mg/kg in the < 0.125 mm fraction. Zinc content ranges from 260 mg/kg to 22,500 mg/kg in the < 0.063 mm fraction and from 264 mg/kg to 37,900 mg/kg in the < 0.125 mm fraction.

The highest contents of Pb and Zn were measured between Žerjav and Mežica (ME-11, ME-13, ME-15) and between Poljane and Prevalje (ME-18, ME-19). The increase in Pb content between Žerjav and Mežica was interpreted as a consequence of heavy metal pollution by air deposition of soil near the smelter in Žerjav, and of the contribution of heavy metal-polluted Helenski potok (ME-5) and mining waste dump in Mežica (ME-15). Elevated concentrations of Pb and Zn between Poljane and Prevalje (ME-18, ME-19) are most probably a consequence

of mine water discharge through a 6 km long tunnel from Mežica mine to the Meža River, since no other source of heavy metal pollution has been found in the area.

The highest contents of Pb and Zn in tributary sediments were measured in Helenski potok (ME-5) and Junčarjev potok (ME-14) and are interpreted as a consequence of discharge from mining waste dumps and tailings in the tributaries area.

### **Cadmium (Cd), Molybdenum (Mo) and Arsenic (As)**

Cd, As and Mo share similar trends with Pb and Zn in upper Meža Valley, because they all occur as trace elements in ore minerals from the Mežica ore deposit (Štrucl 1984; Fux & Gosar 2007).

The second source of these elements are the Ravne ironworks in the lower Meža Valley where the highest contents of Mo are reached in the < 0.063 mm fraction (ME-20) and are higher than the contents in the < 0.125 mm fraction.

Relatively high contents of As in Drava River samples (ME-23 and ME-24) are a consequence of the Drava River catchment area characteristics.

### **Cobalt, Chrome, Copper and Nickel (Co, Cr, Cu and Ni)**

Near Ravne (ME-20) the contents of Co, Cr, Cu and Ni are increased in the < 0.063 mm fraction compared to contents in the < 0.125 mm fraction, which is due to different methods of processing at Ravne ironworks (Kaker & Glavar 2005; Alijagić & Šajn 2006).

### **Individual particle analysis**

Seven stream sediment samples of Meža River with its tributaries (Topla, Helenski potok, Mušenik, Jazbinski potok, Junčarjev potok) (ME-1, ME-5, ME-14, ME-17, ME-18, ME-20) and Drava River (ME-24), were analyzed using SEM/EDS. They contained Pb, Zn, Cr, Ni, Mn, Mo, Cd, Ti, V, W, Zr, Ce, Sb, Cu, Y, Sr, Ba, and Ag, found in different heavy metal-bearing phases.

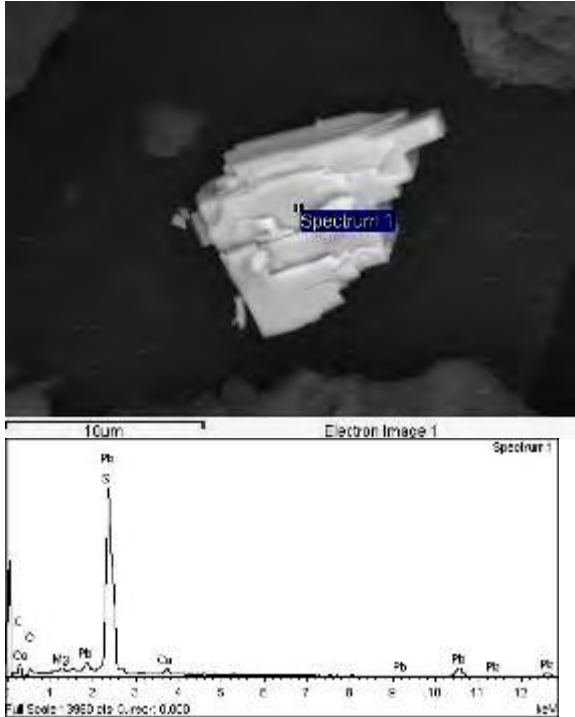


**Fig. 2.** SEM image and EDS spectrum of galena (sampling point ME-14).

The main outcomes of SEM/EDS analysis are as following:

In sediments of the Mežica mining and smelting area, mineral phases such as cerussite ( $PbCO_3$ ), galena ( $PbS$ ) (Fig. 2), pyromorphite ( $Pb_5(PO_4)_3Cl$ ), descloizite ( $PbZn(VO_4)(OH)$ ), bindheimite ( $Pb_2Sb_2O_6(O,OH)$ ), sphalerite ( $ZnS$ ), and smithsonite ( $ZnCO_3$ ) were identified. These minerals are derived from both geogenic and technogenic processes in the Mežica mining district.

Technogenic phases, such as various Fe-alloys ((Cr,Ni)-ferroalloy, (Cu,Ni)-alloy, and (Fe, Si)-alloy), Fe-oxides ((Cr,V,Fe)-oxide, (Mo,W,V,Cr,Fe)-oxide, (Mo,W)-oxide, (W,Cr,Fe)-oxide), and spherical particles ((Cr,Ni)-oxide or chrome-nickel-spinel (Fig. 3), (Cr,Fe)-oxide or chrome-spinel), were recognized in the area of the Ravne ironworks.

Mineral phases of geogenic origin, found in most of the investigated sediments, are barite ( $BaSO_4$ ), strontianite ( $SrCO_3$ ), rutile ( $TiO_2$ ), ilmenite ( $FeTiO_3$ ),

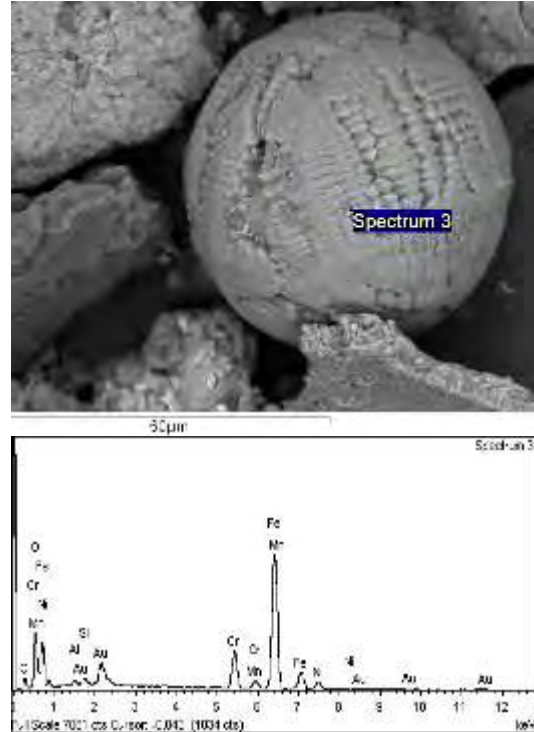


**Fig. 3.** SEM image and EDS spectrum of aerosol particle (sampling point ME-20).

titanite ( $CaTiSiO_5$ ), zircon ( $ZrSiO_4$ ), chalcocopyrite ( $CuFeS_2$ ), monazite ((Ce,La,Nd) $PO_4$ ), and xenotime ( $YPO_4$ ). Their source is most probably weathering of bedrock in the catchment area.

## CONCLUSIONS

Chemical analysis of the Meža River and its tributaries revealed significant heavy metal pollution of the upper Meža River sediments with lead, zinc, and some molybdenum, cadmium and arsenic enrichments. The trend of Cd and As is similar to trend of Pb and Zn, which is in agreement with the fact that Cd and As are associated with Pb and Zn in ore minerals (Štrucl, 1984; Fux & Gosar, 2007). In the lower Meža valley, these heavy metal concentrations decreased somewhat.

In the lower Meža River Valley concentrations of cobalt, chrome, copper and nickel are increased around Ravne as a result of the ironworks industry.

Geogenic and tectogenic heavy metal-bearing phases in sediments of the Meža River were identified by means of SEM/EDS. Knowledge of the mineralogy of heavy metal-bearing phases is important in understanding their stability, solubility, mobility, bioavailability, toxicity and developing remediation strategies.

#### ACKNOWLEDGEMENTS

The authors are grateful for financial support of this study to Slovenian Research Agency (ARRS) and RESTCA European seventh framework program for financial support for attendance to IAGS symposium.

#### REFERENCES

- ACME ANALYTICAL LABORATORIES L.T.D. 2003. Assays and geochemical analysis. *Acme analytical laboratories L.t.d.*, Vancouver B.C., 18.
- ALIJAGIĆ, J. & ŠAJN, R. 2006. Influence of ironworks on distribution of chemical elements in Bosnia and Herzegovina and Slovenia = Vpliv železarn na porazdelitev kemičnih prvin v Bosni in Hercegovini ter Sloveniji. *Geologija*, **49/1**, 123–132
- LAPAJNE, S., ZUPAN, M., BOLE, M., ROVŠER-DREV, A. & JANET, E. 1999. Posnetek obstoječe vodooskrbe in kakovosti površinskih voda na območju Mežiške doline. – In: Ribarič Lasnik, C. et al.: Problem težkih kovin v Zgornji Mežiški dolini: proceedings volume, *Environmental Research & Industrial Co-operation Institute ERICo*, Velenje, 87–95.
- FUX, J. & GOSAR, M. 2007. Vsebnosti svinca in drugih težkih kovin v sedimentih na območju Mežiške doline = Lead and other heavy metals in stream sediments in the area of Meža valley. *Geologija*, **50**, 347–360.
- KAKER, H., GLAVAR, U. 2005. Steel Selector (Version 3.0) [computer software]. Available from <http://www.metalravne.com/selector/selector.html>
- OXFORD INSTRUMENTS, 2006. INCAEnergy EDS X-ray Microanalysis System. *Oxford Instruments Analytical Limited*, Oxfordshire, 19.
- ŠAJN, R. 2006. Factor Analysis of Soil and Attic-dust to Separate Mining and Metallurgy Influence, Meza Valley, Slovenia. *Mathematical Geology*, **38**, 735-747.
- ŠAJN, R. & GOSAR, M. 2004. Pregled nekaterih onesnaženih lokacij zaradi nekdanjega rudarjenja in metalurških dejavnosti v Sloveniji = An overview of some localities in Slovenia that became polluted due to past mining and metallurgic activities. *Geologija*, **47**, Ljubljana, 249-258.
- ŠTRUCL, I. 1984. Geološke, geokemične in mineraloške značilnosti rude in prikamenine svinčevo-cinkovih orudenj mežiškega rudišča = Geological and geochemical characteristics of ore and host rock of lead-zinc ores of the Mežica ore deposit. *Geologija*, **27**, Ljubljana, 215-327.
- VREČA, P., PIRC, S., ŠAJN, R., 2001. Natural and anthropogenic influences on geochemistry of soils in the terrains of barren and mineralized carbonate rocks in the Pb – Zn mining district of Mežica, Slovenia. *Journal of Geochemistry Exploration*, **74**, 99-108.

## Relationship of heavy metals between rice and soils in Zhejiang, China

Zhou Guohua, Wei Hualing, Sun Binbin & Liu Zhanyuan

*Institute of Geophysical and Geochemical Exploration, Langfang Hebei 065000, P.R.China  
(e-mail: [zhouguohua@igge.cn](mailto:zhouguohua@igge.cn))*

**ABSTRACT:** Rice and cultivation-layer soils were collected in the rice harvest season of 2006 in the key agricultural regions of Zhejiang province. Heavy metals and some soil physicochemical indicators were determined. It was demonstrated that heavy metal concentrations in rice were usually related to their concentrations in cultivation soils. In general, the Biologic Accumulation Coefficients (BAC) of heavy metals of rice to soil have a good relationship with physicochemical factors of soils including organic matter, pH, CEC and granularity. The results provide a pathway for making adjustments to soil physicochemical conditions such as organic matter and pH at the areas with higher background of heavy metals or contaminated sites so as to control heavy metal transportation from soil to edible parts of rice.

**KEYWORDS:** *heavy metal, physicochemical factors, soil, rice, bio-accumulation coefficient, Zhejiang*

### INTRODUCTION

Zhejiang province is located in eastern China and has a relatively developed economy. The main plain of the northeastern part of the province was formed by alluvium, and coastal, lake and marsh sediments. There are several small plains along the eastern coastline formed by alluvium and marine sediment. These plains have undergone thousand of years of agricultural cultivation.

A multi-purpose regional soil geochemical survey with a sampling density of one sample every square kilometer for top soils (0-20cm) and one sample every 4 square kilometers for bottom soils (150-200cm beneath surface) was conducted. Organic matter, pH and concentrations of fifty two elements were determined during a 2002-2005 study by the geological survey of Zhejiang province. This survey showed that a number of areas contain elevated concentrations of heavy metals in soils. Compared to the regional geochemical data obtained in the early of 1990's heavy metal (including As, Bi, Cd, Cu, Sb, Se, Tl, V, Zn) accumulation and acidification were apparent at several areas (Zhou *et al.*, 2004). It is likely that recent

industrialization and urbanization has caused degradation of the soil quality.

This study assesses the potential impact of the changes in the soil condition on agricultural product safety and examines the transportation of heavy metals from soils to rice.

### SAMPLING AND ANALYSIS

Sampling sites were selected based on the regional soil survey and a related study in seven sub-areas, each with coverage of several dozen to hundreds of square kilometers and with representative geological setting and geochemical characteristics. Rice and cultivation layer soil at 146 sites were sampled at a density of one site per square kilometer during rice harvest season, October 2006.

Heavy metals in rice and soils as well as several physicochemical indicators of soils including Organic matter (OM), pH, Cation- Exchange Capacity (CEC) and soil granularity were analyzed. As, Cd, Cr, Cu, Hg, Mn, Ni, Pb, Se, Zn and OM of soils, and As, Cd, Cr, Cu, Hg, Mn, Ni, Pb, Se and Zn of rice were determined at the central chemical lab of the Institute of Geophysical and Geochemical Exploration. The CEC of the soils was measured at the analytical institute of

Jiangsu Geological Survey of China. Soil granularity was determined at the China University of Geological Sciences.

**RESULTS AND DISCUSSION**

**Relationship of heavy metals between rice and soils**

The correlation coefficients of heavy metal concentrations between rice and soils for 146 samples are Cd 0.932, Cr 0.172, Cu 0.181, Hg 0.276, Ni 0.410, Se 0.178 and Zn 0.264 respectively, which indicates a fairly good relationship between these elements. As the accumulation of Cd, Cu, Se and Zn in soils increased, the concentrations of the rice also increased. Although the concentrations of these elements in rice are much lower than the safety threshold value in most samples and have no immediate impact on human health, the increase of soil concentration of heavy metals will eventually enhance risk through rice uptake in the food chain. Therefore diminishing the input of heavy metals to soil is urgent to maintaining long-term soil cultivation suitability.

There was no significant relation of the concentrations of As, Mn and Pb between rice and soils. Scatter plot showed that the correlation coefficient of As increases from 0.027 to 0.321 after deleting one set of data outliers (see fig.1 and 2). But the correlation coefficients of Mn and Pb couldn't be improved by deleting anomalous data sets. Several researchers (Lu *et al.*, 2005; Su *et al.*, 2008; Zhou *et al.*, 2007) obtained similar results between

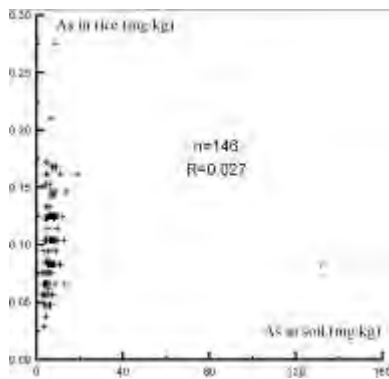


**Fig. 1.** As concentration in rice vs. soils from of 146 sample sets.

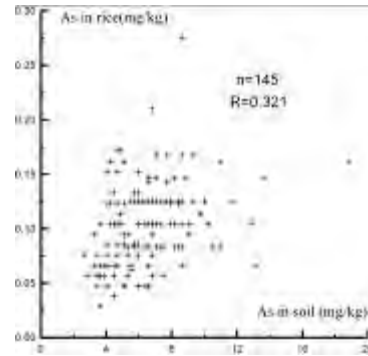


**Fig. 2.** As concentration in rice vs. soils after excluding one anomalous sample set.

crops and soils, and they proposed that Pb in edible parts of crops was mainly from aero-precipitation.

**Physicochemical factors influencing rice's BAC of heavy metals**

Biologic Accumulation Coefficient (BAC) of heavy metals in rice is defined as:

$$BAC = \frac{C_b}{C_s} \times 100\% \quad (1)$$

$C_b$  --heavy metal concentration in rice;  $C_s$  --heavy metal concentration in soil.

BAC values and related statistics are presented in table 1.

It is apparent that rice's BAC values of Cd and Zn are greater than 10%; the BACs of Cu, Mn, Hg, As and Se are much lower; the BACs of Cr, Ni and Pb are the lowest. This can be attributed to elemental

**Table 1.** Statistical parameters of rice's BAC of heavy metals (n=146)

	mean	median	SD	VC
BAC <sub>As</sub>	1.72	1.60	0.71	0.41
BAC <sub>Cd</sub>	26.73	18.22	24.33	0.91
BAC <sub>Cr</sub>	0.26	0.26	0.14	0.54
BAC <sub>Cu</sub>	4.02	3.45	2.76	0.69
BAC <sub>Hg</sub>	3.01	2.59	2.02	0.67
BAC <sub>Mn</sub>	3.45	3.28	1.35	0.39
BAC <sub>Ni</sub>	0.69	0.57	0.45	0.65
BAC <sub>Pb</sub>	0.36	0.27	0.43	1.19
BAC <sub>Se</sub>	1.56	1.17	1.69	1.08
BAC <sub>Zn</sub>	14.59	14.13	5.56	0.38

SD--standard deviation;VC-- variation coefficient.

abundance and bio-geochemical characteristics including bio-available contents and the uptake ability of rice (Salomons *et al.*, 1995; Zhou *et al.*, 2005; Jiang and Zhang, 2002; Wu *et al.*, 1999; Mou *et al.*, 2004). It is also observed that the variation coefficients for most heavy metals are greater than 0.5. This may be because rice species, soil parent material, and soil type are varied greatly between the 146 sampling sites so that the uptake ability of rice to presence of heavy metals is of large difference from site to site.

The correlation coefficients between rice's BAC and soil physicochemical indicators were calculated (see table 2).

**Table 2** . Correlation coefficients of BAC and physicochemical indicators

	OM	pH	CEC	FC
BAC <sub>As</sub>	0.188	-0.230	-0.539	-0.213
BAC <sub>Cd</sub>	0.132	-0.212	-0.307	0.113
BAC <sub>Cr</sub>	0.189	-0.006	0.150	-0.278
BAC <sub>Cu</sub>	-0.041	-0.102	-0.252	-0.203
BAC <sub>Hg</sub>	-0.369	0.269	-0.287	-0.035
BAC <sub>Mn</sub>	0.013	-0.180	-0.215	-0.447
BAC <sub>Ni</sub>	0.160	-0.257	-0.242	0.183
BAC <sub>Pb</sub>	-0.344	0.302	-0.333	-0.121
BAC <sub>Se</sub>	-0.295	0.212	-0.497	-0.161
BAC <sub>Zn</sub>	-0.438	0.301	-0.561	-0.370

FC refers the percentage of fine silt and clay component with grain-size less than 5 µm.

Table 2 illustrates that the BACs of As, Cd, Cr and Ni tend to increase as soil organic matter increases. Although the detailed mechanism needs to be studied, the phenomena may be due to the influence of the soil condition (including OM contents) on the species and bio-ability of these heavy metals. Contrarily the BACs of Hg, Pb, Se and Zn decrease greatly as soil organic matter is increased which provides a possible pathway to control Hg, Pb and Zn transfer into food by adding organic fertilizer.

The effect of pH on BACs of heavy metals is complicated. The BACs of rice of As, Cd, Mn and Ni tend to decrease as pH

increased. It can be supposed that the bio-available contents of heavy metals decreased as pH increased. But the BAC's trend of Hg, Pb, Se and Zn is somewhat anomalous. One possible reason is that sample sites are scattered in large region and soil properties and rice genotype are varied greatly so that pH influence is less than other factors. However Pb concentration in rice may be mainly from atmosphere so that there is no relation in soil-plant system.

CEC and fine silt and clay component (FC) have similar effects on rice's BAC. The competitive uptake of the alkaline-earth cations may result in a reduced heavy metal BAC for rice. Soils with higher percentage of fine silt and clay provided more CEC so that it has similar effect on the BAC.

## CONCLUSIONS

This paper presents some trends for heavy metal patterns in rice-soil systems on a regional scale in Zhejiang province. The major findings are summarized below: (1) Heavy metal concentrations in rice are related to concentrations in soils. Thus soil heavy metal contamination should be strictly controlled.

(2) Biologic Accumulation Coefficients (BAC) of rice are influenced by soil properties such as organic matter, pH, CEC, and granularity component.

(3) Although further study needs to be conducted to determine the effect of other soil properties, the influences of organic matter and pH on rice's BAC provide an important pathway to predict heavy metal risk on the safety of rice and other agricultural products. This may mean that as soil contamination continues soil properties such as pH may need to be adjusted using products such as lime and organic fertilizer.

## ACKNOWLEDGEMENTS

We would like to give our thanks to the analytical technicians for their hard work on the sample analysis and to the geochemical technicians at the Geological Survey of Zhejiang province for their assistance in the field work.

## REFERENCES

- JIANG BIN AND ZHANG HUEI-PING. 2002. Genotypic differences in concentration of Lead, Cadmium and Arsenic in polished rice grains. *Journal of Yunnan Normal University*, **22(3)**, 37-40. (in Chinese).
- LU YUANFA, YANG HONGWEI, ZHOU GUOHUA, MA LIYAN, MEI YUPING AND CHEN XIQING. 2005. Lead isotopes in soil as a tracer of environmental lead pollution in Hangzhou. *Quaternary Science*, **25(3)**, 355-362. (in Chinese).
- MOU REN-XIANG, CHEN MING-XUE, ZHU ZHI-WEI, YING XING-HUA. 2004. Advance in the researches on heavy metals in rice. *Ecology and Environment*, **13(3)**, 417-419. (in Chinese)
- SU YIN, YUAN XINZHONG, CENG GUANGMING, LI HUIMENG AND LI LIAN. 2008. Study on influence factors of transportant and transformations of Pb in soil-plant system. *Journal of Anhui Agricultural Sciences*, **36(16)**, 6953-6955. (in Chinese).
- WU QI-TANG, CHEN LU, WANG GUANG-SHOU. 1999. Differences on Cd uptake and accumulation among rice cultivars and its mechanism. *ACTA Ecologica Sinica*, **19(1)**, 500-501,601,701. (in Chinese)
- W.SALOMONS, U.FÖRSTNER, P.MADER. 1995. Heavy metal: problems and solutions. *Springer*.
- ZHOU GUO-HUA, DONG YAN-XIANG, LIU ZHAN-YUAN, WANG QIANG-HUA, LIU GUO-HUA & SUN BIN-BIN. 2004. Temporal-spatial variation of elements in soils in the Hangjiahu area. *Geology in China*, **31**, 72-79. (in Chinese).
- ZHOU GUOHUA, WU XIAOYONG & ZHOU JIAN HUA. 2005. Available element contents and factors influencing their availability in northern Zhejiang. *Quaternary Science*, **25(3)**, 316-322. (in Chinese).
- ZHOU GUO-HUA, WANG QING-HUA AND DONG YAN-XIANG. 2007. Factors affecting heavy metal concentrations in the soil-agricultural product system. *Computing techniques for geophysical and geochemical exploration*, **29(1)**, 226-231. (in Chinese).

## Anthropogenic Gadolinium as a Micropollutant in Drinking Water

Serkan Kulaksız<sup>1</sup> & Michael Bau<sup>1</sup>

<sup>1</sup>Jacobs University Bremen, Earth and Space Sciences, Campus Ring 8, 28759, Bremen, Germany  
(e-mail: [m.bau@jacobs-university.de](mailto:m.bau@jacobs-university.de))

**ABSTRACT:** Rare earth elements (REE) are often used as geochemical tracers due to their coherent behaviour in natural systems. While studies of REE in geochemistry rely on the assumption that these systems are free from anthropogenic input, they are, however, increasingly affected by anthropogenic micropollutants. Excessive amounts of gadolinium (Gd), a rare earth element, have been reported in rivers and groundwaters from numerous regions with high population density and advanced health care systems. The source of the excess Gd is its usage as a contrast agent in magnetic resonance imaging (MRI). The Gd is stabilized as a water-soluble and highly stable organic complex which is transported unimpeded through sewage systems and waste water treatment plants (WWTP) into rivers and aquifers. We provide data that documents that anthropogenic Gd is also present in municipal drinking water in several cities in Germany. The presence of anthropogenic Gd in drinking water strongly suggests that pharmaceuticals which behave similar to anthropogenic Gd may also be present.

**KEYWORDS:** *anthropogenic gadolinium, rare earth elements, tapwater, contrast agent, nephrogenic systemic fibrosis*

### INTRODUCTION

The rare earth elements (REE) form a group of elements that have coherent geochemical behaviour due to their trivalent charge and similar ionic radii. They can, however, be fractionated from one another as a result of geochemical processes operating under specific physico-chemical conditions. In order to outline general trends within and differences between the individual REE, concentrations are usually normalized to a reference system (e.g. to shale). Deviations of individual elements from the generally smooth trend are referred to as anomalies.

While studies of natural REE and their variation are abundant and their behaviour in natural systems is reasonably well understood, their increased usage in high-tech products and applications that have become essential for our modern life styles is making it harder to conduct research on natural processes.

The increasing demand for REE in applications ranging from petroleum cracking catalysts to fertilizers, or from essential computing hardware to nuclear power plants means that research and

monitoring studies need to be intensified to understand their increasing input into the environment. REE are found in natural waters at ultratrace concentrations, and natural concentrations can be easily masked by small amounts of anthropogenic influence (Bau & Dulski, 1996). Another disadvantage of their low abundance is that even in known cases of contamination there are no emission limits. Presently, there is relatively little work to assess the long-term effects of REE on ecosystem health.

Tapwater, surface water and WWTP effluents were sampled, filtered (0.2µm) and acidified to pH 2.0. REE were separated and preconcentrated following the method described in detail by Bau and Dulski (1996). REE concentrations were determined by inductively coupled plasma mass spectrometry.

### ANTHROPOGENIC GADOLINIUM

Figure 1 shows dissolved REE concentrations normalized to shale (McLennan, 1989) for rivers that are uncontaminated. The general trend is an enrichment of heavier REE as compared to lighter REE, with few minor deviations.

Cerium is insoluble when present in a tetravalent state, and is depleted compared to its neighbouring elements, causing negative Cerium anomalies in oxic systems. Lanthanum, Gd, and Lu have higher complexation stability constants when compared to the other trivalent REE, due to their specific electron configurations. They may therefore be found in slightly higher concentrations, and display small positive natural anomalies. The conclusion from these rivers is that major anomalies are not expected in systems uncontaminated by human impact.

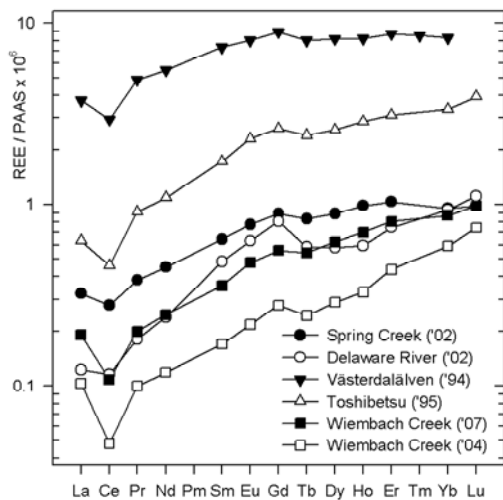


**Fig. 1.** Rare earth element plots of uncontaminated rivers. Samples marked with circles are from Bau *et al.* (2006) and those with triangles from Bau & Dulski (1996). Samples marked with squares are from this study.

Figure 2 shows REE patterns for a selection of rivers showing positive anthropogenic Gd anomalies. These anomalies are found across the world in Japan, Australia, Europe and the U.S., in areas of high population density. The anthropogenic Gd in river waters can be related to the use of Gd compounds as contrast agents in MRI (Bau & Dulski, 1996). Availability of modern medical facilities, therefore, is a prerequisite for producing such Gd anomalies. This is shown by the lack of a positive Gd

anomaly in the Chao Phraya River (Thailand) which passes through the densely populated Bangkok City (Nozaki *et al.* 2000), but lacks readily available MRI facilities.

The effluent waters of a waste water treatment plant (Ruhleben) in Berlin (Fig. 3) show the highest positive Gd anomaly observed to date. Strong positive Gd anomalies are common in effluents of other treatment plants across the world (e.g. Australia, USA, Austria, Germany, and Czech Republic) due to the inability of the treatment processes to remove the highly stable and water soluble Gd complexes. This is also the cause for their presence in river and lake waters and in groundwater which receive these effluent waters either directly (input into rivers) or indirectly (infiltration).

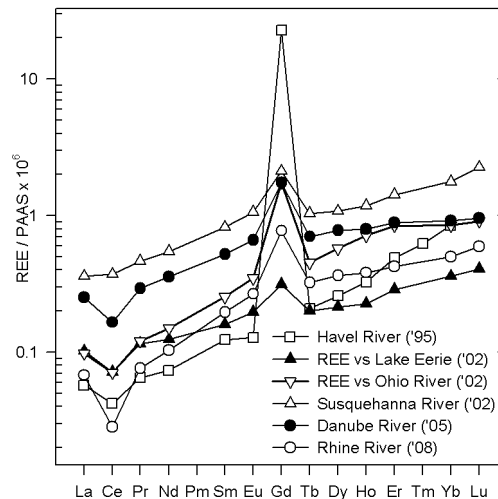


**Fig. 2.** Rare earth element plots of contaminated rivers. Samples marked with triangles are from Bau *et al.* (2006). The sample marked with open squares is from Bau & Dulski (1996). Samples marked with circles are from this study.

**Gadolinium in Tapwater**

While there is little reason to worry about anthropogenic Gd in river or ground water, elevated Gd in tapwater is alarming. Grobner (2006) has described the link between exposure to Gd-based contrast agents and nephrogenic systemic fibrosis (NSF) in patients with kidney failure,

making the issue of anthropogenic Gd in tapwater even more relevant. More cases of NSF have been reported elsewhere, causing the U.S. Food and Drugs Administration to force drug manufacturers in 2006 to include a boxed warning on the product description of Gd-based contrast agents. Figure 4 shows dissolved REE in drinking water from different German cities. The highest positive anthropogenic Gd anomaly is found in Berlin. This is due to a combination of the large contribution of treatment plant effluent to the urban water system compared to the discharge from rivers, and the water recycling policy using bank infiltration to replenish groundwater (Knappe *et al.* 2005).

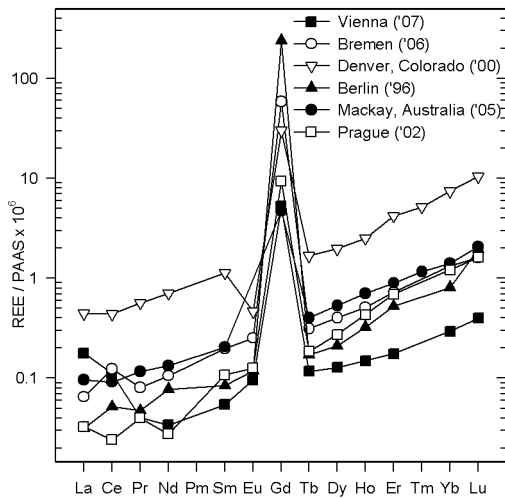


**Fig. 3.** Dissolved REE data for waste water treatment plants in different countries. Notice the orders of magnitude difference in Gd values. Data for Denver from Bau *et al.* (2006), Berlin from Bau & Dulski (1996), Mackay from Lawrence *et al.* (2006) and Prague from Möller *et al.* (2002). Samples from Vienna and Bremen are from this study.

The other cities show varying but nevertheless significant amounts of anthropogenic Gd in their tapwater. With the exception of Bremen (20% anthropogenic Gd), all samples show more than half of total dissolved Gd to be of anthropogenic origin, with up to 95% for the Berlin sample. The anthropogenic

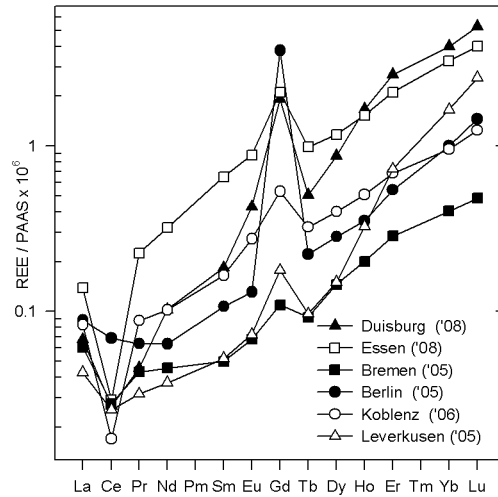


**Fig. 4.** Dissolved REE in tapwater from various German cities investigated in this study.

component is estimated by subtracting the extrapolated natural (background) Gd concentrations from total dissolved Gd as shown in equation 1, where  $N$  denotes a normalized value (to shale) and  $*$  denotes a natural (background) value.

$$\log Gd_N^* = 0.67 \log Tb_N + 0.33 \log Sm_N \quad (1)$$

While this equation can only serve as an approximation of the true anthropogenic content of a sample due to its simplistic binary approach, it is an easy yet useful way of determining the relative contributions of the natural and anthropogenic Gd in a sample. One powerful application of this approach is its use as a tracer for the presence of WWTP effluent in surface water, groundwater and drinking water. Quantifying anthropogenic Gd content in these waters would be a fast and cost-efficient way of screening for other truly dissolved compounds such as antibiotics, steroids and antihistamines. Quantifying the mixing ratios of contaminated to uncontaminated sources in groundwater, for example, has been demonstrated by Knappe *et al.* (2005). Morteani *et al.* (2006) have shown a

correlation between anthropogenic Gd and estrogens in the sewage plants and surface water of Prague, Czech Republic, utilizing this relation as a method for pinpointing sewage leaks.

### CONCLUSIONS

The presence of anthropogenic Gd in water systems in densely populated areas with readily accessible magnetic resonance imaging facilities is by now a widely observed phenomenon, whereas anthropogenic Gd in tapwater is less frequently reported. We have shown that this results not from the lack of anthropogenic Gd in these systems, but rather the lack of research focusing on this issue. The presence of anthropogenic Gd in drinking water should not be overlooked, given preliminary results that link it to diseases, such as nephrogenic systemic fibrosis, and the lack of knowledge about potential other long term effects of exposure. Moreover, quantifying anthropogenic Gd in drinking water can be used as a means of characterizing drinking water quality in urban areas in terms of how well the WWTPs can remove truly dissolved compounds such as Gd complexes or common pharmaceuticals that are used in large quantities.

### ACKNOWLEDGEMENTS

We thank the staff of the Geochemistry Laboratory at Jacobs University Bremen, and Peter Dulski of GFZ Potsdam. This research is funded by the German Science Foundation.

### REFERENCES

- BAU, M. & DULSKI, P. 1996. Anthropogenic origin of positive gadolinium anomalies in river waters. *Earth and Planetary Science Letters*, **143**, 245-255.
- BAU, M., KNAPPE, A., & DULSKI, P. 2006. Anthropogenic gadolinium as a micropollutant in river waters in Pennsylvania and in Lake Erie, northeastern United States. *Chemie der Erde – Geochemistry*, **66**, 143-152.
- GROBNER, T. 2006. Gadolinium - a specific trigger for the development of nephrogenic fibrosing dermopathy and nephrogenic systemic fibrosis? *Nephrology Dialysis Transplantation*, **21**, 1104-1108.
- KNAPPE, A., MÖLLER, P., DULSKI, P., & Pekdeger, A., 2005. Positive gadolinium anomaly in surface water and ground water of the urban area Berlin, Germany. *Chemie der Erde – Geochemistry*, **65**, 167-189.
- LAWRENCE, M.G., JUPITER, S.D., & KAMBER, B. S. 2006. Aquatic geochemistry of the rare earth elements and yttrium in the Pioneer River catchment, Australia. *Marine and Freshwater Research*, **57**, 725-736.
- MORTEANI, G., MÖLLER, P., FUGANTI, A. and Paces, T., 2006. Input and fate of anthropogenic estrogens and gadolinium in surface water and sewage plants in the hydrological basin of Prague (Czech Republic). *Environmental Geochemistry and Health*, **28**, 257-264.
- MÖLLER, P., PACES, T., DULSKI, P., & MORTEANI, G. 2002. Anthropogenic Gd in Surface Water, Drainage System, and the Water Supply of the City of Prague, Czech Republic. *Environmental Science & Technology*, **36**, 2387-2394.
- NOZAKI, Y., LERCHE, D., ALIBO, D.S., & SNIDVONGS, A. 2000. The estuarine geochemistry of rare earth elements and indium in the Chao Phraya River, Thailand. *Geochimica et Cosmochimica Acta*, **64**, 3983-3994.

## Correlation of Atmospheric Soil and Atmospheric Lead in Three North American Cities: Can Re-suspension of Urban Lead Contaminated Soil be a Major Source of Urban Atmospheric Lead and Cause Seasonal Variations in Children's Blood Lead Levels?

Mark Laidlaw<sup>1</sup>

<sup>1</sup>4 Birch Drive, Hamlyn Terrace, NSW, 2259 AUSTRALIA (e-mail: [markas1968@gmail.com](mailto:markas1968@gmail.com))

**ABSTRACT:** Soils in older cities are highly contaminated by lead from past use of lead in leaded gasoline and due to the use of lead in exterior paints. In this study the temporal variations in atmospheric soil and atmospheric lead in three North American cities are examined. This study tested the hypotheses that atmospheric lead and atmospheric soil concentrations obtained from the Interagency Monitoring of Protected Visual Environments (IMPROVE) exhibit statistically significant correlations in three North American cities and that atmospheric soil and atmospheric lead follow seasonal patterns with highest concentrations during the summer and/or autumn. Results indicate that atmospheric soil and atmospheric lead were correlated in Detroit between November 2003 to July 2005 ( $r = 0.47$ ,  $p < 0.001$ ); In Pittsburgh between April 2004 to July 2005 ( $r = 0.40$ ,  $p < 0.001$ ); and in Birmingham between May 2004 to December 2006 ( $r = 0.35$ ,  $p < 0.001$ ). The hypothesis that atmospheric soil and atmospheric lead follow seasonal patterns with highest concentrations during the summer and/or autumn could not be rejected. It is suggested that atmospheric lead and atmospheric soil concentrations are correlated due to re-suspension of urban lead contaminated soils. It is further suggested that in order to decrease urban atmospheric lead concentrations, lead deposition, and children's seasonal exposure via hand to mouth activity, urban lead contaminated soils should be remediated or isolated.

**KEYWORDS:** *lead, soil, re-suspension, blood, poisoning, children*

### INTRODUCTION

In the USA, motor vehicles used gasoline containing tetramethyl and tetraethyl Pb additives from the 1920s to 1986. By the 1950s, Pb additives were contained in virtually all grades of gasoline. By 1986, when leaded gasoline was banned, 5–6 million metric tons of Pb had been used as a gasoline additive, and about 75% of this Pb was released into the atmosphere (Chaney & Mielke 1986; Mielke & Reagan 1998). Thus, an estimated 4–5 million tons of Pb has been deposited into the US environment by way of gasoline-fueled motor vehicles (Mielke 1994). Accumulation of soil Pb created by leaded gasoline is proportional to highway traffic flow (Mielke *et al.* 1997).

In the 1970s, the presumed dominant source of soil Pb contamination was Pb-based house paint (Ter Haar and Aronow, 1974). A subsequent study of garden soils conducted in metropolitan Baltimore,

Maryland, began to raise questions about that assumption. Soil around Baltimore's inner city buildings, predominantly unpainted brick, exhibited the highest amounts of Pb, and soils outside of the inner city, where buildings were commonly constructed with Pb-based paint on wood siding, contained comparatively low amounts of Pb, suggesting that Pb based house paint could not account for the observed pattern of soil Pb (Mielke *et al.* 1983). The same pattern was also found in Ottawa, Canada (Ericson & Mishra 1990).

The quantity and distribution of soil Pb have been studied in numerous places in North America (see Laidlaw & Filippelli, 2008). All these North American cities exhibited the same distance decay characteristic of high soil Pb contamination in the inner city and decreasing contamination toward the outer parts of the city as initially identified

in garden soils of Baltimore (Mielke *et al.* 1983). Further, similarities in this distance decay pattern of soil Pb supports the idea that Pb-based house paint was not the sole source contributing to these observed differences.

Soil lead concentrations have been observed to be associated with children's blood lead concentrations using multiple study designs – cross-sectional, ecological spatial, ecological temporal, prospective soil removal and isotopic (Laidlaw & Filippelli, 2008).

Average monthly blood Pb (BPb) values of children from urban areas tends to increase significantly in summer months (Haley & Talbot 2004; Laidlaw *et al.* 2005; Yiin *et al.* 2000). Early work by Mielke *et al.* (1992), Johnson & Bretsch (2002), and Johnson *et al.* (1996) suggested that blood Pb seasonality may be related to the interaction between climate and Pb contaminated soils. Yiin *et al.* (2000) actually measured seasonal changes in dust Pb levels and correlated blood Pb levels with seasonal dust Pb concentrations. Yiin *et al.* (2000) conducted a study to examine seasonal changes in residential dust Pb content and its relationship to blood Pb in preschool children. The study found that windowsill wipe samples were most correlated with blood Pb concentration and the variation of dust Pb levels for floor Pb loading, windowsill Pb loading, and carpet Pb concentration were consistent with the variation of blood Pb levels, showing the highest levels in the hottest months of the year (June, July, and August).

Laidlaw & Filippelli (2008), Laidlaw *et al.* (2005), and Filippelli *et al.* (2005) have demonstrated that seasonal variations in children's blood lead levels in Syracuse, Indianapolis and New Orleans could be predicted using soil moisture and atmospheric variables suggesting that re-suspension of urban soils contaminated by past use of leaded gasoline and paint were causally related to seasonal variations in blood lead. These papers concluded that urban lead contaminated soil was being re-suspended when soils were dry in the summer and autumn when

evapotranspiration is maximised. Their assumption that soil lead is being re-suspended and is responsible for a large portion of the lead in the atmosphere is supported by lead isotopic analysis of atmospheric lead in Yerevan Armenia (Kurkjian *et al.* 2001) which indicated that following elimination of the use of lead in gasoline, 75% of atmospheric lead in the Yerevan atmosphere was derived from re-suspended soil.

Soil resuspension has the capability of entraining significant volumes of Pb into the air of urban areas. Harris & Davidson (2005) calculated that resuspension of soil is responsible for generating 54,000 kg of airborne Pb each year in the South Coast Air Basin of California (SOCAB) and will remain a major source well into the future. Similarly, Lankey *et al.* (1998) concluded that 43% of Pb emissions in the South Coast Air Basin in California resulted from the resuspension of soil and road dust.

In this study, data from Birmingham, Alabama; Pittsburgh, Pennsylvania; and Detroit, Michigan were selected to assess seasonal patterns and assess seasonal relationships between atmospheric soil and atmospheric lead.

The following hypotheses were tested:

- 1) Atmospheric air lead and atmospheric soil concentrations exhibit statistically significant correlations in three major North American Cities; and

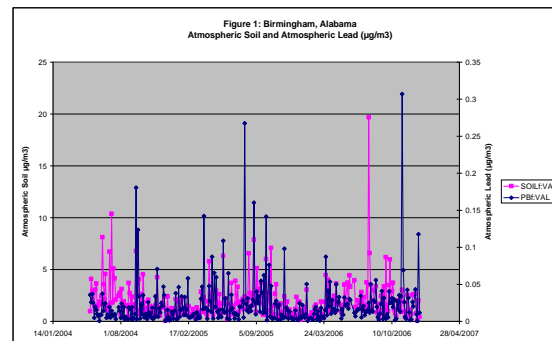


**Fig. 1.** Plot of atmospheric soil and atmospheric lead in Birmingham, Alabama ( $r = 0.35$ ,  $p < 0.001$ ).

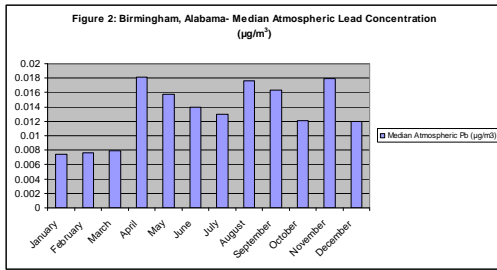


**Fig. 2.** Median atmospheric lead concentrations at IMPROVE air monitoring station in Birmingham, Alabama (May 2004 to December 2006).

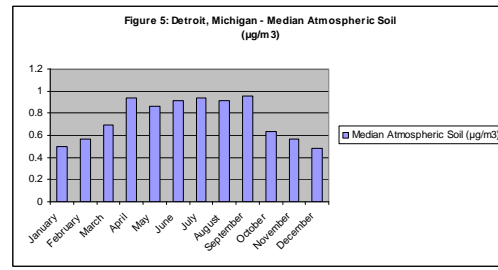


**Fig. 5.** Median Atmospheric soil concentrations at IMPROVE air monitoring station in Detroit, Michigan (November 2003 to July 2005).

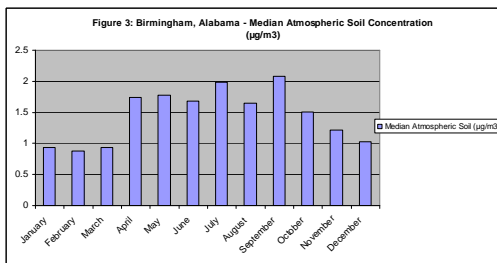


**Fig. 3.** Median Atmospheric soil concentrations at IMPROVE air monitoring station in Birmingham, Alabama (May 2004 to December 2006).

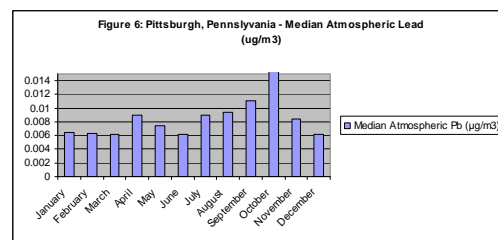


**Fig. 6.** Median atmospheric lead concentrations at IMPROVE air monitoring station in Pittsburgh, Pennsylvania (April 2004 to July 2005).

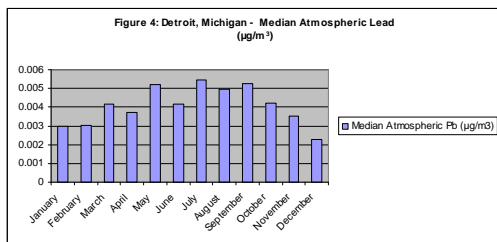


**Fig. 4.** Median atmospheric lead concentrations at IMPROVE air monitoring station in Detroit, Michigan (November 2003 to July 2005).

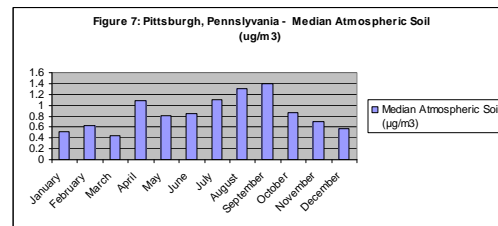


**Fig. 7.** Median Atmospheric soil concentrations at IMPROVE air monitoring station in Pittsburgh, Pennsylvania (April 2004 to July 2005).

- 2) Atmospheric soil and atmospheric lead follow seasonal patterns with highest concentrations during the summer and/or autumn.

## CONCLUSIONS

1) In order to decrease urban atmospheric lead concentrations, lead deposition, and subsequent children's exposure via hand to mouth activity, urban lead contaminated soils should be remediated or isolated.

## REFERENCES

- CHANEY, R.L. & MIELKE, H.W. 1986. Standards for soil Lead limitations in the United States. In: Heamphill, D.D. (Ed.), Trace Substances in 2036 M.A.S. Laidlaw, G.M. Filippelli / Applied Geochemistry 23 (2008) 2021–2039 Environmental Health, vol. XX. University of Missouri, Columbia, 357–377.
- ERICSON, J.E. & MISHRA, S.I., 1990. Soil lead concentrations and prevalence of hyperactive behavior among school children in Ottawa, Canada. *Environment International*, **16**, 247–256.

- FILIPPELLI, G.M., LAIDLAW, M., LATIMER, J., & RAFTIS, R. 2005. Urban lead poisoning and medical geology: an unfinished story. *GSA Today*, **15**, 4-11.
- HALEY, V.B. & TALBOT, T.O. 2004. Seasonality and trend in blood lead levels of New York State children. *BMC Pediatrics*, **4**, 8.
- HARRIS, A. & DAVIDSON, C. 2005. The role of resuspended soil in lead flows in the California south coast air basin. *Environmental Science and Technology*, **39**, 7410–7415.
- IMPROVE (Interagency Monitoring of Protected Visual Environments), 2007. Available: <http://vista.cira.colostate.edu/improve/>. Accessed [15 November 2007].
- JOHNSON, D. & BRETSCHE, J. 2002. Soil lead and children's BLL Levels in Syracuse, NY, USA. *Environmental Geochemistry and Health*, **24**, 375-385.
- JOHNSON, D., MCDADE, K., & GRIFFITH, D. 1996. Seasonal variation in pediatric blood levels in Syracuse, NY, USA. *Environmental Geochemistry and Health*, **18**, 81-88.
- KURKJIAN R., DUNLAP, C., & FLEGAL, R. 2001. Lead isotope tracking of atmospheric response to post-industrial conditions in Yerevan, Armenia. *Atmospheric Environment*. 2002, **36**, 1421-1429.
- LAIDLAW, M.A.S., MIELKE, H.W., FILIPPELLI, G.M., JOHNSON, D.L., & GONZALES, C.R., 2005. Seasonality and children's blood lead levels: developing a predictive model using climatic variables and blood lead data from Indianapolis, Indiana, Syracuse, New York, and New Orleans, Louisiana (USA). *Environmental Health Perspectives*, **113**, 793–800.
- LAIDLAW, M.A. & FILIPPELLI, G.M. 2008. Resuspension of urban soils as a persistent source of lead poisoning in children: A review and new directions. *Applied Geochemistry*. 2008, **23**, 2021-2039.
- LANKEY, R.L., DAVIDSON, C.I., & MCMICHAEL, F.C. 1998. Mass balance for lead in the California south coast air basin: an update. *Environmental Research*, **78**, 86–93.
- MIELKE, H.W., ANDERSON, J.C., BERRY, K.J., MIELKE JR., P.W., CHANEY, R.L., & LEECH, M. 1983. Lead concentrations in inner-city soils as a factor in the child lead problem. *American Journal of Public Health*, **73**, 1366–1369.
- MIELKE, H.W., 1994. Lead in New Orleans soils: new images of an urban environment. *Environmental Geochemistry and Health*, **16**, 123–128.
- MIELKE, H.W. & REAGAN, P.L., 1998. Soil is an important pathway of human lead exposure. *Environmental Health Perspectives*, **106**, 217–229.
- MIELKE, H.W., DUGAS, D., MIELKE JR., P.W., SMITH, K.S., SMITH, S.L., & GONZALES, C.R., 1997. Associations between soil lead and children's blood lead in urban New Orleans and rural Lafourche Parish of Louisiana. *Environ. Health Perspectiv.*, **105**, 950–954.
- YIIN, L.M., RHOADS, G.G., & LLOYD, P.J. 2000. Seasonal influences on childhood lead exposure. *Environmental Health Perspectives*, **108**, 177-182.

## Impact of Evolving Hypoxia on the Remobilization of As and Se in the Lower St. Lawrence Estuary (Québec)

Stelly Lefort<sup>1</sup>, Gwenaëlle Chaillou<sup>2</sup>, Nathalie Molnar<sup>1,3</sup>,  
Alfonso Mucci<sup>1</sup>, & Bjorn Sundby<sup>1,2</sup>

<sup>1</sup>McGill University, 3450 University Street, Montreal, QC, H3A 2A7 and GEOTOP (email: [slefort@eps.mcgill.ca](mailto:slefort@eps.mcgill.ca))

<sup>2</sup>Institut des sciences de la mer de Rimouski, Université du Québec à Rimouski, Rimouski, QC G5L 3A1

<sup>3</sup>IRD, BPA5, 98846 Nouméa, Nouvelle Calédonie

**ABSTRACT:** Dissolved oxygen concentrations in the bottom water of the Lower St. Lawrence Estuary have decreased by more than 50% since the 1930s, and are now < 60µmol/L. This might affect the diagenesis of redox-sensitive elements such as Mn, Fe, As and Se. These metals, which are normally concentrated in the oxic layer of the sediment, could escape to the overlying waters if the sediment oxygen penetration depth were to decrease as oxygen in the bottom water becomes depleted. Fe, Mn, As and Se fluxes across the sediment-water interface were measured as a function of the overlying water oxygen concentration in short-term controlled-laboratory incubations of sediment cores. No significant changes of Fe, Mn and As fluxes (Se analyses are on-going) were observed. Cores sampled between 1982 and 2007 reveal changes in sediment chemistry over the last 25 years. Dissolved and reactive Fe and As concentrations have increased significantly, although their total solid-phase concentrations have remained invariant. This is interpreted as a progressive response of the sediment to the decreasing levels of bottom water oxygen.

**KEYWORDS:** *hypoxia, oxidation, reduction, diagenesis, authigenic*

### INTRODUCTION

Upon burial in the sediments, organic matter is microbially oxidized in a sequence dictated by the Gibbs Free Energy yield of each reaction (Froelich *et al.*, 1979). The oxidants are used in this sequence: respiration of oxygen, denitrification, manganese oxide reduction, iron oxide reduction, sulphate reduction and fermentation (Van Cappellen & Wang, 1996). This leads to a vertical redox zonation of the sediment column.

In coastal environment, detrital and authigenic Fe and Mn oxides, which accumulate in oxic surface sediments, play a pivotal role in determining the geochemical behaviour of arsenic (Mucci *et al.*, 2000) and selenium (Belzile *et al.*, 2000). Arsenic and selenium differ in their affinities for metal oxide surfaces. Although both adsorb onto iron oxides, arsenate (As(V)) adsorbs more strongly than arsenite (As(III)), and selenite (Se(IV)) adsorbs more strongly than selenate (Se(VI)) (Belzile *et al.*, 2000).

Furthermore, Se(IV) is scavenged preferentially by manganese oxides (Belzile *et al.*, 2000), and it is thought that manganese oxides catalyse the oxidation of As(III) to As(V) (Mucci *et al.*, 2000).

Following the reductive dissolution of reactive Fe and Mn oxides during suboxic and anoxic diagenesis, As and Se are released to the sediment porewaters (Aggett & Kriegman, 1998). Dissolved species can thus migrate upwards and be reprecipitated in the oxic layer or escape to the water column. They can also migrate downwards where As may co-precipitate with sulphides under reducing conditions (Mucci *et al.*, 2000; Belzile, 1988) and Se will react spontaneously with dissolved Fe to form FeSe or FeSe<sub>2</sub> (Takayanagi & Belzile, 1988). Hence, As and Se retention in the sediments depends on the availability of Fe and Mn oxides which, in turn, depends on the thickness of the oxic layer. The redox conditions at or near the sediment-water interface will therefore determine whether the sediments serve as a source or a sink

for these elements (Saulnier & Mucci, 2000). In this study we investigate the impact of hypoxia on: 1) the response of Fe, Mn, As and Se fluxes to a decreasing oxygen concentration in the overlying waters and, 2) the long-term evolution of As and Se concentrations in the solids and porewaters of the Lower St. Lawrence Estuary sediments.

### STUDY AREA

The Lower St. Lawrence Estuary (LSLE) occupies the 300 km landward end of the Laurentian Channel with depths of 300-350 m. The water below 150m depth originates in the offshore slope region of the north-western Atlantic and is a mixture of North Atlantic and Labrador Sea waters (Bugden, 1991). This water is isolated from the atmosphere by a permanent pycnocline, and the dissolved oxygen concentration decreases progressively as the water flows landward to the head of the estuary. The oxygen concentration in the LSLE bottom water has decreased from 130  $\mu\text{mol/L}$  in 1930 to about 60  $\mu\text{mol/L}$  today (Gilbert *et al.*, 2005) and is thus hypoxic. Hypoxia is defined by  $[\text{O}_2] < 62.5 \mu\text{mol/L}$ , which is the level necessary to sustain most animal life (Diaz & Rosenberg, 1995).

### METHODS

Sediment cores were recovered on board the R/V Coriolis II in July 2007 at four stations in the LSLE using a Bowers & Connelly Multicorer and an Ocean Instrument Mark II box corer. Upon recovery, box cores were transferred to a specially-designed glove box and sub-sampled under a constant flow of  $\text{N}_2$  to limit oxidation. Porewaters were extracted from the sediment using Reeburgh-type squeezers, filtered through a 0.45  $\mu\text{m}$  filter, acidified with a 2% equivalent volume of ultrapure, concentrated  $\text{HNO}_3$  and kept refrigerated until analysis. Solid sediment samples were kept frozen until freeze-dried and ground for analysis.

Cores recovered with the multicorer were immersed in a water bath kept at 4°C and transferred to an on-land laboratory. Each core remained 7 days in

a controlled oxygen concentration bath followed by 48 hours incubation in the dark. At regular intervals, filtered overlying waters were collected for oxygen and trace metal analyses. The water removed during sampling was replaced by an equivalent volume of bottom water of known composition and oxygen concentration. The incubations were carried out at three different overlying water dissolved oxygen concentrations: 90, 50 and 20  $\mu\text{mol/L}$ .

Total dissolved Fe and Mn were analyzed directly by flame atomic absorption spectrometry (AAS). As was measured by AAS with hydride generation (HG-FIAS). Total dissolved Se concentrations were determined by hydride-generation atomic fluorescence spectrometry (Chen *et al.*, 2005).

The freeze-dried sediments were subjected to both a total dissolution and a selective extraction. The latter, as described in Chester & Hughes (1967), is carried out in a hydroxylamine hydrochloride and acetic acid (HA) solution and designed to isolate reactive phases. With the exception of total Se, extracted metals were determined by the method described for porewaters. Total solid Se concentrations were measured by AAS with HG-FIAS (analysis ongoing).

### RESULTS AND DISCUSSION

Both Mn and As were released to the overlying water during the incubations but no detectable release of Fe was observed in any of the incubations. At the highest oxygen level, the fluxes varied by as much as one order of magnitude between and within the different study sites (Table 1), and no significant trends could be discerned as oxygen concentration evolve towards anoxia. These results imply that the sediments require more than 9 days to respond to chemical changes occurring in the overlying waters. Accordingly, Katsev *et al.* (2007) estimated that it may take on the order of 100 years to reach a new steady state.

Station	[O <sub>2</sub> ] ~ 90µmol/L		[O <sub>2</sub> ] ~ 50µmol/L		[O <sub>2</sub> ] ~ 20µmol/L	
	[Mn]	[As]	[Mn]	[As]	[Mn]	[As]
24 A	-0.13	-0.12	-	-	-	-
24 B	-0.11	-0.08	-	-	-	-
24 C	ND	-0.04	-	-	-	-
23S A	-0.93	-0.45	-	-	-	-
23S B	-0.31	-0.69	ND	ND	-0.24	-0.34
23 B	<dl	-0.08	-	-	-	-
23 C	-0.17	-0.36	ND	ND	-0.55	-0.60
23 D	-0.14	-0.44	ND	ND	-0.14	-0.47
20 B	<dl	-0.26	-0.09	-0.36	<dl	-0.03
20 C	<dl	1.27	-0.18	ND	-0.01	-0.55
20 D	-0.14	-0.32	ND	-0.13	-0.03	ND

**Table 1.** Fluxes of Mn (mmol/m<sup>2</sup>/d) and As (x10<sup>-3</sup> mmol/m<sup>2</sup>/d) in short-term, duplicate and triplicate incubations of cores at three overlying water oxygen concentrations. *ND*: no data, - : core not incubated, <dl: below the detection limit. Negative fluxes are from sediment to water.

Whereas total concentrations of solid Fe and As remained relatively constant over time (not shown), dissolved Fe and As in the porewaters have increased substantially since 1982 (Fig. 1). The concentrations in the suboxic zone have doubled or tripled. Similarly, HA-extractable Fe and As concentrations increased significantly at stations 23 and 24 since 1982 (Fig. 2). This increase is concomitant with an accumulation of AVS in the sediment over the last 10 years (G. Chaillou, unpublished).

Stations 23 and 24, located in the LSLE, have been subjected to hypoxic conditions since the 1980s. With depletion of oxygen in the bottom waters, the sediment oxygen penetration depth decreased, and Fe oxides, concentrated in the oxic sediment layer, were reductively dissolved and released adsorbed arsenic. Hence, the low oxygen levels during the last 25 years in the bottom waters is reflected in more reducing conditions in the sediment and increases in both dissolved and HA-extractable Fe and As.

Preliminary results reveal similar trends for Se at station 23. Ongoing analyses will allow us to estimate the flux of Se at the sediment-water interface.

**CONCLUSION**

The concentrations of dissolved and HA-extractable Fe and As have increased

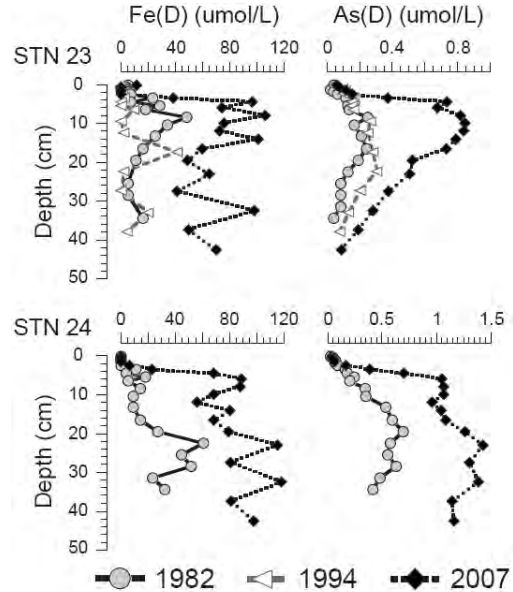


**Fig. 1.** Porewater iron and arsenic concentrations at stations 23 and 24.

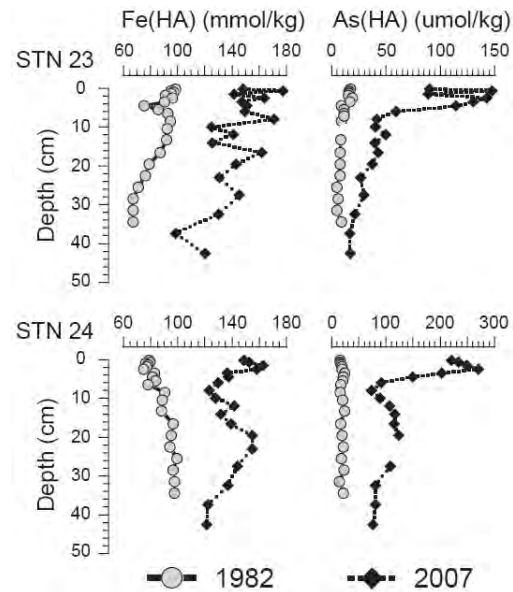


**Fig. 2.** HA-extractable, solid iron and arsenic concentrations at stations 23 and 24.

significantly since 1982 in the suboxic sediment of the LSLE. These changes coincide with the decreasing oxygen concentration in the bottom waters. We attribute the changes in the sediment to both an increase of the AVS content and a thinning of the Fe oxide-rich surface layer. If the bottom water oxygen concentration continues to decrease, the iron oxide layer

will shallow further and the capacity of the sediment to adsorb As and retard the flux of As to the bottom water will diminish. When the sorption capacity of the sediment is exhausted, the sediment will no longer modulate the release of dissolved As from the sediment.

#### ACKNOWLEDGEMENTS

This research was funded by a NSERC Strategic grant to B.S. and A.M. Additional financial support to S.L. was provided by the Department of Earth and Planetary Sciences/McGill and the GEOTOP-UQAM-McGill research centre.

#### REFERENCES

- AGGETT, J. & KRIEGMAN, M.R. 1998. The extent formation of arsenic(III) in sediment interstitial waters and its release to hypolimnetic waters in Lake Ohakuri. *Water Resources*, **22**(4), 407-411.
- BELZILE, N., ET AL. 2000. Early diagenetic behavior of selenium in freshwater sediments. *Applied Geochemistry*, **15**, 1439-1454.
- BUGDEN, G.L. 1991. Changes in the temperature-salinity characteristics of the deeper waters of the Gulf of St. Lawrence over the past several decades. *Canadian Special Publication Fisheries Aquatic Sciences*, **113**, 139-147.
- CHEN, Y.-W., ET AL. 2005. Photochemical behavior of inorganic and organic selenium compounds in various aqueous solutions. *Analytica Chimica Acta*, **545**(2), 142-148.
- CHESTER, R. & HUGHES, M.J. 1967. A chemical technique for the separation of ferromanganese minerals, carbonate minerals and adsorbed trace elements from pelagic sediments. *Chemical Geology*, **2**, 249-262.
- DIAZ, R.J. & ROSENBERG, R. 1995. Marine benthic hypoxia: A review of its ecological effects and the behavioural responses of benthic macrofauna. *Oceanography Marine Biology Annual Review*, **33**, 245-303.
- FROELICH, P.N. ET AL. 1979. Early oxidation of organic matter in pelagic sediments of the eastern equatorial Atlantic: suboxic diagenesis. *Geochimica et Cosmochimica Acta*, **43**, 1075-1090.
- GILBERT, D. ET AL. 2005. A seventy-two-year record of diminishing deep-water oxygen in the St. Lawrence Estuary: The Northwest Atlantic connection. *Limnology and Oceanography*, **50**(5), 1654-1666.
- KATSEV, S., ET AL. 2007. Effect of progressive oxygen depletion on sediment diagenesis and fluxes: A model for the Lower St. Lawrence Estuary. *Limnology and Oceanography*, **52**, 2555-2568.
- MUCCI, A. ET AL. 2000. The differential geochemical behavior of arsenic and phosphorus in the water column and sediments of the Saguenay Fjord Estuary, Canada. *Applied Geochemistry*, **6**, 293-324.
- SAULNIER, I. & MUCCI, A. 2000. Trace metal remobilization following the resuspension of estuarine sediments: Saguenay Fjord, Canada. *Applied Geochemistry*, **15**, 191-210.
- TAKAYANAGI, K. & BELZILE, N. 1988. Profiles of dissolved and acid-leachable selenium in a sediment core from the Lower St. Lawrence Estuary. *Marine Chemistry*, **24**, 307-314.
- VAN CAPPELLEN, P. & WANG Y. 1996. Cycling of iron and manganese in surface sediments: a general theory for the coupled transport and reaction of carbon, oxygen, nitrogen, sulfur, iron and manganese. *American Journal Sciences*, **296**, 197-243.

## Geochemistry of catchment outlet sediments: evaluation of Mobile Metal Ion™ analyses from the Thomson region, New South Wales, Australia

Alan Mann<sup>1</sup>, Patrice de Caritat<sup>2</sup>, and John Greenfield<sup>3</sup>

<sup>1</sup>Consultant, 17 Zenith St, Shelley, WA 6148, AUSTRALIA (e-mail: [awmann@iinet.net.au](mailto:awmann@iinet.net.au))

<sup>2</sup>Geoscience Australia, GPO Box 378, Canberra, ACT 2601, AUSTRALIA

<sup>3</sup>Geological Survey of NSW, 516 High St, Maitland, NSW 2320, AUSTRALIA

**ABSTRACT:** Outlet sediment (or overbank) samples from 99 catchments in the Thomson region have been examined by conventional geochemical analytical methods and by partial digestion using Mobile Metal Ion™ (MMI) extraction. Elements such as Pb have good correlation with known mineral deposits using conventional (near-total digestion) methods, whilst elements such as Cu, Au and Ag show a better correlation with known mineral deposits when MMI concentrations are used. This study shows that very low density sampling of catchment outlet sediments (here 1 site/1540 km<sup>2</sup>) provides useful and possibly predictive geochemical information for mineral exploration in areas dominated by transported regolith.

**KEYWORDS:** *Overbank sediment, geochemistry, mineral exploration, MMI, Thomson Orogen*

### INTRODUCTION

Overbank sediment samples collected near the outlets of large drainage basins are commonly used to obtain regional geochemical information (e.g. McConnell *et al.* 1993; Demetriades 2008). Having been deposited on floodplains in low energy environments adjacent to major drainage channels; they are fine-grained and have the potential to represent large areas of, or the average composition of, entire catchments. Representative sampling of large areas has critical implications for geochemical surveys applying low sampling density strategies. Such a survey is currently being carried out for the whole of Australia (Caritat *et al.* 2008). This paper presents and discusses some of the results from a pilot study conducted in the Thomson region, in northwestern New South Wales, as a forerunner to the national survey.

### GEOLOGICAL SETTING

#### Location

The Thomson project area covers an area of 154,521 km<sup>2</sup> and is located in north-western New South Wales (Figure 1). It contains the Thomson Orogen, one of the most poorly understood orogenic belts in

Australia due to its remoteness and the degree of surficial cover. Named after the Thomson River in central Queensland, it is part of the greater Tasmanides of Eastern Australia.

#### Geology

Various mineral prospects and minor metal occurrences are found in the study area, including Pb, Zn and Sn deposits north-east of Broken Hill, Au deposits near Tibooburra and Au, Cu and Pb deposits north of Cobar (Figure 1).

The area is dominated by transported regolith with minor outcrop of crystalline basement rocks. In the east, black cracking clays, clay pans and gilgai are associated with the expansive Quaternary alluvial plains of the Darling, Barwon, Bogan and Warrego River systems. There is also an area in the north-west around Tibooburra in which cracking clays are common. The alluvium of ephemeral streams in the west and south-east is principally composed of reworked eolian material. Erosional rises and plains in the centre of the study area north of White Cliffs relate to silicified palaeodrainages. Calcareous soils comprise a large part of the landscape in the south-west.



### **Climate**

The western portion of the Thomson project area is classified as desert, with rainfall <250 mm/yr. The eastern portion is classified as grassland, with rainfall 250-500 mm/yr (Caritat & Lech 2007). Summers are hot and dry, winters cool. Highly variable rainfall results in ephemeral streams, particularly in the west, and many of the creeks and rivers flow only during flood events, which can be significant events. The low-gradient, sinuous and anastomosing streams, creeks and rivers broaden to include flood plains often several kilometres wide. It is during these events that fine silts and clays from the upstream catchment are deposited on the floodplains.

### **SAMPLING AND ANALYTICAL METHODS**

Locations for the outlet sediment (overbank) samples are shown in Figure 1. In all, 99 catchments were sampled giving an average sample density of 1 site/1540 km<sup>2</sup>. At most sites three samples were taken: (a) a top outlet sediment (TOS) from 0-10 cm depth; (b) a bottom outlet sediment (BOS) from ~60-90 cm depth; and (c) a shallow outlet sediment (SOS) from 10-25 cm depth specifically for MMI determinations. Two size fractions (<180 µm and <75 µm) were prepared from the TOS and BOS samples. The SOS sample for multi-element MMI (MMI-M) analysis by method ME-MS17 was provided to ALS Chemex in its bulk form.

Field pH, Munsell soil colour (dry & moist), EC 1:5 (soil:water), pH 1:5, XRD, laser particle size analysis, XRF (multiple elements), ICP-MS (after HNO<sub>3</sub>/HClO<sub>4</sub>/HF/HCl digestion for multiple elements), ICP-MS (after HF/HCl/HNO<sub>3</sub> digestion for Se), ISE (for F), GF-AAS (for Au), and ICP-MS after MMI extraction were performed. Full details of the sampling and analytical methods are given in Caritat & Lech (2007).

### **RESULTS AND DISCUSSION**

#### **XRF and Near-Total Analyses**

Areas with high metal concentrations mostly occur close to outcrops of

crystalline basement. There are high Cu values north of the Barrier Ranges (in the south-west of the study area), east of Tibooburra and north of Cobar. Cu concentration is generally higher in the BOS sample for both size fractions. Pb was determined by ICP-MS after four acid digestion and shows elevated concentrations in the <180 µm fraction of the BOS around Cobar, and near the Barrier Ranges in the south-west of the survey area (see Figure 2). Sb, also determined by ICP-MS after four acid digestion, is also high around Cobar and on the Yancannia map sheet in the central-west. Au, determined by GF-AAS, on the other hand does not show the same geochemical patterns in the two size fractions, and there is no consistent pattern across the Thomson region for this element by this method. This also applies to Ag by ICPMS after four acid digest.

#### **Mobile Metal Ion Extraction**

Systematic trends are shown after MMI extraction and analysis for a number of elements, including Cu, Au and Ag. Figure 3 shows the range of MMI values obtained for Cu in overbank (SOS) samples.

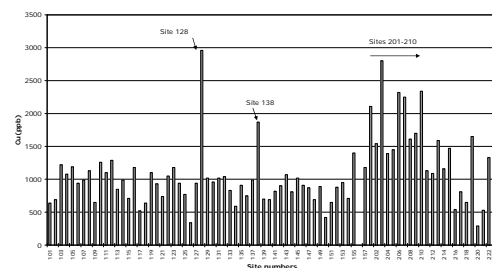


**Fig. 3.** Cu concentration in catchment outlet sediment samples after MMI extraction.

Large variations in catchment outlet MMI Cu values are evident. Sites 201-210, located in catchments with known mineral occurrences north of Cobar (Figure 1), have values above 1500 ppb Cu, over three times the “background” values of the lowest sites. Site 128, which has nearly six times the values of lowest sites, is in the middle west, and Site 138 is within the Tibooburra catchment, which includes the Albert Goldfield, a gold camp

with elevated values measured independently in lag and calcrete.

A multiplicative index is a powerful discriminator where two (or more) elements associated with mineralization are sought as geochemical indicators, since the index will only be strong where all selected elements are well represented. Figure 4 shows the multiplicative Au\*Ag index for overbank outlet sites after MMI extraction.

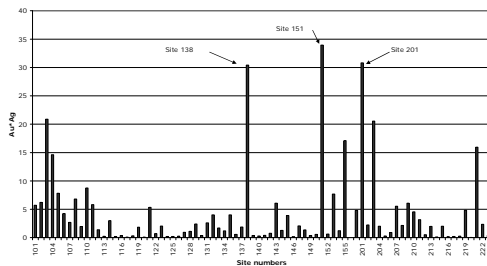


**Fig 4.** Multiplicative Au\*Ag index for catchment outlet sediment samples after MMI extraction.

Again there is considerable variation in values. Site 138, east of Tibooburra, again appears anomalous; this site is some 20 km east of the Albert Goldfield (elevated Au, Ag and Cu) where soils with MMI Au in excess of 100 ppb have been recorded within the same catchment. Sites 151 and 201 also have high Au\*Ag (Figure 4) and are located north of Cobar in the vicinity of known Au, Ag, Cu occurrences.

## CONCLUSIONS

- (1) A number of sites with anomalous catchment outlet sediment geochemistry are associated with catchments containing known outcropping mineral occurrences, confirming the value of the approach.
- (2) Not all catchments with known mineral occurrences have anomalous catchment outlet sediment geochemistry.
- (3) Partial extraction such as MMI analysis provides additional and distinct

geochemical information to that provided by strong acid and XRF analysis. This may be due to an improved signal-to-noise ratio (MMI analysis) for what is effectively 2D (surface) analysis versus three dimensional (bulk) methods.

(4) Active alluvial sites are normally avoided in prospect scale MMI analysis; in this case active alluvium has been used on purpose to obtain information representative of large catchments.

(5) Very low density sampling can provide reliable, representative geochemical information on a regional basis, with total and partial extraction data yielding complementary information.

## ACKNOWLEDGEMENTS

This work is published with the permissions of the Chief Executive Officer, Geoscience Australia, and the Executive Director, Mineral Resources, NSW DPI.

## REFERENCES

- CARITAT, P. DE, & LECH, M.A. 2007. Thomson Region geochemical survey, northwestern New South Wales. *CRC LEME Open File Report*, **145**, 479 pp.
- CARITAT, P. DE, LECH, M.A. & MCPHERSON, A.A. 2008. Geochemical mapping "down under": selected results from pilot projects and strategy outline for the National Geochemical Survey of Australia. *Geochemistry: Exploration, Environment, Analysis*, **8**, 301-312.
- DEMETRIADES, A. 2008. Overbank sediment sampling in Greece: a contribution to the evaluation of methods for the "Global Geochemical Baselines" mapping project. *Geochemistry: Exploration, Environment, Analysis*, **8**, 229-240.
- MCCONNELL, J.W., FINCH, C., HALL, G.E.M. & DAVENPORT, P.H. 1993. Geochemical mapping employing active and overbank stream-sediment, lake sediment and lake water in two areas of Newfoundland. *Journal of Geochemical Exploration*, **49**, 123-143.

## Five-Year History of a Biologically Based Treatment System that Treats High Concentrations of Effluent from an Industrial (Smelter Operation) Landfill

Al Mattes<sup>1</sup>, Bill Duncan<sup>2</sup>, D.Gould<sup>3</sup>, Les Evans<sup>1</sup>, Susan Glasuaer<sup>1</sup>

<sup>1</sup> Land Resource Science, University of Guelph, Guelph, Ontario N1G 2W1, [almattes@rogers.com](mailto:almattes@rogers.com)

<sup>2</sup> University of Victoria, Victoria BC

<sup>3</sup> CANMET/MMSL, Natural Resources Canada, Ottawa, Ontario

**ABSTRACT:** For the past ten years, a biologically based engineered wetlands treatment system has operated in Trail BC, site of the worlds largest integrated lead zinc smelter. Effluent from an historic capped landfill is collected and delivered to a multi-cell engineered wetlands treatment system designed and operated by a private company. The system is unique in treating effluent at high concentrations (mean Zn concentration over 5 years is 268 ppm; mean As concentration is 168 ppm) year-round. A single source of carbon is used. The system is free of plugging (typically with metal sulphides) or short circuiting (effluent by-passing the matrix and therefore not treated). This paper examines metal removal and total loading, considers seasonal differences, analyzes a spike event ([Zn] > 3800, [As] > 3600), and suggests some of the potential biotic and abiotic removal mechanisms operating.

**KEYWORDS:** *treatment, effluent, Industrial smelter, landfill*

### INTRODUCTION

The use of passive systems to treat acid mine drainage was first suggested and studied in bench scale applications as early as 1978, (Government of Pennsylvania website, Science of Acid Mine Drainage), and more than 300 artificial wetlands to treat acid mine drainage were constructed in the U.S. between 1984 and 1990 (Wieder 1989). In 1990, it was suggested that the metabolism of sulfate-reducing bacteria (SRB) was the most useful biological process in wetlands designed to treat metal contaminated water (McIntire 1990). Anaerobic bioreactor systems were designed that maximized sulphate reducing bacterial populations and activity with an organic substrate to promote bacterial growth (McIntyre *et al.* 1990).

Although considerable effort has been applied to the development of these systems, there are many details of their operations that are not understood and longevity remains an issue (Neculita *et al.* 2007). Important characteristics required for a successful ABR design include the following:

1. Near neutral pH
2. Available carbon from an additional organic source
3. A solid matrix, (sand and/or gravel) around which SRB can establish micro-environments
4. An anoxic environment
5. A supply of sulfate sufficient that the sulphate reducing bacteria can out-compete other bacteria for the available carbon.
6. A means to physically retain the metal sulphides that are produced (Neculita *et al.* 2007):

Ideal designs have a depth between 0.6 and 1.5 M (Neculita *et al.* 2007) to reduce short circuiting. Vertical upflow is better than downflow (Tsukamoto *et al.* 2004). A hydraulic retention time of at least 3 – 5 days is optimal (Kuyucak *et al.* 2006). There are no reports on systems operating for extended periods (more than 3-4 years). Failures due to plugging, short circuits, and exhaustion of organic carbon are widely reported (Neculita *et al.* 2007).

This report is a five-year history that describes a system in Trail, British

**Table 2.** Mean concentrations removed over five-year period of operations showing break-down between ABR cells and plant based cells.

<b>Mean Concentrations at Input and Percentage Removed (2003 through 2007)</b>						
	<b>As (ppm)</b>	<b>% Removed</b>	<b>Cd (ppm)</b>	<b>% Removed</b>	<b>Zn (ppm)</b>	<b>% Removed</b>
<b>Input</b>	165.5		5.1		264.4	
<b>1st ABR</b>	18.5	88.8	0.8	84.4	65.3	75.3
<b>2nd ABR</b>	6.9	62.6	0.11	86.3	32.3	50.5
<b>Combined</b>		<b>95.8</b>		<b>97.9</b>		<b>87.8</b>
<b>1st Plant</b>	3.6	47.4	0.02	80.9	65.6	-102.9
<b>2nd Plant</b>	2.2	40.4	0.02	24.1	26.2	60
<b>Typha</b>	2.7	-24.3	0.03	-110.7	12.8	51.2
<b>Pond</b>	0.5	82.9	0.02	52.6	3	76.8
<b>Total %</b>		<b>99.7</b>		<b>99.7</b>		<b>98.9</b>

Columbia designed and operated by Nature Works for Teck Metals Limited. The system was constructed in 1997 and rebuilt in 2002 to operate year-round. It treats effluent from historic capped landfills. It is capable of treating effluent with high concentrations of metals Zn (up to 3800 ppm) and As (up to 3600 ppm). However, mean concentrations over a five-year period are lower (Zn 267.6; As 167.6). The system was designed to treat Zn, Cd, Pb and other metals based on bacterial reduction of sulfate. Bacterial processes for removal of Zn and some other cations were known to occur when the system was designed, but unexpectedly high concentrations of As were also removed. The mechanism for As removal is not yet clearly understood.

### Sampling and Analysis

Flow rate is monitored by in line flow meters. The leachate contains  $Zn_3(AsO_4)_2$  – a highly abrasive, relatively insoluble salt – leading to periodic pump burn-out. This results in a reduction in performance efficiency.

Regular sampling has taken place since 2002. Sampling frequency has not been consistent. It initially took place weekly during summer months; then weekly during spring and summer and bi-weekly during winter (when accessible); finally bi-weekly during summer and monthly during winter operations. Samples are tested in the field for pH, DO, ORP and  $[Fe^{2+}]$ ,

$[FeT]$ , &  $[SO_4^{2-}]$ . Samples are submitted to Teck analytical services where ICP-MS for total and dissolved metals is completed.

The system design is based on two upflow anaerobic bioreactors (ABRs) followed by three horizontal sub-surface flow (HSSF) wetlands cells. The water flows by gravity through the cells. Once treated, the water is stored in a holding pond and subsequently used for irrigation of a tree farm.

### Results

A spike event was used to determine the retention time of the cells. Data from the spike event, flow rate, and changes in metal concentrations in cells were considered, allowing calculation of retention time. Percentages were used as a normalizing function for data analysis.

Removal rates have been consistent over the five-year period showing that removal is not concentration dependent (Tables 1 & 2). The overall percentages of metals removed remain high at close to 99% for all years. The system design allows sampling of two distinct compartments: (ABRs) and the plant based treatment cells. Examining metal removal, it is apparent that much of the As, Cd and Zn are removed in the ABR cells (Table 2). Arsenic and Cd are removed at better than 95% in the two ARB cells, but Zn removal achieves only 88.7%. This table also shows occasional release of Zn and Cd from plant cells.

### Metal Removal and Metal Loading

The system has treated nearly 20,000 m<sup>3</sup> of metal contaminated water over 5 years. The concentrations of metals delivered to the system vary widely, with a drop in metal concentrations after the landfill was capped and after the arsenic was confined to a specially designed storage facility (Table 1).

The system was rebuilt in 2002, resulting in a reduction in the treatment efficiency. Metal removal was lower in 2003 following re-starting. Removal in the

**Table 1.** Mean input concentrations of contaminants showing levels of total and dissolved metals (in brackets).

Year	As	Cd	Zn
2003	108 (53)	4 (2.7)	266 (219)
2004	95 (13)	23 (1.3)	193 (101)
2005	534 (58)	17 (4.4)	709 (158)
2006	83 (27)	2 (0.5)	108 (46)
2007	23 (4)	1 (0.5)	62 (40)
Mean	168 (31)	5 (1.9)	268 (113)

ABR cells in 2003 was reduced by > 5% for As and by >10% for Zn.

Analyzing total metals sequestered in the system gives a measure of effectiveness. The system treats large volumes with high metal concentrations resulting in high total loading with high concentrations of metal retained. The total volume of material sequestered in the treatment system over 5-years is calculated by multiplying the flow rate for each year by the molar concentration of each contaminant. When this is done and the yearly totals are summed, the total weight of metals is 2990 kg of As, 85 kg of Cd and 7698 kg of Zn (more than 10,000 Kg).

### Seasonal Differences

The metabolism of SRB bacteria is not dependent on temperature (Tsukamoto et al, 2004), but there are definite seasonal variations observed in the system. Differences are small but statistically significant. The rates of removal for summer operations for As, Cd and Zn removal are 99.3, 99.4 and 99.2 %

respectively and 99.5, 99.2 and 98% for winter removal.

The One Way ANOVA test was used to determine statistical significance. Input concentrations between summer and the fall winter season were not significant; however, for dissolved As and Zn, total As and Zn differences were significant at  $p < 0.01$ .

### Spike Event

In Nov and Dec of 2005, high concentrations of Zn and As were released to the treatment system. In Nov., the concentration of Zn was 3800 ppm and As 3600. December concentrations were Zn, 3000 ppm and As, 3000. By January, the concentrations were 260 ppm for Zn and 250 ppm for As.

The effect of the spike was to lower ABR removal efficiency from 99.5 to 81.4% for As, 99.5% to 97.2% for Cd and 94.5% to 83.5% for Zn. Overall removal efficiency decreased from 99.9% to 99.6% for As, 99.9% to 99.2% for Cd and 99.7% to 96.8% for Zn. Throughout this period SO<sub>4</sub><sup>2-</sup> continued to be removed and total loading for SO<sub>4</sub><sup>2-</sup> was reduced by 740 ppm. Differences between removal percentages were not statistically significant. Data shows that much of the Zn and As was initially retained in ABRs, but over time these elements were dissolved and released.

### Removal Mechanisms

It is possible that metal removal is the result of a mechanical process, with solid (Zn<sub>3</sub>(AsO<sub>4</sub>)<sub>2</sub>) removed by filtration. To examine this, we modeled mineral stability using a custom designed computer program.

At input concentrations, the results show that Zn<sub>3</sub>(AsO<sub>4</sub>)<sub>2</sub> is stable over a wide pH range (-4 – 9) and is the dominant mineral present. At lower concentrations in subsequent cells it is less dominant. In the pond it is not an important species. Over time in the ABR's and plant cells, Zn<sub>3</sub>(AsO<sub>4</sub>)<sub>2</sub> appears to dissolve. This can be shown by an increase in the concentration of dissolved As species above the levels entering each cell.

### Formation of Sulfides

It is necessary to use statistical procedures to assess chemical dynamics. The amount of Zn, As and  $\text{SO}_4^{2-}$  that are removed were compared using linear correlation analyses. Examining the output from each cell for removal of these metals shows a marked correlation between Zn and  $\text{SO}_4^{2-}$  in the 2<sup>nd</sup> plant cell and *Typha* cell ( $r^2 = 0.8$ ), before decreasing to  $\sim 0.6$  in the pond. This high positive correlation supports that the formation of ZnS (sphalerite) is an important aspect. Values for As are not as high.

### Orpiment Formation

One As removal mechanism is the formation of orpiment ( $\text{As}_2\text{S}_3$ ). To test for it specially constructed flow-through bags containing the same mixture as the cell matrix ("tea bags") were inserted into large vertical piezometers in each ABR cell and left there for a summer. On removal, they were frozen and shipped to the Argonne National Laboratory for analysis using high energy X-rays (XANES). Results confirm the presence of  $\text{As}_2\text{S}_3$  (orpiment) produced only when both As and  $\text{SO}_4^{2-}$  are reduced.

### DISCUSSION

Reports suggest ABRs should have a depth of at least 0.6m and not be more than 1.5m (Neculita *et al.* 2007). In Trail cells are more than 5 m deep operating continuously for six years without plugging or short circuiting. Trail has high [Zn] (268 ppm) without signs of bacterial die off. Neculita (2007) suggests multiple sources of carbon are essential for longevity whereas in Trail a single source of carbon – pulp and paper biosolids - is used. The biosolids are composed of short wood fibres and biota biomass from their biological-based treatment system.

Flow rates to the Trail wetlands are relatively consistent, although there is an overall decline in metal concentrations (Table1). Over a 5-year period the system has treated 20,000m<sup>3</sup> of effluent and sequestered more than 10,000 kg of metals. The high flow rate and concentration of metals sequestered,

combined with reaction of the system to the spike event are evidence of robustness.

Evidence from the spike event indicates that the residency time in our bioreactor is higher than observed in other systems – two weeks during peak summer capacity, longer than for other systems which report 3 – 5 days (Kuyucak *et al.* 2006). Analysis of the spike event showed that despite the potential effects of a short term increase in As concentrations,  $\text{SO}_4^{2-}$  and metals continued to be removed, albeit more slowly.

Data from 2003 shows that there is a period when the system first starts during which metal removal in the ABRs is reduced. But for the full system in 2003, removal rates are consistent with the full 5-year period. This illustrates the advantage of a multi-cell approach.

This ongoing removal of  $\text{SO}_4^{2-}$  shows that SRB metabolism continues despite reports of toxic concentrations of heavy metals (Poulson *et al.* 1997).

A substantial removal of metals during the spike event followed by a release over time from the ABRs is seen, it may be inferred that filtration, adsorption and subsequent mineral formation contribute to metal removal. Although adsorption plays a part in the removal of metals, sites on the organic substrate are likely to be quickly saturated.

Bacterial activity plays an important role in removal. This is shown from analysis of linear correlation statistics for removal of  $\text{SO}_4^{2-}$  and Zn, and  $\text{SO}_4^{2-}$  and As, as well as the formation of orpiment. Dissolution of  $\text{Zn}_3(\text{AsO}_4)_2$  also shows bacterial activity.

The Trail system has shown that it is possible to design and operate a system year-round that treats high concentrations of metals. In Trail, the contaminated water is treated to the degree that from the final holding pond it is used for irrigation of trees to be planted in areas near the smelter.

### REFERENCES

KUYSCAK, N., CHABOT, F., & MARTSCHUK, J. 2006. Successful Implementation and Operation of Passive Treatment System in

- an Extremely Cold Climate, Northern Quebec, Canada. In: *International Conference on Acid Rock Drainage March 26-30*.
- MCINTYRE P.E. & EDENBORN H.M. 1990. The Use Of Bacterial Sulphate Reduction In The Treatment Of Drainage From Coal Mines. Proceedings, Mining and Reclamation Conference, West Virginia University.
- NECULITA, C-M, ZAGURY, G, & BUSSIERE, BRUNO 2007. Passive Treatment of Acid Mine Drainage in Bioreactors, using Sulphate Reducing Bacteria: Critical Review and Research Needs. *Journal of Environmental Quality*, **36**, 1-16
- POULSON S.R., COLBERG, P.J.S., & DREVER, J.I. 1997., Toxicity of Heavy Metals (Ni, Zn) to *Desulfovibrio desulfuricans*. *Geomicrobiology Journal*, **14**, 41-49.  
[http://www.dep.state.pa.us/dep/deputate/minres/bamr/amd/science\\_of\\_amd.htm](http://www.dep.state.pa.us/dep/deputate/minres/bamr/amd/science_of_amd.htm)
- TSUKAMOTO T.K., KILLION, H.A., & MILLER, G.C. 2004. Column experiments for microbiological treatment of acid mine drainage: low-temperature, low-pH and matrix investigations, *Water Research*, **38**, 1405–1418.
- WIEDER, R.K. 1989. A survey of constructed wetlands for acid coal mine drainage treatment in the eastern United States. *Wetlands*, **9**, 299-315.



## Urban geochemistry and health in New Orleans: Soil Pb, blood Pb and student achievement by 4<sup>th</sup> graders

Howard W. Mielke<sup>1,2</sup>, Christopher R. Gonzales<sup>3</sup>, & Eric Powell<sup>4</sup>

<sup>1</sup>Chemistry, Tulane University, New Orleans, LA, USA Email: howard.mielke@gmail.com

<sup>2</sup>Center for Bioenvironmental Research at Tulane and Xavier Universities, New Orleans, LA, USA

<sup>3</sup>Chemistry, Xavier University of Louisiana, New Orleans, LA, USA <sup>4</sup>Lead Lab, Inc., New Orleans, LA, USA.

**ABSTRACT:** Rigorous attention to geochemistry and metal toxicology are critical to healthy and sustainable urban environments. Lead (Pb) is a well known neurotoxin, especially to very young children. During the 20<sup>th</sup> century enormous quantities of Pb were used in consumer products including paint and vehicle fuel additives. As a result, Pb was dispersed into cities worldwide and accumulated in especially large quantities within inner city environments. Using empirical data from New Orleans, this study illustrates the negative correlation between urban Pb geochemistry, children's blood Pb, and scholastic aptitude in elementary schools. In order to become an environment suitably healthy for children, New Orleans requires an extensive remedial effort to control Pb dust.

**KEYWORDS:** *built environments, children, human impact, neurotoxicity, soil survey.*

### INTRODUCTION

Urban environments are increasingly the major location for housing the human population. As a result, it is essential to pay rigorous attention to the geochemical characteristics of urban environments and to assess the contribution that the accumulations of consumer products play on human health. This study evaluates the urban geochemistry and health as it relates to the neurotoxic effects, as indicated by student achievement of 4<sup>th</sup> grade students, and lead (Pb) that has accumulated in New Orleans.

### METHODS

This study examines the relationships of a database consisting of soil Pb, blood Pb (BPb) of children 6 years and younger, and scholastic achievement rates of 4<sup>th</sup> grade students from the Louisiana education assessment program (LEAP 21) in New Orleans. The data was from years 2000-2005 and reflects the pre-Hurricane Katrina conditions of New Orleans. Prior to the flood, schools were organized by attendance districts or neighborhood schools. This arrangement provided the opportunity to conduct a series of statistical tests to evaluate the associations between soil Pb, BPb and

overall 4<sup>th</sup> grade GPA scores matched for 105 schools of pre-Katrina New Orleans (Zahran et al., 2009).

### RESULTS

A significant positive relation exists between soil Pb and blood Pb ( $r^2 = 0.85$ ,  $P < 0.0001$ ) (Zahran et al. 2009).

Figure 1 illustrates that blood Pb is inversely and significantly ( $P$ -values  $< 0.0001$ ) associated to school grade point average (GPA), that is, the average of English language arts ( $r^2 = 0.58$ ), Math ( $r^2 = 0.50$ ), Science ( $r^2 = 0.63$ ), and Social Studies ( $r^2 = 0.61$ ).

### DISCUSSION

Soil Pb is an important pathway of human Pb exposure (Mielke & Reagan 1998). Empirical evaluation between soil Pb and BPb indicated a strong positive and non-linear association between soil Pb and BPb (Mielke et al., 2007a). The soil Pb footprint of New Orleans indicates that in the case of public and private properties an enormous disparity exists between the inner-city and outlying areas of New Orleans that cannot be attributed to older Pb-based paint alone; dust Pb from the previous use of lead additives to gasoline provide a better explanation between

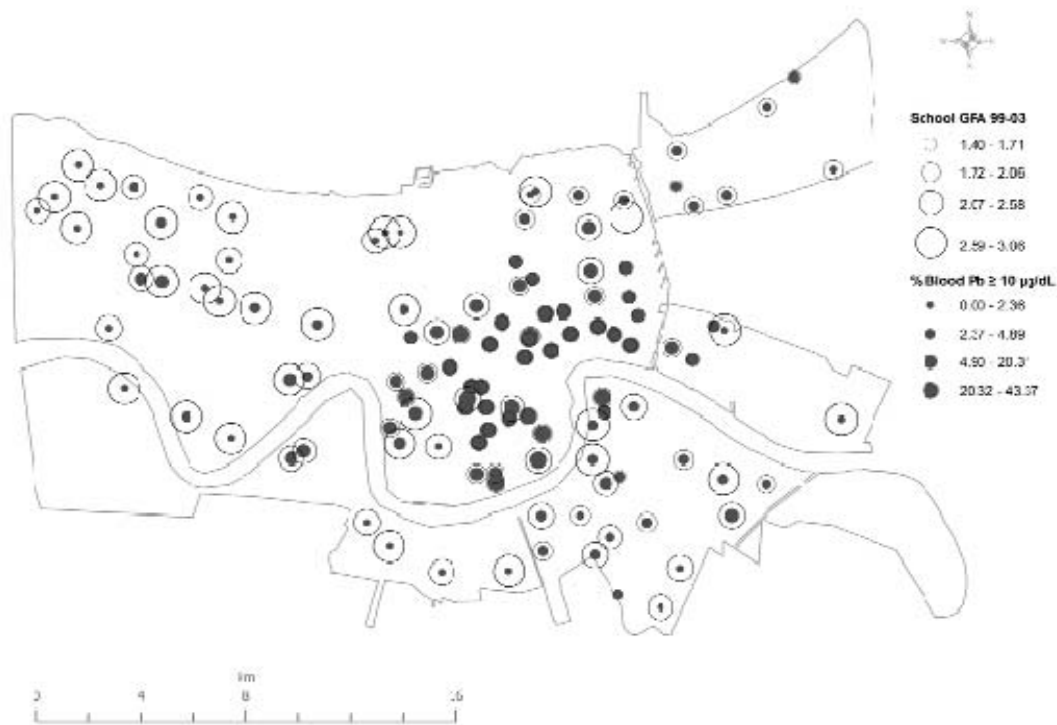


**Fig. 1.** Map of the quartiles of 4<sup>th</sup> grade school GPA and associated census tract % blood lead  $\geq$  10  $\mu\text{g}/\text{dL}$  (Zahran et al. accepted).

various areas of the city (Mielke et al., 2008). Poor African-American populations primarily live in the most Pb contaminated neighborhoods of New Orleans (Campanella & Mielke, 2008). Body burdens of Pb are especially large in the inner city where the childhood prevalence of blood Pb equal to or greater than the CDC 10  $\mu\text{g}/\text{dL}$  guideline is exceeded in many communities (see Fig 1). Within the communities with the highest blood Pb exposures, school failure rates exceed 50% in all subjects of the LEAP 21 scholastic achievement test.

Soil Pb is an enormous reservoir of Pb dust in the city and the quantity of Pb dust on the surface of the soil exceeds the quantity of Pb dust regulated in the interior by orders of magnitude (Mielke et al., 2007b). Soil Pb is mobile and during periods of low soil moisture such as late summer, significant increases occur in children's BPb compared with periods of high soil moisture (Laidlaw et al., 2005). Covering contaminated soil with clean soil is effective in reducing the amount of Pb on the soil surface and the cover appears stable, even after a major flood event (Mielke 2007; Mielke et al 2006a;b). An estimated \$US 76 million per year represents the costs of Pb poisoning in New Orleans (Mielke et al 2006a;b). These costs

underestimate costs related to the inequities of Pb poisoning because they exclude the cost of education and stresses from excessive violence (Zahran et al. 2009). Norway set precedence for a national program to systematically survey and remediate soil Pb and other contaminants which pose a threat to young children (Ottesen et al., 2008). A similar program should yield positive benefits to the children of New Orleans.

### CONCLUSIONS

- (1) The built environment of New Orleans became severely contaminated by the enormous quantities of Pb released in the 20<sup>th</sup> Century.
- (2) Lead is a potent neurotoxin, and because children are exceptionally sensitive to lead dust during their early developmental years they must be protected from exposure.
- (3) The urban geochemistry of Pb is strongly associated with the blood Pb of children which in turn is associated with their learning outcomes.
- (4) During New Orleans post-Katrina recovery, the opportunity exists to improve the environment for the benefit of children's health, and promote education and the sustainability of the city. Norway's clean soil program provides precedence for this action.

(5) Urban environments, as the dominant location for most of the human population must be guarded against excessive accumulation of toxic substances, and the skills of geoscientists can assist with this endeavor.

#### ACKNOWLEDGEMENTS

Funding from Association of Minority Health Professional Schools / Agency for Toxic Substances and Disease Registry Cooperative Agreement 5 U50 TS 473408 to Xavier University of Louisiana; Blood Pb data contributed by Kathleen Aubin & Dianne Dugas, Section Environmental Epidemiology & Toxicology, LA Office Public Health, & Ngoc Huynh, LA CLPPP; LEAP from the Louisiana Department of Education.

#### REFERENCES

CAMPANELLA, R. & MIELKE, H.W. 2008. Human geography of New Orleans' urban soil lead contaminated geochemical setting. *Environmental Geochemistry and Health*, **30**, 531-540.

LIDLAW, M.A.S., MIELKE, H.W., FILIPPELLI, G.M., JOHNSON, D.L., & GONZALES, C.R., 2005. Seasonality and children's blood lead levels: developing a predictive model using climatic variables and blood lead data from Indianapolis, Indiana, Syracuse, New York, and New Orleans, Louisiana (USA). *Environmental Health Perspectives*, **113**, 793-800.

MIELKE, H.W., GONZALES C., POWELL E., & MIELKE PW, JR. 2008. Urban soil lead (Pb) footprint: Comparison of public and private housing of New Orleans. *Environmental Geochemistry and Health*, **30**, 231-242.

MIELKE, H.W., GONZALES. C.R., POWELL, E., JARTUN, M., & MIELKE, P.W., JR. 2007a. Nonlinear association between soil lead and blood lead of children in metropolitan New Orleans, Louisiana: 2000-2005. *Science of the Total Environment*, **388**, 43-53.

MIELKE, H.W., POWELL, E.T., GONZALES, C.R., & MIELKE, P.W., JR. 2007b. Potential lead on play surfaces: Evaluation of the "PLOPS" sampler as a new tool for primary lead prevention. *Environmental Research*, **103**, 154-159.

MIELKE, H.W. 2007. Human actions as a force of change in the livability of the Earth: A case study of the Mississippi River Delta and New Orleans. *Zeitschrift für Geologische Wissenschaften*, **35**, 129-139.

MIELKE, H.W. POWELL, E.T., GONZALES, C.R., & MIELKE, P.W., JR. 2006a. Hurricane Katrina's impact on New Orleans soils treated with low lead Mississippi River alluvium. *Environmental Science and Technology*, **40** (24), 7623-7628

MIELKE, H.W., POWELL, E.T., GONZALES, C.R., MIELKE, P.W., JR., OTTESEN, R.T., LANGEDAL, M. 2006b. New Orleans soil lead (Pb) cleanup using Mississippi River alluvium: need, feasibility and cost. *Environmental Science and Technology*, **40** (08), 2784-2749.

MIELKE, H.W. & REAGAN, P.L. 1998. Soil is an important pathway of human lead exposure. *Environmental Health Perspectives*, **106**, 217-229.

OTTESEN, R.T., ALEXANDER, J., LANGEDAL, M., HAUGLAND, T., & HØYGAARD, E. 2008. Soil pollution in day-care centers and playgrounds in Norway: national action plan for mapping and remediation. *Environmental Geochemistry and Health*, **30**, 623-637.

ZAHARAN, S., MIELKE, H.W., WEILER, S., BERRY, K.J., & GONZALES, C. *Accepted*: Children's blood lead and standardized test performance response as indicators of neurotoxicity in metropolitan New Orleans elementary schools. *NeuroToxicology*.



## Mercury concentrations in fungal tissues, as influenced by forest soil substrates and moss carpets

Mina Nasr & Paul A. Arp

Faculty of Forestry & Environmental Management, 28 Dineen Drive, UNB, Fredericton, NB E3B 6C2, Canada  
(e-mail: [arp2@unb.ca](mailto:arp2@unb.ca))

**ABSTRACT:** This paper summarizes trends in mercury (Hg) concentrations in soils, mosses and fungal fruiting bodies of mixed forest locations in southwestern New Brunswick. The highest soil Hg concentrations occurred within the decomposing and humifying forest litter, but these concentrations decreased rapidly from the forest floor and A layers to the C layers in the mineral soil below. Hg concentrations in mosses and fungal fruiting bodies varied strongly by species, with further variations for the latter due to development stage (emerging, mature, over-mature), tissue type (stalk, cap) and sulphur (S) content, and the total Hg, S and carbon (C) concentrations within the mycelia-preferred soil substrates. All these variations make it difficult to use Hg concentrations in soils, mosses and fungi as broad-based indicators of environmental Hg pollution.

**KEYWORDS:** *Mercury concentration, forest soil, fungi, fruiting bodies, moss*

### INTRODUCTION

Hg is intricately distributed from the forest floor to the underlying mineral soil and subsoil (Grigal 2003). Vegetative uptake of Hg from the soil is generally low, except for some of the soil-based fungi that exploit organic soil substrates for readily metalized carbon (C) and nutrients such as nitrogen (N), phosphorus (P), Potassium (K), etc (Bending *et al.* 1995). The objective of this paper is to statistically relate the highly variable Hg concentrations within the upper soil layers (L, F, H, A) and in the fruiting bodies (mushrooms) of select fungal species to a number of factors. Factors include: (1) location according to a small but increasing atmospheric Hg deposition gradient (increasing from an inland location towards the coast and to an island), (2) soil layer types, namely the litter (L), fermentation (F), humifying (H) layers, and the A layer of the mineral soil, (3) the dominant moss type when present, (4) fungal species commonly found across southwestern New Brunswick.

### GEOLOGICAL AND REGIONAL SETTINGS

The areas selected for the study were forest locations in Fredericton, along the coast along the Bay of Fundy (Lepreau

and New River Beach) and on the island of Grand Manan. Bedrock formations underneath these locations vary but mostly refer to siliceous sedimentary rocks, covered by combinations of ablation till on basal till. Soils vary from thin podsoils on the uplands to gleysols on wetter locations. Forest vegetation is mixed, with red spruce, black spruce, white pine, balsam fir, aspen, white birch, yellow birch, red maple and sugar maple dominating the forest canopies. Moss cover varies from sphagnum on wet locations, feather mosses on moist locations, to plume and cap mosses and no mosses on drier locations. Atmospheric Hg inputs within the study region generally increase from north to south (NADP; Ritchie *et al.* 2006).

### METHODOLOGY

Soil (L, F, H, and A layers), mosses and fungal fruiting bodies were each collected from the same spots at the three locations. The L, F, H samples were ground to pass a 1 cm sieve; the mineral soil was sieved to retain its fine-earth 2mm fraction; mosses were separated into green versus dead tissues; the fruiting bodies were separated by stalk and cap. Subsamples were freeze-dried prior to

DMA-80 total Hg analysis, following the EPA 7473 method. The samples were also analysed for elemental organic C, N and S contents (LECO CNS analyzer). The resulting Hg concentration data were log-transformed, and were subject to multiple regression analyses that were originally developed for this study. The analysis includes using a host of independent variables as potential predictor variables, such as species type (mosses, fungi), tissue type (cap, stalk); development stage (emergent, mature, over mature), soil layer type (L, F, H, A), location (island, coast, inland), and C, N, and S contents.

## RESULTS AND DISCUSSION

Average elemental Hg, C, N, S concentrations and corresponding ratios are listed in Table 1 by tissue type and soil layer. The trends show highest in-soil Hg concentrations in the H layer, presumably on account of combined litter decomposition and strong Hg retention by the humifying substances. Across the soil layers, Hg concentrations and Hg/S ratios decrease strongly from the LFH layers to the C layers, while the Hg/C and Hg/N ratios increase with increasing soil depth. These trends suggest that Hg is concentrating at the soil-vegetation interface, and that Hg transfer into the deeper soil layers through biomixing and soil leaching is quite limited.

The generally high Hg concentrations in green moss tissues suggest an atmospheric source of accumulated Hg (Gjengedal *et al.* 1990). The higher Hg concentrations in Pleurozium under typically moist and dense forest covers would be due to an extra Hg capture by the forest canopy, and subsequent release to the moss carpet by way of throughfall and litterfall (St Louis *et al.* 2001). In this study, the lower Hg concentrations in Sphagnum would be related to more open forest and wetter ground conditions, while the lower Hg concentrations in Ptilium and Polytrichum would be related to the drier ground conditions in the forest interior of the sampling locations.

Across the fungal genera, average Hg concentrations range from 74 to 2161 ppb (Table 1), with large variations within family and species as well (details not shown). The overall trend by species refers to mycelial growth preferences, corresponding to LFH substrates and low Hg concentrations in Cantharellus, Cortinarius, and Russula, and to mineral soil substrates with high Hg concentrations in Amanita, Bankera, Boletus.

The variations of the within-soil Hg concentrations (Table 2) are, mostly significantly related to: (1) layer type, as characterized by the presence of the F and H layer relative to the L and A layers, (2) the combined depth of the L, F, H layer, with Hg concentrations decreasing as this depth increases, (3) location, with increasing Hg concentration from the inland location to the island, likely due to increasing atmospheric Hg deposition, (4) the total C and S concentrations within the soil, with Hg concentrations increasing with increasing S concentrations but decreasing with increasing C concentrations, (5) the carpeted presence of Sphagnum and Pleurozium mosses on the forest floor in comparison to other moss carpets or moss-free locations.

The Hg concentration variations within fungal tissues (Fig. 1) also follow a rather complex pattern (Table 3). For example, Cortinarius, Bankera, Cantharellus and Lactarius accumulate more Hg than what can be accounted for by variables such as: (1) the systematic stalk versus cap differences, (2) the reductions of the Hg concentrations from the emerging to the over-mature mushroom stage, (3) the C, Hg and S contents in the L, F, H, A layers, (4) the reduction of Hg uptake from soils with high S levels, (5) the increased Hg uptake from soils with high Hg concentrations, tempered by increased C concentrations.

The rather complex pattern of Hg concentrations in soils, mosses and fungal fruiting bodies makes it difficult to use Hg concentrations in these substrates as a general and unambiguous indicator of Hg

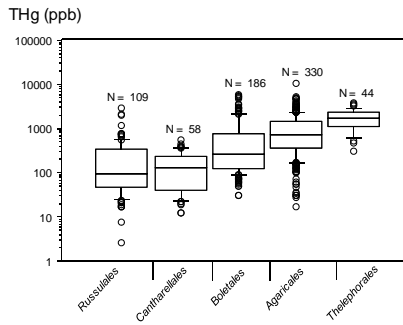


**Fig. 1.** Box plot for Hg concentrations (ppb, dry weight) in fungal fruiting bodies, by order.

toxicity derived from external Hg pollution loads. Among substrates, mosses are likely the best indicators of external Hg stress (Ruhling *et al.* 2004), but only under open, non-forested and non-shrubby conditions. Hg concentrations in fungal tissues are particularly variable, not only by species but also by substrate conditions, within-substrate Hg availabilities, and developmental stage of the short-lived fruiting body. The hyper-accumulation of Hg in the fungal fruiting bodies of *Bankera* and *Boletus* is of general interest in terms of being a notable Hg entry point into terrestrial food chains. In this study we suggest that loss of Hg from decaying fruiting bodies suggests a pathway of soil-retained Hg re-emission back into the atmosphere. The extent of such transfer, however, is not significant in terms of overall Hg gains and losses at the ecosystem level (details not shown).

## CONCLUSIONS

Hg concentrations in forest soils, mosses and fungal fruiting bodies are variable, and are influenced by many factors, such as the extent of forest-based capture of atmospheric Hg deposition, transmission of Hg from the forest canopy to the litter layer whether covered with mosses or not, and type of moss and soil layer conditions and configurations. Within the fungal fruiting bodies, further alternation of the Hg cycle occurs on account of mycelia substrate preferences and Hg allocation to stalk and caps, according to developmental stage.

## ACKNOWLEDGEMENTS

We like to thank Dr. David W. Malloch and the Forest Soil Laboratory team at UNB for valuable support during this study. This work was funded by Collaborative Mercury Research Network (COMERN), sponsored by the National Science and Engineering Council of Canada (NSERC).

## REFERENCES

- Bending, G.D. & Read, D.J. 1995. The Structure and Function of the Vegetative Mycelium of Ectomycorrhizal Plants .5. Foraging Behavior and Translocation of Nutrients from Exploited Litter. *New Phytologist*, **130.3**, 401-09.
- Grigal, D.F. 2003. Mercury sequestration in forests and peatlands: A review. *Journal of Environmental Quality*, **100**, 393-405.
- Gjengedal, E. & Steinnes, E. 1990. Uptake of metal-ions in moss from artificial precipitation. *Environmental Monitoring and Assessment*, **14**, 77-87.
- Nasr, M. 2007. Mercury levels in fungal fruiting bodies from interior and coastal forests of the Bay of Fundy region, New Brunswick, Canada. Thesis, *University of New Brunswick, Fredericton, Canada*.
- National Atmospheric Deposition Program (NADP), *Environment Canada*, 05/03/2006, <http://nadp.sws.uiuc.edu/date>.
- Ritchie, C.D., Richards, W., & Arp, P.A. 2006. Mercury in fog on the Bay of Fundy (Canada). *Atmospheric Environment*, **40**, 6321-6328.
- Ruhling, A. & Tyler, G. 2004. Changes in the atmospheric deposition of minor and rare elements between 1975 and 2000 in south Sweden, as measured by moss analysis. *Environmental Pollution* **131.3**, 417-23.
- St. Louis, V.L., Rudd, J.W.M., Kelly, C.A., Hall, B.D., Rolfhus, K.R., Scott, K.J., Lindberg, S.E. & Dong, W. 2001. Importance of the forest canopy to fluxes of methyl mercury and total mercury to boreal ecosystems. *Environmental Science & Technology*, **35.15**, 3089-98.

**Table 1.** Average Hg, C, N, S elemental composition by soil layer (Nasr 2007).

Substrate	Hg	C	N	S	C/N	C/S	Hg/C	Hg/N	Hg/S
	ppb		%				ppb / %		
<i>Sphagnum</i> ; shrubby, wet	152	50	1.50	0.15	33.3	333	3.0	101	1,013
<i>Ptilium</i> ; forest interior, dry	79	50	1.80	0.14	27.8	357	1.6	44	564
<i>Polytrichum</i> ; forest interior, dry	185	51	1.60	0.17	31.9	300	3.6	116	1,088
<i>Pleurozium</i> ; dense canopy, moist	267	49	2.00	0.18	24.5	272	5.4	134	1,483
L	141	50	1.60	0.13	31.8	419	0.3	9	116
F	260	45	1.60	0.16	29.1	292	0.6	17	169
H	299	37	1.50	0.16	26.2	267	0.8	20	212
A	110	10	0.50	0.05	23.7	235	1.5	28	350
B1	30	1	0.10	0.05	16.0	59	4.0	55	88
B2	18	1	0.10	0.04	11.9	34	4.4	45	56
C	7	0.1		0.06		3	11.4		13
<i>Cantharellus</i>	74	49	3.20	0.12	15.3	407	1.5	23	617
<i>Cortinarius</i>	192	45	4.70	0.17	9.6	273	4.3	41	1,164
<i>Russula</i>	242	48	4.40	0.18	10.8	260	5.1	55	1,322
<i>Hydnum</i>	249	47	3.80	0.12	12.4	396	5.3	66	2,092
<i>Tylopilus</i>	297	49	2.60	0.17	18.7	283	6.1	114	1,727
<i>Fuscoboletinus</i>	326	47	4.30	0.32	11.0	150	6.9	76	1,035
<i>Leccinum</i>	399	41	3.60	0.28	11.4	148	9.7	111	1,430
<i>Suillus</i>	431	49	3.90	0.18	12.5	272	8.8	111	2,394
<i>Lactarius</i>	482	46	3.90	0.13	11.7	341	10.5	124	3,597
<i>Amanita</i>	712	47	5.40	0.22	8.7	218	15.1	132	3,296
Bankera	1761	47	3.50	0.17	13.5	275	37.4	503	10,298
<i>Boletus</i>	2161	41	5.60	0.84	7.4	49	52.2	386	2,560

**Table 2.** Summary of regression results for Hg concentrations (ppb) in L, F, H, A soil layers.

Regression variable	Regr. coef.	Std. error	Std. coef.	t-value	p-value	R <sup>2</sup>	Partial corr.
Intercept	160.8	12.3	160.8	13.1	<0.0001		
F-layer (0,1)	89.5	6.9	0.4	12.9	<0.0001	0.221	0.41
H-layer (0,1)	137.1	14.8	0.3	9.3	<0.0001	0.321	0.31
LFH depth (cm)	-10.9	1.2	-0.3	-9.1	<0.0001	0.391	0.3
Location *	33.8	4.2	0.2	8.1	<0.0001	0.431	0.27
Total S (%)	588.2	76.5	0.3	7.7	<0.0001	0.454	0.26
Pleurozium (0, 1)	58.3	10.6	0.2	5.5	<0.0001	0.468	0.19
Sphagnum (0, 1)	44	8.2	0.1	5.3	<0.0001	0.485	0.18
Total C (%)	-1.2	0.3	-0.2	-4.5	<0.0001	<b>0.498</b>	0.16

Location: -1 for mainland, 0 for coast, 1 for island.

**Table 3.** Summary of regression results for Hg concentrations (ppb) in fungal tissues.

Regression variable	Regr. coef.	Std. error	Std. coef.	t-value	p-value	R <sup>2</sup>	Partial corr.
Intercept	0.8	0.1	0.83	7.99	<0.0001		
Developmental stage	0.3	0.03	0.27	7.81	<0.0001	0.114	0.408
<i>Cantharellus</i>	-0.8	0.11	-0.29	-7.41	<0.0001	0.245	-0.388
<i>Cortinarius</i>	0.3	0.05	0.25	6.75	<0.0001	0.338	0.358
<i>Russula</i>	-0.4	0.06	-0.24	-6.69	<0.0001	0.429	-0.355
Bankera	0.6	0.11	0.21	5.94	<0.0001	0.52	0.32
Cap (0), stalk (1)	-0.2	0.04	-0.19	-5.74	<0.0001	0.556	0.31
Location	0.3	0.05	0.21	5.31	<0.0001	0.582	0.289
<i>Polytrichum</i>	0.3	0.06	0.18	4.92	<0.0001	0.617	0.269
<i>Boletus</i>	0.9	0.18	0.16	4.86	<0.0001	0.641	0.266
Total S (F-layer)	-1.7	0.46	-0.14	-3.7	0.0003	0.654	-0.205

Development stage: 0 for emerging, 1 for mature, 2 for over-mature

## Hydrogeochemical processes governing the origin, transport, and fate of major and trace elements from mine wastes and mineralized rock

D. Kirk Nordstrom<sup>1</sup>

<sup>1</sup>US Geological Survey, 3215 Marine St., Boulder, CO 80303, USA (e-mail: [dkn@usgs.gov](mailto:dkn@usgs.gov))

**ABSTRACT:** The formation of acid-mine or acid-rock drainage is a complex process that depends on petrology and mineralogy, structural geology, geomorphology, surface hydrology, hydrogeology, climatology, microbiology, chemistry, and mining and mineral processing history. The concentrations of metals, metalloids, acidity, alkalinity, chloride, fluoride, and sulphate found in receiving streams, rivers, and lakes are affected by all of these factors and their interactions. Certain generalizations can be made that help to simplify our understanding of the origin, transport, and fate of contaminants released from mineralized areas. Waters of low pH tend to maintain element ratios indicative of the main mineral or group of minerals from which they dissolved, except iron and silica. Estimates of relative proportions of minerals dissolved can be made with mass-balance calculations if minerals and water compositions are known. Releases of drainage waters and ground waters from mines, waste rock, and tailings piles into receiving streams can be identified through synoptic sampling and discharges quantified through tracer-injection studies. Once dissolved, metal and metalloid concentrations are strongly affected by redox conditions and pH. Iron is the most reactive because it is rapidly oxidized by bacteria and archaea and ferric iron hydrolyzes and precipitates at low pH (2.2).

**KEYWORDS:** *acid-mine drainage, trace elements, geochemical modeling*

### INTRODUCTION

The processes governing the production of acid-mine drainage and drainage from unmined but mineralized areas are usually numerous and complex. Although there have been many laboratory studies on the oxidation of sulphide minerals during the last 2 decades, fewer field studies have been done showing the behaviour of major and trace elements during downstream transport in fluvial systems. Of greater concern is the limited transfer of hydrogeochemical research knowledge to remediation teams attempting to alleviate trace element contamination from water supplies. This abstract outlines some of the generalizations that can be made regarding the geochemistry of trace elements mobilized from mineralized areas into surface and ground waters and attenuation processes during down-gradient transport.

### GEOLOGIC CONSIDERATIONS

Element mobility begins with the rock, mineral, and processed mineral materials. Source rocks and host rocks can have a

wide range of composition and mineralogy from silicic to ultramafic igneous rocks and from limestone to black shale sedimentary rocks. Known element associations are helpful (Clarke 1924; Rankama & Sahama 1950): e.g., concentrations of Co, Ni, Cr, Mg, and Fe are higher in mafic to ultramafic rocks whereas Mo, Be, Sn, and W are higher in granitoid (silicic) rocks. Hydrothermal alteration can further concentrate these elements in sulphide minerals to form ore deposits. Understanding these associations is an important foundation for predicting which metals might occur at a given site (Plumlee 1999).

The geology not only provides the chemical source for trace-element mobility but it also provides the physical framework for water-flow paths. The structural properties of the rocks, the porosity, permeable fractures, provide for water-mineral reaction and element mobility. The geomorphology contributes to water-table levels, aquifer permeability, surface-water travel times, and time periods for erosion and sediment transport. Examples of

these can be found in the Questa baseline results (Caine 2007; Vincent 2008).

**HYDROLOGIC CONSIDERATIONS**

Dissolved constituents are driven by chemical reaction and the water flow. Hydrologic processes are particularly difficult to quantify in mountainous, hard-rock terrains but they can be essential for identifying and quantifying natural sources of contaminants (Nordstrom 2008). Streams, lakes, and rivers are the receiving water bodies for acidic drainage, and their water compositions depend on the composition and flow of surface and ground waters into them as well as the in-stream reactions (Kimball *et al.* 1994). In settings where a long-term flow of acidic ground water continues into a river that experiences increasing droughts, the river water quality will decline because of decreasing amounts of clean meteoric recharge (Nordstrom 2009).

**REACTION DURING TRANSPORT**

Elements can be grouped according to whether they react substantially (non-conservative) or react little (conservative) during downstream transport. In acidic waters (pH<4), metal cations stay dissolved generally except ferric iron and the more insoluble metals such as Au, Ag, Pb, and Ba. An example of constant weight ratios for Mn/Zn, Cd/Zn, and Co/Ni relative to changing sulphate concentrations in a single small debris-fan aquifer with pH 3-4 near Red River, New Mexico is shown in fig. 1. Constant ratios indicate there is no attenuation of metals during down-gradient flow while the sulphate concentrations become diluted through mixing.

The composition of the inflow water to the debris fan, natural acid-rock drainage of pH 2.5-3, was computed by mass balances to be derived from the weathering of the following minerals:

Gypsum . . . . .	3.78 mmol/kg
Pyrite . . . . .	8.66 mmol/kg
Dolomite . . . . .	4.64 mmol/kg
Kaolinite . . . . .	1.40 mmol/kg
Oligoclase . . . . .	0.44 mmol/kg
Fluorite . . . . .	0.20 mmol/kg

Sphalerite . . . . .	0.11 mmol/kg
Illite/Sericite . . . . .	0.032 mmol/kg
Chalcopyrite . . . . .	0.029 mmol/kg
Goethite . . . . .	-7.40 mmol/kg
Silica . . . . .	-2.89 mmol/kg

The negative sign refers to mineral precipitation instead of dissolution. Such computations are done with PHREEQC (Parkhurst & Appelo 1999). An inescapable conclusion of mass balances is that during the weathering of pyritiferous hydrothermally altered rock, iron and silica are precipitated.

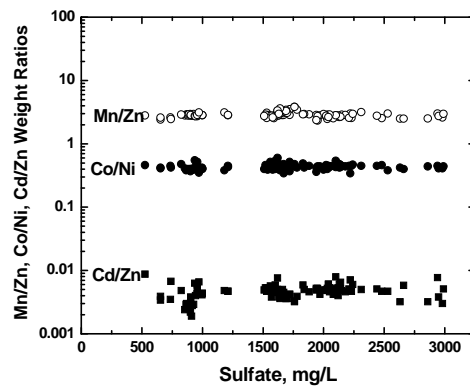
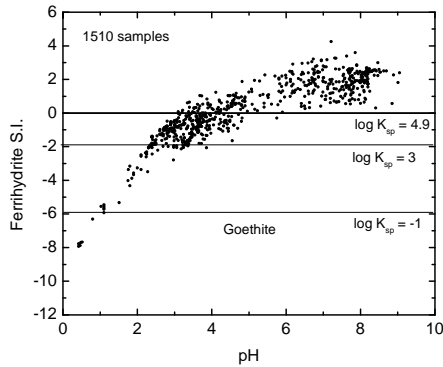


Fig. 1. Weight ratios for dissolved Mn/Zn, Co/Ni, and Cd/Zn in a single debris-fan aquifer of pH 3-4 and sulphate concentrations of 600-3000 mg/L (data from Naus *et al.* 2005).

**Fe(III) precipitation**

Oxidation of Fe(II) occurs rapidly at low pH but at measureable rates of about 1-5 mmol/L/h in surface waters by chemoautotrophic bacteria and archaea (Nordstrom 2003).

During the oxidation of dissolved iron and down-drainage neutralization of the acid water, hydrous ferric oxide (HFO) minerals precipitate, such as micro- to nano-crystalline goethite, schwertmannite, and ferrihydrite. The precipitate is usually a mixture of phases of uncertain composition and crystallinity. Using Fe(OH)<sub>3</sub>, or “ferrihydrite”, as a proxy for HFOs, more than 1500 samples of acid-rock drainage and receiving streams from locations in the western US were selected to calculate ferrihydrite saturation indices using WATEQ4F (Ball & Nordstrom, 1991). The results are shown in fig. 2.



**Fig. 2.** Ferrihydrate saturation indices relative to pH for 1510 screened analyses from western US mine sites.

Supersaturation of up to nearly 4 orders of magnitude is indicated relative to a  $\log K = 4.9$  which reflects freshly precipitated HFO. When elimination of all data points which are below the detection limits for Fe(III) and for electrode measurements, values of Eh measured agree with Eh calculated from Fe(II/III) determinations and speciation calculations and the revised ferrihydrate saturation index diagram looks like fig. 3.

Saturation with respect to HFO is now seen to be maintained and the supersaturation seen previously is an artifact of HFO nanocolloids passing through the filter apparatus.

The 2 elements that are removed from solution most rapidly with iron oxidation and HFO precipitation are arsenic and

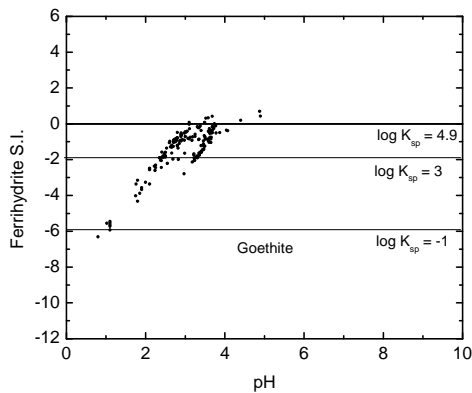


**Fig. 3.** Same as fig. 1 after removing all points below detection limits of Fe(III) and of redox electrode measurements.

thallium (Webster *et al.* 1994; unpublished data).

### Al precipitation

Aluminium also precipitates from acid surface waters when diluted or neutralized to a pH of  $\geq 4.5-5$  (Nordstrom & Ball 1986) because  $pK_1=5$  for  $Al^{3+}$  hydrolysis. For ground waters, there appears to be a buffering and precipitation of aluminium closer to a pH of 4 (Blowes *et al.* 2005; Naus *et al.* 2005). Using the same data set, saturation indices are plotted for  $Al(OH)_3$  in Figure 4. Three ranges of pH can be identified that describe aluminium geochemistry. For pH values  $<5$ , aluminium is conservative; for pH values of 5-7.5 a solubility limit is reached which corresponds to “amorphous”  $Al(OH)_3$  (or microcrystalline basaluminite, Bigham & Nordstrom 2000). For pH values  $> 7.5$  organic complexing likely dominates (Ball *et al.* 2005) and maintains concentrations higher than expected for microcrystalline gibbsite/kaolinite solubility.

Waters in fig. 4 that are substantially below the general trend are dilute surface waters that have not mixed with acid waters.

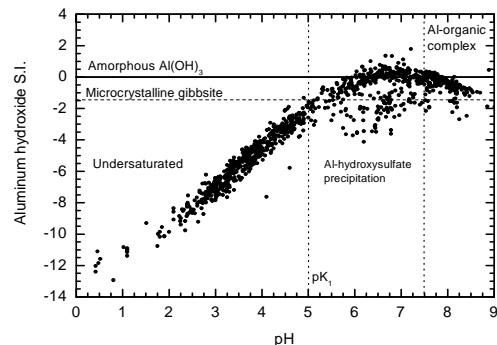


**Fig. 4.** Aluminium hydroxide saturation indices relative to pH for the same samples shown in fig. 1.

### Combining reaction with flow

Numerous codes are available that compute chemical reaction during flow provided that sufficient physical and chemical parameters are available (Nordstrom 2004). A practical approach has been developed by Kimball *et al.*

(1994) and Runkel *et al.* (1996) for surface waters affected by acid-mine drainage, transporting major and trace element contaminants in mountainous stream systems. First, synoptic sampling with tracer injection is used to obtain discharge values and mass loadings (Kimball 1997). Second, this data forms the basis for reactive-transport modelling (e.g., Caruso *et al.* 2008). Third, this approach can be used to evaluate remedial scenarios (Runkel & Kimball 2002; Walton-Day *et al.* 2007).

### CONCLUSIONS

This contribution summarizes state-of-the-science with respect to USGS research on the hydrogeochemistry of trace-element mobilization and attenuation from mineralized areas during transport in surface and ground waters. The primary aspects are:

- (1) geology forms the physical and chemical framework for solid sources of trace elements in mineralized settings
- (2) hydrology forms the physical and chemical framework for fluid mobility of trace elements
- (3) mass balances relates the partitioning of trace elements from mineral sources to the water
- (4) equilibrium solubilities provide an upper limit to dissolved concentrations of trace elements but formation of nanocolloids and organic complexing complicates interpretations.
- (5) combined reaction equilibria with fluid flow can offer practical approaches to understanding contaminant transport and to the evaluation of remediation scenarios.

### ACKNOWLEDGEMENTS

I thank Blaine McCleskey for assisting with preparation of the diagrams, Jim Ball for assistance with collection, analysis, and compilation of data, and the National Research Program and the USEPA for support of much of this research.

### REFERENCES

BALL, J.W. & NORDSTROM, D.K. 1991. User's manual for WATEQ4F, with revised thermodynamic data base and test cases for

calculating speciation of major, trace and redox elements in natural waters. *U.S. Geological Survey Open-File Report* **91-183**.

BALL, J.W., RUNKEL, R.L., & NORDSTROM, D.K. 2005. Questa baseline and pre-mining ground-water quality investigation. 12. Geochemical and reactive-transport modeling based on tracer injection-synoptic sampling studies for the Red River, New Mexico, 2001-2002. *U.S. Geological Survey Scientific Investigations Report* **2005-5149**.

BIGHAM, J.M. & NORDSTROM, D.K. 2000. Iron and aluminum hydroxysulfates from acid sulfate waters. In: P.H. RIBBE (series ed.) *Reviews in Mineralogy and Geochemistry* **40**, *Sulfate Minerals - Crystallography, Geochemistry, and Environmental Significance*, Mineralogical Society of America, Washington, D.C., 351-403.

BLOWES, D.W., PTACEK, C.J., JAMBOR, J.L., & WEISNER, C.G. 2005. The geochemistry of acid mine drainage. In: LOLLAR, B.S. (ed.) *Environmental Geochemistry* **9**, HOLLAND, H.D. & TUREKIAN, K.K. (ed.) *Treatise on Geochemistry*, Elsevier, 149-204.

CAINE, J.S. 2007. Questa baseline and pre-mining ground-water quality investigation. 18. Characterization of brittle structures in the Questa caldera and speculation on their potential impacts on the bedrock ground-water flow system. *U.S. Geological Survey Professional Paper* **1729**.

CARUSO, B.S., COX, T.J., RUNKEL, R.L., VELLEUX, M.L., BENCALA, K.E., NORDSTROM, D.K., JULIEN, P.Y., BUTLER, B.A., ALPERS, C.N., MARION, A., & SMITH, K.S. 2008. Metals fate and transport modelling in streams and watersheds: state of the science and USEPA workshop review. *Hydrologic Processes*, **22**, 4011-4022.

CLARKE, F.W. 1924. The Data of Geochemistry. *U.S. Geological Survey Bulletin* **770**, 5<sup>th</sup> edition.

KIMBALL, B.A. 1997. Use of tracer injections and synoptic sampling to measure metal loading from acid mine drainage. *U.S. Geological Survey Fact Sheet* **FS-245-96**.

KIMBALL, B.A., BROSHEARS, R.E., BENCALA, K.E., & MCKNIGHT, D.M. 1994. Coupling of hydrologic transport and chemical reaction in a stream affected by acid mine drainage. *Environmental Science & Technology*, **28**, 2065-2073.

NAUS, C.A., MCCLESKEY, R.B., DONOHOE, L.C., HUNT, A.G., PAILLET, F.L., MORIN, R.H., & VERPLANCK, P.L. 2005. Questa baseline and pre-mining ground-water quality investigation. 5. Well installation, water-level data, and surface- and ground-water

- geochemistry in the Straight Creek drainage basin, Red River, New Mexico, 2001-2003. *U.S. Geological Survey Scientific Investigations Report 2005-5088*.
- NORDSTROM, D.K. 2003. Effects of microbiological and geochemical interactions in mine drainage. In: JAMBOR, J.L., BLOWES, D.W., AND RITCHIE, A.I.M., (eds.) *Environmental Aspects of Mine Wastes*, Mineralogical Association of Canada **31**, 227-238.
- NORDSTROM, D.K. 2004. Modeling low-temperature geochemical processes. In: DREVER, J.I. (ed.) *Surface and Ground Water, Weathering, and Soils 5*, HOLLAND, H.D. & TUREKIAN, K.K. (ed.) *Treatise on Geochemistry*, Elsevier, 37-72.
- NORDSTROM, D.K. 2008. Questa baseline and pre-mining ground-water quality investigation. 25. Summary of results and baseline and pre-mining ground-water geochemistry, Red River, Taos County, New Mexico, 2001-2005. *U.S. Geological Survey Professional Paper 1728*.
- NORDSTROM, D.K. 2009. Acid rock drainage and climate change. *Journal of Geochemical Exploration*, **100**, 97-104.
- NORDSTROM, D.K. & BALL, J.W. 1986. The geochemical behaviour of aluminium in acidified surface waters. *Science*, **232**, 54-56.
- PARKHURST, D.L. & APPELO, C.A. 1999. User's guide to PHREEQC (version 2) – a computer program for speciation, batch-reaction, one-dimensional transport, and inverse geochemical calculations. *U.S. Geological Survey Water-Resources Investigations Report 99-4259*.
- PLUMLEE, G.S. (1999) The Environmental geology of mineral deposits. In: PLUMLEE, G.S. & LOGSDON, M.J. (eds.) *The Environmental Geochemistry of Mineral Deposits 6A*, Society of Economic Geologists, 71-116.
- RANKAMA, K. & SAHAMA, TH.G. 1950. *Geochemistry*, The University of Chicago Press.
- RUNKEL, R.L., BENCALA, K.E., BROSHEARS, R.E., & CHAPRA, S.C. 1996. Reactive solute transport in streams: 1. Development of an equilibrium-based model. *Water Resources Research*, **32**, 409-418.
- RUNKEL, R.L. & KIMBALL, B.A. 2002. Evaluating remedial alternatives for an acid mine drainage system – application of a reactive transport model. *Environmental Science & Technology*, **36**, 1093-1101.
- VINCENT, K.R. 2008. Questa baseline and pre-mining ground-water quality investigation. 17. Geomorphology of the Red River Valley, Taos County, New Mexico and influence on ground-water flow in the shallow alluvial aquifer. *U.S. Geological Survey Scientific Investigations Report 2006-5156*.
- WALTON-DAY, K., PASCHKE, S.S., RUNKEL, R.L. & KIMBALL, B.A. 2007. Using the OTIS solute-transport model to evaluate remediation scenarios in Cement Creek and the Upper Animas River. *U.S. Geological Survey Professional Paper 1651*, 979-1028.



## Geological controls concerning mercury accumulations in stream sediments across Canada

Jae Ogilvie<sup>1</sup>, Mina Nasr<sup>1</sup>, Andy Rencz<sup>2</sup>, Paul A. Arp<sup>1</sup>

<sup>1</sup>Faculty of Forestry & Env. Mgt, UNB, Fredericton, NB CANADA (email: [arp2@unb.ca](mailto:arp2@unb.ca))

<sup>2</sup>Geological Survey of Canada (GSC), NRCAN, Ottawa, ON CANADA.

**ABSTRACT:** This paper presents Geological Survey of Canada (GSC) data survey for mercury (Hg) concentrations in stream sediments ( $n \approx 144,000$ ) for select areas across Canada based on geological and topographic elevation differences between upland and lowland streams. Hg concentrations vary widely from 5 to 9,400 ppb per sample, with regional averages from 29 (central Nunavut) to 165 ppb (Vancouver Island, BC). An extensive cluster (100x400 km, oriented SE-NW) of Hg concentrations >4000 ppb is located in the east-central portion of the Yukon Territory. Regionally and locally, Hg concentrations tend to be consistently higher in upland streams than in lowland streams. The upland/lowland delineations were derived from coarse-gridded (national, 300 m) and fine-gridded (local, 30 m) digital elevation models (DEMs).

**KEYWORDS:** *Mercury concentrations, stream sediments, geological survey, upland/lowland delineation*

### INTRODUCTION

The upland/wetland transfer dynamics of mercury (Hg) across the landscape via streams and other flow channels pose health threats to aquatic ecosystems (Chasar *et al.* 2009). This paper presents select Geological Survey of Canada (GSC) data for Hg concentrations in stream sediments across Canada, with an overall intent to relate these data to local geographic, topographic, climatic and atmospheric Hg deposition conditions. Here, we explore how Hg concentrations in stream sediments relate to local bedrock type and its physical characteristics such as colour, texture and composition. Next, topographic elevation differences are examined through flow channel and upland/wetland delineations, using (i) the national 300m digital elevation model (DEM) and (ii) higher resolution DEMs including provincial DEMS and bare-ground LiDAR (Light Detection and Ranging) as primary delineation tools.

### GEOLOGICAL SETTING

The general framework for this study builds on national and provincial data layers of digitized, surface water features,

peatland inventory, digital elevation model, and bedrock geology, and raw data for atmospheric deposition (Hg), weather (mean annual precipitation, and mean monthly temperatures). The geological and lithological settings for each stream survey were assigned based on local bedrock type, by survey zone. Topographic flow accumulation, wet-area and cartographic depth-to-water (DTW) assessments were each obtained through DEM derivation (Murphy *et al.* 2009).

### MATERIAL & METHODOLOGY

Data were processed using ArcGIS to extract and interpret zonal statistics comparing Hg concentrations to stream sediment properties through geo-referenced map overlays. The following data-layers are examples: Canadian Landmass DEM (NRCAN 2007); Survey of Hg concentrations in stream sediments (NRCAN 2008); NASA SRTM DEM, CGIAR-CSI (2008); Surficial Materials of Canada (Fulton, 1995); Geological Map of Canada (Wheeler *et al.* 1997). These maps and associated data layers were compiled in ESRI shapefile (.shp) and layer (.lyr) formats within ArcMap GIS project files (.mxd).

**RESULTS**

The regional-based survey pattern of the GSC-determined Hg concentrations (ppb) in stream sediments across Canada is shown in Fig.1. Of particular interest are: (i) the high Hg concentration cluster near the central north-eastern border of the Yukon Territory (Survey Zone 3), (ii) the somewhat elevated background levels in the southern portions of the Canadian Shield along the Great Lakes, (iii) the scattered pattern of similar values throughout British Columbia, Labrador and

the Maritimes, and (iv) the generally low levels across the northern regions and lowland terrains. Average, lowest and highest values and associated standard deviations are listed in Table 1 according to survey region. This table also displays average upland-to-lowland Hg concentrations according to the nationwide upland-lowland, using the 300m DEM-grid delineation process. Fig.2 provides a local example for this process using the 30m DEM-grid delineation process.

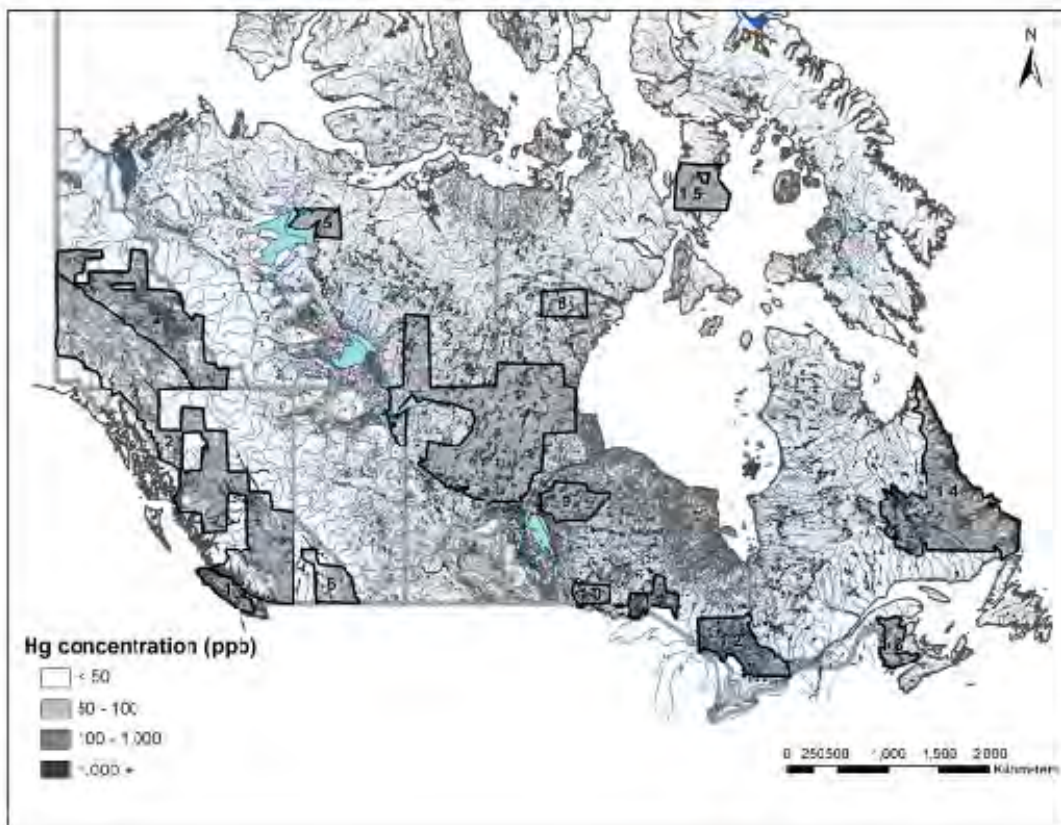


**Fig. 1.** Outline of upland (white) / lowland (grey) delineation plus flow channels and lakes across Canada, based on the national DEM (300 m resolution), plus an overlay of the numbered regions (polyshapes with black outline) for the GSC stream-sediment Hg survey, showing Hg concentrations inside these regions, from white to dark grey.

**DISCUSSION**

The results for the Hg concentrations in stream sediments presented in Fig.1 and Table 1 are preliminary, with more analyses to be done, and more GSC data to be added for Quebec, Newfoundland and Nova Scotia. On the whole, the

patterns are not directly related to the national Hg deposition pattern (details not shown), and are also not related to the global distillation pattern of volatiles, whereby Hg emitted from industrial and natural processes including forest fires from southern locations should incur an

increasing Hg presence within the arctic regions. The pattern of slightly lower Hg concentrations in lowland stream sediments would be due to lowland-specific Hg dilution and volatilization processes (Budd *et al.* 1993). This occurs in spite of the strong affinity between  $Hg^{2+}$  and dissolved organic matter (DOM, Bengtsson *et al.* 2008). However, DOM-transported Hg is subject to photochemically induced volatilization, which should increase with increasing sunlight exposure along widening stream channels and lake and river systems (Meng *et al.* 2005, Hall *et al.* 2008 & O'Driscoll *et al.* 2008). For the most part, in-stream Hg

concentrations are related to local mineralogies, with low concentrations associated with silicate and carbonate bedrock formations with no to few sulphide inclusions. In contrast, high Hg concentrations in stream sediments can be found in areas with elevated S mineralogies, such as Survey Zone 3 (Fig. 1), and areas with known ore deposits and mining activities (e.g., max. value for New Brunswick, Table 1).

The nationwide and regional pattern of Hg concentrations in stream sediments is of general interest because it establishes priority areas for further research

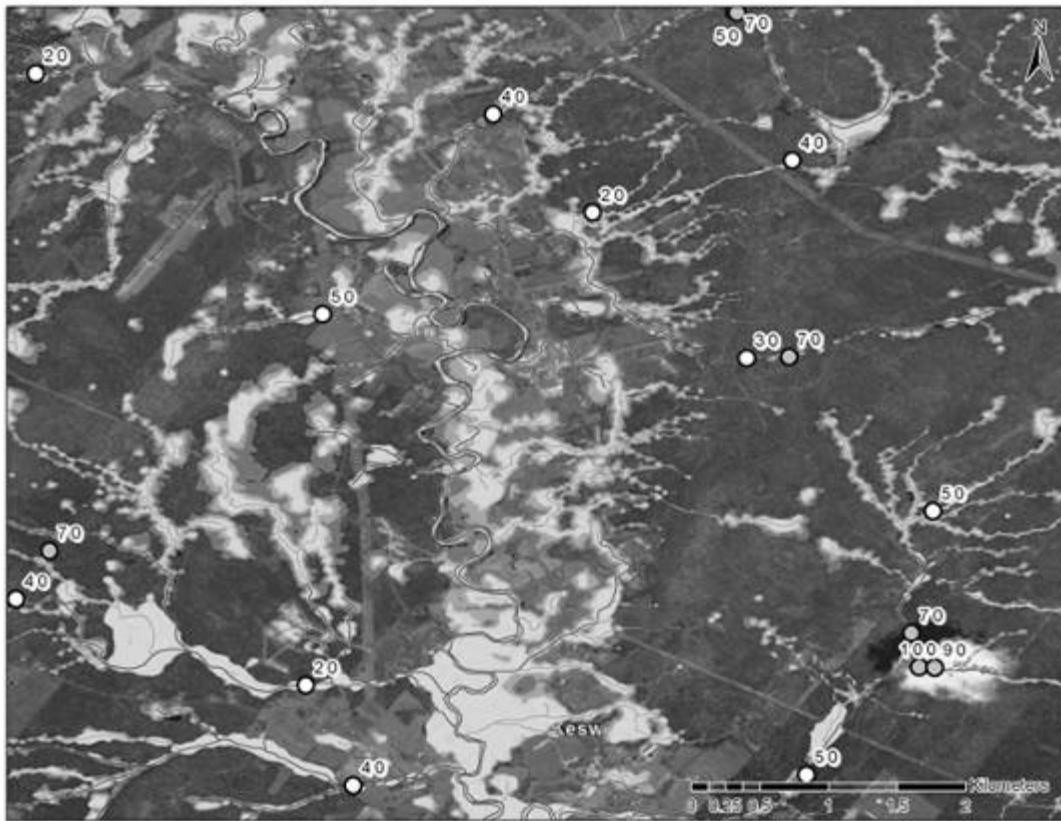


**Fig. 2.** An example of the upland/lowland delineation process, re-sampling the local 30m DEM grid to 10 m, with lowlands shaded from light to dark grey (corresponding to a cartographic depth-to-water index of 0 to 1 m, respectively) overlying the local air-photo mosaic. Also shown are the local GSC stream-sampling points (circles), with the stream-sediment Hg concentrations in ppb. Note the generally close correspondence between sampling points and the DEM-derived flow channels. Location: central New Brunswick, northwest of Fredericton (Keswick). The light area with a dark shadow towards the north-west in the lower right is a cloud.

**Table 1.** Hg concentration profile by survey zones and upland/lowland delineation (CV: coefficient of variation).

Survey zone (number)	n	Hg (ppb)				CV	Average Hg (ppb)		Upland/Lowland Ratio
		Average	Min.	Max.	StdDev		Uplands	Lowlands	
Nunavut, Central (8)	1,232	29	10	110	18	0.62	33	26	1.27
Nunavut, North-east (15)	2,118	44	10	150	20	0.45	45	43	1.04
British Columbia, East (6)	3,972	35	10	2,380	65	1.86	36	35	1.02
Manitoba, East (9)	5,111	45	10	801	21	0.47	49	44	1.1
Central Canada (7)	31,523	55	5	1,560	33	0.60	58	51	1.15
North West Territories, Central (5)	1,298	57	10	295	36	0.63	59	55	1.06
Yukon and BC, Rocky Mountains (2)	41,965	58	5	9,200	125	2.16	60	50	1.2
Ontario, ELA (10)	1,954	80	11	1,047	46	0.58	83	79	1.05
Labrador (14)	20,549	82	8	900	57	0.70	86	74	1.17
New Brunswick (13)	7,771	84	10	6,830	97	1.15	87	74	1.18
Yukon, east of Rocky Mountains (3)	11,372	110	8	5,950	149	1.35	113	96	1.18
Ontario, Central (12)	3,242	115	10	1,020	63	0.55	123	97	1.27
Ontario, Sudbury area (11)	9,157	126	10	5,000	101	0.80	131	117	1.12
British Columbia, Vancouver Island (1)	2,882	165	10	9,400	492	2.98	170	138	1.24
<b>Total</b>	<b>144,146</b>	<b>77.5</b>	<b>5</b>	<b>9,400</b>	<b>95</b>	<b>1.06</b>	<b>81</b>	<b>70</b>	<b>1.16</b>

regarding the transfer of Hg from uplands into rivers, lakes and local food chains, and the link between local geological structures and the health of fish-eating communities. The high-resolution delineation of local flow channels and adjacent wet areas also provides a new tool for (i) metal prospecting and related sampling strategies, (ii) interpreting local Hg deposition patterns, and (iii) hotspot visualization of Hg transfer and Hg methylation along upland-wetland transition zones (Mitchell *et al.* 2008).

### CONCLUSIONS

Mapping the GSC survey data for Hg concentrations in stream sediments in terms of local flow-channel and upland/lowland patterns provides a new means to evaluate these data in relation to local geologic and topographic conditions and configurations. Overlaying other geo-referenced data layers such as climate and atmospheric deposition maps including Hg deposition will reveal additional association-patterns between Hg in stream sediments and surrounding factors.

### ACKNOWLEDGEMENTS

This work is a collaboration between Environment Canada, NRCAN- GSC and UNB, and is financed through the CARA program of Environment Canada. Administrative and general support from T. Clair, CWS, Sackville, NB, is gratefully appreciated.

### REFERENCES

- BENGTSSON, G., & PICADO, F. 2008. Mercury sorption to sediments: Dependence on grain size, dissolved organic carbon, and suspended bacteria. *Chemosphere*, **73.4**, 526-31.
- BUBB, J.M., WILLIAMS, T.P. & LESTER, J.N. 1993. The Behavior of Mercury Within A Contaminated Tidal River System. *Water Science and Technology*, **28.8-9**, 329-38.
- CGIAR-CSI. 2008. NASA SRTM DEM. Retrieved February 08, 2008, <http://srtm.csi.cgiar.org/>.
- CHASAR, L.C., SCUDDER, B.C., STEWART, A.R., BELL, A.H., AIKEN, G.R. 2009. Mercury Cycling in Stream Ecosystems. 3. Trophic Dynamics and Methylmercury Bioaccumulation. *Environmental Science Technology*, **43** (8), 2733–2739.

- FRISKE, P.W.B. & HORNBOOK, E.H.W. 1991. Canada's National Geochemical Reconnaissance programme; *Transactions of the Institution of Mining and Metallurgy*, **100** (B), 47-56.
- FULTON, R.J. 1995. Surficial materials of Canada, *Geological Survey of Canada*, Map 1880A, Scale 1:5,000,000.
- HALL, B.D., AIKEN, G.R., KRABENHOFT, D.P., MARVIN-DIPASQUALE, M. & SWARENSKI, C.M. 2008. Wetlands as principal zones of methylmercury production in southern Louisiana and the Gulf of Mexico region. *Environmental Pollution*, **154**, 124-134.
- MENG, F., ARP, P., SANGSTER, A., BRUN, G.I., RENCZ, A., HALL, G., HOLMES, J., LEAN, D., & CLAIR, T. 2005. Modeling dissolved organic carbon, total and methyl mercury in Kejimikujik freshwaters. In: *Mercury Cycling in a Wetland Dominated Ecosystem: A Multidisciplinary Study*. Society of Environmental Toxicology and Chemistry, Pensacola, FL, 267-284.
- MITCHELL, C.P.J., BRANFIREUN, B.A., KOLKA, R.K. 2008. Spatial characterization of net methylmercury production hot spots in peatlands. *Environmental Science and Technology*, **42**, 1010-1016.
- MURPHY, P.N.C., OGILVIE, J., & ARP, P.A. 2009. Topographic modelling of soil moisture conditions: a comparison and verification of two models. *European Journal of Soil Science*, **60**, 94-109.
- NRCAN 2007. Canada3D – Digital Elevation Model of the Canadian Landmass. <http://www.geogratis.ca/geogratis/en/collect ion/detail.doid=8880>.
- NRCAN 2008. Survey of Hg concentrations in stream sediments (unpublished data).
- O'DRISCOLL, N.J.O, POISSANT, L., CANRIO, J., & LEAN, D.R.S. 2008. Dissolved gaseous mercury concentrations and mercury volatilization in a frozen freshwater fluvial lake. *Environmental Science and Technology*, **42**, 5125-5130.
- O'DRISCOLL, N.J., RENCZ, A.N., & LEAN, D.R.S. 2005. Mercury Cycling in a Wetland Dominated Ecosystem: A Multidisciplinary Study. *Society of Environmental Toxicology and Chemistry (SETAC)*, Pensacola, FL, 267-284.
- WHEELER, J.O., HOFFMAN, P.F., CARD, K.D., DAVIDSON, A., SANFORD, B.V., OKULITCH, A.V., & ROEST, W.R. 1997. *Geological Map of Canada (CD-ROM) Map D1860A*, Geological Survey of Canada.



## Quantifying hydrothermal, groundwater, and crater lake contributions to the hyperacid Banyu Pahit stream, East-Java, Indonesia

Stephanie Palmer<sup>1\*</sup>, Jeffrey M. McKenzie<sup>1</sup>,  
Vincent van Hinsberg<sup>1</sup>, & A.E. Williams-Jones<sup>1</sup>

<sup>1</sup>Earth and Planetary Sciences, McGill University, 3450 University St., Montreal, QC H3A 2A7, Canada  
(e-mail: [stephani@eps.mcgill.ca](mailto:stephani@eps.mcgill.ca))

**ABSTRACT:** Hyperacidic fluids from Kawah Ijen volcano (East-Java, Indonesia) contaminate the surrounding environment with high concentrations of potentially toxic elements. These fluids are released through the Banyu Pahit stream, which is used to irrigate farmland on the outer flanks of the Ijen caldera complex. This study has identified the sources of fluids contributing to stream flow in the uppermost 4 kilometers of the Banyu Pahit, including sources that are unaccounted for in previously reported studies of the Ijen magmatic-hydrothermal system. Detailed chemical analyses of these different source fluids (the crater lake and all neutral and acid springs) and of the stream itself at regular intervals indicate that volcanogenic input to the stream is not limited to seepage from the crater lake, but also includes significant input from the hydrothermal system via hot, hyperacidic springs located 1 and 3 kilometers from the crater. Springs may represent an important source of element flux to the surrounding environment. Their hydrothermal characteristics suggest that hyperacidic fluids may be used as a monitor of volcanic activity.

**KEYWORDS:** *hydrochemistry, volcanogenic pollution, acid brine, Kawah Ijen, Banyu Pahit*

### INTRODUCTION

Active volcanoes are sites of complex and dynamic hydrologic systems involving interactions between hydrothermal and magmatic fluids, groundwater, and surface water. Volcanic activity can produce high levels of natural pollution and often is accompanied by fluids having levels of toxicity similar to those of acid mine drainage, i.e., greatly exceeding WHO guidelines for human health (Edmunds & Smedley 1996; Sriwana *et al.* 1998; Delmelle & Bernard 2000). These fluids flow from crater lakes and hot springs into the surrounding environment and have strong negative impacts on human health and on the ecosystem (Parnell & Burke 1990; Pringle *et al.* 1993; Schaefer *et al.* 2008; Löhr *et al.* 2005). Understanding the hydrologic processes that control the sources, transformations, and distribution of these toxic fluids is necessary to assess their impact on local surface and groundwater resources (Rowe *et al.* 1995). Potentially, the temporal changes

in the chemistry of these fluids can also serve as monitors of volcanic activity.

This study examines the pollution of surface water by Kawah Ijen volcano, Indonesia. The headwaters of the hydrologic system from this volcano, a hyperacid brine lake, are conspicuously different in composition from the downstream waters. The objective of this study is to characterize and quantify the hydrologic processes that control the observed changes in the chemistry of the downstream waters. Results from hydrochemical analyses of the Kawah Ijen Crater Lake, Banyu Pahit stream and adjacent springs, including some previously unstudied springs explains the evolving chemistry of the Banyu Pahit in terms of a clearly identifiable set of sources and sinks.

### STUDY SITE

#### Banyu Pahit Stream System

Kawah Ijen is located on the eastern rim of the Ijen caldera in East Java, Indonesia (Figure 1). The crater of the volcano hosts

the world's largest naturally-occurring hot, hyperacid lake, with a volume of approximately  $32 \times 10^6 \text{ m}^3$  (Delmelle & Bernard 2000; Delmelle *et al.* 2000). Magmatic and hydrothermal fluids continuously condense into the lake, maintaining the very low pH ( $\approx -0.01$ ) and high temperature ( $\approx 38^\circ\text{C}$ ). Heavy metals in the lake water are present in elevated concentrations due to extensive rock dissolution in the acid brine (Delmelle &

Bernard 1994; Delmelle *et al.* 2000). The lake water seeps through the flanks of the crater forming the headwaters of the Banyu Pahit stream (Figs. 1 & 2) which flows northward across the larger volcanic complex, and passes through the town of Blawan 17 km downstream before exiting the caldera and flowing across agricultural plains, where it is used for irrigation, and then to the ocean (Fig. 1). Although hydrochemical measurements show dilution of the toxic lake water by other sources along the Banyu Pahit stream, notably by two major tributaries near the town of Blawan, heavy metal concentrations and pH remain at toxic levels and pose major risks to health of the local population and ecosystems downstream (Delmelle & Bernard 2000; Löhr *et al.* 2005). Fluxes of toxic elements remain high further downstream, but despite this, the waters are still used to irrigate the agricultural plains (Delmelle & Bernard 2000)

Almost nothing is known about the uppermost 4 km of the Banyu Pahit stream due to difficult field access, although differences in stream composition across this interval have been reported. van Hinsberg (2001) suggested three potential explanations for the observed changes: 1) dilution by another fluid source, 2) fluid-rock interaction, and 3) mineral precipitation.

### SAMPLING AND ANALYTICAL METHODS

#### Field Work

Water samples were taken at 23 sites along the uppermost 4 km of the Banyu Pahit stream in July and August 2008 (dry season); from two clusters of acid springs adjacent to the stream (6-9 and 12-15), groundwater in the Banyu Pahit canyon (11) a neutral spring near Paltuding (23), the Kawah Ijen Lake (1), and at regular intervals of the Banyu Pahit stream (Figure 1, 2). Samples were filtered at  $25 \mu\text{m}$  into sample-rinsed 60 mL polypropylene bottles. Neutral samples were acidified with 2 drops of 18% nitric acid when fluid pH was less than 2. At each sampling site, pH, temperature, and electric conductivity were measured. At

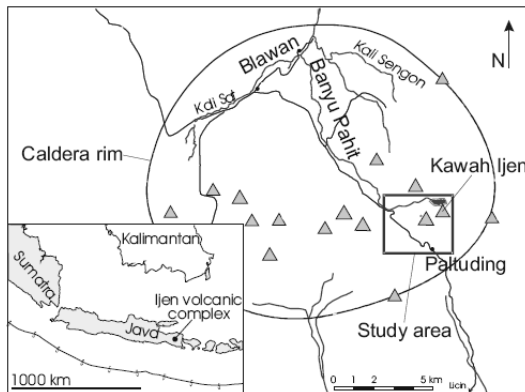


**Fig. 1.** Overview map of the Ijen caldera, East Java, Indonesia.

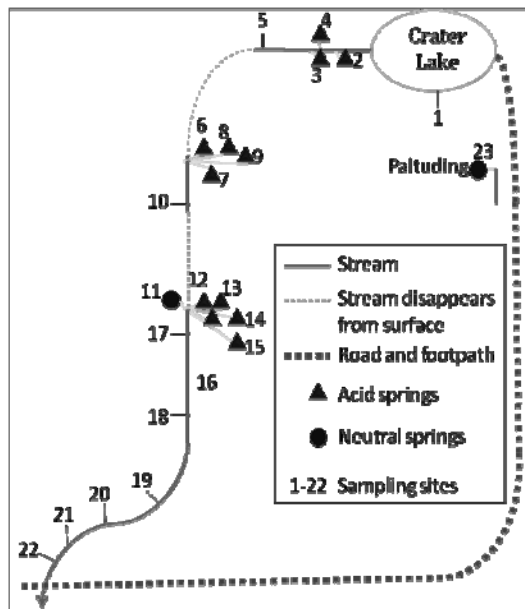


**Fig. 2.** Schematic diagram showing the locations of sampling sites along the Banyu Pahit stream and those of nearby neutral and acid springs. The distance from the lake to Sample site 22 is approximately 4 km.

selected sites, aluminum, iron, and chloride concentrations were determined on-site by colorimetry. Stream discharge was also measured at regular intervals along this stretch of the stream.

**Chemical Analyses**

Concentrations of major cations in all samples were determined by acetylene flame Atomic Absorption Spectroscopy at the Trace Element Analytical Laboratories (TEAL) of McGill University. Analyses of trace element concentrations were carried out using Inductively Coupled Plasma Quadrupole Mass Spectrometry (also at TEAL). Concentrations of anions were determined by Ion Chromatography at the Hydrogeology Laboratory at McGill University.

**Observations and Discussion**

Table 1 illustrates concentrations and estimates of the total daily flux of selected elements out of the Kawah Ijen Lake into the Banyu Pahit stream, based on measurements from the 2008 field season. Also reported are concentrations and estimated daily fluxes for the downstream Banyu Pahit, near the town of Blawan.

Exploration of this remote, previously understudied, section of the Banyu Pahit

**Table 1.** Concentrations and estimated daily fluxes of Al, Cd, and F through the Banyu Pahit stream system, based on approximate stream discharges of 60 L/s (from the Crater Lake) and 4000 L/s (near Blawan; from Delmelle & Bernard, 2000).

	Crater Lake		Banyu Pahit (near Blawan)	
	Concentration (ppm)	Estimated Daily Flux (kg d <sup>-1</sup> )	Concentration (ppm)	Estimated Daily Flux (kg d <sup>-1</sup> )
Al	5740	29,740	25.1	8,600
Cd	0.06	0.3	0.001	0.3
F	727	3,770	7.3	2,520

stream during July and August, 2008, provided two key observations which suggest a more complicated hydrologic system than previously realized. Firstly, the stream flows subterraneously for tens to hundreds of meters along two reaches. Secondly, a number of previously unobserved springs contribute to the flow of the Banyu Pahit stream. Based on preliminary colorimetric measurements, these springs show a distinct chemical grouping (Fig. 3a), which we interpret as neutral groundwater springs, acid springs with a hydrothermal component, and seepage from the crater lake. The Banyu Pahit, downstream of these springs, is demonstrably a mixture of crater lake, groundwater and thermal acid spring fluids (Fig. 3b).

It was also observed that acid fluids seem to be restricted to the Banyu Pahit

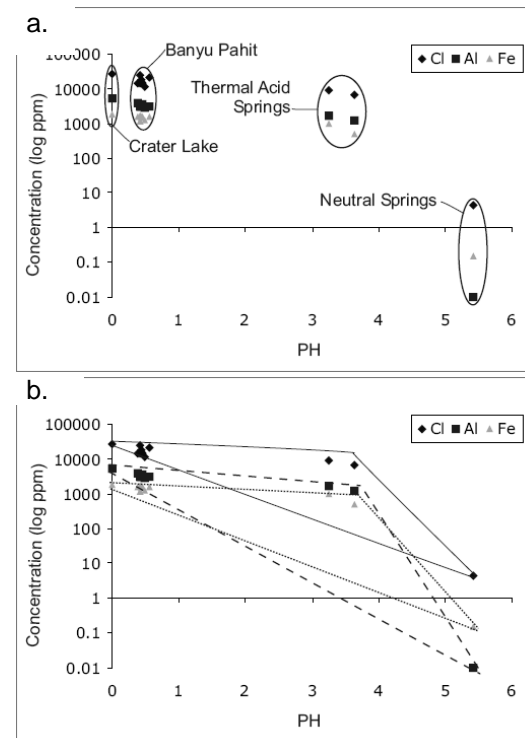


**Fig 3.** Chemical groupings of upstream Banyu Pahit source fluids, based on on-site colorimetry (crater lake, thermal acid springs, neutral spring and stream) (a). Mixing curves for the same groups (b).

stream valley and that springs of acidic composition only emerge along the southern side of the valley. Neutral springs were observed at the same elevation as some of the acid springs, but emerge only on the northern side of the valley. This could have important implications for constraining the boundaries of the hydrothermal system, understanding groundwater flow, and examining groundwater-hydrothermal system boundaries.

### CONCLUSIONS

The main conclusions from the current study are that:

(1) The Banyu Pahit stream is much more complex than previously thought, due to the input of neutral and acid spring water.

(2) Volcanogenic environmental contamination via the Banyu Pahit stream can be attributed to the hydrothermal system as well as Kawah Ijen Lake seepage, and models of the system must account for both.

(3) The hyper-acidic water seems to be contained within the Banyu Pahit stream valley, potentially constraining the extent of the Ijen hydrothermal system and placing important constraints on the hydrology of the Banyu Pahit valley.

Further chemical characterization of different sources of fluids to the upstream Banyu Pahit and quantification of their contributions will follow. These results will be used in conjunction with fluid-rock modeling of this section of the stream and discharge measurements in an end-member mixing analysis to quantify the respective contributions to the Banyu Pahit stream of crater lake seepage, hydrothermal fluids and groundwater. Detailed geological mapping of the stream valley by van Hinsberg during this same field season will help refine models of fluid-rock interaction.

### ACKNOWLEDGEMENTS

We would like to thank Glyn Williams-Jones, Nathalie Vigouroux, Guillaume Mauri, Eline Mignot, and Carole Gilbert for assistance, guidance and inspiration,

Jean-Francois Hélie, Bill Minarik, Glenna Keating, and Isabelle Richer for assistance with various chemical analyses, and Michel Baraer and Bernardo Brixel from the Hydrogeology lab group at McGill University. The research was supported by an NSERC Discovery grant to JMM and AEWJ.

### REFERENCES

- CHRISTOPHERSEN, N., NEAL, C., HOOPER, R.P., VOGT, R.D., & ANDERSEN, S. 1990. Modelling streamwater chemistry as a mixture of soilwater end-member – a step towards second generation acidification models. *Journal of Hydrology*, **116**, 307-320.
- DELMELLE, P. & BERNARD, A. 1994. Geochemistry, mineralogy, and chemical modeling of the acid crater lake of Kawah Ijen Volcano, Indonesia. *Geochimica et Cosmochimica Acta*, **58 (11)**, 2445-2460.
- DELMELLE, P., BERNARD, A., KUSAKABE, M., FISCHER, T.P., & TAKANO, B. 2000. Geochemistry of the magmatic-hydrothermal system of Kawah Ijen volcano, East Java, Indonesia. *Journal of Volcanology and Geothermal Research*, **97**, 31-53.
- DELMELLE, P. & BERNARD, A. 2000. Downstream composition changes of acidic volcanic waters discharged into the Banyupahit stream, Ijen caldera, Indonesia. *Journal of Volcanology and Geothermal Research*, **97**, 55-75.
- EDMUNDS, W. & P.L. SMEDLEY. 1996. Groundwater geochemistry and health: An overview. *Geological Society, London, Special Publications*, **113**, 91-105.
- LOHR, A.J., BOGAARD, T.A., HEIKENS, A., HENDRIKS, M.R., SUMARTI, S., VAN BERGEN, M.J., VAN GESTEL, C.A.M., VAN STRAALLEN, N.M., VROON, P.Z., & WIDIANARKO, B. 2005. Natural pollution caused by the extremely acidic crater lake Kawah Ijen, East Java, Indonesia. *Environmental Science & Pollution Research*, **12(2)**, 89-95.
- PARNELL, R.A. & BURKE, K. 1990. Impacts of acid emissions from Nevado del Ruiz volcano, Columbia, on selected terrestrial and aquatic ecosystems. *Journal of Volcanology and Geothermal Research*, **42**, 69-88.
- PRINGLE, C.M., ROWE, G.L., TRISKA, F.J., FERNANDEZ, J.F., & WEST, J. 1993. Landscape patterns in the chemistry of geothermally-impacted streams draining Costa Rica's Atlantic slope: Geothermal

- processes and ecological response. *Limnological Oceanography*, **38(4)**, 753-774.
- SCHAEFER, J.R., SCOTT, W.E., EVANS, W.C., JORGENSEN, J., MCGIMSEY, R.G., & WANG, B., 2008. The 2005 catastrophic acid crater lake drainage, lahar, and acidic aerosol formation at Mount Chiginagak volcano, Alaska, USA: Field observations and preliminary water and vegetation chemistry results, *Geochem. Geophys. Geosyst.*, **9(7)**, Q07018.
- SRIWANA, T., VAN BERGEN, M.J., SUMARTI, S., DE HOOG, J.C.M., VAN OS, B.J.H., WAHYUNINGSIH, R., & DAM, M.A.C. 1998. Volcanogenic pollution by acid water discharges along Cidiwey River, West Java (Indonesia). *Journal of Geochemical Exploration*, **62**, 161-182.
- VAN HINSBERG, V.J. 2001. *Water-rock interaction and element fluxes in the Kawah Ijen hyperacid crater lake and the Banyu Pahit river, East Java, Indonesia*. M.Sc. Thesis, Utrecht University, Amsterdam.
- VAN HINSBERG, V.J., WILLIAMS-JONES, A., MAURI, G., VIGOUROUX, N., WILLIAMS-JONES, G., PALMER, S., MCKENZIE, J., & NASUTION, A. 2008. Studying the Kawah Ijen volcano-hydrothermal system; merits of an interdisciplinary approach. *IAVCEI conference proceedings*, Reykjavik, Iceland, August 17-22.



## Land use/land cover influences on the estimated time to recovery of inland lakes from mercury enrichment

Matthew J. Parsons<sup>1</sup> & David T. Long<sup>1</sup>

<sup>1</sup>Michigan State University Department of Geological Sciences, 206 Natural Science, East Lansing, MI 48114 (email: long@msu.edu)

**ABSTRACT:** Sediment chronologies have been demonstrated to be reliable archives of the environmental record of mercury (Hg). We questioned if chronologies could be used to investigate the stressors related to time to recovery (TTR) from mercury enrichment to multiple future system states. Sediment cores from 30 inland lakes of Michigan were collected between 1999 and 2005, analyzed for total Hg, and dated using 210-lead. Linear models of recovery were calculated based on most recent decreasing trends of concentration or Hg flux to estimate the time required to reach geochemical background concentration and flux and current rates of Hg deposition. Predicted TTR were then compared to current watershed attributes. Results indicate that estimated TTR for background concentrations is positively influenced by agricultural and forested land use found along flow paths to the lakes. Whereas, urban land use along flow paths and watershed to lake area ratio may be more influential when compared to current wet deposition measurements. There were far weaker relationships between TTR and local Hg emission rates, suggesting that the watershed pathway may play a more significant role in the recovery of these systems.

**KEYWORDS:** mercury, 210-lead, land use, recovery, sediment chronologies

### INTRODUCTION

Anthropogenic activity has lead to Hg contamination of aquatic systems in the most remote places on the surface of Earth (Fitzgerald, *et al.*, 1998). This is due, primarily, to its unique physical properties that allow long range transport of Hg and deposition far from the original source. Due to its threat to ecological and human health in its methylated form it is important to understand the sources and pathways of Hg to aquatic systems. Sediment chronologies have been demonstrated to be reliable archives of the environmental history of lakes (Engstrom, *et al.*, 1994) and have been used to document the enrichment of Hg in aquatic systems due to human activities (Benoit, *et al.*, 1998; Swain, *et al.*, 1992). Sediment chronologies have been useful both for scientific inquiry and environmental management. For example, information from sediment chronologies demonstrates that removal of Pb from gasoline has resulted in the decreased loading to the environment since the enactment of environmental legislation in

the 1970s. Furthermore, it is suggested that abatement technologies for nitrogen and sulphur species has lead to the decreased emission of Hg from coal-fired power plants, this combined with decreased consumption explaining the decreased concentrations and loadings found in recent sediments of inland lakes (Engstrom & Swain, 1997). Therefore, since sediment chronologies have been used to demonstrate the environmental record of Hg accumulation we question whether they can be used to understand environmental recovery of the watershed.

Environmental recovery is commonly defined as a return of the system to a previously undisturbed state. Using sediment geochemical chronologies the previous undisturbed state can be determined graphically as the geochemical background concentration prior to anthropogenic disturbance. In the US, geochemical background concentration is usually defined as the concentration in sediment prior to European settlement ca. 1800. However, until environmental legislation is enacted

worldwide to eliminate Hg emission, geochemical background concentrations may not be an achievable system state. A better approach may be to consider different system states as more achievable scenarios. For this work we consider three separate definitions of system recovery 1) geochemical background concentrations, 2) geochemical background fluxes and 3) current rates of Hg wet deposition. Time to recovery from Hg contamination was then estimated using a linear model based on the most recent decreasing trajectory.

The primary pathway of Hg to aquatic systems is considered to be atmospheric transport and subsequent deposition, which has caused an accumulation of Hg in watershed soils (Mason, *et al.*, 1994). Recent work has shown that watershed disturbance such as clear cutting results in the increased export of Hg from the watershed to aquatic systems (Porvari, *et al.*, 2003) and others have found agricultural and urbanized land use to be important factors influencing Hg export (Fitzgibbon, *et al.*, 2008; Mason & Sullivan, 1998). Thus the recovery of aquatic systems from anthropogenic Hg may depend on watershed characteristics which will differ among watersheds. Therefore we compared time to recovery to watershed attributes (e.g., %urban, susceptibility to erosion, watershed to lake area ratio, etc...) to test the hypothesis that the rate of recovery from Hg enrichment is influenced by watershed controlled pathways and stressors.

### STUDY AREA AND METHODS

The State of Michigan spans a large geographic range and contains more than 10,000 lakes that vary in watershed land use from highly urban in the Southeast to agricultural watersheds midway through the state and highly forested watersheds in its Upper Peninsula. Between 1999 and 2005 30 sediment cores were collected aboard the Environmental Protection Agency R/V *Mudpuppy* or Michigan Department of Environmental Quality M/V *Nibi* using an Ocean Instruments MC-400 Lake/Shelf

Multicorer. The MC-400 collects four simultaneous cores two of which were analyzed for total metals and 210-lead, respectively. Details of field methods, Hg analyses and 210-lead interpretation can be found elsewhere (Parsons, *et al.*, 2007).

Watershed attributes were determined using Arcview. Watersheds were delineated using the *watershed* command in ArcView on National Elevation Dataset digital elevation models (DEM) from the United States Geological Survey (USGS, 2008). Landuse/land cover data were obtained from the Michigan Geographic Data Library (MDNR, 2002). Soils data were taken from the United States Department of Agriculture's State Soil Geographic Database (USDA, 1994). Mercury emissions for the State of Michigan were obtained from the National Emissions Inventory for 2002 (Granke, 2006). Mercury deposition at the lake location was estimated by interpolation of regional wet deposition flux data for 2007 obtained from the Mercury Deposition Network (Illinois State Water Survey, 2008). Statistical analyses were performed in R<sup>®</sup>.

### RESULTS

Of the 30 lakes that were cored 9 reached geochemical background concentrations and had current concentrations and/or fluxes that are decreasing to present. Five additional lakes that did not reach geochemical background were included for comparison to current wet deposition. Linear models of recovery were estimated on the most recent decreasing trend of concentration and/or flux and by ignoring episodic or short term increases in fluxes or concentrations (Fig. 1).

Time to recovery (TTR) was calculated as the difference between the estimated time to system state (e.g., current wet deposition) and the year the lake was sampled. TTR varied from 0 to more than 134 y for recovery to wet deposition, from 8 to 168 y for background flux and from 9 to 70 y for background concentration. There was no consistent pattern among the estimates of TTR, that is, no single

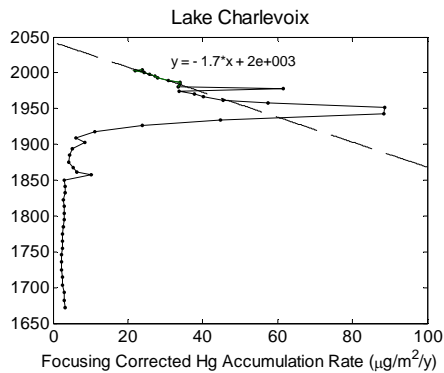


**Fig. 1.** Focusing corrected Hg accumulation rate for Lake Charlevoix.

definition of recovery (e.g., wet deposition) always produced the greatest TTR. However, of the 6 lakes in which all three recovery states were able to be calculated background concentration was greatest in 4 of them.

Correlation coefficient p-values were calculated and are shown in Table 1 for a select group of watershed attributes. Background concentrations were significantly correlated to flow-inverted agricultural land use. Flow-inverted landuse (FLI) is the product of the inverse of the flowlength, determined using the *flowlength* command in ArcView, and individual land use. This calculation provides more weight to those land uses along flowpaths and/or close to the lakeshore. Similarly flow-inverted-squared landuse (FLI2) was calculated as the inverse of the product of the inverse of the squared flowlength and individual land use. Background concentration was also significantly correlated to Forest FLI2. Wet deposition TTR was most highly correlated to Urban FLI2, but only when a subset of the original data was used. There was also a significant correlation between watershed area and TTR to wet deposition. Background flux showed significant correlation to watershed to lake area ratio, but only when the highest TTR was removed from the dataset. Results of Hg emissions, from Michigan industry, within a 25 km radius of the lake centre are shown in Table 1. Although not shown, the 25 km data are consistent with emissions calculated at 10, 50, 75, and

**Table 1.** P-value correlation matrix of TTR for selected watershed attributes. Watershed attributes significant at  $p < 0.05$  are shown

Attribute	Wet	BG	BG
	Dep	Conc	Flux
Ag FLI	0.66	<b>4E-5</b>	0.83
Urban FLI	<b>3E-3</b>	0.10	0.80
Forest FLI2	0.29	<b>8E-3</b>	0.32
Hg.25	0.85	0.11	0.72
Watershed Area	<b>3E-3</b>	0.18	<b>0.015</b>

100 km radii in that no significant correlations at the  $p < 0.05$  level were found. Additionally, no single watershed attribute was consistent across all definitions of recovery at  $p < 0.05$ .

## DISCUSSION

Previous work has shown that urbanization and agricultural land uses increase the flux of Hg to river systems through the increase of impervious surface and erosion of soils, respectively (Mason & Sullivan, 1998). Thus, the correlation of TTR using background concentration to agricultural FLI might be expected, but the relationship was not manifested in the percentage of agricultural landuse within the watershed as it was in previous work (Fitzgibbon, *et al.*, 2008; Lyons, *et al.*, 2006). Rather this work indicates more specifically that it is those agricultural landscapes that lie along flowpaths to the lake that provided the better correlation. This suggests a significant pathway for Hg to inland lakes and may help in the management of watersheds. Although flowpath-based relationships have been found for sediment based work (Randhir & Hawes, 2009), to the authors knowledge these relationships have not been demonstrated for mercury's pathway to lakes. The poor correlation to emission of Hg within the State of Michigan provides further evidence for watershed attributes as important stressors for TTR, but may also indicate that the emission source variable needs to be broadened to regional scales or calculated using geometry other than circular geometry. The absence of a single consistent watershed attribute across all definitions of recovery suggests a change

of source from short (i.e., wet deposition) to long TTR (i.e., background concentration). This may be indicative of long term storage in agricultural and forest landscapes versus short term storage in more urban landscapes.

## CONCLUSIONS

The expected recovery time for lakes enriched by anthropogenic Hg additions varies based on the definition used for recovery. Watershed attributes (e.g., Ag FLI) were found to be important stressors and more highly correlated to TTR than Hg emissions within the State of Michigan. This suggests that a watershed approach should be considered when dealing with the recovery of environmental system and that reducing Hg emissions alone may not result in reduced fluxes of Hg to aquatic systems.

## ACKNOWLEDGEMENTS

We would like to thank: the Michigan Department of Environmental Quality for the funding of this work; the captain and crew of the R/V *Mudpuppy* and M/V *Nibi* for their assistance in core collection and Paul Wilkinson of the Freshwater Institute for help in the analysis and interpretation of 210-lead results.

## REFERENCES

- BENOIT, J. M., FITZGERALD, W. F. & DAMMAN, A. W. H. 1998. The biogeochemistry of an ombrotrophic bog: Evaluation of use as an archive of atmospheric mercury deposition. *Environmental Research*, **78**, 118-133.
- ENGSTROM, D.R. & SWAIN, E.B. 1997. Recent declines in atmospheric mercury deposition in the upper Midwest. *Environmental Science and Technology*, **31**, 960-967.
- ENGSTROM, D.R., SWAIN, E.B., HENNING, T.A., BRIGHAM, M.E. & BREZONIK, P.L. 1994. Atmospheric Mercury Deposition to Lakes and Watersheds - a Quantitative Reconstruction from Multiple Sediment Cores. In: *Environmental Chemistry of Lakes and Reservoirs*. 33-66.
- FITZGERALD, W. F., ENGSTROM, D. R., MASON, R.P. & NATER, E. A. 1998. The case for atmospheric mercury contamination in remote areas. *Environmental Science and Technology*, **32**, 1-7.
- FITZGIBBON, T.O., LYONS, W. B., GARDNER, C.B. & CAREY, A.E. 2008. A preliminary study of the Hg flux from selected Ohio watersheds to Lake Erie. *Applied Geochemistry*, **23**, 3434-3441.
- GRANKE, L. 2006. 2002 Estimates of Anthropogenic Mercury Air Emissions in Michigan. Michigan Department of Environmental Quality.
- Follow: Illinois State Water Survey, NADP Program Office, 2204 Griffith Drive, Champaign, IL 61820, NADP Program Office, Illinois State Water Survey, February 5, 1998, <http://nadp.sws.uiuc.edu/mdn/>
- LYONS, W.B., FITZGIBBON, T.O., WELCH, K.A., & CAREY, A.E. 2006. Mercury geochemistry of the Scioto River, Ohio: Impact of agriculture and urbanization. *Applied Geochemistry*, **21**, 1880-1888
- MASON, R.P., FITZGERALD, W.F. & MOREL, F.M. 1994. The biogeochemical cycling of elemental mercury: anthropogenic influences. *Geochimica et Cosmochimica Acta*, **58**, 3191-3198.
- MASON, R.P. & SULLIVAN, K.A. 1998. Mercury and methylmercury transport through an urban watershed. *Water Research*, **32**, 321-330
- PARSONS, M.J., LONG, D.T., YOHAN, S.S. & GIESY, J. P. 2007. Spatial and Temporal Trends of Mercury Loadings to Michigan Inland Lakes. *Environmental Science and Technology*, **41**, 5634-5640
- PORVARI, P., VERTA, M., MUNTHE, J., & HAAPANEN, M. 2003. Forestry practices increase mercury and methyl mercury output from boreal forest catchments. *Environmental Science & Technology*, **37**, 2389-2393.
- RANDHIR, T.O. & HAWES, A.G. 2009. Watershed land use and aquatic ecosystem response: Ecohydrologic approach to conservation policy. *Journal of Hydrology*, **364**, 182-199.
- SWAIN, E.B., ENGSTROM, D.R., BRIGHAM, M.E., HENNING, T.A., & BREZONIK, P.L. 1992. increasing rates of atmospheric mercury deposition in Midcontinental North America. *Science*, **257**, 784-787.
- Follow: The National Map Seamless Server, <http://seamless.usgs.gov/index.php>

## Potential for contamination of deep aquifers in Bangladesh by pumping-induced migration of higher arsenic waters

**Kenneth G. Stollenwerk**

*U.S. Geological Survey, MS 413, Box 25046, Denver, CO, 80225, USA;*

*(e-mail: [kgstolle@usgs.gov](mailto:kgstolle@usgs.gov))*

**ABSTRACT:** Recognition of arsenic (As) contamination in shallow, geochemically reducing aquifers in the Bengal Basin has resulted in increasing exploitation of groundwater from deeper aquifers that are generally more oxic and contain low concentrations of dissolved As. Pumping-induced infiltration of high-As groundwater could eventually cause As concentrations in the deeper aquifers to increase. Laboratory batch and column experiments on oxic sediments from a site near Dhaka, Bangladesh were used to identify and quantify geochemical reactions that could control transport of As and other constituents in contaminated groundwater through these sediments. Results from these experiments were used to simulate the potential rate of As transport through the oxic aquifer at the sampling site using the reactive-solute transport model PHAST, which couples hydrologic flow with geochemical reactions. Initial As concentrations in the simulations were 900  $\mu\text{g/L}$ . Interstitial velocity of contaminated groundwater through the oxic aquifer ranged from 3 m/yr to 30 m/yr. Modeling results showed that As reactions with sediments slowed the movement of As through the oxic aquifer to a rate of 0.01 m/yr for an interstitial velocity of 3 m/yr, and 0.22 m/yr for a velocity of 30 m/yr. Results from these experiments show that the oxic sediments have a significant but finite capacity to remove As from solution. Therefore, well screen depth below the anoxic/oxic boundary as well as rate of withdrawal need to be considered in locating new wells in low-As aquifers.

**KEYWORDS:** *arsenic, groundwater, Bangladesh, sediment reactions, transport modeling,*

### INTRODUCTION

Arsenic concentrations in shallow alluvial aquifers of the Bengal Delta Plain often exceed 10  $\mu\text{g/L}$  and are a major health concern for the millions of people who rely on these aquifers for drinking water. These aquifer sediments are typically reducing and gray in color. In solution arsenic occurs predominantly as As(III) along with some As(V). Drilling and coring in some parts of Bangladesh by the U.S. Geological Survey and others has revealed the presence of low-As (<10  $\mu\text{g/L}$ ) groundwater in oxidized sediments beneath the high-As aquifers. These oxidized sediments contain iron oxides and have the potential to attenuate As into deeper aquifers that have been proposed as a long-term and safe source of drinking and irrigation water.

### METHODS

Laboratory batch and column experiments were used to identify and quantify

processes affecting transport of arsenic through sediments collected from an oxidized aquifer at a site located about 10 km west of Dhaka, Bangladesh (Stollenwerk *et al.* 2007). Arsenic concentrations in groundwater associated with these oxic sediments were <5 $\mu\text{g/L}$ . The highest As concentrations in contaminated groundwater were 900  $\mu\text{g/L}$  at this site, 650  $\mu\text{g/L}$  as As(III) and 250  $\mu\text{g/L}$  as As(V).

Data from the laboratory experiments were used to calibrate a geochemical model capable of simulating the reactions between constituents in As-contaminated groundwater and oxic sediments. The reactive-solute transport model, PHAST (Parkhurst *et al.* 2004), which couples hydrologic flow with geochemical reactions, was then used to simulate the potential rate of As transport through the oxic aquifer at the sampling site. A range of As concentrations and groundwater velocities were simulated. Results

presented here are for an initial As concentration of 650  $\mu\text{g/L}$  As(III) and 250  $\mu\text{g/L}$  As(V). Simulated interstitial groundwater velocities were from 3 m/yr to 30 m/yr.

## RESULTS AND DISCUSSION

### Laboratory Experiments

Several reactions between constituents in As-contaminated groundwater and oxic sediments controlled As mobility in the laboratory experiments. Adsorption was the primary mechanism for removing As from solution. The adsorption capacity of the oxic sediments was a function of the concentration and oxidation state of As, and the concentration of other solutes that competed for adsorption sites. Although As(III) was the dominant oxidation state in contaminated groundwater, data from the laboratory experiments showed that As(III) was oxidized to As(V) by manganese oxide minerals that are present in the oxic sediment. Phosphate in contaminated groundwater caused a substantial decrease in As(V) adsorption. Silica, bicarbonate and pH caused only a small decrease in As adsorption.

Reactions between Fe(II) in contaminated groundwater (5.8 mg/L) and oxic sediment also affected As mobility. Ferrous iron was oxidized by manganese oxides to ferric iron which precipitated as hydrous ferric oxide, creating additional sorption sites. Evidence for this reaction included an increase in ferric oxide concentrations in reacted column sediments and manganese concentrations in leachate that were greater than in the initial eluent.

Measured concentrations of As(III) and As(V) in leachate from a column experiment are compared with simulated concentrations using the model PHAST in Figure 1. Arsenic concentrations in leachate were below detection for the first 50 pore volumes of contaminated groundwater eluted through the column. Although initial As(III) concentrations were 650  $\mu\text{g/L}$ , oxidation of As(III) to As(V) by manganese oxides resulted in leachate concentrations of As(III) near detection limits for 270 pore volumes. All of the As

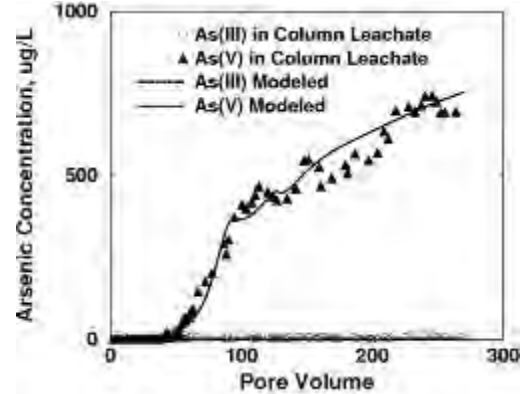


**Fig. 1.** Measured and modeled concentration of As(III) and As(V) in leachate from column experiment. Initial As(III) concentration = 650  $\mu\text{g/L}$ ; initial As(V) concentration = 250  $\mu\text{g/L}$ . (Note: As(III) modeled concentrations were <1  $\mu\text{g/L}$  and plot along bottom of x-axis.)

measured in leachate was present as As(V). The model simulated the As(III) and As(V) concentrations reasonably well.

### Field Scale Modeling

Extrapolation of laboratory results to the field scale is at best qualitative because of the complexity of the geochemical and hydrological systems in the Bengal Basin. Movement of As-contaminated groundwater towards a well screened in the uncontaminated aquifer is likely to contain both vertical and horizontal components of flow. For modeling purposes presented here, a relatively slow interstitial groundwater velocity of 3 m/yr (Stollenwerk et al. 2007) is compared with a more rapid interstitial velocity of 30 m/yr (McArthur et al. 2008).

For groundwater with 900  $\mu\text{g/L}$  As moving into an oxic aquifer similar to our site at an interstitial velocity of 3 m/yr, the rate of transport of an As front defined as a concentration of 10  $\mu\text{g/L}$  was simulated to be 0.01 m/yr. For an interstitial velocity of 30 m/yr, the rate of transport of a 10  $\mu\text{g/L}$  front of As was simulated to be 0.22 m/yr.

## CONCLUSIONS

(1) Transport of As in contaminated groundwater through low-As oxic

sediments is inhibited by a complex set of reactions which include adsorption/desorption, precipitation/dissolution, and rate-controlled oxidation/reduction.

(2) Oxidic sediments have a significant but finite capacity to remove As from solution.

(3) The rate of As contamination of low-As aquifers as a result of pumping for drinking and irrigation water supply increases with As concentration and the rate of groundwater withdrawal.

## REFERENCES

- MCARTHUR, J.M., RAVENSCROFT, P., BANERJEE, D.M., MILSOM, J. HUDSON-EDWARDS, K.A., SENGUPTA, S., BRISTOW, C., SARKAR, A., TONKIN, S., & PUROHIT, R. 2008. How palaeosols influence groundwater flow and arsenic pollution: a model from the Bengal Basin and its worldwide implication. *Water Resources Research*, **44**, W11411.
- PARKHURST, D., KIPP, K., ENGESGAARD, P., & CHARLTON, S. 2004. *PHAST – A program for simulating ground-water flow, solute transport, and multicomponent geochemical reactions*. U.S. Geological Survey Techniques and Methods 6-A8.
- STOLLENWERK, K.G., BREIT, G.N., WELCH, A.H., YOUNT, J.C., WHITNEY, J.W., FOSTER, A.L., UDDIN, M.N., MAJUMDER, R.K., & Ahmed, N., 2007. Arsenic attenuation by oxidized aquifer sediments in Bangladesh. *Science of the Total Environment*, **379**, 133-150.



**CURRENT CAPABILITIES AND FUTURE PROSPECTS OF REAL-TIME, IN-FIELD GEOCHEMICAL ANALYSIS**

EDITED BY:

**RUSSELL S. HARMON  
NANCY McMILLAN**



## LIBS-based geochemical fingerprinting for the rapid analysis and discrimination of minerals – the example of garnet

Daniel C. Alvey<sup>1</sup>, Jeremiah J. Remus<sup>2</sup>, Russell S. Harmon<sup>3</sup>,  
Jennifer L. Gottfried<sup>4</sup>, & Kenneth Morton<sup>2</sup>

<sup>1</sup> U.S. Military Academy, West Point, NY, 10996 USA

<sup>2</sup> Electrical and Computer Engineering, Duke University, Durham, NC, 27708 USA

<sup>3</sup> ARL Army Research Office, 4300 S. Miami Blvd., Durham NC, 27703 USA

(email: russell.harmon@us.army.mil)

<sup>4</sup> U.S. Army Research Laboratory, Aberdeen Proving Ground, MD, 21005 USA

**ABSTRACT:** In this study, statistical classification techniques have been applied to LIBS data for a large suite of garnets of different composition from different places around the world. Each broadband LIBS spectrum contains measured light intensities between 200 and 880 nm collected over 13,600 channels in a CCD spectrometer. The Matlab<sup>®</sup> program was used to perform a high-dimensional principal components analysis (HDPCA) on the data set. Individual garnet LIBS spectra were grouped according to the similarities in the linear combination of their principal components. Because of the large volume of data and the ability of Matlab<sup>®</sup> to display results in multiple dimensions, an accurate model could be created that was able to successfully classify unknown garnet samples of a specific composition type according to their geographic origin.

**KEYWORDS:** *Laser-induced breakdown spectroscopy, garnet, LIBS, multivariate principal components analysis, geochemical fingerprinting*

### INTRODUCTION

The ability to geographically identify the source area of natural gems plays an important role in determining if these stones may have originated from a politically unstable area. Garnet is a semi-precious silicate mineral of variable composition that has been used as a gemstone since the Bronze Age.

In LIBS, a pulsed laser beam is focused on a sample such that energy absorption produces a high-temperature microplasma at the sample surface. Small amounts (nanograms) of material are dissociated and ionized, with both continuum and atomic/ionic emission generated by the plasma during cooling. A broadband spectrometer-detector is used to spectrally- and temporally-resolve the light from the plasma and record the intensity of elemental emission lines. Since the technique is simultaneously sensitive to all elements, a single laser shot can be used to record the broadband LIBS emission spectra, which are unique chemical 'fingerprints' of a material.

### BACKGROUND

The garnet group of minerals can be described by the general compositional formula  $A_3B_2(SiO_4)_3$ , where A and B refer respectively to cation sites 8-fold and 6-fold coordination. The A sites are occupied by rather large divalent cations, whereas the B sites host smaller trivalent cations. Garnets occur in many different geologic settings, which typically determine the particular species of garnet present. The six common species of garnet comprise two groups on the basis of their ideal end-member chemical compositions as follows: The Pyrope Garnet Group consists of Almandine [ $Fe_3Al_2(SiO_4)_3$ ], Pyrope [ $Mg_3Al_2(SiO_4)_3$ ], and Spessartine [ $Mn_3Al_2(SiO_4)_3$ ] whereas the Ugrandite Garnet Group comprises Andradite [ $Ca_3Fe_2(SiO_4)_3$ ], Grossular [ $Ca_3Al_2(SiO_4)_3$ ], and Uvarovite [ $Ca_3Cr_2(SiO_4)_3$ ]. Six other minor species of garnet occur in nature, but are not common.

**RESULTS**

In this study, we acquired broadband LIBS spectra at the Army Research Laboratory for more than 125 garnet samples from 76 different locations worldwide. Sets of 25 single laser shot broadband spectra were for 28 spessartines, 37 andradites, 32 grossulars, 12 pyropes, 26 almandines, and 10 uvarovites. The resultant garnet LIBS spectral database was analyzed by multivariate statistical analysis after averaging the LIBS spectra for each sample.

Broadband LIBS spectra for three garnet types – the Mg-Al pyrope type, the Ca-Al grossular type, and the Mn-Al spessartine type are shown in Figure 1.

The high dimensional nature of LIBS signals can lead to several computational issues when used in conjunction with many machine learning techniques. Dimensionality reduction is the process by which the high dimensional signals are mapped into a lower dimensional space. The resulting lower dimensional space can enable more robust performance when used in conjunction with pattern recognition techniques.

Principal components analysis (PCA) is a standard technique for dimensionality reduction that finds a linear mapping from the high dimensional space to a lower dimension space. The linear mapping is chosen to maximize the variance in the resulting lower dimensional space and is determined by performing an Eigen-decomposition on the covariance matrix of the observation dimensions. Due to memory limitations, the required covariance matrix cannot be calculated when the number of observation dimensions is extremely large, as is the case with LIBS signals. This work utilizes an alternate formulation of PCA that is applicable to datasets with high dimensional observations, high dimensional PCA (HDPCA) (Bishop, 2007). HDPCA calculates the covariance matrix of the observations instead of the observation dimensions. Therefore, for data sets containing fewer observations than observation dimensions, such as LIBS signals, HDPCA provides a tractable

method for performing dimensionality reduction.

The results of the HDPCA analysis for the 4 groups of spessartine garnets from locations in Australia, China, Brazil, and Virginia are shown in Figures 2 and 3. The K-nearest-neighbour analysis (K=5, in two dimensions, 2<sup>nd</sup> and 3<sup>rd</sup>) results in a 93.3% correct sample classification (Fig. 2). The shaded areas corresponding to the symbols in the legend are the areas most likely to find an unknown sample from that region. By comparison, the results of the 'leave-one-out' classification analysis shown in Figure 3 results in a slightly higher classification success at 94.6%. Figure 4 shows the classification

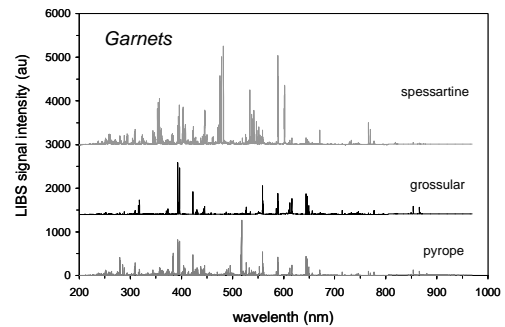


**Fig.1.** Example broadband LIBS spectra for a pyrope, grossular, and spessartine garnet. The clear differences observed in the broadband spectra reflect the chemical differences in the composition of the three garnets.

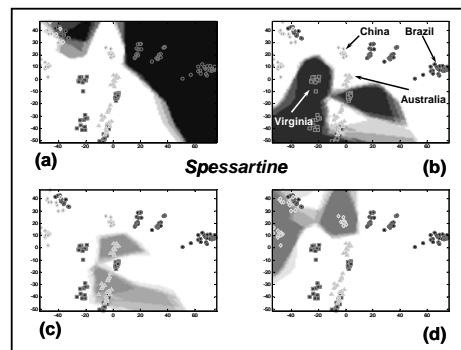
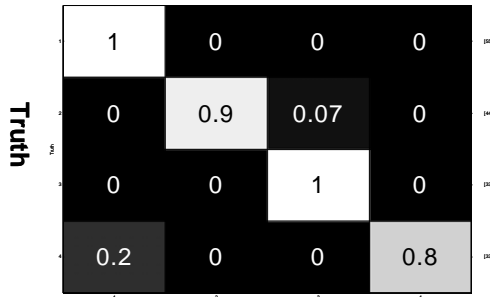


**Fig. 2.** Plots of 2<sup>nd</sup> principal component scores (x-axis) versus 3<sup>rd</sup> principal component scores (y-axis) showing the regions of space where unknown spessartine data points would be classified as originating from one of the four geographic locations: Brazil, Virginia, Australia, and China, clockwise from upper right, respectfully.



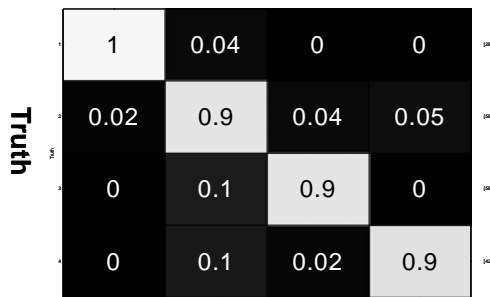
**Classification Assignment**

**Fig. 3.** Confusion matrix for the HDPCA analysis of four spessartine garnets from different locations worldwide. The nth row and column correspond to the nth spessartine type truth and HDPCA statistical assignment, respectively.



**Classification Assignment**

**Fig. 5.** Confusion matrix for the HDPCA analysis of the four grossular garnets. The nth row and column correspond to the nth grossular type truth and HDPCS statistical assignment, respectively.



**Classification Assignment**

**Fig. 4.** Confusion matrix for the HDPCA analysis of the four pyrope garnets. The nth row and column correspond to the nth pyrope type truth and HDPCS statistical assignment, respectively.

confusion matrix for four groups of pyrope garnet from North Carolina, the Kimberly area of South Africa, Arizona, and Bohemia, in the Czech Republic. Figure 5 shows the confusion matrix for four groups of grossular garnet from the Inyo City area of California, Vermont, the Asbestos area of Quebec in Canada, and the Coaluila area of Mexico.

**CONCLUSIONS**

Important attributes of a LIBS sensor system for geochemical analysis include (i) real-time response, (ii) in-situ analysis with no sample preparation required; (iii) a high sensitivity to low atomic weight elements which are often difficult to determine by other techniques, and (iv) standoff detection. LIBS technology is now sufficiently mature, inherently rugged, and affordable to offer a capability for both laboratory and field-deployable analysis. A successful laboratory benchtop feasibility study of garnets has been conducted that highlights the potential of LIBS for mineralogical identification and classification.

**REFERENCES**

BISHOP, C.M. 2007. *Pattern Recognition and Machine Learning*, Springer.



## The U-tube sampling methodology and real-time analysis of geofluids

Barry Freifeld<sup>1</sup>, Ernie Perkins<sup>2</sup>, James Underschultz<sup>3</sup>, & Chris Boreham<sup>4</sup>

<sup>1</sup>Lawrence Berkeley National Laboratory, Berkeley, CA USA (bmfreifeld@lbl.gov)

<sup>2</sup>Alberta Research Council, Edmonton, AB CANADA

<sup>3</sup>CSIRO Petroleum & CO2CRC, Bentley, WA AUSTRALIA

<sup>4</sup>Geoscience Australia & CO2CRC, Canberra, ACT AUSTRALIA

**ABSTRACT:** The U-tube geochemical sampling methodology, an extension of the porous cup technique proposed by Wood (1973), provides minimally contaminated aliquots of multiphase fluids from deep reservoirs and allows for accurate determination of dissolved gas composition. The initial deployment of the U-tube during the Frio Brine Pilot CO<sub>2</sub> storage experiment, Liberty County, Texas, obtained representative samples of brine and supercritical CO<sub>2</sub> from a depth of 1.5 km. A quadrupole mass spectrometer provided real-time analysis of dissolved gas composition. Since the initial demonstration, the U-tube has been deployed for (1) sampling of fluids down gradient of the proposed Yucca Mountain High-Level Waste Repository, Armagosa Valley, Nevada (2) acquiring fluid samples beneath permafrost in Nunuvut Territory, Canada, and (3) at a CO<sub>2</sub> storage demonstration project within a depleted gas reservoir, Otway Basin, Victoria, Australia. The addition of in-line high-pressure pH and EC sensors allows for continuous monitoring of fluid during sample collection. Difficulties have arisen during U-tube sampling, such as blockage of sample lines from naturally occurring waxes or from freezing conditions; however, workarounds such as solvent flushing or heating have been used to address these problems. The U-tube methodology has proven to be robust, and with careful consideration of the constraints and limitations, can provide high quality geochemical samples.

**KEYWORDS:** *geochemical sampling, carbon sequestration, borehole sampling, fluid sampling*

### INTRODUCTION

Obtaining uncontaminated fluid samples from deep geologic aquifers is challenging because of the elevated pressures and temperatures encountered. Entering wellbores that are under pressure and which may contain explosive or sour gas is a complex task that requires the deployment of well-head pressure control equipment along with cranes or workover rigs to utilise wireline conveyed samplers. The technology to maintain fluid sample integrity during recovery has been developed primarily within the oilfield and geothermal service industries, with examples of commercially available instruments being: Schlumberger's MDT fluid sampler; Halliburton's Armada Sampling System; and Kuster Corporation's flow through sampler. All three of these sampling devices are mechanically complex and need to be conveyed into and out of a wellbore to facilitate each sample recovery.

The U-tube was developed to simplify the recovery of fluids from deep boreholes and allow flexibility for post-sampling analysis (Freifeld *et al.* 2005; Freifeld & Trautz 2006). In particular, the ability to repeatedly collect large volume multiphase samples into high pressure cylinders facilitates both real-time field analysis as well as acquisition of sample splits for future laboratory based analysis.

### U-TUBE OPERATION

The U-tube is permanently or semi-permanently deployed in a wellbore to provide the ability to periodically (or continuously) acquire samples. The U-tube is extremely simple, consisting of a loop of tubing, which has a tee at its base, terminating at a check valve that permits fluid to enter the loop of tubing (Fig. 1). A filter at the inlet removes particulates that can interfere with the operation of the check valve. At the surface, the U-tube drive leg is connected to a supply of high pressure N<sub>2</sub> that closes the check valve



**Fig. 1.** Schematic layout of the downhole equipment for deploying a U-tube geochemical sampler.

and forces the sample that collects within the loop of tubing up the sample leg to the surface.

In its most basic form the surface sampling equipment can consist of an open container at which the sample leg terminates. However, for higher purity sampling or accurate dissolved gas chemistry analysis, the sample is directed into N<sub>2</sub> purged and/or evacuated high pressure sample cylinders. After a sample has been acquired, by venting both the sample and drive legs to atmospheric pressure, the check valve is allowed to open and fresh sample enters the U-tube sampling loop.

### U-TUBE DEPLOYMENT

To date, we have deployed the U-tube using several distinct modalities depending on the wellbore completion requirements. As part of Nye County's Nuclear Waste Repository Early Warning groundwater monitoring program, a borehole in the Amargosa Valley, Nevada, USA, was completed with four U-tubes within two sand packs. At depths of 265 m and 350 m, two U-tubes were located within each sandpack and isolated using a bentonite backfill.

At the High Lake Site in Nunuvut Territory, Canada, a 7.5 cm diameter mineral exploration boring was completed with a U-tube to sample sub-permafrost brines (Freifeld *et al.* 2008). Small gage (1/4") stainless steel tubing served as the drive and sample legs of the U-tube as well as functioned as the strength member for lowering the U-tube and pneumatic packer to a depth of ~400 m. To prevent freezing within the sampling lines a heat trace providing 20 W/m was run along the entire length of the borehole completion.

As part of geologic CO<sub>2</sub> sequestration demonstration projects conducted at the Frio Site, Liberty County, TX, USA, and the Otway Project, Nirranda South, Victoria, Australia, U-tubes were deployed for sampling multi-phase mixtures of gas, water and supercritical CO<sub>2</sub>. At both these sites, CO<sub>2</sub> was injected in the subsurface to understand the subsurface movement of the CO<sub>2</sub> plume and geochemical sampling was one of many technologies employed to understand the fate of the CO<sub>2</sub>.

### SAMPLE ACQUISITION & ANALYSIS

The method for U-tube sample retrieval is determined by the end use of the collected fluid. For the relatively shallow fluid collection at Nye County's Amargosa Valley Site and at the High Lake Site, samples were driven to the surface using compressed N<sub>2</sub> gas supplied in standard 'G' size (~8000 l) industrial cylinders. At both the Amargosa and High Lake site, samples were collected at 1 bar and there was no attempt to maintain sterile sampling conditions.

For the CO<sub>2</sub> sequestration programs at the Frio Field Site and the Otway Project, samples were collected in high pressure, large volume (13 l) cylinders for surface processing. To maintain sample integrity the pressure cylinders at the Frio Site were flushed with N<sub>2</sub> and then evacuated using a rotary vane pump prior to filling to formation pressure with fluid from the U-tubes.

Because of difficulty in keeping vacuum pumps operating when they are exposed to significant volumes of moisture laden gas, it was decided that after flushing the sample cylinders with N<sub>2</sub>, they would be allowed to bleed down to 1 bar pressure but not evacuated. The residual 13 l of N<sub>2</sub> in the sample cylinders acted as an internal standard, enabling an accurate estimation of dissolved gas concentration in the sample fluid (Freifeld & Trautz 2006).

**FRIO FIELD SITE**

At the Frio Field Site, because of the need for real-time feedback to guide operational decision making and the ephemeral nature of some of the monitored parameters, significant effort was given toward field analysis. To measure the pH before degassing, a high pressure pH electrode (Model TB567, ABB Inc. Reno, Nevada, USA) was installed on the high pressure sample line. In addition, benchtop measurements were acquired of electrical conductance, pH and alkalinity soon after sample collection (Kharaka *et al.* 2006).

A field deployable quadrupole mass spectrometer (Omnistar, Pfeiffer Vacuum GmbH, Asslar, Germany) was used to detect the arrival of the CO<sub>2</sub> plume in addition to determine CH<sub>4</sub>, O<sub>2</sub>, Ar and N<sub>2</sub> concentrations. Various tracers including Kr, SF<sub>6</sub> and perfluorocarbons were periodically co-injected with CO<sub>2</sub> to aid in determining rates of subsurface transport and changes in CO<sub>2</sub> saturation (Freifeld *et al.* 2005). The gas tracers can be determined to a precision of ±100 ppb or better using the mass spectrometer, although frequent calibration is required to obtain this level of accuracy.

**OTWAY PROJECT**

The Otway Project is using a multilevel completion with three U-tubes to sample above and below the gas-water contact of a depleted gas reservoir, while CO<sub>2</sub> is injected in a well located 300 meters downdip. The uppermost U-tube was installed just below the mudstone cap rock and is sampling predominantly supercritical CH<sub>4</sub>, while the lower two U-tubes initially produced water, but transitioned to predominantly CO<sub>2</sub> and CH<sub>4</sub> as the gas-water contact was pushed down by the increasing volumes of CO<sub>2</sub>.

Early in the sampling program it was observed that there was a decrease in gas flow from the sample leg for the U-tube accessing the residual gas column. This flow restriction was found to be caused by a progressive build-up of wax within the ¼" sample line at the near surface. The wax composition was dominated by a homologous series of n-alkanes, maximizing at n-C<sub>27</sub>, with a melting point of ~41°C; a temperature that would cause it to solidify during surface sampling. Following a solubility study of different commercially available solvents, a product sold by ExxonMobil under the trade name Solvesso-100, composed primarily of C<sub>9-10</sub> dialkyl and trialkylbenzenes, provided the best solution for periodic flushing of wax that collects within the U-tube sampling lines.

Figure 2 shows the molar fraction of CO<sub>2</sub> in the samples for all three U-tubes. Initial small increases in CO<sub>2</sub> appear in July for U-tube 2 (3 ½ months after the

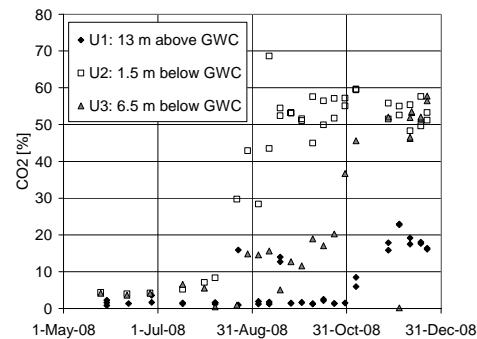


**Fig. 2.** Molar fraction of CO<sub>2</sub> in gas samples collected in U-tubes at the Otway Project.

start of CO<sub>2</sub> injection), and August for U-tube 3. After the initial appearance as a dissolved phase, the CO<sub>2</sub> molar fraction rapidly increases as a free-phase gas component arrives. U-tube 2 became self lifting in September and no further water samples were obtained. Similarly for U-tube 3 the transition to gas occurred at the very end of December 2008, with the samples collected in 2009 containing only small amounts of liquid.

### CONCLUSIONS

The U-tube geochemical sampling system has been demonstrated to operate in varied environmental conditions, from direct burial in sand/bentonite backfill to deep oil and gas reservoirs. As with all borehole sampling methods, careful attention needs to be paid to the type of fluid being sampled, the purpose of the sampling and the interaction of the borehole with the surrounding formation. By addressing potential sampling difficulties and carefully controlling wellbore conditions, U-tubes can provide high purity samples for real-time and laboratory analysis.

### ACKNOWLEDGEMENTS

This work was supported by the Assistant Secretary of the Office of Fossil Energy, U.S. Department of Energy, National Energy Technology Laboratory under contract DE-AC03-76SF00098. The

CO<sub>2</sub>CRC Otway Project is funded by Australian Federal and State governments and industrial and academic partners in Australia and abroad.

### REFERENCES

- FREIFELD, B.M. & TRAUTZ, R.C. 2006. Real-time quadrupole mass spectrometer analysis of gas in borehole fluid samples acquired using the U-tube sampling methodology. *Geofluids*, **6**, 217–224. doi: 10.1111/j.1468-8123.2006.00138.x.
- FREIFELD, B.M., TRAUTZ, R.C., YOUSIF K.K., PHELPS, T.J., MYER, L.R., HOVORKA, S.D., & COLLINS, D. 2005. The U-Tube: A novel system for acquiring borehole fluid samples from a deep geologic CO<sub>2</sub> sequestration experiment. *Journal Geophysical Research*, **110**, B10203, doi:10.1029/2005JB003735.
- FREIFELD, B.M., FINSTERLE, S., ONSTOTT, T.C., TOOLE, P., & PRATT, L.M. 2008. Ground surface temperature reconstructions: using in situ estimates for thermal conductivity acquired with a fiber-optic distributed thermal perturbation sensor. *Geophysical Research Letters*, **35**, L14309, doi:10.1029/2008GL034762.
- KHARAKA Y.K., COLE D.R., HOVORKA S.D., GUNTER W.D., KNAUSS K.G., & FREIFELD, B.M. 2006. Gas-water-rock interactions in Frio Formation following CO<sub>2</sub> injection: Implications for the storage of greenhouse gases in sedimentary basins. *Geology*, **34**, 577–580.
- WOOD, W. 1973. A technique using porous cups for water sampling at any depth in the unsaturated zone. *Water Resources Research*, **9**, 486–488.

## LIBS as an archaeological tool – example from Coso Volcanic Field, CA

Jennifer L. Gottfried<sup>1</sup>, Russell S. Harmon<sup>2</sup>, Anne Draucker<sup>3</sup>,  
Dirk Baron<sup>3</sup>, & Robert M. Yohe<sup>3</sup>

<sup>1</sup>U.S. Army Research Laboratory, Aberdeen Proving Ground, MD, 21005 USA

<sup>2</sup>ARL Army Research Office, 4300 S. Miami Blvd., Durham NC, 27703 USA

(email: russell.harmon@us.army.mil)

<sup>3</sup>Department of Physics and Geology, California State University, Bakersfield, Bakersfield, CA, 93311 USA

**ABSTRACT:** Recently, multi-element chemical analysis of has become a common means for attributing the provenance of archaeological materials. Laser-induced breakdown spectroscopy (LIBS) is a simple atomic emission spectroscopy technique with potential for real-time man-portable chemical analysis in the field. Because LIBS is simultaneously sensitive to all elements, a single laser shot can be used to record the broadband emission spectra, which provides a ‘chemical fingerprint’ of a material. Sets of single-shot broadband LIBS spectra were collected for a suite of 27 obsidians from major sites across the Coso Volcanic Field (CVF), as well as for samples from 4 other California obsidian locations – Bodie Hills, Mt. Hicks, Fish Springs, and Shoshone. Different advanced statistical signal processing techniques were applied to the obsidian data. Although all obsidian samples exhibited quite similar broadband LIBS spectra, the 5 different California obsidian locations could be clearly discriminated. Within the CVF, it is possible to distinguish the five sub-groupings defined on the basis of previous ICP-MS analysis. Samples from the Joshua Ridge are a distinct group, those from the S, SE, and W Sugarloaf locations are strongly correlated, as are samples from the Cactus Peak and E Sugarloaf and the West Cactus Peak and Stewart locations.

**KEYWORDS:** Laser-induced breakdown spectroscopy, LIBS, multivariate spectral analysis, obsidian sourcing, geochemical fingerprinting

### INTRODUCTION

Obsidian is a naturally occurring volcanic glass that has long been used by ancient peoples as a raw material for producing tools. Hydration dating and geochemical studies of obsidian can provide archaeologists with important means of understanding artifact production and past trade patterns (Erickson 1981). In particular, multi-element chemical analysis of obsidian has become an accepted procedure for attributing the provenance of artifacts, particularly obsidian (e.g. Shackley 2005; Negash *et al.* 2006).

### GEOLOGICAL SETTING

The Coso Volcanic Field (CVF) in California, USA (Fig. 1) contains at least 38 high-silica rhyolite domes (Duffield & Bacon 1981), many of which contain obsidian glass that has been quarried for tools by the indigenous population for more than 12,000 years. CVF obsidian

artifacts are found throughout southwestern USA and sourcing of CVF obsidian for archaeological studies by geochemistry has been an important tool in assessing prehistoric trading patterns across the Great Basin (Gilreath & Hildebrandt 1997).

The obsidians of the CVF are crystal-

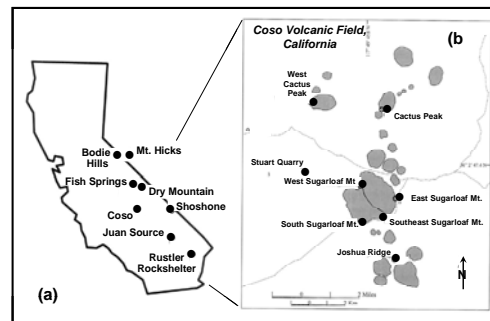


**Fig. 1.** (a) California map showing the obsidian sources analyzed and (b) map of the Coso Volcanic Field (after Duffield & Bacon 1981; Hughes 1988)

poor, high-silica, metaluminous rhyolites that containing 77±0.6% SiO<sub>2</sub> (Bacon *et al.* 1981) that are similar to rhyolites found in California and western Nevada, such as those present at Mt. Hicks, Bodie Hills, Fish Springs, and Shoshone (Fig. 1).

Geochemical studies by Hughes (1988), Ericson & Glascock (2004), and Draucker (2007) employing multivariate statistical analysis have delineated major obsidian sub-sources within the CVF. This study was undertaken to ascertain the extent which LIBS could be applied to the problem of obsidian sourcing through analysis of the same suite of samples that was analyzed by Draucker (2007).

## RESULTS

The emerging analytical technique of laser-induced breakdown spectroscopy (LIBS) is a simple atomic emission spectroscopy technique that has the potential for real-time man-portable chemical analysis in the field. Because LIBS is simultaneously sensitive to all elements, a single laser shot can be used to record the broadband emission spectra, which provides a 'chemical fingerprint' of a material.

We collected sets of single-shot broadband LIBS spectra in the Army Research LIBS Laboratory for 27 obsidian samples from major sites across the CVF as well as for samples from 4 other California obsidian locations – Bodie Hills, Mt. Hicks, Fish Springs, and Shoshone. The resultant obsidian LIBS spectral database was analyzed by multivariate statistical analysis.

A total of 185 emission lines for both major and trace elements were attributed from each LIBS broadband spectrum. Then background-corrected, summed, and normalized intensities were calculated for 18 selected emission lines and 153 emission line ratios were generated. Finally, the summed intensities and ratios were used as input variables to multivariate statistical chemometric models. A total of 3100 spectra were used to generate Partial Least Squares Discriminant Analysis (PLS-DA) models and test sets.

A model was built for discriminating the five distinct obsidian localities (Coso, Mt. Hicks, Fish Springs, Shoshone, and Bodie Hills), the broadband LIBS spectra for which exhibit a high degree of visual similarity; 100% of the 200 test single-shot spectra were correctly classified with that model (Table 1). In other words, obsidian samples from the 5 regions are easily distinguishable with LIBS.

When the 575 remaining Coso spectra (from samples not used in the 5-class model) were tested against the model, 574 out of 575 were correctly classified with the other Coso samples in the model. In other words, the model remains valid even for unknown samples (Table 2).

Subsequently, a more complex PLS-DA model (not shown) was built based on individual classes for each of the 31 obsidian samples in order to identify similarities between samples from different geographical areas. From these results, it was concluded that the South, SE, and West Sugarloaf samples are strongly correlated with each other, as are the Cactus Peak and East Sugarloaf and the West Cactus Peak and Stewart samples. The Cactus Peak, West Cactus, E Sugarloaf and Stewart samples also have similar LIBS features.

## CONCLUSIONS

Although all obsidian samples exhibited quite similar broadband LIBS spectra, the PLS-DA approach was able to clearly discriminate samples from the 5 different California obsidian locations. Within CVF, it is possible to distinguish the five sub-groupings defined on the basis of ICP-MS

**Table 1.** Confusion matrix for the PLS-DA analysis of the California obsidian localities using 600 broadband LIBS spectra and 15 latent variables to produce 5 model classes. Horizontal lines separate the groupings for the Coso Volcanic Field by Draucker (2007) and the other four California obsidian localities

Test Samples	Model Classes							
	165	179	186	176	164	172	173	174
Joshua Ridge (B-J)	165	25	0	0	0	0	0	0
E Sugarloaf (B)	179	25	0	0	0	0	0	0
SE Sugarloaf (2-L)	186	25	0	0	0	0	0	0
South Stewart (L)	176	25	0	0	0	0	0	0
Mt Hicks	164	0	25	0	0	0	0	0
Fish Springs (Inyo)	172	0	0	25	0	0	0	0
Shoshone	173	0	0	0	25	0	0	0
Bodie Hills	174	0	0	0	0	0	25	0

**Table 2.** Confusion matrix for a test of the PLS-DA model for the Coso obsidian locality. The remaining 575 broadband LIBS spectra for Coso (not included in the original model) were assigned with nearly perfect locality classification (99.8%). Only Coso sample #189 from South Sugarloaf had some misclassification with Shoshone sample #173.

Unknown Test Samples	Model Classes							
	165	179	186	176	164	172	173	174
Joshua Ridge (O)	166		25		0	0	0	0
Cactus Peak (2-T)	167		25		0	0	0	0
Cactus Peak (1-J)	168		25		0	0	0	0
Cactus Peak (1-L)	169		25		0	0	0	0
E Sugarloaf (D)	180		25		0	0	0	0
E Sugarloaf (E)	181		25		0	0	0	0
SE Sugarloaf (1-O)	183		25		0	0	0	0
SE Sugarloaf (1-V)	184		25		0	0	0	0
SE Sugarloaf (2-F)	185		25		0	0	0	0
S Sugarloaf (1-L)	182		25		0	0	0	0
S Sugarloaf (3b-l)	187		25		0	0	0	0
S Sugarloaf (2-L)	188		25		0	0	0	0
S Sugarloaf (3a-N)	189		24		0	0	4	0
W Sugarloaf (1-O)	190		25		0	0	0	0
W Sugarloaf (2-R)	191		25		0	0	0	0
W Sugarloaf (3-l)	192		25		0	0	0	0
W Sugarloaf (4-M)	193		25		0	0	0	0
West Cactus (B)	170		25		0	0	0	0
West Cactus (A)	171		25		0	0	0	0
South Stewart (M)	175 (large)		25		0	0	0	0
South Stewart (M)	175 (small)		25		0	0	0	0
South Stewart (K)	177		25		0	0	0	0
North Stewart (J)	178		25		0	0	0	0

analysis. Samples from the Joshua Ridge are a distinct group, those from the S, SE, and W Sugarloaf locations are strongly correlated, as are samples from the Cactus Peak and E Sugarloaf and the West Cactus Peak and Stewart locations.

**REFERENCES**

BACON, C.R., MACDONALD, R., SMITH, R.L., & Baedecker, P.A. 1981. Pleistocene high-silica rhyolites of the Coso Volcanic Field, Inyo County, California. *Journal of Geophysical Research*, **86**, 10223-10241.

DRAUCKER, A.C. 2007. *Geochemical*

*characterization of obsidian subsources from the Coso Range, California using laser ablation inductively coupled plasma mass spectrometry as a tool for archaeological investigations.* MS thesis, California State University at Bakersfield, Bakersfield, California.

DUFFIELD, W.A. & BACON, C.R. 1981. Geologic map of the Coso Volcanic Field and adjacent areas, Inyo County, California. *U.S. Geological Survey Miscellaneous Investigations Map I-1200.*

ERICKSON, J.E. 1981. Exchange and production systems in Californian prehistory: The results of hydration dating and chemical characterization of obsidian sources. *British Archaeological Reports International Series*, **110**, 1-240.

ERICKSON J.E. & GLASCOCK, M.D. 2004. Subsource Characterization: Obsidian utilization of subsources of the Coso Volcanic Field, Coso Junction, California, USA. *Geoarchaeology*, **19**, 779-805.

GILREATH, A.J. & HILDEBRANDT, W.R. 1997. Pregistoric use of the Coso Volcanic Field. *Contributions of the University of California Archaeological Research Facility.*

HUGHES, R.E. 1988. The Coso Volcanic Field Reexamined: Implications for obsidian sourcing and hydration dating research. *Geoarchaeology*, **3**, 253-265.

NEGASH, A., SHACKLEY, M.S., & ALEVE, M. 2006. Source provenance of obsidian artifacts from Early Stone Age (ESA) site of Melka Konture, Ethiopia, *Journal Archaeological Science*, **33**, 1647-1650.

SHACKLEY, M.S. 2005. Obsidian -Geology and archaeology in the North American Southwest. *University of Arizona Press.*



## The application of visible/infrared spectrometry (VIRS) in economic geology research: Potential, pitfalls and practical procedures

Andrew Kerr, Heather Rafuse, Greg Sparkes,  
John Hinchey, & Hamish Sandeman

*Geological Survey of Newfoundland and Labrador, Department of Natural Resources, PO Box 8700, St. John's, NL, A1B 4J6. CANADA (e-mail: andykerr@gov.nl.ca)*

**ABSTRACT:** Portable visible/infrared spectroscopy (VIRS) instruments now have wide application in mineral exploration, exploitation, processing, environmental monitoring and numerous other fields that require characterization of natural and artificial materials. This method utilizes the absorption response of many minerals to electromagnetic radiation in the visible, near infrared and shortwave infrared regions, i.e., from about 350 nm to 2500 nm. Data can be acquired rapidly, and can provide very useful insights, notably with respect to hydrothermal alteration assemblages, which include many minerals with distinctive VIRS patterns. Despite its great potential, there is presently limited published information due to confidentiality issues, and the use of VIRS in research-oriented studies is less common. Our experience since acquiring a VIRS instrument in 2008 has convinced us of its great potential, but results from pilot studies show that the acquisition and interpretation of data is not always simple and direct. There is a need for a collaborative effort to develop and publish procedures, protocols and libraries for such studies; this initiative would facilitate greater use of these methods as standard tools for research in economic geology and other aspects of Earth Sciences.

**KEYWORDS:** *visible/infrared spectrometry, economic geology, alteration, mineralization*

### INTRODUCTION

Over the last 10 years, portable infrared and visible/infrared optical spectrometers have become common tools for both mineral exploration purposes and also in operating mines. These instruments have great potential for the characterization of natural materials in a variety of fields related to environmental science, earth science and archaeology. The most obvious geoscience application is towards understanding hydrothermal alteration in mineralizing systems, and this is the main objective where such instruments are used in exploration (e.g., Thompson *et al.* 1996). Mapping of alteration is critically important as an exploration tool and also as a route to understanding the genesis of mineral deposits, and it follows that VIRS instruments should be widely applicable to economic geology research by both government agencies and academic institutions. The portability of such instruments lends itself to direct application in the field, although the

Newfoundland climate has to date discouraged us from taking our instrument out on traverses.

Despite this obvious potential, there are very few published sources providing case studies or guidelines for data acquisition, processing and interpretation. This absence undoubtedly reflects the proprietary and confidential nature of results obtained in exploration programs.

The Geological Survey of Newfoundland and Labrador (GSNL) acquired a Terraspec Pro<sup>TM</sup> VIRS spectrometer in 2008, and we are currently applying it in several research projects related to diverse styles of mineralization, and also as a practical aid to local prospectors and companies interested in identifying minerals and alteration facies. These studies are to some extent pilot projects, and are linked to the development of methodology and protocols for acquiring and interpreting the data from both empirical and mineralogical perspectives. The results illustrate the great potential of

VIRS methods as pragmatic and scientific tools, but they also point to some of the complications that can influence and in some cases compromise results. This presentation is intended to share some of our experiences in using this remarkable technology, and also to initiate discussion of various ideas that could lead to greater sharing of information amongst research institutions using VIRS instruments.

#### **BACKGROUND AND TECHNICAL ASPECTS OF VIRS ANALYSIS**

VIRS is to a large extent an outgrowth of the space exploration programs of the last 50 years, in which there was a need to develop methods for the remote imaging of the Earth and other planets. The method depends on a well-known phenomenon, i.e., the response of natural materials to electromagnetic radiation. The colour of common minerals results from differential absorption of specific visible wavelengths, although there is only rarely a simple relationship between colour and composition. However, a very large number of minerals have distinct wavelength-specific absorption in the near Infrared (NIR) and short-wave infra red (SWIR) regions of the spectrum. Not all such absorption features are unique to a given mineral, but a combination of such features can be very diagnostic, and may also yield qualitative information about compositional parameters.

Not all minerals are active in the infrared and the common anhydrous rock-forming silicates (e.g., quartz, feldspars, pyroxenes, etc.) are generally unresponsive. This may seem at first sight to be a disadvantage, but it has a good side also, in that it allows the recognition of important alteration minerals in small proportions, often below the threshold of visual identification. Spectra obtained from rocks containing several infrared active species represent mixtures, but they are not necessarily linear mixtures of individual spectra, as minerals vary in their reflectance. The interpretation of data from mixed assemblages is perhaps the greatest challenge in using VIRS

instruments as research tools, and it is almost unavoidable.

#### **SPECTROMETER OPERATION AND DATA COLLECTION ASPECTS**

The spectrometer itself has a relatively simple design, although it is of course complex in its details. A specialized light source within a “probe” irradiates the sample, and reflected light is transmitted into the analytical module by a fibre-optic cable. Three separate spectrometers analyze the response at wavelengths from 350 nm to 2500 nm, and provide digital input to the control system, which is a customized laptop computer. The acquisition of data is very rapid – once the machine is initiated and calibrated, individual spectral measurements take less than 60 seconds. The retention and recording of key information about the location and geological context of the measurement is a significant concern, and careful record-keeping is vital. The use of digital photographs of the sample, upon which the locations of individual measurements can be directly plotted and numbered, is one of the methods that we have adopted.

#### **ISSUES IN DATA PROCESSING AND INTERPRETATION**

The results from VIRS analyses are amenable to several methods of interpretation. In the simplest sense, the spectra can be used as empirical measurements on given rock types or formations, without specific reference to the causative minerals. We have found that superficially identical rock types with different geological contexts can in some cases be effectively characterized and discriminated. The comparison of measured spectra with reference spectra from minerals is the main tool used for identification, and is very effective in cases where samples are monomineralic or dominated by a single infrared active species. The size of the area analyzed is ~ 1 cm in diameter. Computer programs with variable levels of automation can speed the process of identification, but

they need to be used with a measure of caution where spectra are likely to have mixed sources. Our experience is that human observation and reasoning is important if the maximum amount of information is to be gleaned from a dataset.

Some basic data processing is required once the data are acquired. These include “splicing” (to remove small offsets related to the use of three discrete detection systems for different wavelength ranges) and also averaging of individual measurements where appropriate. Our experience is that homogeneous samples produce identical spectra from several measurements, although their total amplitude may vary. These data can be reduced by numerical averaging, although individual spectra must first be closely examined, to be sure that they do not contain a distinct response recording the heterogeneous distribution of some key mineral.

The amount of reflectance from a sample is influenced by factors such as colour and also the nature of the surface. Surprisingly, smooth surfaces such as cut drill core provide lower amplitude spectra than rough or uneven surfaces such as broken core or hand samples. However, the geometry of spectra (ie., the presence of discrete absorption features) is retained even when overall reflectance is reduced. The comparison of measured spectra with reference spectra is hampered by such differences in amplitude, and we have found it advantageous to “normalize” spectra such that all results have the same overall apparent range in reflectance. This is a simple scaling procedure once the maximum and minimum values are obtained, and is easily performed using instrument software or standard spreadsheet programs. It can also be carried out in a more qualitative manner after the results are imported into graphics programs for display.

Dealing with spectral responses from samples that contain mixed assemblages is a significant challenge. If one of the alteration minerals is highly reflective, its

response may drown out that from other species that may also be important. An example of this is provided by results from a VMS alteration zone, in which kaolinite group minerals were independently identified by XRD. In the VIRS data, the response from these species was generally overcome by a strong response from “sericite” (i.e., hydrous muscovites and related minerals). Our experience is that a valuable first step is to seek responses from areas where a single mineral species is dominant; this allows the identification of the “end members” that will contribute to a composite spectrum. These measurements can then be used as input in attempts to broadly quantify the proportions of minerals in mixtures and the progressive development of alteration “facies”.

#### **CASE STUDIES**

In our initial use of VIRS methods, we have chosen a diverse set of projects. These include epithermal-style precious metal mineralization (eastern and central Newfoundland), mesothermal gold mineralization (Central Newfoundland), syngenetic VMS mineralization and related alteration (Central Newfoundland), porphyry-style Mo-Cu mineralization (southern Newfoundland) and uranium mineralization in the Central Mineral Belt of Labrador. Space does not permit detailed discussion of results, but in all cases we were able to recognize distinctive alteration species and document their distribution. In some cases, results provided surprises, eg., the recognition of topaz in quartz-alunite alteration and possible Li-rich micas in VMS alteration influenced by magmatic fluids. In some cases, the resolution of species in mixed assemblages proved to be difficult, but the overall spectral patterns could still be used to discriminate alteration facies and demonstrate their superposition.

Using these techniques has not proved as simple as we might have hoped, but this should come as no surprise given the innovative nature of the technology and the complexity of natural systems. The

methods have great untested potential as research tools, but like any analytical technique, they acquire greater power and significance when they can be linked to other types of independent information, such as lithochemical data, petrographic analysis and XRD measurements.

#### **WHERE SHOULD WE GO FROM HERE?**

The successful use of VIRS methods as research tools requires more than anything a published framework that will provide standards for the collection and interpretation of data, and accessible data libraries that can give examples for comparison and contrast. The spectral libraries used for mineral identification are in part public-domain, but much information remains tied to the instrument software and cannot readily be distributed. Differences in the formats used for spectral files in different libraries complicate their use in standard software and impedes information exchange.

The development of spectral reference libraries geared to specific mineralizing environments or geographic regions (eg., VMS deposits in eastern Canada, or Cordilleran Mo-W deposits) would be a very useful step, especially if such resources were available through a single integrated website. Such reference spectra should not be restricted to individual minerals (although these are important) but should include information from real rocks that contain mixed

assemblages and have known geological and metallogenic contexts. Dealing with mixed responses is an almost unavoidable problem in most situations that we can envisage.

There may also be a need for "standards" that can be used to calibrate instruments, check for progressive shifts in their measurement responses, and ensure that data acquired from different sources are comparable. In most other analytical fields we have standard materials, and these should not be hard to establish. Amongst those that we use is a homogeneous pyrophyllite from the Manuels deposit near St. John's.

Progress towards these objectives requires active collaboration between research organizations using VIRS data, and Government Geological Surveys, with their mandate to provide public information, are ideally poised to lead such an effort.

#### **ACKNOWLEDGEMENTS**

We thank Phoebe Hauff of Spectral International Inc., for her assistance in becoming Terraspec owners, and also for her insight into these methods, their potential and their complications.

#### **REFERENCE**

THOMPSON, A.J.B., HAUFF, P.L., & ROBITAILLE, A.J. 1996. Alteration mapping in exploration: application of shortwave infrared (SWIR) spectroscopy. *SEG Newsletter*, **39**, 15-27.

## **Analysis of gem treatments: comparison of nano-second and pico-second laser-induced breakdown spectroscopy**

**Nancy J. McMillan<sup>1</sup>, Patrick Montoya, Carlos Montoya, & Lawrence Bothern**

<sup>1</sup>*Department of Geological Sciences, New Mexico State University, Box 30001, MSC 3AB, Las Cruces, New Mexico, 88003 USA (email: nmcmilla@nmsu.edu)*

**ABSTRACT:** Gems are routinely treated with a variety of chemical additives to reduce defect visibility, enhance color, and improve stability. The ability to detect treatments is critical for the gem industry but is difficult because the analytical technique must be minimally destructive and sufficiently simple to be used by people throughout the gem industry as well as trained geochemical analysts. This work compares nano-second LIBS (Laser-Induced Breakdown Spectroscopy) to pico-second LIBS analysis of common gem treatments such as Be-diffused sapphires and rubies impregnated with leaded glass. Analytical conditions such as the wavelength of laser light and the environment of analysis (air, He, and Ar) are explored with the goal of determining the optimal analytical conditions. Data richness (amount of trace element information), data reproducibility, and damage to the gem are considered.

**KEYWORDS:** *gem, treatment, LIBS, sapphire, ruby, lead*

### **INTRODUCTION**

Chemical treatments are commonly applied to imperfect gems to improve appearance and/or enhance the color. Although gem treatment is legal, dealers must disclose whether or not a specific specimen has been treated and what treatment has been applied. As treatment technology improves, the gem industry is increasingly aware of and sensitive to the presence of both disclosed and undisclosed treated gems in the marketplace. Thus, there is a need to be able to reliably detect chemically treated gems with a minimally-destructive technique.

### **LASER-INDUCED BREAKDOWN SPECTROSCOPY (LIBS)**

In LIBS analysis, a pulsed laser is focused on the gem surface. The laser energy ablates a small amount of gem material which burns in a short-lived plasma. As the plasma cools, excited electrons decay into lower-energy orbitals, releasing energy in the form of photons in the ultraviolet-visible-infrared range. This light is collected by optic fiber, diffracted, and recorded as a spectrum, generally between 200 and 1000 nm.

This paper explores the trade-offs of gem damage during LIBS analysis and data quality under a variety of analytical conditions. Two lasers, a Big Sky Laser Technology (now Quantel USA) Nd-YAG nano-second laser operated at its fundamental wavelength of 1064 nm, and a Raydiance, Inc., pico-second laser operated at its fundamental wavelength of 1552 nm as well as harmonics at 776, 517.2, and 388 nm, are used in separate LIBS systems. Furthermore, the use of inert gas environment (He or Ar) is explored to increase peak intensities at lower laser power and sample damage.

### **RESULTS**

The pico-second laser causes significantly less damage to the stone than the nano-second laser; however, fewer trace element peaks may be observed in the pico-second LIBS spectra (Fig. 1). The sensitivity of the pico-second LIBS system to trace elements may be enhanced in Ar or He, with a better lens system than currently employed, or by using the harmonic wavelengths. These parameters are under investigation.

The utility of LIBS analysis for two common gem treatments is illustrated

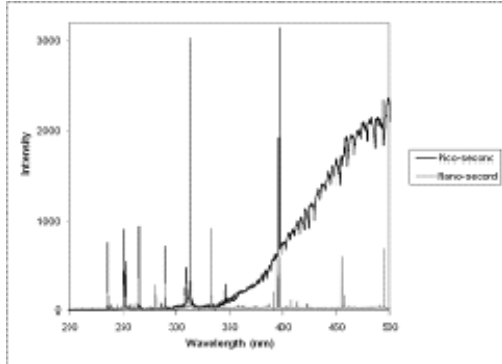


**Fig. 1.** Comparison of pico-second (black) and nano-second (gray) spectra from a faceted and polished aquamarine. Note that the nano-second spectrum has more peaks (from more elements) and far less continuum than the pico-second spectrum.

here using nano-second analyses in air. Rubies are sometimes impregnated with Pb-containing glass to render imperfections invisible (McClure *et al.* 2003). Because natural ruby has very low concentrations of Pb, detection of significant Pb indicates that glass at the gem surface has been analyzed. Fig. 2 presents LIBS spectra of six rubies, three of which have Pb peaks, indicating treatment with glass impregnation.

Since the 1990s, orange sapphires that have been diffused with Be have been found on the gem market (Emmett *et al.* 2003). Similar to leaded rubies, Be-diffused sapphires are easy to detect with LIBS because natural sapphires have low concentrations of Be (Emmett *et al.* 2003). Figure 3 shows LIBS spectra of six sapphires, three of which show the presence of Be at the dominant 313.1 nm peak. Further analyses are underway, in order to compare the pico-second LIBS spectra to their nano-second counterparts, to test different harmonic wavelengths of the pico-second laser, and to explore the use of Ar or He environment to reduce damage and increase peak intensity.

## CONCLUSIONS

LIBS analysis of gem treatments has several advantages over traditional techniques, including:

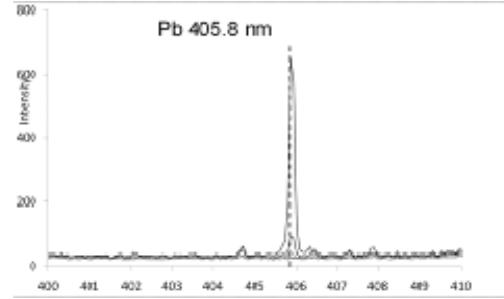


**Fig. 2.** Nano-second LIBS spectra of six rubies. The dominant Pb peak at 405.8 nm is marked.

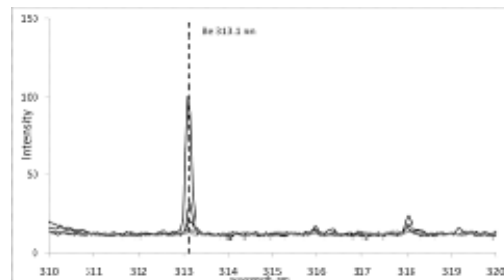


**Fig. 3.** Nano-second LIBS spectra of six sapphires. The dominant Be peak at 313.1 nm is marked.

- (1) immediate and simple analysis;
- (2) minimal damage;
- (3) sensitivity to common gem chemical treatments.

If appropriate analytical protocols are developed, LIBS will have a place in the field of gem analysis to detect and monitor chemical treatments in the gem trade industry.

## ACKNOWLEDGEMENTS

We gratefully acknowledge support from grants from the State of New Mexico Department of Economic Development and the collaboration of Raydiance Inc.

## REFERENCES

- EMMETT, J.L., SCARRATT K., MCCLURE S.F., MOSES T., DOUTHIT T.R., HUGHES R., NOVAK S., SHIGLEY J.E., WANG W., BORDELON O., & KANE R.E. 2003. Beryllium diffusion of ruby and sapphire. *Gems & Gemology*, **39**, 84-135.
- MCCLURE, S.F., SMITH, C.P., WANG, W., & HALL, M., 2003. Identification and durability of lead-glass-filled rubies. *Gems & Gemology*, **42**, 22-34.

## Laser ablation chemical analysis LIBS and LA-ICP-MS for geochemical and mining applications

R.E. Russo<sup>1,2,3</sup>, J. Yoo<sup>2</sup>, J. Plumer<sup>1</sup>, J. Gonzalez<sup>2</sup>, & X. Mao<sup>3</sup>

<sup>1</sup>A3 Technologies, 1201 Technology Dr, Aberdeen, MD, 21001 USA

<sup>2</sup>Applied Spectra 46661 Fremont Blvd, Fremont, CA, 94538 USA

<sup>3</sup>Lawrence Berkeley Lab Berkeley, CA, 94720 USA (e-mail: rerusso@appliedspectra.com)

**ABSTRACT:** Laser ablation has advanced to the stage of providing routine chemical characterization and analysis of solid samples without sample preparation. Advances in precision and accuracy allow a suite of applications from qualitative surveying to accurate quantization to age dating. Real-time in the field measurements without consumables make this approach a modern day 'green technology' for characterization and analysis. Two common implementations of laser ablation chemical analysis include LIBS (Laser Induced Breakdown Spectroscopy) which provides on the order of ppm detection, and LA-ICP-MS (Laser Ablation Inductively Coupled Plasma Mass Spectrometry), which provides ppb level sensitivity for most elements in the periodic table. Significant improvements in accuracy over XRF (x-ray fluorescence) are available for complex geological and mining samples. Commercial LIBS and ICPMS instruments are manufactured with integrated measurement protocols appropriate to a particular application. Data treatment chemometric processes are embedded in software making the laser ablation analysis technology more intuitive for the end-users.

**KEYWORDS:** laser ablation, LIBS, ICP-MS, real-time analysis, instrumentation

### INTRODUCTION

This presentation will summarize developments in laser ablation with emphasis on LIBS (laser induced breakdown spectroscopy) and inductively coupled plasma mass spectrometry (ICP-MS) as analytical tools for real time chemical analysis (Fig. 1) (Russo *et al.* 2005). Laser ablation has become a prominent analytical technique over the past decade with applications crossing into many scientific disciplines, including geoscience, environmental, and forensics, among others (Baudefet, *et al.* 2007; Gonzalez *et al.* 2008). Laser ablation is a direct sampling technique by which a high energy laser is focused on the surface of a material and atoms, ions, and particles are ejected. The particles, which are chemically representative of the bulk sample, are then transported into an ICP-MS for analysis. In LIBS, a luminous, short-lived plasma is created on the sample surface by the focused laser beam and its emission spectra are analyzed to provide both qualitative and quantitative chemical compositional analysis (Cremers

*et al.* 2006; Miziolek *et al.* 2006). Laser ablation based analysis is instantaneous, allowing real-time chemical composition analysis. Commercial systems are available for laboratory and field measurements.

LA offers several advantages over digestion/solution analyses such as 1) reduction in isobaric interferences, 2)

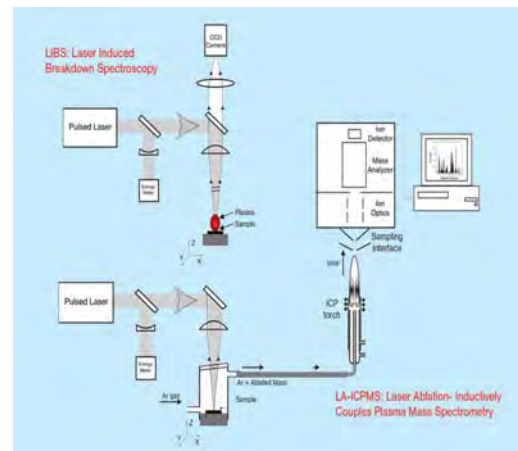


**Fig. 1.** Laser ablation with LIBS and LA-ICP-MS configurations.

reduction in sample size requirements, 3) a reduction in sampling time and 4) and the elimination of the need for acids further reducing potential for contamination and health risks. In addition, when compared to digestion and dissolution methods, researchers have reported similar precision and accuracy in the analysis of numerous samples; as a result, LA-ICP-MS is now the method of choice for elemental analysis, including geochemical analyses (Poitrasson *et al.* 2003).

This paper presents an overview of the current research issues and commercialization efforts related to laser ablation for chemical analysis, discusses several fundamental studies of laser ablation using time-resolved shadowgraph and spectroscopic imaging, and describes recent data using nanosecond laser pulsed ablation sampling for ICP-MS and LIBS. Efforts towards commercialization of field based LIBS systems also will be described.

### LIBS ANALYSIS

Several applications will be described based on measurements obtained with two LIBS system that have been engineered and manufactured for industrial use. Our data illustrate how LIBS can answer a multitude of real-world needs for the rapid chemical analysis of various substances, including geological samples. The experiments were performed using RT100-HP and RT100-B commercial LIBS systems from Applied Spectra, Fremont, CA. These two instruments are similar, both acquire instantly a spectrum from a single laser shots, but they include different optical spectrographs. RT100-HP incorporates a high-performance Czerny Turner spectrograph attached to an image intensifier with timing control to select the gate width and delay for optimal analysis. This spectrograph has a dual grating turret, which allows the user to choose a spectral window with relevant spectral resolution (200 nm at resolution of 0.8 nm; or 40 nm at resolution of 0.1 nm). The other instrument RT100-B incorporates a

broadband Echelle spectrograph with an intensified CCD camera that instantly acquires a wide span of spectrum from 200 to 900 nm at resolution ~0.05 nm. The RT 100-B allows discrimination of classes of compounds whereas the RT 100 HP is ideally suited for quantitative analysis of selected elements. Each model can be configured into a field-portable Pella-case design. We used the RT100-B to perform quantitative determination of lead in 12 different samples; several representative LIBS spectra from are shown in Figure. 2. For these measurements, we used 20 mJ laser pulses focused into 100  $\mu$ m ablation spots.

Even though there seem to be a substantial degree of similarity between the spectra in Figure 2, they are all individually different. We applied a chemometric algorithm known as the principal component analysis (PCA) to compare and categorize these spectra. The results are presented in Figure 3 as a projection of our data from a multicomponent space onto coordinates of the two first principal components. It is evident that separation of high-lead samples from low-lead samples is easily achieved in this way. Therefore, a simple task of classifying samples into high or low lead groups can be fulfilled very rapidly and even without a need for standard calibration.

LIBS can be used for field screening on

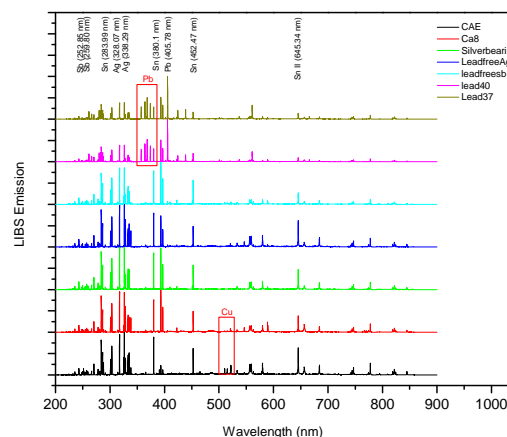
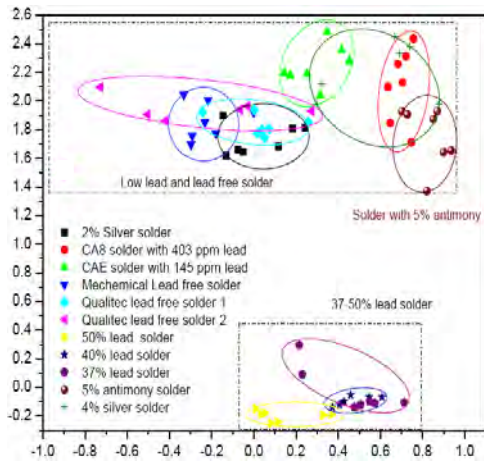


Fig. 2. Example broadband LIBS spectra.



**Fig. 3.** PCA classification of samples.

a qualitative level or for quantitative analysis. As example of quantitative analysis, we utilized the RT100-HP for measuring lead in the NIST 2579 reference sample

A portion of a spectrum that includes emission lines of mercury and lead is shown in Figure 4; the insert is a calibration plot for lead in this sample set. In general, LIBS provides detection on the ppm level for most elements; in this case on the order of 30 ppm for lead in glass based matrices. For higher sensitivity, LA-ICP-MS provide ppb detection.

Both LIBS and LA-ICP-MS offer spatial and depth resolution. A single laser shot provides an instantaneous measurement of approximately several nanograms to micrograms of sample. For spatial analysis, the laser is focused to several tens of microns and scanned across a surface. For depth analysis (including inclusions), the laser is pulsed repetitively at a single location to drill a channel into the sample (Fig. 5).

**CONCLUSIONS**

LA-ICP-MS and LIBS instruments can be used for fast and sensitive analysis of a wide variety of samples of interest to the geochemical and mining industries. Localized microanalysis with lateral and depth profiling is easily realized. Either traditional one-element calibration or

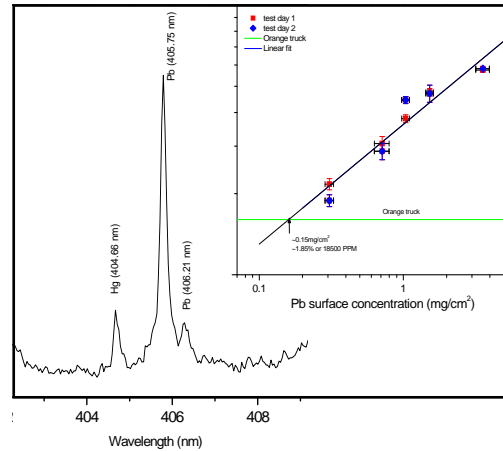


**Fig. 4.** Pb and Hg LIBS emission lines. Insert set is analytical working curve analysis.

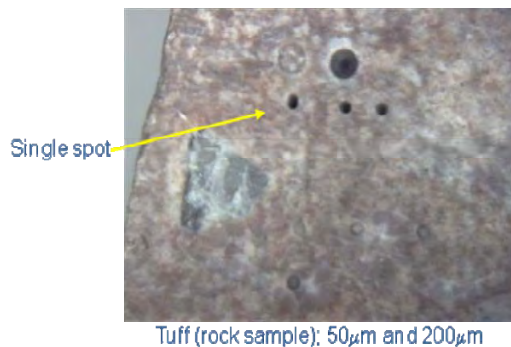


**Fig. 5.** Tuff sample with several laser sampled locations.

multivariate chemometrics can be applied for qualitative or quantitative determination of elements in the samples. LIBS and LA-ICP-MS provide real-time chemical analysis with no sample preparation, across both laboratory and field applications. Companies including Applied Spectra and A3-Technologies have begun marketing LIBS systems for diverse applications. Integrated hardware and software allows user friendly applications within a completely integrated platform.

**REFERENCES**

BAUDELET M., BOUERI M., YU J., MAO S., PISCITELLI V., MAO X., & RUSSO R. 2007. Time-resolved ultraviolet laser-induced breakdown spectroscopy for organic material analysis. *Spectrochimica Acta Part B: Atomic Spectroscopy*, **20**,1329-1334.

- CREMERS, D.A. & RADZIEMSKI, L.J. 2006. *Handbook of Laser Induced Breakdown Spectroscopy*. J. Wiley & Sons, New York
- GONZALEZ, J., OROPEZA, D., MAO, X.L., & RUSSO, R.E. 2008. Assessment of the precision and accuracy of thorium ( $^{232}\text{Th}$ ) and uranium ( $^{238}\text{U}$ ) measured by quadrupole based-inductively coupled plasma-mass spectrometry: comparison of liquid nebulization, nanosecond and femtosecond laser ablation. *Journal of Analytical Atomic Spectrometry*, **23**, 229-234.
- MIZIOLEK, A.W., PALLESCHI, V., & SCHECHTER, I. (eds.) 2006. *Laser-Induced Breakdown Spectroscopy (LIBS), Fundamentals and Applications*. Cambridge University Press, UK.
- POITRASSON, X.L., MAO, S.S., FREYDIER, R., & RUSSO, R.E. 2003. Comparison of ultraviolet femtosecond and nanosecond laser ablation inductively coupled plasma mass spectrometry analysis in glass, monazite, and zircon. *Analytical Chemistry*, **75**, 6184-6190.
- RUSSO, R.E., GONZALEZ, J., & LIU, C.Y. 2005. Laser ablation: LIBS and ICP-MS. *Lab Plus International*.

## In-situ Mössbauer spectroscopy on Earth, Mars, and beyond

Christian Schröder<sup>1</sup>, Göstar Klingelhöfer<sup>1</sup>, Richard V. Morris<sup>2</sup>, Bodo Bernhardt<sup>3</sup>,  
Mathias Blumers<sup>1</sup>, Iris Fleischer<sup>1</sup>, Daniel S. Rodionov<sup>1,4</sup>, & Jordi Gironés López<sup>1</sup>

<sup>1</sup>Institut für Anorganische Chemie und Analytische Chemie, Johannes Gutenberg-Universität,  
Staudinger Weg 9, D-55099, Mainz GERMANY (e-mail: schroedc@uni-mainz.de)

<sup>2</sup>Astromaterials Research and Exploration Science, NASA Johnson Space Center, Mail Code KR, 2101 NASA  
Parkway, Houston, TX 77058, USA

<sup>3</sup>Von Hoerner & Sulger GmbH, Schlossplatz 8, D-68723 Schwetzingen GERMANY

<sup>4</sup>Space Research Center IKI, Moscow RUSSIA

**ABSTRACT:** Iron occurs naturally as Fe<sup>2+</sup>, Fe<sup>3+</sup>, and, to a lesser extent, as Fe<sup>0</sup>. Many fundamental (bio)geochemical processes are based on redox cycling between these oxidation states. Mössbauer spectroscopy provides quantitative information about the distribution of Fe among its oxidation states, identification of Fe-bearing phases, and relative distribution of Fe among those phases. Determination of Fe<sup>3+</sup>/Fe<sub>Total</sub> and the identification of iron hydroxide mineral phases, for example, provide evidence for aqueous activity on the surface of Mars. Metallic iron identified in several rocks investigated on Mars suggests a meteoritic origin. These Mössbauer spectra were obtained with portable, miniaturized spectrometers on board the NASA Mars Exploration Rovers. Because of their backscattering measurement geometry, the instruments are directly placed on the sample surface to be analyzed by a robotic arm. In field studies on Earth, similar instruments have been used for the in situ study of green rust in soil, and as a prospecting tool and process monitor during field testing of precursor hardware for lunar in situ resource utilization (oxygen production). An advanced version of the Mars spectrometer has a new detector system permitting shorter measurement times and the capability for simultaneous acquisition of X-ray fluorescence spectra to determine elemental compositions.

**KEYWORDS:** Mössbauer spectroscopy, MIMOS IIa, Mars Exploration Rover, In-situ resource utilization, X-ray fluorescence spectroscopy

### INTRODUCTION

Iron is one of the most abundant elements in the universe. Mössbauer (MB) spectroscopy is an established laboratory technique and a powerful tool to study Fe-bearing substances. The surface of Mars is Fe-rich compared to Earth, and a miniaturized MB spectrometer (MIMOS II) was developed for its robotic exploration as part of NASA's Mars Exploration Rover (MER) mission (Klingelhöfer *et al.* 2003). The capability of simultaneous acquisition of X-ray Fluorescence (XRF) spectra has been added. This new instrument, capable of both mineralogical and chemical applications (Klingelhöfer *et al.* 2008) is briefly described and then a few examples of extraterrestrial and terrestrial applications are presented.

### MIMOS IIA INSTRUMENT DESCRIPTION Mössbauer Spectroscopy

Available textbooks and reviews provide a detailed introduction to MB spectroscopy (e.g., Hawthorne 1988; Burns 1993). MB spectra provide quantitative information about the distribution of Fe among its oxidation and coordination states (e.g., octahedrally coordinated Fe<sup>3+</sup>), identification of Fe-bearing phases, relative distribution of Fe among those phases, and can help to constrain crystallinity and particle size.

### MIMOS IIa

MIMOS IIa is an advanced version of the MER instruments (Klingelhöfer *et al.* 2003) operating continuously since landing in January 2004. A new detector system has been implemented, inherited from the Alpha Particle X-ray Spectrometer (APXS), also part of the MER payload. This Si Drift Detector system provides higher energy resolution and increased

signal-to-noise ratio relative to the MER instruments, reducing measurement times and enabling the simultaneous acquisition of XRF spectra (Klingelhöfer *et al.* 2008). A <sup>57</sup>Co radioactive source provides the 14.4keV MB  $\gamma$ -rays and other energies for X-ray excitation. Acquisition of both 6keV and 14keV MB spectra enables depth selective measurements because of different attenuation coefficients (Fleischer *et al.* 2008). MIMOS IIa is set up in backscattering geometry to render sample preparation unnecessary; the instrument is simply placed on the surface to be analyzed, which is particularly useful for outdoor and in-situ applications. The instrument has a field of view of ~15 mm in diameter. Its main parts are a sensor head and an electronics board. A PC is necessary to start/stop measurements and for data read out. Wireless connection to the PC is possible. Power can be supplied via the mains in the lab, or a car battery, generator or solar cells in the field. The instrument, excluding PC and power supply, weighs less than 500 g.

### **MARS EXPLORATION**

A "Follow-the-Water" strategy has been adopted for Mars Exploration. Hoehler *et al.* (2007) suggested a "Follow-the-Energy" approach. The primary objective of the MER mission is to explore two sites on Mars where water may once have been present, and to assess past environmental conditions at those sites and their suitability for life (Squyres *et al.* 2003).

### **Rock and Soil Classification**

Rocks and soils (no implication of the presence or absence of organic materials or living matter intended) investigated with MERs *Spirit* and *Opportunity* in Gusev crater and at Meridiani Planum, respectively, were divided into classes on the basis of their chemical composition measured with the APXS and into subclasses on the basis of their Fe-bearing mineralogical composition and  $\text{Fe}^{3+}/\text{Fe}_{\text{Total}}$  ratios determined with the MB spectrometers (Ming *et al.* 2006, 2008; Morris *et al.* 2006a, 2006b, 2008). The

distribution of igneous minerals (olivine and pyroxene) versus secondary minerals (hematite) and  $\text{Fe}^{3+}/\text{Fe}_{\text{Total}}$  ratios are a measure of weathering/alteration (e.g., Schröder *et al.* 2004).

### **Geologic Mapping**

The APXS and MB in-situ dataset from individual stratigraphic units can be placed in a geologic context when reconciled with the MER remote sensing Miniature Thermal Emission Spectrometer (MINI-TES; McSween *et al.* 2008) and Panoramic Camera (e.g. Farrand *et al.* 2008) datasets. Adding orbital imagery enabled the first field reconnaissance geologic mapping on another planetary surface (Crumpler *et al.* 2009).

### **Habitability/Astrobiological Implications**

Olivine in dust and soil suggests that physical rather than chemical weathering processes dominate on contemporary Mars (Morris *et al.* 2004), and the apparent global distribution of olivine-bearing dust and soil (Yen *et al.* 2005) reflects the overall extremely arid conditions on Mars. By contrast, aqueous minerals identified in outcrop rocks such as the Fe oxyhydroxide goethite in the Columbia Hills in Gusev crater (Morris *et al.* 2006a) or the Fe hydroxide sulfate jarosite at Meridiani Planum (Klingelhöfer *et al.* 2004) provide evidence for wet conditions in the past. Jarosite forms only at low pH and constrains environmental conditions. The abundance of ferrous versus ferric minerals provides further astrobiological implications because redox cycling of Fe, for example, can provide energy for microbial metabolism (e.g., Schröder *et al.* 2006).

### **Meteorites**

Several meteorites were identified on Mars on the basis of their Fe metal and troilite contents (Schröder *et al.* 2008, 2009). Compared to the Moon, meteorites have a greater chance to survive impact on Mars because of its atmosphere. Compared to Earth, the current extremely arid climate on Mars lets meteorites

persist for much longer times and thus accumulate. Landis (2009) suggested that iron meteorites may be collected to provide steel as a construction resource on Mars for future human exploration.

#### **LUNAR IN SITU RESOURCE UTILIZATION**

Some essential consumables must be produced from lunar surface materials to enable a sustained, long-term presence of humans on the Moon. Oxygen, for example, can be produced by hydrogen reduction of metal cations (primarily Fe<sup>2+</sup>) bonded to oxygen in the lunar regolith to metal (Fe<sup>0</sup>) with the production of water. The hydrogen source is residual hydrogen in fuel tanks of lunar landers. Electrolysis of the water produces oxygen and hydrogen (which is recycled). Oxygen yield can be calculated by quantitative MB measurements of Fe distribution among oxidation states in the regolith before and after hydrogen reduction. Mounted on a rover, for example, MB spectrometers can also be used as prospecting tools to select the optimum feedstock for the oxygen production plants (e.g., high total Fe content and easily reduced phases). Both applications were demonstrated during the NASA Outpost Precursor for ISRU and Modular Architecture (OPTIMA) field test on Mauna Kea, Hawaii, in 2008.

#### **TERRESTRIAL APPLICATIONS**

##### **Characterization of Particulate Matter**

Airborne particles collected with filters distributed across Vitoria, Brazil were analyzed by MB spectroscopy, whereby certain Fe-bearing minerals indicated different pollution sources. For example, hematite comes mostly from iron ore pellet plants, pyrite from handling and storing coal in the industrial area, and magnetite is related to steelwork plants (de Souza *et al.* 2001).

##### **Monitoring of Fougerite in the Field**

Iron mixed-valence materials such as 'green rust' and fougerite are sensitive to air exposure and soil pollution by nitrates. A MIMOS instrument autonomously lowered or raised within a plexiglas tube, which was put down a bore hole, allowed

to study their formation and distribution in situ as a function of depth in soil (e.g. Rodionov *et al.* 2006).

#### **SUMMARY**

A miniaturized MB spectrometer MIMOS II was developed for the robotic exploration of Mars, where it provided fundamental information about mineralogical composition and alteration processes, helped to classify rocks and soils, aided geologic mapping, was instrumental in assessing habitability of past and present environments, and identified potential construction resources for future human explorers. The applicability of the instrument as a process monitor for oxygen production and prospecting tool for lunar ISRU has been demonstrated. The characterization of air pollution sources and the study of mixed-valence materials as a function of depth in soil are examples of terrestrial in situ applications. MIMOS IIa with additional XRF capability will open up new applications.

#### **ACKNOWLEDGEMENTS**

The development and realization of MIMOS IIa was funded by the German Space Agency DLR under contracts 50QM99022, 50QX0603, and 50QX0802. The project has been supported by the Technische Universität Darmstadt and the Johannes Gutenberg-Universität Mainz.

#### **REFERENCES**

- BURNS, R.G. 1993. Mössbauer Spectral Characterization of Iron in Planetary Surface Materials. In: PIETERS C.M. & ENGLERT P.A.J. (eds.), *Remote Geochemical Analysis: Elemental and Mineralogical Composition*, Cambridge University Press, UK, 539-556.
- CRUMPLER, L. *et al.* 2009. Field Reconnaissance Geologic Mapping of the Columbia Hills, Gusev Crater from MER Spirit Rover and HiRISE Observations. *Lunar and Planetary Science*, **40**, 2045.
- DE SOUZA JR., P.A. *et al.* 2001. On-line and in-situ characterization of iron phases in particulate matter. *Proceedings of the Air & Waste Management Association's 94th Annual Conference*, paper **569**, session AB-2d, 11p.
- FARRAND, W.H. *et al.* 2008. Rock Spectral

- Classes Observed by the Spirit rover's Pancam on the Gusev Crater Plains and in the Columbia Hills. *Journal of Geophysical Research*, **113**, E12S38, doi:10.1029/2008JE003237.
- FLEISCHER, I. *et al.* 2008. Depth selective Mössbauer Spectroscopy: Analysis and simulation of 6.4 keV and 14.4 keV spectra obtained from rocks at Gusev crater, Mars, and layered laboratory samples. *Journal of Geophysical Research*, **113**, E06S21, doi:10.1029/2007JE003022.
- HAWTHORNE, F.C. 1988. Mössbauer Spectroscopy. *Reviews in Mineralogy*, **18**, 255-340.
- HOEHLER, T.M. *et al.* 2007. A "Follow the Energy" Approach for Astrobiology. *Astrobiology*, **7**, 819-823.
- KLINGELHÖFER, G. *et al.* 2003. Athena MIMOS II Mössbauer spectrometer investigation. *Journal of Geophysical Research*, **108**(E12), 8067, doi:10.1029/2003JE002138.
- KLINGELHÖFER, G. *et al.* 2004. Jarosite and Hematite at Meridiani Planum from Opportunity's Mössbauer Spectrometer. *Science*, **306**, 1740-1745.
- KLINGELHÖFER, G. *et al.* 2008. The Advanced Miniaturised Mössbauer Spectrometer MIMOS IIa: Increased Sensitivity and New Capability for Elemental Analysis. *Lunar and Planetary Science*, **39**, 2379.
- LANDIS, G.A. 2009. Meteoritic steel as a construction resource on Mars. *Acta Astronautica*, **64**, 183-187.
- MC SWEEN, H.Y. *et al.* 2008. Mineralogy of volcanic rocks in Gusev crater, Mars: Reconciling Mössbauer, APXS, and MINITES spectra. *Journal of Geophysical Research*, **113**, E06S04, doi:10.1029/2007JE002970.
- MING, D.W. *et al.* 2006. Geochemical and mineralogical indicators for aqueous processes in the Columbia Hills of Gusev crater, Mars. *Journal of Geophysical Research*, **111**, E02S12, doi:10.1029/2005JE002560.
- MING, D.W. *et al.* 2008. Geochemical Properties of Rocks and Soils in Gusev crater, Mars: Results of the Alpha Particle X-ray Spectrometer from Cumberland Ridge to Home Plate. *Journal of Geophysical Research*, **113**, E12S39, doi:10.1029/2008JE003195.
- MORRIS, R.V. *et al.* 2004. Mineralogy at Gusev Crater from the Mössbauer Spectrometer on the Spirit Rover. *Science*, **305**, 833-836.
- MORRIS, R.V. *et al.* 2006a. Mössbauer mineralogy of rock, soil, and dust at Gusev crater, Mars: Spirit's journey through weakly altered olivine basalt on the plains and pervasively altered basalt in the Columbia Hills. *Journal of Geophysical Research*, **111**, E02S13, doi:10.1029/2005JE002584.
- MORRIS, R.V. *et al.* 2006b. Mössbauer mineralogy of rock, soil, and dust at Meridiani Planum, Mars: Opportunity's journey across sulfate-rich outcrop, basaltic sand and dust, and hematite lag deposits. *Journal of Geophysical Research*, **111**, E12S15, doi:10.1029/2006JE002791.
- MORRIS, R.V. *et al.* 2008. Iron mineralogy and aqueous alteration from Husband Hill through Home Plate at Gusev Crater, Mars: Results from the Mössbauer instrument on the Spirit Mars Exploration Rover. *Journal of Geophysical Research*, **113**, E12S42, doi:10.1029/2008JE003201.
- RODIONOV, D. *et al.* 2006. Automated Mössbauer spectroscopy in the field and monitoring of fougurite. *Hyperfine Interactions*, **167**, 869-873.
- SCHRÖDER, C. *et al.* 2004. Weathering of Fe-bearing minerals under Martian conditions, investigated by Mössbauer spectroscopy. *Planetary and Space Science*, **52**, 997-1010.
- SCHRÖDER, C. *et al.* 2006. Fe Mössbauer spectroscopy as a tool in astrobiology. *Planetary and Space Science*, **54**, 1622-1634.
- SCHRÖDER, C. *et al.* 2008. Meteorites on Mars observed with the Mars Exploration Rovers. *Journal of Geophysical Research*, **113**, E06S22, doi:10.1029/2007JE002990.
- SCHRÖDER, C. *et al.* 2009. Santorini, Another Meteorite on Mars and Third of a Kind. *Lunar and Planetary Science*, **40**, 1665.
- SQUYRES, S.W. *et al.* 2003. Athena Mars rover science investigation. *Journal of Geophysical Research*, **108**, 8062, doi:10.1029/2003JE002121.
- YEN, A.S. *et al.* 2005. An integrated view of the chemistry and mineralogy of martian soils. *Nature*, **436**, 49-54.

## Archaeometry in the House of the Vestals: analyzing construction mortar with portable infrared spectroscopy

Jennifer Wehby<sup>1</sup> & Samuel E. Swanson<sup>1</sup>

<sup>1</sup>University of Georgia, Department of Geology, Athens, GA, 30601 USA  
(e-mail: Jennifer.Wehby@gmail.com)

**ABSTRACT:** The aim of this study was to test portable infrared spectroscopy for non-destructive analysis of ancient construction mortar. Mortar samples from the House of the Vestals, in Pompeii, Italy, were initially examined with traditional analytical techniques, including X-ray fluorescence, X-ray diffraction and thin section analysis. These techniques were used to establish mineralogical and chemical profiles of the samples and to verify the results of experimental field methods. Results showed the lime-based binder was composed of calcite, and the volcanic sand aggregate contained clinopyroxene, plagioclase, sanidine and olivine crystals.

Field analysis of the mortar *in situ* consisted of near-infrared (NIR) reflectance spectrometry with a portable FieldSpec®3 spectroradiometer. The instrument's detectors operate in the shorter wavelengths (300nm – 2500nm), which are useful for analysing and identifying carbonates; most of the silicates were not detected within the NIR range. Statistical analysis of NIR spectral data indicated the key variances between samples fell within ~2000 – 2200nm and ~2250 – 2375nm, approximately where the major absorption bands appeared in a reference sample of pure calcite. This suggests the binder component of mortar is potentially useful for distinguishing different mortar types, and that this method of non-destructive analysis of the mortar *in situ* shows some promise.

**KEYWORDS:** near-infrared, portable, spectroscopy, mortar, Pompeii

### INTRODUCTION

Since 1995 the Anglo-American Project in Pompeii (AAPP) has been carrying out excavations and architectural analysis of one of ancient Pompeii's city blocks. This block, labelled insula VI.1, contains a mix of residential, commercial and industrial properties which survive as upstanding walls to a height of up to 3m. In its final phase, the House of the Vestals in Pompeii, Italy, had grown to its full extent by incorporating several smaller properties, evolving into one of the largest domestic structures in Pompeii (Jones and Robinson 2005). One of these smaller properties, VI.1.25 (Fig. 1) contains several different types of mortar, currently distinguished by color, which represent different construction phases. This structure presents a unique opportunity to test if and how the composition of calcium carbonate varies in each mortar type and how well these differences can be distinguished with portable infrared analysis. This mineral is well resolved with

near-infrared spectroradiometers and should show subtle differences in the shape and intensity of absorption spectra because of subtle differences in composition and structure (Ellis 1930).

### METHODS

From July 7-18, 2008, a near-infrared

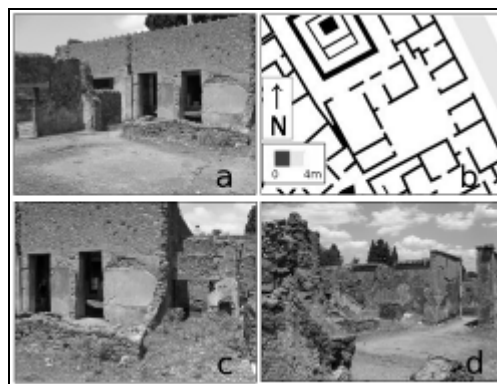


**Fig. 1.** House of the Vestals, structure VI.1.25, various views and plan map.

reflectance spectroscopy study of mortar was conducted *in situ* in the House of the Vestals using a portable spectroradiometer. These dates included three days of equipment set-up and testing and six days of analysis. Following the field tests in Pompeii, portable IR analysis was conducted on reference mortar samples collected during the 2007 field season of the AAPP. The hypothesis tested in this project is that individual construction phases will show differences in the absorption and reflectance features in near-infrared spectra of mortar, especially in the bands associated with CaCO<sub>3</sub>.

Analysis was conducted with a FieldSpec®3 portable spectroradiometer, manufactured by Analytical Spectral Devices, Inc. This instrument measures, in a field setting, infrared energy reflected at short-wavelengths, including the visible and near-infrared (VNIR) and short-wave infrared regions (SWIR). The instrument contains three detectors: a VNIR detector, from 350 – 1050nm, and SWIR 1, from 1000 – 1800nm, and SWIR 2, 1800–2500nm (ASD 1999). The detectors are connected to the instrument with a single fiber optic cable that contains 19 fibers for each detector. The cable is inserted into a “pistol grip”, a device that secures and directs the fiber optic cable during analysis. It can be either hand-held or mounted on a tripod; both configurations were tested (Figs. 2 and 3).

The instrument is controlled by an IBM Think Pad® laptop computer via a wireless network, utilizing ASD's proprietary software package. For this study, reference standard readings were collected before each sample reading to ensure consistent equipment function and to establish atmospheric conditions.



**Fig. 2.** Hand-held configuration of the FieldSpec®3. with the author taking a reference measurement.



**Fig. 3.** Tripod configuration of the FieldSpec 3® with the author taking a target sample reading.

## Fluorescence analysis of dissolved organic matter (DOM) in landfill leachates

Caixiang Zhang<sup>1</sup>, Yanxin Wang<sup>1</sup>, & Zhaonian Zhang<sup>2</sup>

<sup>1</sup>MOE Biogeology and Environmental Geology Laboratory, China University of Geosciences, Wuhan, 430074 CHINA (e-mail:caixiangzhang@yahoo.com)

<sup>2</sup>Environmental monitoring of Yichang, Hubei, 443000 CHINA

**ABSTRACT:** Dissolved organic matter (DOM) in Landfill leachate contains a large number of unknown molecules. Due to its complex chemical compositions, the analysis of DOM in landfill leachates constitutes a major challenge and the questions of their geographic or climatic specificity as well as their evolution in time due to biodegradation processes will not be explained unless some effective characterization methods are designed. After undergoing fractionation by tangential ultrafiltration and resins XAD column, a fluorescence study of DOM originating from a domestic landfill (China) was present here. The distribution of dissolved organic carbon, UV absorbance, and humic-like fluorescence were different among all fractions and organic carbon absorbed on XAD-8 resin (HoN/B) contains more chromophores. Humic-like and fulvic-like fluorescence occurred in all fractions, but protein-like fluorescence only occurred in the colloidal fraction. Subtle differences in synchronous fluorescence spectra were observed among various fractions; this may indicate the occurrence of DOM degradation from higher to lower molecular weight. The results reported here have significance for further understanding the sources and nature of DOM in aquatic environments.

**KEYWORDS:** Colloids, Dissolved organic matter, Fractionation, Fluorescence, Landfill leachate

### INTRODUCTION

Landfill leachate is an important point pollution source to water body, which contains DOM with a large number of unknown molecules that actively involve in biogeochemical and environmental processes (Chin *et al.* 1997). DOM not only plays an important role in freshwater systems for the mobility of toxic heavy metals and other pollutants but also may itself be a groundwater contaminant (Christensen *et al.* 1998).

Municipal landfill leachate typically contains dissolved organic carbon (DOC) concentrations up to several thousand (typically >1700 ppm), even in a landfill that is decades old (Christensen *et al.* 1998). More than 200 organic compounds have been identified in municipal landfill leachate (Paxe'us 2000). Therefore, an effective chemical characterization of landfill leachate by numerous analytical techniques requires a previous isolation procedure in order to remove possible interferences. In our previous study, we tested the advantage of the ultrafiltration

and resins XAD column chromatography to fractionate leachates (Zhang 2007). In this paper, the UV and fluorescence spectroscopies are used to define the spectral prosperities of each group of compounds present in the landfill leachates.

### MATERIALS AND METHODS

Leachates were collected from a landfill site (Wuhan, China), receiving compacted domestic wastes. Samples were pre-filtered by a microfilter device (1µm, Millipore) and sequently fractionated by tangential ultrafiltration into DOM (<0.45µm labelled as R1-3) and <1kDa (labelled as R1-5) fractions. The DOM was separated into relative hydrophilic (HI) and hydrophobic (HO) fractions by XAD columns due to resin's different properties and to hydrophobic/hydrophilic interactions occurring between the resin and organic matter (Zhang 2007), including hydrophilic acids (HiA), hydrophobic acids (HoA), Hydrophobic neutrals and bases (HbN/B), hydrophilic

neutrals and bases (HiN/B) and polar components (pc) (shown in Fig. 1). All fractions were adjusted to pH 6-7 and analyzed for DOC (Elementar Liquitoc, Germany), UV<sub>254</sub>(HP-1800) and fluorescence spectra (PerkinElmer LS55).

The EEM fluorescence spectroscopy involved scanning and recording of 23 individual emission spectra (220–510 nm) at sequential increments of 10 nm of excitation wavelength between 260 and 490 nm. The spectra were recorded at a scan speed of 1000 nm/min using excitation and emission slit bandwidths of 10 nm. Analyses were performed at a constant laboratory temperature of 22±3 °C, and blank water scans were run between every 10-20 analyses using a sealed distilled water cell.

The synchronous spectra (SF) were collected in the 260-460 nm excitation wavelength range using bandwidth of Δλ=20 nm between the excitation and emission monochromators. All SF and emission spectra were recorded with a 10 nm slit width on both monochromators. The scan speeds of spectra were 500 nm/min.

## RESULTS AND DISCUSSION

### Chemical analysis

Table 1 presents the results of fractionations of the DOM. The result of mass balance calculation of the DOC system shows that more than 55 % of the total DOC was retained by XAD-8 resin column, involving the portions of HoA and HbN/B, and DOC concentrations of the portion eluted by blackwashing (HoA) accounted for 47.4 % of total DOC, as compared with 26.25 % hydrophilic acids (HiA) of the total DOC. More than 11% of the total DOC passed through two resin columns, indicating that small molecular weight polar components were not absorbed onto by XAD-8 and XAD-4. The fractionation did cause potential loss of organic matter by permanent adsorption onto resin's polymers, which were 8.34 % for the XAD-8 resin and 6.41 % for the XAD-4 resin, respectively.

### Characteristic peaks position

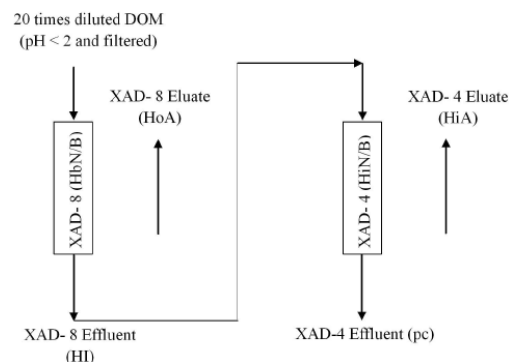


**Fig. 1.** Scheme of the tandem XAD-8/XAD-4 isolation procedure of DOM portion from the landfill leachate

**Table 1**

The chemical properties of the permeate after acidification and the filtered DOM and its fractions<sup>a</sup> isolated by XAD-8 and XAD-4

Parameters	Permeate	HO	HoA	HbN/B <sup>c</sup>	HI	HiA	HiN/B <sup>c</sup>	pc
DOC (mg/l)	355.90	198.39	168.71	29.68	157.51	93.41	22.81	41.29
% <sup>b</sup>		55.74	47.4	8.34	44.26	26.25	6.41	11.60
UV <sub>254</sub> (cm <sup>-1</sup> )	0.913	-	0.302	0.162	0.198	0.046	0.286	0.009

<sup>a</sup> mass balance of DOC formula: HO+HoA+HbN/B; HI=HiA+HiN/B+pc; DOM=HO+HI

<sup>b</sup> percentage over total DOC

<sup>c</sup> estimated by difference in mass balance

A typical fluorescence EEM results for leachate samples from R-landfill demonstrate five distinctive and intense fluorescence peaks in Figure 2, such as at Ex/Em=230–250/400–440 nm (labeled as “A”), which was relative to UV humic fraction identified in location to the diagnostic fluorescence centre observed previously; at Ex/Em=220–230/340–370 nm (labeled as “D”), a poorly understood fluorescent centre widely attributed to a component of the UV fulvic-like (Coble 1996); at Ex/Em=320–350/400–440 nm (labeled as “C”), which can be attributed to aromatic and aliphatic groups in the DOM fraction and commonly labeled as fulvic-like (Coble 1996); at Ex/Em=350–400/420–460 nm (labeled as “E”), which is attributed to humic-like and a final fluorescence centre at Ex/Em= 275–280/350–360 nm (labeled as “B”), which is attributed to the protein tryptophan, and widely observed in polluted river waters (Baker 2001; 2002) and clean estuaries (Mayer *et al.* 1999).

Synchronous fluorescence spectra of all fractions were similar shown in Figure 3, but showed differences in relative intensity of four characteristic peaks at about 285,

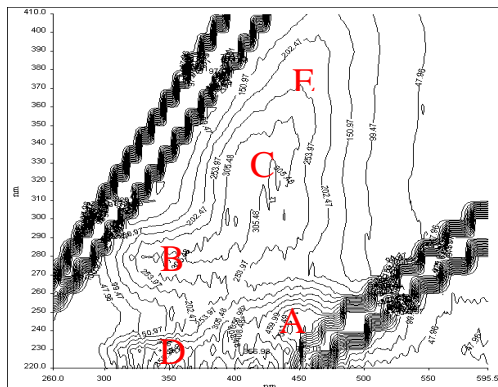


**Fig. 2.** EEM fluorescence contour and surface profile of the DOM isolated from landfill leachate.

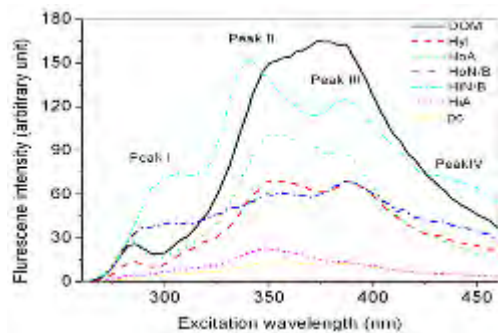


**Fig. 3.** SF spectra for original DOM and its six fractions at offsets of 20nm.

350, 385 and 434 nm. This is most likely caused by different concentrations of fluorophores in the DOM. In addition to possible DOM source differences, the  $\lambda_{max}$  for Peak I (B in Fig. 2 described above) can also depend on the  $\delta\lambda$  used for the synchronous fluorescence (De Souza Sierra & Donard 1994). In our study, the  $\lambda_{max}$  was most commonly observed at about 285 nm, and this wavelength was used throughout the study to characterize Peak I. Peaks II and III are characteristic for fulvic acids and solution humic acids (“C” and “E” in Fig. 2 described above), whereas peak IV is associated with the presence of humic acids (F not shown in Fig. 2).

Synchronous fluorescence has the potential to provide useful information regarding the relative abundance of protein-like vs. fulvic-like DOM (Peak I / Peak II) and humic-like vs. fulvic-like DOM (Peak III/Peak II). Figure 4 shows the

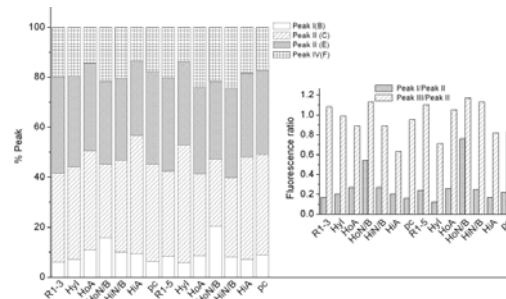


**Fig. 4.** The relative abundance (%) comparison between isolated fraction of R1-3 (05) and of R1-5 by XAD in the synchronous fluorescence spectra and the fluorescence index, Peak I/Peak II, Peak III/Peak II. Peak I-IV: 285, 350, 385, and 430 nm

relative abundance of each fraction isolated from leachate DOM. Fulvic-like acids and solution humic acids are dominant in each fraction isolated from DOM. The XAD resin could separate DOM into different fractions and higher ratio of Peak I/Peak II appeared in HoN/B and HiN/B, suggesting that N-containing chromophores can be adsorbed by XAD resins such as aliphatic amine, protein, amino-acid, pyrimidine.

In synchronous fluorescence spectra (Fig. 3) there are some shifts at 350 and 385 nm to shorter wavelengths as compared with original DOM. This shift in the maxima of fluorescence intensity from longer to shorter wavelengths is associated with a decreasing number of highly substituted aromatic nuclei (Miano & Senesi 1992). The calculated ratios of fluorescence intensity should be a measure of the degree of polycondensation and humification of DOM. Therefore, to the ratio were used as humification index here. Only two clearly distinguishable bands (Peak II and III) are needed to calculate the humification index because all samples were dominated by them (Figs. 3, 4). The greater ratio may be attributed to greater content of higher molecular weight organic matter in samples. The HoN/B fraction with highest humification indices was found in Figure 4. It was reasonable since humification indices of organic compounds adsorbing onto XAD-8 resin (humic substances)

should be higher than those of non-humic substances.

## CONCLUSIONS

Emission-Excitation Matrix (EEM) fluorescence spectroscopy as a non-destructive and sensitive analytical technique was successfully applied in this study to characterize DOM in landfill leachate. The DOM is composed of complex mixture of organic compounds with different fluorescence properties. In particular, the EEM profiles of DOM show two well-defined peaks at Ex/Em=320-350 /400-420 nm, Ex/Em=320-350 /420-450 nm reasonably due to the presence of two different groups of fluorophores. An additional and less intense band at Ex/Em=280-290 /320-350 nm can be assigned to aromatic amino acids and phenol-like compounds.

The EEM profiles of fractions obtained by the isolation procedure of the DOM by the XAD resins showed that a fractionation was effective and the XAD-8 eluate is highly representative of the original DOM. Emission scan spectra of DOM and its fractions are featureless, whereas synchronous scan spectra show that the isolation procedure is efficient in separating the original DOM into fractions with different fluorescence properties. The synchronous scan spectra obtained with a wavelength offset of 20 nm present multicomponent samples such as the DOM fractions from landfill leachate.

The EEM fluorescence allows identifying major differences in fluorescent properties between fractions. However, the EEM fluorescence spectroscopy may become very time-consuming. For quick preliminary analysis, it is recommended that synchronous fluorescence spectra be used for distinguishing samples of DOM with different chemical properties.

## ACKNOWLEDGEMENTS

The research work was financially supported by the National Natural Science Foundation of China (Grant for Outstanding Young Scholars No.40425001), and Wuhan Science and Technology Bureau (200860423203).

## REFERENCES

- BAKER, A. 2001. Fluorescence excitation-emission matrix characterization of some sewage-impacted rivers. *Environmental Science & Technology*, **35**, 948-953.
- BAKER, A. & CURRY, M. 2004. Fluorescence of leachate from three contrasting landfills. *Water Research*, **38**, 2605-2613.
- CHIN, Y.P., AIKEN, G.R., & DANIELSEN, K.M. 1997. Binding of pyrene to aquatic and commercial humic substances: The role of molecular weight and aromaticity. *Environmental Science & Technology*, **31**, 1630-1635.
- CHRISTENSEN, J.B., JENSEN, D.L., GRON, C., FILIP, Z. *ET AL.* 1998. Characterization of the dissolved organic carbon in landfill leachate-polluted groundwater. *Water Research*, **32**, 125-135.
- COBLE, P.G. 1996. Characterization of marine and terrestrial DOM in seawater using excitation-emission matrix spectroscopy. *Marine Chemistry*, **51**, 325-346.
- DE SOUZA SIERRA, M.M., DONARD, O.F.X., LAMOTTE, M., BELIN, C. *ET AL.* 1994. Fluorescence spectroscopy of coastal and marine waters. *Marine Chemistry*, **47**, 127-44.
- MAYER, L.M., SCHICK, L.L., LODER, T.C. 1999. Dissolved protein fluorescence in two main estuaries. *Marine Chemistry*, **64**, 171-179.
- MIANO, T.M., & SENESI N., 1992. Synchronous excitation fluorescence spectroscopy applied to soil humic substances chemistry. *Sci Total Environ*, 117/118, 41-51.
- PAXE'US, N., 2000. Organic compounds in municipal landfill leachates. *Water Science and Technology*, **42**, 323-33.
- ZHANG, C.X. 2007. PhD thesis. China University of Geosciences.

## Innovation for the CHIM method

**Liu Zhanyuan, Sun Binbin, Wei Hualing, Zeng Daoming, & Zhou Guohua**

*Institute of Geophysical and Geochemical Exploration, Langfang, Hebei, 065000, P.R. CHINA  
(e-mail: Liu zhanyuan@igge.cn)*

**ABSTRACT:** The method of the electro-geochemistry extraction (CHIM) for exploration has been continuously improved since it was used in China. The CHIM method is innovated through designing the new cathode receiver with solid absorbents, powered by battery in a low-voltage “dipole” mode with time controller. The innovated method has the following advantages: (1) Power for element receiver is independently supplied by a low-voltage “dipole” battery at each sampling site. The survey scale is not limited by electrical wires. The method can be applied in regional exploration. (2) The equipment is light-weight. (3) The cathode receiver with solid absorbents is easily operated in the field. (4) Time controller adopted is for standard time control at each sampling site.

**KEYWORDS:** CHIM, *dipole mode, time-control function* The cathode receiver with the ‘solid’ absorbents, small scale

### INTRODUCTION

The method of the electro-geochemistry extraction (CHIM) was developed by Yus Ryss.

The CHIM method have been applied in exploration for hidden base metals, gold deposits since CHIM was introduced to China in the beginning of 1980s. The CHIM method became less used since the middle 1990s due to its heavy equipment, complicated operation, expensive cost and low efficiency etc. However the research on understanding of its mechanism and on improvements for its technology is continuously carried out. It was found that CHIM technology extracts signals of mineralization elements from materials surrounding the receiver. The signals are transported from ore deposits at depth to surface by other mechanisms in a long period of past processes, not driven by present electricity force. The renovation of the CHIM technique was based on this new knowledge. The anomalous elements can be extracted by a low voltage dipole focusing on a small diameter area.

### THE NEW CATHODE RECEIVER

The new cathode receiver consists of the graphite pole and solid absorbents fixed in a plastic container (Figs. 1 and 2).

The shape of the new cathode receiver is a flat cylinder with a diameter of 12.8cm and a height of 2.8cm. The solid absorbents can put inside and take out by opening the cover (Fig. 2).

### POWER SUPPLY BY LOW VOLTAGE

#### DIPOLE

The cathode receiver and the anode were composed into a dipole system, powered by a low voltage battery (Fig.3). The distance of the anode-cathode is about 30~40cm. The receiver (cathode) is buried in the soils at a depth of 30~40cm. The anode stainless steel is installed directly over the receiver at the ground surface.

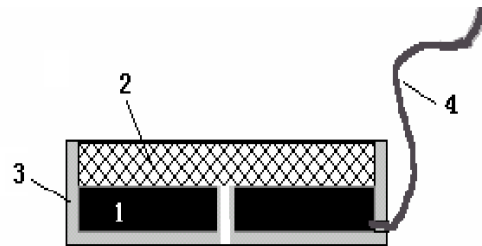


**Fig. 1.** Sketch map of the cathode receiver; 1-graphite-pole; 2-solid absorbent materials; 3-plastic container;4-electrical wire.

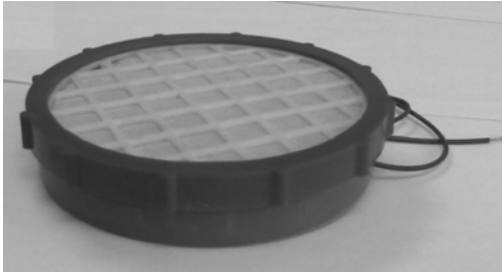


Fig. 2. Photo of the cathode receiver.

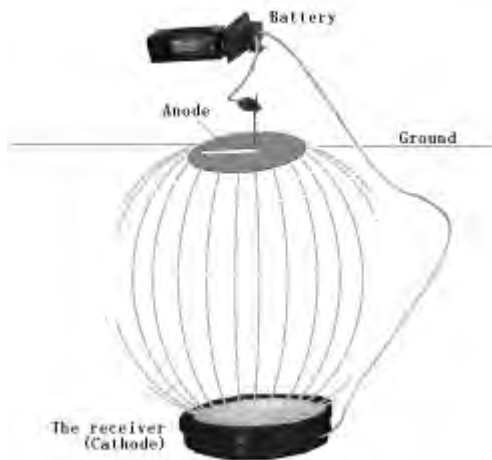


Fig. 3. Sketch of the 'Dipole CHIM' system.

**TIME CONTROLLER**

We designed a time-controller for insuring the same extraction time at each sample station (Fig. 4). The power supply time is automatically controlled between zero to 24 hours.

**A CASE STUDY**

Figure 5 shows the results at Jinwozi gold deposit in Xinjiang (Wang *et al.* 2007). Samples were taken along a 15km long profile across the deposits. Sampling intervals are 500 m in 2001 and 100 m in 2002 respectively. The results indicate that anomalies of Au obtained by different intervals are obviously coexisting over the ore bodies. The previous CHIM powered by electrical generator can not used for such long profile survey.

**CONCLUSIONS**

(1) The innovation CHIM technology is based on extracting elements at a limited



Fig.4. "Dipole CHIM" with time controller

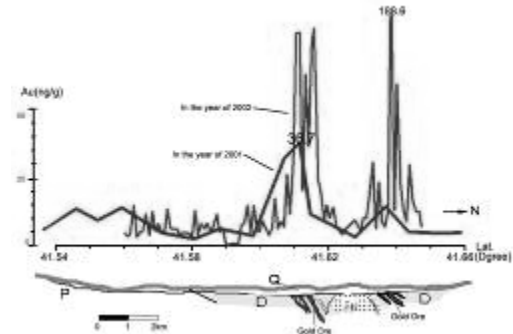


Fig. 5. Gold anomalies obtained by the innovation CHIM technique across the Jinwozi gold deposit in Xinjiang.

area surrounding the cathode, which the elements are transported from ore deposits at depth to surface by other mechanisms in a long past period of processes.

(2) The improved CHIM technology is enable to carry out survey not only at large scale but also at small scale.

(3) The improved CHIM technology with the time-controller can be used for standardization of sampling time.

(4) The improved CHIM technology has light equipment, convenient operation, low cost and high working efficiency, etc.

**ACKNOWLEDGEMENTS**

We would like to give our thanks to Dr. Wang Xueqiu for translating Chinese into English. Thanks are given to the Ministry

of Science and Technology for financial support (project No. 2007AA06Z133).

## REFERENCES

- Hamilton, S.M. 1998. Electrochemical mass transport in overburen: a new model to account for the formation of selective leach geochemical anomalies in Glacial Terren. *Journal of Geochemical Exploration*, **63**, 155-172.
- LEIZ, R.W. 1994. Ideal CHIM with the newly-Developed NEOCHIM electrode, V.S. *Exploration Geochemists*, **83**, P10-15.
- MING, K. & XIAN-RONGCES, L. 2003. Improvement and applied results of geoelectrical chemistry methods. *Geology and Prospecting*, **5** (in Chinese).
- MING, K., KUANG, C., & XIAN-RONGCES, I. 2006. Application of "DIPOLE CHIM" electrified by low voltage. *Geology and Prospecting*, **4** (in Chinese).
- RYSS, Y. 1983. The methods of the electro-geochemistry extraction, *The Geologe Publish of China*, in Chinese, 1986, translating Russian into Chinese by ZHANG ZHAOYUAN & CUI LINPEI.
- WANG, X., LIU Z., & YE, R. *et al.* 2003. Deep-penetrating geochemistry: A comparative study in the Jinwozi Gold Ore District, Xinjiang. *Geophysical & Geochemical Exploration*, **4** (in Chinese).
- WANG, X., WEN, X., YE, R., LIU Z., SUN, B., ZHAO, S., SHI, S., & WEI, H. 2007. Vertical variation and dispersion of elements in arid desert regolith: a case study from the Jinwozi gold deposit, northwestern China. *Geochemistry: Exploration, Environment, Analysis*, **7**, 163-171.
- ZHANYUAN, L., JIMIN, L., & AIMIN, C. 1997. Adiscussion on the action conditions of CHIM process. *Geophysical & Geochemical Exploration*, **2** (in Chinese).
- ZHANYUAN, L., ZHIZHONG, C., & BINBIN, S. 2005. The processed of the carrier material in the cathode receiver. *Geophysical & Geochemical Exploration*, **5** (in Chinese).



# **GEOCHEMICAL ASPECTS OF MINE WASTES**

EDITED BY:

**DOGAN PAKTUNC**  
**U. ASWATHANARAYANA**



## Geochemistry of the Lake George Antimony mine tailings, Lake George, New Brunswick, Canada: Understanding antimony mobility in a tailings environment

Pride T. Abongwa<sup>1</sup> & Tom A. Al<sup>1</sup>

<sup>1</sup>Department of Geology, P.O. Box 4400, University of New Brunswick, NB, E3B 5A3 Canada  
(e-mail: z4v08@unb.ca)

**ABSTRACT:** Sulfide minerals in the Lake George Antimony deposit included stibnite ( $\text{Sb}_2\text{S}_3$ ), arsenopyrite ( $\text{FeAsS}$ ), boumonite ( $\text{PbCuSbS}_3$ ), chalcopyrite ( $\text{CuFeS}_2$ ), cubanite ( $\text{CuFe}_2\text{S}_3$ ), kermesite ( $\text{Sb}_2\text{S}_2\text{O}$ ), pyrite ( $\text{FeS}_2$ ), pyrrhotite ( $\text{Fe}_{(1-x)}\text{S}$ ), senarmontite ( $\text{Sb}_2\text{O}_3$ ), sphalerite ( $(\text{Zn},\text{Fe})\text{S}$ ), stibivanite ( $\text{Sb}_2\text{VO}_5$ ) and tetrahedrite ( $(\text{Cu},\text{Fe})_{12}\text{Sb}_4\text{S}_{13}$ ). Native antimony (Sb) was also found. The major gangue minerals are calcite and quartz, with minor amounts of plagioclase and muscovite, and accessory rutile and zircon (Abbot & Watson 1975). The pore-water geochemistry of the Lake George Antimony Mine tailings was characterized by collecting and analyzing samples at discrete depths throughout the vadose zone. As a consequence of sulfide oxidation and associated mineral-water reactions, the pore water in the near surface tailings is characterized by elevated  $\text{SO}_4$ , Fe, Mn, Ca, Na, Al, K, and Si concentrations. The pH is near neutral throughout the tailings because of acid-neutralization reactions involving carbonate minerals. Relatively low Sb concentrations were recorded in the near-surface tailings pore-water compared to pore-water at greater depth. The results of SEM/EDS analyses indicate the presence of secondary Sb and Fe oxyhydroxide minerals in the near surface tailings. Precipitation of secondary Sb oxide phases presents limitations on Sb mobility, as does adsorption of Sb on the surfaces of Fe oxyhydroxides.

**KEYWORDS:** *Tailings, antimony, Fe-oxyhydroxides, oxidation, sorption*

### INTRODUCTION

The Lake George Antimony Mine is located 39 kilometers west-southwest of Fredericton, New Brunswick, Canada. Stibnite ( $\text{Sb}_2\text{S}_3$ ) and native antimony (Sb) were the main sources of antimony in the 100 year history of the mine (1880-1996).

Many hydrochemical studies of tailings systems have focused on tailings derived from copper, nickel, lead, zinc, and gold deposits (e.g., Dubrovsky *et al.* 1985, Al *et al.* 1994; Jambor & Blowes 1994; McGregor *et al.* 1998a; Johnson *et al.* 2000). Extensive research has been conducted on these types of tailings, which has led to a solid understanding of the geochemical processes that occur. The oxidation of sulfide minerals in tailings piles will lead to significant changes in pore-water geochemistry over time. The tailings from the Lake George Antimony Mine contain abundant arsenopyrite and stibnite which have reached an advanced state of weathering. The weathering of

stibnite and associated antimony minerals in tailings has not been studied previously.

### METHODS

Geochemical data were obtained from vertical cores retrieved using aluminum casing (7.5 cm diameter, 3 m long) that were driven through the unsaturated and saturated zones of the tailings. After collection, the cores were cut into 25 cm lengths and centrifuged to extract pore water. During centrifugation, the pore-water was collected in a  $\text{N}_2$ -purged reservoir and then extracted directly into syringes to prevent contact with the atmosphere. Anion analysis was performed using Ion Chromatography and analysis of cations was performed by both Inductively-Coupled Plasma Mass Spectroscopy (ICP-MS) and Inductively-Coupled Plasma Optical-Emission Spectroscopy (ICP-OES).

Aqueous geochemical modeling was performed using the program PHREEQC

Interactive Version 2.15.0 (Parkhurst & Appelo 1999). The Inl.dat database distributed with PHREEQC was used for all calculations. Geochemical modeling was used to speciate the components of the tailings pore-water at discrete depths and to investigate the thermodynamic stability of mineral phases through out the tailings.

Additional cores were collected in 5 cm diameter aluminum casings for mineralogical analysis. The cores were cut into 50 cm lengths and sealed in the field. They were then frozen upon arrival in the laboratory and analyzed on a later date. The cores were dried in a N<sub>2</sub> atmosphere for three weeks. The cores were then impregnated with low-viscosity epoxy for thin section preparation. The primary mineralogy of the tailings was determined using optical microscopy, X-ray Diffraction (XRD) and Scanning Electron Microscopy/Energy Dispersive Spectroscopy (SEM/EDS).

**RESULTS & DISCUSSION**

In the near-surface tailings, aqueous concentrations of SO<sub>4</sub>, Fe, Mn, Ca, Na, Al, K, Si, and As were elevated with respect to the respective concentrations in the deeper tailings (Fig. 1). The E<sub>h</sub> is relatively high in the near-surface tailings and the pH is near neutral throughout the tailings (Fig. 1). The elevated SO<sub>4</sub> and metal concentrations in the near surface tailings are a result of silicate and sulfide mineral weathering under oxidizing conditions. Acid generated by sulfide oxidation is buffered by neutralization reactions involving carbonate mineral dissolution. The distribution of Ca and alkalinity concentrations versus depth, as well as total C analyses (Fig. 2) with depth are consistent with carbonate consumption in the near-surface oxidation zone. Saturation indices (Fig. 3) indicate that the tailings pore-water is near equilibrium with respect to gypsum, with gypsum expected to precipitate in response to the release of Ca and SO<sub>4</sub> from carbonate dissolution and sulfide-oxidation reactions respectively.

Although elevated Sb concentrations

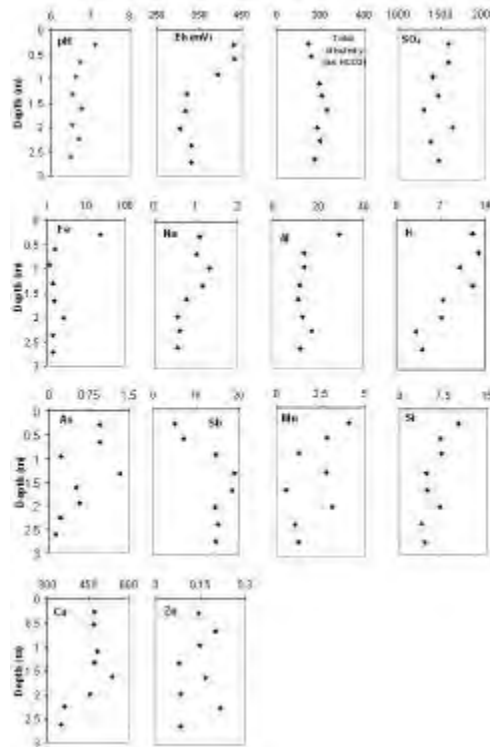
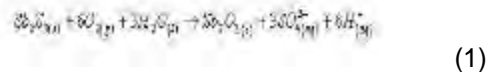


**Fig. 1.** Aqueous geochemical data from the Lake George Antimony Mine tailings. The x-axis represents concentrations in mg/L unless otherwise stated.

might be expected in the near-surface pore-water due to greater stibnite oxidation in contact with oxygen in the unsaturated zone, Sb concentrations are relatively low in the near surface pore-water and increase with depth (Fig. 1).

Geochemical speciation calculations suggest that Sb occurs predominantly as Sb(III) throughout the tailings pore-waters and that Sb concentrations are limited by the precipitation of common Sb(III) minerals, such as sernamontite (Sb<sub>2</sub>O<sub>3</sub>, reaction 1).



The pore-water in the near-surface tailings is supersaturated with respect to stibnite oxidation products sernamontite, Sb<sub>2</sub>O<sub>5</sub>, and Sb(OH)<sub>3</sub> (Fig. 3). Iron concentrations as high as 23.49 mg/L were recorded in the near-surface pore-water with lower concentrations at depth (Fig. 1).

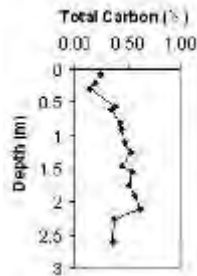


**Fig. 2.** Total inorganic C vs. depth (expressed as wt.% calcite).

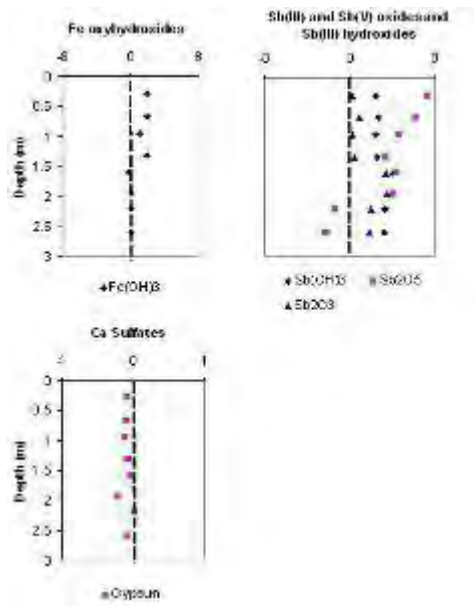


**Fig. 3.** Pore-water mineral saturation indices calculated with PHREEQC (Parkhurst & Appelo 1999) using the Iln.dat database.

The pore-water is undersaturated with respect to siderite but supersaturated with respect to Fe (III) hydroxides such as goethite and amorphous  $\text{Fe}(\text{OH})_3$  (Fig. 3). These results, consistent with SEM/EDS analyses showing Fe oxyhydroxide mineral precipitates in the near-surface tailings (Figs. 4 & 5), suggest that adsorption reactions involving Fe oxyhydroxides may play a role in controlling Sb mobility in the tailings environment. A series of laboratory experiments by Leuz *et al.* (2006), showed that the Fe oxyhydroxide, goethite, ( $\text{FeOOH}$ ) is an important sorbent for  $\text{Sb}(\text{III})$  and  $\text{Sb}(\text{V})$  species in the near-neutral pH range.

However, their results indicate that

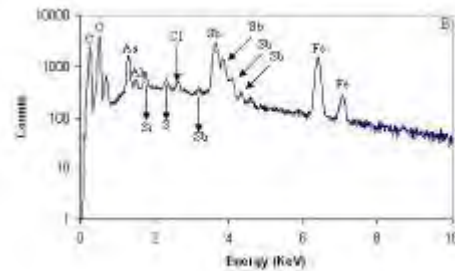
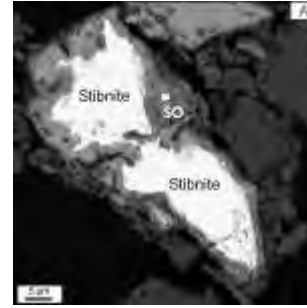


**Fig. 4.** (A) Backscattered electron image (BSEI) showing oxidation of stibnite. (B) SEM/EDS spectra obtained within a secondary oxide (mixture of Fe and Sb oxide). White square is the location of the EDS analysis shown in (B) and SO means secondary oxide.

elevated aqueous Sb concentrations are expected at pH above 7 or 8 because  $\text{Sb}(\text{III})$  may be oxidized to  $\text{Sb}(\text{V})$  by reaction with Fe-oxyhydroxides (Belzile *et al.* 2001), and adsorption of the product  $\text{Sb}(\text{V})$ , decreases above this pH range.

## CONCLUSIONS

Trends in pore-water geochemistry in the near surface tailings of the Lake George Antimony Mine reflect the effects of sulfide-mineral oxidation. The  $\text{SO}_4$ , and most metal concentrations are relatively high in the surficial (oxidation) zone of the tailings. The presence of carbonates in the tailings neutralizes the acidity produced by sulfide oxidation, resulting in near-neutral pH. The relatively low Sb concentration in the near-surface tailings compared to concentrations at depth are thought to result from the combination of secondary Sb-oxide mineral precipitation and adsorption of Sb on secondary Fe oxyhydroxides. Identification of secondary minerals important for controlling Sb mobility will commence in the future with

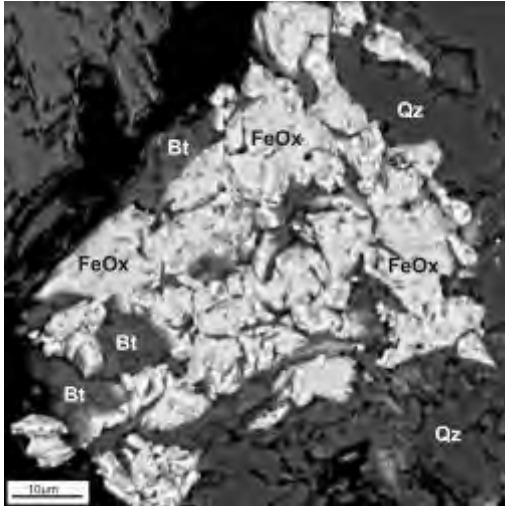


**Fig. 5.** BSEI showing secondary Fe oxyhydroxide minerals. Qz = Quartz, Bt = Biotite and FeOx = Fe oxyhydroxides

detailed, nano-scale mineralogical studies.

#### ACKNOWLEDGMENTS

Funding for this research was provided by an NSERC Discovery grant to Dr. T. Al. The first author would also like to thank the Geological Society of America (GSA) and Dr. J.S Little (J.S Little International Fellowship, administered via the University of New Brunswick) through a student research grant that contributed to this research. The authors would also like to thank members of the Geochemistry research group at the University of New Brunswick for assistance with field and laboratory work.

#### REFERENCES

ABBOT, D. & WATSON, D. 1975. Mineralogy of

- the Lake George Antimony deposit, New Brunswick. *CIM Bulletin*, **68** (July), 111-113.
- AL T.A., BLOWES D.W., JAMBOR J.L., & SCOTT J.D. 1994. The geochemistry of mine-waste pore water affected by the combined disposal of natrojarosite and base-metal sulfide tailings at Kidd Creek, Timmins, Ontario. *Canadian Geotechnical Journal*, **31**, 502-512.
- BELZILE, N., CHEN, Y.W., & WANG, Z.J., 2001. Oxidation of antimony (III) by amorphous iron and manganese oxyhydroxides. *Chemical Geology*, **174**, 379-389.
- DUBROVSKY N.M., CHERRY J.A., REARDON E.J., & VIVYURKA, A.J. 1985. Geochemical evolution of inactive pyritic tailings in the Elliot Lake uranium district. *Canadian Geotechnical Journal*, **22**, 110-128.
- JAMBOR, J.L. & BLOWES, D.W. 1994. Environmental Geochemistry of Sulfide Mine-Wastes. *Mineralogical Association of Canada Short Course* **22**, 438 p.
- LEUZ, A.C., MÖNCH, H., & JOHNSON, C.A. 2006. Sorption of Sb(III) and Sb(V) to goethite: Influence on Sb(III) oxidation and mobilization. *Environmental Science and Technology*, **40**, 7277-7282.
- MCGREGOR, R.G., BLOWES, D.W., JAMBOR J.L., & ROBERTSON W.D. 1998. Mobilization and attenuation of heavy metals within a nickel mine tailings impoundment near Sudbury, Ontario, Canada. *Environmental Geology*, **36**, 305-319.
- PARKHURST, D.L. & APPELO, C.A.J. 1999. User's Guide to PHREEQC (Version 2.15.0)-A Computer Program for Speciation, Batch-Reaction, One-Dimensional Transport and Inverse Geochemical Calculations. *U.S. Geological Survey, Water Resources Investigation Report* **99-4259**.

## Contribution of *Cistus ladanifer* L. to natural attenuation of Cu and Zn in some mine areas of the Iberian Pyrite Belt

Maria J. Batista<sup>1</sup> & Maria M. Abreu<sup>2</sup>

<sup>1</sup>INETI, Apartado 7586, 2721-866, Alfragide PORTUGAL (email: joao.batista@ineti.pt)

<sup>2</sup>Instituto Superior Agronomia-UTL, Tapada da Ajuda, Lisboa PORTUGAL

**ABSTRACT:** The comparison between four groups of soils and rock rose plants (*Cistus ladanifer* L.) developed on these soils was made using three mine areas of different ages (Neves Corvo, Brancanes, Monte dos Mestres) and a control area (Lombador). Copper and zinc soil-plant relationship was different in Neves Corvo, ongoing exploitation of copper and zinc, when compared with the control area of Lombador reflecting the actual influence of the present exploitation. The rock rose plants seem to have contributed to the natural attenuation of Cu in soils of Brancanes area where mining stopped more than a century ago.

**KEYWORDS:** *Cistus ladanifer* L., mining areas, control area, natural attenuation, copper mines

### INTRODUCTION

The role of green plants in natural attenuation is an important way of phytostabilization of degraded areas, especially in the abandoned mine areas where well adapted and tolerant spontaneous plants grow. These plants contribute to decrease soil erosion, the mobility of contaminants in soil and to reduce or eliminate the risk to both human health and the environment.

The rock rose (*Cistus ladanifer* L.) is a typical Mediterranean plant well adapted to thin soils with low nutritional characteristics and water holding capacity as some of those found in the Iberian Pyrite Belt (IPB) (Carvalho Cardoso, 1965). This metallogenetic province is renowned by the existence of important polymetallic massive sulfide deposits and because was exploited for base metals since pre-Roman times.

The objective of this study was to evaluate the role of chemical elements uptake by rock rose (a well adapted plant to mine environments) in natural attenuation by phytostabilization of soils polluted during different periods of mining activity and abandon.

### MATERIALS AND METHODS

The capacity of rock rose to contribute to the natural attenuation of contaminated areas was evaluated by comparison, among different mine areas, the chemical elements in soils and plants. These areas were selected because of the similar geological environment and, the different periods of mining and abandon. The mines are located in the Vulcano Sedimentary formations of Upper Devonian epoch (Carvalho & Ferreira 1993). Three different areas of sampling were chosen. NC area - correspond to the Neves Corvo still active Cu and Zn mine where 19 soils and plants samples were collected. MM area - represent the Monte dos Mestres area which includes the following subareas: Courela das Ferrarias (a mine exploited until 1987), Cerro da Cachaçuda, Herdade do Castelo and Cerro das Guaritas all exploited for Mn (abandoned before 1980) and Cerro do Algaré exploited for copper and pyrite. In MM area were collected 26 samples of soils and plants. The third area, named B – represent the Brancanes mine that was exploited until the end of the XIX century. In this area were collected 11 samples of soils and plants. For comparison, seven samples of soils and plants were collected

in a reference area designated as L - Lombador area, which is located in the northern part of the area in turbidites of the Upper Visean age. The study areas are represented in Figure 1.

A total of 112 samples of rock rose (roots and leaves) and 56 soil samples (fraction <0.18 mm) where these plants were grown were analyzed. Soil pH was determined in a soil/water suspension with 1/2.5 (m/v) proportion. Soils and plants were analyzed for Cu, Zn, Al, Fe, Mn, Ca, K and P by ICP-OES after digestion with four acids ( $\text{HClO}_4 + \text{HNO}_3 + \text{HCl} + \text{HF}$ ).

After analysis of basic statistics and Shapiro-Wilk normality test, it was concluded that the data did not assure the normality conditions necessary to perform certain statistical analysis. To follow usual procedures the data were lognormalised and normality was tested by normal probability curves.

One-way-ANOVA tests were made to control the quality of the data. To achieve the proposed objectives, multiple comparison of means of the four groups was made by Tukey ( $p < 0,05$ ) test. The Dunnett ( $p < 0,05$ ) test was used to compare the means of three groups of mining sites with the control group (Seaman *et al.* 1991). Pearson correlation coefficients were also obtained to confirm the tests results.

## RESULTS AND DISCUSSION

The statistical parameters of central tendency obtained for the four groups of areas which reflect the geochemistry of different periods of the mine abandon are presented in Tables 1A and 1B.

Comparing all the groups (Tukey test) by pairs it was concluded that Brancanes, Lombador and Monte dos Mestres are comparable for Cu and Zn in soils and Fe in leaves of the rock rose plants. None of these groups is comparable with Neves Corvo in what Cu, Zn and Fe is concerned, both in soils and plants. This is due to the present mine exploitation of these metals and the dispersion of newly exploited materials in the surrounding area.

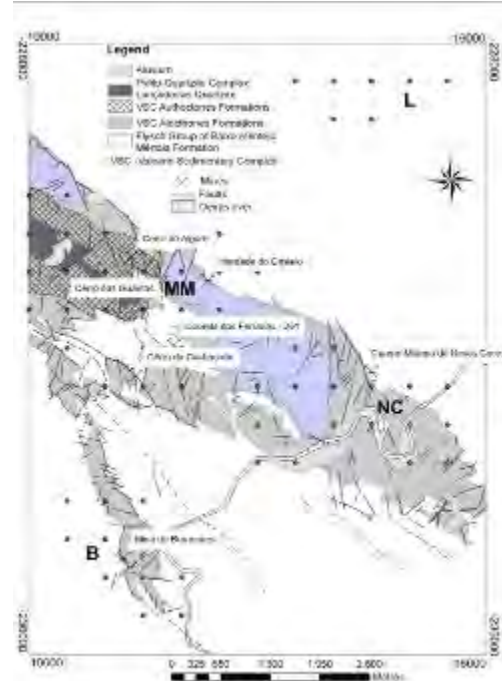


**Fig.1.** The study areas (NC, MM, B, L) of different mine sites with different periods of abandon.

In all the studied areas the concentrations of Mn, Al, K and Mg are statistically comparable among the areas. This indicates that these chemical elements, both in soils and plants, are independent from the mine exploitation.

In the control area, Lombador, the phosphorus, an essential element in plants nutrition, presents, in the relationsoil-plant, a different behavior from the other areas. This can be related to the substratum rock in the Lombador area which is composed of metasediments (turbidites) and are not included in Volcano Sedimentary Complex as the other areas where mining works have occurred.

The correlation coefficients ( $p < 0.05$ ) obtained for Lombador area showed that Cu in roots has good correlation with Zn ( $r=0.81$ ) and Fe ( $r=0.85$ ) in roots and with Al in soil (0.76) and roots ( $r=0.82$ ) and K in leaves (0.90). Zinc in roots is well correlated with Zn in leaves (0.76) and Fe in roots (0.88) meaning that this may be related with the capacity of Zn to be translocated to the aboveground parts of

**Table.1A.** Mean and median (mg kg<sup>-1</sup>) of soil pH and Cu, Zn, Fe, Mn, Ca, P, Mg, Al, K in soil samples (S) and plants (F-Leaves; R-roots) in Lombador (control area) and Monte dos Mestres.

	Lombador (L)		Monte dos Mestres (MM)	
	Mean	Median	Mean	Median
CuS	24	20	74	47
CuF	9	9	34	26
CuR	10	10	12	9
ZnS	49	42	56	49
ZnF	66	63	78	67
ZnR	17	16	23	23
MnS	685	543	1074	776
MnF	835	860	876	727
MnR	304	268	300	289
FeS	27429	23600	28342	29450
FeF	623	593	768	604
FeR	608	600	908	850
CaS	1957	2200	2308	1900
CaF	9600	10100	7692	7150
CaR	6571	5200	6427	6150
PS	437	410	612	590
PF	1530	1460	1455	1505
PR	350	360	386	375
MgS	5429	4500	4046	4500
MgF	2947	2613	2770	2750
MgR	655	699	745	756
AlS	62257	60300	65046	63500
AlF	1286	1200	1462	1350
AlR	1386	1400	1808	1850
KS	13114	11700	16542	15450
KF	5416	6400	5784	6000
KR	1984	2200	2295	2176
pH	6.0	6.2	6.0	6.1

the rock rose plants in Lombador, especially in low pH environment ( $r=0.79$ ). These results showed the importance of Cu and Zn uptake by plants (Wenzel & Jockwer 1999; Kidd *et al.* 2004) as these elements are essential micronutrients. The soil-root relationship, possibly more related with plant uptake, is higher in Cu than in Zn. The relation soil-leaf (possibly more related with

**Table 1B.** Mean and median (mg kg<sup>-1</sup>) of soil pH and Cu, Zn, Fe, Mn, Ca, P, Mg, Al, K in soil samples (S) and plants (F-Leaves; R-roots) in Neves Corvo and Brancanes areas.

	Neves Corvo		Brancanes	
	Mean	Median	Mean	Median
CuS	978	226	46	44
CuF	179	95	9	9
CuR	30	14	9	9
ZnS	165	83	52	54
ZnF	101	107	52	54
ZnR	28	23	20	19
MnS	1420	1017	966	1015
MnF	770	643	765	796
MnR	350	286	323	308
FeS	33479	30800	30945	29300
FeF	1538	1000	615	600
FeR	797	800	874	700
CaS	3000	2000	3418	2900
CaF	7377	7100	8107	8030
CaR	6109	5700	7139	6539
PS	700	600	827	800
PF	1406	1380	1548	1620
PR	387	354	374	330
MgS	5232	5400	4427	4900
MgF	2605	2600	2797	3003
MgR	758	789	695	666
AlS	63853	65000	68455	68500
AlF	1316	1226	1750	1550
AlR	1464	1498	1021	958
KS	15732	15000	18045	18100
KF	5311	5300	4816	6100
KR	2282	2200	2205	2186
pH	5.5	5.7	5.8	5.8

translocation mechanisms is higher in Zn (Alvarenga *et al.* 2004).

In contrast, in the Neves Corvo mining area the correlations between each element (Cu, Zn and Fe) in soil-root, soil-leaf and leaf-root samples, and low pH are high. Therefore, mobility of those elements in the soil-plant system seems to be facilitated in this nowadays mining area.

The Dunett test considers a control area (Lombador) for comparison. In this area,

phosphorus in soils is not comparable with the other mine areas groups which are in accordance with the Tucker test results. Phosphorous is an essential element in plant nutrition and its soil-plant relationship is different between the control area, where soils were developed on Visean age metasediments, and the mining areas whose substrata is composed of Volcano Sedimentary formations. The copper and zinc showed significant differences in the soil-plant system between the control area and Neves Corvo area. These differences indicate the obvious fact that those elements are nowadays mined in Neves Corvo, being present in the superficial environment of the area.

The comparable soil-plant copper relationship between Brancanes abandoned mine area and the Lombador control area, means that the period of more than a century of abandon may have contributed to some natural attenuation of this element in the mining area.

### CONCLUSIONS

The comparison between Tuckey and Dunnett tests indicated that the reference area of Lombador presents significant differences with the ongoing exploitation of Neves Corvo Cu and Zn mine. On the contrary, Cu relationship of soil-plant is similar in the Lombador control area and in Brancanes which is abandoned over a century. This fact suggests that natural attenuation effects on Cu in the soil-plant system have already happened in Brancanes mining area. The rock rose species (*Cistus ladanifer*, L.) seems to play an important role in the natural

attenuation process.

The major elements Mg, Ca, Al, K does not presented significant differences between the areas showing some independency of mining effects in these soil-plant systems. Phosphorus presents a different behavior between control and mining areas what may be related with parent material differences or plant physiology.

### REFERENCES

- ALVARENGA, P; ARAÚJO, M.F., & SILVA, J.A. 2004. Elemental uptake and root-leaves transfer in *Cistus ladanifer* L. Growing in a contaminated Pyrite Mining Area (Aljustrel-Portugal). *Water, Air and Soil Pollution*, **152**, 81-96.
- CARVALHO CARDOSO, J.V.J. 1965. Os solos de Portugal, sua classificação, caracterização e génese – 1- A sul do Rio Tejo-. *Direcção Geral dos Serviços Agrícolas, Lisboa*.
- CARVALHO, P. & FERREIRA, A. 1993. Geologia de Neves Corvo: Estado Actual do Conhecimento". *Simpósio de Sulfuretos Polimetálicos da Faixa Piritosa Ibérica, APIMINERAL, Évora, Portugal Mineral*, **33**, 11-1 to 1.11-21.
- KIDD, P.S; Díez, J., & MONTERROSO MARTINEZ, C. 2004. Tolerance and bioaccumulation of heavy metals in five populations of *Cistus ladanifer* L. subsp. *Ladanifer*. *Plant and Soil*, **258**, 189-205.
- SEAMAN, M.A., LEVIN, J.R., & SERLIN, R.C. 1991. New developments in pairwise multiple comparisons: Some powerful and practicable procedures. *Psychological Bulletin*, **110**, 577-586.
- WENZEL, W.W. & JOCKWER, F. 1999. Accumulation of heavy metals in plants grown on mineralised soils of the Austrian Alps. *Environmental Pollution*, **104**, 145-155.

## The Diavik Waste Rock Project: Design, construction and preliminary results

D. W. Blowes<sup>1</sup>, L. Smith<sup>2</sup>, D. Segó<sup>3</sup>, L.D. Smith<sup>1,4</sup>, M. Neuner<sup>2</sup>, M. Gupton<sup>2</sup>,  
B.L. Bailey<sup>1</sup>, N. Pham<sup>3</sup>, R.T. Amos<sup>1</sup>, & W.D. Gould<sup>1</sup>

<sup>1</sup>Department of Earth and Environmental Sciences, University of Waterloo CANADA  
(email: blowes@uwaterloo.ca)

<sup>2</sup>Department of Earth and Ocean Sciences, University of British Columbia CANADA

<sup>3</sup>Department of Civil and Environmental Engineering, University of Alberta CANADA

<sup>4</sup>Diavik Diamond Mines Inc. CANADA

**ABSTRACT:** Predicting the effluent water quality from waste rock stockpiles at new mines is challenging because of the limited understanding of the subsurface geology and the small volumes of samples available. Testing protocols, based on laboratory tests conducted on small volumes of rock, have been developed to assess the acid generating potential of waste rock. Extending these small scale tests to provide quantitative estimates of the concentrations of dissolved constituents anticipated in effluent water of full-scale stockpiles, the scale up problem, is more challenging. The Diavik waste rock research program includes the measurement and comparison of waste rock characteristics across a wide range of scales, varying from samples of less than a kilogram to the construction of three large-scale waste rock piles (15 m in height × 60 m × 50 m) to assess the evolution of the hydrology, geochemistry, temperature, and biogeochemistry of the waste rock piles over time. The study also provides insight to the hydrologic, geochemical, and thermal behavior of waste rock piles located in areas with continuous permafrost.

**KEYWORDS:** *Diavik Diamond Mine, waste-rock management, scale-up, mine drainage*

### INTRODUCTION

Development of open pits during mining at the Diavik Diamond Mine will result in the excavation of large volumes of country rock. The Diavik Country Rock Management Plan requires that country rock be segregated into three types during deposition: Type I (less than 0.04 wt % total sulfur); Type II (between 0.04 and 0.08 wt % total sulfur); and Type III (more than 0.08 wt % total sulfur). The Type III rock is considered to be potentially acid generating. The proposed reclamation covers for the country rock piles consist of Type I rock and till covers for Type III stockpile, and a Type I cover for Type II stockpile. The Diavik Waste Rock Research Program is designed to evaluate the benefits of the proposed reclamation strategies for the Diavik Country Rock Stockpiles, and to provide information to evaluate techniques used to scale the results of laboratory studies to predict the environmental impacts of full-

scale rock stockpiles. Understanding the relationship between these small-scale tests and full-scale waste rock piles is important to designing mine-waste disposal facilities and in developing management plans for new and operating mines that protect the environment.

### SITE DESCRIPTION

Diavik Diamond Mine Inc. is located on an island in Lac de Gras, 300 km northeast of Yellowknife, NT (Fig. 1). Open pit mining will lead to the eventual development of two 200 Mt permanent stockpiles of waste rock. The country rock consists of granite averaging <0.04 wt.% S and biotite schist averaging >0.08 wt.% S. Both rock types contain low concentrations of carbonate minerals.

### TEST PILE CONSTRUCTION AND INSTRUMENTATION

Three 15 m high test piles were constructed beginning in the spring of

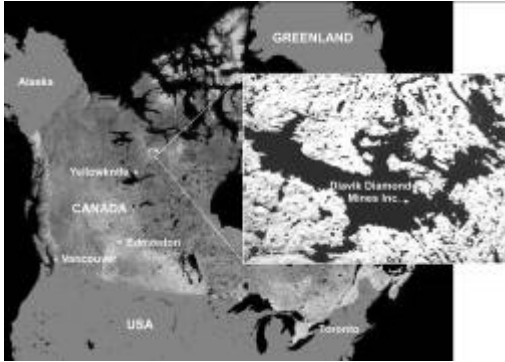


**Fig. 1.** Location of the Diavik Diamond Mine.

2005 and completed in the winter of 2007. These include the Type I pile, the Type III pile, and the Covered pile. The Covered pile consists of a Type III core, covered with a 1 m till layer and a 3 m Type I cap. Each pile was constructed with a basal drainage system for the collection and analysis of all water infiltrating through the piles, and a cluster of basal lysimeters for the collection of sub-samples of the infiltrating water to examine scale-up effects in flow variability and solute loadings.

The test piles were constructed with run-of-mine (ROM) material using standard mining equipment. Four tip faces spaced 5 m apart were instrumented with thermistors, soil water suction lysimeters (SWSS), tensiometers, gas sampling ports, time domain reflectometer (TDR) probes, air permeability probes, and access ports for thermal conductivity profiling and microbiological sampling. Stationary and portable data logging equipment is employed to collect data at frequent intervals. In addition to the three test piles, four continuously-draining collection lysimeters (two Type I and two Type II), each 2 m in diameter, were installed to monitor the flow and geochemistry of the active zone (Smith *et al.* 2009).

## PRELIMINARY OBSERVATIONS

### Physical Characterization

Physical characterization of the test piles has included grain size analysis, hydraulic properties, air permeability, and thermal



**Fig. 2.** Photo showing the basal drainage ditch excavated diagonally across the center of the Type I pad exiting through the SW corner (left side of picture).



**Fig. 3.** Basal drainage ditches excavated around the perimeter of the Type III pad exiting through the SW and NW corners (left side and bottom of picture, respectively). Basal lysimeters are visible in the centre of the photo.



**Fig. 4.** Waste rock sampling at the tip face.

conductivity. Grain size analyses indicate the test pile is representative of a "rock-

like” rather than a “soil-like” system, given the relatively small proportion of material less than 2 mm in diameter. The hydraulic properties of the waste rock have been measured at a number of different scales (Neuner *et al.* 2009). Porosity estimates are all on the order of 25%. Estimates of hydraulic conductivity vary greatly depending upon the scale of the measurement and the measurement technique, and range from  $8 \times 10^{-6}$  to  $1 \times 10^{-2} \text{ m s}^{-1}$  (Neuner *et al.* 2009).

### **Water Flow and Transport**

In the Type III pile, an apparent wetting front created by several artificial rainfall events conducted in late 2006 led to an elevated zone of moisture in the upper 3 m of the pile. Rainfall events late in the summer 2007, linked to two tracer tests, resulted in a wetting front that penetrated to a depth of approximately 8 m. This moisture was subsequently mobilized through the summer 2008 season as the pile warmed above 0°C (Neuner *et al.* 2009).

Outflow at the base of the Type III pile includes components originating as snowmelt on the batters of the pile, and infiltration of rainfall on the batters and, potentially, the top surface of the pile. The Type I test pile has only received natural rainfall events, resulting in cumulative outflow approximately one order of magnitude lower than the Type III pile. The Type I pile is apparently still accumulating water, with only the batters yielding flow at the base (Neuner *et al.* 2009).

### **Gas Transport**

Measurements made in the Type I pile and the Type III pile show no depletion in oxygen or increase in carbon dioxide concentrations, indicating gas transport mechanisms are fast relative to the rate of the oxygen consumption and carbon dioxide production due to geochemical reactions. In the Covered pile, significant depletions in oxygen and increases in carbon dioxide concentration have been observed at some locations, suggesting gas transport rates are limited by the till

cover. Gas pressure measurements in the Type III pile show gas pressure gradients within the pile respond to changes in wind speed and wind direction. The calculated magnitude of oxygen transport due to wind driven pressure gradients is similar to oxygen transport due to diffusion and/or convection observed at other waste rock piles (Amos *et al.* 2009).

### **Thermal Regime**

The air temperature fluctuations at the Diavik site results in ground surface temperatures that vary as much as 10°C during a month. The active layer in the bedrock at the site is about 4 m, as the surface temperatures vary between -28 and 16.5°C throughout the year. At 10 m depth into the bedrock, the temperature is stable at -5°C. In the Type I and Type III test piles, an active layer ranges from approximately 5 to 10 m depth under the influence of surface temperatures. Below a depth of 5 m, the cooling rate of waste rock varies from 2 to 3°C per year.

### **Test Pile Geochemistry**

Geochemical results show that the degree of sulfide oxidation is dependent upon the temperature of the piles and the rock sulfide content. In the basal drain effluent of the Type III pile, a decrease in pH was observed throughout the summer as the pile warmed. Sulfate concentrations also increase with the warming of the pile and decrease as the pile cools. The decrease in pH is correlated with an increase in the concentrations of dissolved metals.

The pH of the effluent from the Type I pile remained near neutral during 2008 with elevated concentrations of sulfate. The pH of the basal drain effluent from the Covered pile was lower than observed at the Type I and Type III piles, potentially as a result of the higher sulfide content of the pile. The Covered pile effluent also had higher sulfate and conductivity (Bailey *et al.* 2009).

### **CONCLUSIONS**

The objectives of the Diavik Waste Rock Research Program are to evaluate the benefits of the proposed reclamation

concepts for the Diavik Country Rock Stockpiles, and to evaluate techniques used to scale the results of laboratory studies to full-scale rock stockpiles. The data collection activities to date including hydrological, thermal, gas transport, and geochemical parameters address these objectives.

#### **ACKNOWLEDGEMENTS**

Funding for this research was provided by: Diavik Diamond Mines Inc. (DDMI); Canadian Foundation for Innovation (CFI) Innovation Fund Award, Natural Sciences and Engineering Research Council of Canada (NSERC); the International Network for Acid Prevention (INAP); and the Mine Environment Neutral Drainage (MEND) program. In-kind support provided by Environment Canada is greatly appreciated. We appreciate the support and assistance we have received from G. MacDonald, J. Reinson, L. Clark, and S. Wytrychowski, DDMI.

#### **REFERENCES**

AMOS, R.T., SMITH, L., NEUNER, M., GUPTON, M., BLOWES, D.W., SMITH, L., & SEGO, D.C. 2009. Diavik Waste Rock Project: Oxygen Transport in Covered and Uncovered Piles.

In: *Proceedings of the 2009, Securing the Future and 8<sup>th</sup> ICARD*, June 22-26, 2009, Skellefteå, Sweden.

BAILEY, B.L., SMITH, L., NEUNER, M., GUPTON, M., BLOWES, D.W., SMITH, L., & SEGO, D.C. 2009. Diavik Waste Rock Project: Early Stage Geochemistry and Microbiology. In: *Proceedings of the 2009, Securing the Future and 8<sup>th</sup> ICARD*, June 22-26, 2009, Skellefteå, Sweden.

NEUNER, M., GUPTON, M., SMITH, L., SMITH, L., BLOWES, D.W., & SEGO, D.C. 2009. Diavik Waste Rock Project: Unsaturated Water Flow. In: *Proceedings of the 2009, Securing the Future and 8<sup>th</sup> ICARD*, June 22-26, 2009, Skellefteå, Sweden.

PHAM, N., SEGO, D.C., ARENSON, L.U., SMITH, L., GUPTON, M., NEUNER, M., AMOS, R.T., BLOWES, D.W., & SMITH, L. 2009. Diavik Waste Rock Project: Heat Transfer in a Permafrost Region. In: *Proceedings of the 2009, Securing the Future and 8<sup>th</sup> ICARD*, June 22-26, 2009, Skellefteå, Sweden.

SMITH, L., NEUNER, M., GUPTON, M., MOORE, M., BAILEY, B.L., BLOWES, D.W., SMITH, L., & SEGO, D.C. 2009. Diavik Waste Rock Project: From the Laboratory to the Canadian Arctic. In: *Proceedings of the 2009, Securing the Future and 8<sup>th</sup> ICARD*, June 22-26, 2009, Skellefteå, Sweden.

## Prediction of acid mine generating potential: Validation using mineralogy

Hassan Bouzahzah<sup>1,2</sup>, Mostafa Benzaazoua<sup>1</sup>, Benoît Plante<sup>1</sup>,  
Bruno Bussière<sup>1</sup>, & Eric Pirard<sup>2</sup>

<sup>1</sup> Université du Québec en Abitibi-Témiscamingue (UQAT), 445 boul. de l'Université, Rouyn-Noranda, QC, J9X 5E4 CANADA (e-mail : Hassan.bouzahzah@uqat.ca)

<sup>2</sup> Université de Liège GeMME, B52 Sart Tilman, Liège 4000 BELGIUM.

**ABSTRACT:** Acid mine drainage (AMD) is a problem of major importance for the mining industry. Its prediction is very important for a proper management and rehabilitation of AMD generating sites. The Sobek test (1978) modified by Lawrence and Wang (1997) is the most used static test to predict the potential to generate AMD (particularly in North America). This method is compared in this work with mineralogy based static tests to evaluate the benefits of knowing the tailings mineralogy in AMD prediction. Three synthetic tailings composed of simple mixtures of well-characterized pure minerals are used. Although basically different in their principles and procedures, the modified Sobek test and mineralogy based static tests provide comparable results. The static prediction results are validated through the use of weathering cell kinetic tests.

**KEYWORDS:** *Tailings, Acid mine drainage, Static and kinetic tests, quantitative mineralogy,*

### INTRODUCTION

Sulfidic mine tailings can generate acid mine drainage (AMD) under atmospheric water and oxygen action. Static tests (also called Acid base accounting ABA tests) are frequently used to predict AMD potential because they are fast and inexpensive. Reliable AMD prediction can help choosing proper mine waste management strategies during mining operation and selecting the appropriate mine closure plan. So, it is imperative to adequately estimate the acid generating potential of tailings especially. However, static tests have an important uncertain zone according to Ferguson and Morin (1991). Materials located in the uncertain zone are tested in this study. The Sobek test (1978) modified by Lawrence and Wang (1997), the most used static prediction test in North America, will be compared with three mineralogical static tests (Kwong 1993; Lawrence & Wang 1997; Paktunc 1999) to compare those different tests and to evaluate the benefits of tailings mineralogical composition knowledge in AMD prediction. For the mineralogy based prediction tests, it is absolutely essential to know the precise mineralogical composition of tailings. For

the relevance of this work, 3 "synthetic" tailings were made from a mixture of pure minerals. A combination of various chemical and mineralogical characterization techniques were used to estimate the mineralogy of the mixtures with sufficient accuracy to give relatively precise results when integrated into mineralogical prediction methods.

### MATERIALS AND METHODS

In order to prepare standard mineral mixtures, pyrite (Py), pyrrhotite (Po), chalcopyrite (Cp), sphalerite (Sp), siderite (Sid), dolomite (Dol), calcite (Cal) and quartz (Qz) were acquired as pure mineral samples through a specialized distributor (Minerobec, Canada). These 8 pure minerals were further cleaned under a binocular microscope and separately crushed to reach 95% under 150µm (typical tailings grain size distribution; e.g. Aubertin *et al.* 2002). Each pure mineral powder was characterized thereafter with a series of chemical and mineralogical techniques. More details can be found in Bouzahzah *et al.* (2008). The relative density of each mineral specimen were measured with an He pycnometer and are

close to the theoretical density of the minerals except for Po ( $D_r = 4.4$ ; theoretical average = 4.61) and Sid ( $D_r = 3.8$ , theoretical 3.96). The XRD was used to identify and quantify the mineral species present in each pure mineral powder and confirmed that the Py, Cp, Dol, Cal, and Qz samples are almost pure. The Sid and Sp powders respectively show a slight contamination with rhodocrosite and quartz. The most impure sample is Po with 24 wt% pyrite and 12 wt% calcite, which explains its relative density discrepancy. The optical and scanning electron microscope observations confirm the XRD results.

The Atomic emission spectrometry (ICP-AES) results on the solids confirm the chemical purity of Py, Cp, Qz, Cal and Dol samples. The Po sample contains calcium which, after conversion into calcite, gives approximately 10 wt% of this mineral. Sid sample contains 10.3 wt% Mn and 1.86 wt% Mg, in agreement with measurements using a Scanning Electron Microscopy coupled to Energy Dispersive X-Ray Spectroscopy (SEM-EDS) analysis; again this explains the difference between the measured and theoretical density of the Sid powder.

Once the pure mineral powders characterized, 3 mixtures were manually prepared and named ML1, ML2 and ML3. They contain each of the 8 minerals in different proportions reproducing 3 mine tailings falling in the uncertainty zone of the static test used. The 3 synthetic tailings were characterized with the same techniques as for the pure minerals. Cp and Sp weight fractions were evaluated from their chemical element tracers (respectively Cu and Zn) obtained from ICP-AES analysis. Qz, Dol, and Sid samples are considered pure and their percentages in the mixtures are not corrected. Table 1 presents the fraction of each mineral in the three mixtures before and after correction taking into consideration the contamination of Po sample by pyrite and calcite, as previously determined. The corrected mineral proportions are used for calculation of the static test parameters based on

**Table. 1.** Corrected mineral composition (corr) of the three standard mixtures as compared to the initial dosing.

	ML1		ML2		ML3	
	Initial %	% corr	Initial %	% corr	Initial %	% corr
Py	6,50	6,86	8,50	9,34	12,00	12,48
Po	1,50	0,92	3,50	2,14	2,00	1,22
Cp	0,80	0,84	0,60	0,62	1,50	1,45
Sp	1,50	1,40	0,90	0,88	0,70	0,64
Dol	8,50	8,50	3,50	3,50	2,00	2,00
Cal	1,00	1,18	14,00	14,43	21,50	21,74
Sid	7,00	7,00	3,00	3,00	20,00	20,00
Qz	73,20	73,20	66,00	66,00	40,30	40,30
Total	100,00	99,90	100,00	99,91	100,00	99,83

mineralogy.

## RESULTS AND DISCUSSIONS

### Static tests

According to the Sobek test (1978) modified by Lawrence and Wang (1997), the acid potential (AP) is calculated from the sulfur content of the sample, and the neutralization potential (NP) is determined by an acid-base titration. For mineralogy based static tests, the calculation methods of Kwong (1993), Lawrence & Wang (1997) and Paktunc (1999) were used. The Lawrence and Wang (1997) method uses the inorganic carbon content for NP calculation. The amount of inorganic carbon and sulfur in samples were deduced from the mineralogical compositions. The Kwong (1993) and Paktunc (1999) methods are based on the summation of individual contributions of the minerals that produce (AP) and neutralize (NP) acid. The net neutralization potential (NNP) of a given tailings is defined as the difference between its NP and AP ( $NNP=NP-AP$ ). The results obtained by the different static tests are listed in table 2 and graphically plotted (Fig. 1) according to the Ferguson and Morin (1991) interpretation. All static tests used in this study classify the tailings in the uncertain zone except for ML1 classified as acid generating with the modified Sobek test.

### Kinetic test

To validate the static tests results presented above, weathering cells (small-

**Table 2.** Compilation of results from chemical and mineralogical static tests used in this study. For the Kwong test, if  $M > 0$ , the sample is considered acid generating, otherwise it is considered non acid generating.

		AP (Kg CaCO <sub>3</sub> /t)	NP (Kg CaCO <sub>3</sub> /t)	PNN (Kg CaCO <sub>3</sub> /t)
Modified Sobek	ML1	139,35	91,9	-47,45
	ML2	197,8	176,3	-21,5
	ML3	238,15	237	-1,15
Lawrence and Wang	ML1	148,63	104,08	-44,55
	ML2	196,11	182,3	-13,81
	ML3	244,6	239,11	-5,49
Kwong M=PA-PN	ML1	0,16	0,08	M=0,08
	ML2	0,22	0,23	M= - 0,01
	ML3	0,31	0,38	M= - 0,07
Paktunc	ML1	122,23	104,18	-18,05
	ML2	176,33	182,24	5,91
	ML3	217,4	239,08	21,68

scale humidity cell tests) were performed (see Cruz *et al.* 2001 for more details on the method). The measured pHs in flushing waters show a slight fluctuation around 8 indicating that the 3 samples did not become acidic during the kinetic tests. The measured oxydo-reduction potentials (Eh) reflect oxidizing conditions as a result of sulfide oxidation. The sulfur measured in leachates (mainly as sulfate) is the product of this sulfide oxidation. Iron was not detected in the leachates since the measured Eh-pH values are favourable for its precipitation as oxyhydroxides minerals in the weathering cells. Trace levels of Mn, Zn and Cu in leachates, and undersaturation of Mn, Zn and Cu secondary minerals (determined by geochemical modeling using VMINTEQ) reflect that Sid, Sp and Cp are not oxidized during the kinetic tests. For more geochemical details see Bouzazhah (2006).

Figure 2 shows that the cumulative sulfur (as SO<sub>4</sub><sup>2-</sup>), Ca and Mg concentrations increase during the weathering cell tests for all samples. The cumulative Ca and Mg leaching is indicative of calcite and dolomite dissolution (related to acid neutralisation). Figure 2 also shows that the sulfide oxidation rate slows down for all tailings after a few days, and that the stabilized oxidation rate is greater for the ML3 sample than for the others, which are

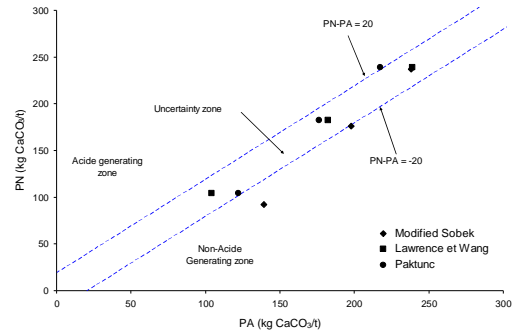


**Fig. 1.** Classification of the tree standard samples in terms of AP and NP according to Ferguson & Morin (1991).

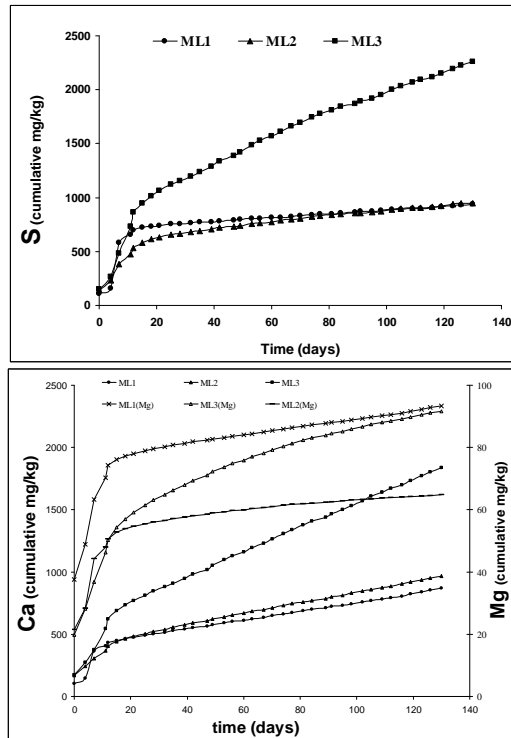


**Fig. 2.** Graphical representations of the evolution of cumulative concentrations of sulfur, calcium and magnesium collected throughout the kinetic test.

similar.

The oxidation-neutralization curve (Fig. 3) gives a long term prediction of AMD generation (see Benzaazoua *et al.* 2001 for more details). Assuming steady-state geochemical behaviour, the oxidation products (sulfates) would disappear before the neutralizing elements (Ca, Mg, and Mn).

## CONCLUSIONS

Many chemical and mineralogical characterization techniques were used to precisely determine the mineralogy of 3 synthetic tailings. Mineralogy based static tests are useful when sample mineralogy is

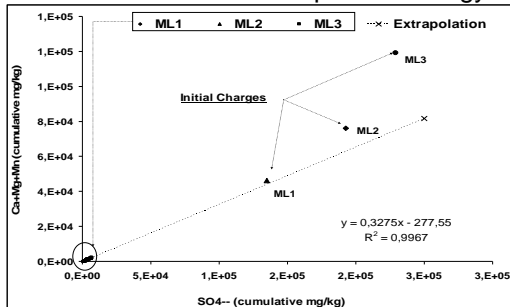


**Fig. 3.** Extrapolated oxidation-neutralization curve for the long-term prediction of acid mine drainage of the tree samples (Benzaazoua & Al 2001)

known with enough accuracy and give in our study comparable results to those of the modified Sobek test. The modified Sobek test seems to overestimate the AP prediction by taking into account the sulfur from sulfides that do not seem to oxidize in the conditions of the weathering cells.

## REFERENCES

- AUBERTIN, M., BUSSIERE, B., & BERNIER, L. 2002. Environnement et gestion des résidus miniers. CD, *Les Editions de l'Ecole Polytechnique de Montréal, CA.*
- BENZAAZOUA, M., BUSSIERE, B., & DAGENAIS, A.M. 2001. *Comparison of kinetic tests for sulfide mine tailings.* In: *Tailings and Mine Waste "01"* Fort Collins, Colorado, January. Balkema, Rotterdam, 263-272.
- BOUZHZA, H. 2006. *Prédiction du potentiel du drainage minier acide des résidus sulfurés.* Master thesis. University of Liege Belgium. 240p.
- BOUZHZA, H., CALIFICE, A., BENZAAZOUA, M., MERMILLOD-BLONDIN, R., & PIRARD, E. 2008. Modal Analysis of Mineral Blends Using Optical Image Analysis Versus X-Ray Diffraction. *Ninth International Congress for Applied Mineralogy* Brisbane, QLD, 8-10 September 2008.
- CRUZ R., BERTRAND, V., MONROY, M., & GONZÁLEZ, I. 2001. Effect of sulphide impurities on the reactivity of pyrite and pyritic concentrates: a multi-tool approach. *Applied Geochemistry*, **16**, 803-819.
- FERGUSON, K.D. & MORIN, K.A. 1991. The prediction of acid rock drainage –Lessons from the data base. *Second International Conference on the Abatement of Acidic Drainage*, Montréal, Canada, **3**, 83-106.
- KWONG, Y.T.J. 1993. Prediction and prevention of acid rock drainage from a geological and mineralogical perspective. *MEND Report 1.32.1* CANMET, Ottawa, 47 p.
- LAWRENCE, R.W. & WANG, Y. 1997. Determination of neutralization potential in the prediction of acid rock drainage. *Proceedings of the 4th International Conference on Acid Rock Drainage, Vancouver*, **2**, 449-464.
- PAKTUNC, A.D. 1999. Characterization of mine wastes for prediction of acid mine Drainage. In: *Environmental impacts of mining activities, emphasis on mitigation and remedial measures*, Springer Verlag, Berlin, Heidelberg, New York, Azcue, J.M., 19-40.
- SOBEK, A.A., SCHULLER, W.A., FREEMAN, J.R., SMITH, R.M. 1978. Field and laboratory methods applicable to overburdens and mine soil. *EPA report no. EPA-600/2-78-054*, 47-50.

## Preliminary investigation into tailings-ground water interactions at the former Steep Rock iron mines, Ontario, Canada

Andrew G. Conly<sup>1</sup>, Peter F. Lee<sup>2</sup>, & Chris Perusse<sup>1</sup>

<sup>1</sup>Department of Geology, Lakehead University, 955 Oliver Road, Thunder Bay, ON, P7B 5E1 CANADA  
(e-mail: andrew.conly@lakeheadu.ca)

<sup>2</sup>Department of Biology, Lakehead University, 955 Oliver Road, Thunder Bay, ON, P7B 5E1 CANADA

**ABSTRACT:** Drainage impacts from mined waste materials on ground water at the former Steep Rock iron mines were investigated at two different sites. Site 1 consists of a goethite-hematite-quartz tailings impoundment that was constructed on top of a bog/wet land. Site 2 consists of a pyritic waste rock dump and a down gradient AMD affected zone, which overlies glaciolacustrine sediments. Ground water from site 1 is pH-neutral and contains moderate sulfate (<1000 mg/L) and low Fe (< 1 mg/L). In contrast, ground water from site 2 has a lower pH (<6) with elevated sulfate (>3000 mg/L) and Fe (>95 mg/L) concentrations. The primary control on ground water chemistry is mineralogy of the waste material. However, carbon and sulfur isotopes indicate that for site 1 ground water chemistry is influenced by waters and gases originating from organic-rich (bog) soils that underlie the tailings. The chemistry of water within catchment basins at both sites is largely controlled by the composition of ground water; however, dilution by surface run-off and precipitation has occurred.

**KEYWORDS:** ground water, tailings, sulfate, pit lake, acid mine drainage

### INTRODUCTION

Flooding since 1979 of two open pits of the decommissioned Steep Rock iron mines near Atikokan, Ontario, has led to the formation of Hogarth and Caland pit lakes (Fig. 1). Distinct differences in water chemistry and quality exist between the two pit lakes: i) Hogarth is non-stratified, oxygenated and highly enriched in dissolved sulfate (1200-2000 mg/L), resulting in chronic sulfate toxicity (Goold 2008); and ii) Caland is not sulfate toxic and has an oxygenated fresh water lens that overlies an anoxic and moderately saline (200-500 mg/L sulfate) water column. The source of dissolved sulfate for both pit lakes is oxidization of pyrite within the buried ore zone; with the difference in sulfate levels reflecting differences in the pyrite content of the ore zones (Conly *et al.* 2008a,b). In addition, both pit lakes have near neutral pH due to reaction with carbonate wall rocks (Conly *et al.* 2008a,b).

However, the contributions of sulfate, acid and metals from ground and surface waters that interact with the numerous tailings and waste rock dumps located

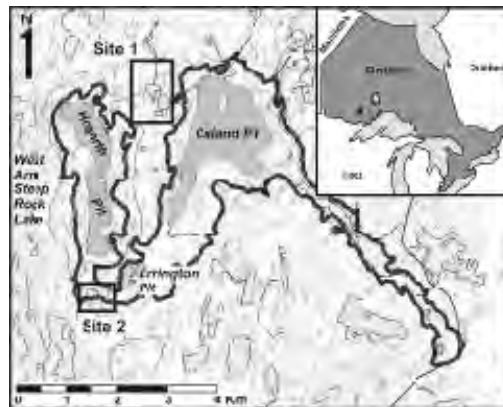


**Fig. 1.** Map showing location of the study sites relative to Hogarth and Caland pit lakes. Black outline represents original lake level (prior to draining for mining). Inset shows location of the Steep Rock iron deposit within Ontario.

throughout the Steep Rock site have not been extensively investigated.

Reconnaissance studies have shown that surface waters originating from waste rock and tailings dumps are typically characterized by low pH, high sulfate levels and variable metal contents. Consequently, the aim of this study is to investigate the nature of ground water interactions with

two different tailing materials, and examine how the products of these reactions interact with adjacent surface water bodies.

### SITE DESCRIPTION

Site 1 (Figs. 1 & 2a) is tailings impoundment that was constructed on top of a bog/wet land. The tailings consist of goethite + hematite + quartz, with little to no pyrite. The tailings are largely contained behind a dam structure, which presently serves as an access road. There is a lateral variation in the grain size of the tailings material: i) on the western side of the bedrock knob the material consists of well-drained, sandy tailings; and, ii) along the northern and eastern side bedrock knob the material consists of water-laden clay-silt tailings. The area south of the dam (~14 m elevation drop) consists of marsh grasses growing in a mixed unit of organic-rich soil and silt-clay tailings. A stream (SW 12) flows along the northwestern margin of the tailings impoundment. Another stream flows southward through the clay-silt tailings into pond 2, and eventually into Caland pit lake.

Site 2 is situated on the south shore of Moore's pit (Figs. 1 & 2b). This site consists of: i) a pyritic waste rock pile, covered with a thin veneer of Fe-oxide tailings; and ii) a down stream acid drainage affected area that is characterized by a Fe oxide + sulfur-rich hard pan surface layer that overlies a stratified unit comprised of intensely altered (Fe-oxide stained) and unaltered Quaternary glaciolacustrine deposits. A small creek (product of beaver activities) flows along the eastern margin of the site into Moore's pond.

### METHODS

Monitoring wells were installed to a depth of 3-4 m into soft tailings at sites 1 and 2. The wells are constructed of 1.5 inch-OD PVC pipe with the lower 1.2 m perforated for collection of ground water. Water was sampled using a LDPE tubing- foot valve assembly. Ground water and surface waters were sampled monthly from August to November 2008. Temperature, pH, and conductivity were measured in the field and

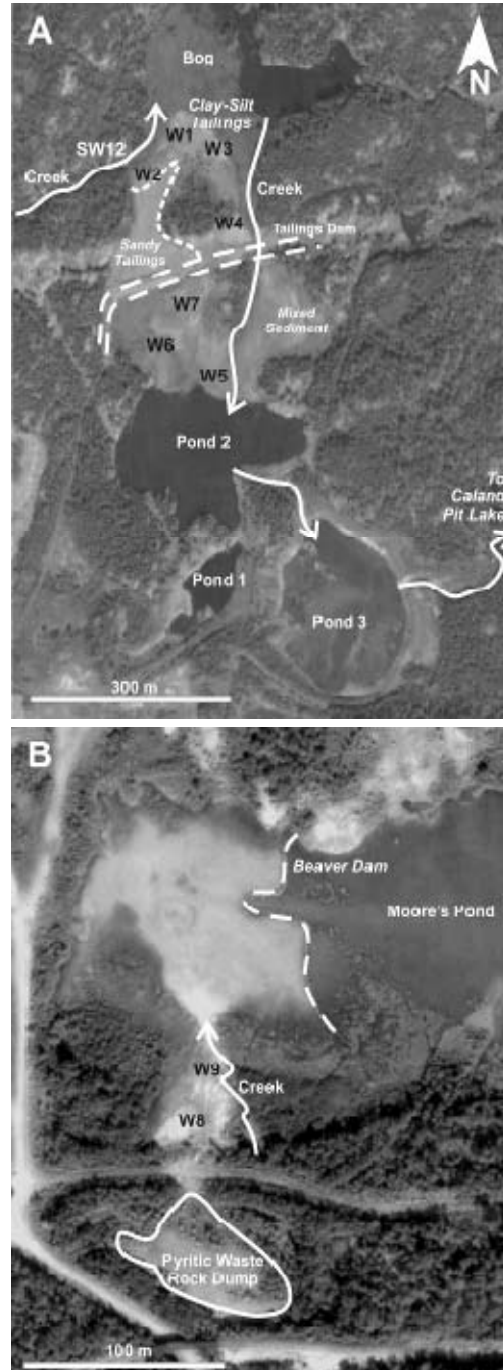


**Fig. 2.** Photo maps showing location of monitoring wells (W#), surface water bodies (flow directions of creeks indicated by arrows) and tailings/waste rock dumps for sites 1 (A) and 2 (B). Base images from Google™ Earth.

laboratory.

The chemical composition of the waters

was determined accordingly: 1) metals in filtered and acidified samples using a Varian ICP-AES; 2) Cl<sup>-</sup> and SO<sub>4</sub><sup>2-</sup> using a DIONEX ion chromatograph; and, 3) alkalinity by carbonate titration.

Stable isotope analyses were performed at the University of Calgary. The δ<sup>34</sup>S ratio of dissolved sulfate (precipitated as BaSO<sub>4</sub>) was determined by elemental analyzer-continuous flow-isotope ratio mass spectrometry (IRMS). δ<sup>13</sup>C<sub>DIC</sub> of water was prepared by phosphoric acid digestion (McCrea1950) prior to IRMS. All isotopic compositions are expressed in per mil notation relative to international standards (δ<sup>34</sup>S: CDT; δ<sup>13</sup>C<sub>DIC</sub>: PDB). Analytical uncertainties are ±0.2‰ for δ<sup>13</sup>C<sub>DIC</sub> and ±0.7‰ for δ<sup>34</sup>S.

**RESULTS AND DISCUSSION**

Figure 3 shows the average composition of major anions and cations, Fe, Mn, total metals and pH for all ground water wells and selected surface waters. Both sites are characterized by sulfate-dominant ground waters, as opposed to the one regional ground water which is chlorine-dominant. Interactions with pyritic waste rock (site 2) produces ground waters with elevated sulfate (>3000 mg/L) low pH (<6) and high Fe (>95 mg/L). Fe-oxide + quartz tailings (site 1) produce pH-neutral ground waters with moderate to high concentrations of sulfate (200-1000 mg/L). The one major difference observed is that ground water from site 1 is highly Fe-depleted (<1 mg/L). The difference in pH, sulfate and Fe levels between the two sites reflects the following: i) the relatively insoluble behaviour of goethite and hematite in pH-neutral waters (site 1); ii) possible occurrence of soluble Fe-sulfates (site 1); and, iii) the relative abundance of pyrite and the rate at which it is oxidized (site 2).

Surface waters parallel the observed trends for ground waters. However, for both sites anion and cation abundances are typically lower, and likely reflect dilution from surface run-off and precipitation.

Figure 4 shows the variation in carbon and sulfur isotopes for Steep Rock ground water and surface water. δ<sup>34</sup>S ratios for

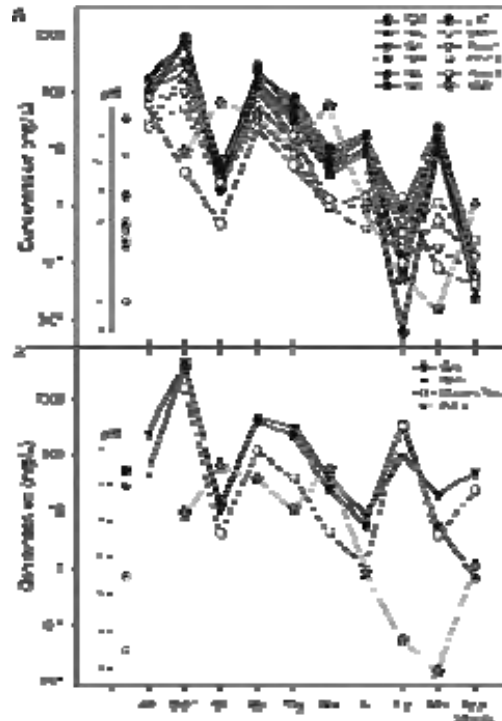


**Fig. 3.** Schoeller diagrams, with pH (inset), showing the average compositions for ground water and surface water from sites 1 (A) and 2 (B). Abbreviations: Alk – alkalinity; AGW – Atikokan ground water.

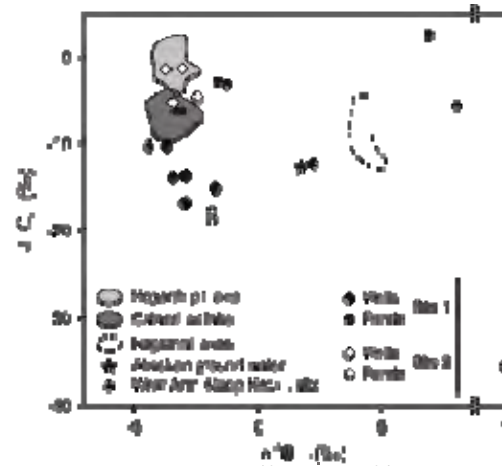


**Fig. 4.** Variation in δ<sup>13</sup>C and δ<sup>34</sup>S of ground water and surface water from sites 1 and 2. Data for other waters (excluding regional water; unpublished) from Conly *et al.* (2008b).

ground water from both sites are within the reported range for the two pit lakes, and indicate that the dissolved sulfate is produced from the oxidation of pyrite

present in waste materials (*cf.* Conly *et al.* 2008b).

Ground water from site 2 displays a narrow range in  $\delta^{13}\text{C}$ , and is within the range reported for the two pit lakes. The  $\delta^{13}\text{C}$  of ground waters from site 2 reflects exchange with atmospheric  $\text{CO}_2$  and carbonate dissolution (*cf.* Conly *et al.* 2008b). In contrast, the  $\delta^{13}\text{C}$  of ground water from site 1 is both more depleted and variable. Such values are interpreted to reflect isotopic exchange with  $\text{CO}_2$  released from buried organic-rich (bog) soils.

The ground water from well 6 (site 1) yielded both the most depleted  $\delta^{13}\text{C}$  and most enriched  $\delta^{34}\text{S}$ . Isotopic compositions of this dual nature are consistent with methanogenesis and bacterial sulfate reduction, arising from interaction with organic-rich (bog) soils from below.

## CONCLUSIONS

The composition of ground water present in tailing impoundments and waste rock dumps is primarily controlled by the mineralogy of the mine waste: i) pyrite-bearing material produces in low pH, sulfate-rich and Fe-rich waters; and, ii) Fe-oxide-bearing material produces neutral pH, moderate sulfate and Fe-poor waters. The water chemistry of tailings catchment ponds is primarily controlled by the chemistry of the inflowing ground water, but has been diluted by run-off and direct precipitation inputs. Sulfur isotopes indicate that sulfate is derived from the oxidation of pyrite in waste materials. Although not reflected in anion, cation and metal concentrations, interactions between

ground water and deeper, bog-derived waters and gases can be inferred from depleted carbon and enriched sulfur isotope ratios. Both ground and surface waters arising from tailings/waste rock interactions contribute, to an unknown degree, to the water quality issues of the pit lakes.

## ACKNOWLEDGEMENTS

We thank the Ontario Ministry of Natural Resources for their assistance with the project and allowing access to the site. Trow Engineering is thanked for their assistance with well installation. Funding for the project is provided through a NSERC Discovery grant awarded to AGC.

## REFERENCES

- CONLY, A.G., LEE, P.F., GODWIN, A., & COCKERTON, S. 2008a. Experimental constraints for the source of sulfate toxicity and predictive water quality for the Hogarth and Caland pit lakes, Steep Rock Iron Mine, Northwestern Ontario, Canada. *Mine Water and the Environment Proceedings*, **10**, 551-554.
- CONLY, A.G., LEE, P.F., GOOLD, A., & GODWIN, A. 2008b. Geochemistry and stable isotope composition of Hogarth and Caland pit lakes, Steep Rock Iron Mine, Northwestern Ontario, Canada. *Mine Water and the Environment Proceedings*, **10**, 555-558.
- GOOLD, A.R. 2008. *Water quality and toxicity investigations of two pit lakes at the former Steep Rock iron mines, near Atikokan, Ontario*. MSc. thesis, Lakehead University, Thunder Bay, Ontario.
- MCCREA, J.M. 1950. On the isotopic chemistry of carbonates and a paleotemperature scale. *Journal of Chemistry and Physics*, **18**, 849-857.

## Long-term fate of ferrihydrite in uranium mine tailings

Soumya Das<sup>1</sup> & M. Jim Hendry<sup>1</sup>

<sup>1</sup> University of Saskatchewan, Department of Geological Sciences, 114 Science Place, Saskatoon, SK, S7N5E2 CANADA (e-mail: sod671@mail.usask.ca)

**ABSTRACT:** The kinetics and mechanisms of the phase transformation of 2-line ferrihydrite to goethite and hematite are being assessed as a function of pH, temperature and Fe/As, Fe/Se, Fe/Mo molar ratios using batch experiments, BET analyses, XRD, and XANES. Initial results from XRD analyses show that ferrihydrite is stable at high pH (~10) for up to seven days at 25°C, but considerable crystallization occurs at elevated temperatures. Specifically, XRD data show that ferrihydrite is transformed to a mixture of hematite and goethite at 50°C (~85% hematite and ~15% goethite) and 75°C (~95% hematite and ~5% goethite) after 24 hours and these ratios remain constant to the end of the experiments (seven days).

**KEYWORDS:** *ferrihydrite, goethite, hematite, phase transformation.*

### INTRODUCTION

Ferrihydrite, a poorly crystalline iron (III) oxide (approximate formula:  $5\text{Fe}_2\text{O}_3 \cdot 9\text{H}_2\text{O}$ ) is typically found in mine drainage environments with pH values >5 (Carlson *et al.* 2002). Ferrihydrite has a large specific surface area (>220 m<sup>2</sup>/g), and therefore can strongly adsorb many environmental pollutants (including As, Mo, and Se) in aquatic systems; consequently it can play a crucial role in the bioavailability and migration of trace metals (Carlson & Schwertmann 1981; Schwertmann & Taylor 1989). Ferrihydrite transforms to thermodynamically more stable and more crystalline products, such as goethite and hematite. This crystallization (phase transformation) is controlled by solution pH, temperature, and solutes present in the system (Johnston & Lewis 1983; Schwertmann & Murad 1983; Paige *et al.* 1997). During this phase transformation, sorbed metal cations desorb as a result of a rapid decrease in the reactive surface area (Ford *et al.* 1997; Arthur *et al.* 1999). In addition, this transformation can have a significant impact on the aqueous concentrations of sorbed ions. Although cation partitioning during phase transformation has been documented, few studies have addressed the impact of this phase change on oxy-anions such as As,

Mo, and Se, which are important elements of concern in uranium tailings.

The goal of this study is to determine the impact of ferrihydrite phase transformations on the long-term source terms for As, Mo, and Se in uranium mine tailings facilities. This is important as arsenic complexation in uranium mine tailings at Rabbit Lake minesite, northern Saskatchewan, Canada is predominantly 2-line ferrihydrite with sorbed arsenate (Moldovan *et al.* 2003). The specific objective of the current study was to investigate the transformation of both natural and synthetic 2-line ferrihydrite to goethite and hematite as a function of temperature. This objective is being met using batch experiments, X-ray Absorption Near Edge Spectroscopy (XANES), X-Ray diffraction (XRD), B.E.T surface analyses, and Surface Complexation Modeling (SCMs). Additional experiments, based on the findings of this study, are underway to elucidate the fate of sorbed As, Mo, and Se onto ferrihydrite during phase transformation as a function of pH, temperature, and the Fe/As,Mo,Se ratio.

### MATERIALS AND METHODS

Initially, synthetic ferrihydrite, goethite and hematite were synthesized using the methods described by Cornell & Schwertmann (2003). These pure phases were analyzed using XRD, BET, and

XANES to ensure the quality of the synthates. Three batches of ferrihydrite were synthesized and precipitates were washed 5-6 times to ensure a chloride-free synthate. Ferrihydrite precipitates were re-dispersed in 200 mL of double deionized (DDI) water at (1) room temperature (25°C), as well as preheated in water baths to temperatures of (2) 50°C and (3) 75°C. For all of these slurries, pH was kept constant at 10 using 1M KOH. 40 mL samples were pipetted from each reaction vessel after 0, 1, 2, 3, and 7 days. Slurries were centrifuged, washed three times with DDI water and air dried for analyses (BET, XRD, and XANES). BET analyses were used to evaluate the decrease in surface areas with increasing crystallinity, and XRD and XANES were used to detail the structural and speciation changes in iron.

**RESULTS AND DISCUSSION**

Measured surface areas (11-point BET analyses) for pure phases such as ferrihydrite, goethite and hematite are in the range as proposed by Cornell & Schwertmann (2003) (Table 1). Preliminary XRD analyses showed that temperature impacts the kinetics of phase transformation of ferrihydrite. Data indicated that after seven days, the rate of transformation from ferrihydrite to more crystalline forms, if it was occurring, was too slow to be measured at 25°C (Fig. 1). In contrast to the 25°C experiment, significant, transformations were observed at 50 (Fig. 2) and 75°C (Fig. 3) after 24

**Table 1.** 11-point BET analyses of pure phases measured in this study. Expected values from Cornell & Schwertmann (2003) are also included to compare the results of present study.

Phase	Surface area (m <sup>2</sup> /g)
Ferrihydrite	347* 200-400 <sup>£</sup>
Goethite	19* 20-30 <sup>£</sup>
Hematite	44* ~30 <sup>£</sup>

\*This study <sup>£</sup>Cornell and Schwertmann (2003)

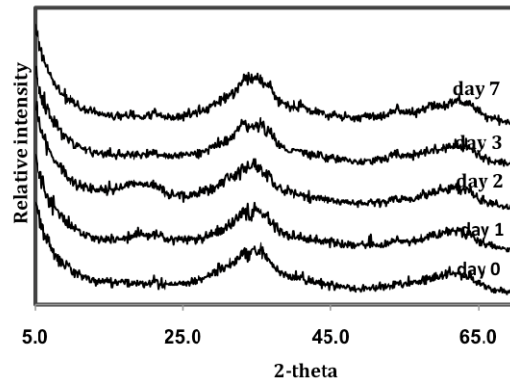


**Fig. 1.** XRD scans of solids at pH 10 and 25°C for day 0, 1, 2, 3, and 7 (from bottom to top). Scans show the dominance of ferrihydrite and lack of hematite and goethite.

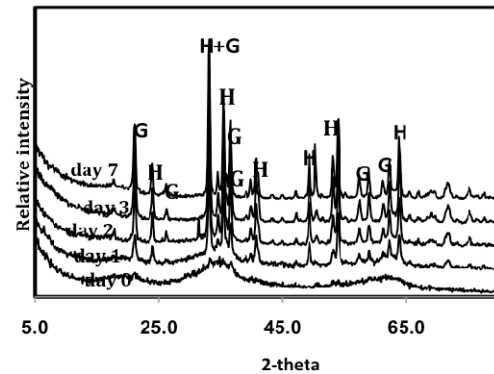


**Fig. 2.** XRD scans of solids at pH 10 and 50°C for day 0, 1, 2, 3, and 7 (from bottom to top). Scans show the dominance of ferrihydrite at day 0 but dominance of hematite and goethite in all subsequent scans.

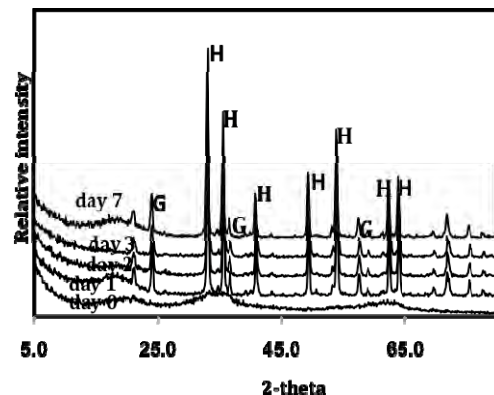


**Fig. 3.** XRD scans of solids at pH 10 and 75°C for day 0, 1, 2, 3, and 7 (from bottom to top). Scans show the dominance of ferrihydrite at day 0 but dominance of hematite and goethite in all subsequent scans.

hours. At both of these temperatures, ferrihydrite was transformed to a mixture of hematite and goethite (~85% hematite and 15% goethite at 50°C and ~95% hematite and 5% goethite at 75°C). These ratios of mixing of hematite and goethite remained constant for the remainder of the experiment (seven days). The transformation of ferrihydrite to hematite in these experiments is not inconsistent with a 2-stage crystallization process, as proposed by Vu *et al.* (2008). According to their findings, in the first stage, goethite is the stable product, but with extended heating, goethite transformed to hematite. These observations contradict with earlier workers (Schwertmann & Murad 1983; Shaw *et al.* 2005) who predicted goethite would be the final product instead of hematite. pH dependent experiments are in progress (pH 2 and 7). Results from these experiments will be of value to define the reaction kinetics of 2-line ferrihydrite in dilute solutions in nature over a wide range of pH and temperature.

#### PRELIMINARY CONCLUSIONS

Although additional analyses of the existing data and additional experiments are required to reach definitive conclusions on the phase changes of ferrihydrite in uranium mine tailings, preliminary XRD data suggest that in deionized water at elevated pH (pH=10) phase transformation of ferrihydrite can occur at elevated temperatures. In both elevated temperature experiments, hematite appeared to be the dominant transformation product. At room temperature, however, ferrihydrite remains stable after the duration of the experiment (seven days).

#### ONGOING WORK

Ongoing experiments are underway to determine:

- (1) pH dependence of crystallization by conducting experiments at pH 2 and 7 and at temperatures of 25, 50 and 75°C.
- (2) the effect of the Fe/As,Mo,Se molar ratio on adsorption and desorption kinetics during phase transformation

#### ACKNOWLEDGEMENTS

We would like to thank T. Bonli for assistance with the XRD and SEM analyses and J. Essilfie-Dughan for assistance with XANES analyses at the Canadian Light Source. This project was jointly funded by Cameco Corporation and NSERC through an IRC grant.

#### REFERENCES

- ARTHUR, S.E., BRADY, P.V., CYGAN, R.T., ANDERSON, H.L., & WESTRICH, H.R. 1999. Irreversible sorption of contaminants during ferrihydrite transformation. *WM'99 Conference*, February 28-March 4.
- CARLSON, L. & SCHWERTMANN, U. 1981. Natural ferrihydrites in surface deposits from Finland and their association with silica. *Geochimica et Cosmochimica Acta*, **45**, 421-429.
- CARLSON, L., BIGHAM, J.M., SCHWERTMANN, U., KYEK, A., & WAGNER, F. 2002. Scavenging of As from acid mine drainage by schwertmannite and ferrihydrite: a comparison with synthetic analogues. *Environmental Science and Technology*, **36**, 1712-1719.
- CORNELL, R.M. & SCHWERTMANN, U. 2003. The iron oxides: *Structure, properties, reactions, occurrences, and uses*. Wiley-VCH.
- FORD, R.G., BERTSCH, P.M., & FARLEY, K.J. 1997. Changes in transition and heavy metal partitioning during hydrous iron oxide aging. *Environmental Science and Technology*, **31**, 2028-2033.
- JOHNSTON, J. & LEWIS, D.G. 1983. A detailed study of the transformation of ferrihydrite to hematite in an aqueous medium at 92°C. *Geochimica et Cosmochimica Acta*, **47**, 1823-1831.
- MOLDOVAN, B.J., JIANG, D.-T., & HENDRY, M.J. 2003. Mineralogical characterization of arsenic in uranium mine tailings precipitated from iron-rich hydrometallurgical solutions. *Environmental Science and Technology*, **37**, 873-879.
- PAIGE, C.R., SNODGRASS, W.J., NICHOLSON, R.V., SCHARER, J.M., & HE, Q.H. 1997. The effect of phosphate on the transformation of ferrihydrite into crystalline products in alkaline media. *Water, Air, and Soil Pollution*, **97**, 397-412.
- SCHWERTMANN, U. & MURAD, E. 1983. Effect of pH on the formation of goethite and hematite from ferrihydrite. *Clays and Clay Minerals*, **31**(4), 277-284.
- SCHWERTMANN, U. & TAYLOR, R.M. 1989. Iron oxides. In: DIXON, J.B. AND WEED, S.B. (eds.) *Minerals in soil environments*, 2ed. Madison, Soil Science Society of America, 379-438.

SHAW, S., PEPPER, S.E., BRYAN, N.D., & LIVENS, F.R. 2005. The kinetics and mechanisms of goethite and hematite crystallization under alkaline conditions, and in the presence of phosphate. *American Mineralogist*, **90**, 1852-1860.

VU, H.P., SHAW, S., & BENNING, L.G. 2008. Transformation of ferrihydrite to hematite: an in situ investigation on the kinetics and mechanisms. *Mineralogical Magazine*, **72**, 217-220.

## Methods for obtaining a national-scale overview of groundwater quality in New Zealand

Christopher J. Daughney, Uwe Morgenstern, Rob van der Raaij,  
Robert Reeves, Matthias Raiber, & Mark Randall

GNS Science, 1 Fairway Drive, Avalon NEW ZEALAND (e-mail: c.daughney@gns.cri.nz)

**ABSTRACT:** This study presents methods developed to summarise groundwater quality in New Zealand, based on data collected since 1990 from over 100 monitoring sites comprising the National Groundwater Monitoring Programme (NGMP). Site-specific groundwater age determinations based on measured concentrations of tritium, CFCs and SF<sub>6</sub> range from less than one year to more than 100 years, with the 25<sup>th</sup>, 50<sup>th</sup> and 75<sup>th</sup> percentiles (across the entire NGMP) being approximately 10, 40 and 100 years, respectively. Hierarchical cluster analysis based on median concentrations of 15 major and minor constituents reveals three dominant water types across the NGMP. At 42% of the monitoring sites, groundwater quality shows some level of human influence, with nitrate, chloride and/or sulphate concentrations in excess of natural background levels. At 32% of the monitoring sites, groundwater quality shows little or no evidence of human influence, but due to high levels of oxygen in the aquifer, any introduced nitrate or sulphate will persist and accumulate. At the remaining 26% of the monitoring sites, the groundwater is oxygen-poor and is not likely to accumulate significant nitrate, but due to natural processes, it commonly accumulates concentrations of iron, manganese, arsenic and/or ammonia.

**KEYWORDS:** *hydrochemistry, groundwater age, multivariate statistics, New Zealand*

### INTRODUCTION

The objective of this study is to provide an overview of groundwater quality across all of New Zealand (NZ). This is achieved by analysis of data collected through the NZ National Groundwater Monitoring Programme (NGMP). The NGMP, established in 1990, is a long-term research programme that aims to identify spatial and temporal trends in NZ groundwater quality and relate them to specific causes. The data analysis methods of interest in this study include hierarchical classification of monitoring sites from hydrochemistry (Daughney & Reeves 2005, 2006), and groundwater age determination based on measured concentrations of tritium, CFCs and SF<sub>6</sub> (Daughney *et al.* 2009).

Hierarchical Cluster Analysis (HCA) is a multivariate statistical method that can be used to assign groundwater samples or monitoring sites to distinct categories (hydrochemical facies). HCA offers several advantages over other methods of grouping or categorising groundwaters.

HCA does not require *a priori* assumptions about the number of groups or the criteria that control the groupings, such as aquifer lithology or confinement. HCA can be based on any number of variables, and these variables can be of any type (chemical, physical, biological; distributed or non-distributed). HCA can thus provide a more holistic approach to sample comparison than most other methods, which are limited in terms of the number of variables that can be simultaneously presented clearly. HCA produces a set of average parameter values (a centroid) for each cluster in the original units of the input variables, and hence the results of HCA can be more readily interpreted in the geological or hydrochemical context than multivariate methods based on transformation, e.g. Principal Components Analysis. The output of HCA can be displayed as a membership table, where each site or sample is unambiguously assigned to a single group. By contrast, for most graphical methods (e.g. Piper diagrams), it is difficult to determine

exactly where the boundaries of each group should be placed, how many groups there should be, or which samples should be assigned to each group.

Determination of groundwater age is valuable for a variety of reasons covering the spectrum from applied resource management to fundamental scientific research. Groundwater dating relies on measurement of one or more tracer substances, followed by fitting of the tracer concentration data with a lumped-parameter model (Zuber *et al.* 2005). Tritium, CFCs and SF<sub>6</sub> are the tracers most commonly used for dating young groundwater (less than about 100 years old).

It is often useful to estimate groundwater age independently of the tracer method in order to overcome ambiguities that can arise in age determinations based on limited tracer data at some sites and in some hydrogeological conditions. Ambiguity in groundwater age can be overcome by fitting the convolution integral to time series tracer data, but it may not be practical to make several measurements over perhaps several years, as might be necessary to permit detection of significant change in the tracer concentrations relative to analytical uncertainty. Major ion hydrochemistry and well construction can be used to estimate groundwater age independently from the direct method of measuring tracer concentrations.

Discriminant Analysis (DA) is a multivariate statistical method that generates a set of classification functions that can be used to predict into which of two or more categories an observation is most likely to fall, based on a certain combination of input variables. DA may be more effective than regression for relating groundwater age to major ion hydrochemistry and well construction because it can account for complex, non-continuous relationships between age and each individual variable used in the algorithm while inherently coping with uncertainty in the age values used for calibration, and there is no need to

assume that the sites involved are within the same aquifer or even within the same catchment.

## METHODS

The NGMP includes 112 long-term monitoring sites across New Zealand; four sites that are no longer included in the NGMP were also considered as part of this study. NGMP sites are situated in discrete aquifers (or on discrete flow lines in large aquifer systems) and are selected to encompass a range of aquifer lithology, confinement and surrounding land use that is representative of New Zealand aquifers in general. Median well depth is 26 m below ground surface (b.g.s.), and the minimum, lower quartile, upper quartile and maximum well depths across all NGMP sites are 3, 10, 55, and 337 m b.g.s., respectively.

Samples are collected quarterly on an on-going basis from each NGMP site according to a standardized protocol. Electrical conductivity, pH and temperature are measured in the field using portable meters, and three different types of samples are collected for laboratory analysis of various parameters. An unfiltered, unpreserved sample is analysed in the laboratory for alkalinity, conductivity and pH using an autotitrator. A filtered (0.45 µm) unpreserved sample is analyzed for Cl, Br, F, SO<sub>4</sub>, NO<sub>3</sub>-N and PO<sub>4</sub>-P by ion chromatography, and for NH<sub>4</sub>-N by automated phenohypochlorite method. A filtered, acid-preserved (HNO<sub>3</sub>) sample is analyzed for Na, K, Ca, Mg, Fe, Mn and SiO<sub>2</sub> by inductively coupled plasma optical emission spectrometry. The length of the historical record differs for each NGMP site but on average covers a period of seven years.

Groundwater age at each NGMP site has been assessed using multiple tracers. Tritium was analyzed in a 1 L unfiltered unpreserved sample using 70-fold electrolytic enrichment prior to ultra-low level liquid scintillation spectrometry (Morgenstern & Taylor 2005). Samples for analysis of CFCs and SF<sub>6</sub> (125 ml and 1 L, respectively) were collected in strict isolation from the atmosphere and

analysed by gas chromatography using an electron capture detector (Busenberg & Plummer 1992; van der Raaij 2003). Dissolved Ar and N<sub>2</sub> concentrations were used to estimate the temperature at the time of recharge and the excess air concentration, which allowed calculation of the atmospheric partial pressure of CFCs and SF<sub>6</sub> at the time of recharge.

The convolution integral and the Exponential Piston Flow Model (EPM) were used to relate measured tracer concentrations to historical tracer input. The tritium input function is based on tritium concentrations measured monthly since the 1960s near Wellington, New Zealand. CFC and SF<sub>6</sub> input functions are based on measured and reconstructed data from southern hemisphere sites. The EPM was applied consistently in this study because statistical justification for selection of some other response function requires a substantial record of time-series tracer data which is not yet available for the majority of NGMP sites, and for those NGMP sites with the required time-series data, the EPM and other response functions yield similar results for groundwater age.

HCA and DA were conducted using log-transformed site-specific median concentrations of various parameters as described by Daughney & Reeves (2005) and Daughney *et al.* (2009). HCA was conducted with median concentrations of Br, Ca, Cl, F, Fe, HCO<sub>3</sub>, K, Mg, Mn, Na, NH<sub>4</sub>-N, NO<sub>3</sub>-N, PO<sub>4</sub>-P, SiO<sub>2</sub> and SO<sub>4</sub> using the Nearest-Neighbour and Wards linkage rules. DA was conducted using electrical conductivity, well depth, and the median concentrations of Ca, Mg, Na, K, HCO<sub>3</sub>, Cl and SO<sub>4</sub>.

## CONCLUSIONS

The range of hydrochemistry encountered across the NGMP can be summarized by assigning each site to one of three categories (hydrochemical facies) defined via HCA. 32% of the NGMP monitoring sites are assigned to the *natural-fresh* category and are typified by oxic groundwater showing little or no evidence of human or agricultural impact. 42% of

the NGMP sites are assigned to the *impacted* category, and are also typified by oxic groundwater, but with evidence of some degree of human or agricultural impact in the form of above-background concentrations of NO<sub>3</sub>-N, often co-occurring with elevated concentrations of Cl and/or SO<sub>4</sub>. The level of impact observed at these sites is variable, with 15% of sites having median NO<sub>3</sub>-N concentration above the guideline for safe human consumption (11.3 mg/L). The remaining 26% of the NGMP sites are assigned to the *natural-evolved* category and are typified by reduced (anoxic) groundwater, often with measurable concentrations of NH<sub>4</sub>-N, dissolved Fe and/or dissolved Mn, and relatively high total dissolved solids concentrations.

Site-specific groundwater age values ranged from less than one year to more than 100 years, with the 25<sup>th</sup>, 50<sup>th</sup> and 75<sup>th</sup> percentiles being approximately 10, 40 and 100 years, respectively, across the entire NGMP. Classification functions derived from DA allowed assignment of 71% of the sites to the correct of four age categories (mean residence time ten years or less, 11 to 40 years, 41 to 100 years, or more than 100 years).

Groundwater age displays a generally expected relationship to well depth, but the age category cannot be predicted from well depth alone. In line with expectation, over all NGMP sites, well depth has a weak positive correlation to groundwater age, with the youngest and oldest age categories generally being associated with shallow and deep bores, respectively. However, shallow wells do not always tap young groundwater: there were a small number of NGMP sites at which groundwater from the oldest age category was found in a well less than 10 m deep. This situation occurred in both confined and unconfined aquifers, corresponding to upward-moving groundwater at the discharge end of a flow system.

Likewise, despite certain expected relationships between groundwater age and hydrochemistry, a particular site's groundwater age category cannot be predicted from its hydrochemistry alone.

For example, the older the groundwater is, the more likely it is to be assigned to the natural-evolved hydrochemical category. This is expected because the longer the groundwater is in the aquifer and isolated from the atmosphere, the more likely it is to become anoxic and to accumulate dissolved substances through water-rock interaction. However, only 85% of the NGMP sites assigned to the oldest age category display the natural-evolved hydrochemical signature, indicating that groundwater can remain oxic in some New Zealand aquifers for more than 100 years. Conversely, the natural-evolved hydrochemical signature is found at a small proportion (5%) of NGMP sites in the youngest age category, indicating that in some situations groundwater can become anoxic in less than a decade. Not surprisingly, this confirms that the rates of hydrochemical reactions are variable, as would be expected for aquifers with varied or mixed lithologies.

There is no significant partitioning of the different age categories between the natural-fresh and impacted hydrochemical categories. In other words, the number of sites having oxic impacted groundwater is always roughly equal to the number of sites with oxic unimpacted groundwater, regardless of groundwater age category. This implies that the impact of human and agricultural activity on New Zealand's groundwater quality is of similar extent over the last ten years as over the previous century.

#### ACKNOWLEDGEMENTS

The authors thank personnel from New

Zealand regional councils for assistance with sample collection. This research was funded by the New Zealand Foundation for Research, Science and Technology (Contract C05X0706).

#### REFERENCES

- BUSENBERG, E. & PLUMMER, L.N. 1992. Use of chlorofluorocarbons (CCl<sub>3</sub>F and CCl<sub>2</sub>F<sub>2</sub>) as hydrologic tracers and age dating tools: the alluvium and terrace system of Central Oklahoma. *Water Resources Research*, **28**, 2257-2283.
- DAUGHNEY, C.J., MORGENSTERN, U., VAN DER RAAIJ, R., & REEVES, R.R. 2009. Groundwater age in New Zealand aquifers: Tracer measurements and age estimation from hydrochemistry. *Journal of Hydrology*, in press.
- DAUGHNEY, C.J. & REEVES, R.R. 2005. Definition of hydrochemical facies in the New Zealand National Groundwater Monitoring Programme. *Journal of Hydrology NZ*, **44**, 105-130.
- MORGENSTERN, U. & TAYLOR, C.B. 2005. Low-level tritium measurement using electrolytic enrichment and LSC. *Proc. Int. Symp. Quality Assurance for Analytical Methods in Isotope Hydrology. International Atomic Energy Agency*.
- VAN DER RAAIJ, R.W. 2003. *Age dating of New Zealand groundwaters using sulphur hexafluoride*. M.Sc. thesis, School of Earth Sciences, Victoria University of Wellington, New Zealand.
- Zuber, A., Witczak, S., Rózański, K., Śliwka, I., Opoka, M., Mochalski, P., Kuc, T., Karlikowska, J., Kania, J., Jackowicz-Korczyński, M., & Duliński, M. 2005. Groundwater dating with <sup>3</sup>H and SF<sub>6</sub> in relation to mixing patterns, transport modelling and hydrochemistry. *Hydrological Processes*, **19**, 2247-2275.

## Mineralogical characterization of arsenic, selenium, and molybdenum in uranium mine tailings

Joseph Essilfie – Dughan<sup>1</sup>, M. Jim Hendry<sup>1</sup>, Ingrid Pickering<sup>1</sup>, Graham George<sup>1</sup>,  
Jeff Warner<sup>2</sup>, & Tom Kotzer<sup>3</sup>

<sup>1</sup>Department of Geological Sciences, University of Saskatchewan, 114 Science Place, Saskatoon, SK, S7N 5E2  
CANADA (e-mail: jim.hendry@usask.ca)

<sup>2</sup>Canadian Light Source Inc. University of Saskatchewan 101 Perimeter Road Saskatoon, SK, S7N 0X4 CANADA

<sup>3</sup> Cameco Corporation, 2121-11th Street West, Saskatoon, SK, S7M 1J3 CANADA,

**ABSTRACT:** High-grade uranium ores from northern Saskatchewan can contain high levels of arsenic (As), selenium (Se) and molybdenum (Mo). A critical environmental issue around the uranium mining industry is the long-term mobilization of As, Se and Mo from its tailings facilities to the nearby groundwater systems. Our goal is to identify and characterize the mineralogical compositions of these elements, and ultimately determine their long-term stability in the environment. In order to meet the objectives we are using synchrotron radiation based X-ray absorption spectroscopy (XAS) techniques along with electron microprobe analysis (EMPA). Bulk XAS is being used to study the oxidation state of these elements as well as their coordination environment, which will allow us to identify their speciation. Electron microprobe analysis (EMPA) and synchrotron-based micro-X-ray fluorescence mapping and absorption spectroscopy ( $\mu$ XRF;  $\mu$ XAS) are being employed to study the spatial distribution and speciation of the elements of concern (EOC) at the micron scale. Understanding of their speciation as well as their distribution will help determine the long-term stability of As, Mo and Se in the aqueous environment in the mine tailings.

**KEYWORDS:** *Mine tailings, Arsenic, Molybdenum, Selenium, XAS, EMPA*

### INTRODUCTION

Uranium mill tailings in northern Saskatchewan can contain elevated levels of arsenic (As), molybdenum (Mo), and selenium (Se). Arsenic is a carcinogen, with exposure via drinking water shown to cause cancer of the bladder, lungs, skin, kidney, and liver in humans (USEPA 1998). Mo and Se are essential trace elements, but with potentially toxic effects at elevated concentrations (Barceloux 1999; Frankenberger & Benson 1994). A critical environmental issue in the U mining industry is preventing mobilization of these elements from tailings facilities and contamination of regional ground water systems. The toxicity and bioavailability of As, Mo, and Se are functions of their chemical form or speciation. Thus, identification of the speciation of these elements in the mine tailings is necessary to determine their mobility, transformation and complexation in the solid and aqueous state.

The objectives of this study are to use synchrotron-based spectroscopic techniques, as well as EMPA, to identify and characterize the mineralogical compositions of As, Mo, and Se in mine tailings, and ultimately assist in determining their long-term stability in tailings containment facilities.

XAS provides a powerful probe of both physical and electronic structure of an element within a sample, and has the ability to determine the molecular level speciation of As, Mo and Se over the concentration range of 50  $\mu$ g/g to several weight percent (typical of mine tailings solids) (Brown *et al.* 1998) at the micron to mm scale.

EPMA is a technique for chemically analysing small selected areas of solid samples, in which X-rays are excited by a focused electron beam. Spatial distribution of specific elements can be recorded as two-dimensional X-ray "maps" using either energy dispersive spectroscopy (EDS) or

wavelength-dispersive spectroscopy (WDS). The spatial scale of analysis, combined with the ability to create detailed images of the sample, allows analyses of fine-grained geological materials such as mine tailings. (Reed 1996).

The accurate identification of As-, Mo-, and Se-bearing minerals in the tailings, as well as their distribution will help elucidate the source chemistry for these potential contaminants. This will facilitate characterization and quantification of the long-term migration of metals, oxyanions and metalloids from mine tailings facilities to adjacent groundwater systems. The information will also ultimately aid in the design of facilities aimed at minimizing migration of these elements into groundwater long after decommissioning.

## METHODS AND RESULTS

### Methods

Four uranium mine tailing samples (collected during the DTMF 2004/2005 drilling program) were selected based on the concentrations of EOC (As, Mo, and Se) as well as redox potential. Standard reference compounds to aid in the identification of the speciation of As, Mo and Se in the mine tailings were also selected based on previous studies in literature and potential mineral phases identified during diagnostic equilibrium modelling (using PHREEQC; Parkhurst & Appelo 1999; Charlton & Parkhurst 2002) using pore water chemical data from the tailings. Both samples and standard reference compounds were prepared using Kapton® tape over a Teflon® sample holder. Arsenic, Mo and Se K-edge X-ray Absorption Near Edge Spectroscopic (XANES) data was collected on both samples and standards using a hard x-ray beamline (HXMA - 06ID-1) at the Canadian Light Source, University of Saskatchewan (CLS) and solid state Germanium and Vortex detectors. Extended x-ray absorption fine structure (EXAFS) was collected where possible, depending on elemental concentrations. Data collected are currently being analysed using EXAFSPAK (George & Pickering 1995)

and IFFEFIT (Ravel & Newville 2005)

Four samples were similarly selected for the EPMA experiments. The samples were dried and embedded in polished epoxy cylindrical plugs. Backscattered electron (BSE) images as well as elemental maps of As, Fe and Ni (EDS/WDS) were collected using a JEOL 8600 Superprobe electron microprobe analyzer (Dept. of Geological Sciences, University of Saskatchewan).

### Results

For As, Mo, and Se all samples displayed well-defined absorption edges, identified by the sharp increase in absorption over a 10 eV interval. The position of the absorption edge is sensitive to the oxidation state of the absorbing atom and thus has been used to determine the oxidation state of As, Mo, and Se in the mine tailings.

Comparison of As K edge absorption spectra for tailings and reference compounds of known oxidation states shows that arsenate ( $\text{As}^{5+}$ ) is the dominant

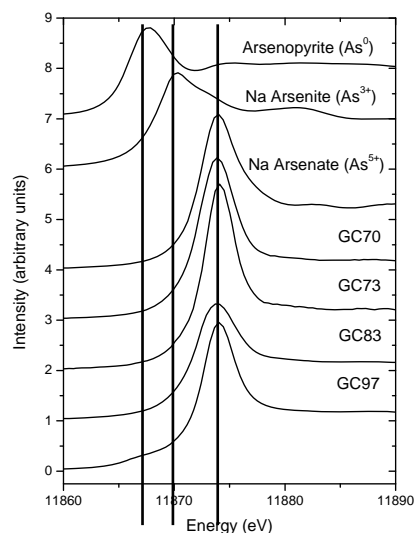


**Fig. 1.** X-ray absorption near-edge structure (XANES) of reference compounds with various As valence states and mine tailings samples. The As K-edge excitation potential for arsenic in the ground state ( $\text{As}^0$ ) is at 11868 eV. The As K-edge excitation potential increases with increasing valence state.

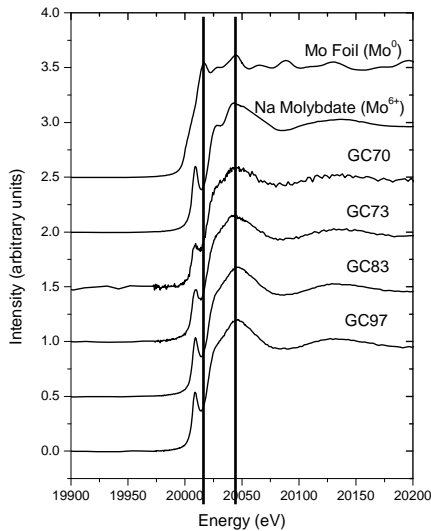


**Fig. 2.** X-ray absorption near-edge structure (XANES) of reference compounds with various molybdenum valence states and mine tailings samples. The Mo K-edge excitation potential for molybdenum in the ground state ( $\text{Mo}^0$ ) is at 20000 eV. The Mo K-edge excitation potential increases with increasing valence state.

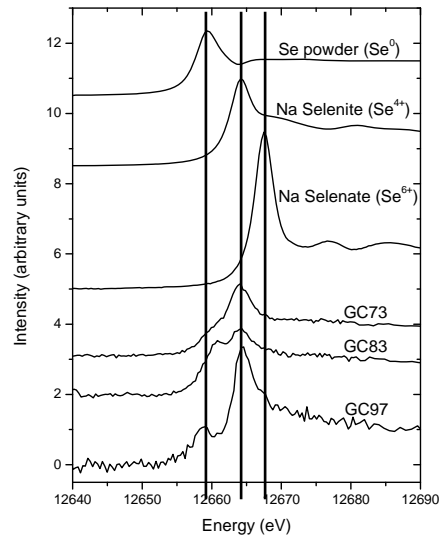


**Fig. 3.** X-ray absorption near-edge structure (XANES) of reference compounds with various Se valence states and mine tailings samples. The Se K-edge excitation potential for Se in the ground state ( $\text{Se}^0$ ) is at 12658 eV. The selenium K-edge excitation potential increases with increasing valence state.

form of arsenic in the mine tailings (Fig. 1).

Similarly, comparison of the Mo K edge absorption spectra for tailings and reference compounds of known oxidation states (Fig. 2), shows that  $\text{Mo}^{6+}$  is the dominant form of molybdenum in the mine tailings. The characteristic pre-edge feature in the near edge spectra indicates that Mo in the tailings occurs mostly as a molybdate.

For Se (Fig. 3), comparison of the Se K edge absorption spectra for tailings relative to reference compounds of known oxidation states shows that selenite ( $\text{Se}^{4+}$ ) was the dominant form of selenium in the mine tailings, along with a considerable amount of reduced Se species (selenide:  $\text{S}^0$ ). These analyses are continuing to further determine the complexation mechanism for selenide and selenite present in the tailings.

Least squares fitting of the near edge spectra of the tailings to that of the standard reference spectra is currently underway to establish the chemical

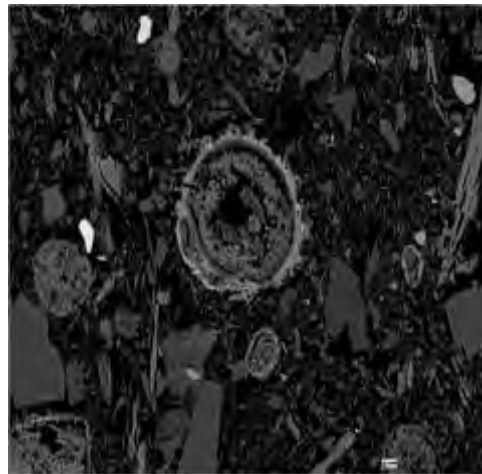


**Fig. 4.** BSE image of mine tailings showing the presence of gypsum nodules with bright rims around them.

complexation or mineralogy of the tailings with respect to As, Mo, and Se.

Electron microprobe analyses of the mine tailings samples (BSE image –Fig. 4) show the presence of notable nodule-like features with bright rims around them.

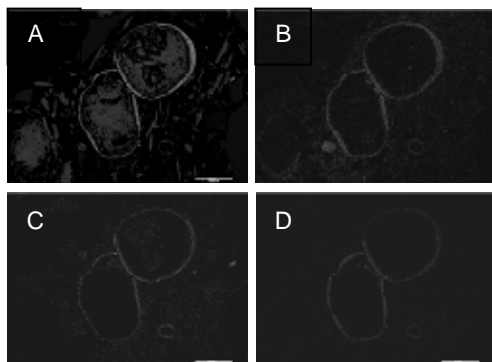


**Fig. 5.** BSE image of gypsum node (A) and elemental maps of As (B), Fe (C), and Ni (D).

Elemental x-ray maps (EDS) indicate the nodules are mainly Ca and S (i.e. gypsum) whereas surrounding rims mainly consist of As, Fe, and Ni (Fig. 5).

Concentration levels of Mo and Se in the tailings were below the detection limit (~ 100 ppm) of the instrument.

Although the EMPA technique provides spatial distribution information on elements of concern, it does not provide any information with regards to their chemical speciation and detailed complexation. The use of synchrotron focused-beam spectroscopy ( $\mu$ XAS) and elemental mapping ( $\mu$ XRF) is currently being explored at the CLS using VESPERS (07B2-1) and HXMA (06ID-1) hard x-ray beamlines. This technique will not only provide information spatial distribution of the elements of concern but their chemical form (speciation/complexation) as well, which is essential in predicting their solubility, mobility and toxicity.

#### ACKNOWLEDGEMENTS

The authors acknowledge the Cameco Corporation and the Cameco-NSERC Industrial Research Chair for financial

support. The authors also thank Tom Bonli Industrial Research Chair for financial support. The authors also thank Tom Bonli for his assistance in the EMPA work.

#### REFERENCES

- BARCELOUX, D.G. 1999. Molybdenum. *Journal of Toxicology- Clinical Toxicology*, **37**, 231-237.
- BROWN, G.E., FOSTER, A.L., & OSTERGREN, J.D. 1998. Mineral surfaces and bioavailability of heavy metals: A molecular-scale perspective. *Proceedings of the National Academy of Sciences of the United States of America*, **96**, 3388-3395.
- CHARLTON, S.R. & PARKHURST, D.L. 2002. PHREEQC-A computer program for speciation, reaction-path, advective transport, and inverse geochemical reactions. *U.S. Geological Surveys Water-Resources Investigations*, **95-4227**.
- FRANKENBERGER, W.T. JR. & BENSON, S.M. (eds.). 1994. *Selenium in the Environment*, Marcel Dekker, Inc., New York.
- GEORGE, G.N. & PICKERING, I.J. 1995. EXAFSPAK: a Suite of Computer Programs for Analysis of X-ray Absorption Spectra. *Stanford Synchrotron Radiation Laboratory*, Stanford, CA, USA.
- PARKHURST, D.L. & APPELO, C.A.J. 1999. *User's guide to PHREEQC (Version 2)—A computer program for speciation, batch-reaction, one-dimensional transport, and inverse modeling*.
- RAVEL, B. & NEWBILLE M. 2005. ATHENA, ARTEMIS, HEPHAESTUS: data analysis for X-ray absorption spectroscopy using IFEFFIT *Journal of Synchrotron Radiation*, **12**, 537-541.
- REED, S.J.B. 1996. *Electron Microprobe Analysis and Scanning Electron Microscopy in Geology*. Cambridge University Press.
- USEPA (UNITED STATES ENVIRONMENTAL PROTECTION AGENCY) 1998. *Arsenic in drinking water: Arsenic Research Plan*; Office of Water.

## Spatial and temporal evolution of Cu-Zn mine tailings while dewatering

D. Jared Etcheverry<sup>1</sup>, Barbara L. Sherriff<sup>1</sup>,  
Nikolay Sidenko<sup>1,2</sup>, & Jamie VanGulck<sup>3</sup>

<sup>1</sup> Department of Geological Sciences, University of Manitoba, Winnipeg, MB, R3T 2N2 CANADA  
(email: jared.etccheverry@gmail.com)

<sup>2</sup> TetreES Consultants Inc., Winnipeg, MB, R3C3R6 CANADA

<sup>3</sup> Arktis Solutions Inc. 186 Steepleridge St., Kitchener, ON, N2P2V1 CANADA

**ABSTRACT:** The Ruttan Cu-Zn mine produced ~30 mT of fine-grained tailings over 30 years. Since the closure of the mine in 2002, the tailings have been systematically dewatered through trenches draining into the open pit and underground workings. This study evaluated the evolution of the reduced tailings, which were underwater until 2002, and also tailings that had been exposed to oxidizing conditions for more than 20 years. The mining process removed most of the sphalerite and chalcopyrite leaving the tailings dominated by pyrite and pyrrhotite. In oxidized tailings, there was extensive alteration of pyrrhotite, and sphalerite but only slight alteration of pyrite. There is very little carbonate to buffer the acidity.

Dewatering the submerged tailings resulted in changes in acidity of pore and shallow groundwater from rapid oxidation of fine grained sulfides. Depth profiles of metal concentrations in dissolved and solid fractions suggest that the tailings are in an early stage of oxidation and that these tailings will produce low pH, metal-laden water for years to come. Hydrated sulphate evaporite minerals formed during dry periods on the surface of the tailings providing a temporary storage for metals that are released during spring runoff and rain events.

**KEYWORDS:** Cu-Zn tailings, acidification, oxidation, dewatering, geochemistry

### INTRODUCTION

From 1973 until 2002, Sherritt Gordon Mines Ltd. and later Hudson Bay Mining and Smelting, extracted copper and zinc ore from volcaniclastic and siliciclastic sequences of the Rusty Lake Greenstone Belt at the Ruttan Mine near Leaf Rapids, Manitoba, Canada.

Flotation refinement of the ore at the Ruttan Mine produced over 30 million tons of fine-grained sulfide rich tailings, some of which were submerged in retention ponds (Fig. 1). Since mine closure, there has been a systematic dewatering of the tailings ponds to allow for more geotechnically stable tailings pile dams. At the time of this study, 2004 and 2005, much of the surface tailings remained in a reduced state due to relatively wet conditions. However, parts of the tailings have been exposed to the atmosphere and oxidizing for many years.

Dewatering of the Ruttan tailings offered the opportunity to observe potentially acid generating tailings as they enter oxidizing

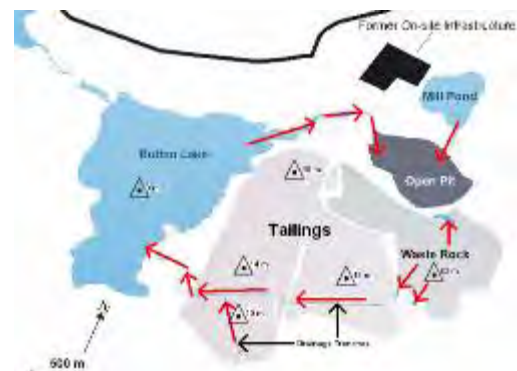


**Fig. 1.** Map of Ruttan mine site showing the drainage trenches in the tailings and flow direction of drainage water.

conditions in a natural setting. The subarctic climate of this region, coupled with the exposure of reduced tailings to oxidizing conditions set this project apart from similar studies.

### METHODOLOGY

Samples of pore water, ground water, surface water and solid tailings were

obtained from similar locations in 2004 and 2005.

Samples of groundwater were obtained from piezometers installed at various locations throughout the tailings. Groundwater was retrieved using a baler. Pore water was squeezed from samples of solid tailings. All water samples were analysed for cations, anions, Eh and pH.

The piezometers were also used to estimate the hydraulic conductivities of the tailings. The Seep/W<sup>TM</sup> software package, was used to model the flow from the tailings into the drainage trenches.

Solid tailings were collected from test-pits and auger cuttings from boreholes in both the oxidized and reduced tailings. The tailings were analyzed for total metals. Sequential extraction of the tailings allowed the mobility of the metals to be assessed. Evaporites were also collected from the surface of the tailings.

The minerals of the solid tailings and evaporites were assessed qualitatively with X-ray diffraction, optical, and scanning electron microscopy.

## RESULTS

### Field Observations

Despite excessively wet conditions encountered in 2005, increases in the level of oxidation in the reduced tailings were observed since 2003. Visible changes were observed <15 cm depth.

In 2003 and 2004, oxidation was patchy as a change of colour from dark grey to orange-brown. The oxidation was usually restricted to one to two centimeter halos along vertical and horizontal cracks. Below 20 cm, the tailings were unoxidized. In 2005, the entire surface was oxidized and the halos of oxidation extended from the cracks, to almost completely oxidize the upper 15 cm. Below 20 cm, the tailings remained unoxidized.

### Solid Tailings

The reduced tailings were found to be comprised of 20-30 % sulfides, and 70-80% gangue minerals and very fine-grained unidentifiable material. Sulfides were 50 -75 % pyrite, 30-40 % pyrrhotite, <5 % chalcopyrite, and <5 % sphalerite.

Gangue constituents included quartz, muscovite, biotite, chlorite, and pyroxene.

In the oxidized tailings, pyrrhotite and sphalerite (Fig. 2) show the most alteration with both minerals being surrounded by iron oxyhydroxides. Pyrite is relatively unaltered.

Chalcopyrite is also unaltered but by virtue of being armored within quartz.

Total metal concentrations in the reduced tailings varied for Fe (18-25 wt. %), Zn (0.2-0.5 wt. %), and Cu (0.03-0.09 wt. %). Similar concentrations were also measured in the oxidized tailings: 17-28 wt. % Fe, 0.04-0.44 wt. % Zn, and 0.03-0.10 wt. % Cu.

White and yellow evaporite minerals form thin crusts on the surface of and within fissures in the tailings. XRD analyses identified the hydrated iron sulphates, melanterite ( $\text{FeSO}_4 \cdot 7\text{H}_2\text{O}$ ), Zn-melanterite ( $(\text{Zn,Fe})\text{SO}_4 \cdot 7\text{H}_2\text{O}$ ), halotrichite ( $\text{FeAl}_2(\text{SO}_4)_4 \cdot 22(\text{H}_2\text{O})$ ) and rozenite ( $\text{FeSO}_4 \cdot 4\text{H}_2\text{O}$ ) (Alpers *et al.* 2000).

Sequential extraction showed that, for both reduced and oxidized tailings, most of the total Fe (75-85%) is in the residual phase with most of the remainder in the iron-hydroxide phase. Less than 1% Fe is in the mobile adsorbed-exchangeable-carbonate and water soluble phases in both reduced and oxidized tailings.

Zinc is primarily split between the residual (30-50%), water soluble (24-30%) and iron-hydroxide (20-28%) phases with

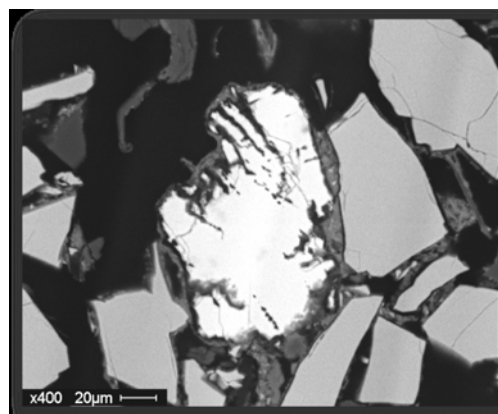


**Fig. 2.** SEM images of oxidized tailings showing altered sphalerite (white) with unaltered pyrite (light grey).

4-8% mobile in adsorbed-exchangeable-carbonate phases. There were higher percentages in the residual and iron hydroxide phases for the reduced than the oxidized tailings.

Copper was shown to be much more mobile with about 28% total Cu being water soluble or easily extractable: 40-50% in iron hydroxide phases and only about 20-30% in the residual.

There was no significant difference in sequential extraction results between 2004 and 2005. The only significant difference with depth was an increase in Fe-hydroxides near the surface.

#### **Pore Water**

The composition of pore water was similar in reduced and oxidized tailings with low pH (>1.8) and high total dissolved solids (~300 g/L) at the surface, and neutral pH and lower dissolved solids with depth. In general, pH values were lower and dissolved metal concentrations higher in 2005 than 2004.

In 2004, the pH of pore water in the reduced tailings was 4.4 at <10 cm depth, increasing to ~7 by 30 cm. Dissolved constituents follow pH, with concentrations of 36,000 ppm  $\text{SO}_4^{2-}$ , 18,000 ppm Fe, and 9,600 ppm Zn at <10 cm depth. These concentrations decrease steadily with depth. Below 30 cm, most metals drop to below detection limits.

In 2005, concentrations of metals increased, with the highest concentrations between 10 and 20 cm depth: 47,000 ppm Fe, 290,000 ppm  $\text{SO}_4^{2-}$  and 1.9 ppm Cu.

#### **Ground Water**

There was a drastic change in groundwater composition from 2004 to 2005. Water within the reduced tailings went from 1 to 800 ppm Fe and 0.2 to 1.3 ppm Zn. The pH values decreased over the same time period from 6.9 to 3.5.

#### **Surface Water**

All mine surface water in direct contact with the tailings is characterized by low pH (2.0-3.5) and a large amount of dissolved solids (1,400-17,000 ppm TDS). Average concentrations of elements in solution

include 7,100 ppm  $\text{SO}_4^{2-}$ , 1,200 ppm Fe, 11 ppm Cu and 180 ppm Zn. The highest TDS were measured in standing pools associated with the least oxidized tailings.

#### **Water Flow Modeling**

A flow model, created with the Seep/W<sup>TM</sup> software, indicated that the trench influences groundwater movement within an area of approximately 25 m, with the fastest flows closest to the trench. Flow rates within the tailings increase towards the trench with maximum flow of  $1.2 \times 10^{-7}$  m/s across the tailings/trench interface. Over a 10 m section this flow rate relates to about  $10^{-5}$  m<sup>3</sup>/s of groundwater, entering the trench.

#### **DISCUSSION**

The objective of this study was to document changes in Cu-Zn tailings during one year of exposure to oxidizing conditions. The primary factor affecting the rate of tailings acidification is the primary mineralogy.

The tailings comprise 5-10 wt. % pyrrhotite; a highly reactive sulfide mineral that releases protons and  $\text{Fe}^{3+}$  into adjacent pore waters on oxidation. Further, the concentration of carbonate minerals in the tailings is low providing little buffering capacity above pH 5. Therefore, the tailings continued to acidify until they reach the pH of  $\text{Al}(\text{OH})_3$  (pH 4-4.5) and  $\text{Fe}(\text{OH})_3$  (pH 2.5-3.5) buffering.

As the reduced tailings continue to de-water and the water table drops, it is expected that oxygen will continue to diffuse deeper into the tailings creating a deepening zone of oxidation. Modeling shows that sulfide-rich tailings with a deep water table can oxidize for centuries (Blowes & Jambor 1990).

The conditions at Ruttan can be compared with Blowes *et al.* (2003) model of the geochemical evolution of tailings as the tailings oxidize. This suggests that much of Ruttan tailings are still in the early to moderate stage of oxidation. In both the reduced and oxidized tailings, there is at least a minor depletion in solid metal concentrations at the surface and a peak in dissolved metal concentrations just

below the top of the tailings. Pore water metal concentrations do not increase with depth; rather, they peak within the first meter of the tailings, further suggesting a juvenile oxidation stage.

Modeling the water flow through the tailings shows that the majority of the metal leaving the tailings is presently coming from surface runoff and dissolved evaporites rather than from the body of the tailings as seepage to the trenches.

### CONCLUSIONS

The purpose of this study was to record the state of the Ruttan tailings during its early stages of oxidation and to observe changes in the tailings from one year to the next. Further, the presence of already oxidizing tailings at the site allowed a comparison between tailings at different stages of oxidation. Anomalous precipitation events in 2005 may have affected the data, however it is clear that the depth of oxidation in the reduced tailings increased and became more pervasive over the course of one year. A very fine grained fraction in the reduced tailings contributed to this rapid oxidation.

Respective weathering rates of sulfide minerals is pyrrhotite/sphalerite>pyrite. The buffering capacity of the tailings is low due to the lack of carbonates, allowing the rapid onset of low pH conditions.

Metals are temporarily attenuated as evaporite minerals on the surface or in secondary oxides and hydroxides in the tailings. The evaporites will re-dissolve in wet weather conditions and the secondary minerals become unstable with acidification of the tailings releasing these metals into the environment.

Large volumes of tailings and slow drainage conditions will lead to ARD conditions at this site for many years.

### ACKNOWLEDGEMENTS

Funding for this project was provided by the Sustainable Development Initiatives Fund of Manitoba and the Natural Sciences and Engineering Research Council of Canada. Neil Ball, Sergio Mejia, and the late Gregg Morden provided assistance with geochemical and mineralogical analyses at the Department of Geological Sciences at the University of Manitoba. We thank Benjamin Edirmanasinghe and Ernie Armitt. Manitoba Mines Branch and Frank Bloodworth, Ruttan Mine for logistical support.

### REFERENCES

- ALPERS, C.N., JAMBOR, J.L., & NORDSTROM, D.K. 2000. Sulfate Minerals: Crystallography, Geochemistry, and Environmental Significance. *Mineralogical Society of America, Geochemical Society: Reviews in Mineralogy and Geochemistry*, **40**, Washington, DC.
- BLOWES, D.W. & JAMBOR, J.L. 1990. The pore-water geochemistry and the mineralogy of the vadose zone of sulfide tailings, Waite Amulet, Quebec, Canada. *Applied Geochemistry*, **5**, 327-346.
- BLOWES, D.W., PTACEK, C.J., & JAMBOR, J.L. 2003. Mill Tailings: Hydrology and Geochemistry. Environmental aspects of Mine Waste. *Mineralogical Association of Canada Short Course series* **31**, 95-116.
- ETCHEVERRY, D.J. 2009. *Spatial and Temporal Variations in the Ruttan Mine Tailings, Leaf Rapids, Manitoba, Canada*. M.Sc. thesis, University of Manitoba, Winnipeg, Manitoba.

## **Adding value to Kinetic Testing Data II – Interpretation of waste rock humidity cell data from an exploration perspective at the Adanac Molybdenum Corporation, Ruby Creek Molybdenum Project, BC, Canada**

**David R. Gladwell<sup>1</sup> & Catherine T. Ziten<sup>1</sup>**

<sup>1</sup>*Wardrop Engineering Inc., 900 – 330 Bay Street, Toronto, ON, M5H 2S8 CANADA  
(david.gladwell@wardrop.com)*

**ABSTRACT:** Kinetic testing is usually applied in predicting the environmental impact of mining activities, however, this data may also be useful in geochemical exploration. Data is presented from kinetic testing of quartz monzonitic waste rock from the Adanac Molybdenum Corporation, Ruby Creek Project. XRD and petrological studies were used to define sample mineralogy, which includes mica, plagioclase, quartz, molybdenite, pyrite, chalcopyrite and minor clay minerals. PHREEQC computer software was used to compute the equilibrium concentrations of ionic species in leachate according to ion pair theory. Consideration of the sample mineralogy and aqueous geochemistry allowed delineation of periods of sulfide oxidation. The observed reaction products provide a suite of potentially anomalous elements which are confirmed by groundwater and surface water geochemistry in the vicinity of the mineralized monzonitic stock. Kinetic data are expensive to acquire; the case history data presented demonstrates that careful data interpretation maximizes return on this investment.

**KEYWORDS:** *Kinetic Testing, Waste Rock, Aqueous Speciation, PHREEQC, Molybdenum, Exploration*

### **INTRODUCTION**

Geochemical exploration and environmental geochemistry are typically not carried out in tandem despite the fact that some data is common to both tasks. This paper examines the potential for using kinetic data collected for environmental purposes in combination with groundwater and surface water geochemistry to enhance the understanding of processes that may be exploited by the exploration geochemist. Kinetic tests are commonly used to predict whether waste rock or tailings will produce acid mine drainage (AMD) and are a precursor to environmental certification and are therefore a critical step in mine development. Kinetic tests are carried out using an elutriated cell or column that are typically operated over a period of about 1 year in carefully controlled laboratory conditions. Kinetic (or humidity cell) testing is a standard protocol (ASTM, 2001) involving periodic rinsing of tailings samples over time to remove all reaction

products that have accumulated following the previous rinsing. The results of kinetic tests provide indication of how waste rock (or tailings) will behave over time with the onset of oxidation, assist in calculating oxidation rates, mineral reaction rates, and with respect to prediction of acid generation facilitate estimation of the rate of NP depletion and the period when AMD is likely to commence (Richie 1994; Day *et al.* 1997; Price *et al.* 1997; Frostan *et al.* 2002; Bowell & Parshley 2005; Ardau *et al.* 2008).

This paper outlines a novel approach to maximising the value of kinetic data by combining mineralogy, aqueous geochemistry and kinetic test data to design ground and surface water exploration programs. The approach is tested on environmental data collected by Adanac Molybdenum Corporation at the Ruby Creek Molybdenum project, Atlin, BC, Canada.

**RUBY CREEK MOLYBDENUM PROJECT**

The Ruby Creek Molybdenum project is located east of Atlin, British Columbia, Canada. Molybdenum mineralization underlies the valley floor near the headwaters of Ruby Creek, (MacLeod 2007). The host plutonic rocks are generally classified as quartz monzonites although sufficient variation exists to distinguish three phases of magma intrusion. The host intrusion, which includes the contact phase between the Cretaceous Fourth of July and Surprise Lake batholiths consists of a highly variably textured unit that grades from “coarse-grained quartz monzonite” (CGQM) south of the Adera fault through a number of texturally transitional phases. North of the molybdenum deposit’s bounding fault (Adera fault) is a quartz monzonite with fewer quartz and feldspar phenocrysts (SQFP or “sparse quartz feldspar porphyry”), containing a higher proportion of pyrite leading to local gossan development at surface. The Mo mineralization is generally confined to fractures in quartz monzonite south of the Adera fault. Kinetic data from three lithologies were examined: an SQFP sample from north of the fault; a CGQM sample with low Mo content and; a sample of low grade molybdenite ore (LGO) from south of the fault. These lithologies were tested in humidity cells HC2, HC3 and HC6 respectively.

**MINERALOGY/PETROGRAPHY**

The mineral assemblages were determined using standard XRD (with Reitveld refinement) and petrographic procedures. Sample HC2 (SQFP) was found to contain quartz (35%), orthoclase (50%), anorthitic plagioclase (12%), muscovite/sericite (1.5%), kaolinite (0.3%) and pyrophyllite (0.9%) together with trace quantities of pyrite, chalcopyrite, marcasite and magnetite. Sample HC3 (CGQM) was found to contain quartz (45%), orthoclase (33%), Ca-rich plagioclase (15%), muscovite/sericite (6.6%) with minor kaolinite and limonite. Petrographic and XRD studies did not find any molybdenite in HC3 although three

repeat analyses yielded 180, 7.3 and 7.9 mg/kg Mo, illustrating a typical nugget effect. HC6 contained a sample of low grade Mo ore (<0.04 % Mo). Petrology for HC6 was not reported although carbonate minerals were found by acid digestion and ICP-MS analysis to be typically very low or absent in these lithologies.

**KINETIC TEST DATA**

Gladwell and Ziten (2009) have demonstrated that PHREEQC computer modelling of ion pairs in kinetic test leachate may be used to delineate periods of testing when sulfides are oxidizing. Figure 1 demonstrates this approach to kinetic test data from HC3 (CGQM) illustrating a period of sulfide oxidation from approximately weeks 37 to 54.  $Al(OH)_2^+$  is also high during sulfide oxidation, probably reflecting reaction of Ca-rich plagioclase with the leachate.

This methodology allowed periods of sulfide oxidation to be identified in all three sets of kinetic test data.

Median leachate water chemistry during periods of sulfide oxidation was calculated for each parameter analyzed, by humidity cell. These data, for parameters that show distinct variation between cells, are presented as Table 1. HC2-SQFP, which contains more pyrite and very low carbonate content, rapidly generates acidic leachate causing its leachate to be higher in all parameters except Mo.

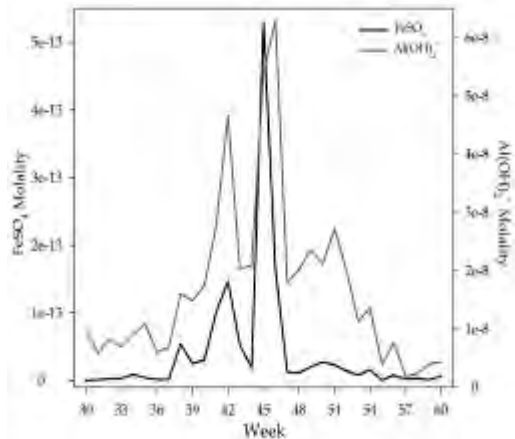


**Fig. 1.** Distribution of  $FeSO_4$  and  $Al(OH)_2^+$  for weeks 30 to 60 from humidity cell 3 (HC3-CGQM).

**Table 1.** Humidity cell data (mg/L) showing variation between periods of sulfide

oxidati	pH	Alkalinity	SO <sub>4</sub>	F	Al	Ba	Be	Cd	Ca	Co	Cu
HC2-SQFP	5.2	1.2	22	9.4	2.8	0.017	0.0036	6.E-04	6.8	0.0033	0.0082
HC3-CGQM	6.2	3.1	1	0.3	0.039	0.0004	0.0001	2.E-05	0.6	0.0001	0.0018
HC6-LGO	7.3	10	3	0.57	0.027	0.0077	4.1E-05	8.E-06	2.06	4.1E-05	0.00037
	Pb	Li	Mg	Mn	Mo	Ni	K	Si	Sr	U	Zn
HC2-SQFP	0.0011	0.0021	0.36	0.980	5.E-05	0.0007	0.98	4.2	0.015	0.14	0.098
HC3-CGQM	0.0004	0.0004	0.06	0.005	0.17	0.0001	0.55	1.3	0.0025	0.001	0.003
HC6-LGO	4.1E-05	0.001	0.01	0.004	4.E-03	4.1E-05	0.2	0.3	0.0084	0.002	0.00062

HC3-CGQM is slightly elevated in Mo and HC6-LGO shows much higher Mo in leachate from kinetic testing. Alkalinity and Mo are the only parameters which are higher in the molybdenite bearing (HC3-CGQM and HC6-LGO) samples

Since the SQFP sample outcrops for a significant portion of the Ruby Creek drainage area, it seems reasonable to expect elevated SO<sub>4</sub>, Al, Ba, Cd, Ca, Co, Cu, Pb, Li, Mg, Mn, Ni, K, Si, Sr, U and Zn in ground and surface waters within the watershed. These high concentrations will not reflect the presence of ore, however, rather just the presence of natural acid rock drainage (Lett & Jackaman 1995). The kinetic testing shows that only the presence of elevated Mo in ground and surface waters within the watershed is likely to reflect the presence of molybdenum mineralization. Examination of the kinetic test data, collected for environmental purposes, thus allows prediction of useful parameters for an exploration survey sampling ground or surface water media.

**GROUNDWATER SURVEY DATA**

Groundwater samples were collected at a series of groundwater springs and artesian wells in the project area through 2004 and 2005 (MacLeod 2007). Groundwater data (Table 2) is grouped into two categories; one for background (BACK) sample sites (n=10); and the second are samples close to the area of molybdenum mineralization (MINER) (n=15). Median concentrations for parameters that were significantly (p=0.95) different between the two groups are presented in Table 2. Clearly, the predicted multi-element signature of HC2-SQFP is in fact observed in groundwater

data in the Ruby Creek watershed. In addition, the predicted elevated Mo levels reflecting the presence of molybdenum mineralization were also observed in groundwater data.

**SURFACE WATER DATA**

Surface water samples were also collected at a number of sites throughout the Ruby Creek watershed although only data collected from active stream flow were utilized here. The surface water data was also categorized into background areas (n=13) and sites downstream from mineralization area (n=21).

Median concentrations for parameters that were significantly (p=0.95) different between the background and mineralized surface water samples are presented in Table 2 under the surface water heading. There are fewer significant differences between surface water compared to ground water parameters. Be, Co, and Pb are anomalous in ground but not in surface water. This may simply be due to dilution by runoff. Both the SQFP multi-element suite associated with natural ARD and the high Mo concentrations associated with mineralization clearly persist into surface water.

**CONCLUSIONS**

Detailed interpretation of kinetic test data collected for environmental purposes has allowed criteria for ground and surface water geochemical exploration to be selected. Parameters predicted from kinetic testing to be anomalous in both ground and surface waters were observed to occur reflecting the presence of both molybdenum mineralization and natural acid rock drainage. Kinetic testing is very expensive and careful use of the acquired

**Table 2.** Significant differences between median (mg/L) background (BACK) and mineralized(MINER) area in ground and surface water in the Ruby Creek Watershed (p=0.95)

	Groundwater		Surface Water	
	BACK	MINER	BACK	MINER
pH	7.57	7.36	7.48	7.15
Alka	22	5.6	36.1	8.3
SO <sub>4</sub>	9.1	17.8	6.7	9.76
F	0.66	0.965	0.1	0.511
Al	0.012	0.1	0.014	0.048
Ba	0.00054	0.0097	0.0051	0.005
Be	0.00003	0.00025	-	-
Cd	0.00003	0.00012	0.00003	0.00012
Ca	6.6	9.12	6.89	4.84
Co	0.00005	0.0001	-	-
Cu	0.00073	0.00069	0.00099	0.001
Pb	0.00003	0.00005	-	-
Mg	2.29	0.79	6.67	1.49
Mn	0.00044	0.0019	0.00061	0.00096
Mo	0.0087	0.05	0.00034	0.024
Ni	-	-	0.0051	0.00094
Si	5.63	3.11	4.31	3.34
Sr	0.018	0.034	0.0152	0.0194
U	0.0013	0.0004	0.0001	0.0003
Zn	0.0013	0.005	0.0027	0.0055
As	0.0051	0.0016	0.002	0.0018

data in geochemical exploration adds considerable value to the investment.

**ACKNOWLEDGEMENTS**

The authors acknowledge the assistance and encouragement of Wardrop Engineering Inc. as they analysed the data and prepared this paper.

**REFERENCES**

ARDAU, C., BLOWES, D.W., & PTACEK, C.J. 2009. Comparison of laboratory testing protocols to field observations of the weathering of sulfide-bearing mine tailings. *Journal of Geochemical Exploration*, **100**, 182-191.  
 BOWELL, R.J. & PARSHLEY, J.V. 2005.

Mineralogical controls on Pit Lake geochemistry, summer Camp Pit. Nevada. *Chemical Geology*, **215**, 373-385.  
 DAY, S.J., HOPE, G., & KUIT, W. 1997. Waste rock management planning for the Kudz Ze Kayah project, Yukon Territory: 1. Predictive Static and Kinetic Test Work. *Proceedings of the 4<sup>th</sup> International Conference on Acid Rock Drainage*. Vancouver, I, 81-98.  
 FROSTAD, S., KLEIN, B., & LAWRENCE, R.W. 2002. Evaluation of laboratory kinetic test methods for measuring rates of weathering. *Mine Water and the Environment*, **21**, 183-192.  
 GLADWELL, D.R. & ZITEN, C.T. 2009. Adding Value to Kinetic Testing Data I-Interpretation of Tailings Humidity Cell Data from the Perspectives of Aqueous Geochemistry and Mineralogy at the Crowflight Minerals, Bucko Lake Nickel Project. In: *24<sup>th</sup> International Applied Geochemistry Symposium*, Fredericton (this volume).  
 LETT, R.E. & JACKAMAN, W. 1995. Application of spring-water chemistry to exploration in the Driftpile Creek area, North-eastern British Columbia. *British Columbia Ministry of Energy, Mines and Petroleum Resources, Geological Fieldwork, 1994*, **1995-1**, 269-275.  
 MACLEOD, M. 2007. Ruby Creek Molybdenum Project "Environmental Assessment Certification Application" [http://a100.gov.bc.ca/appsdata/epic/html/deploy/epic\\_document\\_258\\_22610.html](http://a100.gov.bc.ca/appsdata/epic/html/deploy/epic_document_258_22610.html)  
 PRICE, W.A., MORIN, K.A., & HUTT, N.M. 1997. Guidelines for the prediction of acid rock drainage and metal leaching for mines in British Columbia: Part II. Recommended procedures for static and kinetic testing. In: *Proceedings of the 4<sup>th</sup> International Conference on Acid Rock Drainage*. Vancouver, I, 15-30.  
 RITCHIE, A.I.K. 1994. Sulphide oxidation mechanisms—controls and rates of oxygen transport. In: ALPERS, C.N. & BLOWES, D.W. (eds.), *Environmental Geochemistry of Sulphide Oxidation*, ACS Symposium Series 550. Washington DC.

## Alteration of sulfides within an open air waste-rock dump: Application of synchrotron $\mu$ -XRD, $\mu$ -XRF, and $\mu$ -XANES analyses

Pietro Marescotti<sup>1</sup>, Cristina Carbone<sup>1</sup>, Gabriella Lucchetti<sup>1</sup>, & Emilie Chalmin<sup>2</sup>

<sup>1</sup>DIP.TE.RIS. - Università di Genova, C.so Europa, 26, I-16132 Genova ITALY  
(e-mail: marescot@dipeteris.unige.it)

<sup>2</sup>European Synchrotron Radiation Facility, Grenoble FRANCE

**ABSTRACT:** We have applied a combination of synchrotron-based techniques ( $\mu$ -XRD,  $\mu$ -XRF, and  $\mu$ -XANES) to determine the mineralogy and the elemental distribution of metals in partially altered sulfide-mineralization fragments deposited within an open-air waste-rock dump (Libiola mine, eastern Liguria, Italy). In this dump AMD processes are active and intense and sulfide-mineralized clasts progressively undergo oxidation originating centimetric-thick hardpans cemented by secondary iron oxides and oxyhydroxides. Selected samples, containing the transition from unaltered sulfides to secondary oxidation products have been analyzed along several millimetric transects. The results evidenced that sulfides (pyrite + chalcopyrite  $\pm$  sphalerite) oxidation starts from the crystals rims or from intra-grain microfractures. Sulfide-S firstly oxidizes to sulfate and then is rapidly leached out from the system. The altered layers are composed almost exclusively of Fe-oxides (hematite) and -oxyhydroxides (goethite and minor bernalite) that replace sulfides and fill intra- and inter-grain interstices. Elemental maps and  $\mu$ -XRF transects evidenced that these secondary minerals efficiently and selectively scavenge many of the elements released during sulfides (e.g. Cu, Zn, As) and gangue minerals (e.g. Ni, Cr, Al) alteration.

**KEYWORDS:** sulfide alteration, Acid Mine Drainage, micro-XRD, micro-XRF, micro-XANES.

### INTRODUCTION

Supergenic interaction between sulfide mineralizations and atmospheric agents causes a series of mineralogical reactions that involve sulfides, gangue and host rock minerals, both in natural outcrops and mining sites. These reactions trigger several processes, known, on the whole, as AMD processes (Acid Mine Drainage; Jambor & Blowes 2003 and references therein). AMD processes determine: 1) the acidification of circulating water; 2) the release, the transport and the selective concentration of several ecotoxic elements; 3) the precipitation of secondary minerals within soils and in the stream sediments of the hydrographic basin.

In this case, the mineralogical studies on the mechanism of sulfide alteration and on the genesis and evolution of secondary oxidation products are of paramount environmental relevance because they allow a better understanding of the source and the mechanisms of release of the ecotoxic elements and the effective

scavenging capacity of the authigenic secondary minerals.

In recent years, several techniques based on synchrotron radiation have been applied to determine, with  $\mu$ m-spatial resolution, the elemental distribution and speciation of metals in mine-contaminated soils (Manceau *et al.* 2003; Morin *et al.* 1999, 2001).

With this work we have applied a combination of synchrotron-based  $\mu$ -XRD,  $\mu$ -XRF, and  $\mu$ -XANES analyses to determine the mineralogy and the elemental distribution of metals in partially altered sulfide-mineralization fragments deposited within an open-air waste-rock dump (Libiola mine, eastern Liguria, Italy).

### GEOLOGICAL SETTING

The Libiola Fe-Cu sulfide mine is located 8 km behind Sestri Levante (eastern Liguria, Italy). It was exploited from 1864 until 1962 and produced over 1Mt of Fe-Cu sulfides. The mine covers a surface area of about 4 km<sup>2</sup> and comprises more than 30 km of underground tunnels and 3

major open pits. The sulfide ore has been classified as stratabound Volcanic-associated Massive Sulfide deposit (VMS) and occurs as massive lenses near the top of a pillow basalt sequence that overlies ophiolitic breccias and serpentinized ultramafites (Zaccarini & Garuti 2008). The ore assemblage consists of pyrite and chalcopyrite, with minor sphalerite and pyrrhotite.

Non-mineralized rocks (mainly basalts and serpentinites), non-valuable mineralizations, and tailings were dumped in five main open-air waste-rock dumps and in several small bodies close to the main mine adits.

The sampling site is the main waste-rock dump of the Libiola mine, which is about 100 m in height and covers a surface of over 3 ha. The deposited materials are highly heterogeneous in grain size and in lithology. In this dump AMD processes are active and intense with sulfide-mineralized clasts progressively undergoing oxidation originating centimetric-thick hardpans cemented by secondary iron oxides and oxyhydroxides (Marescotti *et al.* 2008).

## METHODS AND RESULTS

Two samples, representative of different stages of sulfide oxidation have been analyzed: a) mineralized fragment containing the transition from unaltered sulfides to sulfide-free oxidation products (Fig. 1a); b) evolved hardpan characterized by rhythmic alternation of sub-millimetric red- and ochreous-layers (Fig. 1b).

## ANALYTICAL METHODS

Two different experiments have been performed at ID18F ( $\mu$ -XRD and  $\mu$ -XRF) and ID21 ( $\mu$ -XRF and  $\mu$ -XANES) beamlines at the ESRF (European Synchrotron Radiation Facilities, Grenoble, France).

At ID18F beamline simultaneous  $\mu$ -XRF (excitation energy of 28 keV; spectrum collection using a Si(Li) solid state detector with detection limits in the range 0.01 ppm for  $30 < Z < 35$  and  $< 0.1$  ppm for  $Z > 25$ ) and  $\mu$ -XRD (monochromatic X-rays

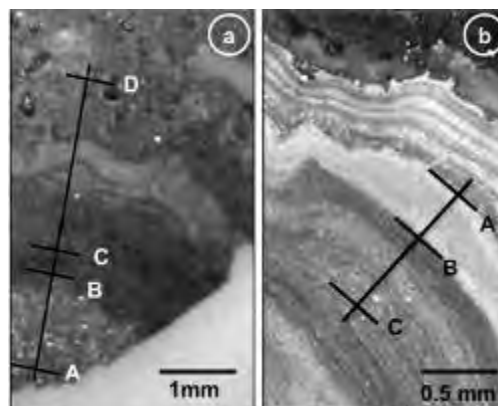


**Fig. 1.** Photomicrograph of the analyzed samples. a) transition from unaltered sulfides (segment AB) to sulfide-free oxidation products (segment CD). The segment BC corresponds to the transition zone. b) layered hardpan with rhythmic alternation of goethite-rich (segment AB) and hematite-rich (segment BC) layers.

of  $\lambda = 0.44285 \text{ \AA}$ ; spectrum collection using a high resolution MAR CCD camera) analyses have been performed on both samples along millimetric transects with analytical steps of  $2 \mu\text{m}$  (Fig. 1a, b).

At ID21 beamline  $\mu$ -XANES and  $\mu$ -XRF maps have been obtained along the same transects analyzed at ID18F. The maps were carried out in area of  $100 \times 100 \mu\text{m}$  with a resolution of  $1 \times 1 \mu\text{m}$ . The sulfur oxidation state was determined by scanning the energy of the exciting beam across the sulfur absorption K-edge (total-S = 2.55 KeV; sulfide-S = 2.472 KeV; sulfate-S = 2.482 KeV).

## RESULTS

Micro-XRD and micro-XANES analyses showed that the earliest stage of sulfide alteration is marked by the progressive oxidation of sulfide-S to sulfate-S that is then rapidly leached out from the system. Sulfide oxidation starts from particle rims or from intra-grain microfractures and is accompanied by a progressive loss of sulfur; sulfides are then pseudomorphically replaced by goethite and minor bernalite. In addition to sulfides, many gangue silicates are efficiently altered and only quartz is preserved within the altered layers.

Elemental maps and  $\mu$ -XRF transects confirmed the high affinity of the secondary minerals to adsorb or incorporate many of the elements released by sulfides or gangue minerals (Fig. 2). In particular, we routinely observed significant concentrations of Ni, Cu, Zn, and As in the goethite-bernalite layers

The evolved hardpans (Fig. 1b) are composed by rhythmic alternation of submillimetric goethite-rich (ochreous) and hematite-rich (red) layers. This layering is the result of a complex evolution of the pristine authigenic Fe-oxides and -oxyhydroxides during which the mineral phases are cyclically involved in transformation processes including recrystallization, dissolution and reprecipitation (Carbone *et al.* 2005).

Micro-XRF transects evidenced a significant mineralogical control on the mobility of several elements released during sulfide and gangue minerals alteration (Fig. 3); in particular goethite-rich layers are enriched in Ni and Zn, whereas hematite-rich layers selectively concentrate As, Se, Mo, and Cu.

## CONCLUSIONS

Synchrotron-based  $\mu$ -XRD,  $\mu$ -XRF, and  $\mu$ -XANES techniques allowed us to determine, with  $\mu$ m-spatial resolution, the mineralogical and chemical variations occurring during the alteration of sulfide mineralizations.

The main results can be summarized as follow:

(1) sulfides and gangue silicates (with the exception of quartz) are completely altered along oxidation fronts and are progressively replaced by secondary Fe-oxyhydroxides (mainly goethite with minor bernalite);

(2) the pristine oxidation products evolve toward well consolidated crusts (hardpans) that are composed by rhythmic alternation of submillimetric goethite-rich and hematite-rich layers;

(3) several ecotoxic elements released during sulfides and silicates alteration are efficiently scavenged by the newly formed Fe-oxide and -oxyhydroxides;

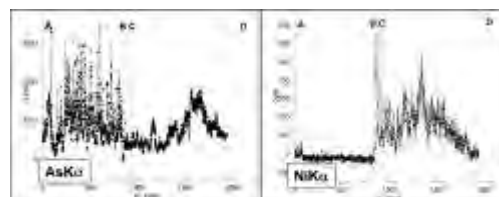


**Fig. 2.**  $\mu$ -XRF line scans evidencing the chemical variations of As (left), and Ni (right), across the transect of Fig. 1a.

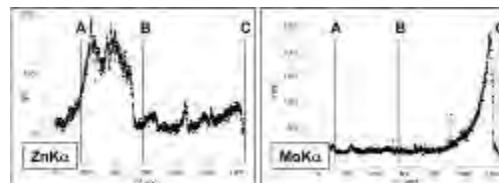


**Fig. 3.**  $\mu$ -XRF line scans evidencing the chemical variations of Zn (left), and Mo (right), across the transect of Fig. 1b. Segment AB = goethite-rich layer; segment BC = hematite-rich layer.

(4) there is a significant mineralogical control on the mobility of these elements; in particular goethite appears to be an effective sink for Ni and Zn, whereas hematite can efficiently scavenge As, Se, Mo, and Cu.

## ACKNOWLEDGEMENTS

The authors wish to acknowledge the financial support of MIUR (Italian Ministero dell'Istruzione, dell'Università e della Ricerca), PRIN-COFIN2006: "The role of mineral phases in the mobilization and storage of contaminant elements within mining sites of eastern Liguria".

## REFERENCES

- CARBONE, C., DI BENEDETTO, F., MARESCOTTI, P., MARTINELLI, A., SANGREGORIO, C., CIPRIANI, C., LUCCHETTI, G., & ROMANELLI, M. 2005. Genetic evolution of nanocrystalline Fe oxide and oxyhydroxide assemblages from the Libiola Mine (eastern Liguria, Italy): structural and microstructural investigations. *European Journal of Mineralogy*, **17**, 785-795.
- JAMBOR, J.L., BLOWES, D.W., & RITCHIE, A.I.M. 2003. Environmental aspects of mine wastes. *Mineralogical Association of Canada, Short Course Series*, **31**, Vancouver, British Columbia.
- MANCEAU, A., TAMURA, N., CELESTRE, R.S., MACDOWELL, A.A., GEOFFROY, N., SPOSITO, G., & PADMORE, H.A. 2003. Molecular-scale

- speciation of Zn and Ni in soil ferromanganese nodules from loess soils of the Mississippi Basin. *Environmental Science Technology*, **37**, 75-80.
- MARESCOTTI, P., CARBONE, C., DE CAPITANI, L., GRIECO, G., LUCCHETTI, G., & SERVIDA, D. 2008. Mineralogical and geochemical characterisation of open pit tailing and waste rock dumps from the Libiola Fe-Cu sulphide mine (eastern Liguria, Italy). *Environmental Geology*, **53**, 1613-1626.
- MORIN, G., OSTERGREN, J.D., JUILLLOT, F., ILDEFONSE, P., CALAS, G., & BROWN, G.E. 1999. XAFS determination of the chemical form of lead in smelter-contaminated soils and mine tailings: importance of adsorption processes. *American Mineralogist*, **84**, 420-434.
- MORIN, G., JUILLLOT, F., ILDEFONSE, P., CALAS, G., SAMAMA, J.C., CHEVALLIER, P., & BROWN, G.E. 2001. Mineralogy of lead in a soil developed on a Pb-mineralized sandstone (Largentiere, France). *American Mineralogist*, **86**, 92-104.
- ZACCARINI, F. & GARUTI, G. 2008. Mineralogy and chemical composition of VMS deposits of northern Apennine ophiolites, Italy: evidence for the influence of country rock type on ore composition. *Mineralogy and Petrology*, **84**, 61-83.

## Arsenic speciation in wastes resulting from pressure oxidation, roasting and smelting

Dogan Paktunc

Mining and Mineral Sciences Laboratories, CANMET, 555 Booth Street, Ottawa, ON, K1A 0G1 CANADA  
(e-mail: dpaktunc@nrcan.gc.ca)

**ABSTRACT:** Arsenic commonly occurs in elevated concentrations in some gold and base-metal deposits. Mining and metallurgical processing of gold and base-metal ores results in solid wastes, effluents, and air emissions containing high concentrations of arsenic. Such wastes form an important source of anthropogenic arsenic in the environment. The nature and occurrence of arsenic in solid wastes are complex and highly variable. A combination of microanalytical tools and techniques including XAFS were used to determine the form and speciation of arsenic in wastes resulting from pressure oxidation, roasting and smelting, and impacted soil. As K-edge and Fe K-edge XAFS analyses of the pressure oxidation residues indicate that arsenic in tetrahedral coordination is corner-linked to 5 to 6 FeO<sub>6</sub> octahedra that are edge- and perhaps face-sharing. During roasting of refractory gold ores, oxidation of As to As<sub>2</sub>O<sub>5</sub> species may be incomplete, which is detrimental to not only gold recovery but also the tailings management options. As K-edge XANES spectra indicate that more than one-third of the arsenic released from a copper smelter stack is composed of As<sup>3+</sup> species. Most likely arsenic species in the smelter-impacted soil include arsenolite, goethite with adsorbed As<sup>5+</sup>, monomethylarsonic acid, and tetramethylarsonium iodide.

**KEYWORDS:** *Arsenic, speciation, mine wastes, impacted soil, XAFS*

### INTRODUCTION

Arsenic is an abundant element in gold and base-metal ore deposits. Mining and metallurgical processing operations result in the accumulation of arsenic-bearing minerals in the tailings and waste rock. Arsenic can be readily released to the environment due to dissolution of the arsenic-bearing minerals under atmospheric conditions. Effluents resulting from mineral processing, refining and smelting operations can carry significant concentrations of As and the effluents have to be treated before they are discharged to the environment. Precipitates that form during processing and effluent treatment include ferric arsenates, ferric sulfoarsenates, ferrihydrite, hematite, and jarosite. These compounds end up in sludge and tailings ponds and their long term stabilities are important in terms of As releases from the wastes. Other sources of arsenic include air emissions in the form of dust and particulates originating from smelters and roasters.

Prediction of arsenic releases from the wastes and their bioavailability and toxicity assessments require solubility and stability tests, as well as speciation and molecular-scale characterization studies.

Several examples of arsenic speciation in wastes resulting from pressure oxidation, roasting and smelting, and impacted soil are given in this manuscript with the overall goal to promote further research in this area.

### METHODOLOGY

Bulk and micro-XAFS analyses were performed at the PNC-CAT's bending magnet (20-BM) and undulator (20-ID) beamlines of the Advanced Photon Source (APS), Argonne, IL, USA. Other microanalytical and mineralogical characterization studies were conducted at CANMET. Details of the methodology can be found in Paktunc (2008) and other publications by the author.

### RESULTS AND DISCUSSION

#### Arsenic in Refractory Gold Ores

Prior to gold extraction by cyanidation, refractory gold ores are either roasted or pressure oxidized to liberate the gold contained as submicroscopic particles or in solid solution in arsenopyrite and arsenic-rich pyrite. Gold extraction from such ores require roasting or pressure oxidation or bacterial oxidation prior to cyanidation to destroy the sulfide structure.

**Pressure Oxidation**

Arsenical compounds that can form during pressure-oxidation of refractory gold ores in the autoclaves include Phase-3, Phase-4, Type 2 and FeOH<sub>2</sub>SO<sub>4</sub> (Fig. 1). In addition, scorodite can form in autoclave with sulfate substituting up to 20% arsenate. Jarosite is another phase with limited arsenate substituting for sulfate (Paktunc & Dutrizac 2003).

Phase-3 has a variable composition (Fe<sub>0.9-1.3</sub>As<sub>0.3-0.6</sub>S<sub>0.4-0.7</sub>O<sub>4</sub>(OH)<sub>0.3-3.3</sub>). As K-edge and Fe K-edge XAFS results indicate that there are about 4 Fe atoms around the central As atom at a distance of approximately 3.33 Å and 2 Fe at ~3.5 Å. In return, there are between 1 and 2 Fe around the central Fe atom at ~2.9 Å, 1-2 As at ~3.3 Å, and 2 As at ~3.5 Å. It appears that two oxygen atoms around As are bridging edge- or face-sharing FeO<sub>6</sub> octahedra.

Phase-4 (Fe<sub>0.9-1.0</sub>AsO<sub>4</sub>(OH)<sub>0.0-0.6</sub>) is identical to ferric orthoarsenate where the central As is coordinated to 5 Fe, three of which are forming edge-sharing FeO<sub>6</sub> octahedra (Fig. 3).

FeOH<sub>2</sub>SO<sub>4</sub> contains minor As (i.e. up to 10% of the S sites in the structure). Its structure is made of corner-linked single chains of FeO<sub>6</sub> octahedra that are linked in turn by SO<sub>4</sub> tetrahedra.

Type-2 has the following composition: (Fe<sub>1.2-1.3</sub>As<sub>0.6-0.8</sub>S<sub>0.2-0.4</sub>O<sub>4</sub>(OH)<sub>2.6-3.5</sub>). It is structurally similar to the As end-member of Phase-3. In accordance with the XAFS spectra shown on Figure 2, XAFS-derived short-ranges of Type-2 and As end-member of Phase-3 are also comparable.

Pressure oxidation residues from the autoclaves display similarities (i.e., XAFS and electron microprobe) to Type-2 and As-rich Phase-3 compounds (Fig.2).

**Roasting**

In the case of roasting, the pretreatment process destroys the sulfide matrix by driving off sulfur from the structure. This results in the formation of iron oxide particles that are made of concentrically zoned and porous hematite and maghemite (Paktunc *et al.* 2006). Arsenic is volatilized as As<sub>2</sub>O<sub>3</sub> and oxidised to

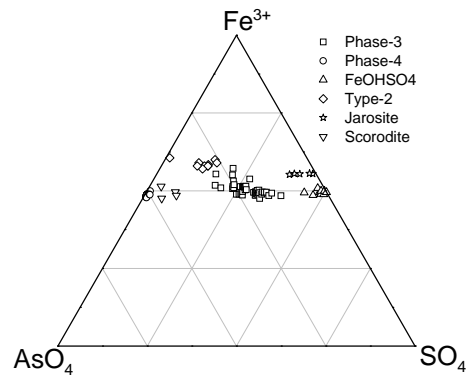


**Fig. 1.** Composition of ferric arsenate-sulfate compounds forming in the autoclaves treating refractory gold ores.

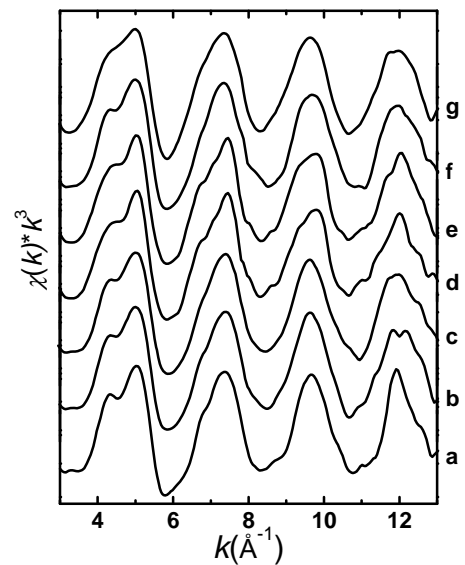


**Fig. 2.** As K-Edge XAFS spectra of Phase-3 (a, b), Type-2 (c), Phase-4 (d,e), autoclave residues (f,g).

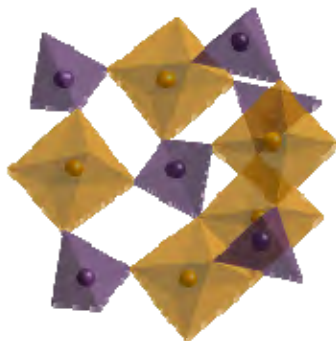


**Fig. 3.** Local structure of Phase-4 showing an arsenate tetrahedron (black) surrounded by 5 FeO<sub>6</sub> octahedra (grey) at 3.34±0.09 Å and 5 arsenate tetrahedra at 4.35±0.23 Å.

As<sub>2</sub>O<sub>5</sub> under the highly oxidizing conditions of a roaster.

Micro-XANES spectra collected from maghemite-rich and hematite-rich domains within Fe-oxide particles indicate the presence of both As<sup>3+</sup> and As<sup>5+</sup> species. This observation is similar to that of Walker *et al.* (2005) in the Giant gold mine tailings. As<sup>3+</sup> species appear to be more common in the maghemite-rich domains, indicating a clear relationship between retarded transformation of Fe-oxide compounds and incomplete oxidation of As species during roasting (Paktunc 2008). This finding is not only important for the recovery of gold (Paktunc *et al.* 2006), but also assessing the stability of the arsenic species in the tailings.

### Arsenic in Smelter Emissions

Recent studies examining the distribution of smelter-derived elements around a copper smelter found that arsenic deposition rates in snow and concentrations in organic soils decrease gradually with distance from the smelter (Henderson *et al.* 2002; Knight & Henderson 2006; Telmer *et al.* 2003; Zdanowicz *et al.* 2006). In order to explore the nature and behaviour of arsenic, a limited number of samples (stack and impacted soil) were characterized.

The sample collected from the middle of a copper smelter stack representing emitted particles was highly complex.

XANES analyses indicated the presence of both As<sup>3+</sup> and As<sup>5+</sup> species in the stack sample and that about one-third of the total As is trivalent (Paktunc 2008). X-ray mapping supplemented by micro-XANES analyses indicated that As is localized along thin rims around spherical Cu particles. These rims have higher As<sup>3+</sup> species ranging from 34 to 40% of the total As.

The soil samples impacted by the copper smelter were selected based on arsenic concentrations, location (i.e., proximity to the smelter) and depth within the soil horizon. XANES spectra of the soil samples collected from 2 to 10 km distances and depths of 0 to 95 cm are dominated by As<sup>5+</sup> species. Least-square analysis of the spectra with the organic As species of Smith *et al.* (2005) indicated the presence of monomethylarsonic acid (CH<sub>3</sub>AsO(OH)<sub>2</sub>) and tetramethylarsonium iodide (C<sub>4</sub>H<sub>12</sub>AsI) in addition to arsenolite and goethite with adsorbed As (Paktunc 2008). Arsenolite (As<sup>3+</sup>) that forms 6 to 13 % of the arsenic species is found only in the near surface samples from 2 to 6 km away from the smelter whereas the samples 10 km away from the smelter are composed of goethite and monomethylarsonic acid (Fig. 4). Considering that monomethylarsonic acid is at least 600 times less toxic than arsenous acid (H<sub>3</sub>AsO<sub>3</sub>) and 60 times less toxic than arsenic acid (H<sub>3</sub>AsO<sub>4</sub>) (Andrewes *et al.* 2004), quantitative speciation of arsenic in the soil profile would have significant implications in risk assessment studies. Although it is premature to draw any conclusion, the preliminary results from this exploratory data set justify the need to undertake a systematic sampling and studies to determine the speciation of arsenic and its methylation within the soil profile and distance from the point source.

### ACKNOWLEDGEMENTS

The XAFS experiments were carried out at the Pacific Northwest Consortium - Collaborative Access Team's (PNC/XOR) beamline at the Advanced Photon Source

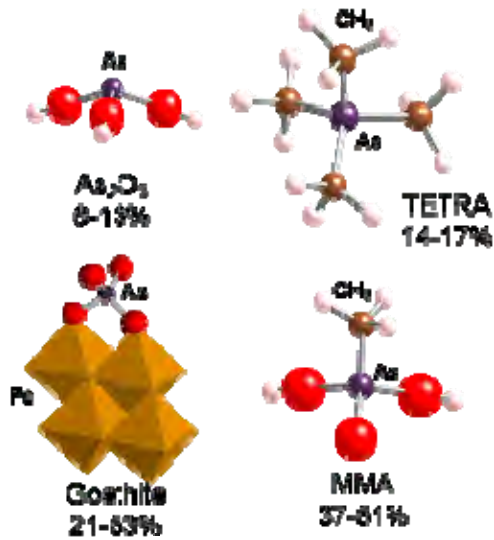


Fig. 4. Arsenic species present in the impacted soil. TETRA:  $C_4H_{12}AsI$ ; MMA:  $CH_3AsO(OH)_2$

(APS) under the user agreement to the author which is supported by the US Department of Energy under contracts W-31-109-Eng-38 (APS) and DE-FG03-97ER45628 (PNC-CAT). The XAFS experiments at PNC/XOR were also supported by the Natural Sciences and Engineering Research Council of Canada through a major facilities access grant.

## REFERENCES

- ANDREWES, P., DEMARINI, D.M., FUNASAKA, K., WALLACE, K., LAI, V.W.M., SUN, H., CULLEN, W.R., & KITCHIN, K.T. 2004. Do arsenosugars pose a risk to human health? The comparative toxicities of a trivalent and pentavalent arsenosugar. *Environmental Science and Technology*, **38**, 4140-4148.
- HENDERSON, P.J., KNIGHT, R.D., & MCMARTIN, I. 2002. Geochemistry of soils within a 100 km radius of the Horne Cu smelter, Rouyn-Noranda, Quebec. *Geological Survey of Canada Open File* **4169**.
- KNIGHT, R.D. & HENDERSON, P.J. 2006. Smelter dust in humus around Rouyn-Noranda, Québec. *Geochemistry: Exploration, Environment and Analysis*, **6**, 203-214.
- PAKTUNC, D. 2008. Speciation of arsenic in an anaerobic treatment system at a Pb-Zn smelter site, gold roaster products, Cu smelter stack dust and impacted soil. Proc. 9th Int. Cong. Applied Mineralogy (ICAM2008) 8-10 Sep 2008, Brisbane, Queensland, *The Australasian Institute of Mining and Metallurgy*, **8/2008**, 343-348.
- PAKTUNC, D. & DUTRIZAC, J. 2003. Characterization of arsenate-for-sulfate substitution in synthetic jarosite using X-ray diffraction and X-ray absorption spectroscopy. *Canadian Mineralogist*, **41**, 905-919.
- PAKTUNC, D., KINGSTON, D., PRATT, A., & MCMULLEN, J. 2006. Distribution of gold in pyrite and in products of its transformation resulting from roasting of refractory gold ore. *Canadian Mineralogist*, **44**, 213-227.
- SMITH, P.G., KOCH, I., GORDON, R.A., MANDOLI, D.F., CHAPMAN, B.D., & REIMER, K.J. 2005. X-ray absorption near-edge structure analysis of arsenic species for application to biological environmental samples. *Environmental Science and Technology*, **39**, 248-254.
- TELMER, K., BONHAM-CARTER, G.F., KLIZA, D.A., & HALL, G.E.M. 2003. The atmospheric transport and deposition of smelter emissions: evidence from the multi-element geochemistry of snow, Quebec, Canada. *Geochimica et Cosmochimica Acta*, **68**, 2961-2980.
- WALKER, S.W., JAMIESON, H.E., LANZIROTTI, A., & ANDRADE, C.F. 2005. Determining arsenic speciation in iron oxides derived from a gold-roasting operation: Application of synchrotron micro-XRD and micro-XANES at the grain scale. *Canadian Mineralogist*, **43**, 1205-1224.
- ZDANOWICZ, C.M., BANIC, C.M., PAKTUNC, D. & KLIZA-PETELLE, D.A. 2006. Metal emissions from a Cu-smelter, Rouyn-Noranda, Quebec: Characterization of particles sampled in air and snow. *Geochemistry: Exploration, Environment and Analysis*, **6**, 147-162.

## Importance of sorption in the geochemistry of nickel in waste rock

**Benoît Plante<sup>1</sup>, Mostafa Benzaazoua<sup>1</sup>, Bruno Bussière<sup>1</sup>, & Donald Laflamme<sup>2</sup>**

<sup>1</sup>Université du Québec en Abitibi-Témiscamingue (UQAT), 445 boul. de l'Université, Rouyn-Noranda, QC, J9X 5E4 CANADA (e-mail: benoit.plante@uqat.ca)

<sup>2</sup>Rio Tinto, Fer et Titane Inc., 1625, route Marie-Victorin, Sorel-Tracy, QC, J3R 1M6 CANADA

**ABSTRACT:** Humidity cell tests were used for contaminated neutral drainage (CND) prediction from waste rock piles of an ilmenite deposit known to occasionally release above-regulatory level nickel loadings. The influence of mineralogy and in-situ weathering degree of waste rock on its geochemical behaviour are investigated in this study, using samples of waste rocks having various mineral compositions and which underwent different alteration levels (fresh and approximately 25 years old waste samples). The rates of sulfide oxidation appear to be of the same order in fresh and weathered waste rock. However, the nickel ions produced by sulfide oxidation do not get leached in the fresh waste rocks while they are leached in the weathered waste rocks. The nickel sorption potential of the studied waste rocks appears to play a significant role on the nickel geochemical behaviour. Batch sorption tests followed by sequential extraction procedures suggest that the number and type of available sorption sites appear to vary between fresh and weathered mine waste rocks.

**KEYWORDS:** *Nickel geochemistry, contaminated neutral drainage*

### INTRODUCTION

Acid mine drainage (AMD) is often characterized by low pH, high acidity, and high metal loadings. The phenomenon received much attention in the past decades in terms of prediction, control, and remediation (e.g., MEND 2001). However, many toxic metals such as Ni, Zn, Co, As, and Sb are soluble at near-neutral pH, and can potentially lead to the contamination of mine effluents without acidic conditions; this phenomenon is called Contaminated Neutral Drainage (hereinafter called CND) or simply Neutral drainage (Nicholson 2004). Since many Canadian mines can potentially face Ni release from waste rock, and Ni geochemistry received much less attention than other CND-related metals (ex. As) in the past years, this work focuses on Ni geochemistry at near-neutral conditions. The present study is performed on waste rock sampled from the Lac Tio mine, an ilmenite deposit near Havre-Saint-Pierre, Québec, Canada, exploited by an open pit operation by Rio Tinto, Fer et Titane Inc. (RTFT) since the early 1950's. The gangue material of the mine is mainly composed of a calcic

plagioclase mineral (approximate formulae  $\text{Na}_{0.4}\text{Ca}_{0.6}\text{Al}_{1.6}\text{Si}_{2.4}\text{O}_8$ ). Water draining from the waste rock piles are near-neutral and sporadically show Ni concentrations slightly higher than those allowed by Quebec regulations. Preliminary studies on this waste rock showed that the material is not acid generating and that Ni is generated mainly from Ni-bearing pyrite ( $\text{FeS}_2$ ) and pentlandite ( $(\text{Fe,Ni})_9\text{S}_8$ ) that seem to be associated with ilmenite in the Lac Tio deposit, and the waste rock benefit from an important metal retention potential occurring most probably via surface sorption (Bussière *et al.* 2005; Plante *et al.* 2008; Pepin *et al.* 2008). This study aims to clarify the sorption importance on Ni geochemistry in mine waste rocks.

### MATERIALS AND METHODS

In this work, 6 Lac Tio waste rock samples are investigated: 3 samples were freshly blasted waste rock and 3 were "weathered" samples from an old waste rock pile (approximately 25 years old) which underwent significant natural alteration. The ilmenite content varies from approximately 20 to 60 wt% in both

the fresh and weathered waste rock samples. The Ni content varies from 0.028 to 0.043 wt% and S content (mainly as sulfide) from 0.142 to 0.384 wt% in the waste rock samples studied. Weathered samples have significantly lower S values (<0.172 wt%) than fresh samples (>0.345 wt%), probably due to previous alteration. The Ni geochemistry was evaluated through the use of humidity cell tests (ASTM D5744-96), which consist of weekly drying-wetting cycles ending with flushing of the studied material (1 kg) with deionised water (1 L), and analysis for various geochemical parameters such as pH and metals (using ICP-AES) on the leachates. These cell tests were performed on the -¼ inch fraction of the mine wastes without grinding, since doing so would generate unwanted fresh surfaces in the weathered waste rock samples.

**RESULTS AND INTERPRETATION**

**Kinetic cells**

The pH values measured in the kinetic tests are shown in Figure 1. The pH of all waste rock samples remain stable between 7 and 8 after 200 days until the end of the test, suggesting conditions will remain near-neutral in the field.

As is often the case in CND generating materials (or in low-acid generating potential materials), the detected metal levels in leachates were generally low, in the order of thousandths to hundredths of mg/L. In fact, the Ni concentrations obtained from the fresh waste rocks are often under the detection limit of the ICP-AES employed (0.004 mg/L). For greater appreciation of the environmental behaviour of the different studied waste rocks, particularly to differentiate the geochemical behaviour of fresh and weathered waste rocks, the release rates were calculated.

The elemental release rates were determined as the slope of the linear regression of the cumulated (from each leachate) and normalized (with regards to total mass in the corresponding cell) metal loads over time (in mg/kg/day); they are summarized in Figure 2. The range of

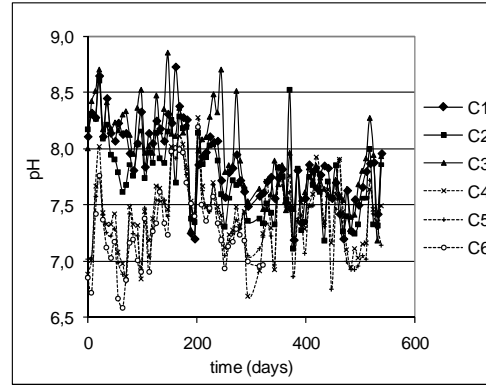


Fig. 1. pH evolution during kinetic cell tests.

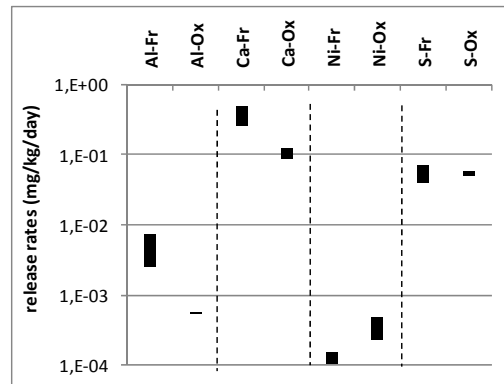


Fig. 2. Ranges of elemental release rates obtained with laboratory kinetic cell tests on fresh (-Fr) and weathered (-Ox). waste rocks.

obtained release rates is shown for Al, Ca, S and Ni for the fresh (labeled “-Fr”) and weathered materials (labeled “-Ox”). The S and Ni releases are associated with sulfides oxidation, while Al and Ca releases are associated with the neutralizing minerals contained in the waste rock (plagioclase).

Plagioclase dissolution is known to be incongruent, with Al and Ca being preferably dissolved at the surface (Blum & Stillings 1995). This dissolution generates an Al-Ca-poor thin layer at the surface, which is consistent with the lower Al-Ca release rates obtained in the leaching waters of the weathered waste rocks. The S release rates obtained from the fresh and weathered waste rocks are of the same order, suggesting that sulfide oxidation occurs at approximately the same rate in both, assuming that all the oxidation products do end up in the

leachates (an acceptable assumption at this pH range). Consequently, the Ni release rates of fresh and weathered waste rocks should be of the same order. However, the Ni release rates from the weathered waste rocks are about half an order of magnitude greater than those from the fresh waste rocks.

Geochemical simulations (not shown) of water quality suggest that Ni is soluble in the test conditions, eliminating secondary mineral precipitation as an explanation for the absence of Ni in leachates. These observations could be explained by the metal retention potential of the Lac Tio waste rock being still active in the humidity cell tests. Consequently, the Ni produced in the humidity cell tests will continue to be retained by the fresh waste rock until saturation of the retention sites.

#### Batch sorption and Sequential Extraction Procedure (or SEP)

In order to validate the hypothesis mentioned above, the Ni retention capacity of the Lac Tio waste rock was estimated using a batch sorption test performed on a fresh (C1) and weathered (C4) sample, followed by a 3-step Sequential Extraction Procedure (or SEP). The batch sorption test was done using a 10 mg/L Ni solution with an initial pH of 6, an ionic force adjusted to 0.05 M with NaNO<sub>3</sub> and with a liquid/solid ratio of 25. Some of the batch sorption results are presented in Figure 3.

Almost 100 % of the Ni was sorbed on the fresh waste rock after 400 minutes, while Ni retention reaches only 50 % after 1500 minutes on the weathered waste rock. The resulting Ni sorption capacities from these batch tests are 0.34 mg/g for the fresh and 0.19 mg/g for the weathered waste rock. However, the Ni sorption capacity of the fresh waste rock is probably greater, since all the Ni was retained in the batch test and the sorption sites were not fully saturated.

Despite strong criticisms on the interpretation of SEP's (Nirel & Morel 1990), they are still recognized as a valuable tool to evaluate metal partition in soils, tailings, and waste rocks. (Wasay *et*

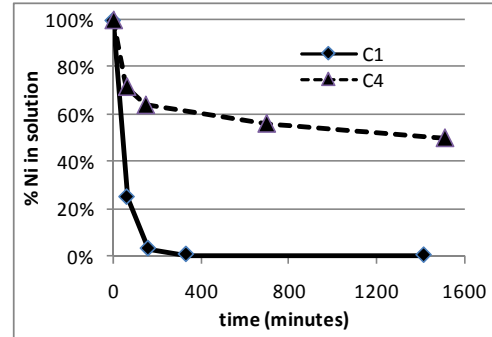


Fig. 3. Batch Ni sorption test.

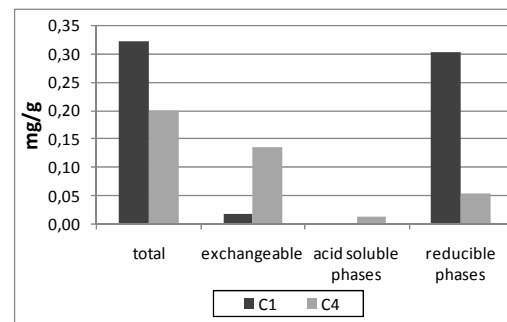


Fig. 4. Distribution of the Ni retention phases in fresh (C1) and weathered (C4) waste rock after a batch sorption test.

*al.* 1998; Zagury *et al.* 1999). The 3-step SEP employed in this study (see detailed procedure in Neculita *et al.* 2008) enabled the determination of the Ni fraction that is 1) soluble and exchangeable, 2) bound to acid-soluble phases and 3) reducible or bound to Fe-Mn oxides. The results are presented in Figure 4: most of the Ni is sorbed on reducible phases of the fresh waste rock (C1) with very few Ni that is easily exchangeable. For the weathered waste rock (C4), about 70 % of the Ni is easily exchangeable, about 25 % of the Ni occurs as reducible phases and the remaining Ni is on acid soluble phases.

#### CONCLUSIONS

This study allows a better understanding of the Ni geochemistry in near-neutral conditions. Kinetic cell tests run for 75 weeks on 6 waste rock samples suggest that the pH will remain near neutral in the waste rock piles. Sorption phenomena seem to drive Ni leaching in laboratory kinetic cells, and the sorption type and capacity vary between fresh and

weathered waste rocks. Applications of these findings to waste rock piles management and remediation are currently being studied.

#### ACKNOWLEDGEMENTS

The Authors would like to thank the NSERC Polytechnique-UQAT Chair in environment and mine wastes management for financial support, and are grateful to QIT-Fer et Titane Inc. for making this research possible and the URSTM personnel for their technical support. The Authors are also grateful to the NSERC Collaborative Research and Development (CRD) Grants.

#### REFERENCES

- BLUM, A.E. & STILLINGS, L.L. 1995. Feldspar dissolution kinetics. In: WHITE, A.F. & BRANTLEY, S.L. (ed.), *Reviews in mineralogy*, **31: Chemical weathering rates of silicate minerals, Mineralogical Society of America, USA, 291-352.**
- BUSSIÈRE, B., DAGENAIS, A.-M., VILLENEUVE, M., & PLANTE, B. 2005. Rapport final: Caractérisation environnementale d'un échantillon de stériles du Lac Tio. URSTM, Rouyn-Noranda.
- MEND, 2001. MEND Manual, Report 5.4.2 CD, CD-ROM: MEND Manual, Ottawa, ON.
- NECULITA, C.-M., ZAGURY, G.J., & BUSSIÈRE, B., 2008. Effectiveness of sulfate-reducing passive bioreactors for treating highly contaminated acid mine drainage: II. Metal removal mechanisms and potential mobility. *Applied Geochemistry*, **23**, 3545-3560.
- NICHOLSON, R.V. 2004. Overview of neutral pH drainage and its mitigation: results of a MEND study. *Proceedings of the MEND Ontario workshop*, Sudbury, 2003.
- NIREL, P.M.V. & MOREL, F.M.M. 1990. Pitfalls of sequential extractions. *Water Research*, **24**, 1055-1056.
- PEPIN G., BUSSIÈRE B., AUBERTIN M., BENZAAZOUA M., PLANTE B., LAFLAMME D., & ZAGURY G.J. 2008. Field experimental cells to evaluate the potential of contaminated neutral drainage generation at the Tio mine, Quebec, Canada. *Proceedings of the 10<sup>th</sup> IMWA Mine Water and the Environment*, Czech Republic, 309-312.
- PLANTE, B., BENZAAZOUA, B., BUSSIÈRE, B., PEPIN, G., & LAFLAMME, D. 2008. Geochemical behaviour of nickel contained in Tio mine waste rocks. *Proceedings of the 10<sup>th</sup> IMWA Mine Water and the Environment*, Czech Republic, 317-320.
- WASAY, S. A., BARRINGTON, S., & TOKUNAGA, S. 1998. Retention form of heavy metals in three polluted soils. *Journal of Soil Contamination*, **7**, 103-119.
- ZAGURY, G.J., DARTIGUENAVE, Y., & SETIER, J.-C. 1999. Ex situ electroreclamation of heavy metals contaminated sludge: pilot scale study. *Journal of Environmental Engineering*, **125**, 972-978.

## Distribution of elements of concern in uranium mine tailings, Key Lake, Saskatchewan, Canada

Sean A. Shaw<sup>1</sup>, M. Jim Hendry<sup>1</sup>, Joseph Esselfie-Dughan<sup>1</sup>,  
Tom Kotzer<sup>2</sup>, & Harm Maathuis<sup>2</sup>

<sup>1</sup>Department of Geological Sciences, University of Saskatchewan, 114 Science Place, Saskatoon SK, S7N 5E2  
CANADA (email: sean.shaw@usask.ca)

<sup>2</sup>Cameco Corporation, 2121-11th Street West, Saskatoon, SK, S7M 1J3 CANADA

**ABSTRACT:** Boreholes were drilled and detailed tailings samples collected through the entire depth profile (76 m) at three locations in the Deilmann Tailings Management Facility, located at the Key Lake Uranium mine in Saskatchewan, Canada. Pore waters and solid phases were separated using piston core squeezing. The concentrations of the elements of concern (EOC: As, Mo, Ni, and Se) as well as other elements were determined for all solid phase (n = 87) and pore water (n=83) samples. Additional analyses, including X-ray Diffraction and Scanning Electron Microprobe were conducted on the solid samples to provide characterization and spatial definition of mineral phases that could influence the distribution of the elements of concern. The pH, Eh and temperature were also measured on core samples and extracted pore waters. The mean concentrations for As, Mo, Ni, and Se were 2,918, 41.9, 3,178, and 9.84  $\mu\text{g g}^{-1}$  in the solid phase and 39.0, 139, 0.63, and 0.83  $\mu\text{mol L}^{-1}$  in the aqueous phase. Results indicated a strong correlation between solid phase As, Mo, Ni, and Se concentrations and aqueous phase As, Mo, and Se values. In addition, comparisons between whole-rock geochemical and micron-scale elemental concentrations suggest a strong correlation between As, Fe, and Ni in the solid phase.

**KEYWORDS:** uranium, mine tailings, geochemistry, mineralogy, Key Lake

### INTRODUCTION

Uranium deposits of the Athabasca basin in northern Saskatchewan, Canada, produce about one-third of the world's uranium. The uranium ores associated with these deposits can contain variable and high concentrations of nickel (up to 5 wt %) and arsenic (up to 10 wt %). Consequently, elevated concentrations of As and Ni have been associated with the tailings facilities for these type of deposits (Donahue & Hendry 2000). The US EPA has set the drinking water limit for As at 0.010  $\text{mg L}^{-1}$ , while the World Health Organization suggests a maximum Ni concentration of 0.070  $\text{mg L}^{-1}$ . Elevated concentrations of additional elements of concern (EOC), including Mo and Se, have also been associated with uranium mine tailings (Morrison *et al.* 2002). At high concentrations, Se compounds are carcinogenic and teratogenic (Ohlendorf *et al.* 1986), while Mo may be toxic as it

leads to a secondary Cu deficiency (e.g., Vunkova-Radeva *et al.* 1988).

The Key Lake uranium mine is located at the southern rim of the Athabasca Basin in north central Saskatchewan, approximately 650 km north of Saskatoon, Saskatchewan (57°13'N, 105°38'W). The Deilmann tailings facility (DTMF) is located on site and has been in operation since 1996.

A 10 Ka criteria for uranium tailings facilities, including the DTMF, has been developed due to elevated concentrations of long-lived transuranic elements (Atomic & Energy Control Board 1987). This 10 Ka criteria is also applied to other elements of concern to prevent their long-term mobilization to the surrounding environment. In order to understand the long-term effects of uranium tailings on the surrounding environment, detailed information on the geochemical and mineralogical controls on the elements of concern are required.

The global objective of this study is to characterize the geochemical characteristics of tailings within the DTMF over the immediate and long term. The specific objective of this study is to quantify the solid and aqueous phase concentrations of the elements of concern within the DTMF and determine the geochemical and mineralogical controls on these observed elemental distributions. This study documents one aspect of a holistic, multi-year scientific program on uranium mine tailings within Cameco Operations, designed to better understand the long-term geochemical behaviour of mine tailings.

### **Tailings Management Facility**

The Deilmann Tailings Management Facility (DTMF) was constructed in the mined out Deilmann pit. The DTMF is characterized by two depositional zones: the east and west cells. Tailings deposition began in the east cell in 1996 and commenced in the west cell once the Deilmann ore body was mined out in 1999. Prior to 1999, the only source of tailings for the DTMF was the Deilmann ore body (Ruhmann & von Pechmann 1989). Since 2000, the tailings have been derived from a mixture of MacArthur River (Delany *et al.* 1998) and low and high-grade wastes from both the Deilmann and McArthur River ore bodies. Therefore, the tailings body can be conceptualized as two separate tailings types, the lower Deilmann and upper McArthur tailings, which are separated at approximately 410 m elevation within the DTMF.

In 1998 the tailings in the DTMF were converted to subaqueous storage by disabling perimeter drains and allowing the facility to naturally flood. Since 2006, the water level has been maintained at approximately 50 m above the top of the tailings.

## **MATERIALS AND METHODS**

### **Sample Collection & Analyses**

Since 1999, boreholes have been drilled into the DTMF tailings for the sole purpose of collecting tailings cores for their geochemical and geotechnical

characterization. Drilling collection periods have previously taken place in 1999, and 2004/2005 with boreholes from all three campaigns proximally-located within several meters of one another.

In June, 2008, boreholes were drilled at three locations in the DTMF east cell using a sonic track mounted drill rig on a floating barge. Boreholes were cored to depths of between 75.3 m and 79.0 m and continuous core samples were collected using a 3.1 m long, 75 mm diameter, core barrel. Following core collection, samples were sealed in containers and stored at temperatures of 4°C. Pore waters were extracted from the tailings samples within 24 h of collection using both centrifugation and piston squeezing techniques. Tailings (n = 87) and pore water (n = 83) samples were analysed for pH, Eh, alkalinity, organic/inorganic C, major cations, major anions, trace metals, and radionuclides.

Geochemical speciation modelling was conducted for all extracted pore waters using PHREEQC (Parkhurst & Appelo 1999). Preliminary mineralogical analysis of selected tailings samples collected in 2004 was conducted using a Philips PW1830 X-ray powder diffractometer and a JEOL JXA-8600 electron microprobe microanalyzer (EPMA). Samples were analyzed by EPMA using electron backscatter imaging, energy dispersive spectrometry, and wavelength dispersive spectrometry.

## **RESULTS AND DISCUSSION**

### **Tailings Solid Phase**

The stratigraphy of the DTMF mainly consists of tailings layers with varying water contents. The water content ranged between 10.3 and 172 %, while the tailings with a particle size < 75 µm ranged between 4.10 and 98.6 %, throughout all three boreholes. The average water content and particle size < 75 µm was 55.6 wt % and 58.8 % in the Deilmann tailings and 49.0 wt% and 42.9 %, in the McArthur tailings. The lower water content and larger grain size observed in the McArthur tailings was mainly attributed to a sand wedge deposited by sloughing events in 2001.

In all boreholes the average concentrations of As, Ni, Mo, and Se were greater in the Deilmann, relative to the McArthur tailings (Table 1). This can be attributed to differences in solid phase compositions of the original Ni-As rich Deilmann ores versus relatively Ni-As poor McArthur River ores.

### Mineralogical Analyses

Major mineral phases identified in the DTMF included several aluminosilicates, quartz, gypsum and hydrobasaluminite. Minor mineral phases identified included ferrihydrite, gersdoffite (NiCoAsS), sulfide phases, and several carbonates.

Preliminary EPMA analyses indicated the formation of As, Fe, and Ni-rich coatings surrounding Ca-SO<sub>4</sub>-rich particles (Fig. 1). A comparison of solid phase As and Ni concentrations demonstrated a good correlation between samples from all three boreholes, which was previously observed by EPMA analyses conducted by Donahue and Hendry (2000) on tailings from a similar facility. This relationship potentially resulted during the neutralization portion of the milling process where a strong pH gradient developed around un-reacted lime particles forming FeO(OH)-AsO<sub>4</sub> complexes along with theophrastite (Ni[OH]<sub>2</sub>).

### Tailings Pore Water

The pH of pore waters, collected by piston squeezing, ranged between 8.0 and 10.7, with an average pH value of 9.9. Measured Eh values ranged between 50 and 525 mV, with an average of 200 mV. Aqueous concentrations for As, Mo, and Se were greater in the Deilmann relative to the McArthur tailings. However, no difference was observed between Ca, Fe, Ni, and SO<sub>4</sub> concentrations between the two tailings types (Table 2) which is largely due to crystallization of gypsum, iron oxy-hydroxides and theophrastite.

Geochemical speciation modelling indicated saturation with respect to gypsum and several carbonates, slight under-saturation with respect to calcium arsenate (Ca<sub>3</sub>[AsO<sub>4</sub>]<sub>2</sub>) and ferrihydrite.

**Table 1.** DTMF tailings average solid phase concentrations for 2008 boreholes.

EOC	Mean ( $\mu\text{g g}^{-1}$ )	Min. ( $\mu\text{g g}^{-1}$ )	Max. ( $\mu\text{g g}^{-1}$ )
<b>McArthur Tailings (n = 42)</b>			
As	406	0.70	1,440
Ni	531	1.60	2,000
Mo	14.0	0.60	32.0
Se	3.20	0.00	8.30
<b>Deilmann Tailings (n = 45)</b>			
As	5,374	165	13,700
Ni	5,764	243	14,300
Mo	69.7	9.00	183
Se	16.3	1.40	27.0

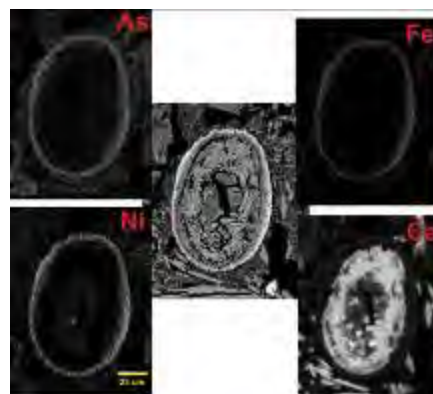


**Fig. 1.** Electron backscatter image of a Ca-SO<sub>4</sub>-rich grain showing a secondary precipitate ring (centre) and individual backscatter images for As, Fe, Ni, and Ca of the same grain.

Additionally, both calcium arsenate and ferrihydrite approached equilibrium with increased depth in each borehole, which was well correlated to the observed increased As aqueous concentrations.

### SUMMARY AND CONCLUSIONS

Solid and aqueous phase geochemical results indicate that tailings derived from the Deilmann ore are different from tailings originating from the McArthur ore body. Significantly greater concentrations of solid phase As, Ni, Mo, and increased aqueous concentrations of As, Mo, and Se are associated with tailings derived from Deilmann ore.

Mineralogical analyses suggest that gypsum and hydrobasaluminite are major secondary precipitates found within the DTMF, with trace amounts of gersdoffite and ferrihydrite also present. Electron microprobe analyses indicates a strong co-location between As, Ni, and Fe, which

**Table 2.** DTMF tailings average pore water concentrations for 2008 boreholes.

EOC	Mean ( $\mu\text{mol L}^{-1}$ )	Min. ( $\mu\text{mol L}^{-1}$ )	Max. ( $\mu\text{mol L}^{-1}$ )
<b>McArthur Tailings (n = 39)</b>			
As	10.8	0.19	33.2
Ni	0.73	0.00	4.38
Mo	50.9	0.00	92.2
Se	0.56	0.00	1.42
Fe	0.18	0.00	0.82
Ca	15,500	6,740	16,700
SO <sub>4</sub>	16,200	11,500	17,700
<b>Deilmann Tailings (n = 44)</b>			
As	67.5	7.34	147
Ni	0.52	0.00	1.45
Mo	227	38.3	433
Se	1.11	0.31	1.85
Fe	0.15	0.00	0.57
Ca	15,700	15,000	16,500
SO <sub>4</sub>	18,400	15,600	21,900

is supported by the linear relationship observed between the solid phase As, Ni and Fe concentrations in bulk tailings.

#### ACKNOWLEDGEMENTS

We would like to thank Andrew Jansen and Virginia Chostner for their assistance with the collection of samples. We would also like to thank Tom Bonli for assistance with the EPMA analyses. This project was jointly funded by Cameco Corporation and NSERC.

#### REFERENCES

ATOMIC ENERGY CONTROL BOARD. 1987. GRegulatory objectives, requirements and guidelines for the disposal of radioactive wastes – long-term aspects. Ottawa, Canada.

DELANY, T.A., HOCKLEY, D.E., CHAMPMAN, J.T., & HOLL, N.C. 1998. Geochemical characterization of tailings at the McArthur River Mine, Saskatchewan. *Tailings and Mine Waste '98*, Balkema, Rotterdam.

DONAHUE, R., HENDRY, M.J., & LANDINE, P. 2000. Distribution of arsenic and nickel in uranium mill tailings, Rabbit Lake, Saskatchewan, Canada. *Applied Geochemistry*, **15**, 1097-1119.

DONAHUE, R. & HENDRY, M.J. 2003. Geochemistry of arsenic in uranium mine mill tailings, Saskatchewan, Canada. *Applied Geochemistry*, **18**, 1733-1750.

OHLENDORF, H. M., HOFFMAN, D. J., SAIKI, M. K., & ALDRICH, T. W. 1986. Embryonic mortality and abnormalities of aquatic birds: Apparent impacts of selenium from irrigation drainwater. *Science of the Total Environment*, **52**, 533-535.

PARKHURST, D.L. & APPELO, C.A.J. 1999. User's guide to PHREEQC (version 2) A computer program for speciation, batch reaction, one dimensional transport, and inverse geochemical calculations. *USGS Survey Water Resources Investigations Report 99-4259*, 310 p.

RUHRMANN, G. & VON PECHMANN, E. 1989. Structural and hydrothermal modification of the Gaertner uranium deposit, Key Lake, Saskatchewan, Canada. *IAEA TECDOC-500*, 363-377.

VUNKOVA-RADEVA, R., SCHIEMANN, J., MENDEL, R.R., SALCHEVA, G., & GEORGIEVA, D. 1988. Stress and activity of molybdenum containing complex in winter wheat seeds. *Plant Physiology*, **87**, 533-535.

## Source, attenuation and potential mobility of arsenic at New Britannia Mine, Snow Lake, Manitoba

Stephanie Simpson<sup>1</sup>, Barbara L. Sherriff<sup>1</sup>,  
Nikolay Sidenko<sup>1,2</sup>, & Jamie Van Gulck<sup>3</sup>

<sup>1</sup> Department of Geological Sciences, University of Manitoba, Winnipeg, MB, R3T 2N2 CANADA  
(email: jared.etccherry@gmail.com)

<sup>2</sup> TetreES Consultants Inc., Winnipeg, MB, R3C 3R6 CANADA

<sup>3</sup> Arktis Solutions Inc. 186 Steepleridge St., Kitchener, ON, N2P 2V1 CANADA

**ABSTRACT:** High concentrations of arsenic (As) (~17 ppm) in a groundwater monitoring well at the gold mine site in Snow Lake Manitoba are either emanating from a Residue Stockpile (ARS) containing arsenopyrite concentrate and/or from an old emergency discharge area used for Nor Acme tailings. Hydrological modelling suggests that As is transported into the aquifer from the ARS by advection and diffusion. The concentration of As in the Nor Acme tailings is <0.1 mg/L, and in the pore water of the tailings <5 mg/L, making the tailings an unlikely source of the contamination. Attenuation of As in surface waters appears to be adsorption of As(V) on Fe-oxyhydroxides such as ferrihydrite, but in the aquifer, the majority of the As is in the more soluble As(III) phase. Arsenic is also attenuated by adsorption on plants either alone or with FeOOH. The objectives of this research were to determine the potential for contamination of Snow Lake, the source of drinking water for the town of Snow Lake, and the local environment. At the time the study was conducted, water quality in Snow Lake met the Canadian Drinking Water Standard of 0.010 mg/L As.

**KEYWORDS:** arsenic, mobility, attenuation, geochemistry, hydrologic modelling

### INTRODUCTION

High concentrations of arsenic are present in the ground water at New Britannia Gold Mine, Snow Lake, Manitoba, Canada. Between 1995 and 2005, ground water samples from a monitoring well (MW 17) had <20 ppm arsenic. This well is installed into an aquifer below a low-lying former Nor Acme Mine emergency tailings disposal area (NATA) (Fig. 1). MW17 is also 100 m down gradient from an arsenopyrite residue stockpile (ARS) that contains pore water concentrations of up to 100 ppm arsenic (Salzsauler *et al.*, 2005).

The objectives of this research were to determine the potential for contamination of Snow Lake which provides drinking water for the town of Snow Lake, and the local environment by identifying the source of arsenic in the ground water at MW17 and the mechanisms by which arsenic is being transported and attenuated.

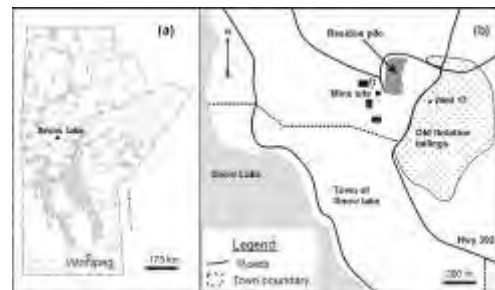


**Fig.1.** (a) map of Manitoba showing the location of Snow Lake (b) diagram of the mine site showing the ARS, MW17 and the emergency tailings.

### SITE DESCRIPTION

From 1949 to 1958, Nor-Acme Gold Mine piped 227,000 tonnes of refractory gold-bearing sulfide concentrate into a rock-walled impoundment (Richardson & Ostry 1996, Salzsauler *et al.* 2005) in hope of finding a means to extract the gold. The ARS remained uncovered until 2000 when a cover was placed to inhibit sulfide oxidation and prevent further contaminated surface runoff. Arsenic is

now suspected to be leaching through the base of the ARS into the local underlying aquifer, which is monitored at MW17. Prior to capping, drainage water from the ARS flowed north into a marshy runoff area (RA) that empties via Canada Creek into Snow Lake. Surface water in the RA has <13 ppm arsenic (Salzsauler 2004). This contamination is suspected to be the result of 50 years of drainage emanating from the ARS and the mine site.

#### **METHODOLOGY**

Cores were collected from the NATA and adjacent wetland. Solid material was obtained from the aquifer beneath the NATA by filtering water samples from MW17. Pore water was squeezed from cores in a hydraulic press. Groundwater, surface and lake water samples were filtered (0.2 µm) in the field. Sub-samples were acidified to preserve cations. Arsenic species were separated on site by passing filtrate through SAX cartridges (Le *et al.* 2000).

Solid and solution samples were analyzed using a combination of induced neutron activation analysis, infrared spectroscopy and inductively coupled plasma, optical emission and mass spectroscopy. Phases controlling water composition were assessed with the geochemical program WATEQ4F (Ball & Nordstrom 1991). Piezometers were installed into the NATA to determine static water table elevations and hydraulic conductivity of the tailings. The hydrology of the site was modelled using the Ogata-Banks analytical solution to assess transport of As. Local water flow directions were approximated using water table data from piezometers in the watershed.

Shoots and roots of the common cattail (*Typha latifolia*) and water sedge (*Carex aquatilis*) were collected and analyzed to examine the passage of arsenic into the plants.

Polished thin sections were made in the absence of water to prevent dissolution of soluble phases. Mineral composition was determined using a combination of X-ray diffraction, electron microprobe analysis, and scanning electron microscopy with

energy dispersive X-ray spectrometry.

## **RESULTS**

### **Hydrology**

The NATA site consists of tailings overlying relatively low permeability clay soil, gravel-sand, and bedrock units. There are two aquifers: one is confined between the bedrock and clay, and another unconfined aquifer which developed within the NATA tailings. Vertical exchange between aquifers is limited due to the clay separation. This is demonstrated by the higher piezometric levels of the unconfined aquifer compared to the confined one.

The surface of the ARS drains NW, however, the base of the ARS dips south (Fig. 2). The ARS is underlain by red-brown clayey soil, which overlies a sand-gravel aquifer.

The water table in the ARS is elevated compared with the aquifer hydraulic heads. This would promote the transport of As from the ARS into the aquifer by advection. Given the higher concentration of As in the ARS compared to the aquifer, As transport could also occur by diffusion through the clayey soil.

Surface and groundwater flow within the Canada Creek watershed is SE from the high level of the mill and ARS to the low lying NATA then north through the wetlands (Fig 3). This path is based on local topography, core log data, and hydraulic head values for the confined aquifer. Hydraulic heads show groundwater in the Canada Creek watershed flowing in the general direction as surface water.

### **Solid phase Geochemistry**

The Nor Acme tailings are composed of 97% quartz and 3% sulfides, which contain <1.5 wt. % As. The clay horizon, 3m below the NATA contains <0.005 ppm As, while the sediments isolated from the aquifer at MW17 have 0.2 ppm As.

### **Aqueous Geochemistry**

The NATA groundwater has a neutral pH, but the surface water varies from 3 to 8. Arsenic concentration at MW17 appears

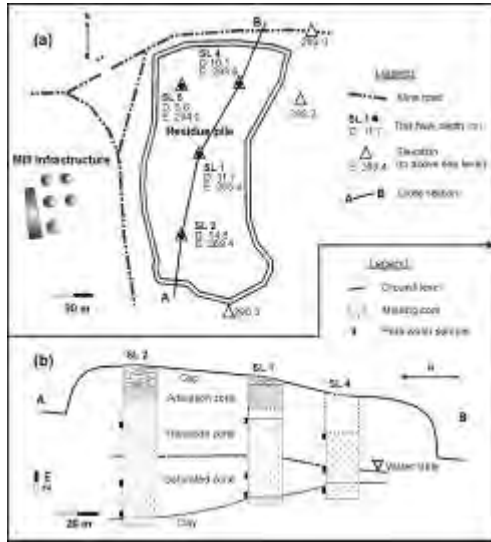


**Fig. 2.** (a) Elevation and location of drill holes in the ARS (b) Cross section of the ARS from S (drill hole SL2) to N (SL4)

to have decreased from 2004 to 2006 (Fig. 4). New Britannia Mines' (NBM) values are consistently <10 mg/L lower than those reported by Salzsauler *et al.* (2005) and Simpson (2007). This may be related to different sampling methods or variation in data incorporated in averages presented per year. Arsenite (As(III)) is the predominant species in groundwater at MW17.

Concentrations of As in surface water range from 1mg/L at the NATA to 11 mg/L in the ARS surface runoff area (RA). Overall, As concentration in the wetlands decreases from the NATA towards Snow Lake (Fig. 3). The lake water contains <0.005 mg/L As, which is well below the Canadian Drinking Water Standards of 0.010 mg/L, however up to 0.016 mg/L was measured at the water-sediment interface.

**Wetland Accumulators**

Concentrations of As are significantly greater in roots of cattails (<1200 mg/L dry weight (dw)) and sedges (<3000 mg/L dw) than in shoots, probably due to adhering soils and sediments, which contain <6800 mg/L As. Both cattails and sedge plants contain significant As in live (<138 mg/L) and dead (<235 mg/L) shoots.

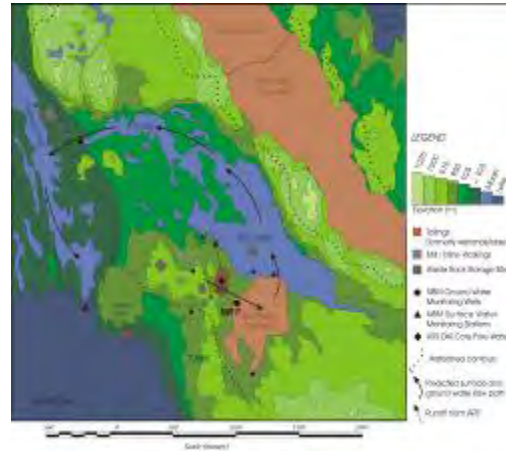


**Fig. 3.** Topographic map of mine site showing the drainage path.

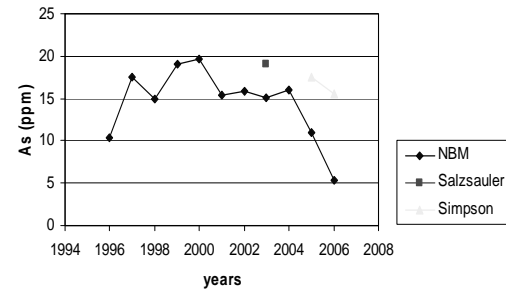


**Fig. 4.** Graph showing total concentrations of As in the groundwater at MW17. Data points represent annual averages.

**DISCUSSION**

The source of As in the ARS and NATA is arsenopyrite, a phase that is stable in low Eh, high pH conditions of unoxidized residue. Oxidation would have been initiated during deposition of the residue and would have progressed in the ARS during the 50 years of exposure. During this time, As rich runoff would have flowed into the runoff area (RA) where As was concentrated by plant material.

With the emplacement of the cover, the atmospheric oxygen that fuelled the precipitation of secondary As phases was essentially eliminated. Secondary phases such as jarosite, scorodite and amorphous iron sulfo-arsenates became unstable in the present conditions in the ARS (Salzsauler *et al.* 2005). Reductive dissolution of the secondary phases and residual arsenopyrite gives rise to 100 mg/L As in pore water at the base of the residue pile (Salzsauler *et al.* 2005).

Arsenic leaches from the base of the ARS, transports through the underlying clayey soil, and into the underlying aquifer producing the high concentration in MW17.

From MW17, the ground water flows initially SE beneath the NATA but due to rock outcrops veers N to combine with surface water in the RA. The sediment in this area has been contaminated with As from the surficial runoff from the ARS as well as earlier mining operations. The As in the surface water is then attenuated by ferric (Fe(III)) oxyhydroxides (HFO) so that by the time it reaches Snow Lake level of As are significantly reduced to <0.005 mg/L.

Aquatic plants can sequester As from soils, sediments and directly from water. Temperature, pH, redox potential and nutrient availability affect this sequestration (Robinson *et al.* 2006), but aquatic plants can control the local conditions. Arsenic is adsorbed to the surface of plant roots via physiochemical reactions. A positive correlation between As and Fe concentrations is consistent with As being incorporated into HFO on the surface of plants. Plant roots at NBM generally have >1000 mg/kg dw As. Plant roots contain 4-5 orders of magnitude more As than surface water or sediments at the same location.

Although the sequestration by plants immobilizes As, it may also facilitate its entry into the food chain and provide an exposure pathway to animals.

## CONCLUSIONS

Covering the ARS at Snow Lake prevented further oxidation and resulting As-rich surface runoff into the environment. However, secondary As

phases are now soluble in the reduced environment of the ARS, resulting in 100 mg/L As in pore water at its base and subsequent transport of dissolved As species into the ground water at MW17. The Nor Acme tailings do not significantly contribute to this contamination. Arsenic may have been mobilized from an earlier runoff from the ARS. Arsenic is absorbed by HFO in soils and plants prior to discharge to Snow Lake.

## ACKNOWLEDGEMENTS

This project was funded by the Manitoba Government through its Sustainable Development Innovation Fund as well as by an NSERC DG to BLS.

## REFERENCES

- BALL, J.W. & NORDSTROM, D.K. 1991. User's manual for WATEQ4f, with revised thermodynamic data base and test cases for calculating speciation of major, trace, and redox elements in natural waters. *US Geological Survey Open-File Report 91-183*.
- LE, X.C, YALCIN, S., & MA, M. 2000. Speciation of sub microgram per liter levels of As in water: On-site species separation integrated with sample collection. *Environmental Science and Technology*, **34**, 2342-2347.
- RICHARDSON, D. & OSTRY, G. 1996. Gold deposits of Manitoba. Manitoba Energy and Mines, Geological Services. *Economic Geology Report ER86 – 1* (2nd edition), 114 p.
- SALZSAULER, K. A., SHERRIFF, B.L., & SIDENKO, N.V. 2005. As mobility in alteration products of sulfide-rich, arsenopyrite-bearing mine wastes, Snow Lake, Manitoba, Canada. *Applied Geochemistry*, **20**, 2303-2314.
- SIMPSON, S. 2007 *The Source, Attenuation and Potential Mobility of As at New Britannia Gold Mine, Snow Lake, Manitoba*. M.Sc Thesis, University of Manitoba.

## Geochemistry and mineralogy of ochre precipitates formed as waste products of passive mine water treatment

Teresa M. Valente<sup>1</sup>, Marcel D. Antunes,  
Maria Amália S. Braga, & Jorge M. Pamplona

<sup>1</sup>CIG-R - Centro de Investigação Geológica, Ordenamento e Valorização de Recursos, Universidade do Minho, Campus de Gualtar, 4710-057, Braga PORTUGAL (email: [teresav@dct.uminho.pt](mailto:teresav@dct.uminho.pt))

**ABSTRACT:** Passive systems with constructed wetlands are designed to simulate natural attenuation processes in order to treat mine water in a long-term and cost-effective manner. In this way, they are especially appropriate to treat mine water discharging from abandoned mines. This paper presents geochemical and mineralogical data obtained from a recently constructed passive system (from Jales abandoned mine, North Portugal). It shows the role of fresh ochre-precipitates, formed as waste products from the neutralization process, in the retention of trace elements. Chemical analysis revealed strong enrichment factors for metals and arsenic, relative to the water from which they precipitate. The mineralogical study shows that ochre-precipitates are poorly ordered iron-rich material, such as ferrihydrites, that occur as small spherical aggregates that are less than 0,1  $\mu\text{m}$  in diameter. Firing experiments on these precipitates gave rise to hematite and to a crystalline arsenate. This provides evidence for the scavenging of arsenic by means of a precursor arsenic-rich amorphous compound. The results revealed that ochre-precipitates are wastes of environmental concern, which should be taken into account when considering the possibilities for reuse or disposal.

**KEYWORDS:** ochre-precipitates, mine water, metals, arsenic, concentration factors.

### INTRODUCTION

The best compromise between regulatory compliance and costs of mine water treatment has being, world-wide, the use of passive systems such as limestone channels and wetlands. There are numerous bibliographic references highlighting the advantages of these approaches (e.g., Skousen *et al.* 1998; Younger *et al.* 2002). Among the advantages, low cost and infrequent maintenance are crucial issues in the cases of abandoned mines. In these passive systems, the production of sludge, although in lesser amounts than in active systems, where chemicals are constantly added, is a major problem.

Sludge formed during initial steps of the treatment process (passive oxidation and neutralization) may affect the overall performance of the plant, especially when they are leached through the biological cells. Therefore, their disposal, or their recovery, as they may have economic value (Hedin 2003), is an issue of concern in the management of the treatment plant.

This paper presents data from a passive system implemented to treat the mine water from the abandoned mining site of Jales, in North Portugal. The layout of the plant comprises initial oxidation and neutralization in a limestone channel. The present work is focused on the resulting products that are generically named ochre-precipitates.

The geochemical and mineralogical properties of the ochre-precipitates are provided in order to demonstrate their ability to concentrate arsenic and metals from the mine water. Additionally, data may support management decisions, regarding disposal or recovery of the wastes, taking into account of their environmental behaviour.

### SITE DESCRIPTION

Jales mine is located near Vila Pouca de Aguiar, North Portugal (Fig.1). It has been exploited since Roman times, in a relatively sulfide-rich deposit. In modern times it was mined for gold and silver between 1933 and 1992.

The mine water to be treated flows from an old adit into the nearby watercourse (Peliteira Creek). Water properties are rather variable, dependent on seasonal variations (Loureiro 2007). Nevertheless, it can be generically described as an acid (pH<4), sulfate and metal-rich solution, especially in iron, arsenic, zinc and manganese.

Figure 1 represents the layout of the treatment plant, which had a start up in 2006. It includes two wetlands, planted with *typha*, and an initial inorganic stage with a reception basin (of which the bottom is filled with limestone), a cascade aeration facility and a limestone channel.

### SAMPLING AND ANALYTICAL METHODS

The ochre precipitates were taken at the end of the limestone channel (Fig. 1). In order to represent diverse seasonal conditions, samples were collected in three sampling campaigns, between 2007 and 2008. At each time, a water sample was collected at the same site.

The samples were air-dried at room temperature, sieved to < 63 µm and analysed by x-ray diffraction (XRD) and scanning electron microscopy combined with an energy dispersive system (SEM-EDS). For chemical analysis, samples were submitted to an extraction with Aqua Regia and analysed by inductively coupled plasma-optical emission spectrometry (ICP/OES). Firing experiments were performed following the procedure described by Brindley & Brown (1980).

Water analysis parameters such as pH, electric conductivity, oxidation-reduction potential and temperature were measured in the field. Ionic chromatography, turbidimetry and ICP-OES were used for anions and metals.

### RESULTS AND DISCUSSION

#### XRD Pattern and Morphology

Figure 2 presents the properties of the ochre-precipitates and the respective firing products, concerning crystallinity pattern, morphology and chemical composition by

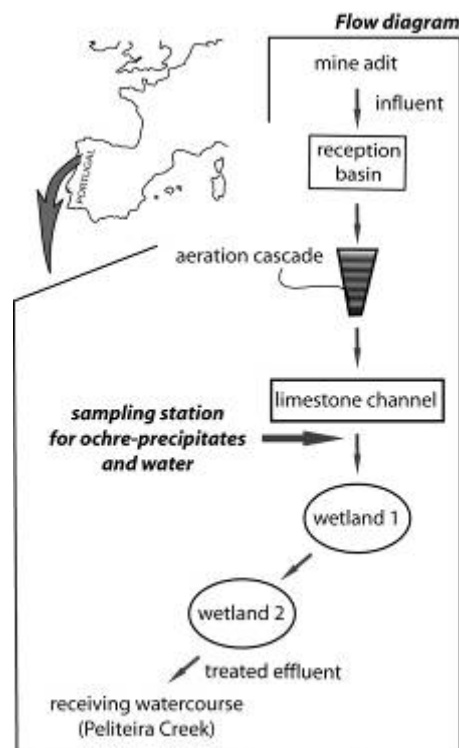


**Fig. 1.** Location and layout of the mine water treatment plant.

SEM-EDS. All the samples of fresh ochre-precipitates exhibit XRD patterns typical of poorly crystalline material, such as ferrihydrite (Schwertmann & Cornell 2000). They present the strongest band centred at 2.56Å, corresponding to the (110) reflection of 6-line ferrihydrite, as well as the characteristic poorly resolved reflections at *d* spacings 1.47 - 1.73 - 1.98 and 2.24Å.

Firing experiments induced thermal transformations on the ochre-precipitates. From these experiments, hematite and a well crystalline arsenate resulted. This indicates that arsenic may be scavenged by an arsenic-rich compound, freshly formed during the initial stages of the water treatment. This is in agreement with the results obtained by Jia & Demopoulos (2008), when performing aging tests on solids precipitated from As(V)-Fe(III) solutions.

SEM-EDS shows that ochre-precipitates are iron-rich particles, with other elements, such as As, Ca, Si and Cu (Fig. 2b). They

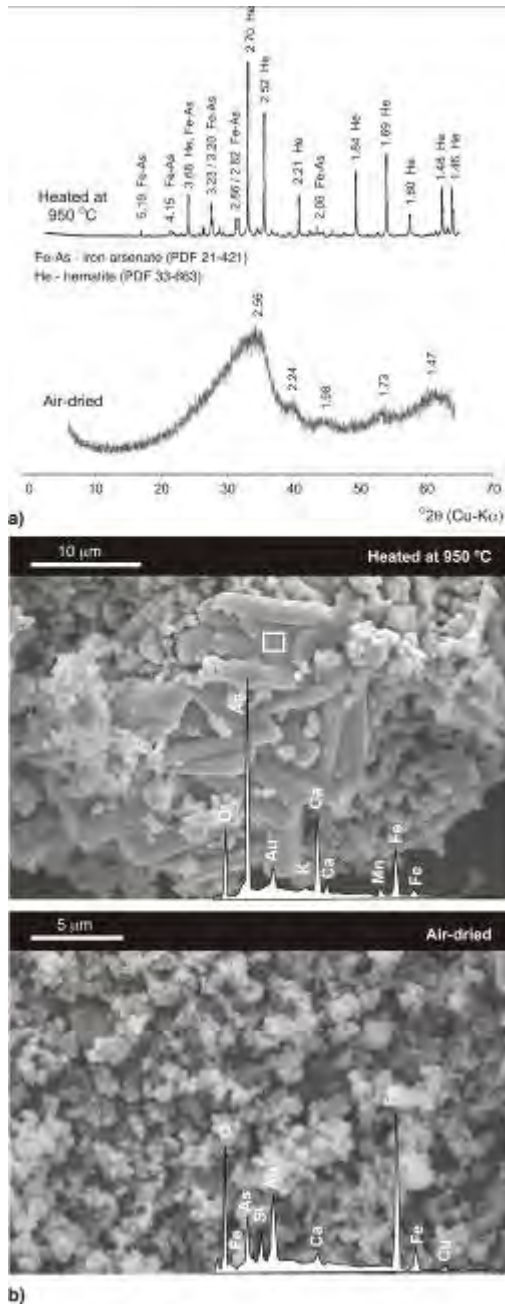


**Fig. 2.** Characteristics of the ochre-precipitates and thermal evolution. a) XRD patterns; b) SEM – SE images, showing the morphology of the aggregates and respective EDS spectra.

occur as aggregates of poorly developed spheres of less than 0.1 µm in diameter. After heating at 950°C, the material transforms to hematite (tabular and

prismatic crystals, often hexagonal dipramids) and an As-rich phase (elongated prismatic grains), that may be corresponding to the arsenic compound detected by XRD (Fig. 2a).

**Chemical Composition and Partitioning**

Chemical analysis shows that iron and arsenic are the major elements, with concentrations around 30% and 5% (average values), respectively.

Combined results on ochre-precipitates and water from which they precipitate indicate strong enrichment regarding several relevant metals (Fig. 3). The concentration factor was estimated using the formulation by Munk *et al.* (2002), which calculates the ratio between the concentration of the elements in the solid and the concentration in the water.

The partitioning of trace elements between the precipitates and the associated water suggests the following trend of affinities for some significant toxic elements: Pb>Cu>As>Cd>Zn>Ni>Mn.

Although there are no universal rules for metal selectivity as it depends on numerous factors, the obtained sequence is in agreement with the results reported in literature for the *Kd* sorption values on fresh precipitates of hydrous ferric oxide (Dzombak & Morel 1990; Munk *et al.* 2002). The lowest factor observed for Mn comes in agreement with the well-known difficulty to remove this metal from mine waters due to its high solubility over a wide pH range (*e.g.*, Hedin *et al.* 1994).

**CONCLUSIONS**

This study, focused on ochre-precipitates from a passive system, can be summarized in the following items:

- (1) the waste-products are iron-rich aggregates that denominated ochre-precipitates;
- (2) the ochre-precipitates are poorly crystalline materials, with XRD patterns typical of ferrihydrite;
- (3) firing experiments confirm this mineralogical precursor, promoting its evolution to hematite;
- (4) Upon heating initial phases transform to hematite and to a well-crystalline

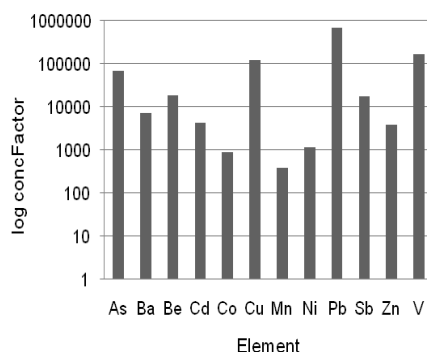


**Fig. 3.** Affinities of metals for ochre-precipitates, estimated by the relation between concentration in the solid and in the water.

arsenate, suggesting that arsenic is retained in the water treatment plant as an amorphous ancestor, co-precipitated with the iron oxy-hydroxide;

(5) the hazardous potential of ochre-precipitates is highlighted by the high enrichment in metals, and especially in arsenic (5%);

(6) Metal contents, as well as the influence of the firing products (thermal behaviour) on the industrial re-use are worthy of further research, as these are environmentally and economically relevant issues.

#### ACKNOWLEDGEMENTS

We thank to EDM (Empresa de Desenvolvimento Mineiro, S.A) for providing access to the water treatment plant. We are also grateful to Lucia Guise and A. Azevedo for assistance with chemical analysis and XRD analysis.

Authors would like to thank Dr Dogan Paktunc for the valuable comments and suggestions.

#### References

- BRINDLEY, G. & BROWN, G. 1980. Crystal structures of clay minerals and their X - ray identification. *London: Mineralogical Society.*
- DZOMBAK, A. & MOREL, M. 1990. *Surface complexation modeling: hydrous ferric oxide.* Wiley-Interscience, New York.
- HEDIN, R. 2003. Recovery of marketable iron oxide from mine drainage in the USA. *Land Contamination & Reclamation*, **11**, 93-97.
- HEDIN, S.; WATZLAF, G., & NARIN, R. 1994. Passive treatment of acid mine drainage with limestone. *Journal of Environmental Quality*, **23**, 1338-1345.
- JIA, Y. & DEMOPOULOS, G. 2008. Coprecipitation of arsenate with iron(III) in aqueous sulfate media: Effect of time, lime as base and co-ions on arsenic retention. *Water Research*, **42**, 661-668.
- LOUREIRO, C. 2007. *Sítios mineiros abandonados – monitorização de efluentes e acompanhamento de uma obra de reabilitação.* BSc Thesis, Universidade do Minho, Braga.
- MUNK, L.; FAURE, G.; PRIDE, D., & BIGHAM, J. 2002. Sorption of trace metals to an aluminum precipitate in a stream receiving acid rock-drainage; Snake River, Summit County, Colorado. *Applied Geochemistry*, **17**, 421-430.
- SCHWERTMANN, U. & CORNELL, R. 2000. *Iron oxides in the laboratory – preparation and characterization.* Wiley-VCH, Weinheim.
- SKOUSEN, J.; ROSE, A.; GEIDEL, G.; FOREMAN, J.; EVANS, R., & HELLER, W. 1998. A handbook of technologies for avoidance and remediation of acid mine drainage. *Natl. Mine Land Reclamation Center*, Morgantown, WV.
- YOUNGER, P.; BANWART, S., & HEDIN, R. 2002. *Mine Water: Hydrology, Pollution, Remediation.* Springer.

## Instability of AMD samples and evolution of ochre-precipitates in laboratory conditions

Teresa M. Valente<sup>1</sup> Lúcia M. Guise, & Carlos A. Leal Gomes

<sup>1</sup>CIG-R - Centro de Investigação Geológica, Ordenamento e Valorização de Recursos, Universidade do Minho, Campus de Gualtar, 4710-057, Braga PORTUGAL (email: teresav@dct.uminho.pt)

**ABSTRACT:** Acid mine drainage is a peculiar focus of environmental impact, due to a combination of the presence of many pollutants and their reactivity. These aspects demand special attention for an accurate characterization of AMD samples in field and in laboratory. The samples are unstable due to the presence of colloidal material such as iron-oxyhydroxides. They induce physical and chemical transformations, even during the transport to the laboratory, which may affect the analytical results. Variations in pH were recorded within the first several hours following their collection as an indicator of the changes in their evolution. The present work presents evidences of the instability of AMD samples, through the results of monitoring experiments performed in different laboratory conditions. Expedient indicators, like pH and electrical conductivity, combined with the analysis of crystallinity, composition and morphology of the resulting precipitates, allow monitoring of the evolution of the samples. The results also provide information about the origin and transformations of the typical ochre-products that precipitate from AMD.

**KEYWORDS:** Acid mine drainage (AMD), chemical instability, ochre-precipitates, schwertmannite, goethite.

### INTRODUCTION

Effluents emerging from sulfide-rich waste-dumps have special characteristics, such as very low pH (< 4), high metal solubility and presence of iron colloids, which provokes water turbidity and precipitation of ochre-products. These effluents are generically named acid mine drainage (AMD), since they result, primarily, from mineral-water interactions involving some sulfide minerals that typically produce acidity upon oxidative dissolution.

AMD are often very heterogeneous and reactive systems. Therefore, to describe their properties is often an issue of analytical concern as it is difficult to obtain representative samples of the affected watercourses. The instability of AMD is related to the formation and transformations of ochre-products, such as jarosite, schwertmannite and goethite (Bigham *et al.* 1996). Mineralogical transformations involving these ochre-precipitates have been the subject of intensive research (Kawano & Tomita 2001; Kim *et al.* 2002; Knorr & Blodau

2006). However, geochemical controls as well as contribution of microorganisms to their evolution still need to be investigated.

This work provides information about the instability of AMD and of AMD-precipitates obtained in a set of experiments carried out with natural and synthetic samples, in different laboratory conditions.

### AMD AT VALDARCAS MINING SITE

The samples are from the abandoned mine of Valdarcas, Northern Portugal (Fig. 1). This mine was exploited for tungsten in a skarn ore deposit rich in sulfides, mainly pyrrhotite, pyrite and minor chalcopyrite and sphalerite. AMD emerges at the base of the enriched-sulfide waste-dumps. It is naturally drained into a small permanent stream (Poço Negro Creek), and, then discharged in the Coura River. Table I presents the pH range at different sites along the system, obtained by monthly monitoring over a two-year period. A complete characterization of the samples is provided by Valente & Leal Gomes (2008).

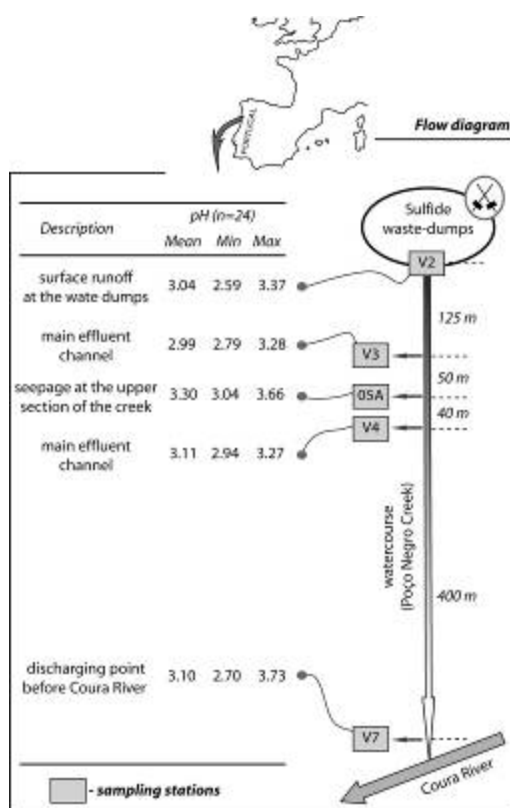


Fig. 1. Location of Valdearcas mine in Northern Portugal and sampling stations for AMD.

## METHODS

### Water Sampling

In order to represent the heterogeneity of AMD, sampling stations included acidic seepages and surface runoff at the waste-dumps, as well as points along the main effluent channel (Poço Negro creek) (Fig. 1).

## EXPERIMENTS

The following experiments were performed: (1) – monitoring of pH of natural AMD, with and without refrigeration, during the first week after collection; (2) – monitoring of water parameters and of the resulted precipitate, for the most instable samples (pH 3.1), over a period of 8 months, with refrigeration (T = 4 °C); (3) - monitoring of water parameters and of the resulted precipitate, at 30°C, in three distinctive reactors: Reactor A – using the same AMD sample as in the experiment (2); Reactor B – using a synthetic AMD solution (prepared accordingly with

Kawano & Tomita 2001); Reactor C – using the synthetic solution, but inoculated with two small fragments of natural schwertmannite (0.05 g).

The pH, EC and Fe<sup>3+</sup> were used as control parameters. The first two were measured with an Orion probe combined pH/ATC electrode Triode and a conductivity cell DuraProbe ref. 0133030. Fe<sup>3+</sup> was determined by molecular absorption (thiocyanate method). Mineralogical composition of the precipitates was determined by X-ray powder diffraction (XRD). Scanning electron microscopy, combined with an energy dispersive system (SEM-EDS), allowed the observation of morphological and compositional aspects of the precipitates.

## RESULTS AND DISCUSSION

Fig. 2 represents the variation of pH in refrigeration conditions (4°C) and at 20°C (average regional temperature). The samples had initial pH in the range 2.7-3.2. For both situations, the samples reported a decrease in pH. Nevertheless, pH was more stable with refrigeration, except for samples with initial pH between 3.0 and 3.1. In fact these were the more unstable samples in both conditions.

This is in agreement with the observations of Valente & Leal Gomes (2008), regarding the precipitation of AMD-precipitates in the Poço Negro creek. They verified that neutralization around pH 3.1 favours the precipitation of schwertmannite, which is also in accordance with the paragenetic relations proposed by Bigham *et al.* (1996) for jarosite, schwertmannite and goethite in AMD systems. For these reasons, samples with pH 3.1 were selected to evaluate their behaviour in a long term base, and especially to monitoring the precipitation of ochre-products. In that context, Fig. 3 shows the pH variations in the experiment performed with refrigeration along 8 months.

This temperature (4 °C) was intended to analyse the transformations in unfavourable kinetic conditions. It is also an adverse temperature to biologic

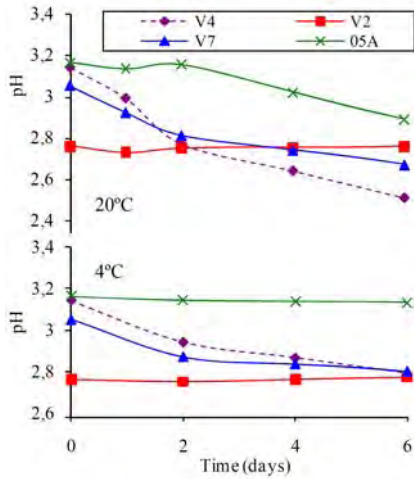


**Fig. 2.** Variation of pH in natural AMD samples.

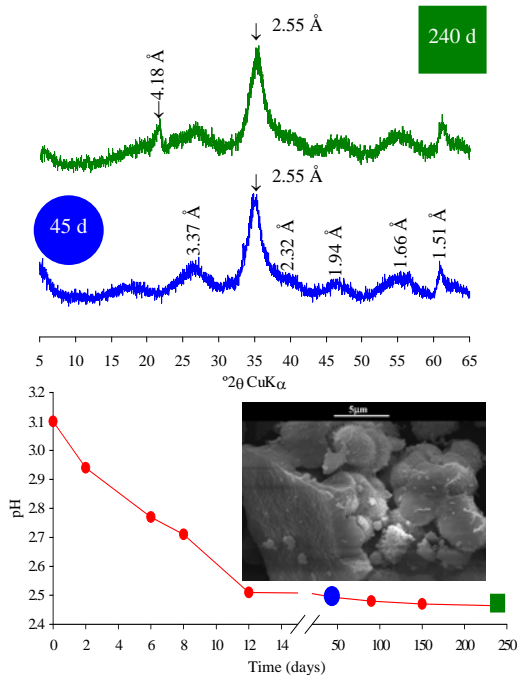
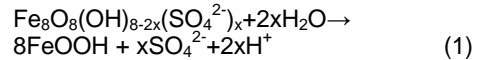


**Fig. 3.** Evolution of AMD at 4°C (sample collected at V4). The moments of withdrawal of precipitate are marked and the respective XRD patterns are presented. SEM-ES image corresponds to the precipitate at 45 days.

reactions that could be inducing precipitation of ochre-precipitates. However, even in these circumstances, pH decreased continuously until the end of the experiment. Such decline was especially sudden during the first 12 days, and can be related to the oxidation of

ferrous iron and subsequent hydrolysis and precipitation of ferric iron. The formation of an ochre deposit on the walls of the reactor was visible during the first week.

After 45 days of experiment, the precipitate showed an XRD pattern typical of a poorly ordered mineral, such as schwertmannite. Identification of this AMD mineral was confirmed by its distinctive spike morphology, observed by SEM-SE (Fig. 3). After 240 days, XRD detected the resolved reflection at *d* spacing of 4.18 Å, which is characteristic of goethite. Therefore, the maintenance of the precipitate in contact with the solution enabled its evolution to a more crystalline state. The trend of decrease in pH that is observed by the end of the experiment reflects the production of acidity, associated with the transformation of schwertmannite into goethite as it was observed by Bigham *et al.* (1996) (eq. 1).



It is expected that schwertmannite would be stable at this low temperature (Kumpulainen *et al.* 2008). Furthermore, Jonsson *et al.* (2005) referred to periods of time of > 514 or even several years to promote transformation at pH 3.0. This experiment confirms that mineralogical evolution may be highly variable in AMD systems and still requires further research.

The effect of temperature and of eventual biological contributions was investigated in the experiment. Observations during the experiment as well as the analysis of the Fig. 4 can be summarized as follows:

- the reactors A and C display similar behavior for pH, EC and  $\text{Fe}^{3+}$ , although initially lagged in time;
- $\text{Fe}^{3+}$  increases initially rapidly, followed by pH decrease, indicating oxidation and hydrolysis of iron;
- After 45 days, XRD indicated the formation of schwertmannite in reactors A and C. There were no significant chemical changes in the reactor B.

These experiments suggest that the addition of schwertmannite to the

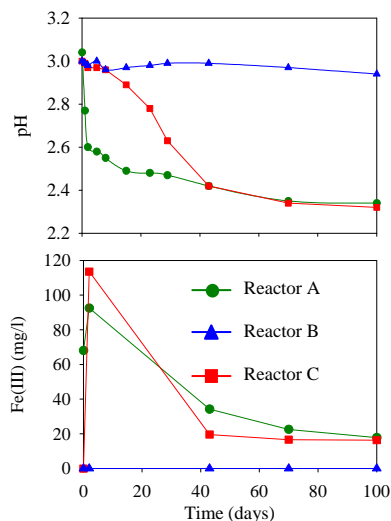


**Fig. 4.** Variation of pH and ferric iron for the experiment at 30°C.

synthetic system promotes oxidation and hydrolysis of iron, which were not detected in the non-inoculated system (reactor B). This can be a strictly inorganic effect, providing nuclei for precipitation, or may be representing an inoculum of acidophilic microorganisms that contribute to the observed changes.

### CONCLUSIONS

The work can be summarized as follows:

- (1) Monitoring of the solution as well as of the ochre-precipitates confirm the instability of AMD from Valdarca;
- (2) Higher instability was detected for samples with pH around 3.0-3.1;
- (3) Ochre-products precipitate from the solution even when samples are preserved at  $T < 4^{\circ}\text{C}$ ;
- (4) Ochre-precipitates displayed the typical XRD patterns of schwertmannite 45 days after collection;
- (5) With time, schwertmannite progressed to a more crystalline mineral (low crystalline goethite), even under unfavourable kinetic conditions ( $T < 4^{\circ}\text{C}$ );
- (6) Addition of natural schwertmannite to a synthetic AMD solution induced similar changes to that observed in the natural

AMD;

(7) These results should be taken into account in the laboratory and field routines for characterizing AMD samples; for instance they demonstrate the need to filtrate samples in the field, since refrigeration does not necessarily preserve this kind of water samples during transport to the lab.

### ACKNOWLEDGEMENT

Authors would like to thank Dr Dogan Paktunc for the valuable comments and suggestions.

### REFERENCES

- BIGHAM, J.; SCHWERTMANN, U.; TRAINA, S.; WINLAND, R., & WOLF, M. 1996. Schwertmannite and the chemical modeling of iron in acid sulfate waters. *Geochimica et Cosmochimica Acta*, **60**, 2111-2121.
- JONSSON, J.; PERSSON, P., SJOBERG, S., & LOVGREN, L. 2005. Schwertmannite precipitated from acid mine drainage: phase transformation, sulphate release and surface properties. *Applied Geochemistry*, **20**, 179-191.
- KAWANO, M. & TOMOTA, K. 2001. Geochemical modeling of bacterially induced mineralization of schwertmannite and jarosite in sulfuric acid spring water. *American Mineralogist*, **86**, 1156-1165.
- KIM, J.; KIM, S.; & TAZAKI, K. 2002. Mineralogical characterization of microbial ferrihydrite and schwertmannite and non-biogenic Al-sulfate precipitates from acid mine drainage in the Donghae mine area, Korea. *Environmental Geology*, **42**, 19-31.
- KNORR, K. & BLODAU, C. 2007. Controls on schwertmannite transformation rates and products. *Applied Geochemistry*, **22**, 2006-2015.
- KUMPULAINEN, S.; RAISANEN, M.-L.; VON DER KAMMER, F.; & HOFMANN, T. 2008. Ageing of synthetic and natural schwertmannite at pH 2-8. *Clay Minerals*, **43**, 437-448.
- VALENTE, T. & LEAL GOMES, C. 2009. Occurrence, properties and pollution potential of environmental minerals in acid mine drainage. *Science of the Total Environment*, **407**, 1135-1152.

## Arsenic mineralogy and potential for bioaccessibility in weathered gold mine tailings from Nova Scotia

Stephen R. Walker<sup>1</sup>, Michael B. Parsons<sup>2</sup>, & Heather E. Jamieson<sup>1</sup>

<sup>1</sup>Geological Sciences and Geological Engineering, Queen's University, Kingston, ON, K7L 3N6 CANADA  
(e-mail: jamieson@geol.queensu.ca)

<sup>2</sup>Natural Resources Canada, Geological Survey of Canada (Atlantic), Challenger Drive, Dartmouth, NS, B2Y 4A2  
CANADA

**ABSTRACT:** Detailed mineralogical characterization of arsenic (As) in near-surface samples of tailings and soil from four Nova Scotia gold mines has revealed a diversity and complexity in both the mineral species within a given sample, and the mineral form and texture at the grain and sub-grain scale. Samples range from arsenopyrite-rich mill concentrates (one of which has almost completely weathered to very fine grey-green aggregates of scorodite), to As-rich tailings containing from four to nine different amorphous to crystalline As host phases, including, but not limited to hydrous ferric arsenate (HFA), hydrous ferric oxyhydroxide (HFO), Ca-Fe arsenate and yukonite. The long-term stability and solubility of these As-bearing phases is critical for understanding the potential human health risk associated with exposure to As-rich mine waste. The variety of As weathering products can be explained by the processing and disposal history of tailings, and subsequent weathering conditions (i.e., carbonate-buffered pH neutral, post-neutral, and acidic). Secondary As forms are all micro- to nano-particulate or crystalline aggregate grains or grain coatings, suggesting that in addition to mineral solubility and grain-size, the grain texture (massive vs. grain coatings) and sub-grain porosity and permeability may control dissolution processes and rates.

**KEYWORDS:** arsenic, tailings, weathering, scorodite, yukonite

### INTRODUCTION

Mining of arsenopyrite-rich gold ores in Nova Scotia in the late 1800s and early 1900s has left a legacy of weathered, As-rich tailings deposits in more than 60 gold districts across the province. Many of these tailings areas are now located close to residential areas and are publicly accessible. The goal of this research was to examine the As mineralogy in a range of near-surface materials collected from several Nova Scotia gold mine sites frequented by the public, and to use the detailed mineralogical characterization to help explain the geochemical fate, mobility and bioaccessibility of As in weathered mine wastes.

Fourteen near-surface tailings samples and one soil from several former gold mines were sieved to <150 µm and mineralogically characterized using conventional techniques (XRD, microscopy and EPMA) and synchrotron micro-analysis (µ-X-ray diffraction, µ-X-ray

fluorescence and µ-X-ray absorption spectroscopy).

### GEOLOGY, PROCESSING, AND SOURCE OF ARSENIC

The Meguma Terrane that covers most of the southern mainland of Nova Scotia (Fig.1) consists of a wedge of folded, greenschist to amphibolite grade, Cambro-Ordovician age, meta-greywacke to slate and meta-siltstone rocks of the Goldenville and Halifax groups (Ryan & Smith 1998). Most of the gold production was from bedding-concordant auriferous quartz veins in the interstratified slate and meta-siltstone sequences.

Tailings were generally deposited close to the mills in low-lying areas and along creeks. Prolonged breaks in production, erosion and reprocessing of tailings have significantly complicated weathering patterns within tailings areas. Changes in ore character and milling processes (especially concentration) over time led to

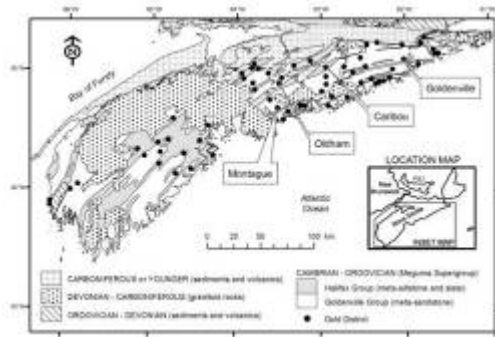


**Fig. 1.** Generalized geological map of southern Nova Scotia showing the location of historical gold districts within rocks of the Meguma Supergroup (after Ryan & Smith 1998; bedrock geology simplified from Keppie (2000)).

heterogeneity in the distribution of arsenopyrite and other sulfides in the tailings. Tailings for the present study were collected from the Goldenville (GD), Caribou (CAR), Montague (MG) and Oldham (OLD) gold districts (Fig. 1).

#### SAMPLING AND ANALYTICAL METHODS

All tailings samples except two were visibly oxidized and were selected based on distinct visual characteristics thought to be indicative of different mineralogy. Of the two unoxidized samples, one was distinctly arsenopyrite rich (CAR02) and another was from saturated tailings beneath a thin organic layer (MG04).

Analyses of major and trace elements were accomplished by digesting the samples using modified *aqua regia* and ICP-MS. Total C and organic C were measured using combustion analysis. Petrographic examination indicated that distinct Fe-As phases could be identified using colour (transmitted and reflected light), transparency, reflectivity, optical relief and texture but in most cases (due to fine-grain size, poor crystallinity or amorphous nature), they could not be uniquely identified by petrography alone. Synchrotron micro-probe and EPMA data when combined with the petrographic observations were able to unambiguously identify a range of As mineralogy in each section. Conventional X-ray powder diffraction analyses were carried out using

a Siemens D-500 X-ray diffractometer with a Co lamp (18 mA, 20 keV). Polished thin-section samples were characterized at Beamline X26A, National Synchrotron Light Source using methods similar to those described by Walker *et al.* (2005). Techniques included micro X-ray Fluorescence ( $\mu$ -XRF), transmission mode micro-X-ray Diffraction ( $\mu$ -XRD) and fluorescence mode micro-X-ray Absorption Near Edge Structure ( $\mu$ -XANES) at a beam spot size of < 10 $\mu$ m.

#### RESULTS AND DISCUSSION

The As content of the sieved (<150  $\mu$ m) tailings ranges from 0.07 wt. % As to over 30 wt. %. The Fe/As ratios of all tailings samples are low on a molar basis (range 1.3 to 5.3) and lower As content samples generally have higher Fe/As ratios (Table 1). These data are consistent with the arsenopyrite-rich source material in relatively Fe-poor gangue. The S/As ratio is usually significantly less than 1 (Table 1), which suggests the preferential leaching of S over As during oxidative weathering of these tailings samples.

Arsenic, Fe, S and Ca are indicative of the underlying geochemical conditions in the Nova Scotia tailings, because of the strong As source influence of arsenopyrite (with near stoichiometric equivalents of Fe, As and S) and the importance of carbonates as the main source of Ca in the tailings (Kontak & Smith 1988). The presence of excess carbonate leads to neutral drainage conditions, while its absence may lead to acid rock drainage in the tailings.

Micro-scale characterization ( $\mu$ -XRF,  $\mu$ -XANES,  $\mu$ -XRD, petrography, and EPMA) was able to confirm As forms identified by bulk XRD and in all cases identify additional As forms. Grain-scale mineralogical analysis unambiguously identified a minimum of two and typically four or more As-bearing phases in each tailings sample (Fig. 2, Table 2).

Micro-XRD confirms that secondary phases are generally aggregates of micro- or nano-scale crystallites, or in some cases amorphous or short-range ordered. Arsenic-mineral associations within

Table 1. Grain Size and Element Concentrations in Tailings and Soil Samples

Sample		% <150 µm	Element Concentrations (mg/kg)				Ratios (mol/mol)				Carbon (% dry wt.)		
ID	Type		As	Fe	S	Ca	Fe/As	S/As	Ca/As	Ca/S	Total	Organic	Inorganic
CAR01	tailings	18.3	76,500	75,200	1,900	<100	1.3	0.06	0.00	0.00	0.12	0.11	0.01
CAR02	mill concentrate	13.7	313,400	364,300	168,200	200	1.6	1.3	0.00	0.00	6.47 <sup>a</sup>	6.47 <sup>a</sup>	0
CAR03	tailings	12.1	21,300	31,900	1,100	700	2.0	0.12	0.06	0.51	0.19	0.13	0.06
CAR04	tailings	12.5	15,200	40,800	10,700	11,300	3.6	1.6	1.4	0.84	0.64	0.09	0.55
GD01	mill concentrate	30.4	210,300	200,400	34,200	<100	1.3	0.38	0.00	0.00	0.17	0.17	0
GD02	tailings	28.6	19,200	36,000	700	1,200	2.5	0.09	0.12	1.4	0.23	0.22	0.01
GD03	tailings	17.7	38,900	48,800	900	900	1.7	0.05	0.04	0.80	0.23	0.23	0
GD04	tailings	7.4	48,700	77,600	2,900	900	2.1	0.14	0.03	0.25	0.25	0.17	0.08
GD05	tailings	61.4	7,209	28,500	1,400	8,400	5.3	0.45	2.18	4.8	0.30	0.09	0.21
MG01	tailings	11.0	62,100	81,800	2,900	600	1.8	0.11	0.02	0.17	0.13	0.11	0.02
MG02	tailings	9.4	24,000	54,800	1,100	1,200	3.1	0.11	0.09	0.87	0.13	0.12	0.01
MG03	tailings	21.4	23,700	58,800	2,100	4,500	3.3	0.21	0.35	1.7	0.55	0.49	0.06
MG04	tailings	18.4	21,400	52,500	16,800	1,400	3.3	1.8	0.12	0.07	0.83	0.81	0.02
MG06 <sup>b</sup>	soil	16.0	318	59,200	1,100	200	250	8.1	1.18	0.15	4.93	3.11	1.82
OLD04	tailings	18.5	33,900	80,100	5,200	600	3.2	0.4	0.03	0.09	2.23	1.89	0.34

<sup>a</sup> Carbon analyses for CAR05-T02 may contain interference from high sulfide content of sample.

<sup>b</sup> B-horizon soil sample collected beneath an up-rooted tree over mineralized bedrock.

individual grains are often complex with up to three As forms associated within an individual grain (10 to 100 µm). The only macro-crystalline (e.g. > 2µm) As-bearing phases identified are the primary arsenopyrite and pyrite, although the spotty nature of diffraction from pharmacosiderite and jarosite suggests the presence of discrete crystallites (> 0.1 µm) for these phases.

**CONCLUSIONS**

Detailed mineralogical characterization of near-surface tailings and soil samples from As-rich Nova Scotia Au mine sites has revealed a diversity and complexity in both the mineral species within a given sample and the mineral form and texture at the grain scale. Gravity concentration of during milling seems to have been a major factor in determining the geochemical fate of As in the Nova Scotia tailings, by altering the ratio of carbonate to arsenopyrite in the tailings.

Secondary As forms are all micro- to nano-particulate aggregate grains or grain coatings. This suggests that in addition to mineral solubility and grain-size, the grain texture (massive or coatings) and sub-grain porosity and permeability may be important in controlling dissolution rates, especially for short reaction times (e.g. dissolution in gastro intestinal fluids by accidental ingestion of tailings). Results from this study are being used by the Province of Nova Scotia to help assess the potential health

risks associated with these high-As mine wastes.

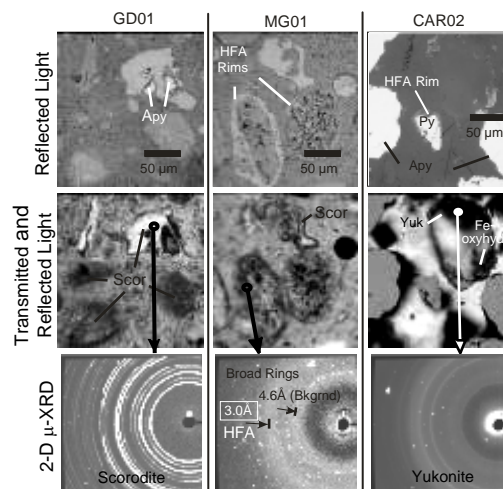


**Fig. 2.** A variety of As phases occur in weathered Nova Scotia gold mine tailings with mixtures of different forms varying from sample to sample. A combination of optical microscopy and µ-XRD allows definitive identification of a range of mineral forms and textures at the micron scale. These As-bearing mineral forms range from finely crystalline transparent to translucent aggregates of scorodite (Scor) (e.g., GD01 and MG01), to amorphous forms that sometimes coat or cement other grains (e.g. MG01 and CAR02). Note the broad diffraction ring at ca. 3 Å (MG01) indicative of amorphous hydrous ferric arsenate (HFA). Yukonite, a Ca-Fe arsenate, occurs most commonly in carbonate-rich samples. In CAR02, it is present in an arsenopyrite(Apy) rich mill concentrate along with other trace oxidized As forms.

Table 2. Mineralogy in Tailings and Soil Samples

Sample	Depth interval (cm)	Minerals		
		Major Gangue <sup>1</sup>	As-bearing Major <sup>2</sup>	As-bearing Minor to Trace <sup>2</sup>
CAR01	0 to 5	Qtz, Ms, Pl, Chl	<b>Scor, Kank</b>	HFA, HFO
CAR02	0 to 4	Qtz, Pl, Ms, Chl	<b>Apy, Py</b>	HFO, Yuk, HFO
CAR03	0 to 8	Qtz, Ms, Pl, Chl	HFA, HFO	Yuk, Gt, Lpc, Akg, Apy, Py
CAR04	0 to 4	Qtz, Ms, Pl, Chl, Ank	Apy, Py	Yuk, HFO
GD01	0 to 5	Ms, Qtz	<b>Scor</b>	Apy, Py
GD02	0 to 5	Qtz, Pl, Ms, Chl	<b>Scor, HFA</b>	HFO, Yk, Apy, Py, Jrs
GD03	0 to 5	Qtz, Ms, Pl, Chl	<b>Scor, HFA</b>	Kank, HFO, Apy, Py
GD04	0 to 5	Qtz, Ms, Pl, Chl	HFA	Gt, Lpc, HFO, Apy, Py
GD05	0 to 5	Qtz, Ms, Chl, Pl, Cal	Ca-FA, Yuk, Apy	Py, HFO
MG01	0 to 6	Qtz, Ms, Pl, Chl	<b>Scor, HFA</b>	Gt, Lpc, HFO, Apy, Py, Tooel
MG02	0 to 5	Qtz, Ms, Chl, Vrm, Pl	HFA	HFO, Apy, Scor, Py, Yk, Phar, Akg, Hm*
MG03	0 to 15	Qtz, Vrm, Ms, Chl, Pl	<b>Phar, Yuk</b>	HFA, Ca-FA, Gt, Lpc, HFO, Apy, Py
MG04	15 to 20	Qtz, Vrm, Ms, Chl, Pl	<b>Apy</b>	HFA, HFO, Py, Rgr
MG06	0 to 5	Qtz, Ms, Pl, Chl	HFO	Gt**
OLD04	0 to 5	Qtz, Ms, Pl, Chl	HFA, <b>Jrs</b>	Gt, HFO, Schw, Tooel

**Bold and Underlined** – indicates As-bearing phase that dominates the sample.

**Bold** indicates detected in bulk XRD.

Ank=ankerite, Cal=calcite, Chl=chlorite, Ms= muscovite, Pl=plagioclase, Qtz=quartz, Vrm=vermiculite

Akg=akaganeite, Apy=arsenopyrite, Ca-FA=amorphous Ca ferric arsenate, Gt=goethite, HFA=hydrous ferric arsenate, HFO=hydrous ferric oxyhydroxide, Hm=hematite,

Jrs=jarosite, Kank=kankite, Lpc=lepidocrocite, Phar=pharmacosiderite, Rgr=realgar,

Schw=schwertmannite, Tooel=tooeleite, Yuk=yukonite

<sup>1</sup> In decreasing order of abundance based on semi-quantitative fitting of XRD patterns.

<sup>2</sup> Estimated decreasing order of abundance.

\* Single more reflective Fe-oxyhydroxide identified appears to be mixture of nano-crystalline hematite and ferrihydrite with relatively low arsenic content (6.7% As<sub>2</sub>O<sub>3</sub>).

\*\* EPMA analysis for As in a single grain was just above detection (0.08%). As was confirmed by synchrotron  $\mu$ -XRF, but not quantified.

Note: Py was confirmed to contain trace As (<0.1%) in some cases, but was not systematically analysed in each sample where present.

## ACKNOWLEDGEMENTS

We are grateful to Paul Smith and Terry Goodwin from the Nova Scotia Dept. of Natural Resources for their capable

assistance during fieldwork for this project. We also thank Karina Lange and Lori Wrye for their assistance in conducting analysis at the synchrotron, and Tony Lanzirrotti at beamline X26A for his continued support and assistance. The authors gratefully acknowledge the support of the NSERC MITHE Strategic Network. A full list of sponsors is available at: [www.mithe-sn.org](http://www.mithe-sn.org). This study was also funded in part through the Environment and Health Program, Earth Sciences Sector, Natural Resources Canada.

## REFERENCES

- KEPPIE, J.D. (compiler) 2000. Geological Map of the Province of Nova Scotia. Nova Scotia Department of Natural Resources, *Map ME 2000-1*, Scale: 1:500 000.
- KONTAK, D.J. & SMITH, P.K. 1988. Meguma gold studies IV: Chemistry of vein mineralogy. In Mines and Minerals Branch Report of Activities 1987, Part B, Nova Scotia Department of Mines and Energy, *Report 88-1*, Halifax, Nova Scotia. 85-100.
- RYAN, R.J. & SMITH, P.K. 1998. A review of the mesothermal gold deposits of the Meguma Group, Nova Scotia, Canada. *Ore Geology Reviews*, **13**, 153-183.
- WALKER, S.R., JAMIESON, H.E., LANZIROTTI, A., ANDRADE, C.F., & HALL, G.E.M. 2005. The speciation of arsenic in iron oxides in mine wastes from the Giant gold mine, N.W.T. Application of synchrotron micro-XRD and micro-XANES at the grain scale. *Canadian Mineralogist*, **43**, 1205-1224.

**GEOCHEMICAL SURVEYS IN GOVERNMENT - NEW DEVELOPMENTS AND  
USES**

EDITED BY:

**PAUL MORRIS  
ERIC GRUNSKY  
CHARLES BUTT**



## Presentation of regional geochemical data via Internet Earth browsers

Stephen W. Adcock<sup>1</sup>, Wendy A. Spirito<sup>1</sup>, & Eric C. Grunsky<sup>1</sup>

<sup>1</sup>Geological Survey of Canada, 601 Booth Street, Ottawa, ON, K1A 0E8, CANADA  
(e-mail: adcock@nrcan.gc.ca)

**ABSTRACT:** The Geological Survey of Canada (GSC) has large amounts of regional geochemical data which are under-utilised both within and outside the organisation. The situation is being rectified by three overlapping activities: (1) cataloguing of the data holdings, to international metadata standards; (2) downloading of the data in a standardised spreadsheet format; (3) simple visualisation of the analytical data using Internet Earth browsers. Regional geochemical surveys have undergone a continuous evolution in sampling and analytical procedures. The resultant multitude of sample media and analytical methods poses several data management challenges, which are being mitigated by developing XML-based data transformation procedures. The GSC geochemical data management system has provisions for detailed metadata describing every aspect of a sample's history. In order to avoid inappropriate merging of disparate data, the analytical data are separated into many distinct datasets. The recent emergence of free, XML-based Earth browser software makes it much easier to visualise and compare the different datasets, without resorting to sophisticated GIS software.

**KEYWORDS:** regional geochemistry, geochemical mapping, web mapping, Canada, New Brunswick

### INTRODUCTION

Many government geoscience organisations have accumulated large quantities of regional geochemical data over the past half-century. Systematic management of the data has posed many problems, due primarily to the continuous evolution in sampling and analytical procedures. Regional geochemical data are typically presented in a spreadsheet format, with each row representing an analysed sample, and each column representing an analytical measurement. This approach works well for individual surveys, but becomes unmanageable for a large collection of disparate surveys. Hence, most organisations have opted to store the data in relational database management systems, and to "normalise" the data to varying degrees. Whilst this makes centralised management of the data much easier, it puts a major obstacle in the way of end-users easily accessing the data.

In the past, accessing these data has usually involved the creation of complex, specialised computer programs, either in-house or via external contracts. Both

approaches are expensive and hard to sustain. The recent emergence of XML-based technologies, coupled with the decreasing costs of computers makes it possible to create much simpler data extraction and manipulation procedures.

This paper outlines one approach that is being developed at the Geological Survey of Canada (GSC), where data are extracted from the database and re-cast as KML files that can be displayed in Google Earth or any other KML-aware application. Examples are presented for a recently-completed compilation of till geochemical data from New Brunswick (Adcock *et al.* 2009).

### MANAGEMENT AND PUBLICATION OF REGIONAL GEOCHEMICAL DATA AT THE GSC

Geochemical surveys at the GSC are generally conceived and executed as individual entities, optimised for the local geography and for the scientific objectives of the funding project. The only major exception to this approach is the National Geochemical Reconnaissance (NGR) program, which has been collecting and

analysing lake and stream sediment samples across Canada since the early 1970s according to a well-defined protocol (Friske & Hornbrook 1991).

Individual surveys are usually published as GSC Open Files, which can be downloaded over the Internet at no cost. Most Open Files include maps of the analytical data, and raw data in the form of a spreadsheet. The maps are typically presented using proportional dot symbology (Bjorklund & Gustavsson 1987), but other approaches, such as contouring, are sometimes used.

The exact format of each Open File is left to the discretion of the authors. This has resulted in a tremendous variability in content and format over the years, which in turn makes it frustrating and time-consuming for end-users to incorporate the data into their own projects. [For a comprehensive listing of GSC geochemical Open Files, see [http://gdr.nrcan.gc.ca/geochem/metadata\\_pub\\_gsc\\_e.php](http://gdr.nrcan.gc.ca/geochem/metadata_pub_gsc_e.php)] Even within the GSC, it is hard to get an accurate idea of what data are available. A further complication arises from the close working relationships between GSC scientists and their colleagues in Provincial agencies (projects are co-managed, samples are shared, publications emanate from different organisations).

The unsatisfactory nature of the current situation has been recognised for many years, but efforts to rectify it have encountered many technical challenges which could not be overcome with the available personnel and financial resources. Recent advances in computing hardware and software have led to new approaches and the development of cost-effective solutions.

A long-term project commenced in 2004 to catalogue GSC and Provincial geochemical surveys. The catalogue conforms to 'Federal Geographic Data Committee' metadata standards (FGDC, 1998) and is publicly accessible over the Internet (Spirito & Adcock 2009). Attention is now focussing on managing the analytical data. Several demonstration projects have been completed as a test of

the data management system, most notably two collections of till geochemistry (Adcock 2009a; Adcock *et al.* 2009).

### **DEVELOPMENT OF A STANDARDISED DATA MODEL FOR REGIONAL GEOCHEMICAL SURVEYS**

Any generalised approach to managing regional geochemical data must be built on top of a well-designed data model. If the model is well-designed, it should be able to adapt easily to ongoing changes in how geochemical surveys are carried out. Poorly constructed models will be harder to adapt, and will become steadily more difficult to maintain. Prior to the late 1980s, geochemical data modelling at the GSC was not consciously undertaken. The emergence of desktop relational database software in the late 1980s led to a serious effort to construct data models, based on methodologies designed specifically for use with relational database software (Halpin 1995). The current data model (Adcock 2009b) has been used successfully in a variety of projects. The most complex of these projects involved the compilation of till geochemical data from across New Brunswick (grouped into 39 surveys, collected and analysed between 1985 and 2006). The final database contains data for 13846 samples, collected from 11841 distinct sites. The database, in MS Access 2003 format, is available as a DVD (or free download) from the GSC or NBDNR (Adcock *et al.* 2009).

The data model is highly normalised, which suits data integrity and manipulation via the SQL language, but creates difficulties for the end-user in terms of accessing the data. Straightforward queries may involve numerous tables which have to be joined together. As a practical work-around, the database includes several very large denormalized tables.

### **XML-BASED TECHNOLOGIES**

Extensible Markup Language (XML), in its various forms, is rapidly emerging as the dominant data format across all computer

systems. Coupled with Unicode (UTF-8), it promises to greatly reduce the problems of interoperability between operating systems and software packages. XHTML is being adopted by all large organisations as the preferred “dialect” of HTML, for use on web sites (W3C 2006). Office productivity software developers are switching to XML as the default file format for word processing and spreadsheets (ISO, 2006; ISO, 2008). KML is becoming a very popular XML syntax for geographic data, partly because of the popularity of Google Maps and Google Earth, but also because it is a relatively easy file format for programmers to work with (in contrast to the SHAPE file format, for example (ESRI 1998)). KML was recently endorsed by the Open Geospatial Consortium as a recognised standard for geographic data visualisation (OGC 2008).

The different dialects of XML (XHTML, KML) are constrained by XML schemas (W3C, 2004). These schemas are critical to the success of XML. They are used to ensure that an XML file adheres to a well-defined structure. Schemas are themselves XML files, which must conform to the XSD specification. Schema designers are free to develop constraints to varying degrees. Forcing an XML file to be compatible with a tightly-constrained schema frees developers from having to write their own data validation procedures. This leads to a great simplification of data manipulation software.

XML files can be manipulated programmatically by a number of different techniques. One of the most powerful and elegant techniques involves yet another XML-based technology – the XSLT programming language (W3C 2007). An XSLT program is itself an XML file. XSLT was designed for the express purpose of transforming XML files into alternative formats. The language includes many constructs to allow efficient restructuring of the data. This leads to programs which are much smaller and easier to write than equivalent programs in more generic languages.

XSD and XSLT working together provide a very powerful technique to take

output from one software package and transform it through intermediate formats, each of which is constrained by its own XSD schema, into a format suitable for end-user display.

### XML TRANSFORMATION IN PRACTICE

All modern relational databases include the ability to export tables as XML files. It is usually possible to apply an XSLT transformation to the data as part of the export procedure. In the interest of simplicity and compatibility across different databases, no special transformation was applied to the tables extracted from the New Brunswick till database. Therefore, after exporting data out of MS Access in a generic XML format, the first XSLT transformation involves restructuring the data to conform to a “Geochemical Survey” XML schema, developed at the GSC (Adcock 2009b). The second transformation produces a set of files which conform to the GML schema (OGC, 2007). KML shares many features with GML, and hence the third and final GML-to-KML transformation is very simple.

Separating the data transformation into three distinct steps enforces a completely modular software design. In practice, the data transformation is executed via command shell scripts, using freely available software for both the XSLT transformation and XSD validation. The raw data contained in the 39 surveys in the New Brunswick compilation are exported into 7,000 individual KML files, which can be viewed online at <http://gdr.nrcan.gc.ca/geochem>.

### REFERENCES

- ADCOCK, S.W. 2009a. The Canadian Database of Geochemical Surveys: Analytical data for till surveys carried out across Canada by GSC staff. *Geological Survey of Canada Open File 5935*, 1 DVD.
- ADCOCK, S.W. 2009b. The Canadian Database of Geochemical Surveys: Technical documentation for the data model. *Geological Survey of Canada Open File 5938*, 1 CD-ROM.
- ADCOCK, S.W., ALLARD, S., PARKHILL, M.A., PRONK, A.G., & SEAMAN, A.A. 2009. The

- Canadian Database of Geochemical Surveys: Analytical data for till surveys carried out in New Brunswick by NBDNR and GSC staff, 1985-2006. *Geological Survey of Canada Open File 5937*, 1 DVD.
- BJORKLUND, A. & GUSTAVSSON, N. 1987. Visualization of geochemical data on maps: New options. *Journal of Geochemical Exploration*, **29**, 89-103.
- ESRI 1998. ESRI Shapefile Technical Description. An ESRI White Paper—July 1998. *Environmental Systems Research Institute, Redlands, California*.
- FGDC 1998. FGDC-STD-001-1998. Content standard for digital geospatial metadata (revised June 1998). *Federal Geographic Data Committee. Washington, D.C.*
- FRISKE, P.W.B. & HORN BROOK, E.H.W. 1991. Canada's National Geochemical Reconnaissance Programme. *Transactions of the Institution of Mining and Metallurgy, Section B*, **100**, 47-56.
- HALPIN, T. 1995. *Conceptual Schema and Relational Database Design*. 2nd edition. Prentice Hall, 547p.
- ISO 2006. ISO/IEC 26300:2006 Information technology -- Open Document Format for Office Applications (OpenDocument) v1.0
- ISO 2008. ISO/IEC 29500-1:2008 Information technology -- Document description and processing languages -- Office Open XML File Formats -- Part 1: Fundamentals and Markup Language Reference
- OGC 2007. OGC 07-036 : OpenGIS Geography Markup Language (GML) Encoding Standard. Version: 3.2.1. Open Geospatial Consortium Inc.
- OGC 2008 OGC 07-147r2: OGC KML Version: 2.2.0. Open Geospatial Consortium Inc.
- SPIRITO, W.A. & ADCOCK, S.W. 2009. The Canadian Database of Geochemical Surveys: Metadata for 600 geochemical surveys across Canada. Geological Survey of Canada Open File 5934, 1 CD-ROM.
- W3C 2004. XML Schema Part 0: Primer Second Edition W3C Recommendation 28 October 2004
- W3C 2006. XHTML 2.0 W3C Working Draft, 26 July, 2006.
- W3C 2007. XSL Transformations (XSLT) Version 2.0 W3C Recommendation 23 January 2007

## The National Geochemical Survey of Australia: 2009 update on progress

Patrice de Caritat<sup>1</sup>, Michelle Cooper<sup>1</sup> & Paul Morris<sup>2</sup>

<sup>1</sup>Geoscience Australia, GPO Box 378, Canberra, ACT 2601 AUSTRALIA (email: Patrice.deCaritat@ga.gov.au)

<sup>2</sup>Geological Survey of Western Australia, Mineral House, 100 Plain Street, East Perth, WA 6004 AUSTRALIA

**ABSTRACT:** Building on method developments achieved during a series of precursor pilot projects, the National Geochemical Survey of Australia (NGSA) project targets catchment outlet (overbank) sediments as a uniform sampling medium. These transported, fine-grained materials are collected (from a shallow and a deeper level) near the lowest point of 1390 catchments, which cover 91% of Australia. Dry and moist Munsell® colour, soil pH and electrical conductivity and pH of 1:5 (soil:water) slurries are recorded and laser particle size analysis and infrared spectroscopy analysis are determined on bulk splits. The dried samples are sieved into two grain-size fractions (<2 mm and <75 µm) that are analysed by x-ray fluorescence (XRF) and inductively-coupled mass spectrometry (ICP-MS) (multi-element, total analyses), by ICP-MS after aqua regia digestion (multi-element, including low level gold), and specialised methods for platinum group elements, fluorine and selenium. At the time of writing, 78% of the samples have been collected and most analyses are completed for the first 25% of samples. The project is due for completion in June 2011.

**KEYWORDS:** *geochemical mapping, overbank sediment, mineral exploration, energy*

### INTRODUCTION

The National Geochemical Survey of Australia (NGSA) project was initiated in late 2006 as part of the Federal Government's Energy Security Initiative (Johnson 2006). It aims to provide pre-competitive data and knowledge to support exploration for energy resources in Australia. In particular, it will improve the existing knowledge of the concentrations and distributions of energy-related elements such as uranium (U) and thorium (Th) at the national scale.

The project is underpinned by a series of pilot surveys recently carried out by Geoscience Australia and the Cooperative Research Centre for Landscape Environments and Mineral Exploration (CRC-LEME) to test robust and cost-effective protocols for sample collection, preparation and analysis. Examples of these are the Riverina (Caritat *et al.* 2005 2007), Gawler (Caritat *et al.* 2008a) and Thomson (Caritat & Lech 2007; Lech & Caritat 2007) projects. Selected results from these geochemical surveys have been presented by Caritat *et al.* (2008b).

The current national project, described below, is being conducted in collaboration

with the State and the Northern Territory geoscience agencies.

### BACKGROUND

The nation-wide geochemical survey was initiated because there is no complete geochemical coverage available for Australia. Experience elsewhere shows that such a data layer is an important complement to other national-scale geological and geophysical datasets.

The current distribution of geochemical data available through the national repository (OZCHEM database) is shown in Figure 1. The map shows that there are vast areas of the country (>60%) that lack any geochemical information. Also, where geochemical data are available, they are often not comparable as a result of incompatible sampling media, inconsistent sample preparation and analysis methods, incomplete quality assessment metadata and/or different analyte suites being reported.

Similarly, the current airborne gamma-ray spectrometric (radiometric) survey coverage available at a resolution deemed appropriate for exploration does not provide a complete national picture of the

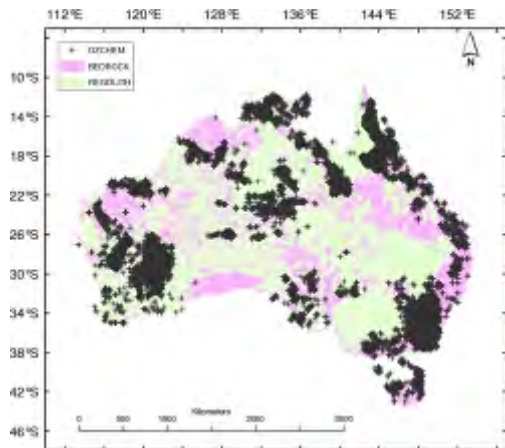


**Fig. 1.** Distribution of whole rock geochemical data in Australia (plus signs) extracted from the OZCHEM national database as at June 2006, overlain on bedrock (pink) and regolith (green) coverages.

distribution of radiogenic elements potassium (K), uranium (U) or thorium (Th). This situation is being remedied by the new airborne geophysics project, which, together with the NGSA, will result in a significantly improved understanding of the distribution of K, U and Th in Australia.

Some regional geochemical surveys have been carried out in parts of Australia, but no national coverage exists. Since the inception of the concept of regional geochemical surveys in the 1960s, they have proven to be a reliable tool for mineral exploration.

## OBJECTIVES

The objectives of the NGSA project are to:

- Collect catchment outlet (overbank) sediment samples from ~1400 large catchments covering >90% of Australia using an ultra low sampling density approach to keep costs down;
- Prepare and analyse the samples to extract the maximum amount of geochemical information (60+ elements) using internally consistent, state-of-the-art techniques;
- Populate the national geochemical database with the resulting new data;
- Compile an atlas of geochemical maps for use by the mineral exploration industry to identify areas

of interest in terms of energy-related resources and other mineral commodities, which can then be the focus of targeted exploration efforts.

## STRATEGY

### Sampling Media

Catchment outlet sediments (similar to floodplain sediments in most cases) are sampled at two depths (0-10 cm below the surface as well as a 10 cm interval at a depth of between around 60 and 90 cm).

### Sampling Sites

1390 catchments covering 91% (or about seven million km<sup>2</sup>) of Australia across all States and Territories have been targeted for sampling. Catchments are sampled as close as possible to their lowest point (usually their outlet). Small coastal catchments and small islands are not included in the survey. The resulting distribution of sites targeted for sampling is shown in Figure 2 and translates to an average sampling density of around 1 site/5500 km<sup>2</sup>.

### Sample Collection

A detailed Field Manual was compiled (Lech *et al.* 2007) and all sampling equipment and consumables were centrally purchased to ensure a standard approach. Sample collection is being undertaken by all State and Northern Territory geoscience agencies following a hands-on, in-field training period. At each locality, a detailed site description, field pH, dry and moist soil Munsell® colours and GPS coordinates are recorded and several digital photographs are taken. All information is recorded digitally to facilitate subsequent uploading into databases.

### Sample Preparation

Samples are dried, split and sieved to <2 mm and <75 µm fractions. The <2 mm fractions is mechanically ground for some analyses, while the finer fraction is not. A bulk split of each dried sample is archived for future investigations.

### Sample Analysis

Bulk parameters routinely recorded at



**Fig. 2.** Distribution of target sampling sites for the National Geochemical Survey of Australia.

Geoscience Australia are pH and electrical conductivity of 1:5 (soil:water) slurries, and laser particle size distribution. Sample analysis has started for 60+ elements using mainly XRF and collision cell ICP-MS at Geoscience Australia. Special analyses not available at Geoscience Australia (e.g., low-level gold and multi-element analysis after aqua regia digestion, fluorine, selenium, platinum group elements, infrared spectroscopy) are obtained externally.

#### **Quality Assessment/Quality Control**

Sample numbers have been randomised to minimise regional bias, help separate false from true anomalies and obtain meaningful estimates of the variance of duplicates. Field duplicates, analytical duplicates, in-house standards and certified reference materials are introduced at regular intervals in the analytical streams.

#### **Data Analysis**

Graphical and statistical data analysis will be carried out at various scales (regional, States/Northern Territory, and National). Non-parametric univariate and multivariate analysis along with the production of geochemical maps will be carried out.

#### **Timeline**

Following planning in the first half of 2007, fieldwork, including initial training, began in mid-2007 and is expected to continue until mid-2009 (allowing for the wet season prohibiting field work in northern

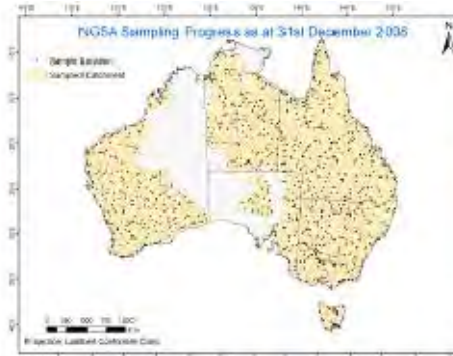


**Fig. 3.** Distribution of catchments sampled for the National Geochemical Survey of Australia, as at 31 December 2008 (1078 catchments, or 78%, completed).

Australia for six months each year, and for time to obtain access permissions for some areas). Figure 3 shows the catchments sampled to 31 December 2008. Sample preparation started in early 2008 and will continue until late 2009. Sample analysis started mid-2008 and will continue until mid-2010. Data analysis and reporting are planned to take place in 2010 and early 2011. The project concludes on 30 June 2011.

#### **DATA DELIVERY**

By 2011, the NGSA project will deliver a National Geochemical Atlas of Australia, which will be available online. In addition, reports on the geochemistry of all States and the Northern Territory will be released, as will separate reports on energy related commodities, on implications for geothermal resources, on comparison with airborne radiometric surveys, and for regions that are the focus of other energy security projects. The national geochemical database OZCHEM will be populated with the new data.

The NGSA will lead to increased knowledge on the concentrations and distributions of geochemical elements in the near-surface environment at the national scale. Further, NGSA results should support increased exploration activity for energy related resources in Australia, particularly using national geochemical survey data to select specific areas for further exploration investment. Finally, it is hoped that the NGSA will be

one of several contributors to success in mineral exploration in Australia. Spin-off benefits in environmental management, land use policy development and geohealth assessment are also expected.

### CONCLUSIONS

A national-scale geochemical survey of Australia is under way. It applies ultra low sampling density to transported and well-mixed outlet sediments, which are expected to represent the average composition of large catchments. The NGSA will provide the first complete, internally consistent geochemical data layer for Australia and is expected to find applications in energy and mineral resources exploration.

### ACKNOWLEDGEMENTS

Funding for the Onshore Energy Security Program is provided by the Australian Government's Energy Security Initiative. We thank our colleagues at Geoscience Australia and within State and Northern Territory geoscience agencies for their collaboration in, and support for, the NGSA. David Champion and Colin Pain provided internal reviews. Published with permission from the CEO of Geoscience Australia.

### REFERENCES

CARITAT, P. de & LECH, M.E. 2007. Thomson Region Geochemical Survey, Northwestern New South Wales. *Cooperative Research Centre for Landscape Environments and Mineral Exploration Open File Report*, **145**, 1021p. + CD-ROM. [http://crcleme.org.au/Pubs/OFRSindex.html]

- CARITAT, P. de, LECH, M., JAIRETH, S., PYKE, J., & LAMBERT, I. 2005. Riverina geochemical survey – A National First. *AusGeo News*, **78**. [http://www.ga.gov.au/ausgeonews/ausgeonews200506/geochem.jsp]
- CARITAT, P. de, LECH, M.E., & KERNICH, A. 2008a. Gawler Region Geochemical Survey, South Australia. *Cooperative Research Centre for Landscape Environments and Mineral Exploration Open File Report*, **211**, 987 pp + CD-ROM. [http://crcleme.org.au/Pubs/OFRSindex.html]
- CARITAT, P. de, LECH, M.E., & MCPHERSON, A.A. 2008b. Geochemical mapping 'down under': selected results from pilot projects and strategy outline for the National Geochemical Survey of Australia. *Geochemistry: Exploration, Environment, Analysis*, **8**, 301-312.
- CARITAT, P. de, LECH, M.E., JAIRETH, S., PYKE, J., & FISHER, A. 2007. Riverina Region Geochemical Survey, Southern New South Wales and Northern Victoria. *Cooperative Research Centre for Landscape Environments and Mineral Exploration Open File Report*, **234**, 843p. + CD-ROM. [http://crcleme.org.au/Pubs/OFRSindex.html]
- JOHNSON, J. 2006. Onshore Energy Security Program underway. *AusGeo News*, **84**. [http://www.ga.gov.au/ausgeonews/ausgeonews200612/onshore.jsp]
- LECH, M. & CARITAT, P. de 2007. Regional geochemical study paves way for national survey – Geochemistry of near-surface regolith points to new resources. *AusGeo News*, **86**. [http://www.ga.gov.au/ausgeonews/ausgeonews200706/geochemical.jsp]
- LECH, M.E., CARITAT, P. de & MCPHERSON, A.A. 2007. National Geochemical Survey of Australia: Field Manual. *Geoscience Australia Record*, **2007/08**, 53p.

## Multi-element geochemical mapping in Southwest China

Zhizhong Cheng<sup>1</sup> & Xuejing Xie<sup>1</sup>

<sup>1</sup>Institute of Geophysical and Geochemical Exploration, Jinguang Road, Langfang, Hebei, 065000 CHINA  
(e-mail: zhizhong9@yahoo.com.cn)

**ABSTRACT:** Southwest China's geochemical mapping project to measure 76 elements was initiated in 2000. 2700 composite samples were analysed by ICP-MS, XRF and ICP-AES, along with other techniques where necessary. The resulting geochemical maps shows the distribution of majority of the elements in the periodic table.

**KEYWORDS:** 76 elements, geochemical mapping, analytical scheme,

### INTRODUCTION

In 1973, J.S. Webb (Webb *et al.* 1973, 1978) published the first geochemical atlas "Provisional Geochemical Atlas of Northern Ireland". From 1973 to now, more than 40 regional and national geochemical mapping projects have been carried out (Reedman 1973; Bowie & Plant 1978a,b; Bolivar 1980; Geological Survey of Canada 1981; Stephenson *et al.* 1982; Weaver *et al.* 1983; Fauth *et al.* 1985; Bolviken 1986; Koljonen *et al.* 1989; Simpson 1993; Varna *et al.* 1997; Laszlo *et al.* 1997; Reimann *et al.* 1998; Salminen 2005; De Vos & Tarvainen 2006).

China's national geochemical mapping project (Regional Geochemistry-National Reconnaissance (RGNR) Project) was initiated in 1978 (Xie 1977, 1978, 1989), involving analysis of 39 elements by a variety of methods. Environmental geochemical monitoring networks (EGMON) Project, (Xie & Cheng 1997) were established in 1993, in which 54 elements were analyzed. In 2000, a project to produce geochemical maps for 76 elements was carried in Southwest China (Xie *et al.* 2008).

### SAMPLE TYPE AND COLLECTION

The RGNR project in Yunan, Guizhou Sichuan and Guangxi provinces were commenced in 1980, and finished in 1995. For the Southwest China regional geochemical mapping program, about 100

RGNR samples from each 1:50000 map sheet were composited into a single sample. The resulting 2700 composite samples were subsequently analysed.

### MULTI-ELEMENT ANALYTICAL SCHEME

The 76 elements analyzed include 39 elements originally analyzed in the RGNR Projects, and 37 new elements. The analytical scheme is based largely on ICPMS, ICPAES and XRF, supplemented with other techniques (Table 1). The lower levels of detection of all elements are less than their crustal abundances (Table 2).

The log deviation are  $\log C \leq 0.1$ , standard deviation (SD) is between 5%~30%. (majority element's standard deviation less than 10%, only that of S and Os are less than 30%)

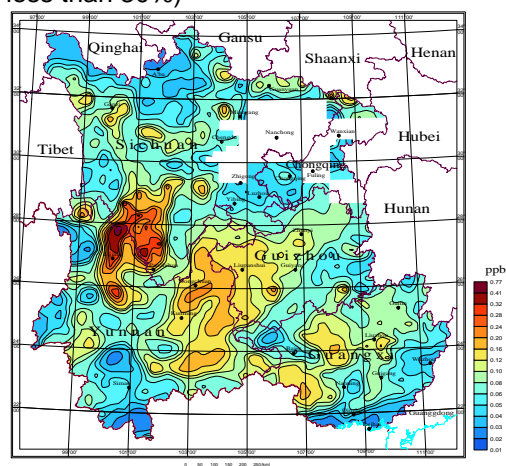


Fig.1. Geochemical map of osmium Os in southwest China.

**Table 1.** Analytical Scheme

Analytical method	Elements
XRF	Si, Al, Fe, Mg, Ca, Na, K, Ba, Ce, Co, Cr, Cu, Ga, La, Mn, Nb, Ni, P, Pb, Rb, S, Sc, Sr, Th, Ti, V, Y, Zn, Zr, Cl, Br
	Pr, Nd, Sm, Eu, Gd, Tb, Dy, Ho, Er, Tm, Yb, Lu
ICP-MS	Be, Bi, Ce, Co, Cs, Cu, Ga, In, La, Mo, Nb, Ni, Pb, Rb, Sb, Th, U, W, Y, Zn, Tl, Ta, Hf, Re Te
ICP-AES	Na, Mg, Al, K, Ca, Fe, Ba, Be, Co, Cr, Cu, Li, Mn, Ni, P, Sr, Ti, V, Zn
GF-AAS	Ag, Au
HG-AFS	As, Sb, Se, Ge
CV-AFS	Hg
SIE	F
ES	Ag, B, Sn,
VOL	C, N,
CF-COL	I
FA-POL	Ir,Rh
FA-ES	Pt, Pd
FA-COL	Os, Ru

**GEOCHEMICAL MAPS FOR 76 ELEMENTS**

All of the geochemical data are loaded into the GeoMDIS system, The data were gridded using the data-gridding function of GeoMDIS, and geochemical maps for each of the 76 elements were generated .

Fig.1 shows a large Os anomaly distributed over an area of approximately 60 000km<sup>2</sup> in north Yunnan and southwest Sichuan possibly indicating widespread platinum group element mineralization. The distribution of In (Fig. 2) shows three large and two small geochemical anomalies .A strong Hf anomaly delineated near Lincang in Yunnan province(Fig. 3), coincides with an extensive area of granitic rocks.

**CONCLUSIONS**

Using samples collected from a more detailed geochemical mapping exercise, the multi-element geochemical mapping exercise carried out in southwest China has indicated regional anomalies which may be related to economic areas of mineralization. Such regional programs illustrate the importance or low-density

**Table 2.** Required lower level of detection

element	D <sub>L</sub>	element	D <sub>L</sub>
Ag	0.02	Mo	0.2
Al <sub>2</sub> O <sub>3</sub>	0.05*	N	20
As	1	Na <sub>2</sub> O	0.1*
Au	0.2	Nb	2
B	2	Nd	0.1
Ba	5	Ni	1
Be	0.2	Os	0.02
Bi	0.05	P	10
Br	1	Pb	2
C	0.1*	Pd	0.2
CaO	0.05*	Pt	0.2
Cd	0.02	Pr	0.1
Ce	2	Rb	1
Cl	20	Re	0.2
Co	1	Rh	0.02
Cr	5	Ru	0.02
Cs	0.5	S	50
Cu	1	Sb	0.05
Dy	0.1	Sc	1
Er	0.1	Se	0.01
Eu	0.1	SiO <sub>2</sub>	0.1*
F	100	Sm	0.1
Fe <sub>2</sub> O <sub>3</sub>	0.05*	Sn	1
Ga	2	Sr	5
Gd	0.1	Ta	0.2
Ge	0.1	Tb	0.1
Hf	1	Te	5
Hg	0.5	Th	2
Ho	0.1	Ti	50
I	0.5	Tl	0.1
In	0.01	Tm	0.1
Ir	0.01	U	0.2
K <sub>2</sub> O	0.05*	V	5
La	1	W	0.3
Li	1	Y	1
Lu	0.1	Yb	0.1
MgO	0.05*	Zn	5
Mn	10	Zr	5

D<sub>L</sub> : detect limit , \* in % , Au, Hg, Ir, Os, Pd, Pt, Re, Rh, Ru in ppb , others in ppm

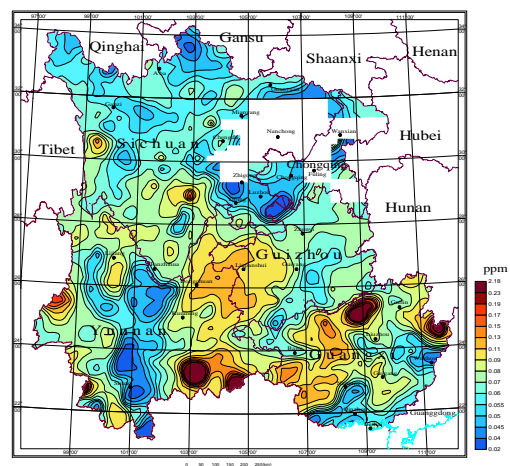


**Fig. 2.** Geochemical map of Indium (In) in southwest China.

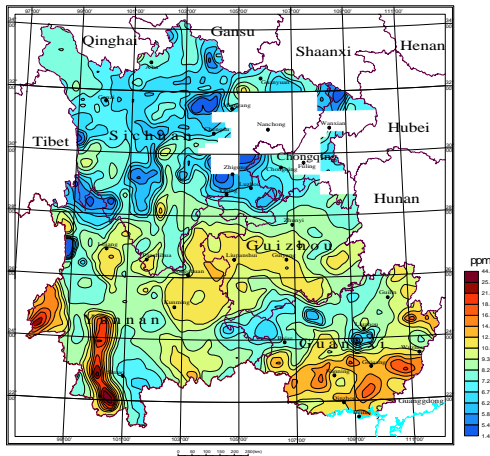


**Fig. 3.** Geochemical map of hafnium (Hf) in Southwest China.

geochemistry as an exploration tool. Furthermore, the analysis of a wide variety of elements to low levels means the data are also suited to environmental management as well as mineral exploration.

**REFERENCES**

BOLIVAR, S.L. 1980. An overview of the National Uranium Resource Evaluation Hydrogeochemical and Stream sediment Reconnaissance Program. Los Alamos Scientific Laboratory. LA-8457-MS, 24 p.

BOLVIKEN B., BERGSTORM, J., BJORKLUND, *et al.* 1986. Geochemical Atlas of Northern Fennoscandia, Scale 1:4 000 000, Mapped by Geological Surveys of Finland, Norway and Sweden with Swedish Geological Co. and the Geological Survey of Greenland. Nordic Council of Ministers.

BOWIE S.H.U. & PLANT, J. 1978a. Regional Geochemical Atlas, Shetland. *Institute of Geological Science, London.*

BOWIE S.H.U. & PLANT, J. 1978b. Regional Geochemical Atlas, Orkney. *Institute of Geological Science, London.*

DE VOS, W. & TARVAINEN, T. (chief editor), 2006. FOREGS Geochemical Atlas of Europe, Part : Interpretation of Geochemical Maps, Additional Tables, Figures, Maps and Related Publications. *ESPOO, Geology Survey of Finland.*

FAUTH, H., HINDEL, R., & SIEWERS, U. 1985. Geochemical Atlas of the Federal Republic of Germany. Federal Office for Geosciences and Raw Materials.

FRISKE, P.W.B. & HORN BROOK, E.H.W. 1991. Canada's National Geochemical Reconnaissance Programme. *Transaction of Institute of Mining and Metallurgy*, **100**, B47-B56.

GEOLOGICAL SURVEY OF CANADA, 1981. National Geochemical Reconnaissance, 1:2,000,000, Colored Compilation Map Series. *Geological Survey of Canada, Open File Report.*, 730-749.

KOLJONEN, T., GUSTAVSSON, N., & NORAS, P. *et al.* 1989. The Geochemical Atlas of Finland, Part 2: Till. *Espoo: Geological Survey of Finland.*

LASZLO, O., ISTVAN, H., & UBUL, F. 1997. Low density geochemical mapping in Hungaria. *Journal of Geochemical Exploration*, **60**, 55-66.

REEDMAN, A.J. 1973. *Geochemical Atlas of Uganda.* Geological Survey of Uganda, Entebbe, 42 p.

REIMANN, C., AYRAS, M., CHEKUSHIN, V., *et al.* 1998. Environmental Geochemical Atlas of the Central Barents Region. ISBN 82-7385-176-1. *NGU-GTK-CKE Special publication*, Geological Survey of Norway, Trondheim, Norway, 745 p.

SALMINEN. R. (chief editor) 2005. FOREGS Geochemical Atlas of Europe, Part : Background information, methodology, and maps. *ESPOO, Geology Survey of Finland.*

SIMPSON, PR. 1993. *Regional Geochemical Atlas, Southern Scotland.* Institute of Geological Sciences, Nottingham.

STEPHENSON, B., GHAZALI, S.A., & WIDJAJA, H. 1982. Regional Geochemical Atlas Series of Indonesia: Northern Sumatra. *Institute of Geological Sciences, Oxford.*

VARNA, K., RAPANT, S., MARSINA, K., *et al.* 1997. Geochemical atlas of Slovak Republic at scale of 1:1,000,000. *Journal of Geochemical Exploration*, **60**, 7-37.

WEAVER, T.A. *et al.* 1983. Geochemical Atlas of Alaska. *U. S. Dept. Energy, Report. GJBX-32* (83).

WEBB, J.S., 1978. *The Wolfson Geochemical Atlas of England and Wales.* Oxford: Oxford University Press.

WEBB, J. S., NICHOL, I., FOSTER, R., LOWENSTEIN, P.L., & HOWARTH, R.J. 1973. Provisional geochemical atlas of Northern Ireland. *AGRG Tech. Comm.* No.60.

XIE, X. 1977. Current problems in regional geochemistry. *Geophys. Geochem. Explor.*, **2**, 1-10 (In Chinese).

XIE, X. 1978. Regional geochemistry-retrospect, present status and prospect. *Ins. Geophys. Geochem. Explor., Res. Rep. No.* 3 (In Chinese).

- XIE, X. & CHENG, H.X. 2001. Global geochemical mapping and its implementation in the Asia-Pacific region. *Applied Geochemistry*, **16**, 1309-1321.
- XIE, X., CHENG, Z., ZHANG, L., FENG, J., YE, J., & ZHU, Y. 2008. *76 Geochemical Elements Atlas of Southwest China*. Geological Publishing House, Beijing, 219p. ( in Chinese).
- XIE, X., HUANZHEN, S, & TIANXIANG, R. 1989. Regional geochemistry -National Reconnaissance project in China. *Journal of Geochemical Exploration*, **33**, 1-9.

## Exploration geochemical surveys of the Taupo Volcanic Region, New Zealand

Anthony B. Christie<sup>1</sup> & Richard Carver<sup>2</sup>

<sup>1</sup>GNS Science, P O Box 30-368, Lower Hutt NEW ZEALAND (e-mail: t.christie@gns.cri.nz)

<sup>2</sup>GCXplore Pty Ltd, 67 Chelmsford Road, Mt Lawley, WA 6050 AUSTRALIA

**ABSTRACT:** Open file mining company exploration geochemical survey data in New Zealand are compiled in the REGCHEM (Regional Exploration Geochemistry) database managed by GNS Science (see <http://maps.gns.cri.nz/website/minmap>). Data for the Taupo Volcanic Region includes 1350 stream sediment (including 163 BLEG analyses), 960 pan concentrate, 2241 rock chip and 510 soil samples from 16 surveys completed between 1983 and 2007. The main exploration target was epithermal gold deposits hosted by volcanic rocks. The usefulness of the conventional stream sediment data is limited by the large number (>90%) of samples with Au and Ag values below the detection limit, and the narrow geographic coverage of the BLEG samples. Pan concentrate stream sediment and rock chip surveys have yielded the best results for reconnaissance exploration.

**KEYWORDS:** stream sediment, BLEG, rock chip, soil, geochemical survey, epithermal, gold, silver, Taupo Volcanic Region

### INTRODUCTION

In New Zealand, there have been no systematic stream sediment geochemical surveys by Government agencies and the only comprehensive data sets are from mining company surveys carried out during mineral exploration activities. These are reported to government as a condition of prospecting and exploration permits. Much of the publicly available archived data has been compiled in digital form in the REGCHEM (Regional Geochemistry) database (Warnes & Christie 1995) and is publicly accessible via the MinMap interface at <http://maps.gns.cri.nz/website/minmap/>. This study describes the REGCHEM data for the Taupo Volcanic Region (Fig. 1), an area highly prospective for epithermal Au-Ag deposits (Crown Minerals 2003).

### REGIONAL GEOLOGY AND MINERAL DEPOSITS

The Taupo Volcanic Region consists of the Taupo Volcanic Zone (TVZ) and large flanking areas of plateau-forming ignimbrite sheets that are up to several hundred metres thick (Fig. 1). The TVZ occupies a 250 km long, 30-50 km wide,

2-4 km deep volcano-tectonic depression striking northeast and filled with Quaternary volcanic rocks overlying a basement of Mesozoic greywacke. The volcanic rocks consist mostly of rhyolite, lesser andesite and dacite, and minor basalt, that form domes, cones, and vents with surrounding and intervening pyroclastic flows (ignimbrite) and airfall deposits, and volcanoclastic sediments. The andesite volcanoes of White Island, Ngauruhoe and Ruapehu are currently active, basalt was erupted at Tarawera in 1886, and the most recent plinian rhyolitic eruption (Taupo Pumice) was deposited in c. AD 233.

Early discoveries of gold in the region included alluvial gold in Onaia Stream, several gold-bearing quartz veins in basement greywacke west of Lake Taupo (e.g. December Reef and Hades Reef in Mangatu Stream), and gold-bearing quartz veins in volcanic rocks at Puhipuhi. Gold-silver mineralisation has also been reported in several of the active geothermal fields, including Kawerau, Waiotapu, Ohaaki and Rotokawa. Mineral exploration from the 1970s discovered several new epithermal Au-Ag prospects including Horohoro, Matahana, Thomsons,

Ohakuri, Wharepapa, Pukemoremore, Umukuri and Forest Road (Fig. 1). These were mostly found by mapping occurrences of hydrothermal breccias, sinters and hydrothermal alteration.

**EXPLORATION GEOCHEMICAL DATA**

Data have been compiled from 15 exploration campaigns between 1982 and 1988 (MR reports 628, 629, 630, 631, 632, 641, 647, 649, 654, 657, 665, 669, 682, 2270, 2532), and one in 2007 (MR report 4307). These included stream sediment, pan concentrate, rock chip and soil sample media (Table 1).

Most of the 1187 stream sediment samples were analysed for Au, Ag, As and Sb, but high detection limits (e.g.,

Au mostly 0.01, 0.02 and 0.05 ppm, but some 0.0002 and 0.002 ppm) result in most samples having concentrations of these elements below their detection limits (Table 1), thus limiting their usefulness.

The 510 soil samples were collected in four small grids over known gold prospects at Ohakuri, Wharepapa, Wharepapa NE and Pukemoremore North.

Weak gold anomalies and trends are present, typically associated with areas of hydrothermal breccias and alteration. Of the other elements analysed, As shows the best contrast with values ranging from 2-2800 ppm.

**Rock Chip Samples**

The 2241 rock chip samples were collected mainly from sinters, veins, hydrothermal breccias or altered rocks. Most were analysed for Au, Ag, As and Sb, and about half were analysed for Hg, Cu, Pb and Zn. About 25% of the Au and Ag assays are below their detection limits. The high values for Au and Ag are in the areas of known prospects (Fig. 2).

**BLEG Samples**

The 2007 survey collected 163 stream sediment samples and analysed them for Au using a bulk leach extractable gold (BLEG) cyanide digestion. The survey extended beyond the TVZ, north into the older Coromandel Volcanic Zone. Despite the low sample density, (1 sample per 9 km<sup>2</sup>), the data outline one anomalous

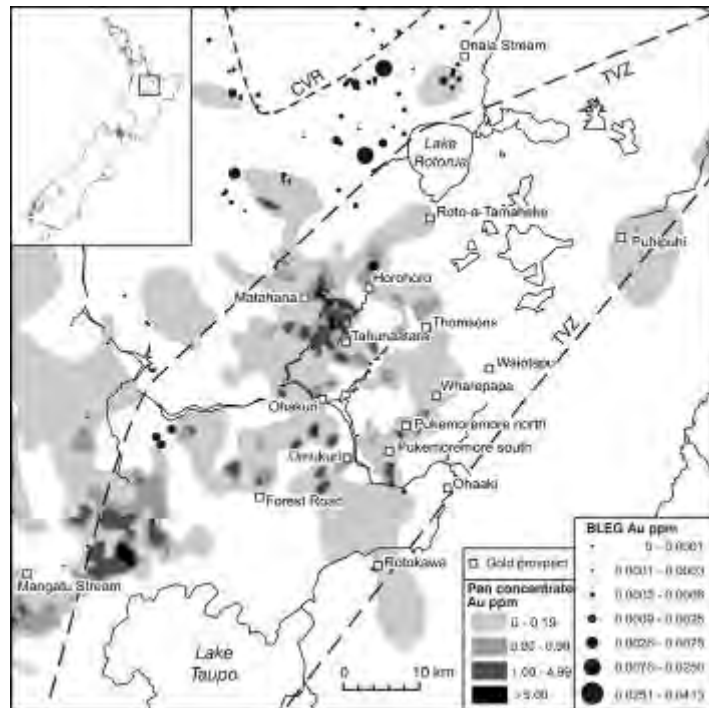


Fig. 1. Au concentrations in pan concentrate and BLEG stream sediment samples. (CVR = Coromandel Volcanic Region; TVZ = Taupo Volcanic Zone).

**Table 1.** Percentile statistics for exploration samples.

Element	n	P 25	P 50	P 75	P 97.5	BLD %
Stream sediment						
Ag ppm	1100	BLD	BLD	BLD	1.50	91
As ppm	947	BLD	BLD	BLD	22	79
Au ppm	924	BLD	BLD	BLD	0.05	94
Cu ppm	33	BLD	8	10	21	24
Pb ppm	101	BLD	BLD	BLD	10	94
Sb ppm	877	BLD	BLD	BLD	BLD	98
Zn ppm	19	30	40	60	80	0
BLEG						
Au ppb	163	0.10	0.20	0.50	1.70	7
Pan concentrate						
Ag ppm	950	BLD	BLD	0.27	5.00	61
Au ppm	960	BLD	0.03	0.74	20.50	46
Rock chips						
Ag ppm	2235	BLD	BLD	BLD	5.50	84
As ppm	2124	BLD	20	80	510	35
Au ppm	2241	BLD	BLD	BLD	0.38	75
Cu ppm	927	BLD	2	3	8	27
Hg ppm	1257	BLD	BLD	1	11	62
Pb ppm	963	BLD	5	9	29	36
Sb ppm	1908	BLD	BLD	3	48	69
Zn ppm	1003	4	12	25	63	18

n = number; BLD = below detection; BLD % = percent of samples below the detection limit  
BLEG = bulk leach extractable gold stream sediment

catchment (25-75 ppb Au), one probably anomalous catchment (8-25 ppb Au) and two other catchments of interest (2-8 ppb Au) (Fig. 1).

#### **Pan concentrates**

More than 900 pan concentrate samples were analysed for Au and Ag. About 50% of the assays are below the detection limits (Table 1). The contrast 97.5/50% ratio for Au is very high (500-683).

#### **DISCUSSION AND CONCLUSIONS**

The young volcanism of the TVZ creates several challenges for geochemical exploration. A thick mantle of young ash and pumice deposits over large areas limits the use of soil geochemical surveys. Exploration in the early 1980s recognised that conventional stream sediment surveys were not effective because target sediments were overwhelmingly diluted by young post-mineral pyroclastics and

volcaniclastics. BLEG and other proprietary stream sediment bulk sampling and analysis techniques appeared more effective, but most explorers concluded that pan concentrate sampling was the most effective reconnaissance geochemical exploration method. Large areas of the region are planted in exotic commercial forests, and clear felling forestry operations have added another complication with the extensive reworking of the erodible surface cover resulting in a very high proportion of young volcaniclastic material in active stream sediments.

Unsuccessful follow-up of some anomalies suggests that erosion and exposure of some deposits may have been temporary and they are now buried beneath younger volcanic rocks.

Work to date has highlighted the Matahana area and two main parallel NE trends of anomalies and prospects, inside

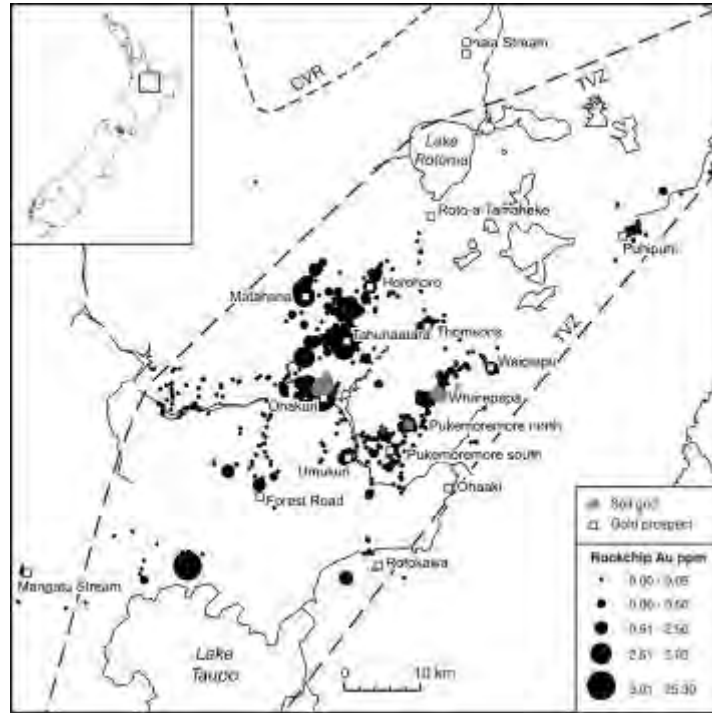


**Fig. 2.** Au concentration in rock chip samples and location of four soil sampling grids. (CVR = Coromandel Volcanic Region; TVZ = Taupo Volcanic Zone).

the margins of the TVZ (Fig. 2), along with several anomalies in other areas with no known cause.

**ACKNOWLEDGEMENTS**

Data were compiled as part of the GNS Science REGCHEM project, and by Crown Minerals (2003), utilising an earlier compilation by Delta Gold. Bob Brathwaite and Paul Morris are thanked for their reviews of the manuscript.

**REFERENCES**

CROWN MINERALS. 2003. Epithermal gold in

New Zealand: GIS data package and prospectivity modelling. Published jointly by Crown Minerals, Ministry of Economic Development and Institute of Geological & Nuclear Sciences.

MR REPORTS. Publicly available mining company exploration reports available from [https://data.crownminerals.govt.nz/MEDMG\\_UEST/system/mainframe.asp](https://data.crownminerals.govt.nz/MEDMG_UEST/system/mainframe.asp).

WARNES, P.N. & CHRISTIE, A.B. 1995. Regional stream sediment geochemistry database (REGCHEM) for selected regions of New Zealand. *The Australasian Institute of Mining and Metallurgy Publication Series*, **9/95**, 611-616.

## The effect of geology on lake geochemical trends in Sudbury, Ontario, viewed through Google Earth

Richard Dyer<sup>1</sup>

<sup>1</sup>Ontario Geological Survey, 933 Ramsey Lake Road, Sudbury, ON CANADA (e-mail: richard.dyer@ontario.ca)

**ABSTRACT:** The Ontario Geological Survey (OGS) lake geochemical sampling program was designed to obtain high quality natural geochemical signals from both greenfield and brownfield regions. An excellent example of this is in the Sudbury area where, despite significant mining activity and disturbance, OGS lake sediment sampling was successful in obtaining relatively uncontaminated deep sediments. The Sudbury area survey is one of many that the OGS has undertaken in the past 22 years. Recent development of 'OGS-Earth', a prototype add-on to Google Earth has allowed very fast and easy visual display of the entire (>60,000 samples) dataset at any scale and viewing angle. Google Earth allows the visualization of geological, topographic and cultural information with overlain geochemistry in virtual 3-D through all scales and view angles. Profound geochemical trends and relationships between geochemistry and geology can be immediately apparent. When viewed in Google Earth, the close association of the lake sediment geochemistry with mineralization and Sudbury Igneous Complex rocks is immediately apparent. Future geochemical data releases by the OGS will include Google Earth (kml) files to allow much easier and quicker viewing of geochemical data than has traditionally been the case.

**KEYWORDS:** *Lake Sediment, Geochemistry, Sudbury Igneous Complex, GIS, OGSEarth*

### INTRODUCTION

The high density (approximately 1 sample per 3 km<sup>2</sup>) lake sediment geochemical program at the Ontario Geological Survey takes advantage of the greater than 250,000 lakes covering almost 1/5<sup>th</sup> of Ontario's 1,000,000 km<sup>2</sup> surface area. The program mandate has always been twofold: 1) to support mineral exploration by sampling in areas of high mineral potential; 2) provide high quality baseline geochemical data of the Province., over 60,000 samples have now been collected across Ontario, covering an area of more than 200,000 km<sup>2</sup> (Fig. 1).

The OGS lake sediment is so large and at such high density that displaying significant portions of the data using conventional geographic information systems (GIS) is sometimes very slow – even with fast computers. To address this problem, the OGS has developed "OGS-Earth", an in-house add-on to Google Earth for the purpose of rapid integration of multiple geochemical datasets. Many of the Province-wide geological layers, including lake sediment data, are now

available on the Geology Ontario website for easy downloading and viewing in Google Earth ([http://www.mndm.gov.on.ca/mines/data/google/default\\_e.asp](http://www.mndm.gov.on.ca/mines/data/google/default_e.asp)). Google Earth allows the visualization of geological, topographic and cultural information with overlain geochemistry in virtual 3-D through all scales and view angles. Even to novice users, profound geochemical trends and relationships between geochemistry and geology can be immediately apparent – and the platform is considerably easier to operate than a typical GIS.

### SAMPLING METHODS

From the outset of the high density lake sampling program in 1987, the application of a robust and consistent sampling protocol was considered paramount and this is still the case. Lake sediment and water sampling is performed by 2-person teams primarily from float-equipped Bell 206B helicopters.

Intact lake cores are retrieved from the lake bottom in a polycarbonate tube. Bottom-up extrusion of the sediment

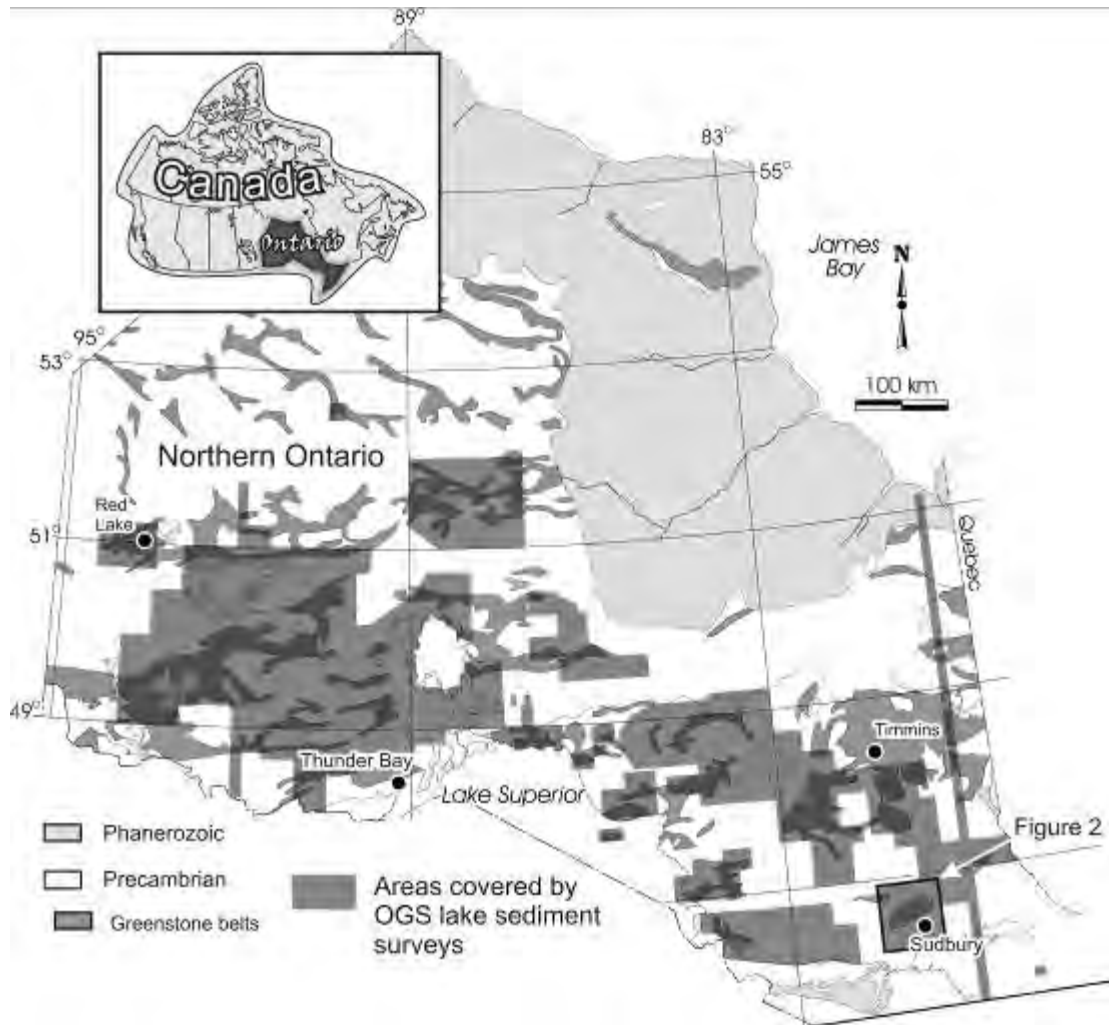


**Fig. 4.** High density lake sediment coverage of northern Ontario.

allows for discrimination between shallow (0-15 cm) sediment and deeper sediment (e.g. >20 cm). All samples are taken from depths >20 cm below the sediment-water interface (SWI) in order to avoid anthropogenic influences and near surface diagenetic effects. Therefore, these deeper sediments more accurately reflect the natural geochemical inputs, which may be traced back to local bedrock geology. If required, the upper (shallow) sediment can also be kept as a separate sample to characterize potential anthropogenic inputs, for example, near industrial areas or existing mines.

**THE USE OF DEEP LAKE SEDIMENT**

The sampling of deep lake sediment has

always been considered an essential part of the OGS lake sediment sampling program. The practice of consistently sampling deep (>20 cm) lake sediment was initially based on studies by Dickman & Fortescue (1984) on the increase/appearance of *Ambrosia* (ragweed) pollen at a sediment depth of 10 to 15 cm within 8 test lakes in the Sudbury and Wawa regions. This increase in the *Ambrosia* pollen corresponds to the onset of extensive deforestation associated with agricultural development during the post-industrial period of the past 100 years. Data from a more recent study in the Sudbury area confirm that a sample depth of >20 cm is adequate to avoid contamination (Hunt 2003). Hunt's



**Fig. 5.** The distribution of nickel in the Sudbury area shown by lake sediment sampling, draped over a regional DEM viewed through Google Earth. Circle size is proportional to concentration, with the largest circle representing >200 ppm Ni. Tear-drop symbols are locations of major Ni deposits. View aspect is northeast toward the direction of last glacial advance.

study involved  $Pb^{210}$  age dating of lake sediment cores obtained with a KB gravity corer from 14 lakes. The sedimentation rate averaged 1.6 cm per decade, therefore a 20 cm depth in lake sediment corresponds to approximately 125 years ago. Eleven of the lakes cored by Hunt (2003) were also sampled by the OGS with the coring torpedo. The geochemical results are very similar indicating that the OGS sampling methodology is successful at obtaining and discriminating between recent and pre-industrial sedimentation (Dyer *et al.* 2004).

**DISTINGUISHING BETWEEN NATURAL & ANTHROPOGENIC SIGNALS AT SUDBURY**  
**Environmental Disturbance in the Sudbury Area**

A significant mining and smelting “footprint” exists in the Sudbury basin which hosts numerous world-class Ni-Cu-PGE deposits. This footprint poses a

challenge for the use of lake sediment geochemistry in the region. Whether the objective is baseline geochemical mapping or mineral exploration, it is difficult to “see” through the ecological disturbance of the past 100 years to understand background geochemical conditions as they would have existed prior to industrial activity.

Environmental impact in Sudbury and the surrounding area is mainly due to smelter emissions. By the early 1970s, these had resulted in vegetation loss or damage over approximately 720 km<sup>2</sup>. This disturbance is manifest as acidified lakes, metal-contaminated lake sediments and indirect effects resulting from damage to vegetation in the lake basins. These disturbances have been amplified due to the presence of Precambrian bedrock that offers very little buffering capacity and the presence of carbonate-poor drift materials over the region, which cannot neutralize

the acidity formed in the by-products of Sudbury's mining industry.

### **The Lake Sediment Geochemical Response in the Sudbury Area**

The distribution of Ni in lake sediment for the Sudbury area is displayed in Figure 2. Most of the regional distribution of Ni is spatially associated with Sudbury Igneous Complex (SIC) rocks, which host most of the Ni mineralization in the Sudbury basin. Anomalies from lakes in close proximity to tailings/slag/waste rock may have, in part, an anthropogenic component due to much higher than average sedimentation rates (resulting in more than 20 cm of young sediments). The pattern of elevated Ni concentrations south of the basin is probably due to the effect of glacial and hydromorphic contributions into the lake basins. The elevated Ni pattern that extends further to the south may be in response to the presence of the Ni-mineralized Copper Cliff offset dike and Nipissing gabbro rocks, in addition to glacial dispersal southward from the Ni deposits contained within the south range of the SIC.

The close association of the lake sediment geochemistry with SIC rocks and Ni mineralization indicates that the OGS protocol of sampling a discrete depth interval of deeper sediments is successful in obtaining relatively undisturbed and uncontaminated sediments in the vast majority of cases.

### **CONCLUSIONS**

The OGS lake geochemical sampling program was designed to obtain a high density, high quality natural geochemical signal from both pristine and disturbed landscapes. It is intended both as a record of natural baseline conditions in pre-industrial sediments and a mineral

exploration tool. An excellent example of this is the high density survey over the Sudbury region, where, despite the significant mining activity and significant ecological disturbance, the OGS lake sediment sampling methodology was successful in obtaining relatively undisturbed and uncontaminated deep sediments in the vast majority of cases. When viewed in Google Earth, the close association of the lake sediment geochemistry and SIC rocks is immediately apparent, as are other geochemical trends that are directly related to the effects of geology.

The ease with which geochemical data can be visualized in Google Earth has important implications to geochemistry beyond the display of OGS data. This platform is not hindered by the size of the geochemical dataset, and it can reach a worldwide audience. As such, Google Earth could be the platform for the integration of other provincial or continental scale geochemical mapping efforts, ultimately leading to a widely and easily accessible geochemical map of the Earth.

### **REFERENCES**

- DICKMAN, M. & FORTESCUE, J. 1984. Rates of lake acidification inferred from sediment diatoms for eight lakes located north of Sudbury. *Verhandlungen Internationale Vereinigung fuer Theoretische und Angewandte Limnologie*, **22**, 345-1356.
- Dyer, R.D., Takats, P., & Felix, V.E. 2004. Sudbury Area Lake Sediment Geochemical Survey; Ontario Geological Survey, *Open File Report 6126*, 106 p.
- HUNT, C. 2003. *Metal concentrations and algal microfossil diversity in pre-industrial (pre-1880) sediment of lakes located on the Sudbury Igneous Complex in Sudbury, Ontario*. Unpublished MSc. Thesis, Laurentian University, Sudbury, Ontario.

## Developing an exploration/environmental geochemical database on a shoestring budget

Ronald R. McDowell<sup>1</sup>, Katharine L. Avary<sup>1</sup>, David L. Matchen<sup>2</sup>,  
James Q. Britton<sup>1</sup>, J. Eric Lewis<sup>1</sup>, & Paula J. Hunt<sup>1</sup>

<sup>1</sup>West Virginia Geological and Economic Survey, 1 Mont Chateau Road, Morgantown, WV 26508 USA  
(e-mail: mcdowell@geosrv.wvnet.edu)

<sup>2</sup>Department of Physical Science, Concord University, Box 1000, Athens, WV 24712 USA

**ABSTRACT:** The West Virginia Geological and Economic Survey (WVGES) has been building a stratigraphic, geochemical database since 1997. Piggybacking geochemical sampling together with field work undertaken for other ongoing Survey research projects, it has been possible to assemble a suite of nearly one thousand rock samples representing approximately 90% of the State's stratigraphic units exclusive of coal-bearing strata (represented geochemically in a separate database). Analytical costs have been kept to a minimum by utilizing a commercial laboratory which caters to the mineral exploration industry. Although data were initially stored in spreadsheet format, the inclusion of geographic coordinates allowed the database to be converted to a form that can be queried, analyzed statistically, and displayed using readily available, GIS software. Since its release to the public in 2001, the geochemical database has been utilized by other State agencies and by the mineral industry to answer specific questions regarding the metal content of the State's bedrock.

**KEYWORDS:** *database, geochemistry, West Virginia, bedrock, metals*

### INTRODUCTION

Since 1997, staff members of the West Virginia Geological and Economic Survey (WVGES) have been building a geochemical database for the State's bedrock units to be used for the dual purposes of mineral exploration and environmental quality assessment. The results of these efforts were first released to the public in 2001 when the number of sample analyses in the database reached approximately five hundred (McDowell, 2001). Prior to the initiation of this project, bedrock geochemical data for West Virginia was only available in print, scattered throughout a variety of WVGES publications. Extant information was limited to geochemical analyses (done principally by *wet chemistry*) of economic materials and minerals such as iron and manganese ore, salt, aggregate, limestone, sandstone, shale, and coal. The only other comprehensive set of geochemical data currently available electronically for West Virginia is data on trace elements in the State's coals (Grady 2002).

Funding for this project has been and continues to be limited by fiscal constraints on State Government spending. Nevertheless, by combining sample collection with geological reconnaissance being done for the United States Geological Survey's (USGS) STATEMAP bedrock mapping program and utilizing commercial laboratories for geochemical analyses, we have been able to create a publicly accessible database containing nearly a thousand samples and representative of a large portion of the State's igneous, metamorphic, and sedimentary rocks. The database comprises a multisheet Excel® workbook. Individual samples within the database are segregated by stratigraphic unit – each worksheet contains all analyses available for samples from a single formation. Because a geographic location is recorded for each sample, it has been possible to migrate all of the information from the database into ARCGIS® allowing the data to be queried, analyzed statistically, and displayed in ways not possible with a simple spreadsheet. The

database continues to grow as samples collected during each year's field work are analyzed and the results added.

### **SAMPLING AND ANALYSIS**

Sampling is done concurrently or as an adjunct to geological reconnaissance; each sample is taken opportunistically during outcrop examination. The standard information recorded at an outcrop in preparation for later making a geologic map is recorded for each sample. This includes a location generated and recorded in the field by GPS unit. Generally, 2 kg samples are collected at each site to insure that enough material is available for repeated geochemical analysis if necessary and thin section preparation if desired. All team members have been trained to collect the freshest possible rock samples, free of debris and organic matter and to assign a unique sample number to each; samples are turned over to the team leader (McDowell) when everyone returns to the office from the field. The team leader is responsible for transcribing field information into the electronic database. This is the most time-consuming step in the entire process because initial data are recorded with pencil and notebook and must be typed into spreadsheet format.

WVGES has not had analytical laboratory facilities since the 1970's so contract geochemical analyses are a necessity. After considering a variety of sources for analytical work including both university and government laboratories, we decided to use a commercial lab, located in Ontario, which specializes in analyses for the mineral exploration industry (they have since expanded into the environmental field as well). For the sake of consistency, each sample is analyzed using the same set of techniques, a combination of Instrumental Neutron Activation Analysis (INAA) and Selective Extraction-Ignition Coupled Plasma spectroscopy that yield results for 49 elements - Au, Ag, As, Ba, Br, Ca, Co, Cr, Cs, Fe, Hf, Hg, Ir, Mo, Na, Ni, Rb, Sb, Sc, Se, Sn, Sr, Ta, Th, U, W, Zn, La, Ce, Nd, Sm, Eu, Tb, Yb, Lu, Cu, Pb, Mn, Cd,

Bi, V, P, Mg, Ti, Al, K, Y, Be, and S.

We have been well pleased with the commercial lab's low cost-per-sample, reliable and consistent turnaround time for analyses, and continuing diligence in maintaining ISO standards of quality control on analytical procedures. Addressing these issues (especially, cost and turnaround time) seems to be a problem for academic and government laboratories. For example, we estimate that the cost-per-sample would double or triple if we used a non-commercial laboratory, assuming we could find one capable of performing comparable analyses. By the same token, turnaround times from non-commercial labs might be as much as five or six times longer than for commercial facilities.

### **COVERAGE AND UTILITY**

Because geochemical sampling was originally conducted exclusively along with bedrock mapping, the initial geographic distribution of samples within the State was limited to Pendleton County, West Virginia (Figure 1). It should be noted that this study area was specifically chosen because of its geologic complexity. Although small in size (approximately 700 ha), it contains rock units ranging in age from Ordovician through Tertiary, excluding only the coal measures. As such nearly 90% of West Virginia's stratigraphic units are found in the initial study area.

As the database has increased in size, interest in expanding its geographic scope to a truly Statewide enterprise (the original intent) has also increased. In 2008, the State's Mapping Advisory Committee recommended just such an expansion. Fortunately, this undertaking can be readily accomplished because the only real requirements for adding samples taken elsewhere in the State are the necessities of identifying the stratigraphic unit being sampled, maintaining consistency in sample description, recording the sample's geographic location, and, of course, collecting the sample. To date, workers from WVGES' Oil and Gas and Coal programs have

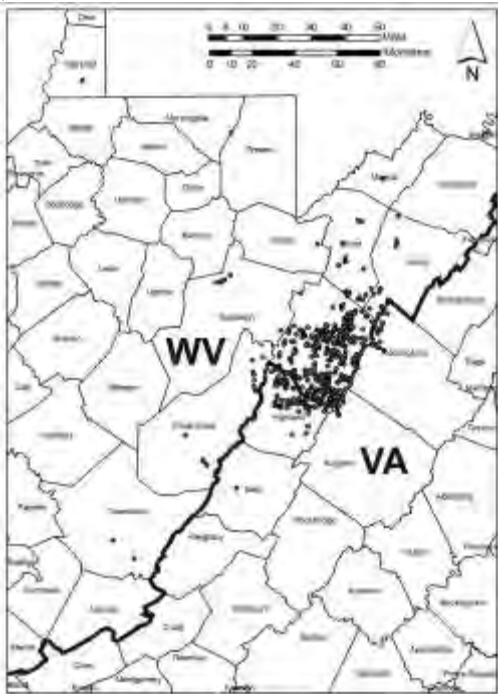


**Fig. 1.** Location of geochemical samples taken during STATEMAP reconnaissance and as part of other WVGES projects, 1997-2008. Initial sampling centered on Pendleton County, West Virginia (indicated by the heavy concentration of sample points) but geographic distribution has been slowly increasing over the past five years due to increased interest in the project and changing focus of bedrock mapping efforts. Notice that a number of geochemical samples were also collected in neighbouring Virginia during cooperative mapping efforts. The results of analyses for those samples have been shared with the Virginia Division of Geology and Mineral Resources (VDGMR).

contributed samples from other parts of the State to the program.

In 2002, the West Virginia Department of Environmental Protection (WVDEP) used analytical data for the Silurian Tuscarora Sandstone in assessing the potential environmental impact of proposed new quarrying operations in that unit. In 2006, the West Virginia Department of Highways (WVDOT), used analytical data for the Devonian Mahantango Formation to evaluate a legal dispute over the valuation of property containing a quarry in that unit. In 2008, a

controversy arose over the levels of selenium in water draining from coal mine spoils in southern West Virginia. Thus far, WVGES has utilized geochemical data on the selenium content in West Virginia coals (Grady 2002) and bedrock (McDowell 2001) to help pinpoint the exact source of the contamination. In addition, one example of a mineral exploration use of the database was a recent industry inquiry as to which rock units in the State were a potential source of both potassium and aluminum for use in making ceramics.

### CONCLUSIONS

By piggybacking sample collection with existing bedrock mapping projects and utilizing the services of commercial analytical laboratories, it has been possible to build a publicly accessible database of geochemical data that has grown over the past eleven years to include the results of analyses for nearly 1,000 samples from 38 of West Virginia's bedrock units. The database is sufficiently populated for each of these units to allow the establishment of elemental background levels in the majority of these stratigraphic units and to perform comparative and discriminatory statistics between units. Consequently, it is now possible to assess new rock samples to determine if their elemental content should be considered anomalous (useful for mineral exploration purposes). By the same token, it is possible to evaluate potential sources of contamination in light of typical concentrations of metals that can be expected in the local bedrock.

### ACKNOWLEDGEMENTS

Partial funding was provided by various USGS STATEMAP contracts. Consultation with the geologists of the Virginia Division of Geology and Mineral Resources is gratefully acknowledged. We would also like to thank numerous private landowners of eastern West Virginia and western Virginia for granting permission to cross property boundaries and collect samples.

**REFERENCES**

Grady, W. (compiler). 2002, Trace Elements in West Virginia Coals, West Virginia Geological and Economic Survey Website: <http://www.wvgs.wvnet.edu/www/datastat/te/index.htm>

McDowell, R. (compiler). 2001, Stratigraphic

Geochemical Database for Portions of Pendleton County, West Virginia and Adjacent Virginia Counties, covering portions of Pendleton Co., WV, Highland Co. VA, and Augusta Co., VA: West Virginia Geological and Economic Survey, Report of Investigations RI-34.

## The value of government-generated geochemical data, and an example of its delivery

Paul Morris<sup>1</sup>

<sup>1</sup>Geological Survey of Western Australia, Department of Mines and Petroleum, 100 Plain Street, East Perth 6004  
AUSTRALIA

(email: paul.morris@dmp.wa.gov.au)

**ABSTRACT:** Regional scale (i.e., sample density of  $10^n \text{ km}^{-2}$ ,  $n > 1$ ) geochemistry are routinely used in mineral exploration, yet the cost and time required to generate do not fit well into company exploration strategies in terms of cost and time. In this context, there is clear role for government to both generate and disseminate geochemical data. The benefit of government involvement is demonstrated by a three-fold increase in exploration activity following release of government geochemistry in Western Australia. Delivery of geochemical data via the web in a standard format using a limited number of queries has been developed by the Western Australian government. The approach combines rigorous data standards for incoming data, the ability to store QAQC information, and coupling the data with validated information for sample location and lithology. The database contains > 24 000 analyses derived from > 300 individual batches generated by eleven government, university and commercial laboratories.

**KEYWORDS:** *Geochemistry, database, government, exploration, world wide web*

### INTRODUCTION

Despite the increased use in mineral exploration of remotely-sensed data (e.g. airborne geophysics, Aster<sup>TM</sup>, Landsat<sup>TM</sup>, Hymap<sup>TM</sup>), there is a continuing demand for regional-scale geochemical datasets, especially those composed of multi-element analyses accompanied by quality control and quality assurance (QA-QC) data, which can be used in the exploration of a variety of commodities. Government organisations have provided these data in Australia (de Caritat *et al.* 2008), the United States and Canada (Kettles *et al.*, 2008), and Europe (Smith & Reimann 2008). In many jurisdictions (including Western Australia), the alternative provider is the mineral exploration industry, where geochemical data form part of exploration reporting requirements, with data subsequently released to the public release after a set time period. Even though these data compare favourably with government-sourced data in some respects (sample media, analytical techniques), there is often some disparity in terms of sample density or extent (i.e. scale), scope, data quality, metadata quality, availability, and QA-QC

(Table 1).

Aside from these issues, several factors can influence whether exploration companies are willing to consider generating their own regional geochemistry datasets. For example, mineral exploration over an area of 1000 km<sup>2</sup> in Western Australia involves costs in the first year of > \$370 000 in terms of an application fee, rent, security, and minimum expenditure requirements, with legislation requiring relinquishment of 50% of the tenanted ground each year. Apart from the additional costs of sample collection and analysis incurred by geochemical programs, surveys must be completed to the stage of data interpretation within a 12 month period following ground acquisition.

In response to the need for regional geochemical coverage, GSWA generated multi-element regolith geochemical datasets based on a one sample/16 km<sup>2</sup> and covering an area > 300 000 km<sup>2</sup> over the period 1994 - 2001 (e.g. Morris and Verren, 2001). As part of its regional mapping program, GSWA routinely generates > 500 multi-element analyses of rocks and regolith. GSWA has embarked

on joint ventures with federal agencies (CSIRO and Geoscience Australia), and the success of these projects can be gauged by a low-density (1 sample/70km<sup>2</sup>) multi-element laterite geochemistry program for 3150 samples over the southwest of Western Australia, which resulted in a three-fold increase in tenement uptake from 5136 km<sup>2</sup> month prior to data release, to 15 102 km<sup>2</sup> in the month following (Cornelius *et al.* 2007).

In addition to generating these data, it is also necessary to ensure that they are disseminated via an easily accessible interface, along with appropriate metadata. A major initiative, undertaken in 2004 by GSWA, was to design and populate a corporate geochemical database of all GSWA geochemical data, and to serve these data to the public via a web interface, in a standard format, free of charge. The resulting corporate database (WACHEM) is accessed by GSWA's web interface, GeoChem Extract (www.dmp.wa.gov.au/geochem).

#### **STRUCTURE OF WACHEM AND GEOCHEM EXTRACT**

WACHEM is a fully relational database on a SQL (structured query language) platform that uses the DataShed™ data management system software model for loading and storage of data. The DataShed™ base model has been customised to GSWA's needs, including the content of various look-up tables to ensure that incoming data are 'clean' in terms of data type (e.g. text versus numeric) and batches contain the minimum requisite amount and type of data. A modification allows the storage of information on pre-analysis sample preparation (i.e. screening, crushing, milling), recognising that results from increasingly sophisticated analytical techniques can be influenced by contamination during sample preparation. To maintain data quality, each analytical batch must list a recognised element or oxide name, unit of measurement, laboratory technique (as a laboratory-specific acronym), and lower level of detection (LLD). The database can also

store related QAQC data for duplicates (i.e. a second analysis of the parent pulp) and reference materials.

GSWA's GeoChem Extract application draws together data from the WACHEM and WAROX databases. The latter is the repository of all field-based point data generated by GSWA, and is used throughout the organisation to automatically create various layers for GSWA maps (e.g. structural symbology), geochronology compilations (sample location, rock, type), and will eventually underlie an online version of map-related explanatory notes.

To date, the WACHEM database contains 24,200 analyses made up of 323 separate analytical batches sourced from eleven laboratories. In order to maintain a dynamic database, the contents of available data are updated daily using a series of stored procedures, with each data download appropriately time stamped.

#### **DATA ACCESSIBILITY**

To achieve a simple user interface, GeoChem Extract relies on a either downloading the whole database, or extracting data according to a limited number of spatial queries (Fig. 1). All selected data are presented as a comma-separated (.csv) file of locational and lithological data (WAROX) and geochemical data (WACHEM), for easy manipulation in third-party software. Embedded in the file is a hyperlink to the batch for each sample. Batch data can be accessed and downloaded, providing information on analytical techniques, detection levels etc and any available QAQC data.

#### **CONCLUSIONS**

Government organisations are well placed to generate regional geochemical datasets, in that they are not subject to the time and cost constraints which form part of mineral exploration legislation. These data are usually multi-element and include QA-QC data which mean the data are well suited to multi-commodity exploration and evaluation in terms of data quality. The

**Table 1.** Comparison Of Government And Exploration Company Geochemical Datasets.

	<b>Government</b>	<b>Exploration Company</b>
Scale (10 <sup>n</sup> km <sup>2</sup> )	1 < n < 4	n typically < 1
Number of elements	Broad (multi-commodity)	Narrow (commodity-focused)
Sample media	Usually limited	Usually limited
Analytical techniques	Varied	Varied
Data quality	Usually good	Variable
Metadata quality	Usually good	Variable
Availability	Good (often digital)	Limited (usually hardcopy)
QAQC	Usually tabulated	Occasionally tabulated

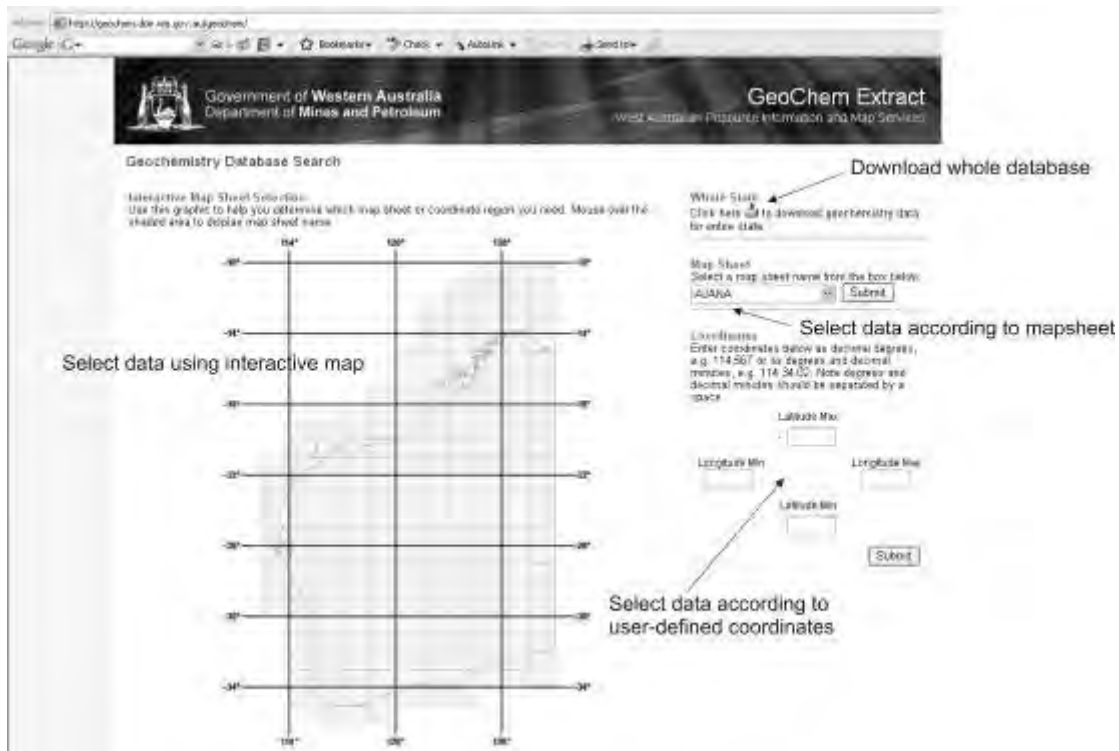


**Fig. 1.** GeoChem Extract introductory screen showing the four options for accessing data.

Geological Survey of Western Australia has combined its regional geochemical data with other lithochemical information in a corporate database, and delivered the data via a customised web application which combines validated locational, lithological, and geochemical data. A series of simple, largely spatially-attributed search tools result in generic file formats that are easily imported into third party software for further manipulation. Hyperlinks in these data provide information on individual

batch conditions. At present, the available data comprise > 24 000 analyses from > 300 analytical batches generated by eleven laboratories.

**ACKNOWLEDGEMENTS**

Darren Wallace, John Cuthbertson, and Trung Tran made major contributions to the construction and maintenance of the WACHEM database.

**References**

CARITAT, P. De, LECH, M.E., & MCPHERSON, A.A.

2008. Geochemical mapping 'down under': selected results from pilot projects and strategy outline for the National Geochemical Survey of Australia. *Geochemistry: Exploration, Environment, Analysis*, **8**, 301-312.
- CORNELIUS, M., ROBERTSON, I.D.M., CORNELIUS, A.J., & MORRIS, P.A. 2007. Laterite geochemical database for the western Yilgarn Craton, Western Australia. *Western Australia Geological Survey, Record*, **2007/9**, 44p.
- CORNELIUS, M., ROBERTSON, I.D.M., CORNELIUS, A.J., & MORRIS, P.A. 2008. Geochemical mapping of the deeply weathered western Yilgarn Craton of Western Australia, using laterite geochemistry. *Geochemistry: Exploration, Environment, Analysis*, **8**, 241-254.
- KETTLES, I.M., RENCZ, A.N. & FRISKE, P.B.F. 2008. The North American soil geochemical landscape project — a Canadian perspective. *Explore*, **141**, 12-22.
- MORRIS, P.A. & VERREN, A.L. 2001. Geochemical mapping of the Byro 1:250 000 sheet. *Western Australia Geological Survey, 1:250 000 Regolith Geochemistry Series Explanatory Notes*, 53 p.
- SMITH, D.B. & REIMMAN C. 2008. Low-density geochemical mapping and the robustness of geochemical patterns. *Geochemistry: Exploration, Environment, Analysis*, **8**, 219-227..

## Using stream sediments for environmental geochemistry in Austria

Sebastian Pfeleiderer<sup>1</sup>, Albert Schedl<sup>1</sup>, & Herbert Pirkl<sup>2</sup>

<sup>1</sup>Geological Survey of Austria, Neulinggasse 38, 1030 Wien AUSTRIA (e-mail: pflseb@geologie.ac.at)

**ABSTRACT:** The dataset of stream sediment analyses in Austria consists of 36,136 samples analyzed for 34 chemical elements. Formerly used for mineral exploration, the data now serve for environmental geochemistry studies. These include the derivation of natural background levels of different rock units, the investigation of chemical fluxes between soil, rock and groundwater and the evaluation of emission risks of historical mine waste. Natural background levels are derived in lithologically homogeneous areas away from mining sites or mineralization. Homogeneity is defined on the basis of catchment areas. Chemical fluxes between soil, rock and groundwater are traced by studying regional distribution patterns as well as temporal dependencies. While most of the major elements in soils and groundwater are lithology-controlled, Cl, NO<sub>3</sub>, SO<sub>4</sub>, Pb, and Cd are strongly affected by precipitation. Within areas of historic mining, univariate and multivariate statistics serve to identify areas with elevated heavy metal concentrations. Lead and zinc mineralizations are easily identified by factor analysis. Detailed mineralogical phase analysis is used to distinguish between natural and anthropogenic sources and to determine the origin and transport of industrial particles in the environment.

**KEYWORDS:** *stream sediment, natural background levels, chemical fluxes, phase analysis, historical mine waste*

### INTRODUCTION

The country-wide dataset of stream sediment analyses in Austria consists of 36,136 samples analyzed for 34 chemical elements (Fig. 1), (Thalman *et al.* 1989). Complemented by local surveys of hydrochemistry, whole rock geochemistry, soil chemistry and mineralogical phase analyses, these data are used to derive natural background levels of different rock units, investigate chemical fluxes between soil, rock and groundwater, and evaluate the emission risks of historical mine waste.

### NATURAL BACKGROUND LEVELS

Natural background levels of different rock units can be derived by either correlating element concentrations of stream sediment analyses with geological maps, or morphological catchment areas (Fig. 2). When using geological maps, statistics for a given unit are calculated using all sample points contained within all the polygons of that unit, whereas when using

catchments, the lithologies within all catchment areas are derived automatically and only point samples in homogeneous areas are used to define natural background levels.

While the first method gives a quick visual overview of ranges, the second, more sophisticated method leads to a more detailed correlation. In both cases, the correspondence between stream sediment and whole rock geochemistry is not perfect since sediments represent only the weathered product of rocks (Pfeleiderer *et al.* 2008). Lithologically homogeneous areas away from mining sites or mineralization are used to derive natural background levels.

### CHEMICAL FLUXES BETWEEN SOIL ROCK AND GROUNDWATER

For long-term quality assurance of drinking water reserves in large karst areas, the chemical characteristics of different soils, rocks, stream sediments and aquifers are analyzed with respect to

the exchange of chemical substances between media (Fig. 3). The origin and mobility of heavy metals are traced and regional as well as seasonal dependencies are studied.

Regional distribution patterns in the data show that lithology is responsible for the amounts of Ca, Mg, K, Na, Al, Si, and SO<sub>4</sub> in soils and groundwater. Cr, Ni and Cu pass from rocks into groundwater, and show up in stream sediments, but do not affect soils. Concentrations of Cl, NO<sub>3</sub> and SO<sub>4</sub> show a temporal dependence on precipitation suggesting rain as the source of input into soil and groundwater. Equally, Pb and Cd originate from emission. (Pirk 2005). These two elements pass through all media and end up in the groundwater, their concentrations occasionally exceeding the limits of drinking water standards.

**MINE WASTE EMISSIONS**

Combining data from stream sediment analyses with data on historic mining areas, the emission risks of old mine waste sites are evaluated systematically throughout Austria. Univariate and multivariate statistics serve to identify areas with naturally, or anthropogenically, elevated heavy metal concentrations (Fig. 4). Lead and zinc mineralization for

example are easily identified by factor analysis (high factor loadings for Ba, Cd, F, Pb, S, and Zn). Natural background levels in the vicinity of historic mining areas, potential risks of emission and maximum possible propagation of pollutants are then estimated.

However, factor analysis cannot always distinguish between naturally elevated heavy metal concentrations and anthropogenic pollution. In specific areas, detailed mineralogical phase analysis is used to make this distinction and to determine the origin and transport distance of industrial particles in the environment (Neinavaie *et al.* 2000).

**REFERENCES**

NEINAVAI, H., PIRKL, H., & TRIMBACHER, C. 2000. Herkunft und Charakteristik von Stäuben. Report **BE-171**, Environmental Agency, Vienna.

PFLIEDERER, S. 2008. Ableitung geogener Hintergrundwerte auf Basis von Einzugsgebiets-bezogenen Auswertungen. In: SCHEDL, A., PIRKL, H., PFLIEDERER, S., LIPIARSKI, P., NEINAVAI, H., & ATZENHOFER, B. (eds.) *Umweltgeochemie Kärnten*. Project report **KC30**, Geological Survey of Austria, Vienna.

PIRKL, H. 2005. Bodengeochemie. In: PFLIEDERER, S., REITNER, H., & HEINRICH, M.

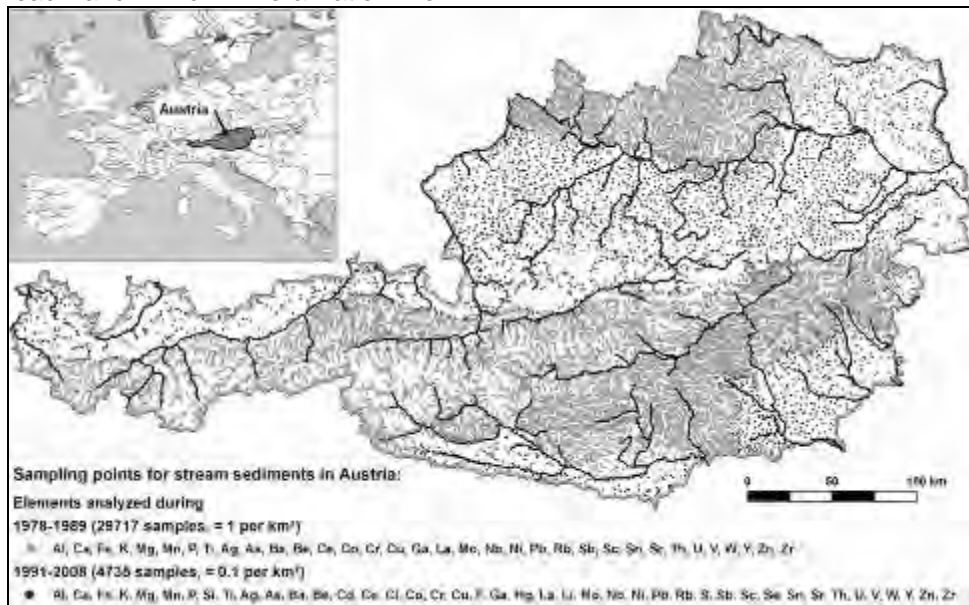
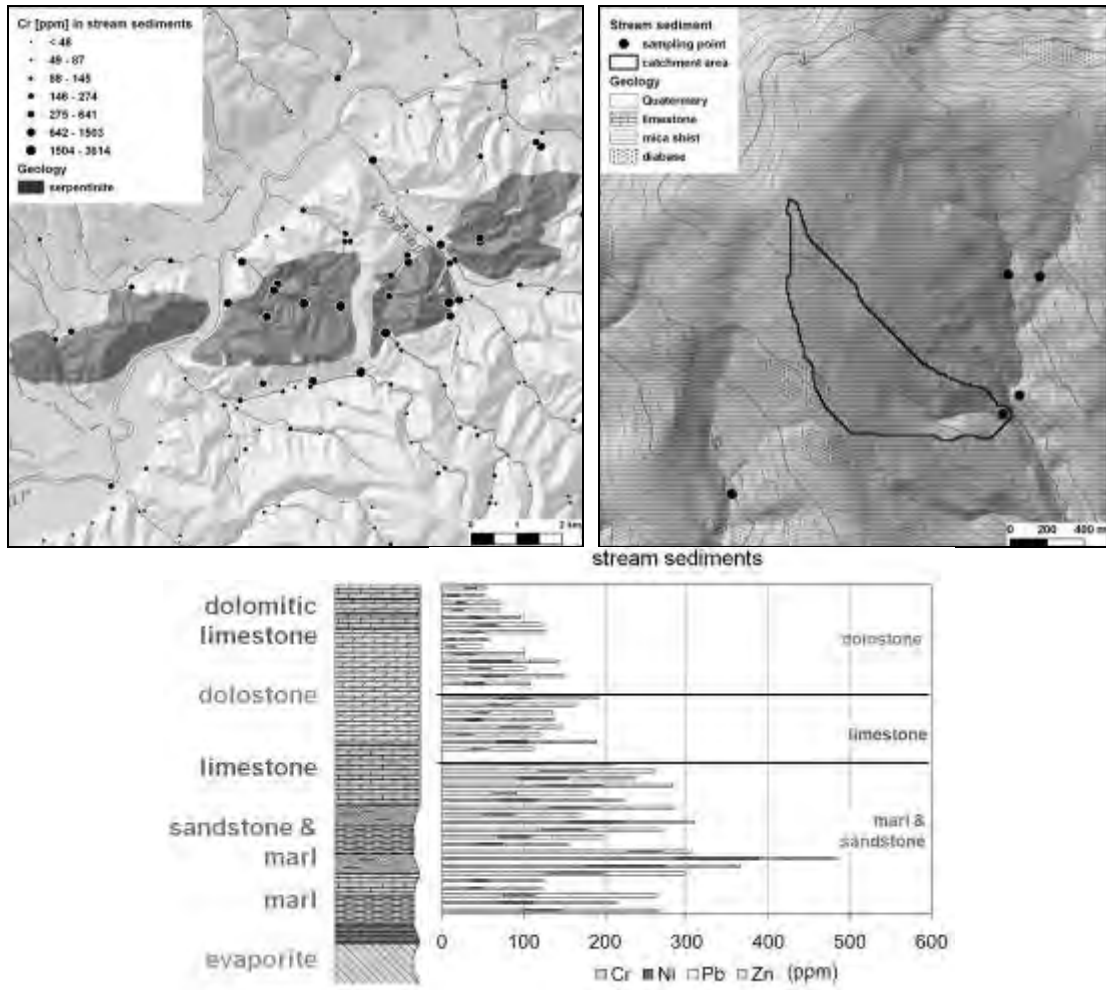


Fig. 1. Location of sampling points for stream sediments, Austria.



**Fig. 2.** Derivation of natural background levels by (a) superimposing sample points on geological units (left) and by (b) relating sample points to catchment areas (right).

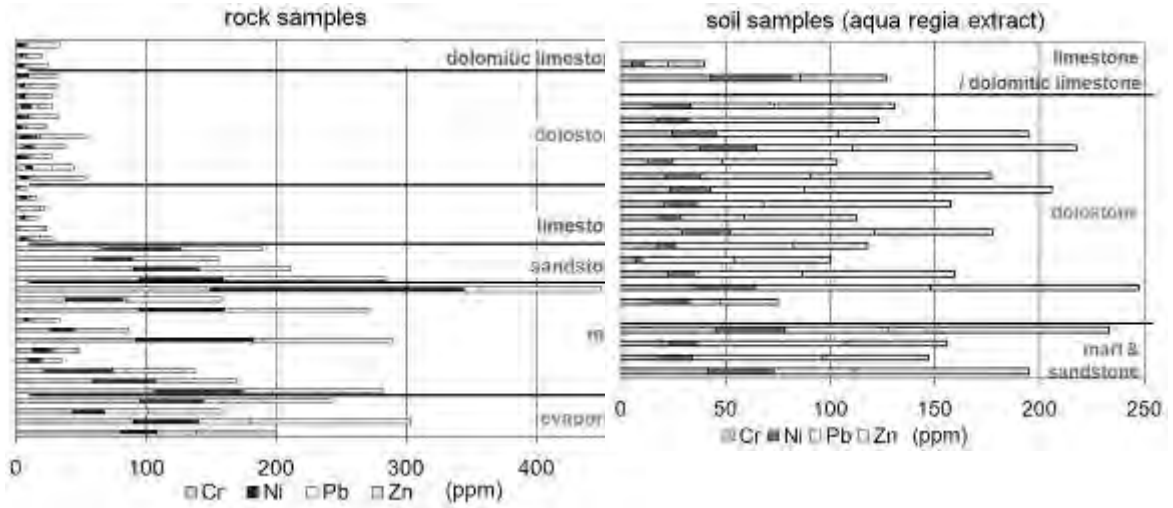


Fig. 3. Chemical analyses of Cr, Ni, Pb and Zn in rocks, soils and stream sediments.

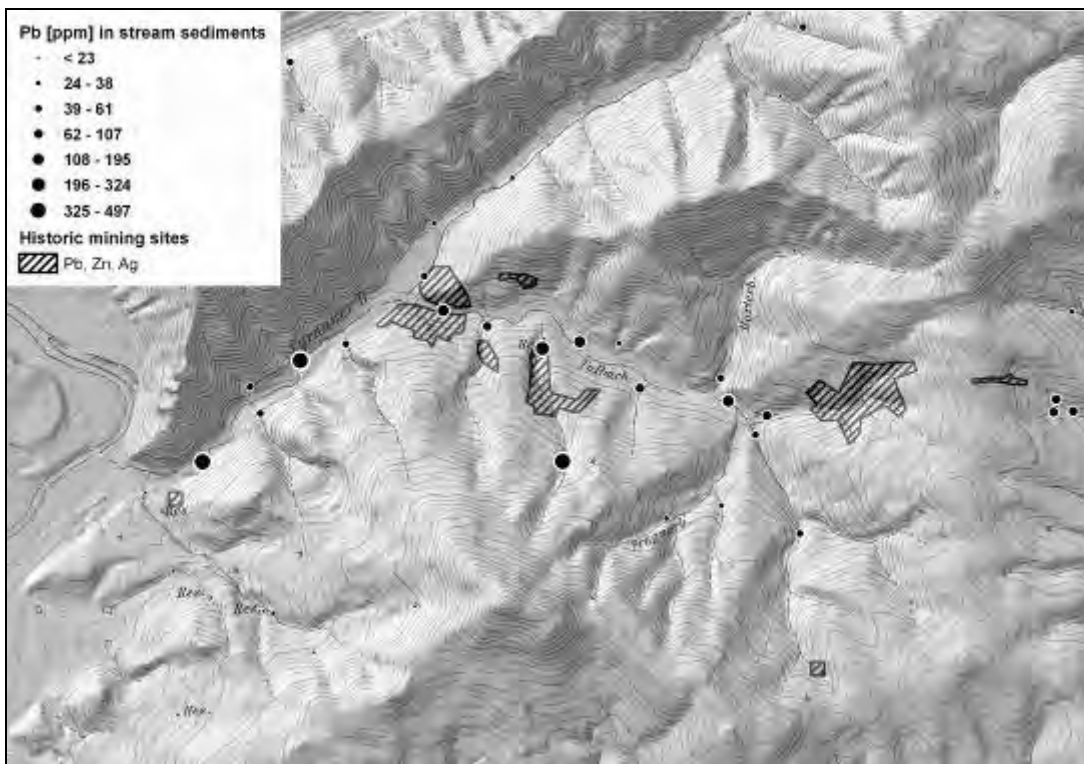


Fig. 4. Elevated Pb concentrations in stream sediments of an historic mining area.

*Hydrogeologische Grundlagen in den Kalkvoralpen im SW Niederösterreichs.* Project report NA6u, Geological Survey of Austria, Vienna.

THALMANN, F., SCHERMANN, O., SCHROLL, E., & HAUSBERGER, G. 1989. Geochemischer Atlas der Republik Österreich 1:1,000,000.

Böhmische Masse und Zentralzone der Ostalpen (Bachsedimente < 0,18 mm). Geological Survey of Austria, Vienna.

## Surficial geochemical studies in support of non-renewable mineral resource assessments, Northwest Territories, Canada

Toon Pronk<sup>1</sup>, Roger C. Paulen<sup>2</sup>, Andrea Mills<sup>3</sup>, & Adrian Hickin<sup>4</sup>

<sup>1</sup>New Brunswick Department of Natural Resources, P.O.Box 6000, Fredericton, NB, E3B 5H1 CANADA  
(email: toon.pronk@gnb.ca)

<sup>2</sup>Geological Survey of Canada, 601 Booth Street, Ottawa, ON, K1A 0E8 CANADA

<sup>3</sup>Newfoundland Geological Survey, Natural Resources Building, P.O. Box 8700, St. John's, NL, A1B 4J6 CANADA

<sup>4</sup>Development and Geoscience Branch, British Columbia Ministry of Energy, Mines & Petroleum Resources, 6<sup>th</sup> Floor, 1810 Blanshard Street (PO 9333 Stn Prov Gov't), Victoria, BC, V8W 9N3 CANADA

**ABSTRACT:** The Non-renewable Resource Assessment is a legislated requirement in the Northwest Territories' Protected Area Strategy and is used to facilitate informed decision making on land use issues, special management areas, protected areas, and the establishment of territorial parks. Two Resource Assessments detailing the Mineral and Petroleum potential of the proposed protected area are completed for each area. If these protected areas are granted as such, it is possible that this study may be last geochemical/mineralogical survey conducted within the boundaries of any area that is a candidate for protection. The NRA process is designed to provide as much information as possible on the mineral potential of the proposed protected area and it covers a multitude of potential mineral deposit targets. Thus, an extensive suite analysis is carried out on tills including geochemical analysis of the -63 micron fraction of the indicator minerals. Indicator minerals from a wide variety of deposit types, e.g. kimberlite, base and precious metals and other pathfinder minerals are being evaluated from bulk glacial sediment samples as well. In areas of low relief, basal till is the targeted sample medium whereas in areas with higher relief, stream sediments, and waters as well as pre-concentrated and screened bulk stream sediments are the target media. Since some of the proposed protected areas are composed of low-relief as well as mountainous areas, sometimes a hybrid approach has been employed. The objective is to provide detailed and pertinent information in support of balanced decision-making.

**KEYWORDS:** *Resource assessment, Northwest Territories, geochemistry, indicator minerals, land use*

### INTRODUCTION

The goal of the Northwest Territories (NWT) Protected Areas Strategy (PAS) is to protect culturally and ecologically important areas within the NWT. The PAS attempts to balance the needs of the present with the needs of the future by providing a process by which communities can identify and protect significant cultural and ecological areas prior to future development (NWT PAS, 2007). It is to be a comprehensive and inclusive process. The NWT's PAS is set with the Mackenzie Valley Action Plan and is sensitive to First Nations land claims. One major issue for both territorial and federal government, as well as communities, is balancing the level of development and/or protection for an area.

The Non-renewable Resource Assessments (NRAs) are part of step 5 in an 8-step process that may ultimately result in (partial or limited) protection of certain areas from development. Phase 1 of an NRA is a desktop exercise that evaluates all existing mineral deposit and survey data for an area from all sources, determines knowledge gaps of the mineral potential, and suggests an approach for Phase 2 follow-up work. Phase 2 of the NRA typically involves field and analytical work designed to lead to a better understanding of the resource potential for a candidate protected area.

Each proposed protected area (PPA) is represented by a Working Group comprising a sponsoring agency, federal, territorial, and band council

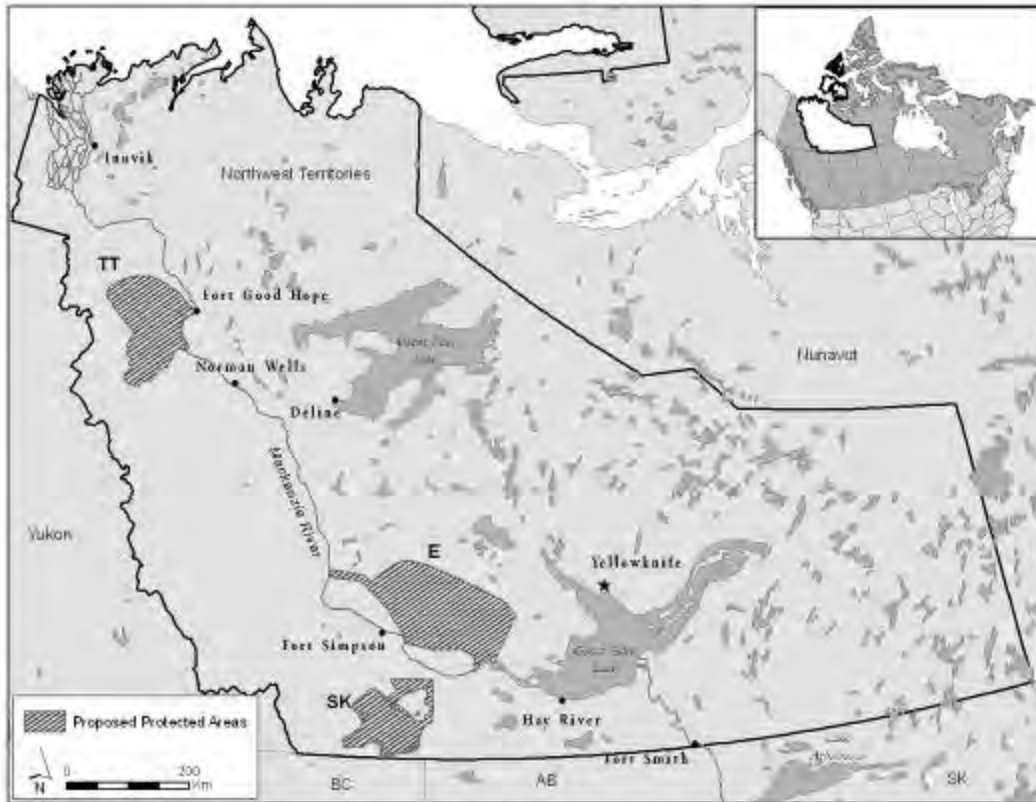


**Fig. 1.** Location of the three Proposed Protected areas in the Northwest Territories: TT = Ts'ude niline Tu'eyeta (Ramparts River wetlands), E = Edehzhie (Horn Plateau), and SK = Sambaa K'e (Trout Lake).

representatives and interested members of neighbouring communities.

Cooperation is imperative in this process, and education and outreach go hand-in-hand with consensus building. Community meetings are part of the process and an understanding of the First Nations cultural landscape is an important asset. Some of the proposed protected areas also play in land claim settlements between the federal government and First Nations people.

This paper deals with three different proposed protected areas that are in different stages with respect to their NRAs; Edehzhie (Horn Plateau), Ts'ude niline Tu'eyeta (Ramparts), Sambaa K'e (Trout Lake). Thus for the three areas different issues and/or stages will be highlighted. All three areas lie (at least partly) within the Western Canada Sedimentary Basin.

### GEOLOGICAL SETTING

The three proposed protected areas lie within the Western Canada Sedimentary Basin (WCSB). This basin is wedged between the Canadian Shield and the Rocky Mountains and consists of largely near-horizontal lying sedimentary rocks of Devonian to Cretaceous aged limestone, dolostone, anhydrite, shale, siltstone, and sandstone (Gal 2007). The Quaternary geology of the Sambaa K'e area was most recently described in Huntley *et al.* (2008) as part of Geological Survey of Canada mapping of the Mackenzie Valley corridor. The late Wisconsin glacial history of the area is relatively simple as the Laurentide Ice Sheet (LIS) moved across the area from the northeast. Ice thickness in excess of 1000m is implied by the presence of granitic erratic boulders at 1588m elevation in the eastern Foothills

(Bednarksi & Smith 2007). The LIS advanced into the WCSB in the Late Wisconsinan. A wood fragment recovered from a till exposure in a riverbank within the Sambaa K'e area dated 35,570 +/- 330BP (AMS date Beta Analytic Inc. - 249392) South of the Sambaa K'e area, Late Wisconsinan Laurentide glaciations is bounded by a younger date of 24,400 +/- 150 BP (Levson *et al.* 2004). During de-glaciation, meltwater and meteoritic drainage was temporarily routed to the south and many outwash channels are present in the landscape around Trout Lake. Huntley *et al.* (2008) provides more detail in regard to the (de-)glacial history and landform assemblages of the area.

The Phase I NRA (Pronk 2008) made an initial assessment of the mineral potential of the area and makes recommendations for the type of survey that should be carried out for further mineral resource assessment (strategy for Phase II).

#### **METHODOLOGY**

Field work methodology follows Paulen (2009) and was closely adhered to for the till survey component of the work, while National Geochemical Reconnaissance protocols (Friske & Hornbrook 1991) were followed in the more mountainous areas of Ts'ude niline Tu'eyeta. These methodologies have both been successfully used throughout the WCSB, in some instances as a single method, or in combination with other methods (Prior *et al.* 2009).

In the till surveys the targeted sample density was one sample/100km<sup>2</sup>. This density was not attained in Ts'ude niline Tu'eyeta; largely because of the presence of unsuitable sample material at the surface (glacio-lacustrine sediments and organic deposits as well as the added caveat of permafrost in some areas). The sample density target was slightly surpassed in the Sambaa K'e PPA (1 sample/92km<sup>2</sup>). Samples were taken at depths between 40 and 110cm in hand-dug pits and in river cuts, below the oxidized soil zones where possible. Sample depth at Sambaa K'e was

considerably more than in Ts'ude niline Tu'eyeta, where permafrost often limited the sampling depth, although frost boils were alternatively used to access relatively unoxidized sample medium. These were especially recognizable in 'recent' areas razed by forest fires where the organic cover was removed.

#### **SOME RESULTS AND CONCLUSIONS**

Results of the Edehzhie survey (a hybrid survey) have been used to adjust suggested protected area boundaries and make compromises in light of mineral potential. There is a high kimberlite potential on the Horne Plateau, as suggested by the presence of indicator minerals and a small diamond recovered from a bulk stream sediment sample (Day *et al.*, 2007).

Potential for diamond-bearing kimberlites is also present Sambaa K'e area. There are basement and structural similarities with the Buffalo Head Hills kimberlite field, Alberta (Prior *et al.* 2007) and there is ongoing diamond exploration within the WCSB to the north as well. Further discussion has altered the potential boundaries for the proposed protected area on the Horn Plateau and discussions are ongoing before any permanent decisions are made by all parties involved. Analytical results for the remaining two areas are pending.

#### **ACKNOWLEDGEMENTS**

The authors would like to acknowledge cooperation with the First Nations people of the NWT. The communities that gave us hospitality during our fieldwork, especially the people of Sambaa K'e and the Sambaa K'e Development Corporation. Field assistance was provided by Lawrence Cesar (Fort Good Hope) and Jessica Jumbo (Trout Lake). Invaluable moral and logistical support and knowledge was provided by Hendrik Falck, Scott Cairns, and Brendan Norman (all NTGO).

#### **REFERENCES**

BEDNARKSI, J.M. & SMITH, I.R. 2007. Laurentide and montane glaciation along the rocky

- Mountain Foothills of northeastern British Columbia. *Canadian Journal of Earth Sciences*, **44**, 445-457.
- DAY, S.J.A., LARIVIERE, J.M.L., MCNEIL, R.J., FRISKE, P.W.B., CAIRNS, S.R., MCCURDY, M.W., & WILSON, R.S. 2007. Regional stream sediment and water geochemical data, Horn Plateau area, Northwest Territories (parts of NTS 85E, 85F, 85K, 85L, 95H, 95I and 95J) including analytical, mineralogical and kimberlite indicator mineral data. *Geological Survey of Canada, Open File 5478*.
- FRISKE, P.W.B. & HORN BROOK, E.H.W. 1991. Canada's National Geochemical Reconnaissance programme. *Transactions of the Institution of Mining and Metallurgy, Section B*; **100**, 47-56.
- GAL, L.P. 2007. Sambaa K'e Candidate Protected Area, Non-Renewable Resource Assessment (phase I) – Petroleum. Northwest Territories Geoscience Office, *NWT Open File 2007-02*.
- HUNTLEY, D., MILLS, A., & PAULEN, R.C. 2008. Surficial deposits, landforms, glacial history, and reconnaissance drift sampling in the Trout Lake map area, Northwest Territories; *Geological Survey of Canada, Current Research 2008-14*, 14 p.
- LEVSON, V., FERBEY, T., KERR, B., JOHNSON, T., BEDNARSKI, J., BLACKWELL, J., & JONNES, S. 2004. Quaternary geology and aggregate mapping in northeast British Columbia: Applications for oil and gas exploration and development. In: *Summary of Activities 2004, British Columbia Ministry of Energy and Mines, Paper 2004-1*, 29-40.
- MILLS, A.J. 2008. Phase II Non-renewable Resource Assessment: analysis and interpretation of regional stream sediment and water sampling results for the Edehzhie Candidate Protected Area, Northwest Territories, Canada, parts of NTS 85E, F, K, L and 95H, I and J; *Northwest Territories Geoscience Office, NWT Open File 2008-03*, 211 p.
- NORTHWEST TERRITORIES PROTECTED AREAS STRATEGY, 2006-2007 Annual Report, 007. Indian and Northern Affairs Canada, 44p. [www.nwtpas.ca](http://www.nwtpas.ca)
- PAULEN, R.C., 2009. Sampling techniques in the Western Canada Sedimentary Basin and the Cordillera. In: R.C. PAULEN & I. McMARTIN (eds.), *Application of Till and Stream Sediment Heavy Mineral and Geochemical Methods to Mineral Exploration in Western and Northern Canada*, Geological Association of Canada, GAC Short Course Notes 18, 41-59.
- PRIOR, G.J., MCCURDY, M.W., & FRISKE, P.W.B. 2007. Stream sediment sampling for kimberlite-indicator minerals in the Western Canada Sedimentary Basin: the Buffalo Head Hills Survey, North-central Alberta. In: R.C. PAULEN & I. McMartin (eds.), *Application of Till and Stream Sediment Heavy Mineral and Geochemical Methods to Mineral Exploration in Western and Northern Canada*, Geological Association of Canada, GAC Short Course Notes 18, 41-59.
- PRONK, A.G. 2008. Sambaa K'e Candidate Protected Area Non-renewable Resource Assessment (Phase I) – Minerals, Northwest Territories Geoscience Office. *NWT Open File 2008-08*.

## Abundances of chemical elements in rocks, sediments, and the continental crust of China

Chi Qinghua<sup>1</sup> & Yan Mingcai<sup>2</sup>

<sup>1</sup>*Institute of Geophysical and Geochemical Exploration, CAGS, Langfang 065000 CHINA  
(e-mail: chiqinghua@igge.cn)*

<sup>2</sup>*Key Laboratory of Applied Geochemistry, CAGS, Langfang 065000 CHINA*

**ABSTRACT:** This paper provides concise data sets of elemental abundances for various kinds of geological media of rocks, soils, stream sediments, and sea sediments in China. The data sets include the abundances of 39-76 elements in igneous rocks, sedimentary rocks, metamorphic rocks, soils, stream sediments, sea sediments, and the continental crust of China. The samples have a good representativity for various media and elements were analyzed by sensitive and accurate analytical methods under strict quality control using geochemical certified reference materials (CRMs). The abundances of many trace and ultra-trace elements such as Au, Hg, PGEs etc. are greatly improved. These data can be widely used for geology, geochemistry, environment and agriculture.

**KEYWORDS:** *Elemental abundance, rocks, sediments, continental crust, China*

### INTRODUCTION

Elemental abundances in various types of geological media such as rocks, sediments and soils of China have been studied since 1980s. These data were published in many literatures (Chi & Yan 2007; Yan & Chi 1997, 2005; Ren *et al.* 1998; Zhao & Yan 1994; Zhu *et al.* 2006). To provide readers with a general overview and convenient use, the authors collected these published data and compiled a concise data set in this paper.

### ABUNDANCES OF 76 ELEMENTS IN ROCKS

2,718 composite rock samples systematically were collected in China. The contents of 76 elements were determined by 15 analytical methods under quality monitoring with CRMs. The arithmetic mean is taken as the elemental abundances by rejecting the data beyond the range of  $X \pm 2s$ . Abundances of 76 elements in igneous rocks of China, sedimentary rocks, metamorphic rocks of the eastern part of China were listed in Table 1 (Chi & Yan 2007; Yan & Chi 1997, 2005).

The estimated abundances of 76 elements in the continental crust based on

a 36 km thickness crustal structure model, rock composition model and contents of elements in the eastern part of China was given in Table 1 (Yan & Chi 1997, 2005).

### ABUNDANCES OF 39 ELEMENTS IN STREAM SEDIMENTS

The systematically representative stream sediments were collected by the regional geochemistry-national reconnaissance (RGNR) project in all over China. 39 elements were determined by 8 analytical methods (Xie & Ren, 1993). An average value is calculated from original data within each 1:25,000 map sheet (about 100 km<sup>2</sup>, with about 25 original data for each element). There are 44,422 1:25,000 map sheets used for this calculation. The arithmetic mean is taken as the elemental abundance by repeatedly rejecting the data beyond the range of  $X \pm 3s$ . The abundances of 39 elements in stream sediments of China are given in Table 1 (Ren *et al.* 1998).

### ABUNDANCES OF 76 ELEMENTS IN SOILS

154 composite soil samples were collected in China. The contents of 76 elements were determined using 15

analytical methods. The arithmetic mean is taken as the elemental abundance by rejecting the data beyond the range of  $X \pm 2s$ . The abundances of 76 elements in soils of China is given in Table 1 (Yan & Chi 1997, 2007).

517 composite soil samples were collected from alluvial plains in the eastern part of China. The contents of 70 elements were determined using 13 analytical methods. The arithmetic mean is directly taken as the elemental abundance for all analytical data with no rejection. The abundances of 76 elements in soils of alluvial plains of the eastern part of China are given in Table 1 (Zhu *et al.* 2006).

#### **ABUNDANCES OF 62 ELEMENTS IN CHINA SEA SHELF SEDIMENTS**

286 sediments of China Shelf Sea were collected under a seawater depth -200 m. The contents of 62 elements were determined using 10 analytical methods. The arithmetic mean is taken as the elemental abundance by rejecting the data beyond the range of  $X \pm 2s$ . Abundances of 62 elements in sediments of China Shelf Sea are given in Table 1 (Zhao & Yan, 1994).

#### **CONCLUSIONS**

The data listed in Table 1 factually reflect abundances of chemical elements in various kinds of geological media of rocks, soils, sediments and in the continental crust of China, because the samples have a good representativity for various media and elements analyzed by high-quality analytical methods under strict quality

control. These data can be widely used for geology, geochemistry, environment and agriculture.

#### **ACKNOWLEDGEMENTS**

The authors would like to thank Dr. Xueqiu Wang for his language translation. Thanks are given to the Ministry of Finance of the People's Republic of China for financial support of the research (Project No. Sinoprobe04).

#### **REFERENCES**

- CHI, Q.H. & YAN, M.C. 2007. *Handbook of Elemental Abundance Data for Applied Geochemistry*. Beijing: Geological Publishing House. 148p. (in Chinese).
- REN, T.X., WU, Z.H., & QIANG, R.S. 1998. *Methods and Techniques of Screening and Follow-up for Anomalies in Regional Geochemical Exploration*. Beijing: Geological Publishing House. 138p (in Chinese).
- XIE, X.J. & REN, T.X. 1993. National geochemical mapping and environmental geochemistry - progress in China. *Journal of Geochemical Exploration*, **49**, 15-34.
- YAN, M.C. & CHI, Q.H. 1997. *The Chemical Compositions of Crust and Rocks in the Eastern Part of China*. Beijing: Science Press, 292p (in Chinese with an English preface).
- YAN, M.C. & CHI, Q.H. 2005. *The Chemical Compositions of the Continental Crust and Rocks in the Eastern Part of China*. Beijing: Science Press. 171p.
- ZHAO, Y.Y. & YAN, M.C. 1994. *Geochemistry of Sediments of the China Shelf Sea*. Beijing: Science Press, 203p. (in Chinese).
- ZHU, L.X., MA, S.M., & WANG, Z.F. 2006. Soil eco-geochemical baseline in alluvial plains of eastern China. *Geology in China*, **33**(6): 1400-1405 (in Chinese with an English abstract).

**Table 1.** Elemental abundances of rocks, soils, sediments, and the continental crust in China

Elements	Detection limits	Whole China				Eastern part of China										Whole China			
		Rocks														Soils		Sediments	
		Acidic rock	Intermediate rock	Basic rock	Ultra-mafic rock	Sandstone	Shale	Carbonate	Gneiss	Leptite	Amphibolite	Metapelite	Marble	Continental crust	Alluvial plain soils	Soils	Stream Sediments	Shallow sea Sediments	
Literatures	A	B, C	A	B, C	B, C	B, C	B, C	B, C	B, C	B, C	A	B, C	B, C	D	B, C	E	F		
N		1249 (693)	198 (130)	184 (128)	91 (73)	425	210	207	201	82	77	149	38	2718	517	154	44422	286	
n		10458 (6665)	1523 (1287)	1756 (1060)	503 (387)	5720	2027	2708	1786	901	628	1571	400	28253					
SiO <sub>2</sub>	0.05	70.85	57.79	48.68	45.11	72.63	60.63	6.49	65.63	66.89	49.72	63.22	8.09	60.62	66.00	65.0	64.74	62.23	
TiO <sub>2</sub>		0.295	0.868	1.578	0.385	0.485	0.761	0.053	0.510	0.507	1.238	0.688	0.044	0.667	0.72	0.72	0.74	0.58	
Al <sub>2</sub> O <sub>3</sub>	0.05	14.20	16.42	15.54	4.69	10.91	16.35	1.14	14.84	14.47	13.72	16.11	0.96	14.83	13.51	12.6	12.73	10.67	
TFe <sub>2</sub> O <sub>3</sub>	0.01	2.98	7.58	11.26	10.41	3.66	5.89	0.70	5.03	4.56	12.74	6.09	0.62	6.53	4.70			4.4	
Fe <sub>2</sub> O <sub>3</sub>		1.22	2.98	4.18	3.85	2.46	4.33	0.35	2.03	2.23	4.38	3.06	0.26	2.45	3.89				
FeO	0.1	1.60	4.18	6.44	5.96	1.09	1.42	0.32	2.73	2.12	7.60	2.75	0.33	3.71	0.74	1.2			
MnO		0.049	0.124	0.167	0.119	0.057	0.059	0.044	0.075	0.068	0.207	0.067	0.045	0.105	0.09	0.08	0.09	0.07	
MgO	0.05	0.94	3.60	7.50	26.98	1.26	1.86	6.53	2.15	1.94	7.35	2.08	10.56	3.16	1.57	1.8	1.56	1.81	
CaO	0.01	1.83	5.81	9.02	7.40	2.52	2.66	42.84	3.26	2.70	9.11	1.59	39.14	5.41	2.91	3.2	2.87	5.19	
Na <sub>2</sub> O	0.1	3.52	3.77	2.80	0.62	1.41	0.80	0.10	3.64	3.19	2.48	1.30	0.11	3.45	1.63	1.6	1.37	2.18	
K <sub>2</sub> O	0.02	4.00	2.09	1.18	0.26	2.40	3.45	0.34	2.87	2.88	1.00	3.90	0.23	2.31	2.47	2.5	2.40	2.23	
P <sub>2</sub> O <sub>5</sub>		0.099	0.275	0.343	0.069	0.094	0.124	0.037	0.163	0.124	0.190	0.110	0.034	0.172	0.10	0.12	0.15	0.12	
H <sub>2</sub> O <sup>+</sup>	0.2	1.07	1.49	1.70	3.25	2.56	4.56	0.74	1.34	1.88	2.10	3.26	1.02	1.50	3.9	4.2			
CO <sub>2</sub>	0.01	0.32	0.38	0.45	0.55	1.72	2.15	40.45	0.31	0.38	0.40	1.02	38.72	1.15	2.0	2.7		4.00	
Corg	0.01					(0.20)	0.38	0.20				0.38		0.34	(0.35)			0.62	
Ag	0.02	0.060	0.053	0.056	0.046	0.052	0.050	0.056	0.057	0.060	0.053	0.054	0.042	0.055	0.072	0.080	0.094	0.063	
As	0.1	1.7	1.7	1.8	1.1	5.0	7.8	3.2	1.3	1.8	1.6	7.2	2.5	2.4	10	10	13.3	7.7	
Au	0.05	0.53	0.85	0.80	0.80	1.0	1.4	0.47	0.65	0.88	1.2	1.1	0.42	0.90	1.6	1.4	2.0	1.1	
B	1	6.2	5.7	7.5	7.0	38	76	13	5.5	15	10	72	6.0	11	48	40	51	58	
Ba	20	700	775	460	90	525	590	63	850	740	260	665	155	620	565	500	520	410	
Be	0.1	2.7	0.91	0.50	0.15	1.6	2.3	0.60	1.4	1.9	0.4	2.3	0.54	1.4	2.3	1.8	2.3	2.0	
Bi	0.05	0.24	0.090	0.085	0.090	0.18	0.34	0.070	0.090	0.14	0.11	0.29	0.064	0.15	0.31	0.30	0.50	0.33	
Br	0.2	(0.2)	(0.3)	(0.4)	(0.4)	(0.3)	(0.4)	(0.5)	(0.2)	(0.2)		(0.3)	(1.0)	(0.25)	2.6	(3.5)		15	
Cd	0.01	0.060	0.092	0.10	0.080	0.081	0.11	0.13	0.070	0.090	0.12	0.080	0.096	0.082	0.118	0.090	0.26	0.065	
Cl	20	58	140	112	120	51	52	124	107	80	164	54	68	112	136	68		3400	
Co	0.2	4.8	22	46	88	8.0	14	1.5	13	11	49	13	1.6	19	13	13	13	12	
Cr	0.5	12	83	190	1630	39	72	7.5	53	48	240	70	5.5	76	65	65	68	60	

Continued

Element	Detection limits	Whole China				Eastern part of China									Whole China			
						Rocks									Soils		Sediments	
		Acidic rock	Intermediate rock	Basic rock	Ultramafic rock	Sandstone	Shale	Carbonate	Gneiss	Leptite	Amphibolite	Metapelite	Marble	Continental crust	Alluvial plain soil	Soil	Stream sediment	Shallow sea sediment
Cs	0.3	3.5	1.9	1.4	0.45	4.3	8.2	0.5	1.8	3.0	1.0	7.2	0.46	2.0	7.5	7.0		6.3
CU	1	8.0	30	55	27	15	29	4.0	22	22	58	26	4.0	26	23	24	26	15
F	50	490	650	485	385	405	775	275	570	510	740	705	310	540	510	480	530	480
GA	1	18.0	20.0	19.9	8.9	13.6	20.5	1.7	18.7	18.4	18.7	21.2	1.6	19	15.7	17.0		14
GE	0.1	1.2	1.1	1.1	0.90	1.4	1.6	0.35	1.0	1.2	1.4	1.7	0.3	1.2	1.4	1.3		
HF	0.2	5.0	4.6	3.5	1.0	5.5	5.8	0.34	4.8	5.2	2.6	5.6	0.29	4.5	8.5	7.4		6.0
HG	2	6.6	6.9	7.8	6.0	15	27	18	6.0	6.7	8.5	11	9.0	7.0	25	40	69	25
I	0.1	(0.05)	(0.13)	(0.1)	(0.15)	(0.1)	(0.4)	(0.2)	(0.05)	(0.05)		(0.1)	(0.14)	(0.1)	2.2	(2.2)		18
IN	0.01	(0.05)	(0.06)	(0.07)	(0.03)	(0.035)	(0.07)	(0.02)	(0.05)	(0.045)	(0.07)		(0.045)	0.054	(0.055)		0.09	
IR	3	(3)	(17)	40	(1350)	18	20	7	(30)	22	(85)	(28)	(6)	(20)		22		
LI	1	19	13	11	4	25	38	9	14	19	11	34	9	17	36	30	34	38
MN	5	380	960	1310	920	440	460	340	580	530	1600	520	350	810	705	600	730	530
Mo	0.1	0.70	0.58	0.63	0.21	0.54	0.93	0.57	0.49	0.50	0.28	0.52	0.36	0.50	0.57	0.80	1.1	0.50
N	10	28	72	80	(50)	170	460	120	37	55	20	222	55	60	440	640		620
NB	1	15	10.4	19	5.2	12	18	(2)	10	12	9	15	(3.4)	10	15.5	16	17	14
Ni	1	7.7	34	100	960	17	34	4.8	24	20	96	29	3.8	31	30	26	29	24
Os	6	(15)	(36)	60	(1300)	32	140	50	35	34	(140)	(50)	27	(40)		40		
P	5	430	1200	1570	310	410	540	160	710	540	830	480	150	750	475	520	655	500
Pb	2	24	15.5	13	8	18	23	8	16	18	12.3	19	8.6	15	23	23	29	20
Pd	0.1	(0.08)	0.42	0.63	2.6	0.30	0.78	(0.16)	0.42	0.50	2.2	0.58	(0.16)	0.75	0.52	0.65		
PT	0.1	(0.06)	0.42	0.72	5.2	0.26	0.50	(0.12)	0.44	0.50	2.6	0.44	(0.15)	0.80	0.48	0.50		
RB	2	140	58	31	7	78	130	9	82	95	29	140	7	70	107	100		96
RE	0.1	(0.25)					(1.4)		(0.4)					(0.1)		(0.1)		
RH	3	(4)	(45)	60	(800)	12	25	4	28	26	150	25	(4)	(40)		17		
RU	4	(7)	(12)	65	(3500)	28	58	15	30	27	(230)	45	(15)	(35)		60		
S	20	120	180	280	210	220	300	240	200	150	270	210	160	250	160	150		510
Sb	0.05	0.16	0.17	0.18	0.14	0.43	0.58	0.24	0.12	0.22	0.14	0.45	0.23	0.18	0.79	0.80	1.42	0.5
Sc	0.1	5.3	19	29	24	8.3	15	1.3	11	9.7	39	16	1.1	17	11	11		10
SE	0.01	0.033	0.058	0.085	0.050	0.073	0.17	0.070	0.060	0.065	0.11	0.12	0.040	0.070	0.10	0.20		0.15
SN	0.2	2.0	1.3	(1.0)	(0.5)	1.6	3.0	0.5	1.2	1.9	1.1	3.1	0.5	1.4	3.1	2.5	4.1	3.0

Continued

Elements	Detection limits	Whole China				Eastern part of China										Whole China			
		Rocks													Continental crust	Soils		Sediments	
		Acidic rock	Intermediate rock	Basic rock	Ultramafic rock	Sandstone	Shale	Carbonate	Gneiss	Leptite	Amphibolite	Metapelite	Marble	Alluvial plain soil		Soil	Stream sediment	Shallow sea sediment	
Sr	2	250	565	510	115	120	110	320	390	265	240	95	225	350	175	170	165	230	
Ta	0.2	1.2	0.56	1.1	0.26	0.76	1.2	(0.1)	0.54	0.7	0.47	1.0	0.080	0.65	1.17	1.1		1.0	
Te	10	(5)	(15)	(10)		(10)	(15)	(5)	(10)			(15)		(6)	40			40	
Th	0.2	14.5	4.9	2.8	0.70	9.2	14	1.1	7.0	8.6	1.5	12.5	0.90	6.0	12	12.5	13.5	11.5	
Ti	10	1770	5200	9470	2650	2910	4560	320	3060	3040	7420	4125	265	4000	4175	4300	4460	3500	
Tl	0.1	0.73	0.36	0.24	0.15	0.51	0.68	0.14	0.47	0.54	0.23	0.76	0.16	0.42	0.66	0.60		0.30	
U	0.2	2.5	1.15	0.70	0.35	2.1	3.1	1.2	1.05	1.45	0.50	2.5	0.77	1.3	2.3	2.7	3.1	1.9	
V	5	33	135	210	110	60	115	13	70	71	260	103	12	112	87	82	87	70	
W	0.2	0.85	0.47	0.50	0.3	1.1	1.7	0.27	0.41	0.72	0.44	1.8	0.56	0.6	1.7	1.8	2.7	1.5	
Zn	2	45	90	110	78	51	80	18	65	65	120	88	18	76	64	68	77	65	
Zr	2	160	180	150	50	195	210	16	175	185	110	200	13	160	250	250	295	210	
Y	0.5	22	18	17	7.0	18	27	4.8	16.5	20	17	26	3.1	17	26	23	26	22	
La	0.2	40	35	24	6.7	34	50	5.5	38.5	37	14	43	5.4	29	37	38	41	33	
Ce	0.5	75	68	47	15.0	63	88	10.3	75	68	28	78	10	57	58	72		67	
Pr	0.2	7.8	7.8	5.3	2.0	6.9	9.8	1.2	8.2	7.6	3.7	8.7	1.2	6.5	7.0	8.2			
Nd	3	30	34	24	7.2	28	40	4.6	32	31	16	37	4.5	26	27	32		29	
Sm	0.1	5.3	6.1	5.1	2.0	5.0	7.2	0.95	5.3	5.4	3.9	6.8	0.80	4.9	5.2	5.8		5.6	
Eu	0.05	0.90	1.7	1.8	0.67	1.05	1.4	0.21	1.3	1.2	1.4	1.4	0.20	1.3	1.1	1.2		1.0	
Gd	0.1	4.9	5.4	4.7	1.7	4.5	6.2	0.88	4.4	4.6	4.3	6.0	0.70	4.3	4.5	5.1			
Tb	0.1	0.72	0.82	0.80	0.39	0.72	1.0	0.13	0.67	0.70	0.71	0.96	0.11	0.69	0.73	0.80		0.73	
Dy	0.1	4.4	4.5	4.3	1.8	3.9	5.8	0.69	3.7	3.7	4.4	5.4	0.55	3.7	3.9	4.7			
Ho	0.03	0.90	0.90	0.85	0.35	0.77	1.2	0.15	0.77	0.77	0.85	1.1	0.11	0.77	0.92	1.0			
Er	0.05	2.6	2.4	2.2	1.0	2.2	3.2	0.42	2.1	2.3	2.6	3.2	0.28	2.2	2.4	2.8			
Tm	0.02	0.39	0.35	0.32	0.16	0.35	0.49	0.065	0.31	0.34	0.90	0.50	0.038	0.34	0.42	0.42			
Yb	0.2	2.4	2.2	1.9	0.99	2.1	3.0	0.42	1.9	2.1	2.4	3.1	0.25	2.2	2.4	2.6		2.2	
Lu	0.02	0.38	0.34	0.31	0.16	0.33	0.47	0.065	0.30	0.33	0.37	0.48	0.035	0.33	0.39	0.40		0.34	

EC: the eastern part of China. Concentration units: major components: %; Au, Hg, Pd, Pt, Re and Te: ppb; Ir, Os, Rh, and Ru: ppt; other elements: ppm.

Literatures: A: Chi & Yan (2007); B: Yan & Chi (1997); C: Yan & Chi (2005); D: Zhu et al. (2006); E: Ren et al. (1998); F: Zhao & Yan (1994)

The number of composite samples for analysis is indicated as "N" and the number of collected individual rock samples is indicated as "n". The number of data without brackets is for major elements, while that with brackets is for trace elements; and those without brackets for the both mean that they are the same. The data of element abundance with brackets in the table are for reference.

Elemental bundance of intermediate rocks in China is average of dioritoids and andesitoids; Elemental bundance of metapelite in the eastern part of China is average of slate, phyllite and micaceous schist.



## **CSIRO Exploration and Mining: the challenge of being pure, applied and relevant**

**John L. Walshe<sup>1</sup>**

*1CSIRO Exploration and Mining, PO Box 1130, Bentley, WA 6102 AUSTRALIA  
(e-mail: john.walshe@csiro.au)*

**ABSTRACT:** CSIRO Exploration and Mining is addressing practical challenges of mineral exploration in the modern era, particularly in Australia. This paper documents some of the scientific opportunities provided by these challenges and some of the progress made. A fundamental problem is to understand “Why the deposit is there and not there?” CSIRO has partnered with Geoscience Australia, state government surveys, universities and industry to develop a mineral systems approach (termed the “Five Questions”) to understanding what controls the location of major resources. The Embedded Researcher is one concept trialled in the Eastern Goldfields, WA, as a mechanism to promote the real-time transfer of concepts, data and promote the uptake of R and D in exploration.

**KEYWORDS:** *exploration, mineral systems, embedded researchers*

### **INTRODUCTION**

Established as the Council for Scientific and Industrial Research (CSIR) in 1926, CSIRO is Australia's national science agency. CSIRO's goals are the pursuit of innovative science and application for industry, society and the environment.

The roots of CSIRO's Division of Exploration and Mining can be traced to the mineragraphic work of Stillwell and Edwards in the 1930s. They provided services directly to exploration, mining and processing companies. Research and development activities spread across the fields of mineralogy, geochemistry and geophysics through the 1960s and 1970s as CSIRO engaged with Australia's expanding minerals industry. A focus on practical outcomes and a willingness to collaborate with industry from the detail of the early exploration stage through to the mining of resources continues with the Minerals Down Under (MDU) initiative. Launched in 2007, MDU is a cross-divisional national flagship enterprise that aims to help sustain and transform the Australian minerals industry with new technologies and ideas through the 21<sup>st</sup> Century.

### **THE CULTURAL DRIVERS**

The close engagement with and direct funding from industry means CSIRO Exploration and Mining operates differently from Geoscience Australia (GA), the national geoscience agency, state government surveys and most, if not all, equivalent agencies around the globe. Engagement with industry has focused on development of new exploration technologies and methodologies, rather than as a provider of pre-competitive data. CSIRO Exploration and Mining has evolved a scientific culture that aims to balance short term practical goals with long terms research goals. Arguably, the most significant catalyst of cultural change within CSIRO was the external earning targets introduced in the early to mid 1980s. The MDU flagship has a projected life through to 2025 and an external earnings target of about 40% of revenue.

The challenge of sustaining long term scientific development while contributing practical outcomes in the near term, in tandem with aggressive external earnings targets, is not only driving internal collaboration between a diverse range of scientific disciplines but also external partnerships with other government agencies, the university sector and

industry. Numerous competitive funding vehicles have been developed over the last two decades by both state and commonwealth governments to encourage cross - institutional R and D. The most significant of these has been the Cooperative Research Centres (CRC) program established by the Australian Commonwealth Government in 1990 to encourage collaboration in R and D between the public and private sector, as well as support world-class research teams and prepare PhD students for non-academic careers.

### **THE PRACTICAL CHALLENGES OF MINERAL EXPLORATION IN THE MODERN ERA**

The challenges of mineral exploration have been widely commented upon in recent times: falling rates of discovery despite increased exploration expenditure, application of a wide range of new science and technology, and unparalleled access to most parts of the globe (Etheridge 2004). In the Australian context, the problems are compounded by perceptions of maturity of mineral fields and the difficulties of exploration under cover. Neil Williams, Director of Geoscience Australia and SEG President for 2008, commented that over the last century we have become very skilled at describing mineral deposits and their genesis, but there is a growing need for research on why known ore deposits occur where they do, and where they do not (Williams 2008). Explorers targeting to depth will be focusing on large high-grade deposits. The research emphasis needs to be the elucidation of the controls on the size and grade of deposits and importantly, their distribution with depth.

The CRC program provided the R and D vehicle to bring together the multi-disciplinary teams across academe and industry to address the fundamental science issues underpinning the question of "Why is the deposit there and not there?" (Jon Hronsky, circa 1998). Inspired by work in the oil industry in the 1980s, the AGCRC (Australian Geodynamics CRC) followed closely by

the *pmd*\*CRC (Predictive Mineral Deposits CRC) worked on developing mineral systems concepts with genuine predictive capacity at any scale. Concurrently, CRC LEME (CRC for Landscape Evolution (later, Environments) and Mineral Exploration) set out to determine the influence of regolith - landscape evolution on mineral exploration; a particularly pertinent problem for explorers in Australia that complemented efforts to better understand the workings of the primary mineral systems. CSIRO Exploration and Mining partnered with Geoscience Australia, state government surveys, universities and industry in developing the cutting-edge science programs to underwrite these endeavours for over a decade and a half.

### **GETTING MORE SCIENCE INTO EXPLORATION: THE MINERAL SYSTEMS PERSPECTIVE**

Traditional exploration strategies focus on finding a proxy for the deposit. The aim is to find geological, geochemical or geophysical anomalies that allow the deposit "to be seen" at a scale somewhat larger than the deposit. The mineral systems methodology aims to focus less on finding proxies for the deposit and more on understanding the critical parts of mineral systems, such as sources of fluids and flow paths, learning to read the rock record for their presence and using that knowledge to direct exploration. From the R and D perspective, in addition to having a robust geological description of the mineral system, there needs to be a numerical view of the system for the purposes of testing and quantifying geological thinking and an exploration view of the system that distils the exploration implications from the geological and numerical descriptions. The geological, numerical and exploration descriptions could be thought of as different but equivalent views of the mineral system.

The 'Five Questions' geological description of a mineral system adopted by the AGCRC and the *pmd*\*CRC (Price & Stoker 2002; Walshe *et al.* 2005) explicitly

highlights the problem of understanding the system in space and the temporal evolution of the system at all scales. Questions 1 and 2 'What is the geodynamic/thermal history of the system' and 'What is the architecture and size of the system?' ensure the issues of 'source(s) of fluids (melts)', 'transport' and 'depositional sites' are addressed within the context of an understanding of the architectural and geodynamic history of the whole system, taking account of information from the deposit to the terrane scale. For systems in which the metal is transported in solution (melt), the mathematical description highlights the importance of physico-chemical gradients to sustain metal transport and promote deposition. From work on Archean gold deposits in the Yilgarn Craton, WA, it seems that understanding the system at the deposit to district scale is mostly a problem in mapping critical fluid pathways and recognising where in the architecture (2 or 3D) fluids have interacted to maximize the key physico-chemical gradients determining Au precipitation. Some judicious combination of geochemical, geophysical, and mineralogical data sets is required to map fluid pathways. Hyperspectral logging is proving a powerful tool for the rapid acquisition of data on mineral distribution.

#### POST SCRIPT

It transpires that getting more science into exploration will require a bit more than a few enthusiastic researchers working with some equally enthusiastic explorers. Technology and concept transfer across the academe – industry interface is a complex, two-way process that is at least as challenging as the science itself. One of the more novel approaches to bridging the divide has been the embedding of researchers within companies to promote the real-time transfer of concepts, data and promote the uptake of R and D in exploration. The health of the interface is

as dependent on supportive and informed managements as it is on those ever-green enthusiastic practitioners. The re-emergence of the bust phase of the boom-bust resources cycle means a testing time for both.

It is the wisdom of the modern era that government funding from "special pots" comes with sunset clauses. Sunset for *pmd*\*CRC and CRC LEME came in 2008. Was sufficient progress made in the allotted time to really make a difference? Will the messages from these CRC programs have a lasting impact on exploration practice? Will the mineral exploration R and D cycle be reinvigorated? The business of being pure, applied and relevant remains a challenge.

#### ACKNOWLEDGEMENTS

In preparing this paper comments by Drs. Charles Butt and Graham Carr, two colleagues with much experience of the various guises of CSIRO Exploration and Mining, were much appreciated.

#### REFERENCES

- ETHERIDGE, M.A. 2004. Research, exploration and predictive mineral discovery: SEG2004: *Predictive Mineral Discovery Under Cover*, Extended Abstracts, Perth, 31p.
- PRICE, G.P. & STOKER, P. 2002. Australian Geodynamics Cooperative Research Centre's integrated research program delivers a new minerals exploration strategy for industry : *Australian Journal of Earth Sciences*, **49**, 595-600.
- WALSHE, J.L., COOKE, D.R., & NEUMAYR, P. 2005. Five questions for fun and profit: A mineral systems perspective on metallogenic epochs, provinces and magmatic hydrothermal Cu and Au deposits. In MAO, J. & BIERLEIN, F. P. (eds.), *Mineral Deposit Research: Meeting the Global Challenge*, **1**, 477-480.
- WILLIAMS, N. 2008. Presidential perspective: The Exploration Crisis – An Industry Perspective. *SEG Newsletter*, **73**, 7p.



## Determination of platinum and palladium for geochemical mapping

Yao Wensheng<sup>1,2</sup>, Yan Hongling<sup>3</sup>, Sun Aiqin<sup>3</sup>, & Wang Xueqiu<sup>1,2</sup>

<sup>1</sup>*Institute for Geophysical and Geochemical Exploration (China), 84 Jinguang Road, Langfang, Hebei Province 065000 CHINA (e-mail: Yaows68@yahoo.com.cn)*

<sup>2</sup>*Key Laboratory of Applied Geochemistry, Chinese Academy of Geological Sciences, 84 Jinguang Road, Langfang, Hebei Province, 065000 CHINA*

<sup>3</sup>*Geoanalysis Laboratory of Henan Province, 28 Jinshui Road, Zhengzhou, 450012 CHINA*

**ABSTRACT:** A procedure including chemical pre-concentration, determination by emission spectrometry or inductively coupled plasma-mass spectrometry, and quality control was developed for platinum and palladium analysis for geochemical mapping samples. Application in multi-scale geochemical mapping projects indicates that: (1) the detection limits, data accuracy and precision can meet the analytical requirements; (2) a sub-sample weight of 10 g is suitable for national- and global-scale geochemical mapping; and (3) sub-sampling errors caused by “nugget effects” could be effectively controlled by the quality control system through the duplicate or triplicate determinations of doubtful samples with relatively high PGE contents.

**KEYWORDS:** *Analysis, Nugget effects, ICP-MS, Sub-sampling, Quality Control*

### INTRODUCTION

Geochemists have a fascinating dream for mapping the whole earth with all elements in periodic table (Wang *et al.* 2006). However many ultra-trace elements such as Platinum Group Elements (PGE) are difficult to determine accurately and precisely. The average concentration of Pt and Pd in most geochemical mapping samples is extremely low, at less than 1 ppb. The detection limits should be below their crustal abundance in order to produce informative geochemical maps (Xie 1995; Xie, Wang *et al.* 2008). The “nugget effect” is another obstacle for the accurate determination of Pt and Pd. Consequently, the complicated chemical pre-concentration steps and sub-sampling are two major sources of error. A procedure of chemical pre-concentration, emission spectrometry (ES) or inductively coupled plasma-mass spectrometry (ICP-MS), and analytical quality control system has been developed for geochemical mapping projects (Wilhelm *et al.* 1997; Yao *et al.* 2003) and more than 50,000 samples have now been analysed using this approach. In this paper, the procedure and its application in multi-scale geochemical mapping projects are

discussed.

### ANALYTICAL METHOD

A 10 g sample is roasted at 650°C and decomposed with hydrochloric acid/hydrogen peroxide. The Pt and Pd in the solution is pre-concentrated using adsorbent materials which are composed of active charcoal and anion resin. The adsorbent materials are washed sequentially with 2% ammonium bifluoride, 5% hydrochloric acid and distilled water, and subsequently ashed in a muffle furnace at 650°C. The total residue of ca. 0.25 mg is dissolved with 2 ml fresh aqua regia, then diluted to 5ml using 10% hydrochloric solution, and determined using ICP-MS, which has a detection limit of 0.2 ppb for Pt and Pd. The residue can also be mixed with a spectral buffer, and determined by DC-arc ES, which has detection limits of 0.3 ppb for Pt and 0.2 ppb for Pd.

### QUALITY CONTROL

#### Reference Materials

The certified reference materials (GPT CRMs) are used for quality control (Yan *et al.* 1998; Gu *et al.* 2007). GPt-1, GPt-2, GPt-7 and GPt-8 are suitable for analytical

quality control in national and global geochemical mapping projects. For local geochemical exploration, use of the GPt CRMs depends on the style of mineralization and PGE contents (Table 1).

### Quality Control Method

A set of CRMs, approximately equal to 5% of the samples, are inserted in each batch of 100 samples during routine analysis.

The relative error (RE%) is used to monitor the between-batch or between-map bias:

$$RE\% = [(C_d - C_s) / C_s] \times 100\%$$

where  $C_d$  is the determined value,  $C_s$  is the standard reference value.

The tolerance of RE% is listed in Table 2. If the RE% results are beyond these limits, analysis of the batch should be repeated.

5-10% samples are randomly selected and coded for duplicate analysis.

The relative deviation (RD%) is used for monitoring sub-sampling error:

$$RD\% = [(C_{d1} - C_{d2}) / C_{d1,2}] \times 100\%$$

where  $C_{d1}$  is the determined value,  $C_{d2}$  is duplicate analysis value, and  $C_{d1,2}$  is the mean of  $C_{d1}$  and  $C_{d2}$ .

The tolerance in RD% is listed in Table 2. If the RD% is beyond these limits, duplicate or triplicate determinations should be undertaken for the doubtful samples.

For local exploration, samples with relative higher PGE contents, about 5% of the total, are selected for the duplicate determination to monitor sub-sampling error.

## RESULTS AND DISCUSSION

### Applications in Geochemical Mapping

The analytical approach and quality control system has been successfully applied in geochemical mapping projects. During the past 15 years, approximately 50,000 samples have been analysed for Pt and Pd. Some examples of applications are as follows:

**Table 1.** PGE reference materials

RM	10 <sup>-9</sup>		Sample type
	Pt	Pd	
GPt-1	0.26	0.26	Soil
GPt-2	1.6	2.3	Stream sediment
GPt-3	6.4	4.6	Peridotite
GPt-4	58	60	Pyroxene peridotite
GPt-5	20	11.3	Chromite
GPt-6	440	570	Low grade ore
GPt-7	14.7	15.2	Soil
GPt-8	0.66	0.66	Soil

**Table 2.** Tolerance of accuracy

Content (ppb)	RE(%)	RD (%)
<1.0	100	100
1~30	66.6	66.6
>30	50.0	50.0

Regional-scale: Pt and Pd mapping of the Bushveld Complex, South Africa (density 1 sample per 1 km<sup>2</sup>) (Wilhelm *et al.* 1997, Lombard *et al.* 1999, Yao *et al.* 2003).

National-scale: The 76-element geochemical mapping pilot project in southwestern China (1 composite sample per 400 km<sup>2</sup>) (Xie, Cheng *et al.* 2008).

Global-Scale: The EGMON project as pilot global geochemical mapping (1 sample per approx. 15 000 km<sup>2</sup>) (Cheng *et al.* 1998; Xie *et al.* 2001).

### Sub-Sampling Errors

The “nugget effect” causes sub-sampling errors in PGE determinations. Previously, large sub-samples (30 g) of all samples were analyzed to decrease sub-sampling errors. This is not cost-effective. Our new approach is: *firstly*, a 10 g sub-sample is used for the routine analysis of all samples; *secondly*, samples with anomalous values are selected for duplicate or triplicate determinations, and the average value of these determinations is considered trustworthy. The selection of these samples is mainly based on the Pt/Pd ratio, statistics of RD% of coded duplicate analyses and total batch data distributions.

Results of the analysis of 105 samples determined from a 10 g sub-sample by the authors' methods and from a 30 g sub-

sample by fire assay ICP-MS in another laboratory are compared in Figure 1. This shows that analysis of a 10 g sub-sample by our analytical and quality control procedure can give as good results as methods using a 30 g sub-sample.

**Accuracy of CRM Analyses**

240 CRMs were inserted into the approximately 3000 samples in the 76-element geochemical mapping pilot project in southwestern China. The RSD% of these determinations and the certified values are listed in Table 3. All the RSD are less than 25% and the analytical data are considered accurate. Data accuracy had also been subsequently justified from the mapping results.

**CONCLUSIONS**

- (1) The detection limits for Pt and Pd can meet the analytical requirements for geochemical mapping.
- (2) A sub-sample weight of 10 g is suitable for national- and global-scale geochemical mapping.
- (3) Sub-sampling errors caused by the

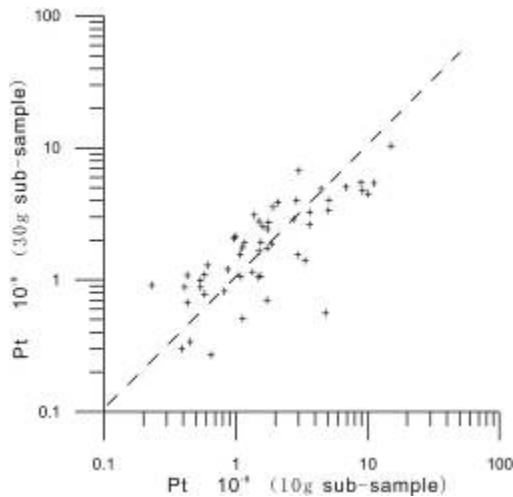


**Fig. 1.** Comparison of analyses using 10 g and 30 g sub-samples

**Table 3.** RSD (%) of CRMs

RM	Pt	Pd
GPt-1	14.58	18.30
GPt-8	21.41	15.03
GPt-2	14.90	13.29
GPt-7	7.03	6.83

PGE “nugget effect” is effectively controlled by duplicate or triplicate determinations of samples with relatively high PGE contents.

**ACKNOWLEDGEMENTS**

Many thanks are given to the geoanalysts at the Henan Geoanalysis Laboratory, particularly for Prof. Chen Fanglun, who had made great contribution to development of the Pt and Pd analytical methods. Thanks are given to the China Geological Survey and the Ministry of Science and Technology for financial support (Projects: Sinoprobe04, and 2007CB411406).

**REFERENCES**

CHENG, H.X., XIE, X.J., & YAN, G.S. 1998. Platinum and palladium abundances in floodplain sediments and their geochemical provinces. *Chinese journal of Geochemistry*, **27**, 101-106.

GU, T.X., SHI, C.Y., PU, W., YAN, W.D., LIU, M., & YAN, M.C. 2007. New Progress on Certified Reference Materials for Platinum-Group Elements: IGGE GPt-8, GPt-9 and GPt-10. *Geostandards and Geoanalytical Research*, **31**, 1-8.

LOMBARD, M. DE BRUIN, D., & ELSENBROEK, J.H. 1999. High-density regional geochemical mapping of soils and stream sediments in South Africa. *Journal of Geochemical Exploration*, **6**, 145-149.

WANG, X.Q. XU, S.F., CHENG, Z.Z., LIU, H.Y., & SHI, S.J. 2006. Progress on international geochemical mapping. *Acta Geological Sinica*, **80**, 1598-1606.

WILHELM, H.J. ZHANG, H. CHEN, F.L. ELSENBROEK, J.H. LOMBARD, M., & DE BRUIN, D. 1997. Geochemical exploration for platinum-group elements in the Bushveld Complex, South Africa. *Mineralium Deposita*, **32**, 349-361.

XIE, X.J. 1995. Analytical requirements in international geochemical mapping. *Analyst*, **120**, 1497-1504.

XIE, X.J. & CHENG, H.X. 2001. Global geochemical mapping and its implementation in Asia-Pacific Region. *Applied Geochemistry*, **16**, 1309-1321.

XIE, X.J., CHENG, Z.Z., ZHANG, L.S., FENG, J.ZH., YE, J.Y., & ZHU, Y.S. 2008. *76 elements geochemical maps in southwestern China*. Geological Publishing House, Beijing.

XIE, X.J., WANG, X.Q., ZHANG, Q., ZHOU, G.H., CHENG, H.X., LIU, D.W., CHENG Z.Z., & XU,

- S.F. 2008. Multi-scale Geochemical Mapping in China. *Geochemistry: Exploration, Environment, Analysis*, **8**, 1-9.
- YAO, W.S., SUN, A.Q., & LIU, Y.C. 2003. Recent development in PGE determination for geological samples. In: ZHOU J.S. (ed.), *Essays in Memory of 50 years of Geoanalysis work in China*. Geological Publishing House, Beijing, 446-462.
- YAN, M.C., WANG, CH.S., GU, T.X., Chi, Q.H., & Zhang, Z. 1998. Platinum-group element geochemical certified reference materials (GPT1-7). *Geostandards Newsletter: The Journal of Geostandards and Geoanalysis*, **22**, 235-246.

## 76 elements geochemical mapping in Southwest China

Zhizhong Cheng<sup>1</sup> & Xuejing Xie<sup>1</sup>

<sup>1</sup>*Institute of Geophysical and Geochemical Exploration, Jinguang Road, Langfang, Hebei, 065000 CHINA  
(e-mail: zhizhong9@yahoo.com.cn)*

**ABSTRACT:** Southwest China's 76 elements geochemical mapping project was initiated in 2000. 2700 composite samples from the 1000,000 RGNR supplement samples were prepared. The 76 elements analytical system using modern analytical instruments such as ICP-MS, XRF, ICP-AES as backbone, supplemented with other techniques was established. The geochemical maps provided the distribution of all the elements in the periodic table.

**KEYWORDS:** 76 elements, geochemical mapping, analytical Scheme,

### INTRODUCTION

In 1973, J.S. Webb (Webb *et al.* 1973, 1978) published the first geochemical atlas "Provisional Geochemical Atlas of Northern Ireland". From 1973 to now, more than 40 regional and national geochemical mapping projects (Reedman 1973; Bowie & Plant 1978a,b; Bolivar 1980; Geological Survey of Canada 1981; Stephenson *et al.* 1982; Weaver *et al.* 1983; Freeman *et al.* 1983; Fauth *et al.* 1985; Bolviken 1986; Koljonen *et al.* 1989; Simpson 1993; Varna *et al.* 1997; Laszlo *et al.* 1997; Reimann *et al.* 1998; Salminen 2005; De Vos & Tarvainen 2006) were carried out.

China's national geochemical mapping project, the "Regional geochemistry-National Reconnaissance (RGNR) Project" was initiated in 1978 (Xie 1977, 1978, 1989). 39 elements were determined by multi-method analytical system. Environmental geochemical monitoring networks (EGMON Project) (Xie & Cheng 1997) was carried out in 1993, 54 elements were analyzed 54 by the new analytical system. In 2000, the 76 elements geochemical mapping was carried in Southwest China.

### SAMPLE COLLECTION AND COMPOSITION

The RGNR project in Yunan, Guizhou Sichuan and Guangxi provinces were started in 1980, and finished in 1995. All

the supplement ones of stream sediment samples for the project were kept in very good condition. About 100 RGNR supplement samples within each 1:50000 map sheet were mixed and composite into 1 samples. 2700 composite samples were submitted for analysis.

### MULTI-ELEMENT ANALYTICAL SCHEME

The 76 elements are analyzed, including the 39 elements originally analyzed in analyzed in RGNR Projects and 37 elements newly added. The 76 elements analytical system were established using ICPMS, ICPAES and XRF as backbone, supplemented with other techniques (Table 1). The Detection limits of all trace and subtrace elements are lowered below their crustal abundance (Table 2). The log deviation are  $\Delta \log C \leq 0.1$ , standard deviation (SD) is between 10%~30%.

### GEOCHEMICAL MAPS FOR 76 ELEMENTS

All of geochemical analytical data for the reasearch area are loaded in GeoMDIS system with Excel format. The geochemical maps are generated by data which are gridded by using data-gridding function of GeoMDIS. 76 elements geochemical maps were generated by GeoMDIS.

The 76 elements geochemical maps show the distribution of all elements in the periodic table, especial for rare and dispersive and precious metals elements.

**Table 1.** The analytical system for 76 elements.

analytical method	elements
XRF	Si, Al, Fe, Mg, Ca, Na, K, Ba, Ce, Co, Cr, Cu, Ga, La, Mn, Nb, Ni, P, Pb, Rb, S, Sc, Sr, Th, Ti, V, Y, Zn, Zr, Cl, Br
ICP-MS	Pr, Nd, Sm, Eu, Gd, Tb, Dy, Ho, Er, Tm, Yb, Lu Be, Bi, Ce, Co, Cs, Cu, Ga, In, La, Mo, Nb, Ni, Pb, Rb, Sb, Th, U, W, Y, Zn, Tl, Ta, Hf, Re Te
ICP-AES	Na, Mg, Al, K, Ca, Fe, Ba, Be, Co, Cr, Cu, Li, Mn, Ni, P, Sr, Ti, V, Zn
GF-AAS	Ag, Au
HG-AFS	As, Sb, Se, Ge
CV-AFS	Hg
SIE	F
ES	Ag, B, Sn,
VOL	C, N,
CF-COL	I
FA-POL	Ir,Rh
FA-ES	Pt, Pd
FA-COL	Os, Ru

Fig.1 show that a Giant Pt geochemical anomaly is distributed over north Yunnan and southwest Sichuan about 60000km<sup>2</sup>. Three large and 2 small In geochemical anomaly areas are delineated in the researched region (Fig. 2). The In anomaly area is of great ore-finding potentialities. A strong Hf anomaly was delineated in Lincang of Yunnan province(Fig. 3). The Hf anomaly zone coincides with the Lincang granitoids area.

**CONCLUSIONS**

The earth is constructed by all elements in the periodic table. Mapping of the spatial distribution of nearly all the elements in the periodic table will get a new overview of the earth surface construction for better stewardship of sustainable environmental management with sustainable mineral resources development.

**REFERENCES**

BOLIVAR, S.L. 1980. An overview of the

**Table 2.** The requirement of method detect limit.

element	D <sub>L</sub>	element	D <sub>L</sub>
Ag	0.02	Mo	0.2
Al <sub>2</sub> O <sub>3</sub>	0.05*	N	20
As	1	Na <sub>2</sub> O	0.1*
Au	0.2	Nb	2
B	2	Nd	0.1
Ba	5	Ni	1
Be	0.2	Os	0.02
Bi	0.05	P	10
Br	1	Pb	2
C	0.1*	Pd	0.2
CaO	0.05*	Pt	0.2
Cd	0.02	Pr	0.1
Ce	2	Rb	1
Cl	20	Re	0.2
Co	1	Rh	0.02
Cr	5	Ru	0.02
Cs	0.5	S	50
Cu	1	Sb	0.05
Dy	0.1	Sc	1
Er	0.1	Se	0.01
Eu	0.1	SiO <sub>2</sub>	0.1*
F	100	Sm	0.1
Fe <sub>2</sub> O <sub>3</sub>	0.05*	Sn	1
Ga	2	Sr	5
Gd	0.1	Ta	0.2
Ge	0.1	Tb	0.1
Hf	1	Te	5
Hg	0.5	Th	2
Ho	0.1	Ti	50
I	0.5	Tl	0.1
In	0.01	Tm	0.1
Ir	0.01	U	0.2
K <sub>2</sub> O	0.05*	V	5
La	1	W	0.3
Li	1	Y	1
Lu	0.1	Yb	0.1
MgO	0.05*	Zn	5
Mn	10	Zr	5

D<sub>L</sub> : detect limit , \* in % , Au, Hg, Ir, Os, Pd, Pt, Re, Rh, Ru in ppb , others in ppm

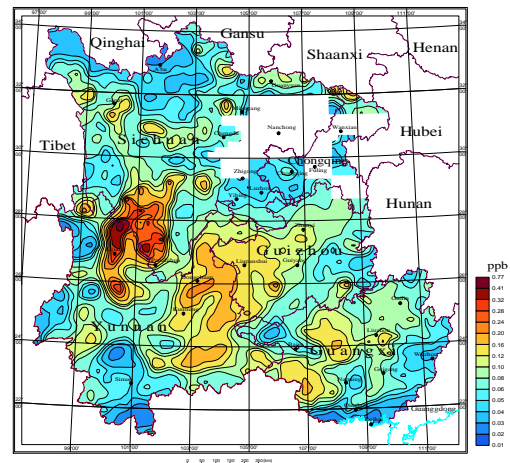


**Fig.1.** Geochemical map of osmium Os in southwest China.

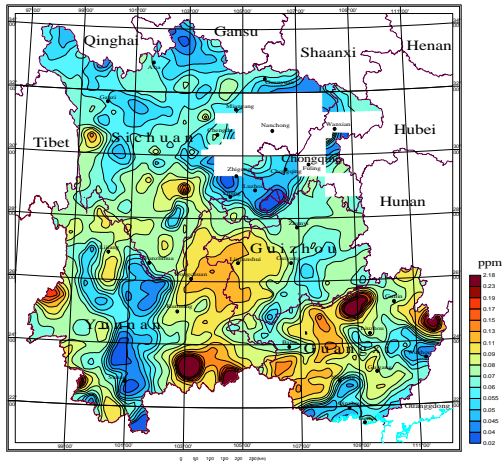


**Fig. 2.** Geochemical map of Indium (In) in southwest China.

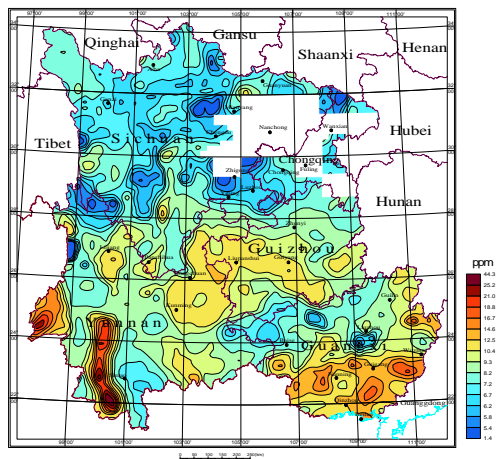


**Fig. 3.** Geochemical map of hafnium (Hf) in southwest China.

National Uranium Resource Evaluation Hydrogeochemical and Stream sediment Reconnaissance Program. Los Alamos Scientific Laboratory, LA-8457-MS, 24 p.

- BOLVIKEN, B., BERGSTORM, J., BJORKLUND, *et al.* 1986. *Geochemical Atlas of Northern Fennoscandia*, Scale 1:4 000 000. Mapped by Geological Surveys of Finland, Norway and Sweden with Swedish Geological Co. and the Geological Survey of Greenland. Nordic Council of Ministers.
- BOWIE, S.H.U. & PLANT, J. 1978a. Regional Geochemical Atlas, Shetland. *Institute of Geological Science, London.*
- BOWIE, S.H.U. & PLANT, J. 1978b. Regional Geochemical Atlas, Orkney. *Institute of Geological Science, London.*

- DE VOS, W. & TARVAINEN, T. (chief editor), 2006. FOREGS Geochemical Atlas of Europe, Part : Interpretation of Geochemical Maps, Additional Tables, Figures, Maps and Related Publications. ESPOO, *Geology Survey of Finland.*
- FAUTH, H., HINDEL, R., & SIEWERS, U. 1985. Geochemical Atlas of the Federal Republic of Germany . *Federal Office for Geosciences and Raw Materials.*
- FREEMAN, T.A., BROXTON, S.H., D.E.M., & BOLIVAR, S.L. 1983. Geochemical Atlas of Alaska. Los Alamos National Laboratory, New Mexico.
- FRISKE, P.W.B. & HORN BROOK, E.H.W. 1991. Canada's National Geochemical Reconnaissance Programme. *Transaction of Institute of Mining and Metallurgy*, **100**, B47-B56.
- Geological Survey of Canada 1981. National Geochemical Reconnaissance, 1:2,000,000, Colored Compilation Map Series. *Geological Survey of Canada, Open File Report*, 730-749.
- KOLJONEN T., GUSTAVSSON, N., & NORAS, P. *et al.* 1989. The Geochemical Atlas of Finland, Part 2: Till. *Espoo: Geological Survey of Finland.*
- LASZLO, O., ISTVAN, H., & UBUL, F. 1997. Low density geochemical mapping in Hungaria. *Journal of Geochemical Exploration*, **60**, 55-66.
- REIMANN, C., AYRAS, M., CHEKUSHIN, V. *et al.* 1998. Environmental Geochemical Atlas of the Central Barents Region. ISBN 82-7385-176-1. NGU-GTK-CKE Special publication, *Geological Survey of Norway, Trondheim, Norway*, 745p.
- REEDMAN, A.J. 1973. Geochemical Atlas of Uganda. *Geological Survey of Uganda, Entebbe*, 42 p.
- SALMINEN. R. (chief editor) 2005. FOREGS Geochemical Atlas of Europe, Part : Background information, methodology, and maps. ESPOO, *Geology Survey of Finland.*
- SIMPSON, PR. 1993. Regional Geochemical Atlas, Southern Scotland. *Institute of Geological Sciences, Nottingham.*
- STEPHENSON, B., GHAZALI, S.A., & WIDJAJA, H. 1982. Regional Geochemical Atlas Series of Indonesia: Northern Sumatra. *Institute of Geological Sciences, Oxford.*
- VARNA, K., RAPANT, S., MARSINA, K. *et al.* 1997. Geochemical atlas of Slovak Republic at scale of 1:1,000,000. *Journal of Geochemical Exploration*, **60**, 7-37.
- WEAVER, T.A. *et al.* 1983. Geochemical Atlas of Alaska. *U. S. Dept. Energy, Rep. GJBX-32* (83).

- WEBB, J. S., NICHOL, I., FOSTER, R., LOWENSTEIN, P.L., & HOWARTH, R.J. 1973. Provisional geochemical atlas of Northern Ireland. *AGRG Tech. Comm. No.60*.
- WEBB, J.S. 1978. The Wolfson Geochemical Atlas of England and Wales. Oxford: *Oxford University Press*.
- XIE, X. 1977. Current problems in regional geochemistry. *Geophys. Geochem. Explor.*, **2**, 1-10 (In Chinese).
- XIE, X. 1978. Regional geochemistry-retrospect, present status and prospect. Ins. *Geophys. Geochem. Explor., Res. Rep. No. 3* (In Chinese).
- XIE X., HUANZHEN, S.. & TIANXIANG, R. 1989. Regional geochemistry -National Reconnaissance project in China. *Journal of Geochemical Exploration*, **33**, 1-9.
- XIE, X. & CHENG, H.X. 2001. Global geochemical mapping and its implementation in the Asia-Pacific region. *Applied Geochemistry*, **16**, 1309-1321.

## A Methodology of source tracking of cadmium anomalies and their quantitative estimation along the Yangtze River Basin, China

Chuangdong Zhao<sup>1</sup> & Hangxin Cheng<sup>1</sup>

<sup>1</sup>*Institute of Geophysical and Geochemical Exploration, CAGS, Langfang, Hebei, 065000, China  
(e-mail: zhaochuangdong@igge.cn)*

**ABSTRACT:** Cd anomalies spreading along almost the whole Yangtze River basin, discovered by the multi-purpose geochemical investigation being carried out in China, have been of the major ecological environmental issue. By taking the Anhui section of the Yangtze River basin as its object, a systematical study on methodology of the source tracking and quantitative estimation of the Cd anomalies has been made in the paper. It is shown that the suspended matters are the main carriers of heavy metals for long distance migrations; the concentration of Cd in the suspended matters is much higher than those of other heavy metals, this may be the main reason for forming the Cd anomalies spreading along the whole Yangtze River basin; The endogenetic mineral deposits, especially Pb-Zn deposits, are the largest suppliers of Cd in the suspended matters. With techniques of layer sampling of sediments on alluvial beds and isotopic age-determination, the geochemical history of sedimentation of Cd and other heavy metals and so resulted pollutions has been primarily reconstructed, with prediction and early warning of evolution of anomalies of Cd and other heavy metals made.

**KEYWORDS:** *Yangtze River basin, source tracking of Cd anomaly, quantitative estimation, suspended matter, sediments on alluvial bed*

### INTRODUCTION

The multi-purpose geochemical investigation on a scale of 1:250,000 has been performed in 7 provinces and 2 cities along the Yangtze River basin since 1999 in China, up to now covering a total of 360,000 km<sup>2</sup>, with a sampling density of 1 sample per 1 km adopted. Results show that element Cd has been anomalously enriched in soils on either bank of Yangtze River, forming Cd geochemical anomalies spreading in a belt of several thousands of kilometres long and tens of kilometres wide. Carrying out systematical studies on the origin, migration course and ecological effects of the Cd geochemical anomalies and predicting their developments in future are not only of scientific significance but also of immediate significance for blocking migrations of Cd in various ecological systems and protecting environments.

### SURVEY OF STUDY AREA

The Anhui section of the Yangtze River basin is located on the middle and lower reaches of Yangtze River and on the

central and southern part of Anhui province, totalling 416 km long and covering 66,000 km<sup>2</sup>, including 10 large basins. It is an important part of the Fe-Cu-S-Au metallogenic belt on the middle and lower reaches of Yang-tze River.

### SAMPLE COLLECTION

A batch of research works indicates that aqueous suspended matters (suspended matters in water) and their sediments-alluvial bad sediments/flood plain sediments could be adopted to quantitatively inverse average chemical compositions for every catchment basin in the studied area. It is thus concluded that aqueous suspended matters and their sediments could be selected as the best sampling media for source tracking of geochemical anomalies along river basins. By determining the element contents in the suspended matters, the output flows of the elements could roughly calculated for corresponding rivers; while with <sup>137</sup>Cs and <sup>210</sup>Pb age-determinations, the rates of sedimentations of alluvial bed sediments/flood plain sediments could

estimated, and combining with content determinations of element in samples, the variations of the elements contents with time could therefore be studied.

**DISTRIBUTIVE FEATURE OF HEAVY METALS IN THE SUSPENDED MATTERS Contents of Heavy Metals in Different Media**

It is seen from the contents of heavy metals in stream sediments, soils and suspended matters for the main basins of the Anhui section of the Yangtze River that the contents of heavy metals in suspended matters are obviously higher than those in stream sediments and soils, indicating that the suspended matters are the main carriers for long distance migrations of heavy metals in the Yangtze River basin.

However obvious differences in enrichment degrees among heavy metals in suspended matters can be observed, the average enrichment degrees of heavy metals in suspended matters are listed in Table 1. It is seen from the table that enrichment degree of Cd in the

suspension, averagely 32.9 times, is obviously higher than those of the other heavy metals.

**OUTPUT FLOW OF HEAVY METALS ALONG THE ANHUI SECTION THE YANGTZE RIVER BASIN**

Table 2 lists the year-output flows of heavy metals for the main tributaries of the Anhui section of Yangtze River.

The data in the table 2 show that the year-discharge of Cd from the main tributaries to Yangtze River in the form of suspended matters is about 1.212 t. The calculations of output flows of Cd for the sections of just getting into and out of Anhui province indicate that the input of Cd into Anhui province from the upper reaches of Yangtze River is about 316.85 t per year, while the output of Cd to the lower reaches of Yangtze River is 313.60 t. The difference between the two is 3.25 t. Considering that the total discharge of Cd to Yangtze River from the tributaries of the Anhui section is 1.21 t, the amount of 4.45 t of Cd is settled in the Anhui section.

**Table 1.** Average enrichment degrees of heavy metals in suspended matters for the main tributary basins of the Anhui section of the Yangtze River basin.

	Cd	Cu	Hg	Zn	Pb	Ni
Suspension/stream sediment	31.2	9.8	6.2	5.7	2.8	2.4
Suspension/soil	34.5	7.7	5.9	6.1	2.4	2.1
Average	32.9	8.8	6.0	5.9	2.6	2.2

**Table2.** Year-output flow of heavy metals for the main tributaries of the Anhui section of Yangtze River (t/a).

Basin of	Cd	Cu	Pb	Zn	As	Hg
Bo Lake	0.092	36.157	8.040	37.978	3.168	0.0384
Wan River	0.069	37.275	3.273	16.570	0.661	0.0081
Caizi Lake	0.007	4.537	0.649	2.654	0.249	0.0045
Qiupu River	0.282	331.382	91.883	23.651	2.368	0.0122
Qingtong River	0.098	19.548	2.117	16.753	0.581	0.0026
Shun'an River	0.144	27.116	0.260	2.135	0.057	0.0004
Yuxi River	0.312	130.325	6.033	23.527	1.805	0.0175
Qingyi River	0.143	67.003	5.156	27.646	2.187	0.0132
Shuiyang River	0.065	47.724	4.009	19.823	1.533	0.0124
Total	1.212	701.067	121.421	170.737	12.609	0.1094

**SOURCE TRACKING OF Cd  
GEOCHEMICAL ANOMALIES**

To track the sources of the geochemical anomalies of heavy metals in suspended matters along the Shun'an River basin (one of the main tributary basins of the Anhui section of the Yangtze River basin), a rock survey was conducted on typical ore deposits and outcrops of main strata and geological bodies along the Shun'an River basin. The results shown in Table 3 indicate the largest source of Cd in suspended matters on the Shun'an River basin is endogenous deposits, especially Pb-Zn deposits.

**PRELIMINARY RECONSTRUCTION OF  
POLLUTION BY HEAVY METALS**

Figure 1 shows the results of age-determination for the sedimentary columns of alluvial beds for the upper reach of the Anhui section of Yangtze River by using <sup>210</sup>Pb and <sup>137</sup>Cs. It could be seen from the figure above that: After 1949, the content of Cd was continuously going up; especially it went up rapidly after 1977 when the policy of reformation and opening was put into effect. The content of Cd came up to 1,037ng/g around 1990, exceeded the

**Table 3.** Contents of heavy metals based on the rock survey along the Shun'an River (µg/g).

Ore deposit	Number of samples	Cd	Cu	Pb	Zn	As	Hg	Ni
Yejiachong Pb-Zn Deposit	3	826.9	260.5	37266.7	100201.8	115.4	7.77	27.0
Fenghuangshan Cu Deposit	5	16.8	99188.1	19.9	4589.2	34.5	0.05	16.7
Xinqiao FeS Deposit	5	14.3	1581.5	505.7	820.3	1834.6	0.28	29.1
Tailing storehouse of Fenghuangshan Cu Deposit	5	2.2	1501.1	76.4	705.5	90.6	0.06	11.0
Lixin coal Mine	3	0.3	34.7	23.4	49.4	8.4	0.15	19.0
Shengchonghe Coal Mine	5	0.5	31.0	54.9	58.1	17.6	0.13	9.4
Fenghuangshan rock bodyock strata	4	0.24	185.96	24.95	92.58	15.1	0.01	13.38
	16	0.38	53.59	90.37	127.92	15.84	0.05	19.04

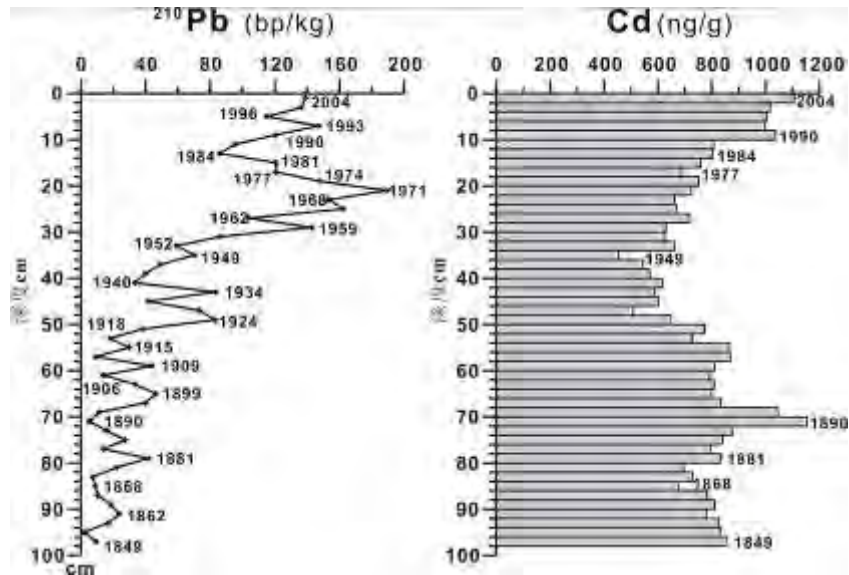


**Fig.1.** The variation of Cd content versus time on the sedimentary column of alluvial beds for the upper reach of the Anhui section of Yangtze River.

state limitation of the third class of soil environment. It even came up to 1,107ng/g in 2004.

If the content of Cd is continuously increasing at the current rate, the content of Cd would be up to 1,574 ng/g for the period of 2040 ~ 2049 at the upper reach of the Anhui section of Yangtze River, and would exceed 2,000 ng/g for the period of 2070 ~ 2079.

#### **PRELIMINARY CONCLUSION**

The measured results of the contents of heavy metals in suspended matters for the Anhui section of the trunk stream and main tributaries of Yangtze River show that the suspended matters have been the main carrier for long distance migration of the heavy metals, the enrichment degree of Cd in the suspended matters has been much higher than those of the other heavy metals. Perhaps it is just the reason for the forming of Cd geochemical anomalies along the basin of Yangtze River. The

calculation results of output flow of heavy metals for the Anhui section of the trunk stream and main tributaries of Yangtze River indicate that the largest output flow of heavy metals has been from Qiupu River, with 4.45 t of Cd per year sedimented along the Anhui section of Yangtze River.

The results of source tracking show that the endogenic deposits, especially Pb-Zn deposits, have been the largest supplier of Cd.

The age-determination results by using <sup>210</sup>Pb and <sup>137</sup>Cs for the sedimentary columns of the alluvia beds along the trunk stream and main tributaries of the Anhui section of Yangtze River show that the variations of the contents of Cd and other heavy metals were basically corresponding closely to major historical events, say the establishment of PRC, the exercise of the policy of reformation and opening and the course of extensive industrialization, etc.

**GENERAL SESSION**

EDITED BY:

**DAVID R. LENTZ**



## Investigation of physical, chemical and microbiological processes in the development of forest rings in Ontario

Kerstin Brauner<sup>1</sup>, Stewart M. Hamilton<sup>2</sup>,  
Keiko H. Hattori<sup>1</sup>, & Gordon Southam<sup>3</sup>

<sup>1</sup>University of Ottawa, 140 Louis Pasteur, Ottawa, ON, K1N 6N5 CANADA (e-mail: [kbrau049@uottawa.ca](mailto:kbrau049@uottawa.ca))

<sup>2</sup>Ontario Geological Survey, 933 Ramsey Lake Road, Sudbury, ON P3E 2G9 CANADA

<sup>3</sup>University of Western Ontario, 1151 Richmond St., London, ON N6A 5B7 CANADA

**ABSTRACT:** Forest rings are large circular features distinctive of Ontario's boreal forest. They are centred on areas of negative redox charge and characterized by a slight depression in the mineral soil around the edge of the ring. A field and laboratory investigation of forest rings is examining the complex relationship between physical, chemical and microbiological processes occurring at the edge of these features. Physical changes that are known to occur include a slight positive electrical field anomaly over the centre of the ring, a negative thermal and hydraulic-conductivity anomaly. Chemical changes are profound and most exemplified by a very sharp redox gradient at the edge of the ring between the chemically reduced interior and the oxidized exterior. Microbiological processes are also occurring and although cause-and-effect relationships are still unproven, they may be crucial in the formation of the rings. A four week laboratory experiment involves the *in vitro* creation of the redox gradients of the two end-member types of rings: one centred on a hydrogen sulfide source and another on a methane source. Test-tubes are being inoculated with bacteria from the highest-gradient ring parts of the respective ring edges. Measurements will provide insight on the role of micro-organisms in ring formation.

**KEYWORDS:** forest ring, thermal conductivity, redox, microbiology

### INTRODUCTION

Forest rings are large circular features commonly observed in the boreal forests of Ontario (Fig. 1). Over 2000 forest rings, ranging from 15 m to 1.5 km in diameter, have been identified on aerial photographs thus far. The circular impression reflects a slight topographic depression (Giroux *et al.* 2001) that forms around centres of negative charge enclosed in the overburden or bedrock. Large accumulations of shallow, biogenic methane are estimated to account for 85% of northern Ontario's forest rings (Hamilton *et al.* 2004). Forest rings have also been reported to form over accumulations of bitumen, coal and dissolved hydrogen sulfide (Hamilton & Hattori 2008). The reducing source imparts electrochemically reducing conditions in overlying and surrounding materials generating numerous physical and chemical changes at the ring edges.

Most notably, subtle positive spontaneous potential (SP) anomalies can be noted in association with strong, negative-inward, redox gradients (Hamilton & Hattori 2008). The goal of our work is to understand the role of micro-organisms in the oxidation process and in the generation of electrical fields.

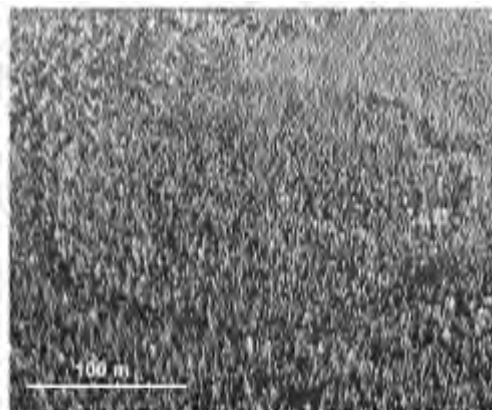


**Fig. 1.** Aerial view of a forest ring near Hearst, Ontario.

The current investigations monitor changes in groundwater temperature across an H<sub>2</sub>S-centered forest ring. The rationale behind the temperature measurements was that microbiological activity and intense oxidation is known to occur at the ring edges and it was thought that temperature data might pinpoint the exact location of the associated exothermic reactions and help with energy and mass budget calculations. However, to our surprise, the results were the opposite of what had been expected; they show a significant *negative* thermal anomaly. Subsequent investigations have (1) confirmed the results, (2) shown them to occur at other rings, and (3) narrowed the location of the temperature anomaly to precisely that of the physical, chemical and microbiological changes that occur at the ring edge. The purpose of this study is to understand these changes and how they are interrelated and to investigate the role of micro-organisms in the oxidation process and generation of electrical fields at the ring edge.

**METHODOLOGY**

Groundwater temperatures and water levels were monitored for a period of 10 months across the edge of an H<sub>2</sub>S-centered forest ring (“Thorn-North”) located 45 km northwest of Timmins, Ontario. Measurements were made using down-hole data loggers installed in existing monitoring wells at a depth of approximately 6.5 m. In addition, the ring edges of two methane-centred forest rings (“Road ring” and “Bean”) were sampled for soil and peat. High-density sampling was done at several depths on transects across the ring edges. Time-sensitive parameters such as pH and oxidation-reduction potential (ORP) were measured at the time of collection.

Clay samples were collected at areas of high-redox gradient at the edge of the Thorn-north ring and the Bean ring, which are H<sub>2</sub>S sourced and methane sourced, respectively. These samples were preserved under anoxic conditions and

are now being used for the test-tube experiments.

Clay from the ring edges was suspended in agar and served as the inoculant and the carbon source for the in-vitro growth of forest ring micro-flora. A redox gradient was established by the steady supply of oxygen at one end and a source of CH<sub>4</sub> or H<sub>2</sub>S at the other end of the test tube. Changes in pH, ORP and SP were monitored over a period of four weeks.

**SELECTED RESULTS**

A detectable drop in groundwater temperature can be measured over the ring edge at Thorn North. Peat-waters collected during the month of July, at 1.5m depth show a minimum of 2°C within the ring edge while outside values peak at 10°C. Although the sampling site is located 200 km south of the southernmost limit of discontinuous permafrost, temperatures have remained low enough to allow the preservation of ice within the peat. The temperature anomaly is propagated to depth, with a 0.35°C anomaly occurring at the same place in groundwater from underlying clay (Fig. 2). In addition, the response of groundwater temperature to seasonal changes in air temperature is higher at the ring edge than in adjacent areas. At 6.5 m depth, the coldest month of the year is August, due to a lag in summer warming. Groundwaters in the ring edge reach their

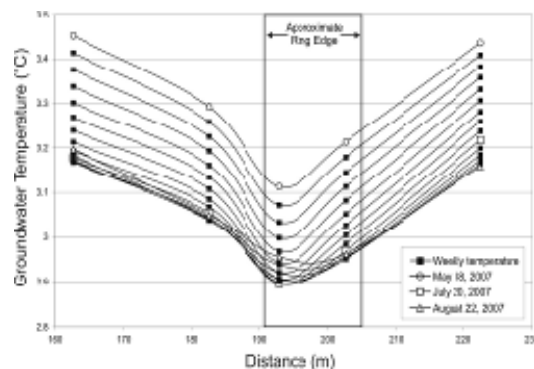


**Fig. 2.** Changes in mean weekly groundwater temperatures (6.5 m depth) across the

northern ring edge of Thorn-North from May to August 2007 (Brauneder *et al.* 2008).

coldest temperature on July 20, whereas groundwaters in adjacent areas reach their coldest state one month later. Similarly, data collected from November to December shows that groundwaters within the ring edge reach their warmest temperature one month earlier than in adjacent areas.

The most likely reason for the thermal anomaly at the ring edge is that it coincides with an area of increased thermal conductivity in the clays. This area also coincides with an area of decreased hydraulic conductivity (Fig. 3).

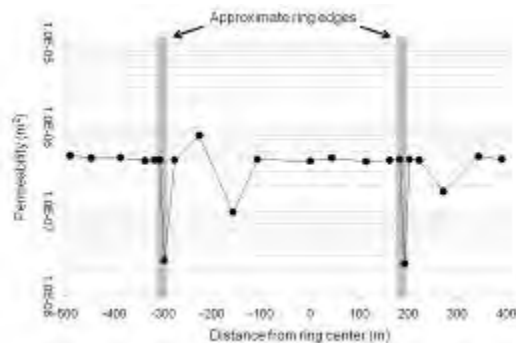


**Fig. 3.** Changes in permeability along a 900 m long transect crossing Thorn-North from south to north.

These physical changes are accompanied by chemical changes. Most notably, a sudden and strong redox gradient, pH gradient and oxygen depletion occur on all investigated ring edges. Similar responses have been noted at other rings. Figure 4 shows an ORP change of 200 mV occurring over a distance of only 3 m at the edge of the Road ring and known to be associated with a pH increase of 0.5 units.

**MICROBIOLOGICAL INVOLVEMENT**

Redox gradients as strong as those observed at the ring edges are potential sources of energy for autotrophic bacteria. Evidence for microbial involvement includes H<sub>2</sub>S consumption, SO<sub>4</sub><sup>2-</sup>

enrichment, oxygen depletion in the

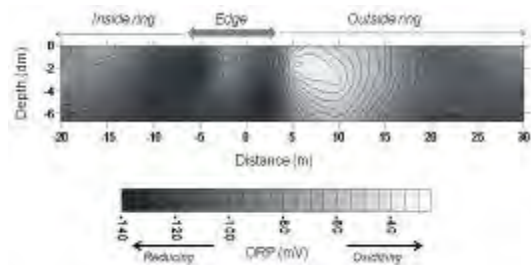


**Fig. 4.** ORP profiling of the top first meter of clay across the northern edge of the Road ring.

**headspace of wells and minor to major biogenic methane production. Additional evidence is given by the generation of hydrocarbons at a number of rings.**

The ongoing microbiological experimentation attempts to re-create *in vitro*, the redox conditions at the edge of two types of forest rings: those centred on methane and H<sub>2</sub>S. A redox gradient is being established between each of these reducing agents and oxygen. Test-tubes will be inoculated with bacteria collected from the highest redox-gradient areas on each ring type. Measurements over the course of the 4 week experiment will help to determine the complex cause-and-effect relationships that exist between the physical, chemical and microbiological processes occurring at the ring edge.

**CONCLUSIONS**

A large number of physical and chemical changes occur in overburden and groundwater at the edges of forest rings. Physical changes include an apparent increase in thermal conductivity and a decrease in hydraulic conductivity. Chemical changes are dominated by a very strong and sudden change from reducing to oxidizing conditions at the ring edge. These changes are all spatially related. Broadly speaking the changes follow the model of Hamilton & Hattori (2008) but unexpected developments, including the thermal anomaly, have been uncovered. Furthermore that model does

not consider the involvement of microflora, which may be an important or even crucial factor in the development of forest rings.

#### **ACKNOWLEDGEMENTS**

This project is part of the first author's Master's thesis. It is supported in part through a Natural Sciences and Engineering Research Council (NSERC) grant to Keiko Hattori at the University of Ottawa, the Ontario Geological Survey, and through grants from the Society of Economic Geologists and the American Association of Petroleum Geologists.

#### **REFERENCES**

BRAUNEDER, K., HAMILTON, S.M., & HATTORI, K.H. 2008. Detailed investigation of chemical

and microbiological parameters over forest-ring edges in northern Ontario. In: *Summary of Field Work and Other Activities 2008*. Ontario Geological Survey, Open File Report, **6226**, 28-1 to 28-8.

GIROUX, J.F., BERGERON, Y., & VEILLETTE, J.J. 2001. Dynamics and morphology of giant circular patterns of low tree density in black spruce stands in northern Quebec. *Canadian Journal of Botany*, **79**, 420–428.

HAMILTON, S.M., BURT, A.K., HATTORI, K.H., & SHIROTA, J. 2004. The distribution and source of forest ring-related methane in northeastern Ontario. In: *Summary of Field Work and Other Activities 2004*. Ontario Geological Survey, Open File Report, **6145**, 21-1 to 21-26.

HAMILTON, S.M. & HATTORI, K.H. 2008. Spontaneous potential and redox responses over a forest ring. *Geophysics*, **73**, B67–B75.

## Geology and Geochemistry of the Lac Cinquante Uranium Deposit, Nunavut

Nathan J. Bridge<sup>1</sup>, Neil R. Banerjee<sup>1</sup>, Craig S. Finnigan<sup>1,2</sup>, Rob Carpenter<sup>2,3</sup>, & Jeff Ward<sup>3</sup>

<sup>1</sup>Department of Earth Sciences, University of Western Ontario, London, ON, Canada, N6A5B7

<sup>2</sup>Kaminak Gold Corporation, Suite 1440 – 625 Howe St., Vancouver, BC, Canada, V6C 2T6

<sup>3</sup>Kivalliq Energy Corporation, Suite 1440 – 625 Howe St., Vancouver, BC, Canada, V6C 2T6

**ABSTRACT:** The Lac Cinquante uranium deposit is located in the Hearne Subprovince of the Western Churchill Province, in the Kivalliq region of Nunavut. Lac Cinquante is hosted in a basement of Archean greenstones that are unconformably overlain by Proterozoic sediments. In this study we present a newly acquired detailed geological map of the Lac Cinquante region that has been coupled with bulk rock geochemistry in an attempt to understand the formation of the Lac Cinquante uranium deposit. This new geological and geochemical information reveal a more detailed geological history than previously reported. Preliminary oxygen stable isotope compositions for the rocks surrounding the main ore zone show an envelope of high  $\delta^{18}\text{O}$  values, possibly related to increased low-temperature water-rock interaction, and compositional changes. Future studies at the Lac Cinquante deposit involving fluid-rock reaction and ore zone formation will be useful in unravelling the metallogenic history for the Lac Cinquante deposit and mineralization in the surrounding region.

**KEYWORDS:** *Unconformity Hosted Uranium Deposit, Nunavut, Geochemistry, Uranium Exploration, Oxygen Stable Isotopes*

### INTRODUCTION

The Lac Cinquante unconformity associated uranium deposit is located in the Kivalliq district of Nunavut approximately 350 km west of Rankin Inlet, and is centered on approximately Latitude 62° 34'33" N, Longitude 98°41'41"W. The deposit is hosted in volcanic Archean greenstones that are unconformably overlain by the northeast trending Angikuni sub-basin. Mineralization is found within the basement volcanics that have undergone hydrothermal alteration along fault zones (Miller et al., 1986). Two major zones of mineralization, and three major styles of mineralization within the Archean greenstones have been identified in previous studies (Miller et al., 1986). Additionally, zones of anomalous uranium concentration have been recognised in the overlying Proterozoic sediments. In this study we present a detailed 1:5000 geological map that has been combined with new stable isotope and bulk rock

geochemical data. Mapping and bulk-rock geochemistry have revealed a suite of Archean tholeiitic basalts and basaltic andesites that transition into a tholeiitic bimodal volcanics to the East. The entire package is unconformably overlain by Proterozoic sediments grading upwards from basal breccia, into conglomerate, and sandstone with a volcanic trachyte unit capping the sedimentary rocks. Oxygen stable isotope geochemistry reveals a zone interpreted to represent high-fluid flow and water-rock interaction associated with the mineralized metasedimentary layer in the Archean volcanics, which is important for understanding the composition, temperature, and amount of fluid responsible for the formation of the uranium deposit.

### REGIONAL GEOLOGY

The Lac Cinquante uranium deposit is located in the Kivalliq Region of the Hearne Subprovince in the Western Churchill Province, Nunavut. The Western

Churchill Province is located in between the Superior province and Slave provinces and is separated from them by the Trans-Hudson and Thelon orogens (Hoffman, 1988). The Western Churchill Province has been subdivided into the Rae and Hearne subprovinces, which are separated by the Snowbird Tectonic Zone (Hoffman, 1988; Berman et al, 2007). The deposit is associated with an Archean greenstone sliver related to the Yathkyed Greenstone belt and is unconformably overlain by the Angikuni sub-basin, one of several northeast trending Proterozoic sub-basins of the Dubawnt Supergroup (Rainbird et al., 2003).

**LOCAL GEOLOGY**

The Lac Cinquante region is characterized by an Archean-Proterozoic unconformity (Figure 1). The area was first mapped by Miller et al. (1986) and was re-mapped in the summer of 2008. Mapping has revealed a basement assemblage of Archean greenstones consisting of a package of tholeiitic meta-basites including gabbros, massive basalts, and pillowed basalts, with interlayered metasedimentary tuffs. This package appears to repeat in a cyclical manner, with gabbros at the base, grading into massive flows with pillowed tops. To the East, the Archean sequence grades into a suite of bimodal volcanics that are comprised of alternating mafic (basaltic-andesite) flows and felsic pyroclastic units. Proterozoic sediments of the Dubawnt Supergroup Baker Sequence, are located above the unconformity in the Lac Cinquante region. This sequence is characterized by a basal breccia unit at the base, overlain by clast-supported conglomerates with interbedded sandstones that fine upwards into sandstones, and siltstones. Conformably overtop of the Proterozoic sediments lies the Christopher Island Formation

**MINERALIZATION**

Two major zones of mineralization, the Main zone and the South Zone have been

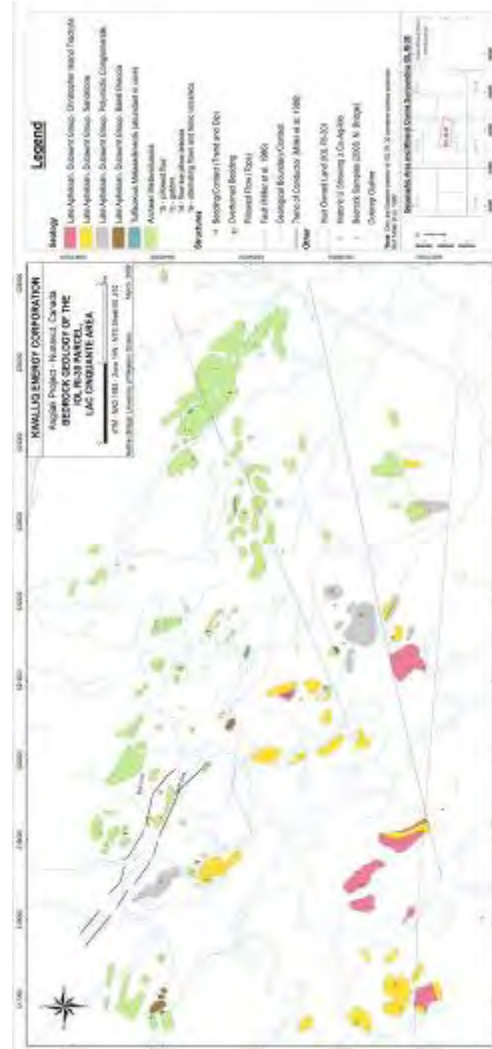


**Fig.1.** Geology of the Lac Cinquante region shows Archean (green rocks) and Proterozoic rocks (yellow, grey, brown, and pink) separated by an unconformity (dashed line). The location of the two major zones of mineralization, the main zone and south zone, documented by Miller et al. (1987) are noted on the map.

documented in previous studies. These are characterized by graphitic exhalative horizons, and in drill core appear as tuffaceous metasediments (Miller et al., 1986). In the region, three major styles of mineralization have been documented in the Archean greenstones, including: disseminated pitchblende with base metals in tuffaceous metasediments, discrete pitchblende veins that cut across

the metasediments, and quartz, carbonate, sulphides, and pitchblende in gash veins trending 040 to 060 along fractures (Miller et al., 1986). Future studies of the mineralization will aim to document the age of mineralization, timing of mineralization, and composition and temperature of the fluids responsible for mineralization.

**BULK ROCK AND STABLE ISOTOPE GEOCHEMISTRY**

Bulk rock geochemistry of the Lac Cinquante deposit shows that the Archean volcanic rocks (both the mafic volcanic flows and the bimodal volcanic suite) are dominantly tholeiitic high-Fe basalts and basaltic andesites. The alternating felsic units in the bimodal suite are dacitic and rhyolitic in composition (Fig. 2).



**Fig. 2.** Jensen cation plot for the classification of volcanic rocks in the Lac Cinquante region according to their Al, Mg, and Fe+Ti cation ratios.

Preliminary oxygen isotope data from bulk rocks in a drill core that crosses the main zone (Fig. 3) show that the rocks surrounding the main ore zone at the Lac Cinquante deposit are elevated above normal magmatic values. This has been interpreted to preserve the signature of elevated fluid flow surrounding the ore zone. The trend is characterized by a

steady increase in  $\delta^{18}\text{O}$  to a peak at the ore zone, and a steady decrease in  $\delta^{18}\text{O}$  to more typical magmatic values after the ore zone. This may have resulted from low-temperature alteration (< 250°C) of basalt leading to the formation of secondary phyllosilicate (and other) minerals with elevated  $\delta^{18}\text{O}$  values. It is also evident from this data that focused fluid flow around the deposit is likely linked to the chemistry of the rocks hosting the ore zone. Future studies will investigate additional detailed isotope studies to resolve fluid-rock interaction values, and fluid temperatures.

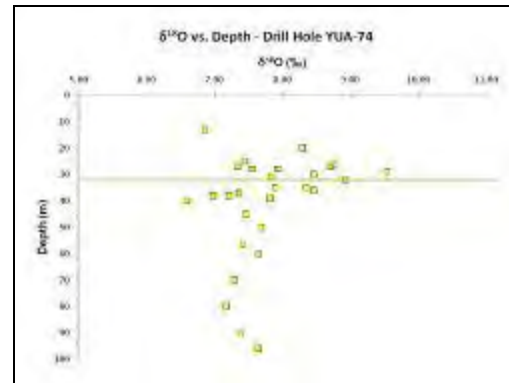


**Fig. 3.** Oxygen stable isotope data from drill hole YUA-74 showing an elevated  $\delta^{18}\text{O}$  envelope surrounding the main ore zone.

**CONCLUSIONS**

New mapping and bulk rock geochemistry of the Lac Cinquante uranium deposit has revealed a more detailed geological history than previously reported. The combination of geology and geochemistry have provided important preliminary results that will be important for understanding the metallogenesis and formation of this unconformity associated uranium deposit. Future studies at Lac Cinquante will focus on dating the mineralization, constraining the fluid temperatures and composition responsible for mineralization, and more detailed mineral chemistry of the alteration halo around the deposit.

### ACKNOWLEDGEMENTS

We would like to thank Kivalliq Energy Corporation, Kaminak Gold Corporation and the Natural Sciences and Engineering Research Council of Canada for funding the project. NJB would like to thank the Society of Economic Geologists for an SEG Graduate Student Fellowship, as well as the Mineralogical Association of Canada, the University of Western Ontario Northern Research Committee and Graduate Thesis Research Awards Fund for additional research funds.

### REFERENCES

- BERMAN, R.G., DAVIS, W.J., & PEHRSSON, S., 2007. Collisional Snowbird tectonic zone resurrected: Growth of Laurentia during the 1.9 Ga accretionary phase of the Hudsonian orogeny. *Geology*, **35**, 911-914.
- HOFFMAN, P.F., 1988. United Plates of America, the Birth of a Craton: Early Proterozoic Assembly and Growth of Laurentia. *Annual Reviews in Earth and Planetary Science*, **16**, 543-603.
- MILLER, A.R., STANTON, R.A., CLUFF, & G.R., MALE, M.J., 1986. Uranium deposits and prospects of the Baker Lake Basin and subbasins Central District of Keewatin, Northwest Territories. In: Evans, E.L. (Ed.) Uranium Deposits of Canada. Canadian Institute of Mining and Metallurgy, Special Volume 33, 263-285.
- RAINBIRD, R.H., HADLARI, T., ASPLER, L.B., DONALDSON, J.A., LECHÉMINANT, A.N., PETERSON, T.D., 2003. Sequence stratigraphy and evolution of the Paleoproterozoic intracontinental Baker Lake and Thelon basins, western Churchill Province, Nunavut, Canada. *Precambrian Research*, **125**, 21-53.

## The New Brunswick Groundwater Chemistry Atlas: a geographical representation of groundwater quality in New Brunswick

Annie E. Daigle<sup>1</sup>, Mallory Gilliss<sup>1</sup>, & Darryl A. Pupek<sup>1</sup>

<sup>1</sup>New Brunswick Department of Environment, 20 McGloin St., Fredericton, NB E3A 5T8 CANADA  
(e-mail: [annie.daigle@gnb.ca](mailto:annie.daigle@gnb.ca))

**ABSTRACT:** Under the Potable Water Regulation of the *Clean Water Act*, the Province of New Brunswick maintains a database of groundwater quality data collected from domestic water wells drilled since 1994. Privacy regulations prohibit the distribution of these data by any method which identifies the individual well owner or associated property. In order to make these data publicly available, the New Brunswick Department of Environment recently released the New Brunswick Groundwater Chemistry Atlas (Atlas). The Atlas was created using the results from approximately 10,500 inorganic chemistry samples collected from domestic water wells drilled between 1994 and 2007. The 28 parameters in the standard inorganic chemistry analysis conducted at the Department of Environment Analytical Services Laboratory are individually mapped in the Atlas. Each map presents the range in concentrations along with information pertaining to the distribution of the data and their relationship to applicable Health Canada drinking water quality guidelines. In addition to providing a baseline measurement of groundwater quality in the Province, the Atlas makes the information in New Brunswick's domestic water well database more accessible to the public. The geographical representation of these data facilitates trend analysis and serves as a valuable resource for many user groups, most notably health professionals, geologists, groundwater researchers, and land use planners.

**KEYWORDS:** *groundwater quality, domestic well logs, inorganic chemistry, database, New Brunswick.*

### INTRODUCTION

Under the Potable Water Regulation of the *New Brunswick Clean Water Act*, the Province of New Brunswick maintains a database of groundwater quality data collected from domestic water wells drilled since 1994.

New Brunswick privacy regulations prohibit the distribution of these water quality data by any method which identifies the individual well owner or associated property. These data can only be provided to researchers and other interested parties in aggregate form with all identifying coordinate data removed.

In 2006, as a means of making these data available in a spatial format to various user groups, the New Brunswick Department of Environment (DENV) began development of a series of thematic maps of groundwater quality using information in the domestic water well database. The goal was to develop a series of maps, which could be publicly

released without compromising privacy regulations. Based in part on the previous work done by Rivard *et al.* (2005) in the Maritimes Carboniferous Basin, the resulting New Brunswick Groundwater Chemistry Atlas (Atlas) was published in December 2008 and is available on-line at [www.gnb.ca/env](http://www.gnb.ca/env).

### BACKGROUND

When a domestic water well is drilled in the Province of New Brunswick, the well driller completes a Water Well Driller's Report outlining the well location, construction details, estimated water yield, and geology encountered. The report is forwarded to the DENV where the information is entered into the domestic well log database.

The well owner is also given a copy of the Water Well Driller's Report and is required by law (under the *Potable Water Regulation – New Brunswick Clean Water Act*) to purchase a Water Quality Analysis

Voucher at the time of drilling. The well owner then redeems the voucher by collecting the necessary water samples, using the bottles and a methodology provided by the DENV, and submitting them to the DENV Analytical Services Laboratory for a standard inorganic chemistry analysis.

Results are entered into the DENV water quality database and a report with the results is sent to the well owner by the New Brunswick Department of Health (NB Health). A flow chart of this process is illustrated in Figure 1.

**METHODOLOGY**

The results of water quality analyses were extracted from the water quality database for the period of January 1, 1994 to December 31, 2006. This resulted in 10,664 usable water chemistry results, although not every parameter was analysed in each case resulting in variations in the sample size. The domestic well log database reported

20,478 usable well logs for the same time period.

The discrepancy between the number of well logs and the number of water chemistry results indicates that roughly 50% of well owners did not submit a water quality sample to the DENV for analysis and redeem their Water Quality Analysis Voucher over the reporting period.

In all 28 parameters were individually mapped: alkalinity, aluminum, antimony, arsenic, barium, boron, bromide, cadmium, calcium, chloride, chromium, conductivity, copper, fluoride, hardness, iron, lead, magnesium, manganese, nitrate, pH, potassium, selenium, sodium, sulphate, thallium, uranium, and zinc. These parameters constitute the standard inorganic analysis conducted at the DENV Analytical Services Laboratory.

Along with individual chemical parameters the Atlas also includes a plot of well depths and maps of NB surficial geology (modified from Rampton, 1984) and bedrock lithology (modified from Fyffe & Richard, 2007).

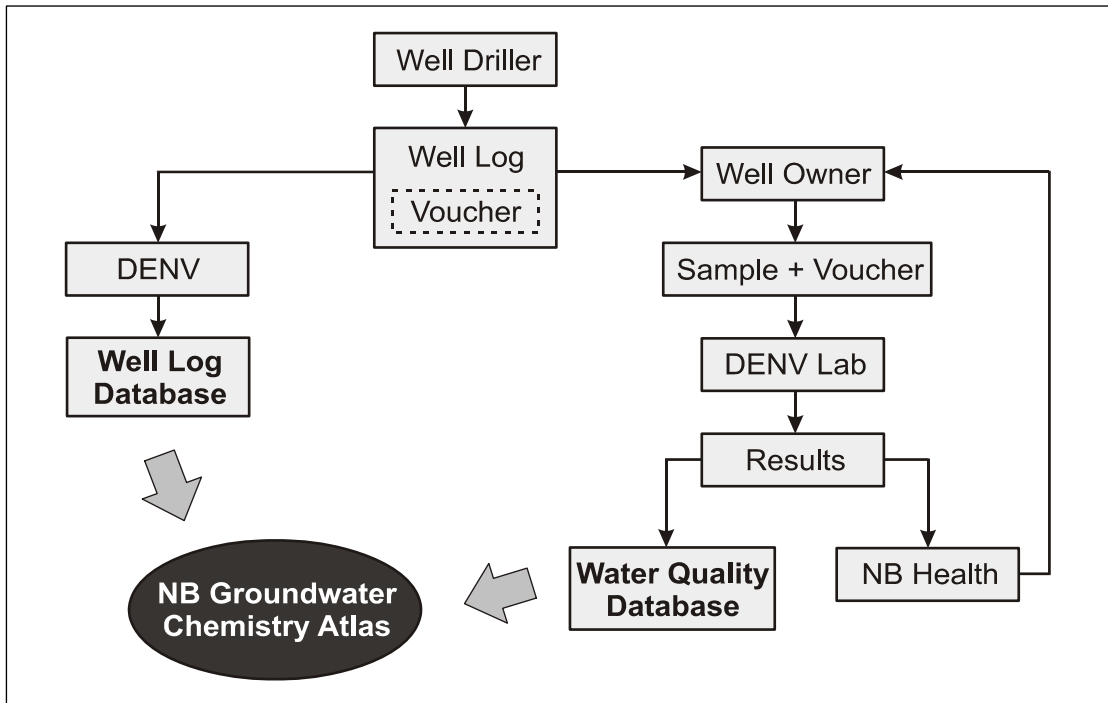


**Fig. 1.** Flow chart of water quality analysis voucher process for newly drilled domestic water wells in New Brunswick.

## RESULTS

For each individual parameter, the Atlas plate indicates the range in concentrations of the parameter along with information pertaining to the distribution of the data and their relationship to the Health Guidelines for Canada Drinking Water Quality (Health Canada, 2008).

The following tables provide a detailed breakdown of the compliance of water well samples with health-based guidelines (Table 1) and aesthetic guidelines (Table 2). These results indicate that in general the water quality of domestic water wells in New Brunswick is very good. The most common water quality issues in New Brunswick are due to excessive iron and manganese in well water, which is attributable to the natural geology of the province.

**Table 1.** Compliance of samples with health-based guidelines

Parameter	Samples in compliance
Antimony	99.4%
Arsenic	94.1%
Barium	98.6%
Boron	100%
Cadmium	99.9%
Chromium	99.8%
Fluoride	95.0%
Lead	97.3%
Nitrate	99.4%
Selenium	98.9%
Uranium	97.9%

**Table 2.** Compliance of samples with aesthetic guidelines.

Parameter	Samples in compliance
Chloride	96.7%
Copper	99.9%
Hardness	89.2%
Iron	71.2%
Manganese	60.2%
pH	86.3%
Sodium	96.6%
Sulphate	99.4%
Zinc	99.9%

In certain instances, the Atlas indicates a relationship between a water chemistry parameter and the bedrock geology, the geological history, or general land use of the area. For example, higher concentrations of iron and manganese are encountered in the Carboniferous Basin, higher nitrate concentrations are seen in agricultural areas along the Saint John River valley, and elevated sodium and chloride can indicate areas that are vulnerable to salt water intrusion but can also outline inland areas where relic sea water from the late Quaternary is found at depth.

In the future, additional data analysis will be conducted on the dataset in order to further examine the relationships between groundwater chemistry and well depth, surficial and bedrock geology, and structural features such as fault zones.

## CONCLUSIONS

Since its release in December 2008, the New Brunswick Groundwater Chemistry Atlas has proven to be a useful tool to help educate New Brunswickers about general groundwater quality in the province and identify areas with potential water quality concerns. The Atlas can be used in conjunction with other information by planners and developers to make informed decisions about land use planning and sustainable development. The data are also being used in environmental health research and mineral exploration by groundwater researchers and geologists.

The Atlas provides a basis for further research into factors that affect natural groundwater chemistry. It also serves as a baseline for comparing shifts in water quality overtime due to climatic changes and other factors.

Since the Atlas only includes water chemistry data up to December 31, 2006, it is intended to be periodically updated as additional well water quality data become available.

The Atlas should be used for general information purposes only, and independent confirmation of groundwater quality for specific sites is recommended.

### ACKNOWLEDGEMENTS

The New Brunswick Groundwater Chemistry Atlas was completed under the Canada-New Brunswick Water Quality Monitoring Agreement with contributions from Environment Canada and the New Brunswick Department of Environment. Additional support was provided by the New Brunswick Department of Natural Resources and the Maritimes Groundwater Initiative of the Geological Survey of Canada. We would like to thank Rockflow Geoscience Consultants Inc., in particular Norah Hyndman, for data analysis and Jeff Stymiest of the Information Technology Branch of the New Brunswick Department of Local Government for his technical support in map development.

### REFERENCES

- FYFFE, L.R. & RICHARD, D.M. 2007. Lithological map of New Brunswick. *New Brunswick Department of Natural Resources; Minerals, Policy and Planning Division*. Plate **2007-18**.
- HEALTH CANADA 2008. Follow: Environmental and Workplace Health, Guidelines for Canadian Drinking Water Quality, 30/05/08, <http://www.hc-sc.gc.ca>.
- RAMPTON, V.N. 1984. Generalized surficial geology map of New Brunswick. *New Brunswick Department of Natural Resources and Energy; Minerals, Policy and Planning Division*, **NR-8**.
- RIVARD, C., DEBLONDE, C., MICHAUD, Y., BOISVERT, V., CARRIER, C., CASTONGUAY, S., & LEFEBVRE, R. 2005. Hydrogeological Atlas of the South-Central Areas of the Maritimes Carboniferous Basin. *Geological Survey of Canada*, Open File **4884**, 54 p.

## Spatial geochemical trends of beach and dune sands from the Northeastern coast of Mexico: implications for provenance

Juan Jose Kasper-Zubillaga<sup>1</sup>, John S. Armstrong-Altrin<sup>1</sup>,  
& Arturo Carranza Edwards<sup>1</sup>

*1 Instituto de Ciencias del Mar y Limnología, Universidad Nacional Autónoma de México, Circuito Exterior s/n, Coyoacan, México DF, México 04510 (e-mail kasper@icmyl.unam.mx)*

**ABSTRACT:** A geochemical analysis of major, trace and rare earth elements was carried out in beach sands collected from the Northeastern coast of Mexico in order to observe the spatial trends along three different beaches. Results show that major elements patterns along the beaches are controlled by heavy minerals and plutonic and sedimentary input towards the coast. In addition, trace elements tendencies indicate that the beach sands are influenced by the presence of magnetite. Finally, the differences in Eu anomalies indicate a mix of felsic to mafic and intermediate rocks and feldspar weathering.

**KEYWORDS:** *beach, sand, provenance, Mexico*

### INTRODUCTION

Beach and dune sediments are compositionally controlled by physical, chemical and mechanical factors such as waves, wind, and long shore currents, climate, relief, source composition, transport and river discharges among others (Folk 1974, Ibbeken & Schleyer, 1991; Carranza-Edwards *et al.* 1994; Critelli *et al.* 1997; Carranza-Edwards *et al.* 1998; Armstrong-Altrin *et al.* 2003; Armstrong-Altrin *et al.* 2004; Kasper-Zubillaga & Carranza-Edwards 2005; Kasper-Zubillaga *et al.* 2008a). A wide range of techniques are used for geochemical determinations to investigate the compositional differences of the beach and dune sediments. Such techniques are defined by major, trace and rare earth elements analyses. Furthermore, these techniques allow to understanding the multi-factorial roles that control the composition of coastal sediments. In this paper we focus our attention in showing the spatial trends of geochemical data obtained during the dry season in the northeastern coast of the Gulf of Mexico to discuss the provenance implications.

### STUDY AREA

The study area is located in the coastal area of the state of Tamaulipas, Mexico (22°10' 24°00'W; 98°00'N). The sampling was carried out in three main localities: Playa Miramar, Boca del Tordo and La pesca (Figs. 1&2).

Main rivers discharging in each site are Panuco, Carrizal and Soto La Marina.

The geology of the study area comprises mainly: limestones, shales, alluvial deposits and basic extrusive and intrusive rocks.

### MATERIALS AND METHODS

Sand samples were dried at 110 °C and treated with lithium meta and tetraborate to make pressed powder pellets. They were analysed using a X-ray fluorescence Siemens SRS3000 equipment for major and trace elements. For major and trace elements precision is valued in terms of relative standard deviation being < 1% (Sutarno & Steger 1985).

The REE analysis was carried out in twenty two sand samples by using 0.1 g of dried sample (mesh 200) and digested with strong acid. Digestion was performed in teflon vessels using 4 ml of HCl O<sub>4</sub> and 10 ml HF. This mixture was heated and residue dissolved in distilled water.

Residue was incorporated to a volumetric flask. Determinations of REE were carried out with an ICP mass spectrometer VG Elemental model PQ3. Detection limits were calculated as the concentration equivalent to three times the standard deviation of five replicates of the blank

solution. It was better than 200ppt for all elements determined. Calibration of the apparatus was done with a 0.1, 1 10 and 100 ppb multi elemental standard solution (SPEX- High Purity) and a blank solution of de-ionized water all containing HNO<sub>3</sub> at 2%. Results were observed for international standards (JG-2). The validity of the analytical procedure was assessed by means of accuracy and precision tests. They were calculated by comparing measured and reference values (JA-2). All elements determined had a better than 10 % relative standard deviation (RSD) precision. Data resulted for BCU-3 or "in house standard indicated good agreement with the certified values.

Chondrite-normalized REE patterns were based on values by Evensen *et al.* (1978) averaging the samples firstly determined in ppm for each site.

**RESULTS & DISCUSSION**

From Figure 3 it can be observed that among the major element trends Ti shows various peaks from localities 10 to 22 that correspond to some beach areas from Playa Miramar, the whole area of Boca del Tordo and one sample from the La Pesca. This suggests that this area might have influenced by heavy minerals and plutonic and sedimentary outcrops as it has previously reported in dune sands from Mexico (Kasper-Zubillaga *et al.* 2008a). The rest of the major elements do not show differences in their trends along the coast. However, Ca shows a dynamic behavior represented by oscillations along the coast probably produced by the amount of biogenic debris.

Trace elements show that V exhibit high peaks in Boca del Tordo beach probably associated with the presence of some heavy minerals like magnetite (Kasper-Zubillaga *et al.* 2008a).

Rare earth elements patterns show differences in Eu anomalies for the samples studied from Boca del Tordo (Fig. 5) that can be attributed to the mix of felsic and mafic sources. This variation can also be explained due to the impoverishment of feldspars due to weathering (Kasper-Zubillaga *et al.* 2008b). Also Boca del

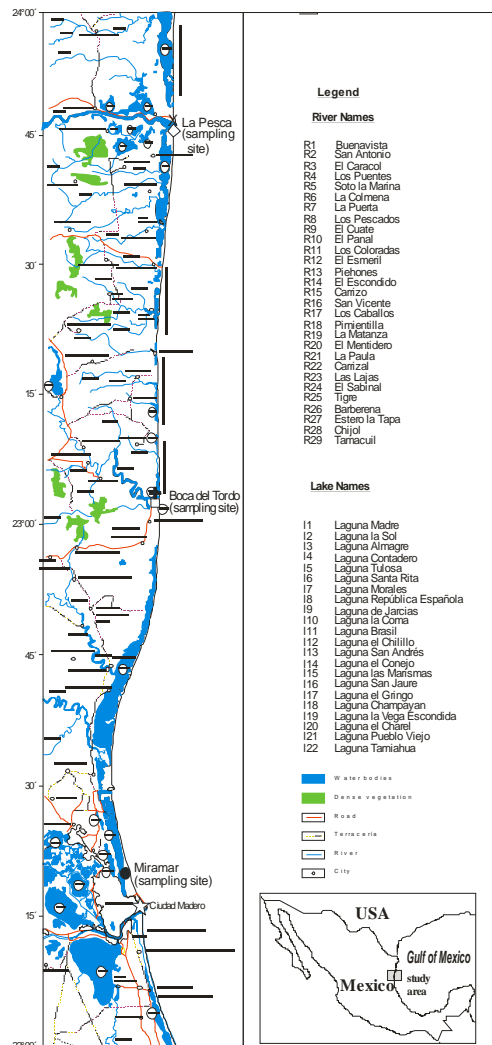


Fig. 1. Study area and sampling sites.

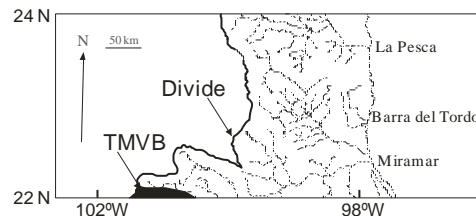
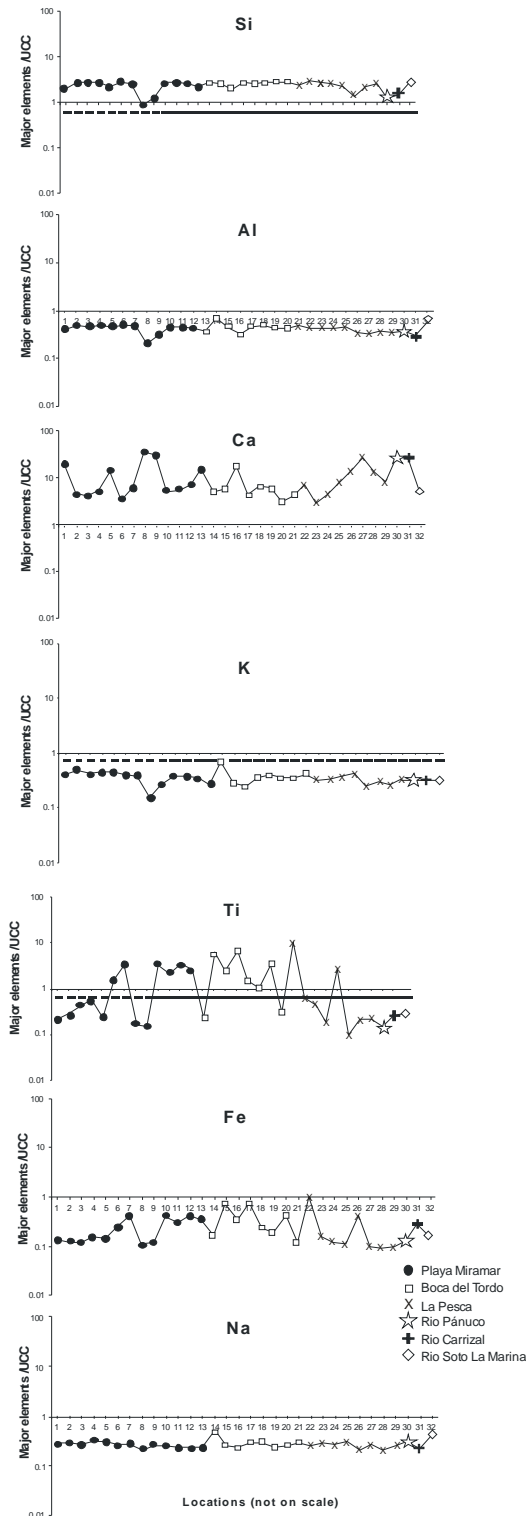
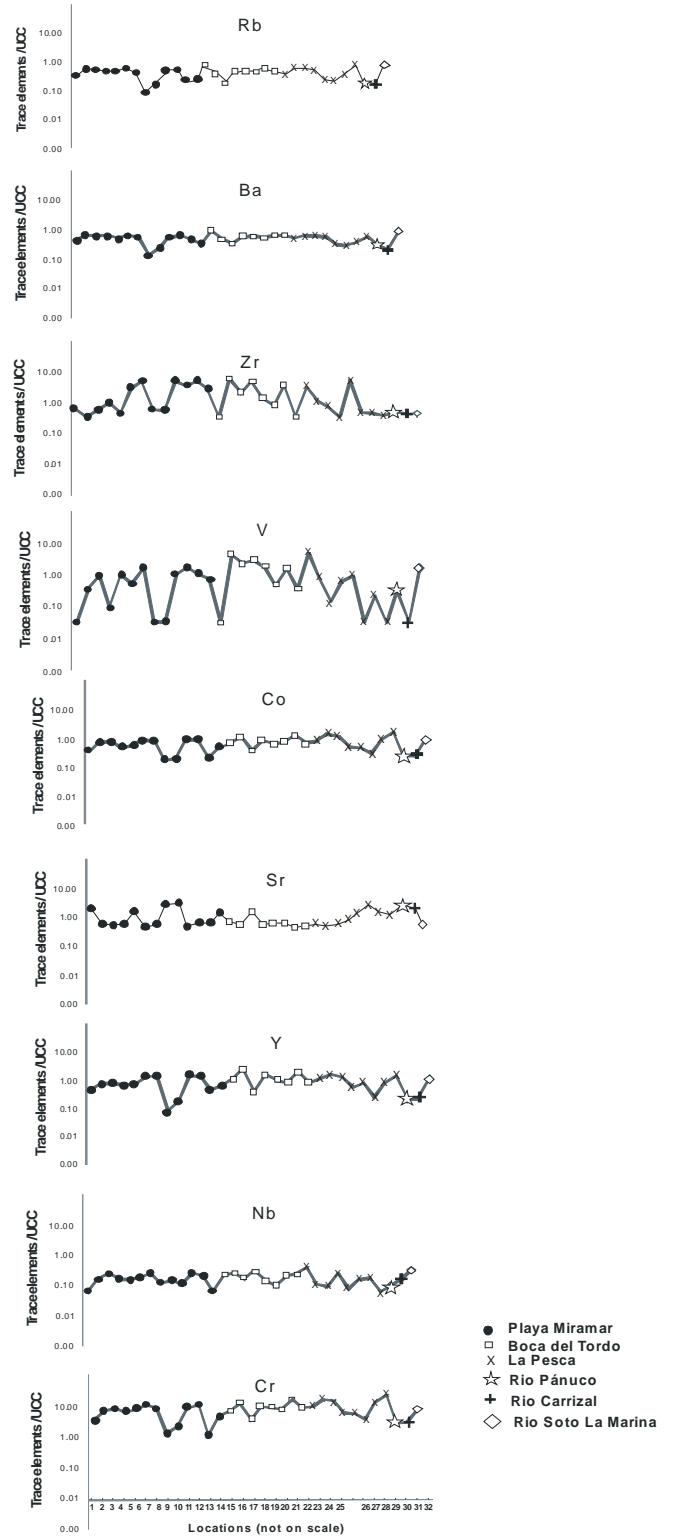


Fig. 2. Map of showing the Trans-Mexican Volcanic Belt (TMVB) near to the study area.



**Fig. 3.** Spatial trends of major elements at beach and dune sands from the northeastern coast of Mexico.



**Fig. 4.** Trace elements tendencies along the northeastern coast of Mexico.

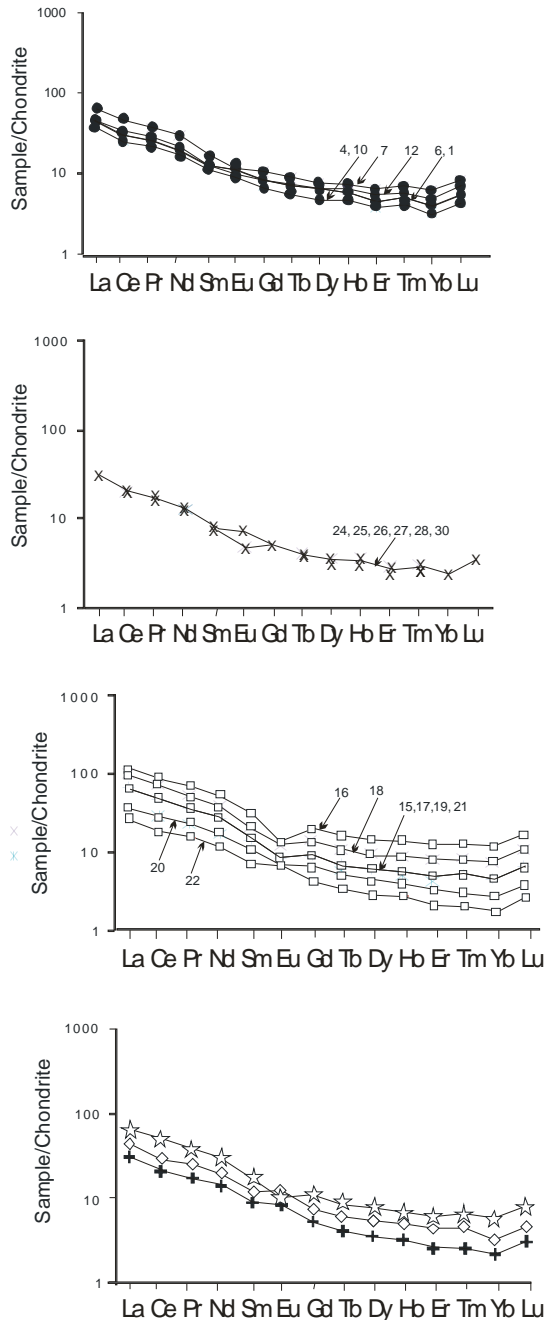


**Fig. 5.** Rare earth elements in the northeastern coast of Mexico.

Tordo concentrates more rare earth elements especially in samples 16 and 18 which is probably due to the presence of some heavy minerals that are potential carriers of rare earth elements (Kasper-Zubillaga *et al.* 2008b). The possible

source of volcanic is mainly through the Panuco River that intersects volcanic from the Trans-Mexican Volcanic Belt.

**CONCLUSIONS**

- (1) Major elements trends show that Northeastern Mexican beaches are influenced by heavy minerals and plutonic and sedimentary outcrops.
- (2) Trace elements tendencies suggest that the Boca del Tordo beach is more influenced by the presence of magnetite than other beaches.
- (3) Rare earth elements trends show a negative and positive Eu anomalies in some samples studied from the Northeastern beaches suggesting a mix of felsic and mafic source rocks and feldspar weathering.

**ACKNOWLEDGMENTS**

We are indebted to Rufino Lozano and Ofelia Morton for the geochemical analyses carried out at the Instituto de Geologia and Instituto de Geofisica respectively from the Universidad Nacional Autónoma de Mexico, Mexico.

**REFERENCES**

ARMSTRONG-ALTRIN, J.S., VERMA, S.P., MADHAVARAJU, J., LEE, Y.I., & RAMASAMY, S. 2003. Geochemistry of upper Miocene Kudankulam limestones, southern India. *International Geological Review*, **45**, 16-26.

ARMSTRONG-ALTRIN, J.S., LEE, Y.I., VERMA, S.P., & RAMASAMY, S. 2004. Geochemistry of sandstones from the Upper Miocene Kudankulam Formation, Southern India: implications for provenience, weathering and tectonic setting. *Journal of Sedimentary Research*, **74**, 285-297.

CARRANZA-EDWARDS, A., ROSALES-HOZ, L., & SANTIAGO-PÉREZ, S. 1994. Provenience memories and maturity of holocene sands in Northwest Mexico. *Canadian Journal of Earth Sciences*, **31**, 1550-1556.

CARRANZA-EDWARDS, A., BOCANEGRA-GARCIA, G., ROSALES-HOZ, L. & DE PABLO GALÁN, L. 1998. Beach sands from Baja California Peninsula, México. *Sedimentary Geology*, **119**, 263-274.

CRITELLI, S., LE PERA,, E., & INGERSOLL,R.V. 1997.The effects of source lithology, transport, deposition and sampling scale on

- the composition of southern California sand. *Sedimentology*, **44**, 653-671.
- EVENSEN, M.N., HAMILTON, P.J., & ONIONS, P.K., 1978. Rare earth abundance in chondrite meteorites. *Geochimica et Cosmochimica Acta*, **42**, 1199-1212.
- FOLK, R. L., 1974. Petrology of Sedimentary Rocks. *Hemphill Publishing Co., Austin, TX*.
- IBBEKEN, H. & SCHLEYER, R., 1991. Source and Sediment. *Springer Verlag, Berlin*.
- KASPER-ZUBILLAGA, J.J. & CARRANZA-EDWARDS, A., 2005. Grain size discrimination between sands of desert and coastal dunes from northwestern Mexico. *Revista Mexicana de Ciencias Geológicas*, **22**, 383-390.
- KASPER-ZUBILLAGA, J.J., ACEVEDO-VARGAS, B., MORTON-BERMEA, O., & ORTIZ-ZAMORA, G., 2008a. Rare earth elements of the Altar Desert dune and coastal sands, Northwestern Mexico. *Chemie Der Erde Geochemistry*, **68**, 45-69.
- KASPER-ZUBILLAGA, J.J., CARRANZA-EDWARDS, A., & MORTON-BERMEA, O. 2008b. Heavy minerals and rare earth elements in coastal and inland dunes of El Vizcaino Desert Baja California Peninsula, Mexico. *Marine Georesources and Geotechnology*, **26**, 172-188.
- SUTARNO, R. & STEGER, H.F., 1985. The use of certified reference materials in the verification of analytical data and methods. *Talanta*, **32**, 439-445.

## Biogeochemistry of Iron

A.L. Kovalevskii<sup>1</sup> & O.M. Kovalevskaya<sup>1</sup>

<sup>1</sup>Geological Institute Siberian Branch of Russian Academy of Sciences Sakhyanova Street, 6a, Ulan-Ude-47, 670047  
RUSSIA (e-mail: [koval@gjin.bsnet.ru](mailto:koval@gjin.bsnet.ru))

**ABSTRACT:** 9070 samples of plants and 1060 samples of soils, rocks and iron ores were studied when research was done on four iron ore deposits. This allowed for the first time to get a considerable volume of fact data about the iron accumulation by a large number of studied bioobjects of plants not only in Angaro-Ilimskii iron ore region, but also in other regions of the East Siberia, particularly in Buryatia and Chita area. The main result of the research is revealing the System of Nonbarrier-Barrier Accumulation (SNBBA) of plants and external layers of bark of trunks of various species of trees as bioobjects, nonbarrier in relation with iron.

**Keywords:** *biogeochemistry, plants, iron, beryllium, nonbarrier-barrier*

### INTRODUCTION

The objects of biogeochemical researches were four iron-ore deposits of Angaro-Ilimsk ore-bearing region of Irkutsk area: Rudnogorskoe, Oktyabr'skoe, Tat'yaninskoe and Zmeinogorskoe. All deposits are explosion tubes of rounded and oval form. Magnetite and seldom gematite iron-ore bodies, which are of practical interest, have mainly ring-shaped, seldom secant, linear form on them. Ring-shaped ore bodies are situated on peripheries of explosion tubes. Their thickness is measured by meter and tens of meters, iron content changes from 20 to 60 % and on average is close to 30-35%. Explosion tubes break through Ordovician and Cambrian sedimentary rocks and are of Triassic age. On their contacts with carbonate rocks the complex processes of scarning are widely developed.

### THE SYSTEM OF NONBARRIER-BARRIER ACCUMULATION (SNBBA) OF PLANTS IN RELATION TO IRON

The first data about nonbarrier iron accumulation by external layers of tree trunk bark were received by us on Ermakovskii fluorite-beryllium deposit in Zabaikalye. Detailed research of chemical element (CE) distribution in cross-sections of trees trunks and in their other parts and species of plants were conducted here for

the first time, the aim of which was – SNBBA of plants in relation with beryllium and companions of its deposits (Kovalevskii & Kovalevskaya, 1979). Here suddenly it was established that over a fluorite-beryllium ore body, the average content of iron for four specimens were anomalously high. In the external layer of pine trunk bark it was 4.1 %, in suberous cones and roots – 5 %. These contents in nonbarrier bioobjects of pine were higher than in soils (2 % in horizon A, 3 % in B, and 1 % in C). For these nonbarrier bioobjects plant-soil coefficient (PSC) of iron were unusually high 2-2.5. According to Perel'man (1989), iron is referred to the elements of average and weak biological capture with the coefficients of biological absorption (CBA=PSC) 0,n – 0,0n. Minimal content of iron at the considered key point of Ermakovskii beryllium deposit – 0.8 % was established in bast (cambiums) of pine with the contents in twigs, needles and green cones equal to 1.2; 2.1 and 1.4 %. For given four barrier bioobjects PSC were received equal to 0.4; 0.6; 1.0; 0.7 considering an average iron content in soil equal to 2 % – considerably less, than its clark, which was equal approximately to 5 %. Established high PSC of iron on beryllium deposits are connected with pyrite form of iron in fluorite-beryllium ores containing to 50-70 % of fluorite. On this beryllium

deposit, it was established that iron like Be, F, Li, Pb, Zr, Ti, Si, Al, has the highest relative concentrations in external layers of tree trunk bark in comparison with other layers of bark, noticeably (in 2.5 – 4 times) enriches the small fraction of crushed pine and larch bark and forms its own minerals in the bark: pyrite, magnetite (?) and ilmenite. These data were completely confirmed and supplemented when biogeochemistry of iron on its deposits in Angaro-Ilimskii ore region was researched.

Iron in cross-sections of larch, pine, birch, cedar, fir tree, rowan-tree trunks turned out to be distributed in the same type (Fig. 1). For all studied species of trees the maximal contents of iron in the external layer of bark, and minimal – in internal layer of the youngest bast cells consisting mainly of dividing cambial cells were established. For all species of trees in 1.5-2 times greater content of iron is established in “young” sap-wood in comparison with “old” nucleus wood in the central part of trunk. According to concentration curves (Fig. 2) in the system: “external layers of trunks bark – other bioobjects of the same species of trees” and comparison of iron contents in various species and parts of plants on the most intensive biogeochemical haloes of iron 213 studied bioobjects of plants were

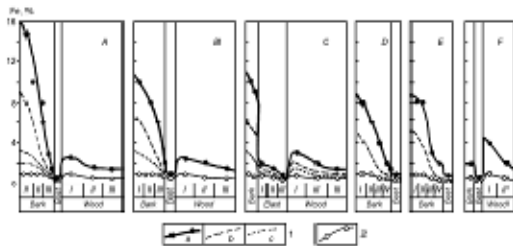


**Fig. 1.** Distribution of iron in trees trunk on the background and the haloes of iron ore bodies (deposit Oktyabr'skoe, Tat'yaninskoe, and Zmeinaya gorka). A – larch (*Larix dahurica* Turcz.); B – pine (*Pinus silvestris* L.); C – birch (*Betula platyphylla* Sukacz.); D – cedar (*Cedrus sibirica* (Rupr.)); E – fir-tree (*Picea obovata* Ledeb); F – rowan-tree (*Sorbus sibirica* Hedl.). 1 – on the haloes (a – the most intensive, b – of middle intensive, c – the less intensive); 2 – on the background.

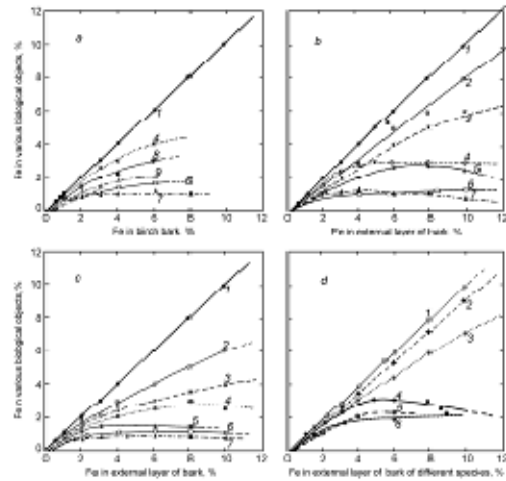


**Fig. 2.** Concentration dependence in the system: the known nonbarrier biological object – the studied biological object for iron on the Oktyabr'skoe iron ore deposit.  
a – birch: 1 – bark, 4 – sap-wood, 6 – nucleus wood, 7 – bast, 8 – leaves, 9 – twigs.  
b – larch: 1 – external layers bark, 2 – middle layers of bark, 3 – internal layers of bark, 4 – sap-wood, 5 – twigs with needles, 6 – nucleus wood, 7 – bast.  
c – pine: 1 – external layers of bark, 2 – average layers bark, 3 – internal layers bark, 4 – sap-wood, 5 – twigs with needles, 6 – nucleus wood, 7 bast.  
d – external layers of bark of different species: 1 – of larch, 2 – of pine, 3 – of birch, 4 – of cedar, 5 – of fir-tree, 6 – of aspen.

grouped for the first time according to their prospecting informativeness to this chemical elements (Kovalevskii, 1991).

From 213 studied bioobjects overgrowing bioobjects of plants – external layers of trunks layers of trunks bark and Siberian larch and ordinary pine stumps, their suberficated cones and birch bark and also roots of all studied species of trees: larch, pine, and birch and green moss are mostly informative. Iron concentrations in their ash on its most intensive haloes exceed 10% according to data of the spectral analyses and reach 12-16% according to data of X-ray-radiometric and chemical analyses. In these 16 (7% of 213 studied) most informative bioobjects haloe concentrations of iron exceed the background in 5-20 times, which approximately corresponds to contrast of

primary litho-geochemical haloes of iron in its ore bodies. That is why these biological objects can be considered nonbarrier, quantitatively-informative in relation to iron. They, first external layers of bark of larch, pine, cedar and fir tree trunks and also birch bark, are recommended for various researches of iron biogeochemistry. Especially if it concerns iron is used as element-indicator of magnetite ores and also of pyritization and sideritization zones, iron of which is more available to plants in comparison with iron of magnetite ores.

**RELATIVE CONTENT OF IRON IN VARIOUS BIOLOGICAL OBJECTS (BIOOBJECTS) OF PLANTS (RCBO)**

The second quantitative parameter, necessary for interpretation of received biogeochemical data is relative content of iron in bioobjects selected on the same points of observation – RCBO. Meanings of RCBO established for bioobjects of the studied iron ore deposits show inconsiderable differentiation between them exceeding ± 20% (Table 1).

**Table 1.** Relative content (RCBO) of iron in bioobjects recommended for biogeochemical researches for this element.

Biological objects	Iron ore deposits			Average
	Oktyabr'skoe	Tat'yanskoe	Zmeinaya gorka	
Trunks bark:				
pine (standard)	1,0	1,0	1,0	1,0
larch	1,1	1,1	1,1	1,1
cedar	1,2	1,3	1,1	1,2
fir tree	0,9	1,0	0,9	0,9
birch	0,8	0,9	0,8	0,8
Suberificated cones:				
pine	1,1	1,1	1,2	1,1
larch	1,2	1,3	1,1	1,2
fir tree	0,7	1,3	0,8	0,9
Young underwood of pine	0,7	0,9	0,8	0,8

**INTENSITY OF BIOLOGICAL ABSORPTION OF IRON**

On all four studied iron ore deposits and on all other key sites the data of which were used in this report, iron absorption by plants take place according to

lithobiogeochemical model (Kovalevskii, 1991). According to this model there are no free ground waters in the rootinhabited zone, and chemical elements (CE) are absorbed only from its solid phase. Intensity of biological absorption in this case is determined with the help of plant-soil (PSC) and plant-rock (PRC) coefficients. During last years PRC was introduced by us for conditions, characteristic for vein ore deposits. On them often the horizon of plant nutrition, which is determined according to special methodics (Kovalevskii, 1991), of the studied CE turned out to be arranged to the lowest soil horizon D – elluvium of bedrocks.

We determined PSC of CE as its contents ratio in ash of nonbarrier plant bioobject and in soil on the horizon of its nutrition, that is of great significance for easily-mobile chemical elements, which often enrich lower and rarely upper (nitrogen, phosphorus, manganese) soil horizons. For watershed elluvium landscapes essential differentiation of iron contents in soil sections wasn't observed. For slope landscapes over not thick iron ore bodies depletion of upper soil horizons was observed due to their horizontal displacement concerning eluvium. Therefore is why also as for other ore elements we used usually the lower soil horizon C at the standard depth of our soil sections 0,8-1 m to calculate PSC.

According to data we have values of PSC depend on mineral and chemical forms of the studied CE. The main ones are dependence on solubility of minerals and size of their grains. Four main forms of iron in soils: magnetite (main), hematite, pyrite and isomorphous (non-mineral) were studied by us. Easily soluble siderite (carbonate) form of iron is of great interest, but in the studied conditions such iron ores known on Ozernyi pyrite-polymetal deposit were oxidized to the significant depth and converted into hydroxide forms in the rootinhabited zone.

On all studied by us iron ore deposits in Baikal-Amur main line (BAM) region magnetite iron dominates in ores. Only on Oktyabr'skii deposit hematite-magnetite

ore bodies are known. Magnetite ores have various structure, texture and size of grains that was displayed in intensity of iron absorption by nonbarrier bioobjects of plants. The most disperse hardly enriched magnetite was found on Tat'yaninskii deposit. Biogeochemical anomalies of iron in nonbarrier bioobjects, which are here external layers of bark (crust) of pine, larch and birch trunks correspond well to iron ore bodies. At background contents of iron in trees bark ash 0.4-1,6 %, but in soils – 2-8%, its PSC on the background was equal to in average 0,2. Over iron ore bodies with concentrations 25-45 % biogeochemical anomalies of iron with its concentrations in ash of nonbarrier bioobjects 10-16 % at average value of PSC=0.3 were established, i.e., here availability of iron of disperse magnetite to plants was in 1.5 times higher than on the background, that is very favourable when using iron anomalies in plants for iron ore mineralization indication.

On the Oktyabr'skii deposit biogeochemical anomalies of iron are characteristic not for all known ores. Such anomalies were not revealed over dominating here massive gematite-magnetite ore bodies that evidenced inaccessibility to plants of iron being in composition of gematite and massive magnetite. Average PSC of iron over gematite-magnetite ore bodies were made 0.01-0,02 at its contents in birch, pine and larch bark 0.2-1.0 %, which were not different from background contents, and in gematite-magnetite ores – 25-55 %. Biogeochemical anomalies of iron with its contents 3-7 % reaching 8-10 % were observed over various varieties of magnetite ores with contents 25-45 %. PSC of iron is here 0.1-0.4; approximately in 20 times higher than over massive gematite-magnetite ores. Over disperse magnetite ores of Oktyabr'skii deposit the average values of PSC of iron were the same as on Tatyankinskii deposit and were 0.3-0.4. Unexpectedly four mostly

intensive biogeochemical anomalies with 7-12 % iron were revealed outside the known iron ore bodies. These anomalies appeared to be connected with three zones of pyritization and chalcopyritization inside the diatreme and with one zone of pyritization outside its limits. When iron contents in these zones are 5-7 %, its PSC over zones of pyritization is 1.4-1.7, in average 1.5. So, on Oktyabr'skii iron ore deposit for the first time a precise dependence of PSC of iron on its three mineral forms was established. Minimal PSC over massive gematite-magnetite ores (0.01-0.02), when there are no biogeochemical anomalies, evidence practical inaccessibility of gematite and massive magnetite to plants. Average PSC = 0.1-0.4 correspond to ores with disperse magnetite, and maximal 1.4-2.5, in average 2 – to zones of pyritization, i.e., sulphide forms of iron in the root inhabited zone. For sites with non-mineral, isomorphic forms of iron, typical for the background, an average PSC = 0.2 when its contents in ash of nonbarrier bioobjects 0.5-1 %, and in soils – 3-6 % at clark close to 5 %.

## CONCLUSIONS

- (1) Received data evidence that iron, like the majority of chemical elements, is characterized by nonbarrier accumulation in suberificated tissues of trees, in particular, in external layers of trunk bark.
- (2) Availability of iron to plants according to the lithobiogeochemical model of root nutrition depending on to its mineral forms in the root inhabited zone changes in 10-100 times.

## REFERENCES

- KOVALEVSKII, A.L. 1991. Biogeochemistry of plants. *Novosibirsk: Nauka*. (In Russian).
- KOVALEVSKII, A.L. & KOVALEVSKAYA, O.M. 1979. Biogeochemical prospecting for beryllium deposits. *Novosibirsk: Nauka*. (In Russian).
- PEREL'MAN, A.I. 1989. Geochemistry. *Moscow: Visshaya shkola*. (In Russian).

## **Correlation of atmospheric soil and atmospheric lead in three North American cities: can re-suspension of urban lead contaminated soil be a major source of urban atmospheric lead and cause seasonal variations in children's blood lead levels?**

**Mark Laidlaw<sup>1</sup>**

<sup>1</sup>4 Birch Drive, Hamlyn Terrace, NSW, 2259 AUSTRALIA (e-mail: [markas1968@gmail.com](mailto:markas1968@gmail.com))

**ABSTRACT:** Soils in older cities are highly contaminated by lead from past use of lead in leaded gasoline and due to the use of lead in exterior paints. In this study the temporal variations in atmospheric soil and atmospheric lead in three North American cities are examined. This study tested the hypothesis that atmospheric lead and atmospheric soil concentrations obtained from the Interagency Monitoring of Protected Visual Environments (IMPROVE) exhibit statistically significant correlations in three North American cities. Results indicate that atmospheric soil and atmospheric lead were correlated in Detroit between November 2003 to July 2005 ( $r = 0.47$ ,  $p < 0.001$ ); In Pittsburgh between April 2004 to July ( $r = 0.40$ ,  $p < 0.001$ ); and in Birmingham between May 2004 to December 2006 ( $r = 0.35$ ,  $p < 0.001$ ). The hypothesis that atmospheric soil and atmospheric lead follow seasonal patterns with highest concentrations during the summer and/or autumn could not be rejected. It is suggested that atmospheric lead and atmospheric soil concentrations are correlated due to re-suspension of urban lead contaminated soils. It is further suggested that in order to decrease urban atmospheric lead concentrations, lead deposition, and children's seasonal exposure via hand to mouth activity, urban lead contaminated soils should be remediated or isolated.

**KEYWORDS:** *lead, soil, re-suspension, blood, poisoning, children*

### **INTRODUCTION**

In the USA, motor vehicles used gasoline containing tetramethyl and tetraethyl Pb additives from the 1920s to 1986. By the 1950s, Pb additives were contained in virtually all grades of gasoline. By 1986, when leaded gasoline was banned, 5–6 million metric tons of Pb had been used as a gasoline additive, and about 75% of this Pb was released into the atmosphere (Chaney & Mielke 1986; Mielke & Reagan 1998). Thus, an estimated 4–5 million tons of Pb has been deposited into the US environment by way of gasoline-fueled motor vehicles (Mielke 1994). Accumulation of soil Pb created by leaded gasoline is proportional to highway traffic flow (Mielke *et al.* 1997).

In the 1970s, the presumed dominant source of soil Pb contamination was Pb-based house paint (Ter Haar and Aronow, 1974). A subsequent study of garden soils conducted in metropolitan Baltimore, Maryland, began to raise questions about

that assumption. Soil around Baltimore's inner city buildings, predominantly unpainted brick, exhibited the highest amounts of Pb, and soils outside of the inner city, where buildings were commonly constructed with Pb-based paint on wood siding, contained comparatively low amounts of Pb, suggesting that Pb based house paint could not account for the observed pattern of soil Pb (Mielke *et al.* 1983). The same pattern was also found in Ottawa, Canada (Ericson & Mishra 1990).

The quantity and distribution of soil Pb have been studied in numerous places in North America (see Laidlaw & Filippelli, 2008). All these North American cities exhibited the same distance decay characteristic of high soil Pb contamination in the inner city and decreasing contamination toward the outer parts of the city as initially identified in garden soils of Baltimore (Mielke *et al.* 1983). Further, similarities in this distance decay pattern of soil Pb supports the idea

that Pb-based house paint was not the sole source contributing to these observed differences.

Soil lead concentrations have been observed to be associated with children's blood lead concentrations using multiple study designs – cross-sectional, ecological spatial, ecological temporal, prospective soil removal and isotopic (Laidlaw & Filippelli, 2008).

Average monthly blood Pb (BPb) values of children from urban areas tends to increase significantly in summer months (Haley & Talbot 2004; Laidlaw *et al.* 2005; Yiin *et al.* 2000). Early work by Mielke *et al.* (1992), Johnson & Bretsch (2002), and Johnson *et al.* (1996) suggested that blood Pb seasonality may be related to the interaction between climate and Pb contaminated soils. Yiin *et al.* (2000) actually measured seasonal changes in dust Pb levels and correlated blood Pb levels with seasonal dust Pb concentrations. Yiin *et al.* (2000) conducted a study to examine seasonal changes in residential dust Pb content and its relationship to blood Pb in preschool children. The study found that windowsill wipe samples were most correlated with blood Pb concentration and the variation of dust Pb levels for floor Pb loading, windowsill Pb loading, and carpet Pb concentration were consistent with the variation of blood Pb levels, showing the highest levels in the hottest months of the year (June, July, and August).

Laidlaw & Filippelli (2008), Laidlaw *et al.* (2005), and Filippelli *et al.* (2005) have demonstrated that seasonal variations in children's blood lead levels in Syracuse, Indianapolis and New Orleans could be predicted using soil moisture and atmospheric variables suggesting that re-suspension of urban soils contaminated by past use of leaded gasoline and paint were causally related to seasonal variations in blood lead. These papers concluded that urban lead contaminated soil was being re-suspended when soils were dry in the summer and autumn when evapotranspiration is maximised. Their assumption that soil lead is being re-suspended and is responsible for a large

portion of the lead in the atmosphere is supported by lead isotopic analysis of atmospheric lead in Yerevan Armenia (Kurkjian *et al.* 2001), which indicated that following elimination of the use of lead in gasoline, 75% of atmospheric lead in the Yerevan atmosphere was derived from re-suspended soil.

Soil resuspension has the capability of entraining significant volumes of Pb into the air of urban areas. Harris & Davidson (2005) calculated that resuspension of soil is responsible for generating 54,000 kg of airborne Pb each year in the South Coast Air Basin of California (SOCAB) and will remain a major source well into the future. Similarly, Lankey *et al.* (1998) concluded that 43% of Pb emissions in the South Coast Air Basin in California resulted from the resuspension of soil and road dust.

In this study, data from Birmingham, Alabama; Pittsburgh, Pennsylvania; and Detroit, Michigan were selected to assess seasonal patterns and assess seasonal relationships between atmospheric soil and atmospheric lead.

The following hypotheses were tested:

- 3) Atmospheric air lead and atmospheric soil concentrations exhibit statistically significant correlations in three major North American Cities; and
- 4) Atmospheric soil and atmospheric lead follow seasonal patterns with highest concentrations during the summer and/or autumn.

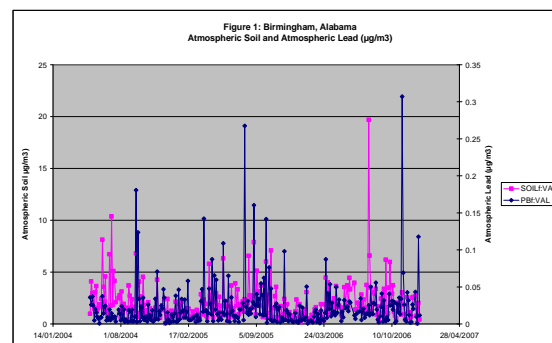


**Fig. 1.** Plot of atmospheric soil and atmospheric lead in Birmingham, Alabama ( $r = 0.35$ ,  $p < 0.001$ ).

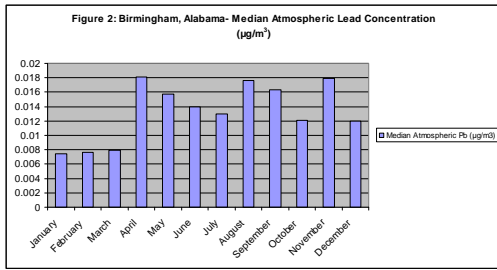


**Fig. 2.** Median atmospheric lead concentrations at IMPROVE air monitoring station in Birmingham, Alabama (May 2004 to December 2006).

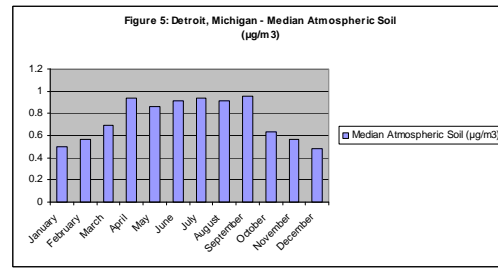


**Fig. 5.** Median Atmospheric soil concentrations at IMPROVE air monitoring station in Detroit, Michigan (November 2003 to July 2005).

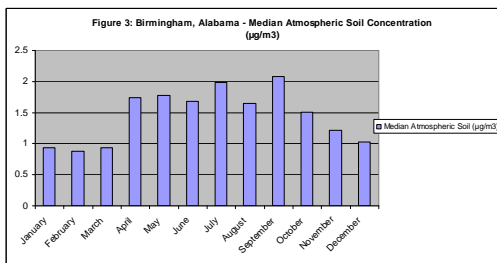


**Fig. 3.** Median Atmospheric soil concentrations at IMPROVE air monitoring station in Birmingham, Alabama (May 2004 to December 2006).

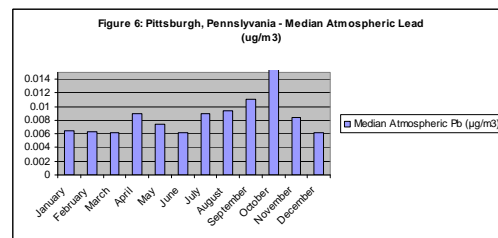


**Fig. 6.** Median atmospheric lead concentrations at IMPROVE air monitoring station in Pittsburgh, Pennsylvania (April 2004 to July 2005).

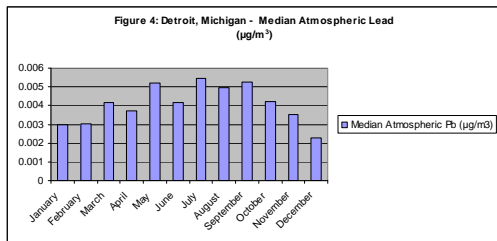


**Fig. 4.** Median atmospheric lead concentrations at IMPROVE air monitoring station in Detroit, Michigan (November 2003 to July 2005).

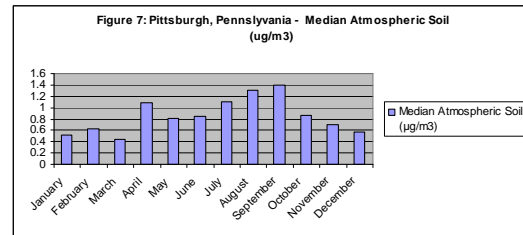


**Fig. 7.** Median Atmospheric soil concentrations at IMPROVE air monitoring station in Pittsburgh, Pennsylvania (April 2004 to July 2005).

**CONCLUSIONS**

1) In order to decrease urban atmospheric lead concentrations, lead deposition, and subsequent children’s exposure via hand to mouth activity, urban lead contaminated soils should be remediated or isolated.

**REFERENCES**

CHANEY, R.L. & MIELKE, H.W. 1986. Standards for soil Lead limitations in the United States.

In: HEAMPHILL, D.D. (ed) Trace Substances in 2036 M.A.S. Laidlaw, G.M. Filippelli / Applied Geochemistry 23 (2008) 2021–2039 Environmental Health, University of Missouri, Columbia, 357–377.

Ericson, J.E. & Mishra, S.I., 1990. Soil lead concentrations and prevalence of hyperactive behavior among school children in Ottawa, Canada. Environ. Internat. 16, 247–256.

FILIPPELLI, G.M., LAIDLAW, M., LATIMER, J., & RAFTIS, R. 2005. Urban lead poisoning and

- medical geology: an unfinished story. *GSA Today*, **15**, 4-11.
- HALEY, V.B. & TALBOT, T.O. 2004. Seasonality and trend in blood lead levels of New York State children. *BMC Pediatrics*, **4**, 8.
- HARRIS, A. & DAVIDSON, C. 2005. The role of resuspended soil in lead flows in the California south coast air basin. *Environmental Science Technology*, **39**, 7410–7415.
- IMPROVE (Interagency Monitoring of Protected Visual Environments), 2007. Available: <http://vista.cira.colostate.edu/improve/>. Accessed [15 November 2007].
- JOHNSON, D. & BRETSCH, J. 2002. Soil lead and children's BLL Levels in Syracuse, NY, USA. *Environmental Geochemistry and Health*, **24**, 375-385.
- JOHNSON, D., MCDADE, K., & GRIFFITH, D. 1996. Seasonal variation in pediatric blood levels in Syracuse, NY, USA. *Environmental Geochemistry and Health*, **18**, 81-88.
- KURKJIAN R., DUNLAP, C., & FLEGAL, R. 2001. Lead isotope tracking of atmospheric response to post-industrial conditions in Yerevan, Armenia. *Atmospheric Environment*, **36**, no. 8, 1421-1429.
- LAIDLAW, M.A.S., MIELKE, H.W., FILIPPELLI, G.M., JOHNSON, D.L., & GONZALES, C.R., 2005. Seasonality and children's blood lead levels: developing a predictive model using climatic variables and blood lead data from Indianapolis, Indiana, Syracuse, New York, and New Orleans, Louisiana (USA). *Environmental Health Perspectives*, **113**, 793–800.
- LAIDLAW, M.A. & FILIPPELLI, G.M. 2008. Resuspension of urban soils as a persistent source of lead poisoning in children: A review and new directions. *Applied Geochemistry*, **23**, no 8, 2021-2039.
- LANKEY, R.L., DAVIDSON, C.I., & MCMICHAEL, F.C. 1998. Mass balance for lead in the California south coast air basin: an update. *Environmental Research*, **78**, 86–93.
- MIELKE, H.W., ANDERSON, J.C., BERRY, K.J., MIELKE JR., P.W., CHANEY, R.L., & LEECH, M. 1983. Lead concentrations in inner-city soils as a factor in the child lead problem. *American Journal of Public Health*, **73**, 1366–1369.
- MIELKE, H.W., 1994. Lead in New Orleans soils: new images of an urban environment. *Environmental Geochemistry and Health*, **16**, 123–128.
- MIELKE, H.W. & REAGAN, P.L., 1998. Soil is an important pathway of human lead exposure. *Environmental Health Perspectives*, **106**, 217–229.
- MIELKE, H.W., DUGAS, D., MIELKE JR., P.W., SMITH, K.S., SMITH, S.L., & GONZALES, C.R., 1997. Associations between soil lead and children's blood lead in urban New Orleans and rural Lafourche Parish of Louisiana. *Environmental Health Perspectives*, **105**, 950–954.
- YIIN, L.M., RHOADS, G.G., & LIOY, P.J. 2000. Seasonal influences on childhood lead exposure. *Environmental Health Perspectives*, **108**, 177-182.

## Using Ground Penetrating Radar to delineate sub-surface calcrete in the Great Victoria Desert, South Australia: implications for gold exploration

Melvyn J. Lintern<sup>1</sup>, Anton W. Kepic<sup>2</sup> & Matthew Josh<sup>3</sup>

<sup>1</sup>CSIRO Exploration & Mining, P.O. Box 1130, Bentley, 6102 WESTERN AUSTRALIA (e-mail: [mel.lintern@csiro.au](mailto:mel.lintern@csiro.au))

<sup>2</sup>Head of Department, Exploration Geophysics, Curtin University, 26 Dick Perry Avenue, Kensington, 6151 WESTERN AUSTRALIA.

<sup>3</sup>CSIRO Petroleum Resources, P.O. Box 1130, Bentley, 6102 WESTERN AUSTRALIA

**ABSTRACT:** Exploration in southern Australia is commonly hampered by the presence of exotic cover such as aeolian sand and alluvium. Calcrete (caliche), present within the cover, has been shown to assist mineral explorers searching for Au deposits as it is an easily identifiable material that can accumulate Au. However, in large areas of South Australia, the location of calcrete within the cover is hampered by overlying sand. Here, we use ground penetrating radar to expose the location of calcrete at the Edoldeh Tank Au deposit, suggest how calcrete can form in the sub-surface, and demonstrate how Au in calcrete can extend the surficial geochemical footprint of Au deposits and thus provide a broader target for explorers.

**KEYWORDS:** *calcrete, gold exploration, ground penetrating radar, mineral exploration, calcium carbonate*

### INTRODUCTION

Calcrete (caliche) or pedogenic carbonate sampling is an important technique for gold exploration, particularly in Australia. In South Australia, mineral explorers use augers or manually dig holes and collect calcrete from the near surface. Typically, calcrete accumulates in arid/semi-arid conditions in South Australia as a result of wind blown dust, rainfall and aerosol derived from marine sources. As calcrete forms sub-surface its appearance in undisturbed environments is commonly disguised by soil and other regolith materials. Calcrete may be ubiquitous in some areas but in sand dune environments its precise distribution in the landscape is not well known. Augering or digging for calcrete here is a hit and miss procedure and add significantly to exploration expenditure. Therefore, an appreciation of calcrete distribution in the landscape is important to mineral exploration.

### METHOD AND RESULTS

The distribution and possible processes of formation of calcrete was investigated at Edoldeh Tank Au prospect in the western

Gawler Craton, located on the edge of the Great Victoria Desert (GVD). In this part of the GVD, regolith landforms are comprised of scarce hills of weathered bedrock outcrops surrounded by sand spreads, dunes and colluvial materials; the hills act as windows to the otherwise covered weathered bedrock. The outcrops themselves have been silicified and, more recently, have been overprinted with calcrete. Calcrete sampling is relatively easy on the exposed outcrops and is preferentially sampled by mineral explorers due to its near-surface location (<10-20 cm depth). However, calcrete on the colluvial slopes and in the swales is not as easily located because of concealment by GVD sand and colluvium.

Ground Penetrating Radar (GPR) was selected to be the primary technique for mapping the calcrete extent because it has very good resolution (less than 0.3 m for a 250 MHz system) and in dry sand/rock can map geological features down to about 10 m (at 250 MHz) depth before attenuation and scattering reduce the signal. Other geophysical techniques generally lack sufficient contrast or resolution to be useful. Seismic methods

can detect consolidated layers very well and have reasonable resolution at shallow depths, but are at least an order of magnitude slower in this environment and cannot detect the base of the calcrete easily. Data were collected for 250 and 500 MHz antenna, and spatial sampling was set by constant time interval and a slow, but steady rate of progress with markers set in the data for 20 m tape intervals. A stack of 32-64 pulses were recorded every 5 cm or less. A surprise in the GPR data was its lack of penetrating power through the cover. The GPR data required more than usual gain adjustment and signal processing to preserve the amplitude variations of reflectivity that mark the calcrete boundaries. As the signal was often at the level of residual systematic noise a long interval 2D subtraction filter was used to extract the reflectivity variations. Whilst the calcrete itself seems fairly transparent, although irregular, it appears that the very dry quartz sand (>90% silica) highly attenuates GPR signals; possibly due to a thin coating of iron rich clay over each silica particle. Surveys upon a nearby track over small sand dunes appear to confirm this characteristic.

Five E-W and N-S transects were selected for the GPR survey. These were located below the flanks of a low hill strewn with silcrete and silicified weathered bedrock cobbles and gravels. Previous limited drilling indicated that the thickness of exotic sandy cover was about 5 m and that calcareous materials may be patchily distributed.

The GPR survey data showed a consistent zone of resistance located at ~0.5-1 m below the surface for each of the five E-W transects. Stacking the graphical images of the transect data, according to their locations on the plan, reveals a tongue-shaped structure of resistance that extends southwards (down slope) at least 200 m visible on all five transects. The depth of resistance is consistent with a sub surface enrichment of calcrete.

In order to test this hypothesis, 25 shallow pits were dug along the transect lines through the sand in areas of high

and low resistance. The zones of high resistance were coincident with the appearance of a near-surface hard laminated calcareous hardpan while the zones of low resistance either had poorly-developed calcareous materials, powdery pedogenic carbonate and/or nodular calcrete.

The often smooth top surface to the calcrete suggests that the calcrete formed by the precipitation of Ca (as carbonate) from sub-surface laterally and vertically flowing vadose water sourced from rainfall, which penetrates easily through the overlying sand. The sub-surface has been plugged with calcrete preventing vertical downwards penetration of vadose water. Instead, vadose water would move laterally until it evaporates or is removed by transpiration. Precipitation of calcium carbonate at the surface of the calcrete would occur, thus contributing to the laminated occurrence of the calcrete.

## DISCUSSION

The tongue-shaped calcrete structure delineated by the GPR has likely to have been formed in one of two ways: either it is the remnant of a more widespread calcrete platform that once covered the entire study area as a result of horizontal movement of fluids and detritus downslope of the hill or it signifies a palaeochannel formed as a result of vadose water preferentially flowing and precipitating in confined zone. The current topography shows a gradient from the NW to the SE within which ephemeral drainages have developed. There is an absence of laminar calcrete accumulation in the near surface of the ephemeral drainages. Deep trenching through the calcrete and sedimentological analysis is required to further investigate these possible explanations of the calcrete tongue formation. Either way, Ca has been transported downslope.

The significance of the calcrete tongue became apparent after geochemical analysis of samples from the test pits showed elevated Au concentrations. Importantly, the highest concentrations (>50 ppb Au) were confined to the laminar

calcrete of the tongue. The source of the Au is from the hill where elevated Au concentrations have been found in the weathered basement. The Au in calcrete down slope of the hill represents a significant extension to the surficial geochemical anomaly and provides a broader target for exploration both at Edoldeh Tank and for similar landscape settings in the GVD. It suggests that Au anomalies in calcrete can be transported but still retain their anomalous signature and thus provide a vector to mineralisation.

### **CONCLUSIONS**

Ground Penetrating Radar was

successfully used to delineate an otherwise undetectable sub-surface calcrete structure. The origin of the structure is a result of surficial processes related to rainfall and topography. Elevated Au concentrations in the calcrete provide a broader target for exploration and suggest that “transported” chemically-mobilised pedogenic carbonate can retain a geochemical signature developed above upslope mineralisation sources.

### **ACKNOWLEDGEMENTS**

We thank David Gray and Nathan Reid for commenting on earlier versions of the manuscript.

## A new direction in searching for the atmospheric CO<sub>2</sub> sink: considering the joint action of carbonate dissolution, global water cycle and the photosynthetic uptake of DIC by aquatic organisms

Zaihua Liu<sup>1,2,\*</sup>, Wolfgang Dreybrodt<sup>3</sup>, & Haijing Wang<sup>4</sup>

<sup>1</sup> The State Key Laboratory of Environmental Geochemistry, Institute of Geochemistry, Chinese Academy of Sciences, Guiyang 550002 CHINA (e-mail: [liuzaihua@vip.gyig.ac.cn](mailto:liuzaihua@vip.gyig.ac.cn))

<sup>2</sup> Karst Dynamics Laboratory, Institute of Karst Geology, Guilin 541004 CHINA

<sup>3</sup> Institute of Experimental Physics, University of Bremen, Bremen 28334 GERMANY

<sup>4</sup> School of Geographical Sciences, Southwest University, Chongqing 400715 CHINA

**ABSTRACT:** The locations, magnitudes, variations and mechanisms responsible for the atmospheric CO<sub>2</sub> sink are uncertain and under debate. Previous studies concentrated mainly on oceans, and soil and terrestrial vegetation as sinks. Here, we show that there is an important CO<sub>2</sub> sink in carbonate dissolution, the global water cycle and photosynthetic uptake of DIC by aquatic ecosystems. The sink constitutes up to 0.82 Pg C/a: 0.24 Pg C/a is delivered to oceans via rivers and 0.22 Pg C/a by meteoric precipitation, 0.12 Pg C/a is returned to the atmosphere, and 0.23 Pg C/a is stored in the continental aquatic ecosystem. The net sink could be as much as 0.70 Pg C/a, may increase with intensification of the global water cycle, increase in CO<sub>2</sub> and carbonate dust in atmosphere, reforestation/afforestation, and with fertilization of aquatic ecosystems. Under the projection of global warming for the year 2100, it is estimated that this CO<sub>2</sub> sink may increase by 22%, or about 0.18 Pg C/a.

**KEYWORDS:** atmospheric CO<sub>2</sub> sink, carbonate dissolution, global water cycle, aquatic photosynthesis, organic matter storage/burial

### INTRODUCTION

An important problem in the science of global change is the imbalance of the atmospheric CO<sub>2</sub> budget (Melnikov & O'Neill, 2006). Of the CO<sub>2</sub> added to the atmosphere from burning of fossil fuels, ~half stays in the atmosphere and ~half is absorbed into the oceans and terrestrial biosphere. Some is "missing". Without correct accounting, predictions resulting from CO<sub>2</sub> emission scenarios are uncertain and the uncertainty affects energy policy decisions.

Previous studies addressed oceans and terrestrial vegetation as CO<sub>2</sub> sinks. Here, we describe an important CO<sub>2</sub> sink in carbonate dissolution, the global water cycle (GWC), and uptake of dissolved inorganic carbon (DIC) by aquatic. The sink is larger than previous estimates (Meybeck 1993; Gombert 2002).

### METHODS

The CO<sub>2</sub> hydrologic sink (J<sub>T</sub>) is:

$$J_T = Q_{MP} \times C_{DIC,MP} + Q_{RO} \times C_{DIC,RO} \quad (1)$$

where Q<sub>MP</sub> is meteoric precipitation and Q<sub>RO</sub> is continental runoff (Shiklomanov 1993), C<sub>DIC,MP</sub> is the mean observed meteoric precipitation DIC concentration, and C<sub>DIC,RO</sub> is the calculated DIC in equilibrium with world mean soil CO<sub>2</sub> and/or calcite.

C<sub>MP,DIC</sub> was based on MP falling on oceans. C<sub>DIC,RO</sub> is computed, using the DIC of soil pore water in equilibrium with a soil air pCO<sub>2</sub> and/or calcite (Dreybrodt 1988). Global mean soil pCO<sub>2</sub> was calculated as (Brook *et al.* 1983):

$$\log(pCO_2) = -3.47 + 2.09(1 - e^{-0.00172 AET}) \quad (2)$$

where AET is annual evapotranspiration, and weighted for carbonate (~15% of the land area; Ford & Williams 1989; Gombert 2002) and non-carbonate regions.

The net CO<sub>2</sub> sink for RO (J<sub>N,RO</sub>) is:

$$J_{N,RO} = J_{TC} - J_{DG,RO} \quad (3)$$

where J<sub>TC</sub> is CO<sub>2</sub> sink by the dissolution of carbonate and CO<sub>2</sub>, and J<sub>DG,RO</sub> is CO<sub>2</sub> degassed from RO waters (Einsele *et al.* 2001; Lerman & Mackenzie 2005).

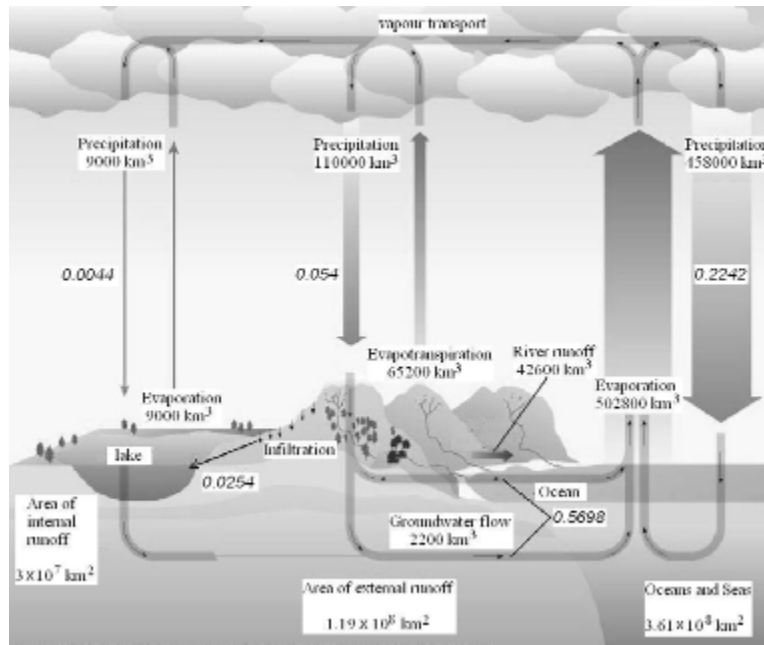
**CALCULATION OF GWC CO<sub>2</sub> SINKS**

Figure 1 presents the model. Precipitation rates are: 9000 km<sup>3</sup> between atmosphere and continental interior (CI), 110000 km<sup>3</sup> between atmosphere and continental margins (CM), and 458000 km<sup>3</sup> between atmosphere and oceans. Mean DIC for global precipitation is 81.59 μmol/l. Thus, the atmospheric CO<sub>2</sub> sink is 0.0044, 0.054, and 0.22 Pg C/a, respectively (Fig. 1). Annual global CI RO and CM RO are 2000 and 44800 km<sup>3</sup>, respectively (Baumgartner & Reichel 1975; Shiklomanov 1993). Using global mean soil pCO<sub>2</sub> of 6393 ppmv and global mean surface temperature of 15°C, the equilibrium values of DIC are 300 and 3640 μmol/l for the non-carbonate and carbonate terranes, respectively. Thus, CO<sub>2</sub> sinks by CI and CM RO are 0.013 and 0.28 Pg C/a, respectively. The total calculated CO<sub>2</sub> sink of 0.30 Pg C/a is very close to that of Gombert (2002; 0.302 Pg C/a), who used a different approach. Although our method seems valid, in terranes with large amounts of pedogenic carbonate (48% continental

area; Adams & Post 1999), the continental-RO CO<sub>2</sub> sink will be larger. Using 50% of land area as a conservative estimate of karst regions and soil with pedogenic carbonate, CO<sub>2</sub> sinks by CI and CM RO are estimated to be 0.025 and 0.57 Pg C/a, respectively (Fig. 1). Therefore, the total atmospheric CO<sub>2</sub> sink as DIC by the GWC could be 0.82 Pg C/a.

DIC is removed during photosynthesis (the “biological pump”; Maier-Reimer 1993) or returned to the atmosphere. Lerman and Mackenzie (2005) found that net storage of organic carbon counteracts CO<sub>2</sub> production by carbonate precipitation:  $Ca^{2+} + 2HCO_3^- \leftrightarrow CaCO_3 + CH_2O + O_2$ . Iglesias-Rodriguez *et al.* (2008) studied phytoplankton calcification in a high-CO<sub>2</sub> world, finding that calcification and net primary production in the coccolithophore *Emiliana huxleyi* are increased by high CO<sub>2</sub> partial pressures: over the past 220 years there has been a 40% increase in average coccolith mass.

River- and lake-surface areas are small compared with those of land and ocean, and so direct exchange of carbon



**Fig. 1.** The global water cycle and its CO<sub>2</sub> sinks (italic numbers, in Pg C/a; water fluxes from Shiklomanov 1993).

between rivers/lakes and atmosphere is possibly less important (Kling *et al.* 1991). However, the rivers of the world are conduits between the land and ocean or inland lakes, carrying large amounts of carbon to the ocean or inland lakes (Kempe 1984; Meybeck 1993).

If 0.24 Pg C/a represents riverine DIC delivered to oceans (Meybeck 1993) and if the flux of carbon from rivers/lakes to the atmosphere is 20% (Kling *et al.* 1991) of the total (i.e., 0.12 Pg C/a), then 0.23 Pg C/a remains in inland lakes and rivers, and in slowly cycled groundwater. Cole *et al.* (2007) estimated that about 0.2 Pg C/a is buried in inland water sediments. Groundwater may have a greater carbon storage capacity due to its large volume and greater load of carbon than rivers (Kempe 1984).

Carbon flux from the oceans to atmosphere can be neglected, because oceans are a large net atmospheric CO<sub>2</sub> sink (Sabine *et al.* 2004).

#### **FUTURE OF THE GWC SINK**

The GWC sink for CO<sub>2</sub> may increase with intensification of the hydrologic cycle (Huntington 2006), including increase in MP DIC (increase in atmosphere pCO<sub>2</sub> and carbonate dust) and in RO DIC (due to reforestation; Liu & Zhao 2000).

Climate-warming enhanced RO could be 2~5% per degree (Huntington 2006). Climate models predict average global surface temperature rise of 1.1 to 6.4 °C during the 21<sup>st</sup> century. Using a temperature increase of 3.75°C and precipitation increase of 13%, the GWC CO<sub>2</sub> sink may increase by 13% if the DIC of MP and RO are unchanged. For an increase in atmosphere pCO<sub>2</sub> from 350 ppmv to 700 ppmv, MP DIC is estimated to increase by 21% (CaCO<sub>3</sub>-CO<sub>2</sub>-H<sub>2</sub>O system) to 83% (CO<sub>2</sub>-H<sub>2</sub>O system). Increases in AET and reforestation/afforestation may cause soil CO<sub>2</sub> to increase (Liu & Zhao 2000). Assuming AET also increases 13%, world mean soil pCO<sub>2</sub> will increase from 6393 ppmv to 7936 ppmv (formula by Brook *et al.* 1983; ~24% increase), a conservative estimate in that it ignores potential soil CO<sub>2</sub>

increase by fertilization and reforestation. Macpherson *et al.* (2008) determined that groundwater pCO<sub>2</sub> in Konza Prairie, USA increased by about 29% (2100ppmv) from 1991-2005. RO DIC is thus estimated to increase by 3.57%. Taking all these into account, the GWC CO<sub>2</sub> sink may increase by ~22% (~0.18 Pg c/a) by the year 2100. Raymond *et al.* (2008) found that the bicarbonate flux from the Mississippi River increased from 0.01 Pg c/a to 0.015 Pg c/a (46% increase) during the past 50 years. This change was attributed mostly to land-use changes rather than climate change.

#### **CONCLUSIONS AND PERSPECTIVE**

We have shown an important potential CO<sub>2</sub> sink by joint action of carbonate dissolution, GWC and the photosynthetic uptake of DIC by aquatic. The sink constitutes up to 0.82 Pg C/a: 0.47 Pg C/a goes to sea via continental rivers and precipitation over sea, 0.12 Pg C/a is returned to the atmosphere, and 0.23 Pg C/a is stored in the continental aquatic ecosystem. The net sink, then, could be 0.70 Pg C/a, or ~9% of the total anthropogenic CO<sub>2</sub> emission and 25% of the missing CO<sub>2</sub> sink (Melnikov & O'Neill 2006).

This sink, a negative climate feedback mechanism, may increase with the global-warming-intensified GWC, the increase in CO<sub>2</sub> and carbonate dust in atmosphere, reforestation/afforestation, and fertilization of the aquatic ecosystems. Using the global warming projection for the year 2100 by IPCC, it is estimated that the CO<sub>2</sub> sink by the GWC will increase by ~22%, or ~0.18 Pg c/a.

Important, poorly-constrained variables in this carbon balance include temporal and spatial variations in precipitation and RO DIC, carbonate dust, and pedogenic carbonate and soil CO<sub>2</sub>. In addition, ocean and lake response to river carbon input is not well known. Although marine and freshwater aquatic organisms can be fertilized by increases in N, P, Si, Fe, Zn and CO<sub>2</sub> (Cassar *et al.* 2004; Zondervan 2007), it is not clear how much of the

carbon is trapped in lakes, estuaries and coastal zones, and how much is returned to the atmosphere through respiration (Zondervan 2007).

This paper presents an estimate of the CO<sub>2</sub> sink by carbonate dissolution, GWC and photosynthetic uptake of DIC by aquatic ecosystems, and suggests a new direction in balancing the global C budget.

#### ACKNOWLEDGEMENTS

This work was supported by the Hundred Talents Program of Chinese Academy of Sciences, and National Natural Science Foundation of China (Grant No. 40872168).

#### REFERENCES

- ADAMS, J.M. & POST, W.M. 1999. A preliminary estimate of changing calcrete carbon storage on land since the Last Glacial Maximum. *Global and Planetary Change*, **20**, 243–256.
- BAUMGARTNER, A. & REICHEL, E. 1975. *The World Water Balance*. Elsevier, Amsterdam.
- BROOK, G.A., FOLKOFF, M.E., & BOX, E.O. 1983. A world model of soil carbon dioxide. *Earth Surface Processes and Landforms*, **8**, 79–88.
- CASSAR, N., LAWS, E.A., BIDIGARE, R.R., & POPP, B.N. 2004. Bicarbonate uptake by Southern Ocean phytoplankton. *Global Biogeochemical Cycles*, **18**, doi: 10.1029/2003GB002116.
- COLE, J.J. & PRAIRIE, Y.T. *et al.* 2007. Plumbing the global carbon cycle: Integrating inland waters into the terrestrial carbon budget. *Ecosystems*, **10**, 171–184.
- DREYBRODT, W. 1988. *Processes in karst systems*. Springer, Heidelberg.
- EINSELE, G., YAN, J., & HINDERER, M. 2001. Atmospheric carbon burial in modern lake basins and its significance for the global carbon budget. *Global and Planetary Change*, **30**, 167–195.
- FORD, D.C. & WILLIAMS, P.W. 1989. *Karst Geomorphology and Hydrology*. Unwin Hyman, London.
- GOMBERT, P. 2002. Role of karstic dissolution in global carbon cycle. *Global and Planetary Change*, **33**, 177–184.
- HUNTINGTON, T. G. 2006. Evidence for intensification of the global water cycle: Review and synthesis. *Journal of Hydrology*, **319**, 83–95.
- IGLESIAS-RODRIGUEZ, M.D. & HALLORAN, P.R. *et al.* 2008. Phytoplankton calcification in a high-CO<sub>2</sub> world. *Science*, **320**, 336–340.
- KEMPE, S. 1984. Sinks of anthropogenically enhanced carbon cycle in surface fresh waters. *Journal of Geophysical Research*, **89**, 4657–4676.
- KLING, G.W., KIPPHUT, G. W. & MILLER, M.C. 1991. Arctic lakes and streams as gas conduits to the atmosphere: Implications for tundra carbon budgets. *Science*, **251**, 298–301.
- LERMAN, A. & MACKENZIE, F.T. 2005. CO<sub>2</sub> air-sea exchange due to calcium carbonate and organic matter storage, and its implications for the global carbon cycle. *Aquatic Geochemistry*, **11**, 345–390.
- LIU, Z. & ZHAO, J. 2000. Contribution of carbonate rock weathering to the atmospheric CO<sub>2</sub> sink. *Environmental Geology*, **39**, 1053–1058.
- MACPHERSON, G.L. & ROBERTS, J.A. *et al.* 2008. Increasing shallow groundwater CO<sub>2</sub> and limestone weathering, Konza Prairie, USA. *Geochimica et Cosmochimica Acta*, **72**, 5581–5599.
- MAIER-REIMER, E. 1993. The biological pump in the greenhouse. *Global Planet Change*, **8**, 13–15.
- MELNIKOV, N.B. & O'NEILL, B.C., 2006. Learning about the carbon cycle from global budget data. *Geophysical Research Letters*, **33**, doi:10.1029/2005GL023935.
- MEYBECK, M. 1993. Riverine transport of atmospheric carbon: sources, global typology and budget. *Water, Air, and Soil Pollution*, **70**, 443–463.
- RAYMOND, P.A. & OH, N.H. *et al.* 2008. Anthropogenically enhanced fluxes of water and carbon from the Mississippi River. *Nature*, **451**, 449–452.
- SABINE, C.L. & FEELY, R.A. *et al.* 2004. The oceanic sink for anthropogenic CO<sub>2</sub>. *Science*, **305**, 367–371.
- SHIKLOMANOV, I.A. 1993. World fresh water resources. In: Gleick, P.H. (ed) *Water in Crisis: A Guide to the World's Freshwater Resources*. Oxford University Press, New York, USA, 13–24.
- ZONDERVAN, I. 2007. The effects of light, macronutrients, trace metals and CO<sub>2</sub> on the production of calcium carbonate and organic carbon in coccolithophores—A review. *Deep-Sea Research II*, **54**, 521–537.

## Groundwater CO<sub>2</sub>: is it responding to atmospheric CO<sub>2</sub>?

**G. L. Macpherson**

*Department of Geology, University of Kansas, 1475 Jayhawk Blvd., Lawrence, KS 66044, USA  
(e-mail: [gilmac@ku.edu](mailto:gilmac@ku.edu))*

**ABSTRACT:** Carbon dioxide in groundwater is typically 10-100 times higher concentration than the atmosphere. In a shallow, thin limestone aquifer in the central USA, dissolved CO<sub>2</sub> varies seasonally, lagging the atmosphere's CO<sub>2</sub> cycle by about 6 months. Besides the annual cycle, dissolved CO<sub>2</sub> has increased at this tallgrass prairie research site during the monitoring period of the past 20 years. Although the precise mechanism is unknown, the similarities in the annual trends of atmospheric CO<sub>2</sub> and groundwater CO<sub>2</sub> at this site suggest there is a tight link between the two CO<sub>2</sub> reservoirs. These similarities include the peak width at CO<sub>2</sub> minima, peak width at CO<sub>2</sub> maxima, and the 20-year trend of overall increase. Groundwater CO<sub>2</sub> at this site has been increasing at a rate that is ~100 times greater than the increase in atmospheric CO<sub>2</sub>, suggesting that groundwater may be a significant and active sink for CO<sub>2</sub>. The most probable source for the shallow groundwater CO<sub>2</sub> at this site is soil respiration; soil respiration must be responding to climate change or atmospheric CO<sub>2</sub>, thus creating the similar trends in atmospheric and groundwater CO<sub>2</sub>.

**KEYWORDS:** *CO<sub>2</sub>, groundwater, climate change, sequestration, soil respiration*

### INTRODUCTION

The global C budget is acknowledged to have a large impact on Earth's climate (IPCC 2007), and yet, as we currently understand it, there is a large mismatch between C sources and sinks, with at least 1 Pg C yr<sup>-1</sup> having no apparent sink. Until recently (e.g., Cole et al. 2007; Liu et al. 2008), the involvement of the terrestrial water cycle in the global C budget had been largely ignored.

Estimates of CO<sub>2</sub> sequestration in groundwater, both from incorporation of soil CO<sub>2</sub> and transformation to dissolved inorganic carbon (DIC), vary over an order of magnitude. Kessler and Harvey (2001) estimate the global flux of C to groundwater to be 0.02 Pg C yr<sup>-1</sup>. This estimate is based on only 44 CO<sub>2</sub> measurements that are biased to western North America. Andrews and Schlesinger (2001), based on data from the Duke Forest Free Air CO<sub>2</sub> Enrichment (FACE) experiments, estimate that under ~1.5X present CO<sub>2</sub>, the global C flux to groundwater would increase to 0.12 Pg C yr<sup>-1</sup>. The estimate for increased C flux to groundwater by Andrews and Schlesinger (2001) is nearly equal to the estimate of

Liu et al. (2008) for the current global flux of 0.13 Pg C yr<sup>-1</sup> to the continental aquatic ecosystem. In effect, based on the above estimates, the flux of C to groundwater could account for ~2% to ~12% of the missing carbon sink in the global carbon budget.

The recent finding (Macpherson et al. 2008) that groundwater CO<sub>2</sub> is increasing ~100 times faster than atmospheric CO<sub>2</sub> draws attention to our limited understanding of the link between the atmosphere and shallow groundwater in terms of gas transfer and storage. This abstract investigates this link and presents evidence for a tight coupling between atmospheric and groundwater CO<sub>2</sub>.

### SETTING

The study area is the bottom fourth of a 1.2 km<sup>2</sup> upland watershed within the 35 km<sup>2</sup> Konza Prairie (fig. 1). The Konza Prairie is located within the Flint Hills physiographic province, which is an unplowed, ~50,000 km<sup>2</sup> remnant of original tallgrass prairie; 99% of the original prairie has been plowed. The study area climate is temperate mid-continental. Annual meteoric precipitation

is  $835 \pm 190$  mm and 75% of precipitation falls during the growing season (Knapp et al. 1998).

Bedrock at the Konza Prairie is Permian-aged, alternating, thin (1-3 m) limestones and thicker (2-12 m) shales. Soils are mostly less than 1 m thick, and form on bedrock, Pleistocene-aged loess, and alluvium and colluvium.

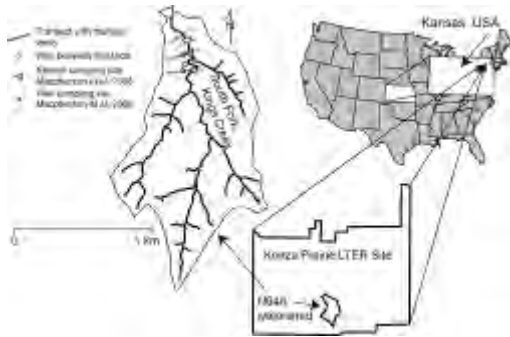


**Fig. 1.** Study area is the Konza Prairie Long-Term Ecological Research Site and Biological Station, a native tallgrass prairie.

### HYDROGEOCHEMISTRY

The essentially unconfined limestone aquifers at the Konza Prairie respond rapidly to precipitation and supply base flow to, and are recharged by, the stream draining the watershed (Macpherson 1996). One aquifer, the subject of this paper, has been sampled almost every 4-6 weeks since 1991. The ~5 cm diameter PVC well used in this abstract is ~12 m deep and is screened only in the limestone. Other wells at the site have similar chemistry to the well used here. (Details about sampling and analysis protocols can be found in Macpherson et al., 2008.) Increasing alkalinity (fig. 2), alkaline earth cations, and groundwater  $\text{CO}_2$  suggest increasing weathering of carbonate minerals (Macpherson et al. 2008), a significant portion of which may be allochthonous carbonate dust that has more radiogenic Sr than the bedrock (Wood & Macpherson 2005).

### CARBON DIOXIDE

The annual cycle of higher and lower

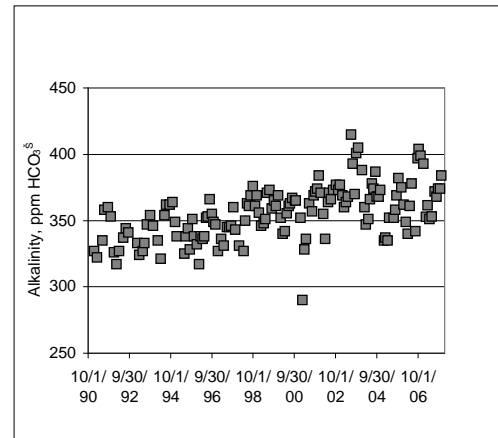


**Fig. 2.** Increase in titration alkalinity of groundwater from a thin limestone aquifer in the central USA over the study period is accompanied by increasing groundwater  $\text{CO}_2$  and decreasing pH (not shown).

groundwater  $\text{CO}_2$  (Macpherson et al., 2008) mimics the Niwot Ridge, Colorado, atmospheric  $\text{CO}_2$  annual cycle (Tans & Conway 2005), the atmosphere monitoring station closest to the study area. The groundwater cycle lags the atmosphere cycle by ~six months (fig. 3). Groundwater  $\text{CO}_2$  is ~10 to 100 times higher concentration than atmosphere  $\text{CO}_2$ , so a direct transfer of  $\text{CO}_2$  from the atmosphere to groundwater is unlikely.

The patterns in the atmosphere  $\text{CO}_2$  cycle, with longer duration of  $\text{CO}_2$  maxima and shorter duration of  $\text{CO}_2$  minima, are repeated in the groundwater  $\text{CO}_2$  cycle (fig. 3). In addition, when the atmosphere cycle has a longer  $\text{CO}_2$  minimum (e.g., August-September, 1998, on fig. 3) then the groundwater cycle has a longer  $\text{CO}_2$  minimum (e.g., February-April, 1999, on fig. 3). Similarly, when the atmosphere has a short period of minimum  $\text{CO}_2$ , (e.g., August, 1999, on fig. 3), the lagged groundwater signal also has a short period of minimum  $\text{CO}_2$  (e.g., March, 2000, on fig. 3). Similarities in curve shape also occur at times of  $\text{CO}_2$  maxima.

### DISCUSSION

The higher partial pressures of  $\text{CO}_2$  in the groundwater preclude simple transport

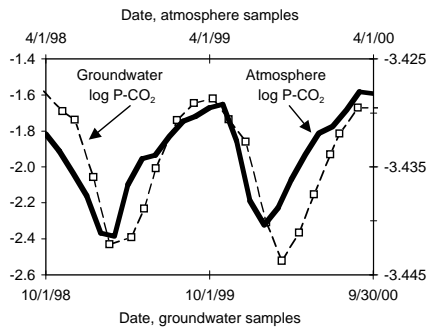


**Fig. 3.** Example of similarity between atmospheric CO<sub>2</sub> and groundwater CO<sub>2</sub> annual cycles. The groundwater cycle lags the atmosphere cycle by ~ 6 months.

of lower partial pressure CO<sub>2</sub> from the atmosphere to the higher partial pressure CO<sub>2</sub> in the aquifer. Stable carbon isotope data (unpublished) suggest that respiration-derived CO<sub>2</sub> dissolving marine limestone is one reasonable explanation for the source of CO<sub>2</sub>. Although aboveground net primary productivity (ANPP) does not show a trend over the time period of this study (Macpherson et al. 2008), ANPP has a large standard deviation, in that it responds primarily to moisture. Meteoric precipitation in this region is highly variable (annual variability ~20-25%; monthly variability > 100%; Macpherson, 1996), and so ANPP correlates strongly with annual precipitation. The ANPP data set is not long enough to show a long-term trend on top the annual variability.

Belowground biomass is greater than aboveground biomass in grasslands, and yet the BNPP is difficult to quantify, so it is unknown whether belowground biomass has changed at the site. In addition, if microbial activity is stimulated by higher ambient CO<sub>2</sub>, as it is in experiments (Williams et al. 2000), and if microbes breakdown recent organic matter more rapidly than old organic matter (Cardon et al. 2001), then ANPP or BNPP might not change even as total primary productivity and respiration increase. This scenario increases respiration-derived CO<sub>2</sub> that

might be delivered to the groundwater as well as to the atmosphere.

## CONCLUSIONS

Groundwater CO<sub>2</sub> at the Konza Prairie LTER Site, an unplowed, mid-continental, mesic tallgrass prairie used for ecological research, has increased over the past 20 years, along with alkalinity and alkaline earth cations. The change in groundwater CO<sub>2</sub> over the study period has been about 100 times larger than the change in atmospheric CO<sub>2</sub> concentration over the same period. The annual groundwater CO<sub>2</sub> cycle has a pattern similar to the annual pattern of CO<sub>2</sub> in the atmosphere, with longer periods of high CO<sub>2</sub> than low CO<sub>2</sub> in any year, as well as similar durations of low-CO<sub>2</sub> periods, the length of which change from year to year. A direct transfer of CO<sub>2</sub> from the atmosphere to groundwater is unreasonable, because groundwater CO<sub>2</sub> concentrations are always 10 to 100 times higher than atmospheric concentrations. An increase in soil respiration, with or without increases in ANPP or BNPP, is proposed as a more reasonable explanation for the increasing groundwater CO<sub>2</sub>. The increase in groundwater CO<sub>2</sub> strongly suggests that shallow groundwater is a significant sink for CO<sub>2</sub>.

## ACKNOWLEDGEMENTS

I thank the Konza Prairie LTER for funding through the NSF LTER Program, the Dept. of Geology at the University of Kansas, and the Geology Endowment Fund of the University of Kansas for supplementary funding. I also am grateful to Marios Sophocleous for providing Palmer Drought Index data for the region, and to the numerous students over the years who helped with data collection for this project.

## REFERENCES

- CARDON, et al. 2001. Contrasting the effects of elevated CO<sub>2</sub> on old and new soil carbon pools. *Soil Biology and Biochemistry*, **33**, 365-373.
- COLE, J.J. et al. 2007. Plumbing the global carbon cycle: Integrating inland waters into

- the terrestrial carbon budget. *Ecosystems*, **10**, 171-184. DOI: 10.1007/s10021-006-9013-8.
- INTERGOVERNMENTAL PANEL ON CLIMATE CHANGE (IPCC). 2007. *Climate change, 2007, the fourth IPCC assessment report*. IPCC.
- KESSLER, T.J. & HARVEY, C. S. 2001. Global flux of CO<sub>2</sub> into groundwater. *Geophysical Research Letters*, **28**, 279-282.
- KNAPP, A.K. et al., eds. 1998. *Grassland Dynamics*. Oxford University Press, New York.
- LIU, Z., et al. 2008. A possible important CO<sub>2</sub> sink by the global water cycle. *Chinese Science Bulletin*, **53**, 402-407.
- MACPHERSON, G.L. ET AL. 2008. Increasing shallow groundwater CO<sub>2</sub> and limestone weathering. *Geochimica et Cosmochimica Acta*, **72**, 5581-5599. doi:10.1016/j.gca.2008.09.004
- MACPHERSON, G.L., 1996. Hydrogeology of thin limestones—the Konza Prairie LTER Site. *Journal of Hydrology*, **186**, 191-228.
- TANS P.P. & CONWAY T.J. 2005. Monthly atmospheric CO<sub>2</sub> mixing ratios from the NOAA CMDL Carbon Cycle Cooperative Global Air Sampling Network, 1968-2002. In *Trends: A Compendium of Data on Global Change, Carbon Dioxide Information Center*. Oak Ridge National Laboratory, U.S. Dept. of Energy, Oak Ridge, Tenn., USA.
- WILLIAMS M. A. et al. 2000. Carbon dynamics and microbial activity in tallgrass prairie exposed to elevated CO<sub>2</sub> for 8 years. *Plant and Soil*, **227**, 127-137.
- WOOD, H. K. & MACPHERSON, G.L. 2005. Sources of Sr and implications for weathering of limestone under tallgrass prairie, northeastern Kansas. *Applied Geochemistry*, **12**, 2325-2342; doi:10.1016/j.apgeochem.2005.08.002.

## Lithological Identification of Rocks in Cape Smith Fold Belt Region; New Quebec Using Remote Sensing Applications

Yask N. Shelat<sup>1</sup> & James E. Mungall<sup>1</sup>

<sup>1</sup>*Department of Geology, University of Toronto, Earth Science Centre; 22 Russell Street, Toronto ON M5S 3B1  
(e-mail: [yask.shelat@gmail.com](mailto:yask.shelat@gmail.com))*

**ABSTRACT:** A study was performed to validate use of remote sensing data for the identification of rock units at Cape Smith fold belt region, New Quebec, Canada. Remote sensing advancement has facilitated to characterise the properties of rock units over a large area with a lot less time than traditional field work. The study area is mainly composed of peridotite, gabbro, metabasalt, metasediments etc and mapped previously by the second author. Landsat Enhanced Thematic Mapper (ETM+) imagery (30 m spatial resolution; bands 1 to 5 and 7) was used to perform various remote sensing techniques such as Band Ratio, Principal Component Analysis, and Supervised Classification. The Remote Sensing image results showed good agreement with the available geological map.

**KEYWORDS:** *Remote Sensing Geology, Landsat Enhanced Thematic Mapper, Band Ratio, Principal Component Analysis, Supervised Classification*

### INTRODUCTION

Remote sensing technology is now becoming an increasingly important means for resource exploration. Use of satellite imagery, image processing, and the correlation of processed images with geological map have been emerging as an effective tool for creating and refining geological map with further structural and lithologic information. (Krishnamurthy 1997; Sabins 1999; Gad *et al.* 2005; Khan *et al.* 2006).

A study was performed to identify rock units in the Cape Smith fold belt, New Quebec orogen, using remote sensing techniques. This region was studied and mapped (Mungall 2007). Enhanced Thematic Mapper (ETM+) image, having 30 m spatial resolution with 8 bit data format, (acquired during the year 2000, Path/Row-20/17 at UTM N 61.48/ W 074.42) was used in this study. The orthorectified satellite imagery of concerned area was supplied by Canadian Royalties Inc. The Landsat data was processed by several different image enhancement techniques, such as Band Ratio analysis and Principal Component Analysis. Supervised Classification was also applied for the same purpose on

resultant RGB image (5,4,2) obtained from PCA analysis (Krishnamurthy 1997; Sabins 1999; Gad *et al.* 2005; Lillesand *et al.* 2007)

### GEOLOGICAL SETTING

The geology description of Cape Smith fold belt is separated into two domains, namely the northern allochthonous and southern parautochthonous (see Mungall 2007). These domains were highly affected by the Trans-Hudson orogeny (~1830-1840 Ma). The southern part of the domain contains Povungnituk and Chukotat groups. The geological map and stratigraphy of the area is presented in Figure 1.

The Dumas Formation is unconformably overlying the Archean Superior Province. It hosts metasediments and intercalated iron formations, as well as peridotite and gabbro bodies, which were identified and separated with the help of both Band ratio and Principal Component Analysis.

The Beauport Formation is produced during major volcanic activity that occurred between 2038 and 1991 Ma. It consists of upper, middle, and lower members composed of sheet and pillowed

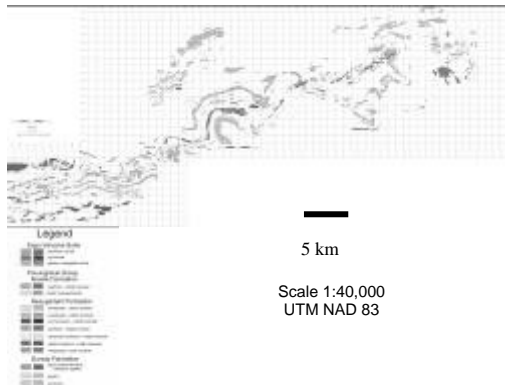


**Fig. 1.** Geological Map of the Cap Smith fold belt and Expo Intrusive Suite (see Mungall 2007).

basalts with metasedimentary intercalations. Magnetic highs occur in the middle member of the formation.

The Expo Intrusive Suite is for the most part composed of mafic and ultramafic intrusions, shaped as tabular-shaped discordant bodies, so are referred as dykes. The Expo suite is economically important due to the presence of sulfide mineralization in the internal part of the intrusion. It is composed of gabbro norite, pyroxenite, peridotite, and dunite.

## METHODS & RESULTS

The flow diagram (Fig. 2) outlines the methods used for the review and separation of the rocks present in the area. Image enhancement is done to increase the variance in the dataset. Contrast manipulation, spatial feature manipulation, and multi-image manipulation are used as digital enhancement techniques (Lillesand *et al.* 2007). In this study multi-image manipulation is used, which includes Band Ratio and Principal Component Analysis.

### Band Ratio

The Band ratio approach for the lithology identification was taken previously by many authors (Sabins 1999; Gad *et al.* 2005; Khan *et al.* 2006).

The Band Ratio enhancement technique can be used to remove the brightness variation caused by topographic effects in a region. (Gad *et al.* 2005; NASA Remote sensing tutorial by Dr. Nicholas Short)

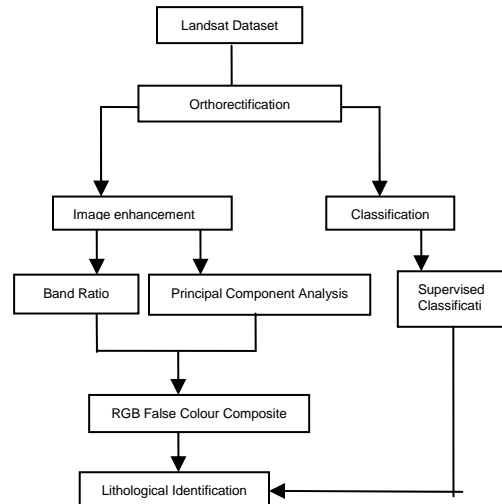


**Fig. 2.** Flow Chart showing the methods used for the identification of the rocks.

Two objects with different spectral properties, i.e., variation in the slope of spectral reflectance curve of two bands, can be separable with the help of ratio images (Lillesand *et al.* 2007). In this study standard reflectance data of USGS Spectral Library and John Hopkins University spectral library (Available in ENVI) have been used. To enhance the dissimilarity between different rock types in the scene, plots with a higher reflectance were kept in the numerator and plots with low reflectance were kept in the denominator, while taking the band ratios. Using this approach, a ratio of 5/3 was taken for basalt, 7/3 for peridotite, and 4/2 for vegetation.

Figure 3 displays a Band Ratio image (5/3, 7/3, 4/2), in which peridotite appears dark yellowish black colour. It is difficult to distinguish between gabbro and basalt, due to their similar reflectance properties.

In general, the spectral band ratio technique is helpful to identify the peridotite, but basalt and gabbro are not uniformly separable over the entire region.

### Principal Component Analysis

Principal Component Analysis (PCA) is a complex statistical approach for highlighting the variance in the image using multiplication of original data with eigenvectors. (NASA Remote Sensing

Tutorial by Dr. Short S.; Lillesand *et al.* 2007). ETM+ data of the study area (band 1 to 5 & 7) have been processed in ENVI 4.4 to produce six new PCA bands.

PCA analysis helps to identify the spectral differences of the rock. Every specific rock appears in a divergent colour in RGB composite image of PCA bands (Krishnamurthy 1997). False colour composite image of PCA bands 5, 4, and 2 have been generated as RGB. Geological information of the previously mapped region (Mungall 2007) was compared with the corresponding area within the resultant PCA image (Fig. 4). Uniform correlation between the specific colour and rock type was observed

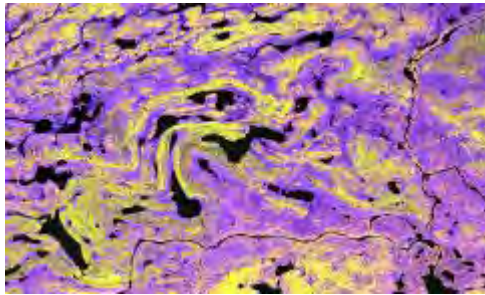


**Fig. 3.** Band ratio image of 5/3, 7/3, 4/2 as RGB false colour composite.

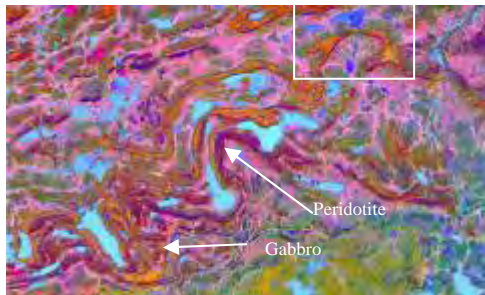
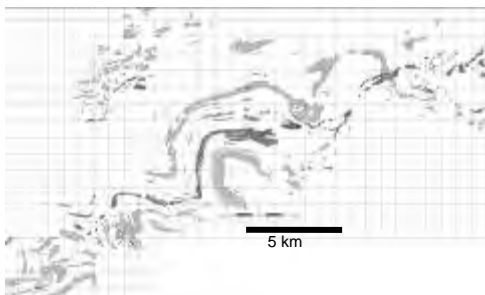


**Fig. 4.** Comparison of Geological Map and PCA image with Bands 5, 4, 2 as RGB

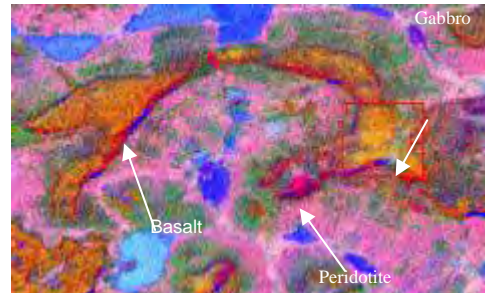
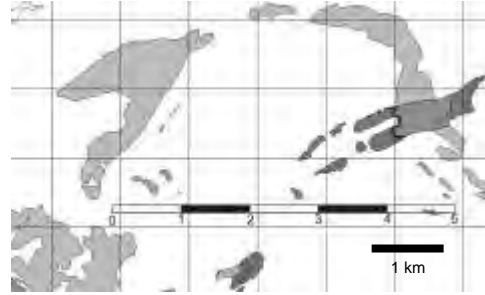


**Fig. 5.** Comparison of Geological Map and PCA image showing distinction between gabbro, peridotite (Expo Intrusive Suite), metabasalt (Upper Beuparlant Formation).

throughout the previously mapped area. It validates the possibility of locating the similar rocks in the unmapped neighbouring region with acceptable accuracy.

As displayed in Figure 4, basalt, gabbro, and peridotite has distinctly different spectral signature and shows texture variations between different rock types.

A small subset (within Marked square) of Figure 4 is expanded in Figure 5. Gabbro unit of Expo Intrusive suite (appears light orange) is clearly differentiated from metabasalt (appears orange-black) of the Beuparlant Formation and peridotite (appears dark magenta) of the Expo Intrusive Suite in Figure 5.

### Supervised Classification

Supervised Classification was used for accurately categorizing lithology in the study area. PCA bands were used as a basis for identifying the presence of peridotite, gabbro, metabasalt and metasediments and defining the training areas for performing Supervised Classification (Lillesand *et al.* 2007). Area

(pixels) with the preponderance of peridotite, gabbro, metabasalt and metasediments are displayed in red, green, blue and white colours respectively in the output image. The Mahalanobis distance classifier has been run in Envi 4.4 for extracting the similar statistical data pertaining to each class. A small section of the resulting output image is represented in Figure 6, depicting presence of various rocks. At some places, mixing of classes has been observed due to similar appearance of gabbro and basalt in the available ETM+ data.

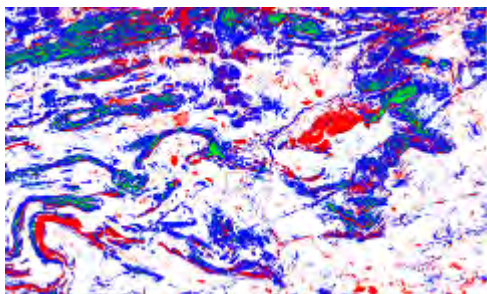


**Fig. 6.** Supervised Classification image with peridotite, gabbro, metabasalt, metasediments, are shown as Red, Green, Blue, and Yellow.

### CONCLUSIONS

Remote sensing techniques have been successfully applied for the identification of rocks in Cape Smith fold belt region. Principal Component Analysis is very effective for the separation of gabbro, metabasalt and peridotite. Band Ratio was helpful for the preliminary identification of peridotite. Supervised Classification approach is taken to verify the results obtained by Principal Component Analysis and Band Ratio. It is also useful to remap the unknown regions once the results are verified.

### ACKNOWLEDGEMENTS

I am sincerely thankful to the Canadian

Royals Inc for providing Landsat images of the study area. To Dr. Derek Rogge; Research Associate University of Victoria for clarifying my doubts in the fundamental remote sensing principals.

### REFERENCES

- GAD, S. & KUSKY, T. 2005. Lithological mapping in the Eastern Desert of Egypt, the Barramiya area, using Landsat thematic mapper (TM). *Journal of African Earth Sciences*, **44**, 196-202.
- KHAN S.D., KHALID MAHMOOD, K, & CASEY, J.F. 2006. Mapping of Muslim Bagh ophiolite complex (Pakistan) using new remote sensing, and field data. *Journal of Asian Earth Sciences*, **30**, 333-343.
- KRISHNAMURTHY, J. 1997. The evaluation of digitally enhanced Indian Remote Sensing Satellite (IRS) data for lithological and structural mapping. *International Journal of Remote Sensing*, **18**, 3409-3437
- MUNGALL J.E. 2007. Crustal Contamination of Picritic Magmas During Transport Through Dikes: the Expo Intrusive Suite, Cape Smith Fold Belt, New Quebec. *Journal of Petrology*, **48**, 1021-1039.
- SABINS, F.F. 1999. Remote sensing for mineral exploration. *Ore Geology Reviews*, **14**, 57-183.
- LILLESAND, T.M., KIEFER, R.W., & CHIPMAN, J. W. 2007. Remote sensing and Image Interpretation, 6th Edition, Chapter seven: *Digital image interpretation and analysis*, pp. 482-623.
- Shelat, Y. 2008. Lithological separation using Remote Sensing applications. Undergraduate Research Project Report, University of Toronto, Toronto, ON.
- NASA Remote Sensing tutorial by Dr. Short N. <http://rst.gsfc.nasa.gov/U>
- USGS Spectral Library <http://speclab.cr.usgs.gov/spectral.lib06/ds231/datatable.html>

## Selective geochemical extraction patterns in Cyprus soils: responses to geology and land use variations

Nyree Webster<sup>1</sup>, David Cohen\*<sup>1</sup>, Neil Rutherford<sup>1,2</sup>,  
Andreas Zissimos<sup>3</sup>, & Eleni Morisseau<sup>3</sup>

<sup>1</sup>School of BEES, University of New South Wales, Sydney, NSW, 2052, AUSTRALIA  
(e-mail: [d.cohen@unsw.edu.au](mailto:d.cohen@unsw.edu.au))

<sup>2</sup>Rutherford Mineral Resource Consultants, Coogee, NSW, 2034, AUSTRALIA

<sup>3</sup>Geological Survey Department of Cyprus, Strovolos, CYPRUS

**ABSTRACT:** The regolith of Cyprus has been highly disturbed due to a long history of human occupation and resource exploitation. Selective extraction analysis of surface and subsurface regolith samples from a NE trending transect across Cyprus indicates soil characteristics to be dominated by parent geology material with current land-use having little significant impact on element concentrations.

**KEYWORDS:** Soil, selective extractions, Cyprus, atlas

### INTRODUCTION

Cyprus is divided into four east-west trending geological terrains (GSD 2002) ranging from the mafic-ultramafic Troodos Ophiolite Complex and mixed lithologies of the Mamonia terrain to the calcarenite-dominated Circum-Troodos Sedimentary Succession (CTSS) and the volcanic Kyrenia terrain in the north. The Troodos Ophiolite Complex contains a core of ultramafic rocks surrounded by a large sequence of sheeted dolerites, gabbro dykes and overlying pillow basalts which host a number of Cyprus-style Cu sulfide deposits. The geology is the result of a series of multifaceted and inter-related tectonic processes over the period of the Late Cretaceous – Pleistocene.

The Mediterranean region has supported a population dependent upon agriculture for more than eight millennia (Butzer 2005). As a result of a long history of human occupation and resource exploitation the regolith in Cyprus exhibits significant disturbance. Cyprus has been subjected to increasing development over the last thirty years (Robertson & Xenophontos 1997). The lowlands areas are heavily terraced and dominated by agricultural activities, the lower mountain slopes utilised for vineyards, orchards and grazing and the higher elevations are

dominated by forests. Soil and regolith profiles from the coast to Troodos vary with skeletal A horizons directly overlying the C horizon in some areas (Cohen & Rutherford 2007).

### SAMPLING AND EXPERIMENTAL

Regolith samples were collected from 68 sites along a transect extending from the CTSS in the SW of the island (near Πέτρα του Ρωμίου), across Troodos and into the CTSS and fanglomerates on the NE side of Troodos (near Λευκωσία). ICP-MS trace elements concentrations were determined following two conventional (sequential) leaches on the <2mm fraction of the upper (0-25 cm) and lower (50-75 cm) parts of the profile: 1M ammonium acetate in pH 5 acetic acid and 1M hydroxylamine.HCl in pH 1 HCl.

Multivariate analytical methods were applied to investigate any relationships between soil characteristics, geology and land use.

### RESULTS

The major geological boundaries correspond with sharp changes in the selective extraction geochemical patterns (Fig. 1). The Troodos ultramafics are characterised by much higher AAC-

extractable Al than other lithologies which may be related to the high proportion of clays derived from the breakdown of plagioclase. AAC Ca is consistently between 12 and 16% in the CTSS unit SW of Troodos (Pakhna Fmn calcarenites) but less than 0.1% in the soils derived from the sheeted dykes. Median extractable Cu is generally higher in the subsoil sample (50-75cm depth) than the surface sample, and higher in the AAC than the subsequent HXL extraction. Extractable Cu is generally highest in the zone extending SW from Troodos across the sheeted dykes and pillow lavas compared with other lithologies (Fig. 2).

Multivariate analysis emphasises the geochemical differences between geological terrains in Cyprus (e.g., Troodos versus CTSS). Factor analysis of

the (post-AAC) HXL extraction for the subsoil samples (Fig. 3) indicates strong separation between samples grouped by parent geology, but a lack of clustering evident when viewed from the perspective of landuse except the clustering associated with forests as these areas are largely restricted to the mafic and ultramafic rocks of the central Troodos region.

**CONCLUSION**

Geology appears to be the main determinant of trace-element contents and mineralogical form – as defined using selective extractions. There is no indication that landuse *per se* has had a significant general effect on soil trace element geochemistry.

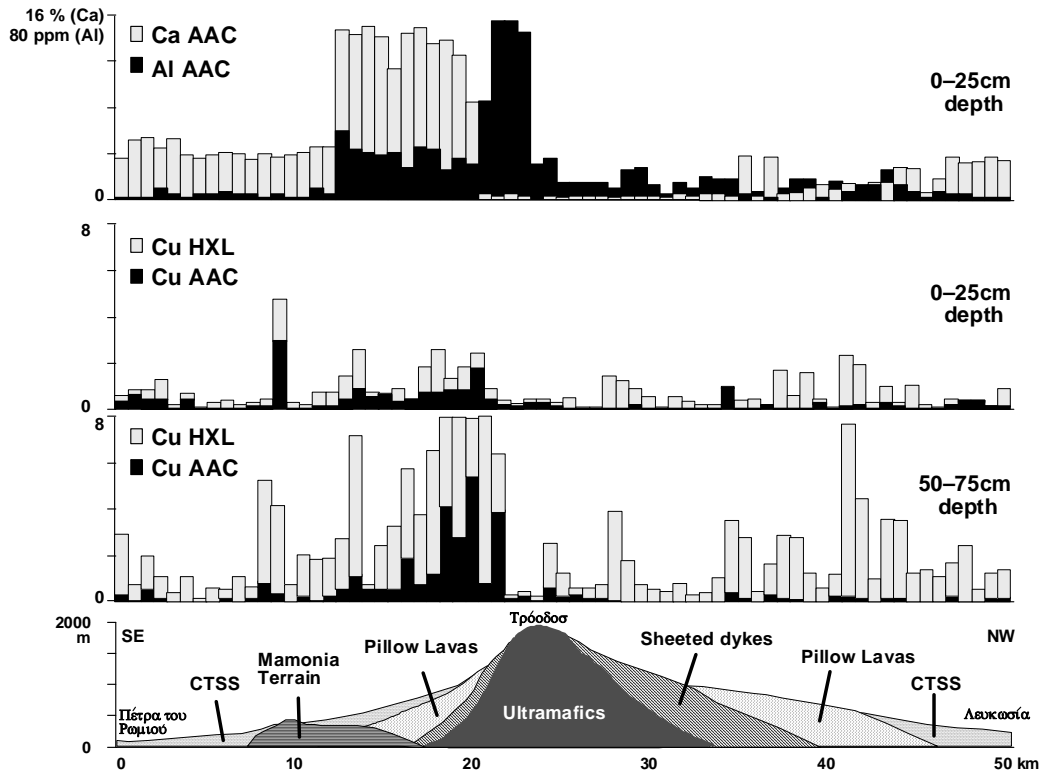


**Fig 1.** Variation in AAC-extractable Ca, Al and Cu, and HXL-extractable Cu in soils from a NW-trending traverse across Cyprus.

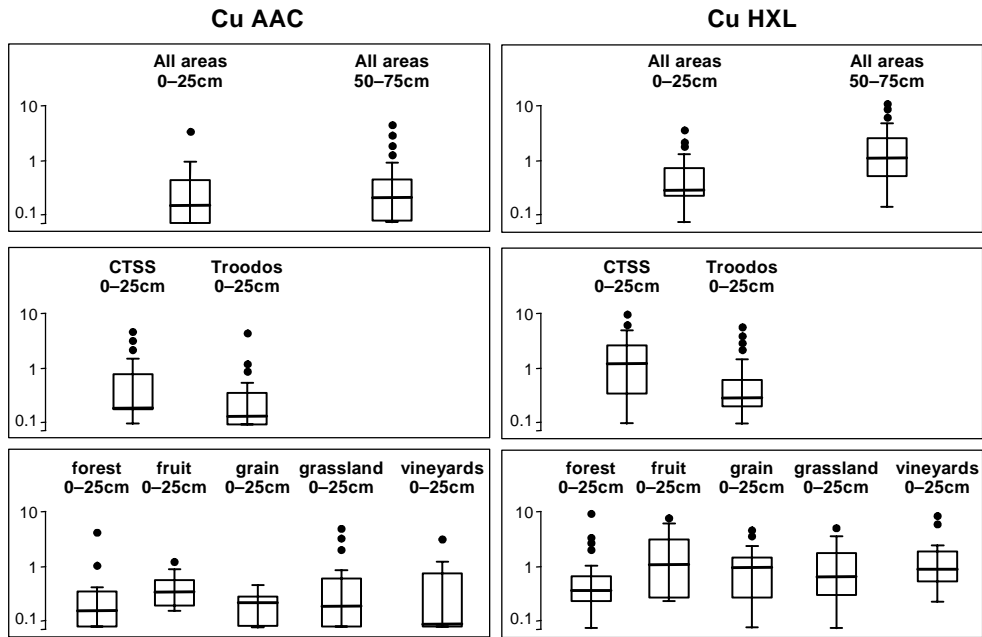


Fig 2. Boxplot comparison of various groupings of AAC and HXL Cu values.

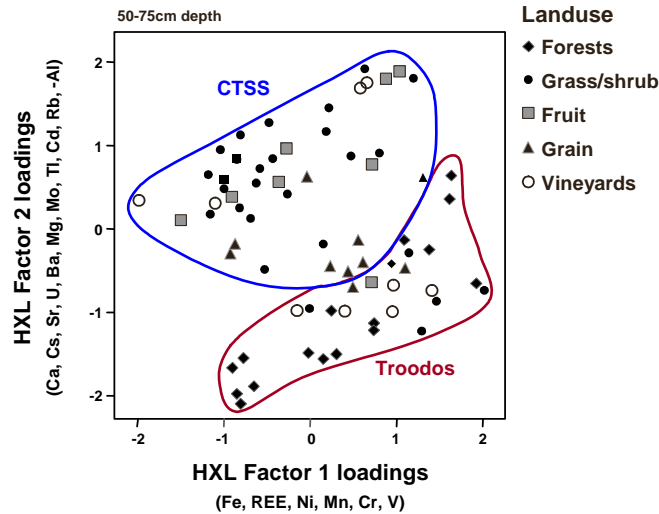


Fig 3. Factor 1 and 2 scores for (post-AAC) HXL-extraction data from the sub-soil samples.

**REFERENCES**

BUTZER, K.W. 2005. Environmental history in the Mediterranean world: Cross-disciplinary investigation of cause-and-effect for degradation and soil erosion. *Journal of Archaeological Science*, **32**, 1773-1800.

COHEN, D.R. & RUTHERFORD, N. 2007. *Geochemical Atlas of Cyprus, Progress Reports*. UNSW Global.

GEOLOGICAL SURVEY DEPARTMENT OF CYPRUS 2002. *The Geology of Cyprus*. G. Petrides (ed). GSD Publication no. 10,.

ROBERTSON, A.H.F & XENOPHONTOS, C. 1997. Cyprus. In: M.M. Eldridge and W.F. Rhodes (eds), *Encyclopedia of European and Asian Regional Geology*. Chapman & Hall.



## The petrogenesis of the Ulsan carbonate rocks from the southeastern Kyongsang Basin, South Korea

Kyoungee Yang

*Division of Earth Environmental System, College of Science, Pusan National University,  
Pusan, 609-735 SOUTH KOREA (e-mail: [yangkyhe@pusan.ac.kr](mailto:yangkyhe@pusan.ac.kr))*

**ABSTRACT:** The petrogenesis of the Ulsan carbonate rocks in the Mesozoic Kyongsang Basin of South Korea, which have been previously interpreted as limestone of Paleozoic age, is reconsidered. A small volume of carbonate rocks containing a magnetite deposit and spatially-associated ultramafic rocks is surrounded by sedimentary, volcanic and granitic rocks of the Mesozoic age. The simple crosscutting relationships and other outcrop features indicate that the carbonate rocks are an intrusive phase and younger than the other surrounding Mesozoic rocks. The Ulsan carbonates have low concentrations of REEs and trace elements with the carbon and oxygen isotope values in the range of  $\delta^{13}\text{C}_{\text{PDB}}=2.4$  to  $4.0\text{‰}$  and  $\delta^{18}\text{O}_{\text{SMOW}}=17.0$  to  $19.5\text{‰}$ . The outcrop evidence and geochemical signatures indicate that the Ulsan carbonates were formed from crustally-derived carbonate melts, which were generated by the melting/fluxing of crustal carbonate materials owing to the emplacement-related processes of alkaline A-type granitic rocks. Compared to typical mantle-derived carbonatites associated with silica-undersaturated, strongly peralkaline systems, the relatively small size and geochemical characteristics of the Ulsan carbonates may reflect carbonatite genesis in a silica-saturated, weakly alkali intrusive system.

**KEYWORDS:** *Ulsan carbonate rocks, Kyongsang Basin, magnetite deposit, melting/fluxing of crustal carbonate melt, Alkaline A-type granitic rocks*

### INTRODUCTION

The Ulsan carbonates (Fig. 1) have long been interpreted as limestone of Paleozoic age or "age unknown" and as the host of a skarn-type iron (magnetite) deposit due to the intrusion of Cretaceous granitic rocks (Park & Park 1980; Choi *et al.* 1999). However, a Paleozoic marine limestone hypothesis fails to explain the spatial association or the relationship between carbonate and ultramafic rocks in a concentric, ellipsoidal shape surrounded by Cretaceous sedimentary, volcanic, and granitic rocks. The sedimentary hypothesis also fails to explain the isolated exposure of a funnel-shaped Paleozoic marine limestone where no marine limestone has been previously observed within the Mesozoic Kyongsang Basin.

Carbonatites have been defined as rare-metal-bearing rocks composed mainly of carbonate of mantle origin, formed in close association with alkaline rocks (Woolley & Kempe 1989). However, there

remains a debate regarding crustal- and mantle-derived carbonate magma or between magmatic differentiation and primary mantle melt. Lentz (1999) postulated a genetic relationship and a possible geochemical continuum between magmatic-hydrothermal skarn systems and some carbonatite systems suggesting a limestone melting/fluxing hypothesis.

Re-evaluating the origin of the Ulsan carbonates can be very important in understanding the geology and petrogenesis in the Mesozoic Kyongsang Basin, South Korea. This present work is summarized and reviewed from the Yang *et al.* (2003).

### GEOLOGICAL SETTING

The geology of the study area consists of Cretaceous sedimentary, volcanic, granitic, ultramafic (serpentinite), and carbonate rocks containing a magnetite-rich pipe and basic dykes (Fig. 1). The sedimentary rocks are intruded by felsic volcanic, granitic and ultramafic rocks,

whereas volcanic rocks occur between granitic and sedimentary rocks. Granites are, classified as I-type, intruded by ultramafic rocks showing sharp contacts. Albitite composed of albite and nepheline observed at the contact between granitic rock and the ultramafic rocks (Choi 1983). In addition, one exceptional A-type alkali granite is exposed 4-5 km northwest from the carbonate rocks; it defined as a hypersolvus alkali feldspar granite containing F-enriched sodic amphibole, riebeckite-arfvedsonite, fluorite, and ferriannite (Koh *et al.* 1996). The ultramafic rocks consist of partly serpentized dunite and harzburgite containing amphiboles, chromite, magnetite, and chlorite with numerous crosscutting small faults and calcite and dolomite veins.

The Ulsan carbonates hosting the magnetite pipe are surrounded by the ultramafic and volcanic rocks (Fig. 1). Various sized xenoliths of hornfels fragments (volcanic rocks) and ultramafic rocks are often enclosed by the carbonates. The carbonates are massive without any evidence of bedding. They consist of two types of calcites: One is well-crystallized, fine- to medium-grained calcite, whereas the other is large, pure, white calcite crystals (up to 4-5 cm in diameter), which is associated with basic dykes, massive main magnetite ores and metasomatic minerals, implying that they have recrystallized due to the intrusion of dykes. The very contact between carbonate rocks and sedimentary, granite, and serpentinite could not be observed at the surface, but was found in core samples described below. Metasomatic minerals are found along the contacts between the carbonates and volcanic rocks, as well as sedimentary rocks. They include garnet, clinopyroxene, amphiboles, apatite, chlorite, and epidote. The ore pipe is nearly vertical and extends more than 300 m below the surface. The ore minerals are mainly magnetite with small amounts of scheelite and arsenopyrite. Most of the magnetite ore is associated with pyroxene and garnets. Annual production was 100,000 tonnes of magnetite concentrates (60% of Fe) and

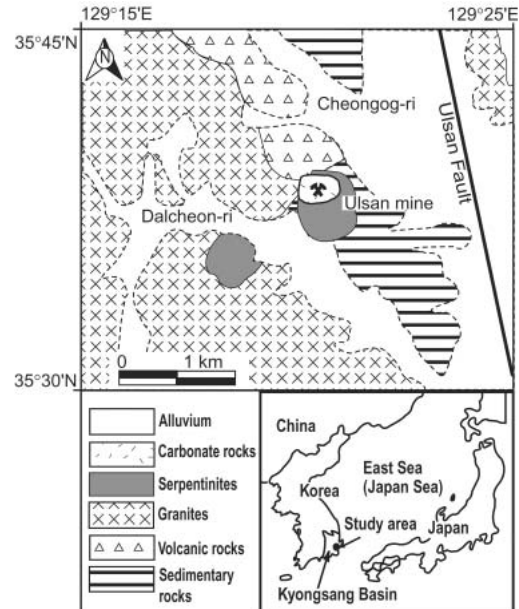


**Fig. 1.** Geologic map of the Ulsan mining area, South Korea (after Park & Park 1980).

1,200 tonnes of scheelite (74% of  $WO_3$ ) in 1984.

#### **UNDERGROUND GEOLOGY FROM DRILL CORES**

Data from seventy-six exploration drilling core samples collected by Korea Mining Promotion Corporation during 1972-1990 were analyzed in order to understand underground geology in the Ulsan mining area, especially focusing on the relation between the carbonates and the surrounding rocks. The depths of the drill holes reached up to 650 m. Based on the analyses of drill core data, field observations, and previous studies (Park & Park 1980; Choi 1983), a schematic cross-sectional view is constructed. This section clearly shows the ore pipe and carbonate rocks in a funnel-shape surrounded by serpentinite. Most of the magnetite mineralization is observed within the carbonate rocks with only small or trace amounts of magnetite within the serpentinites and hornfels. The carbonates and magnetite pipe are found at the bottom of cores drilled 650 and 300 m deep (Choi 1988), respectively, suggesting they continue farther at depth.

The shape and structure of the carbonates and surrounding rock types suggest the carbonates are an intrusive structure rather than representing a sedimentary sequence.

### STABLE ISOTOPES

The carbon and oxygen isotope compositions of the calcites show a bimodal distribution: Group I (fine- to medium-grained calcites) is in the range of  $\delta^{13}\text{C}_{\text{PDB}}=2.4$  to  $4.0\text{‰}$  and  $\delta^{18}\text{O}_{\text{SMOW}}=17.0$  to  $19.5\text{‰}$ , whereas Group II (coarse-grained calcites) is  $\delta^{13}\text{C}_{\text{PDB}}=-10.3$  to  $-11.1\text{‰}$  and  $\delta^{18}\text{O}_{\text{SMOW}}=9.8$  to  $11.2\text{‰}$ . Group II values are thought to be modified from Group I. This interpretation is based on their large crystal size and spatial association with dykes. The large calcite crystals possibly resulted from the local recrystallization of fine- to moderately coarse-grained calcite owing to the intrusion of basic dykes. The possible depletion of  $\delta^{13}\text{C}$  and  $\delta^{18}\text{O}$  in Group II can be produced by decarbonation or (and) contribution of  $^{13}\text{C}$ -depleted carbon from graphite or organic matter in sedimentary wall rocks. Alternatively, the incorporation of significant amounts of  $\text{CH}_4$  can be caused by the intrusion of basic dykes.

Compared to typical values from marine limestone, the  $\delta^{18}\text{O}$  values of Group I are slightly lower, while both  $\delta^{13}\text{C}$  and  $\delta^{18}\text{O}$  of Group I are far from those usually associated with carbonatite (Bowman 1998).

### RARE-EARTH ELEMENTS AND TRACE ELEMENTS

Trace elements and rare-earth elements (REEs) of the same calcite samples used for the stable isotope analysis have significantly lower concentration of REE as well as most trace elements relative to typical carbonatites. The total REE contents of the Ulsan carbonates range from 3 to 17 ppm, which are much lower than any igneous rocks and even lower than those of some sedimentary rocks. REE and trace-element abundances may have changed sufficiently due to alteration, thus, affecting petrogenetic

interpretations for the Ulsan carbonate rocks.

The REE data suggest that these carbonate rocks cannot be carbonatites of mantle origin. However, it is noteworthy that the range of compositional variations of typical carbonatite family rocks overlaps with those of sedimentary, metamorphic, and endogenic carbonate rocks (Samoilov 1991). Samoilov (1991) explained that one reason for the significant compositional variations of the carbonatites were due to different types of the associated alkaline rocks under different geologic-tectonic settings.

### DISCUSSION AND CONCLUSION

The Kyongsang basin is composed mainly of Cretaceous-early Tertiary rocks. Paleozoic limestone is reported only in the northern part of the Korean Peninsula up to the present time. Thus, it suggests that the Ulsan carbonates may have been uplifted by the intrusion of granite or transported via a strike-slip fault from the nearest outcrop of limestone 120 km to the south. However, the Kyongsang basin has not experienced any severe deformation since the Mesozoic, rather only sedimentation, uplift, and igneous activity. Moreover, many outcrop observations and cross-cutting relations are inconsistent with the previous ideas. A transportation of a funnel-shaped part of Paleozoic limestone without any of the associated rocks found in the region is geotectonically problematic.

Recent studies regarding carbonatite genesis suggest volatile fluxing and limestone/marble syntectonic relationships and crustal carbonate melt generated by intrusion-related pneumatolytic skarn processes may result in geochemical or isotopic compositions that vary within a spectrum of sedimentary crustal to mantle-like igneous sources for carbonatites (Lentz 1998). It is worth noting that an increasing trend of carbonatite magmatism with time has been explained in two different ways: One is due to recycling of more and more crustal carbon (as carbonates) into the mantle since Early Proterozoic (Ray *et al.*

2000), while the other is due to the increased availabilities of intrusion-related syntectonic processes with time (Lentz 1999); either assumption reveals more incorporation of crustal carbonate materials with time. In addition, the rare occurrence of carbonatites from oceanic settings was interpreted that crustal carbonate may serve as the source for at least some carbonatites (Hoernle *et al.* 2002).

In conclusion, this study suggests that the Ulsan carbonate rocks are an intrusive phase probably formed by crustal carbonate melt that was generated by the emplacement-related processes of an A-type granitic magma. If an entire spectrum of geochemistry and mineralization can be generated in between two end members, crustal and mantle carbonatite, according to a limestone melting/fluxing theory (Lentz 1999), outcrop evidences obtained from the spatial and simple cross-cutting relations can be decisive criteria for establishing the origin of carbonate rocks of the Ulsan mining area. If the limestone melting/fluxing theory (Lentz 1999) is correct, the relative proportion of carbonate melt generated in the study area is less, reflecting minor carbonatite genesis in association with the silica-saturated, weakly alkalic system.

## REFERENCES

- BOWMAN, J.R. 1998. Stable-isotope systematics of skarn. In LENTZ, D.R. (ed.) *Mineralized intrusion-related skarn systems*, 99-145. Mineralogical Association of Canada Short Course 26.
- CHOI, S. 1983. *Skarn evolution and iron-tungsten mineralization and the associated polymetallic mineralization at the Ulsan mine, Republic of Korea*. Unpublished PhD. Dissertation, Waseda University, 271 p.
- CHOI, S., SO, C., YOUM, S. & KIM, M. 1999. Stable isotope and fluid inclusion studies of iron-tungsten mineralization at Ulsan skarn deposit (Abstract). *Economic and Environmental Geology*, **32**, 148-9.
- CHOI, S.Y. 1988. *A study of the origin of serpentinite in Ulsan mine area*. Unpublished PhD. Dissertation, Pusan National University, 87 p (in Korean with English abstract).
- HOERNLE, K., TILTON, G., LE BAS, M.J., DUGGEN, S., & GARBE-SCHONBERG D. 2002. Geochemistry of oceanic carbonatites compared with continental carbonatites: mantle recycling of oceanic crustal carbonate. *Contributions to Mineralogy and Petrology*, **142**, 520-542.
- KOH, J.S., YUN, S.H. & LEE, S.W. 1996. Petrology and geochemical characteristics of A-type granite with particular reference to the Namsan granite, Gyeongju. *Journal of Petrology of Society of Korea*, **2**, 142-60 (in Korean with English abstract).
- LENTZ, D.R. 1998. Late-tectonic U-Th-Mo-REE skarn and carbonatitic vein-dyke systems in the southwestern Grenville Province: a Pegmatite-Related Pneumatolytic Model linked to Marble Melting (limestone syntexis). In: LENTZ D.R. (ed) *Mineralized intrusion-related skarn systems*, 519-657, Mineralogical Association of Canada Short Course 26.
- LENTZ, D.R. 1999. Carbonatite genesis: A reexamination of the role of intrusion-related pneumatolytic skarn processes in limestone melting. *Geology*, **27**, 335-38.
- PARK, K.H. & PARK, H.I. 1980. On the genesis of Ulsan Iron-Tungsten deposits. *Journal of Korean Institution of Mining Geology*, **13**, 104-16 (in Korean with English abstract).
- RAY, J., RAMESH, R. & PANDE K. 2000. Carbon isotopes in Kerguelen plume-derived carbonatites: evidence for recycled inorganic carbon. *Earth and Planetary Science Letters*, **170**, 205-14.
- SAMOILOV, V.S. 1991. The main geochemical features of carbonatites. *Journal of geochemical Exploration*, **40**, 251-262.
- WOOLLEY, A.R. & KEMPE, D.R.C. 1989. Carbonatite: Nomenclature, average chemical compositions, and element distribution. In: BELL, K. (ed) *Carbonatites: Genesis and evolution*, Unwin-Hyman, London, 1-14.
- YANG, K., HWANG, J. & YUN, S. 2003. The petrogenesis of the Ulsan carbonate rocks from the southeastern Kyongsang Basin, South Korea. *The Island Arc*, **12**, 428-439.

## Alteration-Mineralization Pattern and Geochemical Characteristics of Samli (Balikesir) Fe-Oxide-Cu-(Au) Deposit, Turkey

Erkan Yilmazer<sup>1\*</sup>, Nilgün Gulec<sup>1</sup>, & İlkey Kuscu<sup>2</sup>

<sup>1</sup>Middle East Technical University, Department of Geological Engineering, Ankara TURKEY

<sup>2</sup>University of Muğla, Department of Geological Engineering, Muğla TURKEY

(e-mail: [erkanyil@metu.edu.tr](mailto:erkanyil@metu.edu.tr))

**ABSTRACT:** Şamlı Fe-oxide deposit is one of the major iron-oxide producing mines in western Anatolia (Turkey) (with calculated reserve of 96 000 tonnes @ of 50 to 53% Fe, and >1% of copper (locally as high as 6.78% and 7.74% Cu). Gold and Ag range from 5 to 8 ppm, and 23.8 to 66.9 ppm, respectively. The Şamlı deposit is a typical magmatic-hydrothermal system related to emplacement, crystallization and cooling of Tertiary Şamlı pluton. The alteration and mineralization in Şamlı Fe-oxide deposit are formed in 3 major successive stages; pre-, syn-, and post-ore stages. Geochemical (+ isotopic) results for altered and fresh rock samples show that the mineralization in the region is accomplished by hydrothermal fluid(s) derived from a magmatic source during the emplacement of the Samli pluton. The Şamlı pluton was derived from a mantle source, which was either previously enriched by small degree partial melts, and/or metasomatized by an ancient subduction. The field characteristics, mineralizing events and alterations, the oxide and sulfide mineralogy, morphology and distribution of the iron-oxide deposits at Şamlı (Balikesir) deposits suggest that it shows characteristics similar to Fe-oxide-Cu-Au deposits.

**Keywords:** IRON OXIDE-CU-AU DEPOSITS, NA-CA ALTERATION, ŞAMLI PLUTON, ŞAMLI, BALIKESIR

### INTRODUCTION

The Samli Fe-oxide deposit (Balikesir, Western Anatolia-Turkey) is one of the iron-oxide producing mines in western Anatolia. This deposit has long known as a skarn-type Fe-oxide deposit. However, our recent research has revealed that the alteration hosting the iron-oxide mineralization also contains some unusual assemblages, and the sulfide mineralogy with abundant gold content, should not be related to skarn systems.

### GEOLOGY

The Şamlı deposit is located within the Sakarya Zone of Turkey, which is made up of arc-trench sequence of Permo-Triassic age, known as Karakaya Formation or Karakaya complex (Okay *et al.* 1990) (Figure 1). This complex was formed during the closing of Paleo-Tethys and unconformably overlying Jurassic-Cretaceous sediments (Akyüz & Okay 1998). The Karakaya Complex consists of a volcanic-volcaniclastic sequence consisting of mafic pyroclastics and tuffs

that alternate with carbonates, turbiditic graywackes, and olistoliths of Permian and Carboniferous ages cut across by the Şamlı pluton (Leo & Genç 1986; Okay *et al.* 1990).

In the deposit site, Karakaya Complex is characterized by metapelitic rocks, metadiabase, and recrystallized limestone. The metadiabase and recrystallized limestone occur either as blocks within the Karakaya Complex, or as roof-pendants within the Şamlı pluton. The Şamlı pluton is a large, intermediate to mafic intrusive body emplaced into the rocks of Karakaya Complex. The reported K/Ar geochronology on biotite range from 23.5±1.5 Ma to 18.4±2.2 Ma (Watanabe *et al.* 2003; Karacık *et al.* 2008). Aplite, quartz, and rare pegmatite dykes and veins cut both the main granitoid body and the country rocks.

### ALTERATION & MINERALIZATION

The alteration and mineralization in the Şamlı deposit is result of a series of 3 overlapping stages (Fig. 2); The pre-ore

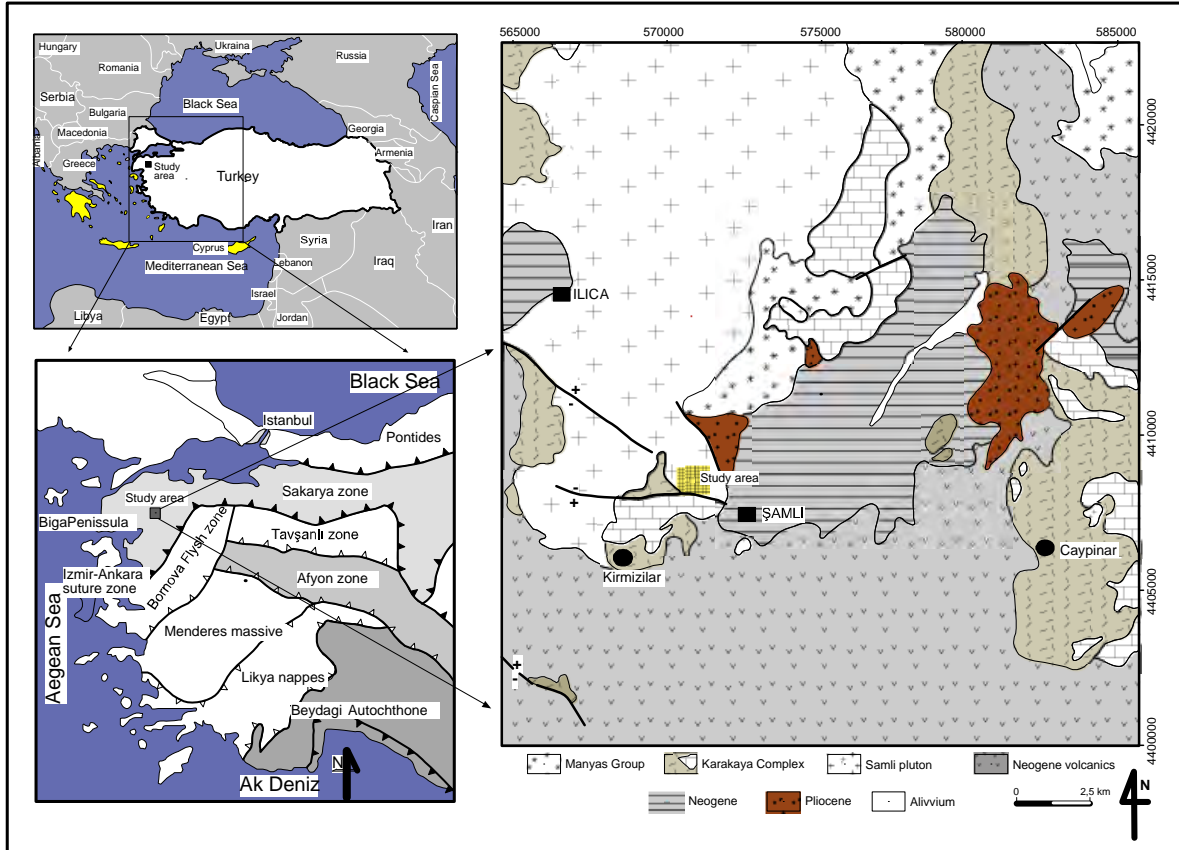


Fig 1. Location & Geological map of Samli-ironoxide deposit.

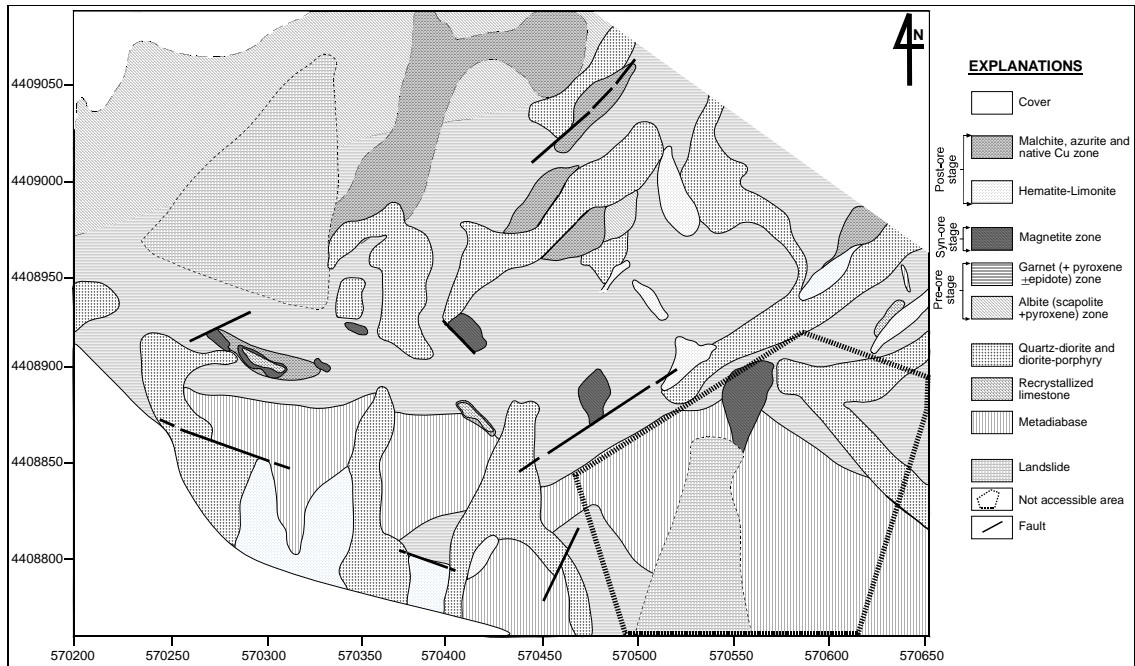
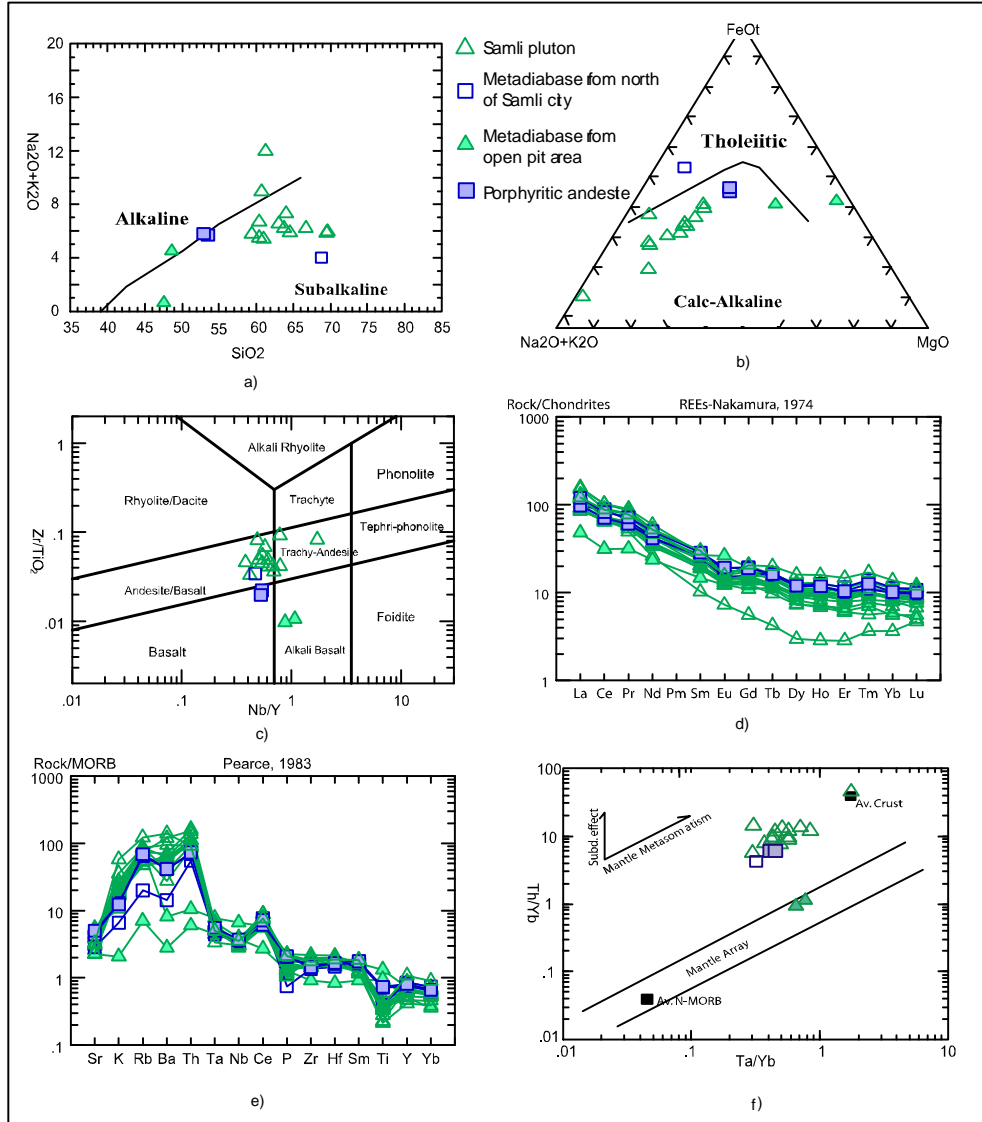


Fig. 2. Alteration-mineralization pattern of Samli Fe-oxide deposit, Turkey.



**Fig. 3.** Total alkalis versus silica (TAS) and (b) AFM plot of Irvine and Baragar (1971), (c) modified Zr/TiO<sub>2</sub>-Nb/Y plot (Pearce, 1996) of Winchester and Floyd (1977), (d) Rock/chondrite-normalized REE diagram for rocks of Şamlı-İlica pluton and (e) rock/MORB-normalized spidergrams, (f) Th/Yb vs Ta/Yb diagram.

stage refers to Na-Ca alteration including albite (+ scapolite + pyroxene) and garnet-pyroxene (± epidote) alteration assemblage. Syn-ore stage consisting mainly of K-Fe-(Ca) alteration includes magnetite, hydrothermal biotite, epidote, and actinolite. The main magnetite-hematite mineralization is hosted by the syn-ore assemblage. This stage is traced along the pluton-metadiabase/metapelite and pluton- recrystallized limestone

contacts and hosted by garnet - pyroxene (± epidote) zone with superimposed albitic alteration. The post-ore stage overprints the Na-Ca and K-Fe assemblages, and consists of chalcopyrite (+epidote +actinolite) hematite-limonite, and Cu-rich (malachite, azurite and native copper) zones. Chalcopyrite, being the most common sulfide, is usually observed as micro-veinlets, together with pyrite in

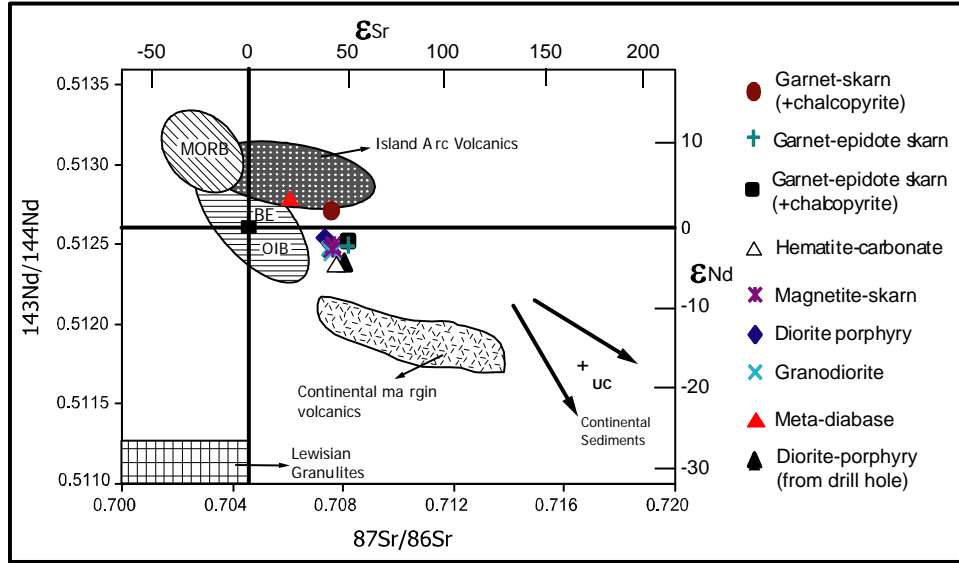


Fig. 4. Nd-Sr isotope correlation diagram.

garnet pyroxene ( $\pm$  epidote) and magnetite zones, while hematite-limonite and Cu-carbonates is only seen as structurally controlled veins and patches in oxidation zones.

**GEOCHEMISTRY**

The Şamlı pluton is subalkaline and calc-alkaline, and mainly diorite porphyry, granodiorite, quartz monzonite, and granite-porphyry in composition (Fig. 3). The metadiabase is alkali basalt in composition, based on the major- and trace-element contents. The REE and multielement patterns with significant depletion of Nb and Ta and enrichment of Th and Ba is suggestive of mantle metasomatism or crustal contamination. Likewise, Th/Yb vs Ta/Yb ratios suggests a mantle source, which was either previously enriched by small degree partial melts (displacement along the mantle array), and/or metasomatized by an ancient subduction (Fig. 3).

**$^{87}\text{Sr}/^{86}\text{Sr}$ ,  $^{143}\text{Nd}/^{144}\text{Nd}$ , &  $^{34}\text{S}$**

**GEOCHEMISTRY**

Results of  $^{87}\text{Sr}/^{86}\text{Sr}$  and  $^{143}\text{Nd}/^{144}\text{Nd}$ , and  $^{34}\text{S}$  isotope analyses (for both altered and fresh rock samples) range between

0.512361-0.512793 for  $^{143}\text{Nd}/^{144}\text{Nd}$ , 0.706056 – 0.708167 for  $^{87}\text{Sr}/^{86}\text{Sr}$  and 0.4-2.6‰ for  $^{34}\text{S}$  respectively (Figure 4).

All samples belonging to Şamlı pluton have a similar  $^{87}\text{Sr}/^{86}\text{Sr}$  isotope ratio (except for metadiabase characterized by low Sr isotope ratio), suggesting the effect of fractional crystallization process in the genesis of the rocks, although the possibility of crustal contamination can not be entirely ruled out. Sr-Nd isotope ratios of almost all altered samples show similarity to that of the Şamlı pluton, implying a magmatic source for hydrothermal fluid(s), as is suggested by S-isotope compositions of sulfide samples.

**CONCLUSIONS**

The Na-Ca and K-Fe-(Ca) alteration assemblage hosting iron-oxide, copper and gold mineralization and spatial and temporal relationship between mineralization and alteration, as well as the oxide and sulfide mineralogy at Şamlı (Balıkesir) suggest that it has characteristics more akin to Fe-oxide-Cu-Au systems.

### ACKNOWLEDGEMENTS

This work is part of ongoing research project and supported by Middle East Technical University (METU), Project No: BAP-03-09-2007-04. We would like to express our sincere thanks to METU.

### REFERENCES

- AKYÜZ, H.S. & OKAY, A.İ. 1998. The Geology Of The South of Manyas (Balıkesir) and Tectonic Significance of Blueschists. *Mineral Res. Expl. Bull.*, **120**, 81-95.
- IRVINE T.N. & BARAGAR, W.R.A. 1971. A guide to the chemical classification of the common volcanic rocks. *Canadian Journal of Earth Sciences*, **8**, 523-548.
- LEO, G.W. & GENÇ, M.A. 1986. Geology and iron deposits of the Şamlı area, Balıkesir Province, MTA, Türkiye.
- OKAY, A.İ., SIYAKO, M., & BÜRKAN, K.A. 1990. Geology of the Biga Peninsula and its tectonic evolution. *TPJD Bull.* (Turkish Association of Petroleum Geologists Bulletin) **2/1**, 83-121 (in Turkish).
- KARACIK, Z., YILMAZ, Y., PEARCE, J.A., & ECE, Ö.I. 2008. Petrochemistry of the south Marmara granitoids, northwest Anatolia, Turkey, *International Journal of Earth Sciences*, **97**, 1181-1200.
- PEARCE J.A. 1996, A user's guide to basalt discrimination diagrams. In: WYMAN, D.A. (ed) *Trace Element Geochemistry of Volcanic Rocks: Applications for Massive Sulphide Exploration*. Geological Association of Canada, *Short Course Notes*, v.12, p.79-113.
- WATANABE, Y., MURAKAMI, H., CENGİZ, İ., SARI, R., KÜÇÜKEFE, S., & VE YILDIRIM, S. 2003. Study on Hydrothermal Deposits and Metallogeny in Western Turkey MTA, Ankara.
- WINCHESTER, J.A. & FLOYD, P. A. 1977, Geochemical discrimination of different magma series and their differentiation products using immobile elements. *Chemical Geology*, **20**, 325-343.



## Total and soil organic carbon, and total sulfur determinations of soils from Cyprus

Andreas Zissimos\*<sup>1</sup>, Eleni Morisseau<sup>1</sup>, Eleni Stavrou<sup>1</sup>, & David Cohen<sup>2</sup>

<sup>1</sup>Geological Survey Department of Cyprus, Strovolos CYPRUS (email: [azissimos@gsd.moa.gov.cy](mailto:azissimos@gsd.moa.gov.cy))

<sup>2</sup>School of BEES, University of New South Wales, Sydney, NSW, 2052 AUSTRALIA

**ABSTRACT:** This study is part of the detailed Soil Geochemical Atlas of Cyprus project, involving analysis of 5,520 sites. The general aim of the project is to establish controls on baseline soil geochemical parameters for application in a range of environmental and resource studies. A method has been developed for measuring total carbon (TC), soil organic carbon (SOC) and total sulfur (TS), yielding a limit of quantification of 0.006% TC and 0.003% TS.

**KEYWORDS:** Soil, Cyprus, atlas

### INTRODUCTION

Soils are complex materials, containing components of mixed origins with differing physical, chemical and biological properties. The form and concentrations of C and S in soils are important indicators of the environmental status of soils, their agricultural potential and their ability to filter and buffer contaminants (Nuwer & Keil 2005; Rawlins *et al.* 2008; Sylvia *et al.* 2005).

Soils sequester large amounts of C and their capacity to store large amounts of organic carbon (OC) is of considerable importance to modeling the global carbon cycle and, at national scales, allow estimation of soil-related CO<sub>2</sub> emissions as part of commitments to the United Framework Convention on Climate Change (Panagos *et al.* 2008). Modeling requires accurate determination of the portion of inorganically-bound C in soil that is of geogenic origin and tightly bound in various mineral forms (Sahrawat 2003). Carbon is also present in soil biota, micro-organisms and debris of plants, as soil or total organic carbon (SOC or TOC) (Parton *et al.* 1987).

Sulfur enters the current geochemical cycle with the weathering of rocks and conversion to either SO<sub>2</sub> or SO<sub>4</sub><sup>2-</sup>-bearing species, and subsequent uptake by plants and microorganisms and conversion into a variety of organic forms. Despite the

importance of soil C and S in environmental monitoring and modeling, there are no commonly-agreed standards for differentiation of the forms of C and S in soils, and a plethora of measurement methods have been published (Essington 2004; Lorenz *et al.* 2006; Schumacher 2002; Tabatabai & Bremner 1970).

This study forms part of the Geochemical Atlas of Cyprus project, aimed at determining factors broad geological and land-use that control TC, TOC and TS in the soils of Cyprus.

The geology of Cyprus is dominated by four distinct terranes - the Troodos Ophiolite Complex composed of mafic and ultramafic rocks, the Circum-Troodos Sedimentary Sequence containing calcarenites, siltstones and carbonates, the Mamonia Complex composed of igneous, sedimentary and metamorphic rocks and the Kyrenia Terrain containing a series of allochthonous massive and recrystallised limestones dolomites and marbles. These terranes generate highly varied landscapes (Fig 1).

### EXPERIMENTAL

The methods for the analyses for TOC and SOC have been developed based on the international standard ISO 10694:1995 and ISO15178:2000.

Soil samples have been collected from



**Fig 1.** View from edge of Messaoria Plain at Tseri towards dissected palaeo-fan surfaces in middle ground and the Troodos Ophiolite Complex mountains in the background.

the upper 25 cm and the 50 to 70 cm section of regolith profiles at each of 5,520 sites across Cyprus, and sieved to <2mm and milled. A bulk soil sample (CYP-A), derived from a calcarenite is being used as an in-house reference material for testing the analytical protocols.

Samples are oven dried at 100°C after which they are weighed in order to measure water content. TC and TS are measured by introducing dried samples to the Carbon Sulfur (CS) automatic analyzer (Eltra CS-800) instrument. Subsequently, 2g of each sample is introduced in pre-weighed high temperature porcelain crucibles and is introduced to a high temperature muffle furnace for the removal of carbonates at 900°C. Samples are then introduced to the CS automatic analyzer for measurement of organic residual carbon.

For every batch of 20-30 samples a quality control reference material is analysed - either NIST SRM 2711 or CYP-A.

## RESULTS AND DISCUSSION

The QC results indicate that the methods developed deliver consistent measurements of TC and TS (Table 1). Measurement of SOC has proven less reliable with a lack of externally certified materials with known values of SOC, or accepted standards to determine SOC.

However, a measure of the overall internal precision of our method for measuring SOC indicates reasonably reproducible results (Table 2).

**Table 1.** Estimates of repeatability (CVr) and reproducibility (CVR) for TC and TS in soil reference materials NIST2710 and 2711.

	TC (%)	TS (%)	TC (%)	TS (%)	TC (%)	TC (%)
CRM	NIST 2711	NIST 2711	NIST 2711	NIST 2711	NIST 2710	NIST 2710
N	76	76	10	10	7	6
Mean	1.739	0.045	1.797	0.041	2.983	0.269
Std Dev	0.044	0.012	0.025	0.002	0.562	0.023
CVR (%)	2.5	26.0			18.8	8.7
CVr (%)			1.4	5.4		

Soil certified reference materials: NIST 2711 *Montana II Soil* %S 0.042 cert. value, %C 2.0 recom. value; NIST 2711 *Montana I Soil* %S 0.240 cert. value, %C 3.0 recom. value

**Table 2.** Estimates of reproducibility (CVR) for TC, TS and SOC results on in-house soil reference material CYP-A.

	TC (%)	TS (%)	SOC (%)
<b>N</b>	30	29	30
<b>Mean</b>	10.887	0.053	0.171
<b>Std Dev</b>	0.129	0.016	0.047
<b>CVR</b>	1.2	31.0	27.4

Limits of detection (LOD) and limits of quantification (LOQ) for C and S have been evaluated through consecutive measurements of blank crucibles containing accelerator reagents without any sample (Table 3).

The results show good correlation between primary lithological compositions of geological terrains. For example, areas of known sulfide deposits in the Kalavassos area (Fig. 2) show elevated concentrations of TS. Of the ~1000 samples analysed so far in the study, the average TC is 5.304% and average SOC is 1.1%. These values are consistent with data from previous studies on soils in

Cyprus. The average TS value in the soils tested is 0.188%.

The techniques will now be applied to the full sample set collected from 5,520 sites, at an average density of one site per km<sup>2</sup> covering the Republic of Cyprus.

**Table 3.** LOD and LOQ assessment using blanks.

	TC (%)	TS (%)
<b>N</b>	10	10
<b>Mean</b>	0.0015	0.0009
<b>SD</b>	0.0007	0.0005
<b>LOD</b>	0.002	0.001
<b>LOQ</b>	0.006	0.003

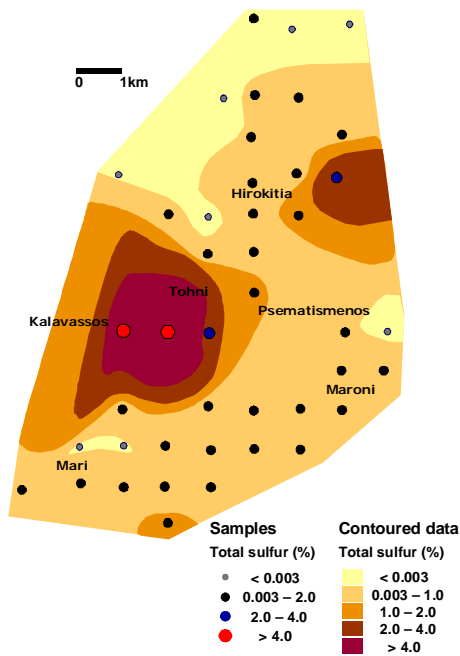


**Fig 2.** Variation in TS in the top 25cm of soil in the vicinity of the Kalavassos sulfide deposit.

**REFERENCES**

ESSINGTON, M.E., 2004. *Soil and Water Chemistry: An interactive Approach*, CRC Press.

ISO, 1995. *Soil quality - Determination of organic and total carbon after dry combustion*. ISO standard 10694:1995.

ISO, 2000. *Soil quality – Determination of total sulfur by dry combustion*. ISO standard 15178:2000.

LORENZ, K., PRESTON, C.M., & KANDELER, E. 2006. Soil organic matter in urban soils: Estimation of elemental carbon by thermal oxidation and characterization of organic matter by solid-state <sup>13</sup>C NMR spectroscopy. *Geoderma*, **130**, 312–323.

NUWER, J.M. & KEIL, R.G., 2005. Sedimentary organic matter geochemistry of Clayoquot Sound, Vancouver Island, British Columbia. *Limnology and Oceanography*, **50**, 1119–1128.

PANAGOS P., VAN LIEDEKERKE, M., MONTANARELLA, L., & JONES, R.J.A. 2008. Soil organic carbon content indicators and web mapping applications. *Environmental Modelling & Software*, **23**, 1207-1209.

PARTON, W.J., SCHIMEL, D.S., COLE, C.V., & OJIMA, D. 1987. Analysis of factors controlling soil organic matter levels in the Great Plains grasslands. *Soil Science Society of America Journal*, **51**, 1173–1179,

RAWLINS, B. G., VANE, C.H., KIM, A.W., TYE, A.M., KEMP, S.J., & BELLAMY, P.H., 2008. Methods for estimating types of soil organic carbon and their application to surveys of UK urban areas. *Soil Use and Management*, **24**, 47–59.

SAHRAWAT K. L. 2003. Importance of inorganic carbon in sequestering carbon in soils of the dry regions, *CURRENT SCIENCE*, **84**, (7), 10 April.

SCHUMACHER, B.A. 2002. Methods for the determination of total organic carbon in soils and sediments. US EPA Report, NCEA-C-1282, EMASC-001.

SYLVIA, D.M., FUHRMANN, J.J., HARTEL, D.P.G., & ZUBERER, A., 2005. *Principles and Applications of Soil Microbiology*, Pearson Prentice Hall.

TABATABAI M.A. & BREMNER, J.M., 1970. Comparison of Some Methods for Determination of Total Sulfur in Soils. *Soil Science Society of America Journal*, **34**, 417-420.





# Sponsors



## Symposium bags sponsor



## Platinum sponsors



**ANGLO  
AMERICAN**

## Gold sponsors



## Silver sponsors



## Bronze sponsors

